



**This electronic thesis or dissertation has been
downloaded from Explore Bristol Research,
<http://research-information.bristol.ac.uk>**

Author:
Smith, Giles A

Title:
Palynology of the Jurassic/Cretaceous boundary interval in the Volga Basin, Russia.

General rights

Access to the thesis is subject to the Creative Commons Attribution - NonCommercial-No Derivatives 4.0 International Public License. A copy of this may be found at <https://creativecommons.org/licenses/by-nc-nd/4.0/legalcode>. This license sets out your rights and the restrictions that apply to your access to the thesis so it is important you read this before proceeding.

Take down policy

Some pages of this thesis may have been removed for copyright restrictions prior to having it been deposited in Explore Bristol Research. However, if you have discovered material within the thesis that you consider to be unlawful e.g. breaches of copyright (either yours or that of a third party) or any other law, including but not limited to those relating to patent, trademark, confidentiality, data protection, obscenity, defamation, libel, then please contact collections-metadata@bristol.ac.uk and include the following information in your message:

- Your contact details
- Bibliographic details for the item, including a URL
- An outline nature of the complaint

Your claim will be investigated and, where appropriate, the item in question will be removed from public view as soon as possible.

**Palynology of the Jurassic/Cretaceous boundary
interval in the Volga Basin, Russia.**

Giles A. Smith

**A dissertation submitted to the University of Bristol in
accordance with the requirements of the degree of Ph.D. in
the Faculty of Science.**

Department of Earth Sciences, December 1999.

80,000 words.

Acknowledgements

There seem to be an inordinate number of people who deserve my gratitude. Firstly, I wish to thank those people who assisted in the organisation of my field trips, and gave up their time to act as guides in each area. Natasha Bakhurina and Dave Unwin helped on many occasions with on-the-spot translations to and from Russian, and similarly Gilles Cuny was only too happy to offer his services in respect to the French language. Beef issues never entered into it!

I wish to express my gratitude to Vladimir Efimov and family for their co-operation and continued interest in my study of the Volga geological preserve. Without that, this Ph.D. would simply never have been started! Many thanks indeed for supplying me with reams of appropriate documentation, so that I could fly out of Sheremitzayevo airport laden with fossils, and not be arrested! Thanks also to Drs Alifanov and Sennikov for their kind hospitality during my brief visits to Moscow.

To Dr Philip Hoedemaeker I wish to express my deepest admiration and gratitude for his work on Tethyan:Boreal correlation, and his willingness to discuss such matters with me. Thanks for spending time on Section Z with me, despite the fact that I have not been able to use any of the data we collected together in the summer of '96. My best wishes go to both him and the 'ammonite digging team'.

Thanks also to Prof. Taj-Eddine and Dr Aoutem for donating their time to my field season in Morocco. I'm disappointed that it didn't pay off, but it was certainly an experience!

Next I would like to thank all those who have offered snippets of advice, or helped in a more hands-on way during the course of this project. A big thank you must go to Mr Shir Akbari of Southampton University for his willingness to let me take over his lab at various stages during the processing of my samples. He has always found time to assist me when needed, and has taken a keen interest in my progress at every stage. Thank you.

Similarly, I owe a debt of gratitude to Dr John Marshall of the same institution. He unselfishly allowed me to use his microscope for the photography, and has been kind enough to offer tid-bits of advice and assistance whenever they were requested. Oh, and thanks for getting me onto the 'friends and family' rate when using the elemental analyser!

Clearly, many thanks are owed to my advisor, Professor Michael J Benton. Particularly I want to thank him for his general availability whenever I had questions, and his enduringly positive opinions about whatever it was that I wanted to do. Arguably, this was not always what I needed, but when things weren't going right, this certainly helped to keep me productive! Also thanks for sliding so many little pots of money my way, whenever I needed a few quid for either processing or fieldwork. Financially, it would have been impossible to complete this work without him!

I am most deeply indebted to Ian Harding, also of the University of Southampton. He was always keen and willing to help, even before being officially recognised in the supervisory role. I don't even know how many times he helped me out with one thing or another. I couldn't fit this thesis into one volume if I listed them all here, so I won't attempt it! I know he'll call in the favours some day; that's fine, I need to address the balance somehow! I really am grateful for all his help. Thanks.

At this point I would like to take the unusual step of thanking those jolly but short-sighted fellows at NERC for refusing to sponsor me. Free from the 'burden' of official sponsorship, I have been able to develop and steer this project in the directions I saw fit. Ironically, that potentially saved this Ph.D.!

Finally, I would like to recognise all those people who have helped outside the science. I am enormously appreciative of my grandparents, who have offered both moral and financial assistance throughout my education (and probably before that). Their influence will always be embedded in everything I achieve. Similarly, thanks go to my mother, who has remained almost doggedly optimistic, encouraging and embarrassingly proud throughout. I don't always understand it, and sometimes even get irritated by it, but it certainly kept me plugging away during tough times! Actually, its almost entirely due to my family as a whole that I didn't pack this PhD in after the first year. I just hope I don't disappoint them!

For my loving partner Rebecca, a special note is also required. Only she knows how much stress she has had to put up with, especially during the write-up stage of this PhD. She really has been a rock through all this (no pun intended!), and her love and support have helped me more than I can adequately express. I hope that I can be similarly effective during the latter stages of her own doctorate!

I can't finish these acknowledgements without a short thank you to a few friends. I'm not going to do a Gwyneth Paltrow and thank everyone I've ever met, but suffice to mention my good friend Adrian Steele, who himself knowing just what it takes to get *the title*, has been a continuous source of moral support. Finally, thanks to Rob and Dave Carr, who were able to offer physical support, particularly at the end of many a long evening out during my first year in Bristol. It was, after all, a difficult time for me!

AUTHOR'S DECLARATION

I declare that the work in this dissertation was carried out in accordance with the regulations of the University of Bristol. The work is original except where indicated by special reference in the text and no part of the dissertation has been submitted for any other degree.

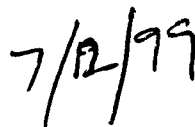
Any views expressed in the dissertation are those of the author and in no way represent those of the University of Bristol.

The dissertation has not been presented to any other University for examination either in the United Kingdom or overseas.

SIGNED:

A handwritten signature in black ink, appearing to be 'G. R. D.', written over a horizontal line.

DATE:

A handwritten date '7/12/99' in black ink, written in a vertical orientation.

Contents

Section	Description	Page
Abstract.....		I
Acknowledgements.....		II
Author's Declaration.....		IV
List of Figures.....		VIII
List of Tables.....		X
Contents of floppy disc (back pocket).....		XII
1	Introduction to Jurassic/Cretaceous boundary studies.....	1
1.1.	Introduction to Jurassic/Cretaceous boundary studies.....	2
1.1.2.	Rationale, aims, and evolution of the project.....	11
1.2.	Review of Jurassic/Cretaceous boundary marine palynology.....	15
1.2.1.	The United Kingdom and NW Europe.....	15
1.2.2.	Scandinavia, 'Scandinavian Arctic'.....	30
1.2.3.	Canada, Canadian Arctic.....	32
1.2.4.	Eastern Europe, Russia, Russian Arctic.....	36
1.3.1.	Tethyan: Western Europe; S. Germany, Switzerland, SE France, Portugal, Spain.....	39
1.3.2.	NW Africa, eastern North Atlantic.....	46
1.3.3.	California, western North Atlantic.....	47
1.3.4.	East & Central Africa, the Middle East, India, China.....	49
2.	Review of the palynofacies literature.....	52
2.1.	Review of published classification schemes.....	53
2.2.	Terminology used in this report.....	64
2.3.	Interpretation of palynological matter components.....	73
2.3.1.	Woody phytoclasts.....	73
2.3.2.	Cuticle.....	79
2.3.3.	Sporomorphs.....	79
2.3.4.	Dinoflagellate cysts.....	81
2.3.5.	Acritarchs.....	86
2.3.6.	Prasinophytes.....	86
2.3.7.	AOM.....	87
3.	Methods.....	89
3.1.	Sample collection and processing.....	90
3.1.1.	Sample collection.....	90
3.1.2.	Sample processing methods.....	91
3.1.3.	Choice of sieve apparatus.....	93
3.1.4.	The use of <i>Lycopodium clavator</i> spore spikes.....	94
3.2.	Analytical methods.....	96
3.2.1.	Methods employed in biostratigraphic analysis.....	96
3.2.2.	Methods employed in relative taxonomic abundance, diversity, and dominance analyses.....	97
3.2.3.	Methods employed in palynofacies analysis.....	99
3.2.4.	Methods employed in total organic carbon (TOC) analysis.....	102
3.2.5.	Preparation of materials for the scanning electron microscope (SEM).	104
3.2.6.	The use of cluster analysis.....	104
3.3.	Testing the processing procedure: effects of nitric acid oxidation and ultrasonic vibration on the palynologic matter assemblages.....	107
3.3.1.	Rationale and technique.....	107
3.3.2.	Effects of processing procedure on the major components of palynological matter.....	108
3.3.3.	Effects of processing procedure on the absolute abundance of palynological matter.....	115
3.3.4.	Effects of processing procedure on the dinocyst assemblages.....	118
3.3.5.	Effects of ultrasonic treatment on woody phytoclast particle size.....	124
3.3.6.	Effects of processing procedure: summary.....	127

Section	Description	Page
4.	Biostratigraphy	129
4.1.	Introduction.....	130
4.1.1.	Location.....	130
4.1.2.	Sedimentology.....	130
4.1.3.	Previous work on the Volga Sections.....	141
4.2.	Dinocyst biostratigraphy and zonation of the Volga Basin	150
4.2.1.	Introduction.....	150
4.2.2.	Dinocyst biostratigraphy of the Gorodische section.....	150
4.2.3.	Dinocyst biostratigraphy of the Kashpir section.....	162
4.2.4.	Comparison of the dinocyst biostratigraphy of the two sections.....	173
4.2.5.	General comparison of the dinocyst assemblages encountered in the present study with other palynological investigations of the Volga Basin.....	177
4.2.6.	Comparison and correlation of the important dinoflagellate cyst ranges and biohorizons in NW Europe and elsewhere in the Russian Platform with those from the Volga Basin.....	179
4.2.7.	Summary of important dinocyst markers.....	195
4.2.8.	Dinoflagellate cyst age of the unzoned deposits at Gorodische and Kashpir.....	197
4.2.9.	Dinoflagellate cyst zonation of the Volga Basin.....	199
4.2.10.	Summary.....	211
4.3.	Dinocyst species list and systematics	212
4.3.1.	Introduction.....	212
4.3.2.	Species list.....	212
4.3.3.	Formal description of new taxa.....	218
4.3.4.	Systematics of selected dinoflagellate cysts.....	236
5.	Volga Basin palynofacies investigation	264
5.1.	Gorodische palynofacies investigation	265
5.1.1.	Total organic carbon (TOC) content.....	265
5.1.2.	Bulk palynological matter.....	267
5.1.3.	Analysis of structured components.....	275
5.1.3.1.	Relative abundance data (%SM).....	275
5.1.3.2.	Detailed analyses of the phytoclast assemblages (%Phyt).....	278
5.1.3.3.	Absolute abundance analysis.....	291
5.1.4.	Interpretation of depositional environments for the Gorodische section based on palynofacies and sedimentological data.....	301
5.2.	Kashpir palynofacies investigation	309
5.2.1.	Total organic carbon (TOC) content.....	309
5.2.2.	Bulk palynological matter: A-P-D plots.....	309
5.2.3.	Analyses of the structured components.....	315
5.2.3.1.	Relative abundance data (%SM).....	315
5.2.3.2.	Detailed analysis of the phytoclast assemblages (%Phyt).....	321
5.2.3.3.	Analyses of particle size data.....	323
5.2.3.4.	Absolute abundance of structured components.....	329
5.2.4.	Interpretation of depositional environments for the Kashpir section based on palynofacies and sedimentological data.....	331
5.3.	Assessment of the dinoflagellate cyst assemblages	344
5.3.1.	Diversity and dominance.....	344
5.3.1.1.	Gorodische.....	345
5.3.1.2.	Kashpir.....	345
5.3.1.3.	Summary.....	347
5.3.2.	Chorate/cavate/proximate groups.....	348
5.3.2.1.	Gorodische.....	348
5.3.2.2.	Kashpir.....	353
5.3.2.3.	Absolute abundance data.....	360
5.3.2.4.	Summary.....	364

Section	Description	Page
5.3.3.	Detailed morphological subdivision.....	364
5.3.3.1.	Gorodische.....	368
5.3.3.2.	Kashpir.....	374
5.3.3.3.	Discussion.....	380
5.3.3.4.	Summary.....	384
5.3.4.	Taxonomic abundance.....	384
5.3.4.1.	Gorodische.....	385
5.3.4.2.	Kashpir.....	389
5.3.5.	Summary of the dinocyst investigation.....	406
6.	Summary and conclusions.....	407
6.1.	Biostratigraphy; summary.....	407
6.2.	Biostratigraphy; conclusions.....	408
6.3.	Sedimentology and palynofacies analysis; summary.....	411
6.4.	Sedimentology and palynofacies analysis; conclusions.....	412
6.5.	Analysis of the dinocyst assemblage; summary & conclusions.....	413
6.6.	Recommendations for future work.....	415
	References.....	417
	Appendix A: Location & log of Section Z, Barranco de Tollo, SE Spain.....	454
	Appendix B: Location, logs and data from the Agadir Basin, Morocco (see also floppy disc).....	457
	Plates.....	462

List of abbreviations used:

cm	centimetre(s)
km	kilometre(s)
µm	micrometre(s)
mm	millimetre(s)
%Phyt	% of total phytoclast assemblage
%SM	% of total structured components of palynological matter
TOC	Total organic carbon
Wt%	Weight % (of total organic carbon)

List of figures:

Figure	Section	Description	Page
1.1.	1.1.	Correlation of Boreal and Tethyan ammonite sequences (A3 foldout).....	6
1.2.	1.2.1.	Correlation of Boreal dinocyst zonation schemes (A3 foldout).....	19
1.3.	1.3.1.	Correlation of Tethyan dinocyst zonation schemes (A3 foldout).....	43
2.1.	2.1.	Comparison of palynological matter classification schemes.....	57
2.2.	2.2.	Comparison of palynological matter terminology used in the present report with that of Tyson (1995) and Batten (1996).....	63
2.3.	2.2.	Morphological subdivision of dinoflagellate cysts.....	70
3.1.	3.1.2.	Flow diagram of palynological processing procedure.....	92
3.2.	3.1.4.	Equations for calculating absolute abundance with <i>Lycopodium</i> spores.....	95
3.3.	3.2.2.	Fisher α diversity diagram.....	98
3.4.		Calculation of PhytOC and AmexOC.....	100
3.5.	3.2.4.	Calculation of TOC.....	103
3.6.	3.2.6.	Methodology of cluster analysis.....	106
3.7.	3.3.2.	Effects of processing procedure on relative abundance of AOM and dinocysts.....	111
3.8.	3.3.2.	Effects of processing procedure on relative abundance of woody phytoclasts.....	113
3.9.	3.3.2.	Effects of processing procedure on major palynological matter groups.....	114
3.10.	3.3.3.	Effects of processing procedure on absolute abundance of palynological matter components.....	116
3.11.	3.3.4.	Effects of processing procedure on the relative abundance of dinocyst morphological groups.....	120
3.12.	3.3.4.	Effects of processing procedure on the number of dinocyst species per morphological group.....	121
3.13.	3.3.4.	Effects of processing procedure on Fisher α diversity and Goodman dominance values.....	123
3.14.	3.3.5.	Effects of ultrasonic treatment on the phytoclast size measurements.	126
4.1.	4.1.	Location map of Volga Basin sections.....	131
4.2.	4.1.3.	Correlation of Gorodische sedimentary log with previously published logs.....	143
4.3.	4.1.3.	Correlation of Volgian and Boreal Standard ammonite sequences.....	145
4.4.	4.1.3.	Correlation of Kashpir sedimentary log with previously published logs.....	149
4.5a.	4.2.2.	Dinocyst range chart, Gorodische.....	154
4.5b.	4.2.2.	Dinocyst range chart, Gorodische; continued.....	158
4.6a.	4.2.3.	Dinocyst range chart, Kashpir.....	167
4.6b.	4.2.3.	Dinocyst range chart, Kashpir; continued.....	169
4.7.	4.2.5.	Comparison of Volga Basin Jurassic dinocyst data with those of NW Europe (A3 foldout).....	181
4.8.	4.2.6.	Comparison of Volga Basin Cretaceous dinocyst data with those of NW Europe (A3 foldout).....	188
4.9.	4.2.9.	Comparison of the Volga Basin dinocyst zonation with that of NW Europe.....	200
4.10.	4.3.1.	Measurements performed on new dinocyst species.....	217
4.11.	4.3.3.	Exploded paratabulation of <i>Lithodinia distincta</i> sp. nov.	222

Figure	Section	Description	Page
4.12.	4.3.3.	Direction of paraplate overlap in <i>Lithodinia distincta</i> sp. nov.	222
4.13.	4.3.3.	Inferred apical paratabulation and archeopyle type in <i>Cyclonephelium bulbosum</i> sp. nov.....	226
4.14.	4.3.3.	Exploded paratabulation of <i>Rhynchodiniopsis magna</i> sp. nov.....	231
4.15.	4.3.3.	Exploded paratabulation of <i>Rhynchodiniopsis undoryensis</i> sp. nov.....	231
5.1.	5.1.1.	TOC and AOM at Gorodische.....	266
5.2.	5.1.2.	Ternary A-P-D plot.....	270
5.3.	5.1.2.	Cluster analysis of A-P-D data.....	272
5.4.	5.2.2.	A-P-D plot by sequence of deposition.....	274
5.5.	5.1.3.1.	Relative abundance of structured components.....	277
5.6.	5.1.3.2.	Relative abundance of phytoclast components.....	279
5.7.	5.1.3.2.	Phytoclast size data.....	282
5.8.	5.1.3.2.	Phytoclast roundness and sorting (STDEV).....	285
5.9.	5.1.3.2.	Ternary plots of relative abundance data.....	287
5.10.	5.1.3.2.	Ternary plot of 'fresh' vs. oxidised materials.....	289
5.11.	5.1.3.2.	Cluster analysis of relative abundance data.....	290
5.12.	5.1.3.3.	Major component absolute abundance.....	294
5.13.	5.1.3.3.	Minor component absolute abundance.....	296
5.14.	5.1.3.3.	Cluster analysis of absolute abundance data.....	297
5.15.	5.1.3.3.	PhytOC.....	300
5.16.	5.2.1.	TOC and AOM at Kashpir.....	310
5.17.	5.2.2.	Ternary A-P-D plot.....	313
5.18.	5.2.2.	Cluster analysis of A-P-D data.....	314
5.19.	5.2.3.1.	Relative abundance of structured components.....	317
5.20.	5.2.3.1.	Ternary plot of relative abundance data.....	319
5.21.	5.2.3.1.	Cluster analysis of relative abundance data.....	320
5.22.	5.2.3.2.	Relative abundance of phytoclast components.....	322
5.23.	5.2.3.3.	Phytoclast size data.....	325
5.24.	5.2.3.3.	Phytoclast roundness and sorting (STDEV).....	327
5.25.	5.2.3.3.	Ternary plots of phytoclast data.....	328
5.26.	5.2.3.4.	Major component absolute abundance.....	332
5.27.	5.2.3.4.	Minor component absolute abundance.....	333
5.28.	5.2.3.4.	Cluster analysis of absolute abundance data.....	334
5.29.	5.2.3.4.	PhytOC.....	336
5.30.	5.3.1.	Dinocyst diversity and dominance (both sections).....	346
5.31.	5.3.2.1.	Chorate/cavate/proximate groups at Gorodische.....	350
5.32.	5.3.2.1.	Ternary plot of chorate/cavate/proximate group data from Gorodische.....	352
5.33.	5.3.2.2.	Chorate/cavate/proximate groups at Kashpir.....	355
5.34.	5.3.2.2.	Ternary plot of chorate/cavate proximate group data from Kashpir.....	356
5.35.	5.3.2.2.	Robust vs. delicate cysts (both sections).....	359
5.36.	5.3.2.3.	Absolute abundance data (both sections).....	363
5.37.	5.3.3.1.	Relative abundance of skolochorate and proximochorate groups, Gorodische.....	370
5.38.	5.3.3.1.	Relative abundance of cavate and proximate groups, Gorodische.....	373
5.39.	5.3.3.2.	Relative abundance of skolochorate and proximochorate groups, Kashpir.....	376
5.40.	5.3.3.2.	Relative abundance of cavate and proximate groups, Kashpir.....	379
5.41.	5.3.3.2.	Cluster analysis of the groups data from Gorodische.....	381
5.42.	5.3.3.2.	Cluster analysis of the groups data from Kashpir.....	383

Figure	Section	Description	Page
5.43.	5.3.4.1.	Cluster analysis of the generic abundance data from Gorodische.....	387
5.44.	5.3.4.2.	Cluster analysis of the generic abundance data from Kashpir.....	391
5.45.	5.3.4.	Relative abundance 'strip-logs' of taxa with a stratigraphically influenced distribution, Gorodische..	394
5.46.	5.3.4.	Relative abundance 'strip-logs' of taxa with a stratigraphically influenced distribution, Kashpir.....	395
5.47a.	5.3.4.	Relative abundance 'strip-logs' of taxa with a potentially palaeoecologically controlled distribution, Gorodische.	397
5.47b.	5.3.4.	Relative abundance 'strip-logs' of taxa with a potentially palaeoecologically controlled distribution, Gorodische; continued.....	398
5.47c.	5.3.4.	Relative abundance 'strip-logs' of taxa with a potentially palaeoecologically controlled distribution, Gorodische; continued.....	399
5.48a.	5.3.4.	Relative abundance 'strip-logs' of taxa with a potentially palaeoecologically controlled distribution, Kashpir.	400
5.48b.	5.3.4.	Relative abundance 'strip-logs' of taxa with a potentially palaeoecologically controlled distribution, Kashpir; continued.....	401
5.48c.	5.3.4.	Relative abundance 'strip-logs' of taxa with a potentially palaeoecologically controlled distribution, Kashpir; continued.....	402
Enclosure 1		Sedimentary log of the Gorodische section showing sample positions and ammonite zonation (back pocket, Volume 1).	
Enclosure 2		Sedimentary log of the Kashpir section showing sample positions and ammonite zonation (back pocket, Volume 1).	

List of tables

Table	Section	Description	Page
1.1	1.1.	10 arguments by Hoedemaeker (1991) for the position of the Jurassic/Cretaceous boundary.....	9
3.1.	3.3.2.	Relative abundance of palynological matter components in the experimental residues.....	110
3.2.	3.3.3.	Absolute abundance of palynological matter components in the experimental residues.....	116
3.3.	3.3.4.	Detailed dinocyst data from the experimental residues.	119
3.4.	3.3.5.	Phytoclast size data: summary table.....	125
4.1.	4.1.2.	Gorodische sedimentology.....	132
4.2.	4.1.2.	Kashpir sedimentology.....	136
4.3.	4.2.2.	Relative abundance and ranges of dinocyst taxa at Gorodische.....	151
4.4.	4.2.3.	Relative abundance and ranges of dinocyst taxa at Kashpir.....	163
4.5.	4.3.3.	Measured dimensions of <i>Aprobolocysta pustulosa</i> sp. nov.....	219
4.6.	4.3.3.	Measured dimensions of <i>Lithodinia distincta</i> sp. nov...	224
4.7.	4.3.3.	Measured dimensions of <i>?Cyclonepheulium bulbosum</i> sp. nov.....	224
4.8.	4.3.3.	Measured dimensions of <i>Rhynchodiniopsis magnifica</i> sp. nov.....	230
4.9.	4.3.3.	Measured dimensions of <i>Rhynchodiniopsis undoryensis</i> sp. nov.....	235

Table	Section	Description	Page
4.10.	4.3.3.	Measured dimensions of <i>Thalassiphora robusta</i> sp. nov.....	235
5.1.	5.1.2.	TOC, and A-P-D data from Gorodische.....	269
5.2.	5.1.3.1.	Relative abundance data (%SM & %Phyt) from Gorodische.....	276
5.3.	5.1.3.2.	Phytoclast size data from Gorodische (summary table).	280
5.4.	5.1.3.3.	Absolute abundance data from Gorodische.....	292
5.5.	5.2.2.	TOC, and A-P-D data from Kaspir.....	311
5.6.	5.2.3.1.	Relative abundance data (%SM & %Phyt) from Kaspir.....	316
5.7.	5.2.3.3.	Phytoclast size data from Kaspir (summary table).....	324
5.8.	5.2.3.4.	Absolute abundance data from Kaspir.....	330
5.9.	5.3.1.1.	Diversity & dominance and chorate/cavate/proximate group relative abundance data from Gorodische.....	349
5.10.	5.3.1.2.	Diversity & dominance and chorate/cavate/proximate group relative abundance data from Kaspir.....	354
5.11.	5.3.1.2.	Separation of common dinocyst taxa into 'robust' and 'delicate' groups.....	357
5.12.	5.3.2.3.	Absolute abundance of dinocyst groups; Gorodische.....	361
5.13.	5.3.2.3.	Absolute abundance of dinocyst groups; Kaspir.....	362
5.14.	5.3.3.1.	Detailed morphological groups data; Gorodische.....	369
5.15.	5.3.3.2.	Detailed morphological groups data; Kaspir.....	375
5.16.	5.3.4.1.	Generic abundance data; Gorodische.....	386
5.17.	5.3.4.2.	Generic abundance data; Kaspir.....	390
5.18.	5.3.4.	Summary of the ecological distribution of key genera....	404

Contents of floppy disc (back cover)

Archive	Contents	File names	File types	File size
appb.zip	Data from the Agadir Basin, Morocco.	Mrelpal.xls	MS Excel	65KB
		Mtaxa.xls	MS Excel	112KB
appc.zip	Additional data from the experimental residues; particle size data	expdat.xls	MS Excel	318KB
appd.zip	Additional data from Gorodische; raw TOC data; dinocyst count data; particle size data	gorodps.xls	MS Excel	1464KB
		gtaxa.xls	MS Excel	65KB
		gtox.xls	MS Excel	16KB
appe.zip	Additional data from Kaspir; raw TOC data; dinocyst count data; particle size data	kashps.xls	MS Excel	1099KB
		ktaxa.xls	MS Excel	63KB
		ktoc.xls	MS Excel	13KB

**CHAPTER 1. Introduction to Jurassic/Cretaceous
boundary biostratigraphy**

1. Introduction.

1.1. Introduction to Jurassic/Cretaceous boundary studies.

The Jurassic-Cretaceous boundary, and in particular the terminal stage of the Jurassic, has been reported as representing one event in a series of periodic mass extinctions to have affected the history of life (Raup & Sepkoski, 1984; Benton, 1995; Sepkoski & Raup, 1986). Although there is widespread acceptance that this stage was witness to a rapid faunal turnover and global minimum in species diversity, Hallam (1986a) questioned the validity of its mass extinction status. He maintained that the noticeable biotic turnover was an 'apparent' extinction related to profound, globally recognisable, marine to terrestrial facies changes. In essence this suggested that the marine taxa not found above the transition were absent due to facies change rather than true extinction resulting from reduction in epicontinental sea area. So did those marine species really become extinct, or did they 'migrate' to stay within the requisite marine conditions? The question is an obvious one: the answer requires there to be a highly controlled system of correlation across wide geographical areas (and preferably across the globe), allowing the critical assessment of such apparent events, and a judgement on whether they are truly synchronous.

One might be surprised to learn then, that there is no such correlation system (at least none which has unanimous acceptance), and furthermore that despite more than a century of vigorous debate, biostratigraphers are still unable to reach consensus on the best stratigraphic position for the system boundary. This is in part due to the difficulty of correlating the base of the Neocomian (which should be the base of the Cretaceous) in its original type area, the Jura Mountains (Hoedemaeker, 1991). Perhaps more fundamental though, is the profound faunal provinciality which has plagued wider correlations of both Jurassic and Cretaceous Systems since the outset of biostratigraphy. So strong is this regionality, that Arkell (1956) in his study of the Jurassic System, first divided the faunas into the now widely recognised Boreal (high latitude) and Tethyan (low latitude) Realms. Since then, it has been shown that each realm can be

further compartmentalised into sub-realms or regions, and there have been various attempts to define these (see for example Jeletzky, 1971; Saks *et al.*, 1971; Saks & Nalnyaeva, 1973; Krimgolts *et al.*, 1988; Shul'gina *et al.*, 1994). This picture is further complicated by the temporal variations in geographic scope of these realms, first noted for the ammonite faunas of the Jurassic System by Arkell (1956), and later for the Early Cretaceous by Rawson (1973).

From the current state of our knowledge, ammonites provide the finest-scale and most reliable means of subdividing stratigraphic sequences through the Mesozoic, and the Jurassic-Cretaceous boundary interval is no exception. Indeed, so well studied are the ammonite successions of the various stage stratotypes making up this interval, that many authors have argued for an elevation of the 'zones' they define to informal 'chronozones' in recognition of their strong temporal control (Holland *et al.*, 1978; Calloman, 1984; Barron, 1989; Riding & Thomas, 1992). The present author accepts this distinction for the Boreal and Tethyan standard schemes, but retains the 'zone' nomenclature. Informal ammonite chronozones are written in Roman font with an initial capital (Riding & Thomas, 1992).

Our reliance on ammonites, coupled with faunal provinciality both between and within the realms has led to the development of numerous chronostratigraphic schemes and regional stage nomenclature. The uppermost Jurassic Stage has three regional names which in their present context do not represent the same stratigraphic interval. The Portlandian Brogniart 1829 and the Volgian Nikitin 1881 are both recognised from the Boreal realm, and the Tithonian Opper 1865 should be exclusively Tethyan, although it has been extensively applied to the uppermost Jurassic of Canada. The choice of whether to use the 'Volgian' or 'Portlandian' names as the definitive terminal Jurassic stage in the Boreal area has been debated at length. Wimbledon (1984) suggested that 'Portlandian' has publication priority over 'Volgian', and that it should therefore stand as the stratotype for the terminal stage. This might be acceptable if the two stages had

bases corresponding to the same stratigraphic horizon. Gerasimov & Mikhailov (1966) however, showed that the Volgian Stage in fact includes a substantial part of the underlying Kimmeridgian (*sensu anglico*), and its base should therefore be approximately equivalent to the base of the Tithonian Stage in France.

The top of the Kimmeridgian Stage is thus diachronous both between the Tethyan and Boreal realms, and also between the English and Russian Platform areas (Figure 1.1). Casey (1967, 1968) proposed that the Volgian Stage should be reduced to that part referred to as the Upper Volgian by Gerasimov & Mikhailov (1966), whilst the Lower Volgian be included within the Kimmeridgian. He also suggested that the base of the Portlandian be extended down to include the Pavlovia beds (correlated to the English Pallasoides Zone by Cope, 1978), which would thus encompass the whole of the Middle Volgian. The top of the Portlandian should then be drawn at the base of the Upper Volgian, equivalent to the top of the Oppressus Zone and base of the fulgens Zone respectively. Whilst this concept neatly solves the problem of upper Kimmeridgian diachroneity, it proposes that the terminal Jurassic stage in both areas be the Volgian. Since in this reworked definition the Volgian Stage in its type area would be defined at both its upper and lower limits by hiatuses, this seems entirely inappropriate; especially since the uppermost Volgian should further represent the Jurassic-Cretaceous system boundary. Moreover, the upper Volgian Substage has been previously suggested to be of Lower Cretaceous age (Krimgolts *et al.* 1988), although more recently Zacharov *et al.* (1997) re-asserted that the entire Volgian Stage belongs to the Jurassic System.

Cope (1993) also argued towards isochroneity of the terminal Kimmeridgian. He promoted the use of an intervening stage in the UK area termed the Bolonian (Gerasimov & Mikhailov, 1966), which would correspond with the Kimmeridgian (*sensu anglico*)-Volgian overlap. In this sense the Kimmeridgian Stage would represent the same stratigraphic interval in all areas (i.e., including Tethyan). Whilst it is certainly undesirable to have diachroneity within a stage, it is equally unacceptable to have an

Figure 1.1 Legend

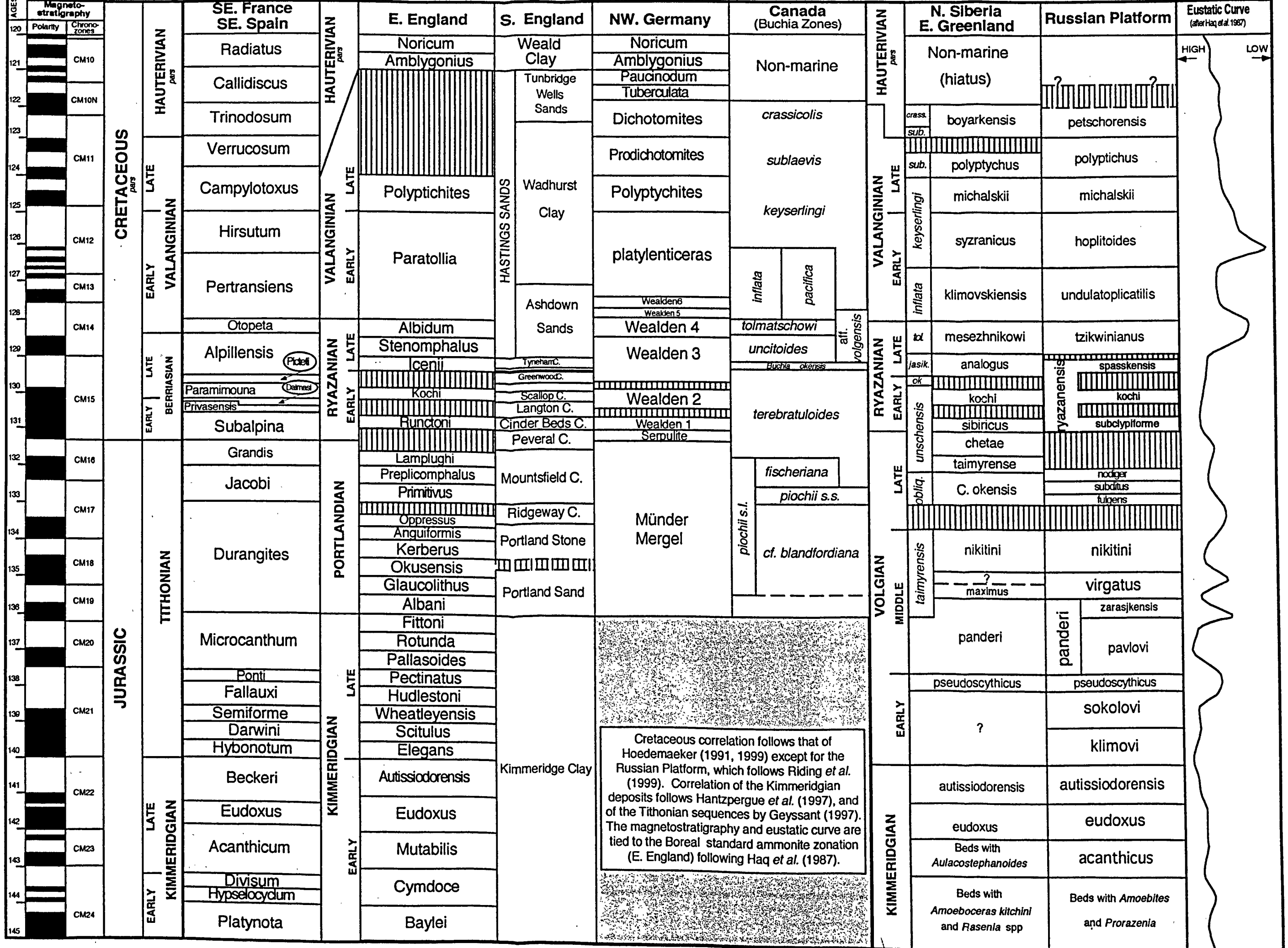
Correlation of Tethyan and Boreal standard zonation schemes

Correlation of the Portlandian to Hauterivian interval follows that of Hoedemaeker (1991, 1999) apart from the Nikitini and older zones of North Siberia and the Russian Platform which follow Riding *et al.* (1999). Correlation of the Tethyan and Boreal standard ammonite zonation additionally follows Geysant (1997: Tithonian Stage) and Hantzpergue (1997: Kimmeridgian Stage). Eustatic curve and magnetostratigraphy are correlated to the Boreal standard ammonite zonation following Haq *et al.* (1987). Zone names in italics are *Buchia* zones.

Abbreviations are as follows;

<i>crass.</i>	...	<i>crassicolis</i>
<i>sub.</i>	...	<i>sublaevis</i>
<i>tol.</i>	...	<i>tolmatschowi</i>
<i>jasik.</i>	...	<i>jasikovi</i>
<i>obliq.</i>	...	<i>obliquitus</i>
<i>ok.</i>	...	<i>okensis</i>

Figure 1.1: Correlation of Tethyan and Boreal standard chronozonation schemes including geomagnetic polarity and relative eustatic curve



additional stage in one area which is not consistently recognisable within an entire realm. Indeed, it is probably for this reason that Cope's (1993) suggestion has not met more widespread acceptance.

The assertion that the Boreal ammonite fauna exhibits a common "community of character" (Wimbledon, 1984), is supported by the fact that some of these shared aspects can be used to correlate certain horizons (for example the Albani Zone of southern England with the nikitini zone of the Volga Basin by the purported co-occurrence in these horizons of the genus *Epivirgatites*: Casey, 1967). Nevertheless, the literature indicates that profound differences in the fauna remain, and this is exemplified in the disparity between the two sets of chronostratigraphic index taxa. Therefore, as undesirable as it is to have two different stages representing the same stratigraphic interval of the same realm, their synonymisation is virtually as inappropriate as it would be to equate the Portlandian and Tithonian Stages. The present author thus prefers to retain both stages in their original regional context.

The same story is seen for the basal stage of the Cretaceous, known from the Boreal Realm as Ryazanian and from the Tethyan area as Berriasian. It is also represented in large parts of NW Europe by the predominantly terrestrial and marginal marine facies of the Wealden, for which correlation has proved problematic outside the UK (although see Fig. 1.1, after Hoedemaeker, 1991). The highly condensed nature of the Ryazanian stratotype has prevented this from being a widely accepted stage name (Casey & Rawson, 1973), many workers actually preferring to adopt the term Berriasian for Boreal areas (Jeletsky, 1973; Saks *et al.* 1975). Using terminology later adopted by Wimbledon (1984) for the uppermost Jurassic, Casey (1973, p. 228) suggested that the basal Cretaceous ammonite faunas "have a community of character that requires expression in stratigraphical terms". Casey & Rawson (1973) noted that the 'Ryazanian transgression' was sufficiently broad as to be recognisable in both southern England and the Russian Platform, suggesting eustatic control. This remark was later corroborated by the work Haq *et al.* (1987). Therefore, following Casey & Rawson (1973), the present

author adopts the binomial stage nomenclature of Ryazanian/Berriasian until stratigraphic correlation allows a globally acceptable basal Cretaceous stage.

There have been many publications attempting to effect Tethyan-Boreal correlation, and thus come to agreement on the position of the System boundary, see for example: Rawson (1973), Saks & Shul'gina (1973a, b; 1974), Anonymous (1975), Shul'gina (1975), Allemann *et al.* (1975), Saks *et al.* (1975), Gerasimov *et al.* (1975), Kutek & Zeiss (1975), Yegoyan (1975), Wiedmann (1975), Casey *et al.* (1977), Rawson *et al.* (1978), Luppov *et al.* (1979), Cope *et al.* (1980), Kemper *et al.* (1981), Sazonova & Sazonov (1983), Baumgartner (1983), Jeletsky (1984), Zeiss (1986), Hoedemaeker (1987, 1991, 1993, 1999), Détraz & Mojon (1989), Oloriz & Tavera (1989), Allen & Wimbledon (1991), Hancock (1991), Cope (1993), and Sey & Kalcheva (1999). In addition, an excellent review of the early history of Jurassic-Cretaceous boundary studies was presented by Saks & Sazonova (1975).

In the present author's opinion, by far the most persuasive arguments for both Tethyan-Boreal correlations and the best position for the boundary are given in the various contributions of Hoedemaeker (in particular, 1987 & 1991, 1999). His conclusions are therefore adopted in this report (see Fig. 1.1). It should be noted though, that the correlation he proposed, whilst robust and based in several cases on the observations of previous authors, still leaves a choice of two candidate horizons for the system boundary. There is no ubiquitous acceptance for either. The level used here is obviously the one favoured by Hoedemaeker (1991), and the reader is referred to the set of ten arguments made by him in defence of this decision (Table 1.1, below). Thus the boundary is drawn at the base of the Tethyan Subalpina Zone, which corresponds to the hiatus between the Lamplugh and Runctoni chrons of southern England, the top of the Chetae Zone of northern Siberia and Greenland, and the base of the Serpulit Member of NW Germany. It also physically corresponds to the top of the Volgian of the Russian Platform, which as described above also falls at an hiatus or disconformity.

1	It has been demonstrated that [the base of the Subalpina Zone] is chronostratigraphically closest to the base of the 'Unité inférieure oolitique', which since the introduction of the Neocomian has always been considered the base of the Cretaceous, even by d'Orbigny (1840-42)
2	[The base of the Subalpina Zone] is therefore also closest to the top of the Tithonian by definition (Oppel, 1865: 535)
3	[The base of the Subalpina Zone] does not violate the original diagnosis of the Tithonian, because none of the ranges of perisphinctean ammonites listed by Oppel (1865) as characteristic for that stage, nor those described by Zittel (1868) from the Stramberger Schichten (which attained a kind of stratotypical appreciation for the upper Tithonian) do cross the boundary.
4	[The base of the Subalpina Zone] corresponds to the base of the Subthermannia boissieri Zone sensu 'Colloque sur le Crétacé inférieur', which is equivalent to the 'Hoplites' boissieri Zone sensu Kilian (1888), but also equivalent to the original concept of the Berriasian of Coquand (1869, 1870, 1871, 1875). Not one of the ammonite species characteristic of the 'H'. boissieri Zone occurs below [the base of the Subalpina Zone].
5	It has been demonstrated that [the base of the Subalpina Zone] is also chronostratigraphically closest to the boundary between the Volgian and the Ryazanian in Siberia. The basal ammonite zone of the Siberian Ryazanian correlates with the basal zone of the Ryazanian in England. [The base of the Subalpina Zone] therefore fulfills the ideal condition of the Tethyan Tithonian-Berriasian boundary being synchronous with the Boreal Volgian-Ryazanian boundary.
6	If [the base of the Subalpina Zone] is the Jurassic-Cretaceous boundary, the Portlandian can remain the uppermost stage of the Jurassic System, even if it is conceived (Cope <i>et al.</i> , 1980: 85) to include the <i>Swinnertonia primitivus</i> , <i>Subcraspedites preplicomphalus</i> , and <i>Volgidiscus lamplughii</i> zones.
7	If [the base of the Subalpina Zone] is the Jurassic-Cretaceous boundary, also the base of the Cinder Beds can be retained as the base of the Cretaceous System in England.
8	If [the base of the Subalpina Zone] is the Jurassic-Cretaceous boundary, the totality of the Ardescian Substage, which according to the original concept of Toucas (1890) comprises the Calcaires Blancs in the Ardèche department of France, remains in the Jurassic. The bulk of the Calcaires Blancs was deposited during the B. jacobi Subzone (Cecca <i>et al.</i> , 1989).
9	If [the base of the Subalpina Zone] is the Jurassic-Cretaceous boundary, the American <i>Paradontoceras-Substeueroceras-Proniceras</i> beds and the Argentine <i>Substeueroceras koeneni</i> Zone remain in the Tithonian. Only non-typical ' <i>Paradontoceras</i> ' <i>reedii</i> and ' <i>Substeueroceras</i> ' <i>disputabile</i> occur in younger beds.
10	If [the base of the Subalpina Zone] is the Jurassic-Cretaceous boundary, everything approximately remains as it was and the interpretation of most geological maps and literature remains virtually unchanged.

Table 1.1: Hoedemaeker's (1991: p 54-55) ten arguments that the base of the Subalpina Zone is the best candidate for the Jurassic-Cretaceous boundary.

Unfortunately, the interval given attention by Hoedemaeker (1991, 1999) does not include the majority of the Jurassic strata under consideration here. For this reason, correlations of the standard Tethyan and Boreal ammonite biozonations have been adopted from the work of Geysant (1997) for the Tithonian-Portlandian interval, and of Hantzpergue *et al.* (1997) for the Kimmeridgian Stage. To the author's knowledge, these represent the most recent publications in the field. The dating adopted here is also that chosen by Hoedemaeker (1991) and Riding & Thomas (1992) from the work of Haq *et al.* (1987), and is closely tied in with the 'standard' Boreal ammonite succession.

Correlation of the Volgian and Boreal standard ammonite chronology for the Russian Platform and Northern Siberia (Figure 1.1) follows that of Riding *et al.* (in

press), which again represents the most recent publication in the field. It should be noted however, that correlation of panderi to nikitini zones adopted from Riding *et al.* (in press) contrasts with that presented by Lord *et al.* (1987) and Casey (1967) who correlated the nikitini Zone with the basal Portlandian Albani Zone. The continued dispute over the correlation of these schemes, and the relatively poor level of chronostratigraphic resolution attainable from the Russian sequences prevents the latter being treated as informal chronozones. Thus they will continue to be referred to as zones in the text, and following the example of previous investigations in the Volga Basin, the index ammonite species is written in Roman font, without an initial capital.

Literature on the ammonite faunas aside, other contributions to Jurassic-Cretaceous biostratigraphy and correlation, particularly of strata close to the boundary, are beyond count. They include donations from all other disciplines of biostratigraphy, as well as studies of isotope signatures, magnetostratigraphy, sequence stratigraphy, lithostratigraphy, and even the analysis of changes in clay mineralogy. Until recently however, there have been relatively few accounts which attempted to unite these often disparate disciplines. Studies like those of Le Hégarat & Remane (1968: ammonites & calpionellids), Bolli (1980: calcisphaerulids & calpionellids), Baumgartner (1983: radiolaria & calpionellids), Vasicek *et al.* (1983: radiolaria & calpionellids), Ascoli *et al.* (1984: foraminifera, ostracods & calpionellids), Morter (1984: molluscs & calpionellids), Bralower *et al.* (1989: nannofossils and magnetostratigraphy), Gradstein *et al.* (1992: dinocysts, foraminifera, nannofossils, magnetostratigraphy), Borza & Petercáková (1994: radiolaria & calpionellids), Magniez-Janin & Dommergues (1994: ammonites & foraminifera), Tavera *et al.* (1994: ammonites, calpionellids & nannofossils), Benzaggagh & Atrops (1996: ammonites & calpionellids), Housa *et al.* (1996: calpionellids & magnetostratigraphy), amongst others have attempted to alleviate this shortcoming.

It is disappointing that relatively few of the studies mentioned above address the calibration of the rapidly growing micropalaeontological (including palynological)

database with the appropriate ammonite chronostratigraphy. Part of this is indubitably due to the dominance of micropalaeontological studies in analysis of offshore cores, where for obvious reasons the ammonite control is much less well developed. Nevertheless the stratotypes have not been investigated as extensively using micropalaeontological techniques as might be expected. Where such studies have been completed, particularly when setting resultant zonations against the ammonite chronostratigraphy, good results have been achieved. Such studies include Memmi & Salaj (1975: Tunisia), Busnardo *et al.* (1976: Tunisia), Habib & Drugg (1983: North Atlantic & SE France), Woollam & Riding (1983: NW Europe), Ogg *et al.* (1991: UK & Tethyan area), Jan du Chêne *et al.* (1993: SE France), Hoedemaeker & Leereveld (1995: SE Spain), Leereveld (1997: western Mediterranean).

Although studies integrating ammonite and dinoflagellate cyst data indicate that much finer stratigraphic division can be attained using the macrofauna alone, the potential for using dinoflagellate cysts in biostratigraphic analyses and correlation has been repeatedly stressed (Clarke, 1967; Riley & Sarjeant, 1972; Sarjeant, 1975; Riding & Sarjeant, 1985). Their planktonic state makes the living dinoflagellate much less provincial than benthic microfossils due to their distribution by ocean currents. Therefore they represent an excellent tool for correlation and extended studies of these organisms integrated with the ammonite biostratigraphy should go some way towards a more united chronostratigraphy.

1.1.2. Rationale, aims, and evolution of the project.

As originally conceived, this study was focused on an assessment of the Jurassic-Cretaceous boundary mass extinction event. The areas of concern were SE England and the Volga Basin, being two regions known to exhibit facies changes of different magnitude at the system boundary. It was hoped that detailed study of these areas, along with a third section which did not incorporate such facies change, would test Hallam's

(1986a) theory of 'apparent' extinction. Comparison of ammonite stratigraphy from the two localities indicated that detailed correlation would have to be improved before any extinction analysis was undertaken. However, from previous analyses conducted on the macrofaunas it was clear that further study would not improve correlation, thus micropalaeontological investigation was considered the most appropriate technique to apply in addressing this problem. Therefore a suite of palynological samples from the two most important Jurassic/Cretaceous boundary sections in the Volga Basin was collected. The aims of this project were therefore modified, with the following goals defined:

- 1: To undertake the most detailed palynostratigraphic analysis of the Volgian lectostratotype yet completed, substantially enhancing our knowledge of dinocysts from Jurassic deposits of the Russian Platform.

- 2: To construct a new dinocyst zonal scheme for the Jurassic-Cretaceous of the Volga Basin, using, as far as is practicable, species in common with other Boreal areas in order to conduct critical comparisons with dinocyst zonations of contemporaneous sequences developed for the UK, North Sea and NW European regions (see Section 2.2.). It was hoped that it would then be possible to integrate these observations with the ammonite chronostratigraphy, and thereby verify and strengthen previous correlations of the Russian Platform and NW European successions.

- 3: To make detailed palynofacies observations, combine these with the new sedimentological information collected in the field, and in this manner make an interpretation of the depositional environments in which the Volga Basin sequences were deposited.

- 4: To determine the characteristics and composition of the dinoflagellate cyst assemblages, and to compare these with the new palaeoenvironmental information in order to advance our understanding of factors controlling the distribution of these

microfossils, and thus highlight strengths or limitations in the application of certain taxa to the development of regionally applicable biozonation and correlation schemes.

5: To combine the palynofacies, dinoflagellate, sedimentological, and macrofaunal data to allow the recognition of any previously unidentified disconformities or hiatuses, and thus give an indication of how complete a stratigraphic record the Volgian lectostratotype succession represents.

Attempts to extend the study into the Tethyan Realm.

It was hoped to extend correlation aspect of this study by undertaking similar analyses of contemporaneous Tethyan successions. First-hand observations from both realms should enforce consistency and enhance similarities between the floral assemblages. Palynology of the Berriasian stratotype or 'paratypes' from SE France has already been studied extensively (see for example; Milloud, 1969; Habib & Drugg, 1983; Jardiné *et al.* 1984; Monteil, 1990, 1993; Gorin & Steffen, 1991; Jan du chène *et al.* 1993; Steffen & Gorin, 1993a, b). Another excellent section, suggested as a replacement stratotype for the Berriasian Stage (Hoedemaeker, 1996, pers. commun.), is to be found near Caravaca, SE Spain. Palynology of Lower Cretaceous sections in this area had previously been considered by Hoedemaeker & Leereveld (1995), although these authors were unable to extend their study into Lower Berriasian strata due to 'poor palynological recovery'. However, no further documentation of the palynological recovery from this interval was forthcoming, either the position of their sample horizons, or the number of samples they collected. Thus, during a field excursion early in the present project to collect macrofossil data from Caravaca, the present author attempted to expand on the work of Hoedemaeker & Leereveld (1995) by collecting a suite of 30 samples from the boundary and Lower Berriasian strata of Section Z. Unfortunately, upon processing, all samples proved to be barren of palynomorphs. A lithostratigraphic log of this section and position of samples taken by the present author can be found in Appendix A.

Subsequent to the Russian and Spanish fieldwork, the logistical and financial arrangements required to complete the mass extinction aspect of the study were reviewed. This part of the project was no longer considered to be feasible, especially since the expertise required for accurate and consistent identification of the macrofossil faunas from the study areas were not readily available. Thereafter the project focused exclusively on sedimentological and palynological techniques, and further Tethyan study areas were sought.

Numerous sections exposing Lower Cretaceous strata, as well as several which span the Jurassic-Cretaceous boundary exist in the Agadir Basin of Morocco. Two sections from this area were studied palynologically by Below (1981a, 1982a,b). To expand this work, a suite of 200 samples was collected from six sections in this area in 1997. Unfortunately, all the samples from five of these sections proved to be barren of palynomorphs. Sedimentary logs of these sections can be found in Appendix B, the sampled horizons shown to provide information on the palynologically barren intervals. 100 samples were collected from the section at Aït Hamouch, of which only 40 yielded palynomorphs. In most of these samples preservation was extremely poor, making accurate taxonomic determinations virtually impossible.

Comparison with material figured by Below (1981a, 1982a,b) suggests that such poor preservation is due to surface weathering rather than taphonomic processes, despite the extensive trenching undertaken during sample collection. Therefore significant advances in the dinocyst biostratigraphy of this area did not prove possible. Furthermore, suggestion that the palynological assemblages have been profoundly affected by surface weathering renders the palynofacies investigation on this locality much less meaningful, and so the Moroccan samples are not considered in this report. However, the data collected can be found in Appendix B of the floppy disc.

Chapter 1.2. Review of Jurassic/Cretaceous boundary marine palynology.

1.2.1. The United Kingdom and NW Europe.

By far the greatest wealth of literature on Jurassic palaeontology is drawn from this region. This is in no small part due to the position of several of the stage stratotypes in the UK area, most notably from the point of view of this study, that of the Kimmeridgian and Portlandian (both in the south of England).

This situation is also reflected in the abundance of palynological literature. Earliest studies of Late Jurassic marine palynology of this region focused on taxonomy and systematics of the flora, with only incidental remarks being made on dinocyst or acritarch palynostratigraphy (Downie, 1956; Lantz, 1958; Sarjeant, 1959, 1960, 1962a,b, 1975; Norris, 1970). Gitmez (1970) considered the dinoflagellate cyst and acritarch floras from Kimmeridgian deposits of England, Scotland and France. This paper concentrated on assemblages from the lowermost Kimmeridgian Baylei Zone, although it was later reconsidered by Riley & Sarjeant (1977), and the assemblage re-attributed to the younger range of *Mutabilis* to *Hudlestoni* chrons. Gitmez & Sarjeant (1972) extended Gitmez's (1970) work into the Upper Kimmeridgian. Both papers focused on dinoflagellate cyst and acritarch systematics, although indications of biostratigraphy were given in simplified occurrence charts. Ioannides *et al.* (1976) produced an account of the marine palynomorph assemblages and biostratigraphy of the *Wheatleyensis* Zone (Late Kimmeridgian *sensu anglico*) at Clavell's Hard (Dorset), and placed this within the range data given by Gitmez (1970) and Gitmez and Sarjeant (1972)(see Ioannides *et al.*, 1976; text-figure 7). The palynology of the *Cymdoce* to *Pallasoides* chrons from the Brora Outlier (NE Scotland) was considered by Lam & Porter (1977), in an integrated study of both sporomorphs and marine palynomorphs. The account concentrated on biostratigraphy, with ranges of the many marine taxa found to be common with contemporaneous strata from southern England. Davey & Riley (1978) gave a generalised account of Mid to Late Jurassic dinocyst biostratigraphy, and a total

of 27 ranges were given for dinoflagellate cyst species occurring in the Kimmeridgian - Volgian interval. In particular they noted that the range tops of selected taxa within the Kimmeridgian could be used as a clear distinguishing factor between the two stages (important taxa were very clearly illustrated), although at that time there were no distinctive datums available for the Kimmeridgian-Volgian boundary.

Drugg (1978) made a major study of Mid to Late Jurassic dinoflagellate cyst material from England, France and Germany, erecting 17 new species, with 5 of the holotypes being drawn from the Kimmeridgian Stage. Raynaud (1978) outlined the main species characteristic of the Upper Jurassic strata of northern Europe. Riding (1987) studied the Hettangian to Late Kimmeridgian dinocyst biostratigraphy of the Nettleton Bottom Borehole in Lincolnshire. The ranges of taxa occurring between the *Baylei* and *Hudlestoni* chrons were given, and variation in the floral assemblage discussed. No attempt was made to link the Nettleton Bottom biostratigraphy to the zonation developed by Woollam & Riding (1983)(see later). Thomas & Cox (1988) published on the palynology of the Oxfordian-Kimmeridgian Stage boundary (*Serratum* to *Cymdoce* chrons). Their work suggested that several of the taxa previously used to demark the boundary in fact had ranges which crossed it. They were unable to demonstrate whether this phenomenon represented true regional diachronism or simply the paucity of information from sections with good stratigraphic control, prompting the need for further work.

A summary of important dinoflagellate cyst biohorizons through the Jurassic and Cretaceous systems was published by Haq *et al.* (1987). This information was integrated with magnetostratigraphy, chronology, sequence stratigraphy and eustatic levels, as well as standard biozonation developed for ammonites and calcareous microfossils. This work was enhanced by Partington *et al.* (1993), who calibrated 33 maximum flooding surfaces (MFSs) in the North Sea Jurassic (Hettangian to Ryazanian) with ammonite biozones and the existing occurrence data for dinoflagellate cysts. Of these, 14 MFSs fall within the range Kimmeridgian - Ryazanian. MFSs tied to ammonite zones show that the boundaries

of the Kimmeridgian and Portlandian, and Portlandian/Ryazanian stages coincide with the termination of second and third order eustatic cycles respectively (Partington *et al.*, 1993). Therefore if these sequences can be recognised elsewhere they may be useful correlation tools.

Dörhöfer & Norris (1977) integrated previous work by various authors on the Jurassic - Cretaceous boundary palynofloral successions in northern Germany (Dörhöfer, 1977; Döring, 1965), England (Hughes & Moody-Stuart, 1969; Hughes & Croxton, 1973; Norris, 1969; Batten, 1973a; Hughes & Norris, 1974, 1975), and Holland (Burger, 1966). Using both marine and terrestrial palynomorphs they were able to discriminate three suites of floral assemblages from the Portlandian to Early Valanginian of England and one Neocomian assemblage containing dinoflagellate cysts from NW Germany (see Fig. 1.2).

Davey (1979) produced one of the first reports which dealt with dinoflagellate cyst biostratigraphy and zonation across the Jurassic-Cretaceous transition in north-west Europe. Sections studied included the Portlandian stratotype in Dorset, and the Portlandian-Ryazanian transitions in Norfolk, Lincolnshire (the only area in the north of England where the Jurassic-Cretaceous boundary can be traced with ammonite faunas; Casey, 1973) and Denmark, as well as the Portlandian - Barremian succession of the North Sea Basin. Ranges of stratigraphically important dinoflagellate cysts occurring through this interval were plotted, and a series of interval zones based on first and last occurrence data developed. He proposed 5 dinocyst zones in the Portlandian (Albani Zone) to topmost Valanginian interval, with the *Paraeodinia dasyforma* Zone spanning the Jurassic - Cretaceous boundary. Work in north-west Europe (outside the UK) was continued in a short paper by Herngreen *et al.* (1980) on the Jurassic/Cretaceous boundary palynofloras of Holland. Prevailing facies in the area were more conducive to the study of sporomorphs than marine palynomorphs, but nevertheless the ranges of certain key taxa were plotted across the Malm - Neocomian interval.

Figure 1.2 Legend

Correlation of previously published Boreal dinoflagellate cyst zonation schemes

Wherever possible the exact position of the zone boundaries relative to the standard ammonite zonation has been shown. Where this information was not provided, correlation has been made to the nearest ammonite zone, or to the stage boundaries as defined by Hoedemaeker (1991, 1999), Geysant (1997) and Hantzpergue *et al.* (1997).

Abbreviations are as follows;

<i>Dichad. sp.</i>	...	<i>Dichadogonyaulax sp.</i>
<i>D. nanna</i>	...	<i>Discorsia nanna</i>
<i>D. pan.</i>	...	<i>Dichadogonyaulax pannea</i>
<i>E. tory.</i>	...	<i>Egmontodinium torynum</i>
<i>E. polyplac.</i>	...	<i>Egmontodinium polyplacophorum</i>
<i>Egmont. sp. A.</i>	...	<i>Egmontodinium sp. A.</i>
<i>E. pharo</i>	...	<i>Endoscrinium pharo</i>
<i>F. warling</i>	...	<i>Fromea warlinghamensis</i>
<i>G. jurassica</i>	...	<i>Gonyaulacysta jurassica</i>
<i>G. juras.</i>	...	<i>Gonyaulacysta jurassica</i>
<i>G. mutabilis</i>	...	<i>Gonyaulacysta pennata</i>
<i>G. penn.</i>	...	<i>Gochteodinia mutabilis</i>
<i>Kleith. sp. A.</i>	...	<i>Kleithriasphaeridium sp. A.</i>
<i>K. simpl.</i>	...	<i>Kleithriasphaeridium simplicispinum</i>
<i>L. egem.</i>	...	<i>Leptodinium egemenii</i>
<i>M. extens.</i>	...	<i>Muderongia extensiva</i>
<i>P. nuda</i>	...	<i>Pareodinia nuda</i>
<i>R. thula</i>	...	<i>Rotosphaeropsis thula</i>
<i>S. crystallinum</i>	...	<i>Scriniodinium crystallinum</i>
<i>Syst.</i>	...	<i>Systematophora spp.</i>

Fisher & Riley (1980) attempted to analyse the distribution of dinoflagellate cysts (and acritarchs) at the Boreal Jurassic/Cretaceous boundary, and construct a zonal scheme spanning the interval from the early Kimmeridgian to the late Valanginian. Primary data was collected from northern France, numerous localities in England, Arctic and offshore eastern Canada, east Greenland, the North Sea Basin, Denmark, and 'other northern European areas' (Fisher & Riley, 1980). This was supplemented by the incorporation of previously published data from Russia, Norway and Canada (Vozzhennikova, 1967; Thusu & Vigran, 1975; Williams, 1975; amongst others). Their zonation comprised 7 zones and 12 subzones, correctly termed "concurrent range biozones" (Fisher & Riley, 1980)(see Fig. 1.2). It was not precisely characterised in the text, and they were unable to calibrate their zonation to reliably dated ammonite chronology, hampering correlation to other microfloral zones. Interestingly, this is one of the few works to propose a formal zone nominated by an acritarch taxon (*Pterospermopsis aureolata*). Care is needed when defining geographically wide zones, especially on the occurrence of taxa for which are thought to have strongly ecologically controlled distribution (Fisher & Riley, 1980).

Rawson & Riley (1982) presented a dinocyst zonation for the Oxfordian to Albian interval closely tied in with the standard ammonite zonation. This was not explicitly described in the text, but was modified from an earlier zonation developed by Robertson Research Ltd (1978). The scheme is presented in Figure 1.2.

Woollam and Riding (1983) were the first to propose a dinocyst zonation for the entire English Jurassic (and the basal Cretaceous) calibrated to standard ammonite biozonation. They recognised six zones which correspond to the interval from the base of the Late Oxfordian Rosenkrantz Zone to the lowest part of the Valanginian (unzoned). The framework developed here has been variously described as dominated by assemblage- or Opper zones (with sub-zones being mostly interval zones)(Woollam & Riding, 1983; Riding, 1984), or with both termed as interval zones (Stover *et al.*, 1996).

If the guidelines in the International Subcommission on Stratigraphic Classification (Salvador, 1994) are adhered to, the term 'interval zone' is in fact inappropriate here, and since a distinction can be made between assemblage zones and Oppel zones, the latter can be most accurately applied to the majority of Woollam & Riding's zones. Two Cretaceous zones were adopted from the work of Davey (1979, 1982), and will be discussed later. With the exception of the SI Zone, all of the dinocyst zones proposed were further divided into subzones on the basis of first and last appearance data for relevant taxa. As such, they are somewhat specific to the UK Boreal area and selected definitions will be discussed (where appropriate) below, and in Chapter 4). All of the dinocyst zones and subzones were extended to coincide with ammonite chronozone boundaries, reflecting a relatively coarse palynological sampling regime.

The work of Woollam & Riding (1983) was supplemented by Riding (1984), who gave a biostratigraphic account of the dinoflagellate cyst range-tops between the latest Triassic and the earliest Cretaceous of north-west Europe. A formal zonal scheme was not proposed here, as approximately 20 percent of the noted range-tops were considered to be in "questionable stratigraphic position" (Riding, 1984: p.196). The majority of the dinocyst Last Appearance Data (LADs) were related to the upper boundaries of the corresponding ammonite zones, again reflecting inaccuracy in the spot-sampling interval (Riding, 1984). These data were then compared to the dinocyst zonation proposed by Woollam and Riding (1983), resulting in a slightly inaccurate, but nevertheless readily-refineable sequence of dinocyst data, particularly useful for correlation.

Riding & Sarjeant (1985) produced a timely review paper discussing the role of dinoflagellate cysts in the stratigraphic subdivision of the Jurassic System, and potential of the group to form a reliable biostratigraphic framework in the future. They plotted ranges of the fifty biostratigraphically most important dinocyst taxa in the Jurassic, of which 14 fell within the Kimmeridgian to Portlandian range.

Nøhr-Hansen (1986) made an extensive review of literature pertaining to Early Kimmeridgian palynology. This work proposed the separation of Woollam & Riding's (1983) *Scriniodinium luridum* Zone into two subzones, termed the *Stephanelytron scharburghense* and *Perisseiasphaeridium pannosum* Subzones in ascending stratigraphic order. The zonal index species was re-assigned to the more appropriate genus *Endoscrinium*.

Woollam & Riding's (1983) dinocyst zonation was applied to four North Sea cores of Late Oxfordian to Late Kimmeridgian age by Cox *et al.* (1987). It was demonstrated here that although overall the zonation of Woollam & Riding could be applied to the North Sea area, the extended ranges of certain taxa (namely *Dingodinium tuberosum*, *Scriniodinium crystallinum* and *Endoscrinium luridum*) suggested the need to adjust the upper bounds of the *Gonyaulacysta jurassica* - *S. crystallinum* and *E luridum* zones into the younger *Mutabilis* and *Autissiodorensis* zones respectively. It was thought that the range extensions seen here represented true diachronism rather than re-working of the assemblages, and thus any zone adjustments would only be valid for the North Sea area (Cox *et al.*, 1987).

The dinocyst stratigraphy of Woollam & Riding (1983) was subsequently revised by Riding & Thomas (1988), in a paper published on the Kimmeridge Clay. To simplify the otherwise cumbersome '1983' biozonation, Riding & Thomas reduced the dual-indexed biozones to a single taxon name. Thus the basal zone of this interval, 'Gj/Sc', simply became the *Scriniodinium crystallinum* Zone (Sc), etc. (Riding & Thomas, 1988)(see Fig. 1.2). In addition, the ranges of several of their original zones (as related to the ammonite chronostratigraphy) were altered to accommodate new occurrence data, and the zone-interval (and subzone-interval) definitions revised as appropriate. Nøhr-Hansen's (1986) re-named *Endoscrinium luridum* Zone was accepted, although the subdivision of this zone was redefined to include three subzones. The reported occurrences of *E. luridum* from the *Autissiodorensis* Zone (Cox *et al.*, 1987) were incorporated in this revision, and the zone-top extended accordingly. Other important

changes to the initial zonation of Woollam and Riding (1983) included the re-definition of the three original subzones of the Gd Zone into five newly defined subzones, and the re-naming of the *Ctenidodinium culmulum* - *Ctenidodinium panneum* Zone in line with the proposed generic re-assignment of the second index species into the genus *Dichadogonyaulax* (Benson 1985).

Barron (1989) considered the Kimmeridgian to basal Portlandian dinocyst biostratigraphy of the Helmsdale region, Scotland. The ranges of 51 dinocyst taxa were presented, and suggested some degree of similarity to ranges presented from other NW European areas. Nevertheless the appropriate portion of Woollam & Riding's (1983) zonation could only be applied loosely to the Helmsdale area. Van der Zwan (1990) detailed the Late Oxfordian to latest Ryazanian dinocyst zonation of the Draugen Field, offshore Mid Norway. The Kimmeridgian zones were adopted from the work of Whitaker *et al.* (1984) on the Troll field. All the zones and subzones described by Van der Zwan (1990) are assemblage zones, although range data were supplied. Their dinocyst zones were not calibrated to the standard ammonite biozonation, making detailed comparison to other published schemes impossible.

The Kimmeridgian (*sensu anglico*) dinocyst zonation of Riding & Thomas (1988) was left largely unchanged by Riding & Thomas (1992), except for the alteration in definition of the *Scriniodinium crystallinum* Zone (see below). Additional information on floral assemblage characteristics and 'provincialism' was also provided. Their definition for the dinocyst biozones of the Late Jurassic to earliest Cretaceous (1992 edition) is by far the most comprehensive and widely accepted zonation for the NW European area, and is therefore the one adopted in the current work. The classification of each of the zones is given below, and can be compared to other schemes in Figure 1.2.

The basal (*Scriniodinium crystallinum*) biozone of this interval spans the Oxfordian-Kimmeridgian boundary (Glosense to Baylei ammonite zones). It is defined as:

"The interval between the LADs of *Leisbergia scarburghensis* and *Rigaudella aemula*, and the FADs of *Cribopteridinium longicorne*, *Oligosphaeridium patulum* and *Systematophora daveyi* and LADs of *Nannoceratopsis pellucida* and *Scriniodinium crystallinum*. " (Riding & Thomas, 1992: p. 38).

The Biozone is further divided into four sub-biozones labelled 'a' to 'd'. The Scr Biozone was updated from Riding & Thomas (1988) to reflect additional data showing that the range base of *Glossodinium dimorphum* was stratigraphically lower than previously reported (thus its appearance could no longer be used to mark the base of the Scr Biozone). Superior to the Scr Biozone lies the Elu or *Endoscrinium luridum* Biozone. It spans the ammonite zones Cymdoce to Autissiodorensis, and is defined as:

"The interval between the FADs of *Cribopteridinium longicorne*, *Oligosphaeridium patulum* and *Systematophora daveyi* and LADs of *Nannoceratopsis pellucida* and *Scriniodinium crystallinum*, and the LAD of *Endoscrinium luridum*." (Riding & Thomas, 1992: p. 42).

The biozone is left unchanged from Riding & Thomas' (1988) definition, although they modified the definitions of the three sub-biozones (a - c), building also on the subdivision of this biozone by Nøhr-Hansen (1986). Assemblages from the Scr and Elu biozones of the Isle of Skye have recently been considered by Riding & Thomas (1997).

The Late Kimmeridgian (Elegans to Fittoni ammonite zones) is marked by the *Glossodinium dimorphum* (Gdi) Biozone, which is thus:

"The interval between the LAD of *Endoscrinium luridum* and the FAD of *Dichadogonyaulax culmula* and LAD of *Occisucysta balios*." (Riding & Thomas, 1992: p. 43).

The definition of the biozone and its comprising sub-biozones (a - e) were left unchanged from the Riding & Thomas (1988) (Riding & Thomas, 1992). This is superseded by the *Dichadogonyaulax? pannea* (Dpa) Biozone, which is the basal zone of the Portlandian *sensu anglico* (Albani to Anguiformis zones). It was characterised as:

"The interval between the FAD of *Dichadogonyaulax culmula* and the LAD of *Occisucysta balios* , and the FAD of *Gochteodinia villosa* and the LADs of *Dichadogonyaulax? pannea* and *Glossodinium dimorphum*." (Riding & Thomas, 1992: p. 44).

The FAD of *Gochteodinia villosa* was later described by Stover *et al.* (1996: p.662) as being the "most significant biohorizon in the Portlandian". Its definition was not changed from Riding & Thomas (1988), and the original subzones (a & b) were retained. The terminal biozone of the Jurassic, spanning *Opressus* (Portlandian) to *Stenomphalus* (Ryazanian) zones, was retained as the *Gochteodinia villosa* Biozone. According to Riding & Thomas (1992), the zone's definition was not altered from Woollam & Riding's (1983), having only adjusted the position of the a-b sub-biozone boundary (Riding & Thomas, 1992). This is not correct however, since Woollam & Riding's (1983) definition was based on Davey's (1979) original diagnosis, which used the FAD of *Pseudoceratium pelliferum* (amongst others) to mark the zone top. Since this zone was not considered by Riding & Thomas (1988), the remastered definition stands as:

"The interval between the FAD of *Gochteodinia villosa* and the LADs of *Dichadogonyaulax? pannea* and *Glossodinium dimorphum*, and the FAD of *Lagenorhytis delicatula*." (Riding & Thomas, 1992: p. 48).

Of the three sub-biozones described, 'a' was confined entirely within the Portlandian, 'b' spanned the Portlandian - Ryazanian and thus the Jurassic - Cretaceous

boundary, and 'c' was exclusively of Ryazanian age. Since these three span the critical interval under review, their definitions are reproduced below:

Sub-biozone a: "The interval between the FAD of *Gochteodinia villosa* and the LADs of *Dichadogonyaulax? pannea* and *Glossodinium dimorphum*, and the LADs of *Dingodinium tuberosum* and *Egmontodinium polyplacophorum*." (Riding & Thomas, 1992: p. 48).

Sub-biozone b: "The interval between the LADs of *Dingodinium tuberosum* and *Egmontodinium polyplacophorum*, and the LAD of *Rotosphaeropsis thula*." (Riding & Thomas, 1992: p. 49).

Sub-biozone c: The "Interval from the extinction of *Cannosphaeropsis* sp. A [now *Rotosphaeropsis thula*] to the extinction of *C. culmulum* (and *G. villosa*)". (Woollam & Riding, 1983: p.13)

Stover *et al.* (1996) summarised the previous work on Jurassic (and Cretaceous) marine palynomorph biostratigraphy, and composed correlation charts of the zonations proposed as well as of important biohorizon data from Riding & Thomas (1992) and Haq *et al.* (1987). The diversity and nature of the dinoflagellate cyst assemblages was also discussed.

Literature dealing with the latest Jurassic palynology of Germany includes several of the papers already discussed (see Gitmez, 1970; Gitmez & Sarjeant, 1972). Additionally, Lund & Ecke (1988) studied the Mid and Late Jurassic palynology of Bavaria, up to strata of Oxfordian age. Dürr (1987) studied the Mid Kimmeridgian dinoflagellate cyst assemblage of southern Germany (*Mutabilis* and *Eudoxus* chrons), presenting ranges for several taxa which are known to be biostratigraphically important in other parts of northern Europe. Amongst these were the species *Cribroperidinium longicorne*, *Perisseiasphaeridium pannosum* and *Occisucysta balia*. This was rapidly

followed by a more comprehensive survey of the Kimmeridgian to Tithonian of southern Germany by the same author (Dürr, 1988).

The Oxfordian - Kimmeridgian interval in NW Germany was considered by Kunz (1990). This study took into account dinoflagellate cyst biostratigraphy as well as palynofacies, and resulted in the definition of three formal zones for the area, of which one, the *Occisucysta balia/Cribroperidinium* spp. Zone spanned the Early and Mid Kimmeridgian. This contrasts markedly in both nomenclature and resolution with the contemporaneous zones from England and the North Sea. Analysis of the floral assemblage revealed that although there are indeed some taxa in common between the two areas, the German flora was strongly affected by prevailing ecological conditions (Kunz, 1990). An early study of the northern and central German palynology by Alberti (1961) indicated that the floras recovered from here shared many similarities with coeval floras in Poland and Bulgaria, which are a mix of Tethyan and Boreal affinities. Below (1981b) correlated the Lower to Middle Valanginian strata of Suddendorf (NW Germany) with the dinoflagellate cyst zonation of Davey (1979), particularly with the *Pseudoceratium pelliferum* and *Spiniferites ramosus* zones (see later).

Other, less voluminous works on the Late Jurassic palynology include an analysis of Kimmeridgian to Volgian species of the genus *Cribroperidinium* (Bailey, 1993), and a paper on dinoflagellate cysts from the Kimmeridge Clay of Yorkshire (Bailey *et al.* 1997).

In contrast to the Upper Jurassic, none of the Lower Cretaceous type localities (up to and including the Albian) are within the British Isles, and only the Ryazanian stratotype is situated within the Boreal Realm (Costa & Davey, 1992). In consequence, literature on the palynology of the NW European Lower Cretaceous is far more sparse, and to some extent overlaps with that outlined above (see Davey, 1979; Hengreen *et al.* 1980; Fisher & Riley, 1980; Woollam & Riding, 1983; Riding, 1984).

Amongst the latter, surely the most influential work on the dinoflagellate cyst zonation of the Early Cretaceous interval is that of Davey (1979). Although the zones he proposed for the Jurassic and the basal zone of the Cretaceous (the *Paraeodinia dasyforma* Zone) were later amended by subsequent investigations (Woollam & Riding, 1983; Riding & Thomas, 1988, 1992), his two zones of the Late Ryazanian and Valanginian are still widely accepted and utilised by other authors (Woollam & Riding, 1983; Iosifova, 1996; Stover et al. 1996). The zone superceding that of *P. dasyforma* (subsequently referred to as *G. villosa*, see above) was named after the taxon *Pseudoceratium pelliferum*. It was defined as the:

"Interval from the first appearance of *Pseudoceratium pelliferum* to the first appearance of *Spiniferites ramosus* (Ehrenberg) Loeblich & Loeblich 1966". (Davey, 1979: p.71).

This zone spanned the interval from the Late Ryazanian Albidum ammonite Zone to the Early Valanginian bed D4D of the Speeton section of northern England (Davey, 1979). This was followed by the *Spiniferites ramosus* Zone (beds D4B to D2E of Speeton), defined as the:

"Interval form the first appearance of *Spiniferites ramosus* to the first appearance of *Discorsia nanna*." (Davey, 1979: p.71).

Although both zones could be described as Interval zones according to the ISSC (Salvador, 1994), information on other important taxon datum levels and floral characteristics were included, and they can therefore also be loosely referred to as OppeL zones using the same guide. The zonation is shown in Figure 1.2 using the ammonite calibrations rather than the Speeton lithostratigraphic units after the revision given by Davey (1982) from the Haldager borehole of Denmark.

Norris' (1963) Ph.D. thesis was the first contribution to describe dinoflagellate cysts from the Lower Cretaceous of southern England. The first works on the Speeton Clay (Yorkshire) were taxonomic appraisals by Neale & Sarjeant (1962a), and various papers in Davey *et al.* (1966). These were followed some years later by a similar study of the Barremian part, by Davey (1974), of the Hauterivian by Duxbury (1979), and a dinocyst calibration of the Speeton Barremian by Harding (1990). Duxbury's (1977) assessment of the dinoflagellate cysts from the Berriasian to Barremian of the Speeton Clay was the first concerted attempt to constrain Neocomian dinoflagellate cyst biostratigraphy in this region. Biostratigraphic data were analysed to produce a zonation scheme of which two zones (A & B) encompass the interval from Berriasian to earliest Hauterivian Stages (Duxbury, 1977). This was followed by Duxbury's (1978) paper summarising Cretaceous dinoflagellate cyst biostratigraphy. He charted the ranges of 24 taxa with known occurrences in the Volgian to latest Valanginian interval, and was able to demonstrate that the Ryazanian-Valanginian and Valanginian-Hauterivian Stage boundaries could be readily identified using dinoflagellate cysts.

A similar summary work on the dinocyst stratigraphy was published by Costa & Davey (1992), who plotted the ranges of 46 taxa in the first two stages of the Cretaceous. The work also contains information on assemblage characteristics for the two stages, and a note on the gap in our knowledge of latest Valanginian dinoflagellate cyst floras from the British Isles. The paucity of Neocomian dinoflagellate assemblages of offshore SW Ireland was briefly indicated by Colin *et al.* (1992). Riley *et al.* (1992) proposed a dinocyst zonation for the North Sea Lower Cretaceous Valhall Formation. Four abundance zones (Salvador, 1994) spanned the interval from the latest Ryazanian to top Valanginian. These are presented in Figure 1.2.

The latest comprehensive review of both palynostratigraphy and dinoflagellate cyst biozonation was given by Stover *et al.* (1996). They plotted 28 of the most biostratigraphically useful dinoflagellate cyst ranges within the Ryazanian -

Valanginian interval, and compared zonal schemes from the North Sea, Canada, and the Netherlands.

1.2.2 Scandinavia, 'Scandinavian Arctic'.

In his study of the Haldager no. 1 borehole (Denmark), Davey (1982) revised his '1979' zonation scheme, and in particular substituted the Speeton Clay divisions for ammonites zones, making his framework more broadly comparable with other areas, particularly the North Sea (see Fig. 1.2). Piasecki (1984) made a study of the Lower Cretaceous Jydegård Formation from Bornholm, Denmark. The microfloral assemblages recovered proved to be directly correlateable with the *G. villosa* and *P. pelliferum* zones of Davey (1979, 1982). Heilmann-Clausen (1987) gave a thorough review of stratigraphically important dinoflagellate cyst ranges presented in publications from NW Europe and Scandinavia, as well as detailed biostratigraphy of the Danish Central Trough. The dinoflagellate cyst zonation schemes proposed by Davey (1979, 1982) and Woollam & Riding (1983) were not applied. A series of papers by Poulsen (1986, 1991, 1992, 1994, 1996) made a significant contribution to palynological knowledge of the Danish Central Trough. The first paper looked at the Callovian to Volgian dinocyst biostratigraphy of several wells, but did not attempt any zonation. This was rectified in 1991 when he applied appropriate portions of the schemes developed by Davey (1979, 1982), and Riding & Thomas (1988), and tailored them to fit the Central Trough assemblages (see Fig. 1.2). Comparison of the Danish Subbasin material with that of England (Poulsen, 1992, 1994, 1996) supported the correlations made for the Central Trough (Poulsen, 1991), proving that the microfloras of Denmark and the British Isles are directly related.

A brief palynological study by Vigran & Thusu (1975) was probably the first work to illustrate Mid and Late Volgian dinoflagellates from Norway. Birkelund *et al.* (1978) took this a little further, noting three palynological assemblages within the

Kimmeridgian to basal Ryazanian interval of Andøya. Characteristic taxa appear similar to coeval assemblages from the British Isles and Denmark, although much lower diversity was noted. This was also noted in a study of the Mid Volgian to Barremian palynology of Andøya by Løfaldi & Thusu (1979). Further work on the Lower Cretaceous deposits of Andøya combined with similar palynological investigations of Sklinnabanken by Århus (1986) show the assemblages to indeed to be comparable with North Sea equivalents, the latter more so than the former. Floras from both areas contain certain elements of the 'borealis' assemblage (of Brideaux & Fisher, 1976) however, and do appear to be somewhat intermediate between the typical 'sub-boreal' and boreal (Arctic) assemblages.

Palynology of the Oxfordian to Volgian interval from the Barents Sea area was considered by Wierzbowski & Århus (1990), and Bjærke (1980), the Jurassic-Cretaceous boundary interval by several authors (Bjærke *et al.*, 1976; Bjærke & Thusu, 1976; Bjærke, 1977; Kelly *et al.*, 1990), and the Lower Cretaceous by Århus *et al.* (1990) and Århus (1992). The Oxfordian to Volgian part of the succession bears a marine palynomorph assemblage akin to that of the 'borealis' assemblage of Canada, with few similarities to coeval assemblages in the British Isles (Wierzbowski & Århus, 1990; Bjærke, 1980). Slightly younger strata bear impoverished and poorly preserved assemblages largely dominated by a few long ranging taxa, making direct correlation to other Boreal areas problematic. However, figured specimens (Bjærke *et al.*, 1976; Bjærke, 1977) do show some similarity to assemblages from the British Isles and the Russian Platform (*pers. obs.*).

Fensome (1979) prepared a largely taxonomic work on the marine palynomorphs of East Greenland. He was able to demonstrate however, that the uppermost Oxfordian and Kimmeridgian rocks bear dinoflagellate assemblages similar to those from the North Sea. Håkansson *et al.* (1981) described the Oxfordian to Valanginian dinoflagellate cysts from northern Greenland. They noted that although the Oxfordian and Valanginian assemblages were similar to those typical of the North Sea proper, the Volgian and

Ryazanian strata bore assemblages dominated by long ranging taxa only. Furthermore, the flora recognised from this part of the column showed distinct similarity to the Canadian 'borealis' assemblage of Brideaux & Fisher (1976; Håkansson *et al.*, 1981). The presence of this flora in the boundary rocks of Greenland (as well as Svalbard, if indeed it can be recognised from there) emphasises the truly Arctic nature of this assemblage proposed by its discoverers (Håkansson *et al.*, 1981). Lund & Pedersen (1985) focused on slightly older rocks of eastern Greenland, terminating their study in the lowermost Kimmeridgian. The assemblage they recovered from this interval was somewhat impoverished, dominated by species of *Leptodinium* and *Scriniodinium*. They were able to correlate these strata with Assemblage E of Bjærke (1977)(see Fig. 1.2).

1.2.3. Canada, Canadian Arctic.

A series of papers by Pocock (1962, 1967, 1972, 1976, 1980) made a major contribution to the volume of northern and western Canadian palynological literature, although a significant number of the taxa erected by him were subsequently either emended or dismissed by Jansonius (1986). Pocock (1962, 1967) considered terrestrial as well as marine palynomorphs, making only brief comments on the nature of the dinocyst assemblages, but nevertheless indicating that they are of Boreal affinity. Pocock's (1972) biostratigraphic work was tied with the zonal subdivision made in Russia on the basis of changes in pollen assemblages, not on marine macrofauna, making direct comparison with the NW European area impossible. Pocock (1976) proposed a palynological zonation of Arctic Canada, erecting one informal and four formal zones spanning the Tithonian to Valanginian interval. Poor preservation in the Berriasian sediments precluded anything more than informal zone nomenclature. Once again it was noted that correlations could not be made to NW European biostratigraphic schemes, since many of the taxa were endemic, or had contrasting ranges (Pocock, 1976).

Williams (1975) presented a combined dinoflagellate and spore stratigraphy and zonation scheme for the Bathonian (Middle Jurassic) to Pleistocene (Tertiary) of the Scotian Shelf and Grand Banks areas, offshore eastern Canada. The four stages of the interval studied (Kimmeridgian, Tithonian, Berriasian, Valanginian) were composed of three dinocyst zones, named after the taxa *Gonyaulacysta cladophora*, *Ctenidodinium panneum*, and *Phoberocysta neocomica*, the latter of which spanned both the Berriasian and Valanginian Stages. The zonation proposed was also adopted in complementary (and overlapping) studies of the same area by Bujak & Williams (1977) on the Jurassic strata, Bujak & Williams (1978 : Cretaceous strata), and Barss, et al. (1979 : Jurassic & Cretaceous strata). The dinocyst assemblage noted as typifying the Canadian *C. panneum* Zone is similar to that of the NW European *C. culmulum* - *C. panneum* Zone described by Woollam & Riding (1983), although it appears a little less diverse and in addition contains examples of the genus *Amphorula* (Bujak & Williams, 1977) normally associated with sediments of more Tethyan aspect. Similarly, the *P. neocomica* Zone assemblage shares much in common with coeval flora from Boreal Europe, not least the nominative taxon, but the presence within it of the *Biorbifera johnewingi* assemblage Subzone (Williams, 1975) again suggests strong Tethyan inheritance. Overall many similarities in the floral assemblages were noted between the Scotian Shelf residues and those described from both Tethyan and Boreal Europe, although there appeared to be great disparity between the former and the contemporaneous assemblages of western Canada described by Pocock (1967, 1972, 1976) and of California by Warren (1967)(Williams, 1975).

An area just north of the Grand Banks region studied by Williams and co-workers was considered by Van Helden (1986), who assessed the Kimmeridgian to Valanginian dinoflagellate cyst biozonation of offshore Newfoundland. It was proposed that the interval corresponding to the *C. panneum* Zone of Williams (1975) be split into two shorter divisions, termed the *Amphorula metaelliptica* and *Endoscrinium campanulum* zones, although the position of the boundary between the two was left unclear.

Brideaux & Fisher (1976) considered the dinoflagellate cyst assemblages of the Jurassic-Cretaceous boundary in Arctic Canada. They discovered that within this interval (more precisely, Upper Oxfordian to Berriasian) a single floral assemblage, which they called the '*Paraeodinia borealis*' or just the '*borealis*' assemblage, could be traced across the Canadian Arctic. Individual species within it, most particularly *Gonyaulacysta cladophora*, *Psaligonyaulax dualis*, and *Lanterna saturnalis* could be used to variously determine Upper Oxfordian to Upper Kimmeridgian strata with some degree of consistency across the whole area (Brideaux & Fisher, 1976). Stratigraphic correlation of these indices (and the '*borealis*' assemblage as a whole) to other areas was made impossible by the combination of three factors:

1) The taxa mentioned above were endemic to the Canadian Arctic area (Brideaux & Fisher, 1976).

2) Although other taxa within the '*borealis*' assemblage could be compared with similar forms from NW Europe, western Canada, or North America, their ranges were in marked contrast in those areas (Brideaux & Fisher, 1976).

3) The biostratigraphy used above was tied to bivalve zonation commonly in use for the Canadian region, and since no agreement had been reached on how to correlate this scheme with the ammonite based chronology of NW Europe, calibration using macrofauna was not a possibility.

Brideaux & Myhr (1976) studied the marine palynomorph biostratigraphy of the Parsons' Lake area in the District of Mackenzie. They were able to date rocks from Oxfordian to Valanginian age using the occurrence data of key taxa for which ranges were already well known. Due to the poor preservation of the Jurassic-Cretaceous boundary interval, together with the presence of well cavings, they were unable to define the base of the Berriasian with any degree of certainty (Brideaux & Myhr, 1976).

Fisher & Riley's (1980) review of the distribution of dinocysts at the Jurassic/Cretaceous boundary (see section 1.2.1.) also included material from Canada and the Canadian Arctic, and the zonation scheme they proposed has several parallels with that of Williams and his co-worker (Williams, 1975; Bujak & Williams, 1977a, 1978). Pocock's 'progress report', also published in 1980 summarised the zonal schemes and biostratigraphic data which had been published at that time. He concentrated on the Canadian literature, but also took into account the data from California and NW Europe. He concluded that comparisons could be made between these areas on the basis of taxa common to all, and that in each the ranges of said taxa were "identical, or very close" (Pocock, 1980). This is in contrast to the data presented in the publications he reviewed (including several of his own papers), which shows the ranges of such taxa to be 'similar'.

Davies (1983) made an excellent contribution to the field with his proposed Opeel zonation of the Sverdrup Basin. Nine of his seventeen zones coincide with the Kimmeridgian to Valanginian interval, and each was carefully defined by its floral characteristics. His zones 'L' and 'M' overlap, and span the Jurassic Cretaceous boundary, with the dinocyst zonation being tied to the accepted macrofaunal zonation based on ammonites and pelycopods. He compared his framework to that of Johnson & Hills (1973) and Pocock (1976), and found that although there were indeed some similarities, fine correlations became difficult as a result of either the use of single-range zones (Johnson & Hills, 1973) which are prone to lateral facies variations, or incorrect identifications (Pocock, 1976).

Late Jurassic microplankton from the Canadian Western Interior (British Columbia) were analysed by Davies & Poulton (1986). Five loosely defined assemblages were reported, correlated to the earlier dinocyst zonation of Davies (1983). Although the assemblages they noted as typical of Upper Oxfordian to Lower Kimmeridgian strata shared many elements in common with other Boreal localities outside Canada, younger

assemblages were dominated by forms endemic to the North American continent (Davies & Poulton, 1986).

Other (predominantly taxonomic) works from this area include consideration of Jurassic - Cretaceous boundary microplankton from Canada by Brideaux (1977) and McIntyre & Brideaux (1980), and Alaska (USA) by Wiggins (1969, 1972).

1.2.4. Eastern Europe, Russia, Russian Arctic.

Beju (1971) built on earlier taxonomic accounts (Baltes, 1959, 1963, 1966) to give the first zonation scheme for the Jurassic deposits of Romania. He divided his interval of study into four zones, of which Zone J₄ correlated with the uppermost Oxfordian to Kimmeridgian Stages (Fig. 1.2). The assemblage was described as being very close to those noted from southern Germany, Poland and Bulgaria. Antonescu & Avram (1980) discussed the Early Cretaceous (Berriasian to Barremian) dinocyst assemblages from the Murguceva and Svinita Formations (Romania). They were able to construct a dinoflagellate cyst zonation for this interval, the two zones falling within the Berriasian and Valanginian Stages (see Fig. 1.2), being concurrent range zones. The assemblages recovered showed elements in common with Boreal assemblages (in agreement with the work of Beju, 1971), but also a strong Tethyan influence, particularly indicated by some of the zonal indices.

Dodekova (1967, 1969, 1992, 1994) analysed the Late Jurassic microplankton assemblages of Bulgaria. Her work indicated that the flora showed a mix of Boreal and Tethyan assemblages, with a much stronger influence from the latter. Biostratigraphy of the Oxfordian-Kimmeridgian and Tithonian was considered in the latter two papers with short-ranging taxa from both realms plotted.

Early studies of the Late Jurassic palynomorphs of Poland focused on taxonomy and systematics (see for example Górká, 1965). Poulsen (1992, 1993, 1994a, 1996) gave further consideration to the uppermost Jurassic to Lower Cretaceous deposits of Poland, and indicated that the recoverable dinocyst floras are comparable to contemporaneous assemblages from Denmark and other NW European areas. Details of the stratigraphic ranges of several taxa are in contrast to their known occurrences in the western European area, particularly in the Late Oxfordian to Kimmeridgian (Poulsen, 1993). Additionally the Late Jurassic floras from Poland contain elements in common with more Tethyan assemblages, and even Austral components are noted (Poulsen, 1992, 1993, 1994a, 1996). Difficulties in precise correlation of the ammonite chronostratigraphy between these areas may well account of some of the observed range discrepancies, although there would appear no reason to discount diachronism. Despite the ready application to the Polish area of the NW European palynological zonation developed by Riding & Thomas (1988) and Davey (1979, 1982), especially with the modifications made by Poulsen (1991), the dinoflagellate cyst assemblages from Poland were described with ammonite rather than dinocyst zone control in these papers.

Major taxonomic works on the Jurassic, Cretaceous and Tertiary palynomorphs of Russia were completed by Vozzhennikova (1960, 1963, 1967), and the material restudied by Lentin & Vozzhennikova (1990).

Theodorova (1980) studied the Neocomian dinoflagellate cyst assemblages from the Pechora and Precaspian Basins, north-eastern Siberia. She found that Lower Cretaceous strata of these basins were deposited in a period of 'maximum transgression' (peak sea-level), and thus the dinocyst flora was diverse. Additionally she suggested that many of the elements of the flora were in common with coeval assemblages from NW Europe, and that the depositional basins must therefore have been interlinked for at least part of this time. In contrast, many other 'early' studies of Siberian palynology suggested that prevailing facies in the Lower Cretaceous were shallow marine to continental, and the dominant palynomorphs were of terrestrial derivation. For example, Rovnina *et al.*

(1986) showed that in samples collected from the Upper Kimmeridgian to Volgian strata of western Siberia, the only recoverable marine taxa were species of the prasinophyte alga *Tasmanites*, known to be commonly associated with near-shore conditions. Similarly Smelror (1986) was only able to retrieve marine palynomorphs from the Mid Jurassic of Arctic USSR, the Late Jurassic and Early Cretaceous palynofloras being exclusively composed of sporomorphs. Ilyina (1986) was able to construct the first (informal) palynological zonation of the Siberian Jurassic, based largely on sporomorphs, but including some marine palynomorphs. Assemblages recovered from the uppermost Jurassic (Volgian) to basal Berriasian successions were of low diversity but included taxa found in northern Europe and Arctic Canada (particularly elements of the '*borealis*' assemblage).

Federova *et al.* (1993) studied the reference sections of the Boreal Berriasian on the north coast of Siberia in terms of micropalaeontology. Dinoflagellate cyst assemblages were described for each ammonite zone. Range charts were not provided, and the apparent assemblages recovered were of very low diversity, although all of the elements could be compared to the NW European area and appeared to be of similar age. In common with the findings of Rovnina *et al.* (1986), one of the reference sections studied (Boyarka River) was devoid of dinocysts, marine palynomorphs being represented only by typically near-shore acritarchs and prasinophytes. Shul'gina *et al.* (1994) described the north Siberian dinoflagellate cyst assemblage of Boreal Berriasian to Boreal Valanginian age (with passing reference to material of older, Volgian sediments). The sampling interval did not permit a detailed study to be made, and prevailing facies certainly played a part in the recovery of a rather low diversity assemblage (Shul'gina *et al.*, 1994). However, the microfloral characteristics would seem to suggest much in common with North Atlantic (UK area) and Arctic 'sub-provinces'. Several elements of the '*borealis*' assemblage were noted from the residues, including the nominative taxon. They revised the 'sub-province' division suggested earlier by Saks *et al.* (1971), based on ammonite provincialism, but made little attempt to correlate this with observable regionalism in the dinoflagellate cyst floras.

From the Volga Basin (Russian Platform) there have been three previous palynological studies of the Volgian lectostratotype at Gorodishche. Lord *et al.* (1987) considered the micro-biostratigraphy of both the Gorodishche and Kashpir sections, although their observations were limited by the small number of available samples. This work was much extended by the largely taxonomic work of Hogg (1994, unpublished). More recently, Riding *et al.* (in press) have continued this work by formulating a new dinocyst zonation scheme for the Russian Platform and Pechora Basin (northern Siberia) areas. This was compared to that of NW Europe, and indeed is similar in many respects. These three contributions will be discussed in more detail in Chapter 4.

Lower Cretaceous palynology of the Russian Platform and surrounding area was considered by Iosifova (1996). This work focused on the Ryazanian to Aptian interval of Tchernaya Retchka (Moscow Basin), and gave a detailed account of dinoflagellate cysts and their biostratigraphy. Iosifova (1998, pers. comm.) made a study of the Lower Cretaceous (Ryazanian) dinocysts from the section at Kashpir, but the work is as yet unpublished. It indicated however, that the assemblages from Kashpir and Tchernaya Retchka were very similar. The Late Ryazanian deposits of the Russian Platform have also been studied by Federova & Grjazeva (1984) and Jakovleva (1993) who, along with Riding (in press) were able to recognise a new (currently unnamed) dinocyst interval between the *Gochteodinia villosa* and *Pseudoceratium pelliferum* zones (see Figure 1.2).

1.3.1 Tethyan: Western Europe; S Germany, Switzerland, SE France, Portugal, Spain.

The Jurassic of the western European Tethyan area is extremely poorly understood in terms of dinoflagellate cysts (and indeed palynology in general). This is in part due to the incomplete nature of this portion of the Tethyan succession, and in a

large part due to the typical Upper Jurassic Tethyan facies not being conducive to palynomorph preservation.

Klement (1960) was the first to describe the marine palynofloras of the southwest German Malm in detail, several of his type specimens later being restudied by Sarjeant (1984). In a short paper, Dürr (1987) described the dinoflagellate cyst assemblage from the Middle Kimmeridgian (Weißjura δ) of southern Germany. Lund & Ecke (1988) loosely described the Mid to Late Jurassic dinocyst stratigraphy of Bavaria, in a manner offering only local utility.

Shortcomings in our palynostratigraphic knowledge of southern Germany were much reduced by Dürr's (1988) work on the Kimmeridgian and Tithonian. She was able to distinguish four dinocyst zones (see Fig. 1.3), which can be described as a combination of range, assemblage, and abundance zones (after Salvador, 1994). Her *Meirogonyaulax bejui* Zone marked the boundary between the Oxfordian and Kimmeridgian strata, but the uppermost Kimmeridgian and Tithonian were barren of palynomorphs and the corresponding Stage boundaries could therefore not be defined. She also noted that the assemblages recovered, whilst containing elements in common with the Boreal floras, were clearly of Tethyan affinity, although the area has been suggested as Boreal in other reviews of provinciality (Riding & Ioannides, 1996; Stover *et al.*, 1996), and is chronologically zoned by Boreal ammonite taxa. Review of the dinocyst taxa encountered and of the relative abundance data presented suggests that indeed there is a mix of Tethyan and Boreal characteristics, with a stronger influence from the latter. However, in view of the fact that the dinocyst zonation scheme cannot easily be correlated to either realm, and in deference to the original authors comments, the area is here considered to be Tethyan.

The Upper Oxfordian to Middle Kimmeridgian interval of southern Germany was again considered by Dürr (1989). In the latter work she was able to define three

'dinoflagellate cyst intervals' of which the uppermost corresponded to the *M. bejui* and *Prolixosphaeridium mixtispinosum* zones previously defined by her (Dürr, 1988)

Palynological assessment of the Jurassic deposits of Alsace (SE France) by Rauscher & Schmidt (1990) showed that although the Oxfordian assemblages were reasonably diverse and well preserved, those from Kimmeridgian strata were very much impoverished, and composed only of long ranging taxa. Millioud (1967) made a preliminary palynological assessment of the type sections of the Valanginian and Hauterivian Stages. This study indicated that dinocysts may in fact be very useful in fine scale biostratigraphic assessments of such sections, although a good proportion of the Valanginian stratotype proved to be barren of palynomorphs. A more detailed study of these sections, together with the Berriasian stratotype was completed by Millioud (1969), where the ranges of stratigraphically useful dinoflagellae cysts were plotted. In common with his preliminary account, the study was very much restricted by the barren nature of the Berriasian and Valangian intervals, having encountered only three palyniferous horizons from each of the two stratotypes.

Habib & Drugg (1983) considered the palynostratigraphy of the Berriasian to Hauterivian stratotypes along with numerous other important sections of Early Cretaceous age in SE France and Switzerland. The zonation they proposed was exactly that suggested for the western (central) North Atlantic (Habib, 1977, 1978; Habib & Drugg, 1983), although this study had the advantage of tying palynomorph data to ammonite biozonation (see Fig. 1.3). Four zones corresponded to the Berriasian to Valanginian interval, with the widely recognised *Biorbifera johnewingii* Zone defined as early Late to terminal Berriasian. Further study of the Hauterivian stratotype was made by Fauconnier (1989). The Cretaceous dinoflagellate cyst stratigraphy and zonation for the SE of France was summarised by Jardiné *et al.* (1984). The zonation they proposed differs in many respects from other zonations within the Tethyan realm (see Fig. 1.3). They went on to suggest that the floras came under increasing Boreal influence at the top of the Valanginian.

Figure 1.3 Legend

Correlation of previously published Tethyan dinoflagellate cyst biozones

Wherever possible the exact position of the zone boundaries relative to the standard ammonite zonation has been shown. Where this information was not provided, correlation has been made to the nearest ammonite zone, or to the stage boundaries as defined by Hoedemaeker (1991, 1999), Geyssant (1997) and Hantzpergue *et al.* (1997).

Abbreviations are as follows;

<i>B. johnewingii.</i>	...	<i>Biorbifera johnewingii</i>
<i>O. asterigium</i>	...	<i>Oligosphaeridium asterigium</i>
<i>D. warreni</i>	...	<i>Dapsilidinium warreni</i>

Whilst undertaking an investigation of the Berriasian stratotype, Monteil (1990) revised the definition of the typically Tethyan species *Amphorula*. Having done this, he attempted to create a zonation for the Upper Oxfordian to Lower Valanginian interval based on his new concept of 'morphostratigraphy'. In this concept, zonation is developed using a single phyletic group. Certain morphological characters are assigned Boolean values (ie. Yes or No) for each specimen, and single zones then formulated according to their 'Character-Yes' or 'Character-No' quality. Complex zonations can therefore be built up using the concurrence of 'morpho-zones' from different phyletic groups.

A further zonation of the Tithonian to Valanginian interval of south-east France was given by Monteil (1992) and subsequently revised/updated by Monteil (1993) (see Fig. 1.3). Of particular interest here is the definition of Monteil's (1992) *Biorbifera johnewingii* Zone, which was proposed as lying across the Tithonian-Berriasian boundary, in contrast to numerous other studies (Habib, 1976, 1977, 1978; Habib & Drugg, 1983, 1987; Jardiné *et al.*, 1984). Indeed, there appears to be widespread disagreement about the stratigraphic extent of this zone, with other reports suggesting that the first occurrence of this species is indeed in the Late Tithonian (Jan du Chêne *et al.*, 1993; Dodekova, 1994; Leereveld, 1997). Since these all post-date the work of Habib & associates, it is perhaps safest to assume that additional occurrences of the nominative taxon have now been noted within the Tithonian (and Early Berrisian), effectively extending its range into older strata. If this is the case, a strong argument could be made for the redundancy, or at least relegation to sub-zone level, of Habib & Drugg's (1983) *Phoberocysta neocomica* Zone.

In addition to the zonation, results of the Vocontian Trough Early Cretaceous Working Group's research into the correlation of sequence- and dinoflagellate cyst stratigraphy were presented. Monteil's work was included in a summary study of the biostratigraphic and sequence stratigraphical knowledge of SE France given by Jan du Chêne *et al.* (1993).

Masure (1988) reported on the dinocyst biostratigraphy of the Berriasian to Aptian interval from the Galicia Margin, offshore Spain. The boreholes studied revealed numerous taxa in common with Boreal areas, especially *Achomosphaera neptunii*, *Phoberocysta neocomica*, and *Pseudoceratium pelliferum*, the co-occurrence of which was used to indicate a late Berrisian age for the cores. The Tethyan species *Biorbifera johnewingii* was only encountered in Valanginian deposits from the Spanish coast, in marked contrast to its apparent first occurrence in SE France and the western Atlantic (see for example Monteil, 1993; Habib & Drugg, 1983; etc).

Dinocyst biostratigraphy of the Berriasian to Aptian of the Río Argos succession, SE Spain was given by Leereveld (1989) Hoedemaeker & Leereveld (1995), and Leereveld (1997). A dinocyst zonation was proposed in Hoedemaeker & Leereveld (1995), and formally defined for the Berriasian to Valanginian interval in Leereveld (1997). The zonation in both publications was calibrated with well dated ammonite and calpionellid data. Four zones were proposed in the latter paper (see Fig. 1.3), the upper three being further subdivided into seven subzones. The base of the *Biorbifera johnewingii* dinocyst Zone is not defined in the Río Argos succession since it apparently extends into an unpalyniferous interval, and Leereveld (1997) was forced to use the base defined by Jan du Chêne *et al.* (1993) for the Broyon section, SE France. The zone could not be subdivided because of 'poor palynological recovery' from that interval (Leereveld, 1997). The work also correlates the Río Argos zonation to those proposed for the western Atlantic, SE France, NW Europe, Libya, Romania, Morocco, the Boreal Arctic, and various localities in the southern hemisphere.

The earliest accounts of microplankton in Portuguese deposits of Kimmeridgian age were in the largely taxonomic studies of Deflandre (1938, 1941). Berthou & Leereveld (1990) considered the Berriasian to Albian palynology of Portugal. Their biostratigraphic charts appear to show numerous 'biohorizons' corresponding to the FADs of several taxa, although since not all of the collected samples are included within

these (presumably because they were barren of palynomorphs), the strength of such events may have been over-emphasised. Overall the flora recovered was dominated by taxa of Boreal aspect (Berthou & Leereveld, 1990), with few direct correlations with other Tethyan assemblages possible (none from the Berriasian - Valanginian strata). Since the ammonite data strongly suggests Tethyan descent, the authors were able to propose several correlations between Boreal and Tethyan ammonite stratigraphy based on the dinoflagellate cyst biohorizons.

1.3.2. NW Africa, eastern North Atlantic.

The literature on north African (onshore) palynology is limited. The Lower Cretaceous sequence of south-west Morocco was considered by Below (1981a, 1982a,b). These contributions were primarily taxonomic in nature, but biostratigraphy was briefly considered in 1981 (Below, 1981a) and in slightly more detail, with comparisons to other areas in his 1982 papers. No zonation was proposed since many of the taxa encountered by him were considered to be long-ranging, although direct comparisons with the zonations of other areas were made. Neocomian palynology of northern Morocco was studied by Gübeli *et al.* (1984), from the turbiditic sediments of the Rif Mountains. The dinoflagellate cyst assemblage was of very low diversity, and the zonation they proposed was defined by sporomorphs. However, the presence of biostratigraphically important taxa was noted allowing approximate correlation of the Berriasian and Valanginian sediments with other Tethyan areas (see Fig. 1.3).

Williams (1978) performed a palynological analysis of two Deep Sea Drilling Project Sites (367, 370) off the western coast of Africa. The assemblages recovered were most favourably compared to contemporaneous floras from the Scotian Shelf, but contained taxa of both Boreal and Tethyan affinity. Biostratigraphic analysis was unable to separate the Berriasian and Valanginian strata with any degree of certainty, and the limited amount of information from the latest Jurassic precluded any meaningful

interpretation of the Jurassic-Cretaceous boundary. Despite some similarities between this flora and that of the onshore Lower Cretaceous localities studied by Below (1981a, 1982, a,b), a substantial portion of the offshore assemblage was not comparable. Williams & Bujak (1985) extended this work with a study of the Kimmeridgian to Hauterivian strata at Site 416 (adjacent to Site 370 of Williams, 1978). Dinoflagellate cyst assemblages were described from each Stage, and compared to those of the Scotian Shelf and the western North Atlantic.

Gradstein *et al.* (1992) used a variety of microfossil and palaeomagnetic data from areas in the eastern and western North Atlantic to construct a probabilistic zonation for the early Cretaceous (including Tithonian) interval. Detailed comparison of their zonation scheme with those proposed for dinoflagellate cysts is difficult, since they did not include ammonite data. However, their zonation is broadly correlated against other data in Figure 1.3. An extensive re-study of central North Atlantic material, and comparisons to the work of Habib & Drugg (1983) and Gradstein *et al.* (1992) was undertaken by Ogg (1994). Nine deep sea sites were re-examined, and it was shown that the succession of taxa used to defined the zonation scheme (and thus the succession of zones themselves) of Habib & Drugg (1983) was the same in the eastern and western areas of the Central North Atlantic. This being the case, it was also shown that the timing of these appearances was slightly younger in the eastern area based on calibration with calcareous nannofossil and foraminiferal data (Ogg, 1994).

1.3.3 California, western North Atlantic.

Literature on the North American marine palynology of this interval is limited. According to Riding & Ioannides (1996), the most comprehensive study of the Upper Jurassic of California is the unpublished thesis of Warren (1967), and suggests that many forms described by Warren (1967, 1973) are of Boreal affinity. However, the

Tethyan nature of the Californian sections (at least of key biostratigraphic taxa) is presented by Habib & Warren (1973).

The Kimmeridgian (*sensu gallico*) sediments of the Blake-Bahama Basin were considered by Zotto *et al.* (1987). This short account was able to demonstrate the position of the Oxfordian-Kimmeridgian boundary palynologically, with particular reference to first occurrence data. Taxa chosen for this biostratigraphic analysis were those known to originate in contemporaneous sediments of the Kimmeridgian stratotype. In comparison to the eastern North Atlantic, there is a wealth of information available on the Jurassic-Cretaceous boundary palynology of the western side, mostly contributed by Habib and associates. Habib (1972) noted four distinct dinoflagellate cyst associations (E-H) which corresponded to the Oxfordian-Valanginian interval. Habib (1976) focused on the Early Cretaceous assemblages, and constructed the first dinocyst zonation for the region, with four zones being defined from the Berriasian to Valanginian-Barremian interval, although as just suggested the stratigraphic control, particularly on the youngest zone, was not precise.

Habib (1977) reviewed this zonation with a study of six additional Deep Sea Drilling Project Sites from the western North Atlantic. The uppermost *Oligosphaeridium complex* Zone of Habib (1976) was replaced by the elevation of its two subzones to zonal status. This was accompanied by greater stratigraphic control showing that in fact the preceding *Druggidium deflandrei* Zone spanned the late Valanginian to Hauterivian interval. Whilst the *B. johnewingii* Zone was characterised as an Interval Zone, the three succeeding zones were Lineage zones (or Phylozones as termed by Habib, 1977), within the genus *Druggidium*. Habib was also able to demonstrate the validity (if not the chronostratigraphic resolution) of his zonation scheme in biostratigraphic assessments of cores from the western Bermuda Rise (Habib, 1977), and Blake-Bahama Basin (Habib, 1978; Habib & Drugg, 1983, 1987). Habib & Drugg (1983) compared the zonation of the Blake-Bahama Basin with new work from the Neocomian stratotypes, showing that the two areas were almost identical in this respect. In this study they were able to place the

first ammonite chronostratigraphic control on their dinocyst zones from the onshore European localities, which was then transferred to the western Atlantic area by Habib & Drugg (1987).

Riley & Fenton (1984) analysed samples collected from Lower Cretaceous rocks of the Gulf of Mexico. The study focussed on the stratigraphic distribution of dinoflagellate cysts, and the assemblages proved very similar to those previously identified by Habib. The notable exception to this was the absence of *B. johnewingii* from the site. Habib's zonation scheme was not applied, although some comparisons were made.

1.3.4. East & Central Africa, Middle East, India, China.

Late Jurassic dinoflagellate assemblages from Kenya were reported by Jaing *et al.* (1992). The small stratigraphic interval studied was approximately equivalent to the *Beckeri* and *Hybonotum* ammonite chrons of the Kimmeridgian - Tithonian boundary (*sensu gallico*), and the Kimmeridgian *Autissiodorensis* - *Elegans* transition (*sensu anglico*). The sequence was split into three dinocyst zones, the first an assemblage zone, and subsequently two interval zones. The uppermost zone was further divided into three subzones. In terms of floral characteristics, they were able to demonstrate that approximately 25% of the taxa were endemic to the African-Arabian-Indian region (of which half were endemic to Africa), and the remainder suggested a mix of European Boreal, Tethyan and Austral characteristics. Jaing *et al.* (1992) also compared the Kenyan assemblage to those of Chen (1978, 1982) from Madagascar, and found them to be strongly comparable.

Upper Jurassic palynological studies of Israeli successions are restricted to Oxfordian and older strata (Conway, 1990, 1996). A basal Cretaceous to ?Portlandian interval was examined by Conway (1996), but the interval proved barren of marine

palynomorphs until Hauterivian/Barremian part of the section (also dated by sporomorphs).

Late Jurassic to early Cretaceous marine palynomorphs from Iran were first reported by Thusu & Vigran (1985), and Thusu & Van der Eem (1985) and again in much more detail by Thusu *et al.*, (1988). The latter work proposed a dinocyst zonation for the Aelian (Early Jurassic) to Barremian (Early Cretaceous) interval, of which four zones correspond to strata of Kimmeridgian to Valanginian age (Fig. 1.3), calibrated to calpionellid data. Comparison of the floral characteristics to other areas show that the Late Jurassic part was broadly similar to the successions of NW Europe (although there were some substantial differences). Neocomian assemblages from Iran were significantly different to those of Tethyan Europe, although they were able to recognise the *Phoberocysta neocomica* Zone, which has additionally been noted from eastern Canada (Bujak & Williams, 1978). Overall the Neocomian assemblages were noted as being more diverse than those recovered from Jurassic sediments. Kimmeridgian palynomorphs were noted by Wheeler & Sarjeant (1990) from a single sample collected in the Alborz Mountains area. The assemblage was not diverse, and poorly preserved, but nevertheless the taxa identified were directly comparable to those isolated from contemporaneous sediments in Boreal NW Europe.

Marine palynomorphs from Afghanistan were reported by Ashraf (1979). He divided the Malm-Neocomian interval into two dinocyst zones (B & C), which were directly correlated to his sporomorph zones published earlier (Ashraf 1977). Once again the flora was shown to have strong Boreal influence.

A short initial report on the Late Jurassic dinoflagellate cysts of Kutchchh (West India) was given by Ventkatchala & Kar (1968). The exact stratigraphic position of the recovered assemblage was not given, but compared to Deflandre's (1938) work on the Portuguese Kimmeridgian sediments. The Upper Jurassic (Oxfordian to Kimmeridgian) of the Kutchchh area was also considered in a short paper by Jain *et al.* (1986) and

Kumar (1986a, 1987a, 1987b). Similarly aged marine palynomorph assemblages from the Spiti Shale Formation (Himalaya) were described by Jain *et al.* (1978, 1984). Five assemblage zones were proposed, although a low level of stratigraphic control was attained, and in many cases the suggested dinocyst ranges conflicted with the ammonite data. The assemblages appear to be a mix of Boreal and Austral characteristics (pers. obs.) in conflict with their assertion that the sediments are 'Tethyan' (Jain *et al.*, 1978). A review of Indian marine palynology was undertaken by Garg *et al.* (1987) re-examining all of the earlier work, and the dinoflagellate biostratigraphy was set in a stronger chronostratigraphic framework.

The available literature on the dinoflagellate assemblages of China is essentially limited to the taxonomic study of Yu Jingxian (1982), who concentrated on the Early Cretaceous of the Heilongjiang Province. Ogg (1992) gave a brief account of the marine palynomorphs of the western Pacific. She noted that all of the Lower Cretaceous sediments proved barren of palynomorphs (independent of facies), and that the earliest recoverable dinoflagellate cysts came from the Aptian/Albian. Sarjeant *et al.* (1992) reviewed the Jurassic palynology of the Pacific region, concluding that due to aspects of preservation in the majority of areas, the marine palynology of the SE Asian region was extremely poorly known. Riding (1996) supported this by asserting that the paucity of data from China and south-east Asia prevents meaningful comparison with other well known areas.

CHAPTER 2. Introduction to palynofacies analysis.

2. Introduction to palynofacies analysis.

2.1. Review of published classification schemes.

The term palynofacies was coined by Combaz (1964), although organic matter occurring in palynomorph preparations had been studied earlier by Muller (1959). As originally defined, the term relates to all the acid-resistant organic materials recovered using palynological processing techniques (HCl & HF acids) as visible under the light microscope. Subsequent workers have not always adhered to this definition, often using it in association with only part of the recoverable organic matter (see for example, Bint & Helby, 1988, Lenoir & Hart, 1988, Hart *et al.*, 1988, and Traverse, 1988, who all focused on palynomorphs; Andrews & Walton, 1990, who concentrated solely on structured components; Rahman *et al.*, 1994, who only considered the shape and nature of the phytoclast debris; and Sittler & Olivier-Pierre, 1994, who considered palynofacies elements to be all organic particles excluding palynomorphs). Batten (1996) noted that the terms 'sedimentary organic matter' (SOM) and 'palynofacies' have often been treated as synonymous by palynologists, although in reality SOM encompasses a much larger range of materials. The term was redefined by Powell *et al.*, (1990) to relate it more closely with sedimentary environments, although Batten (1996, p. 1020) commented that determination of such environments on the basis of palynofacies is often equivocal, even where a palynofacies is well characterised. In most preparations there is probably a difference between the 'palynofacies' which existed in the sedimentary environment and 'palynofacies' in the sense of Combaz (1964), whether it was generated by diagenetic alterations, weathering, sample collection bias, or simply destructive processing techniques. Since in many cases palynofacies analysis is aimed at determining the environment of deposition, the definition of Powell *et al.* (1990) might be regarded as circular reasoning.

Debate about the use of the term 'palynofacies' aside, the terminology used in reference to the constituents of organic matter has also been both appropriately and inappropriately developed. As noted by Tyson (1995) the terms 'kerogen' and

'palynological organic matter' (or palynological matter) are largely synonymous (although see Batten, 1981: p. 202), but in the context of the present work, the author prefers to use the latter term. This is because 'kerogen' can also take on geochemical connotations, for example the characterisation of 'kerogen types' by Tissot *et al.*, (1974) on the basis of elemental analysis. Other terms synonymous with palynological matter include: dispersed organic debris, palynodebris (Manum, 1976; Habib, 1979a; Boulter & Riddick, 1986; Pocock *et al.*, 1988; van Waveren & Visscher, 1994), organoclasts (Courtinat, 1989), and palynoclasts (Powell *et al.*, 1990).

One of the most widely used terms referring to the constituents of palynologic matter assemblages is 'particulate organic matter' (POM). Various authors differ in their usage of this term. For example Tyson (1984, 1989, 1993, 1995) has routinely included amorphous organic materials within this group (thus making it synonymous with palynologic matter), whilst Harding & Allen (1995) and Cole & Harding (1998) exclude AOM. The Oxford English Dictionary defines the word *particle* as a "very small bit or piece (of something)". Thus it does not connote any qualities of structure or organisation, and can acceptably be used in conjunction with AOM. Palynomorphs, being entities unto themselves, are not in the strictest sense particles, but have been ubiquitously accepted as being members of POM.

Numerous formal classification schemes for the various components of palynological matter have been developed, but none has met widespread acceptance. There are several apparent reasons for this. Palynofacies investigations typically fall into two categories: those aimed at assessing hydrocarbon potential, and those focused on (palaeo)environmental interpretations. Tyson (1995) noted that studies of hydrocarbon potential concentrate on the identification of inert, gas-prone, oil-prone, and very oil-prone elements within the palynological matter assemblages, and for this reason the classifications developed tend to be simple with a small number of categories. Conversely, palaeoenvironmental assessments need to consider a far greater set of

variables, and are altogether more complex to interpret. This dichotomy prevents a united classification from being acceptable.

In addition, many classifications have used unsuitable or ambiguous terminology, and more still have proposed new terms for what Tyson (1995, p. 341) described as a "relatively familiar set of components". Typically confusion has arisen over the use of organic petrological (reflected light) terminology in transmitted light studies. Whilst comparisons can be drawn between macerals determined in reflected light and various palynofacies components proper, the fundamental difference in optical technique must force the terminology to remain separate. Thus the application of the maceral term 'inertinite' to opaque particles identified in transmitted light microscopy (for example, Habib, 1979a,b; Habib *et al.*, 1988; Gorin *et al.*, 1989; Gorin & Monteil, 1990; Gorin & Steffen, 1991) is unacceptable. The use of poorly defined terms such as 'herbaceous' (Burgess, 1974; Hunt, 1979; Powell *et al.*, 1982; Tissot & Welte, 1984)(which is also inappropriate in this context as it is a botanical term used to describe non-woody flowering plants; Tyson, 1995), or those which unnecessarily group components of different provenance, such as 'phyrogen' (Bujak *et al.*, 1977), have made subsequent comparisons of palynofacies components difficult. So too has the development of terminology such as the 'palynomacerals' of Whitaker (1984)(and subsequently Van der Zwan, 1990 and Whitaker *et al.*, 1992) and the palynofacies concepts of Habib (1979a, 1982, 1989), as well as studies based on preservation state of palynological matter (Hart, 1986), all of which have proved difficult to apply consistently.

Nevertheless, several classification schemes dealing with the majority of palynologic matter types have been presented. The most commonly cited of these are shown in Figure 2.1 and reviewed below, followed by a comparison with the choice of terminology adopted in this report. In addition, numerous studies have dealt with relatively simple palynofacies composed of a small number of components. These include studies such as Piasecki (1986), Barron (1989), Nøhr-Hansen, (1989), Van Waveren (1989), Benson (1990), Kunz (1990), Davies *et al.* (1991), Sittler & Schuler

(1991), Courtinat (1993), Hssaïda & Morzadec-Kerfourn (1993), Mussard *et al.* (1994), Sittler & Ollivier-Pierre (1994), Van Waveren & Visscher (1994), Harding & Allen (1995), Oboh-Ikuenobe (1996), Oboh-Ikuenobe *et al.*, (1997), and Cole & Harding (1998). Additionally, some authors have preferred to relate their observed palynofacies to palaeoenvironment using the simplified systems developed for estimating hydrocarbon potential (see for example, Manum & Thronsen, 1978; Venkatachala, 1981b; Hoelstad, 1986; Pocknall & Beggs, 1990; Riley *et al.* 1992). Since the aims of the current investigation do not involve estimation of hydrocarbon potential, review of the formal classification schemes associated with this concept is not made here. The reader is referred to the summaries made by Tyson (1995, Chapter 20) and Batten (1996), and the references cited therein.

Staplin (1969) was the first to present a formal classification for palynologic debris. He grouped all the recognisable components into 'primary' and 'modified materials', thus recognising the importance of distinguishing between 'fresh' and reworked matter, and in particular the partial oxidation of some materials prior to deposition (after Spackman & Thompson, 1963, who made observations on coal constituents). He also separated materials of terrestrial and marine origin, recognising various components of phytoclast material. Little attempt was made to further itemise the different phytoplankton groups or to make a detailed study of the 'sapropelic indicators' ('AOM'). Such shortcomings were addressed by Combaz (1980), although his subdivision of the amorphous group was not widely applicable as none of his categories were well defined.

Habib (1979a)(although actually published earlier in Deroo *et al.*, 1978) used an informal classification for his observed palynological matter from the North Atlantic, which was subsequently used to develop a set of formal 'organic facies types'. He grouped this material into structured and amorphous categories, and included within the latter particles which he later (at least in part) re-attributed to oxidised tracheidal

PAGE
NUMBERING
AS ORIGINAL

matter (Habib, 1983). The inclusion of phytoclast material within his amorphous group in his early papers (Habib 1979a,b) led to some degree of inconsistency. Indeed, the characterisation of his amorphous group is somewhat jargonised and in places poorly defined (Tyson, 1995: p. 361). His 'organic facies types' have been applied in several other studies (Habib, 1982, 1983; Deroo *et al.*, 1978; Poulsen, 1986; Courtinat, 1989; Habib & Miller, 1989, Benson, 1990), most successfully in relation to the deep sea environment.

Masran & Pocock (1981) published a much more widely utilised classification scheme (for examples of its application see Summerhayes, 1981; Pocock, 1982; Masran, 1984; Venkatachala, 1984; Venkatachala *et al.*, 1984; Mukherjee & Chopra, 1987; Pocock *et al.*, 1988; Firth, 1993). They proposed nine major categories which encompassed both well preserved and degraded terrestrially-derived materials as well as an amorphous group (*sensu stricto*). Tyson (1995) however notes that there are several terminological problems with their classification, not least of which is the formal substitution of the term 'marine' by 'aqueous'. They greatly expanded on Staplin's (1969) acknowledgement of modified materials, placing some emphasis on the geochemical subdivision of amorphous matter (Tyson, 1995). Further they introduced the intermediate 'semi-amorphous' category for biologically degraded organic matter with traces of original structure remaining. Their division of the phytoclast group was the most detailed yet published, although their use of the terms 'root', 'stem' and 'leaf' were unqualified and perhaps over interpretative for primary data collection. A dichotomy in the 'charcoal' group into 'degrado-' and 'pyro- varieties' was presented in line with the recognisable maceral equivalents.

From work on the North Sea palynofacies, Parry *et al.* (1981) constructed a relatively simple classification scheme. The nature of their palynofacies assemblages meant that much attention was paid to phytoclast material. Despite this they did not distinguish between blocky brown wood with little internal structure (cf. gellified; Tyson, 1995) and wood possessing longitudinal thickenings, which clearly represents

tracheid material. The palynomorph group was well separated in their scheme, into marine, terrestrial, and freshwater components, and further discriminated to the level of dinoflagellate cysts, prasinophytes, spores and pollen.

Perhaps the most widely used of all classification schemes is that of Whitaker *et al.* (1984) based on palynofacies characterisation of the Troll Field, offshore Norway. Their relatively autochthonous (structured) fraction was finely divided (Whitaker *et al.*, 1984: Figure 7), and they separated chorate, cavate and proximate dinoflagellate cysts. Tyson (1995) notes that their use of the acronym S.O.M. for 'structureless sapropelic organic matter', was inappropriate as it has also been used for 'sedimentary organic matter'. Additionally, their SOM appears to be analogous with the AOM of most other workers (Tyson, 1995). Conversely, the AOM of Whitaker *et al.* (1992) seems to represent the homogeneous degraded remains of terrestrial material.

The main problem with the classification of Whitaker *et al.* (1984) is that they did not describe it in the text, referring only to an iconified key. As a result, later attempts to qualify the various categories, particularly of the 'relatively allochthonous' phytoclast material have not always been consistent (see Bryant *et al.*, 1988; Van der Zwan, 1990; Whitaker *et al.*, 1992). This group is divided into 'palynomacerals' 1-4, on the basis of hydrodynamic properties (Whitaker *et al.*, 1992). Of the four, only Palynomaceral 3 can be consistently separated, and appears to be largely cuticle material. Palynomacerals 1 and 2 appear to relate very loosely to the brown wood category of Parry *et al.* (1981), although both appear to include 'humic gels', 'resinous substances', and 'algal detritus', thus including amorphous components (Van der Zwan, 1990; Whitaker *et al.*, 1992). Quite what 'algal detritus' was in this respect was never qualified, although Tyson (1995) suggests it may have been *Botryococcus* colonies, at least in Palynomaceral 1. The main difference between these two is supposedly contrasting buoyancy, with Palynomaceral 2 particles tending to be thinner, more lath shaped and less dense. The key as drawn by Van der Zwan (1990) would suggest that Palynomaceral 2 includes fragments of tracheids, which would perhaps explain why this

palynomaceral is represented by more 'lath shaped' fragments. He also compares Palynomaceral 1 with the brown wood component of Boulter & Riddick (1986), which is indeed roughly comparable to that of Parry *et al.* (1981).

Palynomaceral 4 of Whitaker *et al.* (1984) appears to be approximately equivalent to the black wood component of Parry *et al.* (1981) and Masran & Pocock (1981), although they included particles which are both black and 'almost black' within this category. It is not clear what colour the 'almost black' material would be, and thus whether it represents extremely thin (grey) pieces of true black wood, or whether they include particles with brown rims. If the latter is the case, they appear to follow Batten's (1973b) inclusion of oxidised brown wood within 'black wood' group. The present author agrees with Tyson's (1995) comment that doing so raises problems with consistent discrimination of the two types, and should therefore be avoided. Furthermore Van der Zwan's (1990: p. 175) assertion that the blade shaped component is "usually uniformly opaque and structureless" seems a little unfortunate since the internal structure of opaque particles (or lack thereof) cannot be assessed using transmitted light.

Although the palynomacerals of Whitaker *et al.* (1984) can be loosely compared to other classifications, they also used a system of superscript notations to indicate aspects of shape and preservation of the various components. These included indications of bleaching and darkening of the particles, which Van der Zwan (1990) attributes to preservational processes. However it is not clear whether these phenomena relate to pre- or post-depositional changes (including artefacts of processing procedure), and must be treated with caution. Whitaker's (1984) classification was also used by Van de Laar & Fermont (1990), Blondel *et al.*, (1993), Steffen & Gorin (1993a,b), Mussard *et al.*, (1994), and Sawyer & Keegan (1996).

An informal nomenclature for palynological matter was presented by Boulter & Riddick (1986). They noted 17 "artificial categories" varying from readily identifiable

palynomorphs and phytoclast material through to amorphous materials and degraded debris. Additionally they proposed two categories termed "comminuted debris" and "specks", which were essentially very fine material for which it was difficult to define a source. Since they did not oxidise their residues, much of this may in fact have been pyrite (Boulter & Riddick, 1986). Their black matter is probably comparable to the black wood of other authors (Boulter & Riddick, 1986), although they note that since it is opaque, there is no way to definitively state its nature. This terminology was restated by Boulter (1994).

A very different type of organic matter classification was presented by Hart (1986). He proposed that degradation state and biological origin should be combined. However, the separation of several of his categories appears to be somewhat "subjective and difficult to apply consistently" (Tyson, 1995: p. 364). In reality a complete spectrum of preservation states exists, and his categories would appear to be very artificial stages within this spectrum. The supposition that degradation is controlled by biological origin is surely not ubiquitously applicable. Hart's system has subsequently been used by Pasley *et al.* (1991), Gregory & Hart (1992), Darby & Hart (1994), and Hart (1994), amongst others.

Van Bergen *et al.* (1990) presented a simple classification scheme which was split into three major categories of 'palynomorphs', 'structured palynodebris' and 'unstructured palynodebris'. The 'wood remains' division of structured palynodebris includes the brown and black wood and tracheid material of other authors. The palynomorph group is subdivided in a familiar way, and although they did not present formal groups for dinoflagellate cysts, acritarchs or prasinophytes, these were itemised within the unicellular component of 'algae'. This has also been used by Van Bergen & Kerp (1990).

















Highton *et al.* (1991) took the shape classification concept of Whitaker *et al.* (1984) much further by completely defining kerogen components on this basis. Little or

no attention was paid to the biological origins of the material (although miospores were used as a separate grouping). Their material was drawn from marginal Westphalian coal-measure environments, and their assemblages were thus lacking in marine material (i.e. phytoplankton and marine zoomorphs). This makes their classification conceptually difficult to compare with those of other workers, but has been broadly attempted in Figure 2.1.

Williams (1992) prepared a very simplified classification for the Brent Group palynofacies, where all the components were split into humic or sapropelic kerogen, with amorphous matter noted as degraded humic or sapropelic material. Humic kerogen was solely constituted of 'blackwood' and 'brownwood' (*sic*), with plant cuticle being assigned to sapropelic kerogen. The majority of Williams' components are comparable to those of other workers.

More recently Tyson (1995) and Batten (1996) presented informal classifications for palynological matter, although Tyson's (1995) was simply intended as a key to the terminology. Although there are differences in the way the major categories are structured, the individual components recognised are quite similar (Fig. 2.2). The main difference is that Batten (1996) used 'palynomorphs' as a major category alongside structured and unstructured organic matter groups whereas Tyson (1995) preferred to include it as a sub-unit of the structured category. Tyson (1995) then used a three-fold subdivision of the palynomorph group into phytoplankton, sporomorph and zoomorph subgroups, whereas Batten (1996) listed individual components without this subdivision. The present author adopts the structure of Tyson (1995), whilst the detailed sub-division of the palynomorph group used here more closely follows that of Batten (1996)(Fig. 2.2).

Figure 2.2: Comparison of the palynological matter terminology used in the present report with that of Tyson (1995) and Batten (1996).

Structure	THIS STUDY		MACERAL GROUP		MACERAL		TYSON 1995		BATTEN 1996	
	Terrestrial	Marine	Terrestrial	Marine	Sclerotinite	Inertinite	Sclerotinite	Phytoclast group	Phytoclasts	Other tissues
Structured	Terrestrial	?	Sporomorphs	'Tubes'		Sclerotinite	Melanised fungal hyphae	Fungal hyphae		
				Black wood	Type 1 	Degradatinites	Oxidised or carbonised woody tissues including charcoal	Black wood		
				Brown wood	Type 2 	Pyrofusinite	Highly gellified woody tissue	Brown wood		
				Tracheids		Teinites	Wood tracheid	Tracheids		
				Cuticle		Cutinite	Cuticle	Cuticles		
				'Sheets'		Fauna?	Non-cellular sheet			
				Spores		Liptinite	Sporomorph subgroup	Spores and pollen grains		
				Saccate pollen		or	Palynomorph group	Miscellaneous		
				Asaccate pollen		Exinite		Dinoflagellate cysts		
				'Simple sacs'		Faunal relics	Amorphous group	Lamalginites	Phytoplankton subgroup	Miscellaneous
Dinoflagellate cysts		Tealaginites	Phytoplankton	Dinoflagellate cysts						
Acritarchs		Lipinite or exinite Vitrinite or Huminite Lipinite or exinite	Structureless	Resinite Collinite Hebamorphinite Lipodetrinite	Zoomorph subgroup	Acritarchs				
Prasinophytes						Prasinophytes	Prasinophyte algae			
Amorphous	Marine	?	Zoomorphs	Zoomorphs		Zoomorphs	Zoomorphs	Scolecodonts	Scolecodonts	
				Resin		Resin	Resin (and amber)			
				AOM		AOM	AOM of terrestrial derivation (AOMT) Amorphous organic matter (AOM)			
Structureless	Marine	Type 1	Type 1	Lipinite or exinite		'AOM'	Unstructured organic matter (USTOM)			
Structureless	Marine	Type 2	Type 2	Lipinite or exinite						

2.2. Terminology used in this report

Structured organic particles

Phytoclasts

'Fungi'

These are yellow to orange-brown thin walled tubular structures interpreted as being fungal hyphae. They can be correlated with the coal maceral sclerotinite of the inertinite group. They are extremely rare in the residues studied here, and will not be discussed further.

Black wood

Opaque black particles, blocky equant to lath-shaped or extremely angular in outline. This category is broadly comparable to the 'charcoal' of Staplin (1969), the 'carbons' of Combaz (1980), 'Palynomaceral 4' of Whitaker *et al.*, (1984), the 'black wood' of numerous authors (Batten, 1973b, 1996; Parry *et al.*, 1981; Williams, 1992), and is directly comparable to the 'charcoal' of Masran & Pocock (1981) and Tyson's (1995, p. 354) "oxidised or carbonised woody tissues including charcoal". Two types can be recognised. The subdivision of both types using long-axis : short-axis relationships follows Frank & Tyson (1995).

Type 1: Equidimensional (length:width ratio $<2:1$), well rounded to angular particles. They are regarded as being directly comparable to the 'degradocharcoal' of Masran & Pocock (1981). Hence they are also comparable to the coal maceral degradofusinite of the inertinite group.

Type 2: Very angular, 'splintery', or elongate lath-shaped particles (length:width ratio $>2:1$). Lath shaped examples often have rows of perforations suggesting tracheid origin. The structure apparent at the edges of some of these particles, together with their 'splintery-shard' like nature was used by Batten (1973b,

1981, 1996) to suggest that they represent true charcoal, and are therefore equivalent to the coal maceral pyrofusinite. This cannot be entirely verified since their opaque nature precludes the observation of internal biostructure known to be typically preserved within this maceral type (Cope, 1981; Masran & Pocock, 1981; Sander & Gee, 1990). Nevertheless, it is here regarded as directly equivalent to the 'pyrocharcoal' of Masran & Pocock (1981).

Brown wood

Orange-brown to black with brown edges. Occasionally equant, but usually more elongate to irregular in shape. The majority of this material displays no discernible internal structure, and it is therefore interpreted as gelified woody tissue. Rarely it forms blocky masses with evidence of cellular structure (equivalent to the 'suberized phellem tissue' of Tyson, 1995: p. 354), but its lack of abundance does not warrant separate consideration here. The presence of variably oxidised (blackened) material suggests a complete gradation from brown to black wood, supporting the notion that the majority of Type 1 black wood observed here is equivalent to degradofusinite. It is at least in part equivalent to the 'brown wood' of Parry *et al.*, (1981) and 'Palynomaceral 1' of Whitaker (1984).

(Brown) Tracheids

Yellow to light brown particles with length-parallel dark brown to black striations. The lighter areas frequently bear bordered or simple pits. The darker striations are clearly thicker and represent 'triple junctions' with adjacent tracheids (Tyson, 1995). The particles are occasionally equant, but are usually elongate and lath-shaped. They are directly comparable to 'Palynomaceral 2' of Whitaker (1984). Tracheids combined with brown wood compose the 'lignified wood' of Staplin (1969), the 'bois ecorses vaisseaux' of Combaz (1980), and the 'brownwood' (*sic*) of Williams (1992). These two components also make up the coal maceral tellinite. Tracheids combined with

brown and black wood components make up the 'wood remains' of Van Bergen *et al.*, (1990).

Cuticle

Colourless to orange-brown sheet-like fragments typically less than 2 μm thick. Particles identified as cuticle always show cellular structure, which frequently includes stomata. Particles of this nature are extremely rare in the residues studied here, although the author has observed that where present the stomata are generally arranged in rows, suggesting derivation from gymnospermous plants (after Boulter & Riddick, 1986). This component is directly comparable to the 'cuticle' of most authors (Staplin, 1969; Combaz, 1980; Parry *et al.*, 1981; Van Bergen, 1990; Williams, 1992; Tyson, 1995; Batten, 1996), and 'Palynomaceral 3' of Whitaker (1984). It almost certainly corresponds to the 'leaf' component of Masran & Pocock (1981). It is also at least in part comparable to the coal maceral cutinite.

'Sheets'

Colourless to orange-brown sheet-like particles generally with no internal biostructure. Colourless sheets tend to be very thin (up to 1 μm thick) and are thus often crumpled in the residues. They also often reach relatively large size (up to 200 μm in diameter) and occasionally have a granulate appearance. The more deeply coloured sheets tend to be thicker (up to 3 μm) and occasionally curved or curled. The two types clearly represent different biological origins, but have not been separated because of the lack of observable biostructure. The colourless material appears to correspond with the 'transparent S.O.M.' of Van Bergen *et al.*, (1990) and possibly the 'unstructured membranes' of Highton *et al.*, (1991), although thicker particles might also be included in the latter. It is uncertain whether they represent phytoclasts or fragments of large marine algae. The thicker sheets may represent fragments of palynomorphs, particularly zoomorphs, and would thus be comparable with the 'zooclast' component of

Tyson (1995). They might also be comparable to the 'sheets' of Highton *et al.*, (1991), although the latter authors indicate a thicker (greater than 5 μm) nature to their component.

Palynomorphs

Sporomorphs

Spores

Yellow to brown sub-circular to triangular in outline, typically with a trilete mark. Megaspores and monoletes do not occur within the residues studied here, but are accepted as additional components of this group. This component is equivalent to the 'spores' category of Parry *et al.*, (1981), Van Bergen *et al.*, (1990) and Williams (1992).

Saccate pollen

Orange-brown bisaccate pollen grains, which are of gymnosperm origin. The component is directly comparable to the 'bisaccate' group of Parry *et al.*, (1981) and Van Bergen *et al.*, (1990), and the 'saccate sporomorphs' of Whitaker (1984).

Asaccate pollen

Includes the colourless to yellow gymnosperm circumpolle *Classopollis*. The tetrads frequently break up to leave isolated spheres, some thin walled examples of which may be mistaken for the 'simple sac' component, although most do show identifiable markings left from the adjacent pollen in the tetrad.

The asaccate component is therefore at least in part equivalent to the 'asaccate' group of Van Bergen *et al.*, (1990), and the 'pollen grains' of Parry *et al.*, (1981) The three sporomorph components together are comparable to the 'spores and pollen' *sensu*

lato of most authors (Staplin, 1969; Combaz, 1980; Masran & Pocock, 1981; Batten, 1996), and are equivalent to the coal maceral sporinite.

'Simple Sacs'

Colourless sub-spherical to ovoidal sacs. Two types are found in this study: small sub-spherical sacs between 30 and 60 μm in diameter, occasionally with a linear or equatorial rupture. These may represent phytoplankton cysts (most likely of simple acritarchs or dinoflagellates) or unornamented sporomorphs, possibly gymnosperm pollen (Harding, 1999, pers. commun.). The second variety are much larger, between 100 and 300 μm . The walls are usually thin and 'hyaline', but may have a fibrous to slightly granular appearance. They are of unknown origin, although it seems unlikely that such large fragile palynomorphs could have been transported from a terrestrial source. This grouping has not been dealt with directly in any of the citations given above, although in his key Whitaker (1984) placed a simple spherical object within his acritarch component. This was not discussed by Van der Zwan (1990) or Whitaker *et al.* (1992). However the term 'simple sacs' has been used previously by Harding & Allen (1995) in their study of the non-marine Wealden deposits. Only the smaller variety found in the present study is equivalent to the 'simple sacs' grouping of these authors.

Phytoplankton

Dinoflagellate cysts

Colourless to dark-brown resting cysts of dinoflagellates. This grouping is equivalent to the 'dinoflagellates' of Combaz (1980), Masran & Pocock (1981), Parry *et al.*, (1981), and Whitaker (1984), the 'dinocysts' of Williams (1992), and the 'dinoflagellate cysts' of Van Bergen *et al.*, (1990) and Batten (1996). In common with the key presented by Whitaker (1984), but here also recognised separately, the group has been further subdivided in recognition of the morphological variation within the group.

Figure 2.3a shows the simplest subdivision of the group into the three most widely recognised gross morphological categories: chorate, cavate, and proximate cysts. Figure 2.3b expands on this simple model, acknowledging intermediates between these main morphologies. In addition, dinoflagellate cysts can also be divided by paratabulation into the gonyaulacoid, ceratioid and peridinioid groups (Fig. 2.3c). These subdivisions follow numerous other studies relating to the distribution of modern and fossil dinoflagellates (see for example, Vozzhennikova, 1965; Downie & Sarjeant, 1966; Scull, 1966; Downie *et al.*, 1971; Harland, 1973; Riley, 1974; Sarjeant, 1982; Dale, 1983; Sarjeant *et al.*, 1987; Tyson, 1989; Farr, 1989; Powell *et al.*, 1990; Steffen & Gorin, 1993a).

Acritarchs

Colourless, thin walled, presumably algal cysts. The only type observed here are the spinose forms of the acanthomorph genus *Micrhystridium*. This component is at least partially equivalent to the 'acritarch' group of most authors, except Staplin (1969) and Tyson (1995) who did not separate these from their phytoplankton groupings. The acritarch and dinoflagellate cyst groups taken together are equivalent to the coal maceral lamalginite.

Prasinophytes

Colourless to orange-brown phycmata of prasinophyte algae. In the present study this category is further subdivided into two components:

Pterospermellids: colourless, thin-walled, sub-spherical phycmata with broad, usually crenulated equatorial flange or ala.

Tasmanitids: yellow to orange-brown thick walled spherical phycmata with randomly distributed pore canals. The distribution density of the pore canals is very variable. This group is directly comparable to the 'tasmanitids' of Parry *et al.*, (1981).

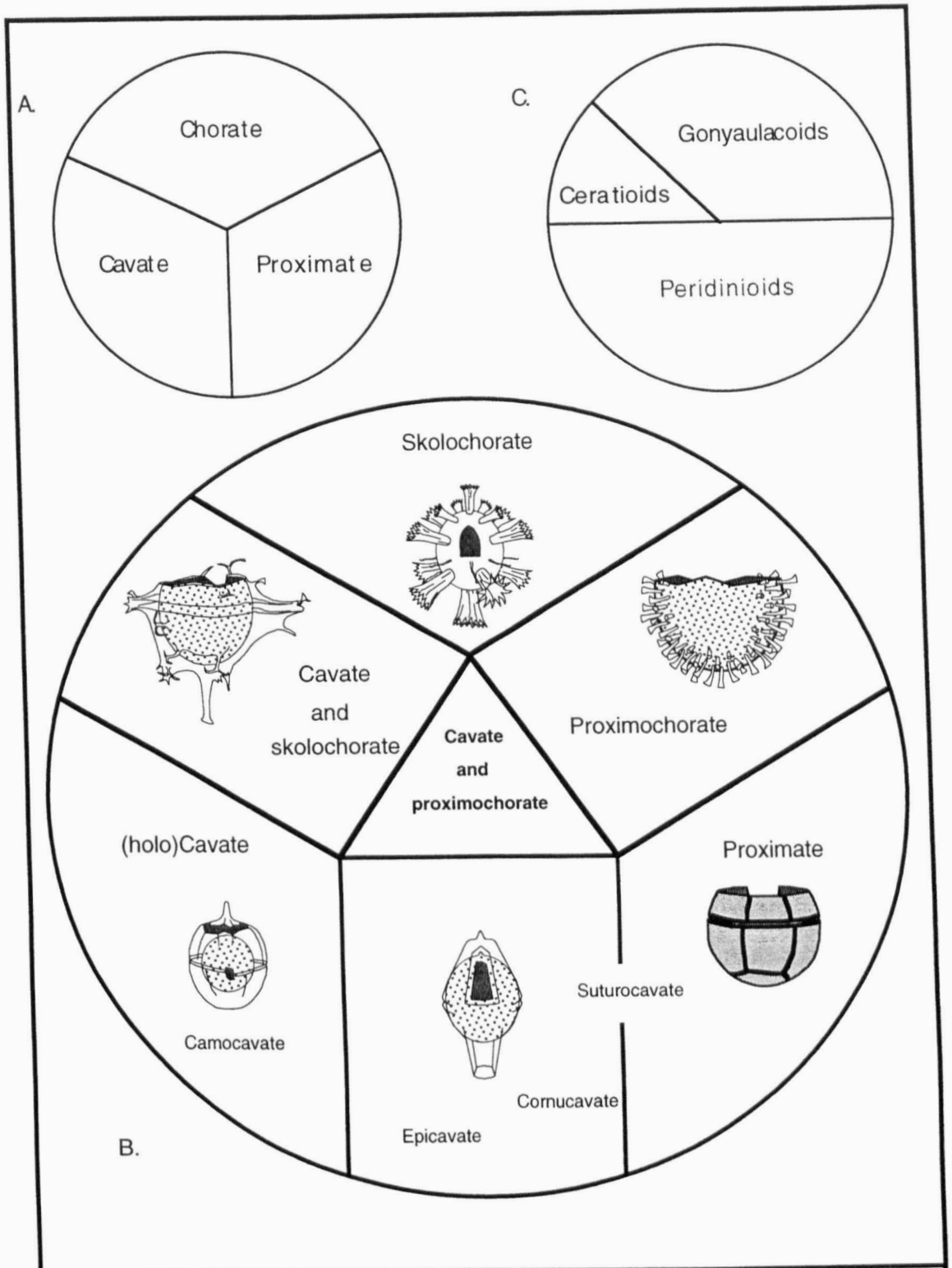


Figure 2.3: **A.** Idealised morphological separation of Jurassic-Cretaceous boundary dinoflagellate cysts into chorate, proximate and cavate categories. **B.** More detailed morphological division showing examples of each group. **C.** Separation of dinocysts into peridnioid, gonyaulacoid, and ceratioid groups.

The prasinophyte category as a whole is equivalent to the 'prasinophytes' of Van Bergen *et al.*, (1990) and the 'prasinophyte algae' of Batten (1996). The group also corresponds to the coal maceral telalginite.

The phytoplankton group taken together is equivalent to the 'marine phytoplankton' of Staplin (1969), the 'phytoplankton subgroup' of Tyson (1995), and the 'unicellular algae' of Van Bergen *et al.*, (1990), and in part equivalent to the 'marine palynomorphs' of Parry *et al.*, (1981).

Zoomorphs

Zoomorphs encountered in the present study fall into two groups.

Scolecodonts: described by Tyson (1995, p. 205) as the "(chitinous) mouth parts... of benthic polychaete annelid worms". They are usually dark brown in colour, and extremely rare in the residues observed here.

Microforams: chitinous linings of foraminifera. Typically orange-brown to dark brown and planispiral, although biserial and uniserial forms have also been noted, and in addition they occur as isolated (fragmentary) chambers. This group has been recognised by several of the authors cited above (see Figure 2.1). Following the work of De Vernal *et al.*, (1992), Tyson (1995) suggests that fossilised linings were largely, if not entirely produced by benthic foraminifera.

Unstructured organic particles

Resin

Yellow to reddish-brown blocky to globular translucent particles. Frequently heavily fractured. This component is extremely rare in the material studied here, but is

comparable with the 'resin' or 'resins' of most authors. It is also equivalent to the coal maceral resinite.

Amorphous organic matter (AOM)

Detailed study of the AOM fraction has not been undertaken here, but general observations provide the basis for this component to be split into three distinct types.

Type 1: usually grey, occasionally brown, fairly robust, irregularly shaped particles, with sharp to diffuse edges. Distinctly granulate, and typically contains a variety of inclusions from small globules to marine phytoplankton and occasionally Type 1 black wood. This is probably directly equivalent to the 'granuleuse' amorphous component of Combaz (1980), and at least in part to the typical 'AOM' of Tyson (1995), the 'AOMA' of Batten (1996), the 'sapropelic amorphous' and 'degraded sapropelic matter' components of Staplin (1969) and Williams (1992) respectively, and the 'structureless organic matter' of Whitaker (1984). Tyson (1995) equates 'AOM' with the coal maceral liptodetrinite, but it is probably also equivalent to the sapropelinite of Mukhopadhyay *et al.*, (1985). It is generally considered to be the product of algal decay (Tyson, 1995).

Type 2: fibrous grey 'whispy' particles. Either occurs as delicate isolated fragments or as 'shrouds' partly or completely obscuring marine algal palynomorphs. Probably poorly preserved equivalent of Type 2 AOM, and may indicate reworking. This is not considered to be directly equivalent to any other previously reported AOM type, but is probably included within the marine amorphous grouping of most authors.

Type 3: yellow to orange-brown robust but irregularly shaped particles with sharp edges. Occasionally some evidence of internal structure can be seen, which is probably of biological origin, although such indications are rare. More commonly the particles are homogenous to slightly fibrous in appearance. These have been shown to

fluoresce, and are probably bituminous. Thus there are probably two origins for this type, having been derived from both the degradation of woody plant and algal material. This component is probably partly equivalent to the 'gelifée' of Combaz (1980), the degraded portions of Whitaker's (1984) 'palynomacerals' 1 and 2, the 'yellow-amber amorphous' material of Masran & Pocock (1981), and in combination with resin, to the 'degraded humic matter' of Williams (1992). Similarly it is partly comparable to the 'humic gel' and 'pseudo-amorphous phytoclast' components of Tyson (1995).

2.3. Interpretation of palynologic matter components

2.3.1. Woody phytoclasts

Review of the palynofacies literature suggests that distinction between brown and black wood components, and of the two different types of black wood, have not always been made consistently. Several studies have combined black and oxidised (carbonised) brown wood (see, for example Whitaker *et al.*, 1992), often terming this group 'inertinite' (Habib & Miller, 1989). Few attempts have been made to distinguish between charcoal fragments and other opaque particles which might correspond to the maceral degrado-inertinite. Batten (1973b, 1981, 1996) has repeatedly suggested that black elongate fragments with 'pits' (which are clearly derived from tracheids) along with 'splintery shards' (probably of the same origin) "may commonly be identified as charcoal" (Batten, 1996 p. 1033). He does note, however, that minute particles are often impossible to separate (using only transmitted-light microscopy) from opaque wood oxidised at lower temperatures in soils or by reworking. Although it is not quite clear what he means by 'minute' within the present frame of study, one can presumably include within this internally 'inseparable' category, all opaque equidimensional particles which show no indication of biostructure. However, as will shortly be demonstrated, there appears to be some justification for the separation of equidimensional and lath-shaped particles, whether or not such separation reflects a generic difference between true charcoal and degrado-inertinite.

There appears to be a complete gradation from 'fresh', unoxidised but gelified woody tissues to 'black wood', and any distinction made between the two is thus in danger of being over-subjective and arbitrary. Several authors have suggested that following mild oxidation during palynological processing, some of the material which would otherwise have been treated as 'inertinite' is in fact revealed to be heavily carbonised brown wood (Batten, 1981, 1996). As Tyson (1995) suggested, it would seem that the only way to distinguish consistently between these two types is to include within the black wood category, only those particles which are completely opaque. One can then make note of the proportions of carbonised to 'fresh' brown wood, although any interpretations made using these subjective observations should only be used in conjunction with other information.

Most studies of 'opaque' particles or black wood from ancient sediments possibly include true charcoal, although disappointingly few reports attempt to make the distinction between this and woody material oxidised under 'normal' conditions (= degrado-fusinite, or 'degrado-charcoal' of Masran & Pocock, 1981). Generally speaking, there appears to be congruence between the distribution of woody palynological matter in modern and in ancient sediments, and they are therefore discussed together.

Despite the porous nature of true charcoal which potentially makes it highly buoyant (Whitaker, 1984; Sander & Gee, 1990), studies of the distribution of this component in modern marine environments suggest that it is extremely rare beyond coastal sediments (Herring, 1985). Small particles become water-logged more rapidly because of their high surface area:volume ratio (Davis, 1967), whereas 'larger' (macroscopic) particles which in theory can stay buoyant for longer periods, are more readily trapped or ponded in estuarine environments. Particles which are transported offshore are efficiently dispersed, and therefore occur in sediments with apparently lower frequency (Skolnick, 1958; cited in Tyson, 1995: p. 240).

Numerous studies have indicated that ancient coarse-grained sediments deposited within deltaic or estuarine environments also frequently contain high relative percentages of terrestrially derived 'opaque' material. Tyson (1995) noted that this has often been attributed to low buoyancy of this matter, in contrast to studies of modern charcoal. However, the comparatively higher density of ancient inertinite in comparison to associated vitrinite is difficult to interpret, since it doesn't necessarily indicate density at the time of deposition (Tyson, 1995). Therefore this apparent concentration in ancient sediments could indeed be a reflection of the factors affecting modern charcoal distribution as described above. It would appear though, that both pre- and post-depositional oxidisation can play a key role in the dominance of inertinite in these environments. High input of inertinite material supposedly oxidised in sub-aerial conditions and soil profiles (Tyson, 1995) has been noted in Jurassic fluvio-deltaic facies by numerous authors (Fisher, 1980; Dennison & Fowler, 1980; Batten, 1982; Nagy *et al.*, 1984; Van Bergen & Kerp, 1990; Oboh-Ikuenobe, 1992). A similar story has also been cited for distributary channel, levee, and proximal delta front facies (Parry *et al.*, 1981) as well as other near-shore and littoral areas (Bujak *et al.*, 1977; Manum & Thronsen, 1978; Claret *et al.*, 1981; Hellem *et al.*, 1986, Pocock *et al.*, 1988; Williams, 1992).

Whether this truly represents heightened production of 'inertinite-like' material under these conditions, the selective removal of less refractive organic matter (either by '*in situ*' oxidation/degradation or extended periods of reworking), or the reduced input of other terrestrial matter remains to be seen. For example, Smythe *et al.* (1992) indicate that substantial oxidation of woody phytoclast material occurs during transport, generating higher proportions of opaque material in the offshore delta facies. High inertinite contents attributed to reworking have also been noted from Late Carboniferous coal facies (Scheidt & Littke, 1989) and in glacial sediments (Ceratini *et al.*, 1983; Wrenn & Beckman, 1981). Additionally, Baird (1992) noted that concentrations of opaque material were apparent at unconformity or 'reworking' surfaces. Habib & Miller (1989) considered the sum of their "carbonised 'woody' remnants" from coastal plain

deposits to be 'recycled inertinite'. They attributed palynofacies dominated by this material (in this case apparently brown and black wood) as being formed in non-marine to coastal environments during marine regression, areas which additionally represented highly oxidising conditions. Furthermore, arid climate has also been suggested as a cause for high inertinite content in near-shore facies, where low rainfall and runoff contribute lower quantities of 'fresh' phytoclasts and clastic sediment generally, reducing the 'dilution' of organic matter, and allowing prolonged oxidation times (Taylor, 1981; Boltz *et al.*, 1981).

Conversely, numerous authors have documented a general distal increase in the relative abundance of 'black wood' within the phytoclast component (Summerhayes, 1987; Tyson, 1989). Boulter & Riddick (1986) and Powell (1990) noted the presence of this material in submarine fan channels, although there were higher proportions in inter-channel facies, where the sediment supply rate was lower. Study of recent fan facies (Mississippi area) by Marzi & Rullkötter (1986) showed a similar relationship, and Tyson (1995) noted that the reduced supply of 'fresh' phytoclasts in conjunction with buoyancy-related sorting affects were most likely responsible for this trend. Ceratini *et al.* (1983) have reported both coarse and fine 'opaque particles' in sediments from offshore Senegal. They suggested that the larger particles were redeposited from more 'proximal' areas via sub-marine canyons, whilst the fine material was wind-blown charcoal. Additionally Masran (1984) proposed that high relative abundance of oxidised phytoclast material, which he considered to be wind-blown charcoal and reworked woody debris (black and brown) characterised both slope and basin facies.

Reworking and subsequent re-deposition of woody material appears to play an important role in the formation of relatively inertinite-rich palynofacies, both in proximal and distal environments. This seems to be particularly true of transgressive facies, especially if depositional conditions remain oxic (Tyson, 1995), where reworked oxidised material from coastal sediments can dominate the assemblages (Smelror & Leereveld, 1989; Whitaker, 1984; Hellem *et al.*, 1986). Indeed, much of the opaque

matter of deep sea and distal sediments may be contributed from the reworking of more proximal facies. For example, Habib (1982) showed that palynofacies dominated by small equidimensional opaque particles were typical of deep-sea shales deposited during transgressive phases. Comparatively more proximal 'exinitic' facies contained larger opaque, and partially opaque phytoclasts, which had apparently been oxidised prior to redeposition and were thought to have been reworked from neritic or slope facies.

Studies of the distribution of brown wood and tracheid material occurring in modern sediments suggests that highest proportions of these components are also to be found in near-shore environments and/or sub-marine canyons (Cross *et al.*, 1966; Gross *et al.*, 1972; Ceratini *et al.*, 1979; Marzi & Rullkötter, 1986). Tyson (1995) noted that for ancient sediments, the scarcity of well quantified studies on the distribution of this group precludes detailed remarks, but that in general higher abundances of this material are noted from near-shore and redeposited sediments. Several studies of deeper marine facies show that positive fluctuations in the 'absolute' content of larger tracheidal material (albeit oxidised) can be correlated with phases of low sea-level (Habib, 1983; Firth, 1993). Tyson (1984) suggested that this may alternatively correspond to the increased frequency of turbidite deposition, although the two need not necessarily be mutually exclusive.

The separate assessment of brown and black wood components probably represents an unnecessarily artificial approach. For example, despite the apparent similarity in distribution of these two woody components, several studies show that increased black wood:brown wood ratio (or 'lability index' of van Waveren & Visscher, 1994) can be used to indicate more distal deposition (Summerhayes, 1987; Tyson, 1987; Smythe *et al.*, 1992). This measure has also been used (in conjunction with other aspects of the palynofacies) in the development or refinement of sequence stratigraphic frameworks (Gorin & Steffen, 1991; Tribollivard & Gorin, 1991; Steffen & Gorin, 1993a,b; Partington *et al.*, 1993; Cole & Harding, 1998) Studies of phytoclast relative abundance combined with assessment of the total organic carbon content (TOC) has been

used to indicate the absolute abundance of terrestrially derived organic matter (Tyson, 1989). The resultant PhytOC value has then been used to reflect relative proximal-distal trends by numerous authors (Tyson, 1989; Dybkjær, 1991; Scotchman, 1991; and Tuweni & Tyson, 1994). It should be noted that periodic reductions in terrestrial input (unrelated to sea-level) could also generate reduced PhytOC values.

In addition to the relative composition of the woody phytoclast material, the size and shape of the particles has also been considered (although the focus has traditionally been on black wood in this respect). From modern sediments, Caratini *et al.* (1983) used variations in maximum phytoclast size to reflect source-proximity in deep-marine sediments. They noted that a decrease in the maximum size from 500 to 5-20 microns was concomitant with a drop in the relative phytoclast abundance from 95% to 5% in an offshore direction. Similarly Nwachukwu & Barker (1985) showed that in the modern Orinoco Delta, large woody debris was concentrated in coarse-grained proximal sediments, and smaller (microscopic) material in more distal silt-grade deposits. This trend is also traceable in ancient sediments, particularly of the opaque particles, the size of which again decreases with increasing distance from the terrestrial source (Habib, 1982; Caratini *et al.*, 1983; Gorin & Monteil, 1990) whilst rounding and sorting of the particles is seen to increase (Denison & Fowler, 1980; Parry *et al.*, 1981; Tyson, 1987; Van der Zwan, 1990; Gorin & Steffen, 1991). Whilst Habib (1982) notes that deep sea inertinite material tends to be small and equidimensional, several other studies indicate a distal increase in the proportion of lath-shape particles (Parry *et al.*, 1981; Whitaker, 1984; Van Waveren, 1989; Gorin & Steffen, 1991; Oboh-Ikuenobe, 1992). Whitaker (1984) suggested that during transgressive, high energy phases, large equidimensional particles were absent, even from areas relatively proximal to source, presumably because of diminished supply and fragmentation during reworking (Tyson, 1995), whilst the proportion of lath shaped particles to equidimensional ones increased distally. This phenomenon has been interpreted as a relatively increased 'buoyancy' of the lath-shaped particles (Gorin & Steffen, 1991). However, Tyson (1995) notes that particle size plays a more influential role on hydrodynamic properties than shape: the

distal lath-shaped particles are usually smaller than their proximal equidimensional counterparts (Whitaker, 1984). Several studies have illustrated a proximal increase in the number of lath-shaped particles, where the elongate grains tend to be larger (Van der Zwan, 1990; Baird, 1992; Frank & Tyson, 1995). Hart (1986) and Tyson (1987) caution that bioturbation can also influence the breakdown of black wood ('inertinite').

2.3.2. Cuticle

Studies of both the modern and ancient distribution of cuticle debris in marine rocks suggest that it is most common in deltaic environments, particularly the delta front (Smythe *et al.*, 1992; Parry *et al.*, 1981) prodelta (Parry *et al.*, 1981; Nagy *et al.*, 1984), and general shoreline areas (Claret *et al.*, 1981;) with abundances decreasing basinwards (Muller, 1959). However, it has also been shown that this material can be exported to the deep sea via sub-marine channel systems (Cross *et al.*, 1966; Stanley, 1986), and in this environment is most abundant in and adjacent to the high energy parts of the sub-marine fans (Boulter & Riddick, 1986; Habib, 1982).

As an alternative to the addition of exotic marker grains, Tyson (1989) proposed the parameter PhytOC as an absolute abundance measurement of the gross phytoclast component. Relative percentage phytoclast particle abundance was thus multiplied by the Total Organic Carbon (TOC) content. Tyson (1989) was then able to demonstrate an intuitive trend between PhytOC content and areas with high influx of terrestrially derived sediment.

2.3.3. Sporomorphs

The data available on sporomorph distribution overwhelmingly show a decrease (often exponentially) in abundance with increasing distance from the terrestrial source (see for example, Hughes & Moody-Stuart, 1967; Darrel & Hart, 1970; Paproth & Streel, 1970; Reyre, 1973; Mudie, 1982; Heusser, 1983; Davies *et al.*, 1991). Modern studies

suggest that proximity to a river-mouth or delta source is more influential on high sporomorph content than proximity to a shoreline *per se* (Stanley, 1965; and the data of Cross *et al.*, 1966; Mudie, 1982). This is because the river transport of sporomorphs is much more prevalent than aeolian or wind transport (Muller, 1959; Mudie, 1982; Heusser, 1988; Clark, 1986). However their distribution is also strongly affected by hydrodynamic properties, and they tend to be concentrated in silty sediments (Muir, 1964) of medium to coarse grade (Cross *et al.*, 1966; Hughes & Moody-Stuart, 1967; Batten, 1974). Although sporomorph content in sandstones tends to be low (or at least lower than in sediments of siltstone grade) (Rossignol, 1961), there is often some correlation with coarser facies due to the generally larger grain size of sediments with fluvio-deltaic influence (Tyson, 1995). This grain-size effect, which presumably reflects energy levels, also has some control over the nature of the sporomorph content, with thin-walled pollen most common in siltstones (Muir, 1964) and thick-walled, often heavily ornamented spores being concentrated in the higher energy facies (Lund & Pederson, 1985; Mutterlose & Harding, 1987a, b; Dybkjær, 1991), although this may also be a sporomorph size effect (Tyson, 1995) rather than a morphological one. Despite common origin from a terrestrial source, there is often a complicated or even inverse relationship between the abundance of woody phytoclasts and sporomorphs as a result of this granulometric control (Courtinat, 1989; Reyre, 1973).

Although the absolute abundance of sporomorphs generally decreases offshore, it has been shown that they can be transported to the deep sea in sub-marine canyons and fans (Heusser, 1988, Habib & Drugg, 1987), turbidites (Manten, 1966; Groot *et al.*, 1967), or by redeposition during episodes of reduced sea-level (Habib, 1982; Tyson, 1995).

The trends observed in the distribution of bisaccate pollen often differ from those of non-saccate sporomorphs. Several studies show that the buoyancy of bisaccate pollen is much higher than that of non-saccate sporomorphs (Hopkins, 1950; Hughes & Moody-Stuart, 1967; Traverse, 1988), and that the amount of time bisaccates can stay

afloat is directly influenced by the size of the sacci (Hopkins, 1950). As a result the relative bisaccate:non-saccate ratio increases offshore, whilst 'absolute' abundance decreases (Cross *et al.*, 1966; Heusser & Balsam, 1977). Similarly, studies of ancient marine sediments suggest that saccate pollen are relatively less abundant than other sporomorphs in areas close to the terrestrial source (Reyre, 1973; Habib, 1979a; Mutterlose & Harding, 1987a, b; Barron, 1989; Prauss, 1989; Tyson, 1989; Tribollivard & Gorin, 1991).

Numerous studies have utilised the ratio of terrestrial to marine components ('T/M index') as an intuitive gauge of proximity to siliciclastic source and sea-level (van Waveren & Visscher, 1994; Cole & Harding, 1998)

2.3.4. Dinoflagellate cysts

Fossil organic-walled dinocysts are only known from dinoflagellates with a meroplanktonic lifestyle (Tyson, 1995), and it has been suggested that between only 7 and 10 percent of modern dinoflagellate species produce preservable cysts (Dale, 1976; Evitt, 1985). This picture is made more complex by the fact that some modern cyst-forming dinoflagellates produce a higher proportion of cysts than others (Dodge & Harland, 1991). For example, Dale (1976) found that in the Woods Hole area, some 50% of the motile *Protoceratium reticulatum*, and only 0.2% of *Gonyaulax digitalis* actually formed cysts. Moreover some environmental (particularly inner neritic) regimes appear to be conducive to higher percentages of cyst production (Dale, 1976, 1983). Typically, cysts are produced during seasonal disruption to water column stratification, and thus pelagic dinoflagellates only rarely produce preservable cysts. The presence of numerous dinocysts in deep marine sediments has therefore been used to indicate redeposition from adjacent shelves (Wall, 1971; Tyson, 1995).

Furthermore, dinoflagellate cysts are known to be strongly hydrographically and sedimentologically (granulometrically) sorted, potentially obscuring any relationship

with the distribution of the motile thecae (although see Blanco, 1995). They have been shown to be particularly concentrated in fine grained (silt to clay) sediments (Davey, 1970; Wall, 1971; Dale, 1976; Wall *et al.*, 1977; Rogers & Bremner, 1991), and 'depleted' in coarser (often inner neritic) sediments (White & Lewis, 1982), although sediment dilution effects may also play a part in this relationship (Wall *et al.*, 1977). The factors affecting the distribution of modern dinocyst thanatocoenoses were neatly summarised by Reid & Harland (1977) as being a combination of latitude, water depth (onshore-offshore differentiation), water mass (upwelling, convergence etc.) and sedimentary factors (selective concentration, siliciclastic dilution). Indeed, Harland (1983) noted that only rarely have cyst thanatocoenoses been linked to thecal biocoenoses. However, despite the complex and often obscure distribution relationship between the cysts and their 'parent' thecae, numerous studies show that generalised trends in dinocyst abundance, diversity, and morphology can be observed.

The work of Wall *et al.* (1977) shows that dinocyst diversity ('species richness') generally increases offshore (up to and including slope facies, see also; Muir & Sarjeant, 1978; Mutterlose & Harding, 1987; Lister & Batten, 1988; Van Pelt & Habib, 1988; Edwards, 1989; Habib & Miller, 1989; Smelror & Leereveld, 1989, Gorin & Steffen, 1991; Habib *et al.*, 1992; Hssaida & Morzadec-Kerfourn, 1993; Moshkovitz & Habib, 1993, Tyson, 1995: although see Masure, 1984; and Dodge & Harland, 1991). Nevertheless, several studies have shown that in some instances, peak diversity can be correlated with the onset of transgression rather than at times of maximum onlap (Habib *et al.*, 1992; Courtinat, 1993; Li & Habib, 1996). Moreover, diversity values tend to be tightly clustered onshore, but become increasingly variable towards the open ocean (Wall *et al.*, 1977). Blanco (1995) suggested that there was significant correlation between high dinocyst diversity and finer-grained sediments in the Recent deposits of offshore Spain. This suggests that diversity trends may be more accurately correlated with sediment grain-size rather than distance from a shoreline *per se*. However, salinity-stressed environments commonly found in near-shore or estuarine facies often exhibit dinocyst assemblages of low diversity-high dominance nature (Wall *et al.*, 1977;

Morzadec-Kerfourn, 1977; May, 1980; Piasecki, 1986; Goodman, 1987; Hunt, 1987; Lister & Batten, 1988; Andrews & Walton, 1990; Courtinat *et al.* 1991; Harding & Allen, 1995). Indeed, Hunt (1987) suggested that salinity might be the most important control on the distribution of dinoflagellate cysts. Nevertheless, high-dominance assemblages have been noted in areas of upwelling (Davey & Rogers, 1975; Fauconnier & Slansky, 1980; Honigstein *et al.*, 1989).

Taken alone, absolute dinocyst abundance is difficult to interpret consistently, as in addition to the factors mentioned above, it is increasingly influenced by terrigenous sediment influx in an onshore direction (Tyson, 1995). However, studies like those of Davey (1970), Davey & Rogers (1975), and Wall *et al.* (1977) suggest highest abundance 'near-shore', with a general decline towards the outer shelf and slope.

A more robust measurement involving dinocyst abundance is the dinocyst:sporomorph ratio (where the dinocyst abundance is 'normalised' against the sporomorph content, which has been repeatedly shown to decrease offshore or away from the terrestrial source). Intuitively, the ratio increases offshore (Muller, 1959; Williams & Sarjeant, 1967; Davey, 1970; Davey & Rogers, 1975; Manum, 1976; Mutterlose & Harding, 1987; Van Waveren, 1989; de Vernal & Giroux, 1991), and can be used to trace eustatic cycles (Mebradu, 1978; Habib, 1979a; Lister & Batten, 1988; Smelror & Leereveld, 1989).

Caution is required when using indices like those mentioned above, since their values are subject to accurate observations of 'in situ' as opposed to reworked specimens (cf. Tyson, 1995), and this together with high AOM content of deep sea sediments can lead to significant deviation from the 'expected' values (Tyson, 1995).

The relative proportions of peridinioid and gonyaulacoid cysts with the assemblages has also been considered. Typically, two measurements have been used: the 'gonyaulacacean ratio' of Harland (1973), which compares the number of gonyaulacoid to

peridinioid species; and the 'P/G ratio' Powell *et al.* (1990) which utilises the number of specimens of each group. Numerous studies show that restricted marine, often salinity-stressed regimes often have peridinioid-dominated assemblages (Downie *et al.*, 1971; Wang *et al.*, 1982; de Vernal & Giroux, 1991). In general though, the two measurements suggest that high peridinioid content is typical of 'onshore' assemblages, whilst relative gonyaulacoid abundance suggests more open marine conditions (see for example, Davey, 1970; Mutterlose & Harding, 1987; Lister & Batten, 1988; Courtinat, 1989; Habib & Miller, 1989). This trend can be obscured in areas of upwelling, where cyst assemblages are typically dominated by the peridinioid group (Wall *et al.*, 1977; Fauconnier & Slansky, 1980; Bujak, 1984; Rauscher *et al.*, 1986, 1990; Powell *et al.*, 1992). There is currently no evidence to suggest that ceratioid cysts can be recognised as a subgroup of the gonyaulacoids in terms of their distribution.

Studies of the distribution of the common cyst morphotypes are hampered to some extent by the fact that (holo)cavate and intratabular (skolo)chorate morphologies are not represented in modern floral assemblages (Tyson, 1995). Furthermore it is unclear whether the trends observed represent passive hydrodynamic sorting or *bona fide* morphological distribution of the cysts in response to ecological conditions (cf. Tyson, 1995). Nevertheless, there appears to be a general gradation from thick-walled and robust proximate cysts in near-shore facies to chorate cysts with delicate processes typical of more open oceanic (distal) environments (Vozzhennikova, 1965; Scull *et al.*, 1966; Davey, 1970; Riley, 1974; Davey & Rogers, 1975; Morzadec-Kerfourn, 1983; Sarjeant *et al.*, 1987; Tyson, 1985, 1989; Courtinat *et al.*, 1991; Tribollivard & Gorin, 1991; Hssaïda & Morzadec-Kerfourn, 1993; Sittler & Olivier-Pierre, 1994; Al-Ameri & Batten, 1997). Whilst this generally holds true on the scale of an onshore-offshore transect, wider geographical distribution seems to suggest the association of proximate forms with cold water (high latitude) areas, and the dominance of chorate morphologies in warmer water, lower latitudes (Davey, 1970; Davey & Rogers, 1975; Norris, 1978; Davies & Norris, 1980). It is unclear how much of this pattern reflects the association of peridinioid (typically proximate) forms with cold water upwelling systems (Tyson,

1995). However, Davies & Norris (1980) have suggested that Boreal dinocyst assemblages are dominated by proximate forms throughout the Jurassic. Suggestions that cavate morphologies are common to inner-neritic environments (Scott & Kidson, 1977) or colder waters (Courtinat, 1989; Courtinat *et al.*, 1991) are difficult to separate objectively from the observed peridinioid trends (Tyson, 1995).

Studies of dinocyst taxonomic composition for palaeoenvironmental interpretation need to eliminate stratigraphically-imposed (evolutionary) trends (Dimter & Smelror, 1990). To this end, several studies have combined like taxa into dinocyst groups (see Downie *et al.*, 1971; Brinkhuis & Zachariasse, 1988; Courtinat *et al.*, 1991; Courtinat, 1993; Brinkhuis, 1994; Wilpshaar & Leereveld, 1994; Li & Habib, 1996; Lamolda & Mao, 1999). In this respect two approaches have been used. Courtinat *et al.* (1991) analysed the dinocyst assemblages from the Cenomanian-Turonian anoxic event in France, and were able to discriminate several dinocyst associations. These they compared to the known palaeoenvironmental conditions, in particular to see if variations in water column oxygenation was reflected in the dinocyst assemblages.

In contrast, Wilpshaar & Leereveld (1994) constructed seven Early Cretaceous dinocyst groups by comparison with selected reports on the distribution of certain genera (see also Brinkhuis & Zachariasse, 1988, and Brinkhuis, 1994 for similar approaches). Thus each group was associated with a particular marine setting. They named each group after a representative genus: *Muderongia* Group; *Systematophora* Group; *Cribroperidinium* Group; *Circulodinium* group; *Oligosphaeridium* Group; *Spiniferites* Group; and *Pterodinium* Group (Wilpshaar & Leereveld, 1994: p. 124). The latter was considered analogous to the morphologically similar modern genus *Impagidinium*, and thereby interpreted as representative of open ocean conditions. Interestingly, they used the *Systematophora* Group as an indicator of inner neritic conditions, which contrasts with the expected skolochorate distribution noted above. Using these pre-defined groups, they were able to construct palaeobathymetric patterns

in the Valanginian-Cenomanian interval of the Vocontian Trough, although their observations were not tested against variation in lithology and other aspects of the palynological matter assemblages. Similarly Li & Habib (1996) used ratios of the Spiniferites and Cyclonephelium groups, taken as indicators of open-marine and near-shore conditions respectively, to track sea-level change at the Cenomanian-Turonian boundary.

2.3.5. Acritarchs

The majority of available information on the distribution of *Micrhystridium* and associated acanthomorph acritarchs, suggests a strong association between the abundance of this group and marginal marine or generally inner neritic conditions (Hughes & Moody-Stuart, 1967; Davey, 1970; Downie *et al.*, 1971; Burger, 1980; Erkman & Sarjeant, 1980; Dimter & Smelror, 1990; Kunz, 1990; Davies *et al.*, 1991; Al-Ameri & Batten, 1997; Cole & Harding, 1998). They occur in more offshore sediments, but are 'diluted' by the relative abundance of dinocysts further from the shoreline. They may also be abundant in AOM dominated deep-water assemblages (Habib, 1979a,b; Tyson, 1984). Tyson (1995) notes that accurate abundance observations of this group are strongly affected by sieving techniques since the acritarchs are often smaller than 20 μm .

2.3.6. Prasinophytes

Analyses of the distribution of the prasinophyte group focus (in terms of the taxa recognised in the present work) on the genus *Tasmanites*. Although several studies indicate an association with near-shore or brackish environments (Combaz, 1967; Prauss, 1989; Kunz, 1990), the majority of evidence suggests high relative abundance of this genus in organic-rich shales deposited in open-marine settings, often with anoxic bottom waters (Wall & Dale, 1974; Loh *et al.*, 1986; Tyson, 1989; Prauss *et al.*, 1991; Tyson & Pearson, 1991). Palaeoecological interpretations involving the occurrence of

pterospemellids are scarce, but Weller (1988) notes their association with marine as opposed to brackish conditions from Oligocene deposits. Conversely, Sittler & Olivier-Pierre (1994) note a strong association between the abundance of *Pterospermella* and proximate dinocysts, in an environment which they interpret as being restricted marine/brackish. In this case, the development of euxinic conditions within these same facies may have been a stronger influence on the prasinophyte abundance than proximity to the shoreline.

Neither group is particularly volumetrically abundant, and abundance peaks may be due to the relatively low siliciclastic input of pelagic environments (Tyson, 1995). Prasinophytes, and particularly *Tasmanites*, are also known to be concentrated at condensed horizons (Leckie *et al.*, 1990), common in cold waters and high latitudes (Prauss & Riegel, 1989; Peniguel *et al.*, 1989), and generally where other phytoplankton are scarce (Tappan, 1980). Batten (1996) suggests that euxinic conditions may have been more influential on the distribution of prasinophytes than temperature.

2.3.7. AOM

Autochthonous AOM is known to be most common in dysoxic or anoxic environments, classically the deep-sea (Dow & Pedersen, 1975; Venkatachala, 1981a; Bellet *et al.*, 1982), although its preservation is not necessarily dependant on anoxia (Calvert & Pedersen, 1992). Bujak *et al.* (1977) have shown that the relative proportion of AOM is generally low in shelf (neritic) facies, but increases offshore. It is also associated with fine-grained (organic-rich) sediments (Bellet, 1982; Ceratini *et al.*, 1983; Masran, 1984; Tyson, 1989; Nøhr-Hansen, 1989; Tribollivard & Gorin, 1991) characteristic of low-energy deposition. However, it can occur in a large variety of environments, providing that conditions are suitable for its preservation. Summerhayes (1983) and Powell *et al.* (1990) have noted that even neritic bioturbated sediments with generally low organic content can have AOM dominated palynofacies, although this is as much to do with the low input of phytoclast material as oxygen-poor conditions.

Furthermore, numerous authors have shown that AOM can often dominate palynofacies in carbonate environments, whether or not they are organic-rich (Reyre, 1973; Hunt; 1979).

Measurement of the abundance of AOM is problematic since it has a tendency to disaggregate into smaller particles during slide preparation. For this reason many reports have relied on visual estimation of AOM abundance rather than particle counts. Tyson (1984, 1989, 1993, 1995) on the other hand, has routinely counted AOM particles alongside other palynological matter components, preferring to count those particles which fall within the observed modal size range (Tyson, 1984). Such an approach allows relative quantification of the AOM abundance to be more directly comparable to other types of palynological matter, although the selected size range for observation is inherently subjective.

As an alternative to the addition of exotic marker grains, Tyson (1989) proposed the parameter AmexOC as an absolute abundance measurement of the marine palynomorph plus autochthonous AOM components. To generate this parameter, the relative percentage particle abundances were summed, and subsequently multiplied by the TOC content. The term is derived from 'amex', originally defined by Senftle *et al.* (1987)(Tyson, 1989) in relation to the areal percentage of the maceral equivalents of these two palynological matter components. Thus, strictly speaking AmexOC values can only be derived by accurate determination of the AOM prevalence, and thereby only with the use of UV light. Tyson (1989) demonstrated that the AmexOC parameter does not necessarily show opposing trends to PhytOC, since variation in primary productivity, degree of bioturbation and clastic sediment dilution all affect the abundance of marine components. Nevertheless, highest AmexOC values were recorded from sediments deposited in most distal facies of the Kimmeridge Clay Formation (Tyson, 1989).

CHAPTER 3. Methods.

3. Methods

3.1. Sample collection and processing:

3.1.1. Sample collection:

Of fundamental importance in the collection of samples for palynological analysis is selection of the least weathered or oxidised material available. In this respect sample collection from all of the study areas (the Volga Basin, Russia, and the Agadir Basin, Morocco, and the Río Argos, SE Spain) first required the removal, or 'trenching' of the exposed sediment surface. This has been shown to be effective not only in the maximisation of the palynological yield (Leereveld, 1997, pers. commun.), but also in the reduction of contamination by plant roots and contemporary palynomorphs (Funkhouser, 1969; Traverse, 1988; Wood *et al.*, 1996). The depth of surface-sediment removal was largely dependent on lithology as well as degree/length of surface exposure. At the Volga sections surface erosion is relatively rapid, and only the top 20 - 25 cm of sediment was removed prior to sample collection. Particularly friable lithologies (such as that immediately above the phosphorite deposit) are prone to more intensive weathering, and to compensate for this a thicker layer of surface sediment was removed before sampling. By contrast weathering at the Moroccan and Spanish localities was much more intense due (at least in part) to a much slower erosion rate. Here the removal of surface sediment was hampered by the greater abundance of hard marly - limestone lithologies less conducive to removal of surface material, although these are probably less prone to weathering. Samples from this type of lithology were taken from areas of no (or reduced) jointing/fracturing. Softer lithologies were trenched to a depth of 50 centimetres.

Discrete horizons and lithologies expected to be organic poor (e.g. recrystallised limestones, and friable clastic sediments with haematitic matrices) were avoided, thus obtaining a sample set with the maximum organic yield (hence, in theory, the most complete floral assemblage). This approach was preferred over maintaining a consistent sampling interval. The quantity of material collected was solely dependent on lithology.

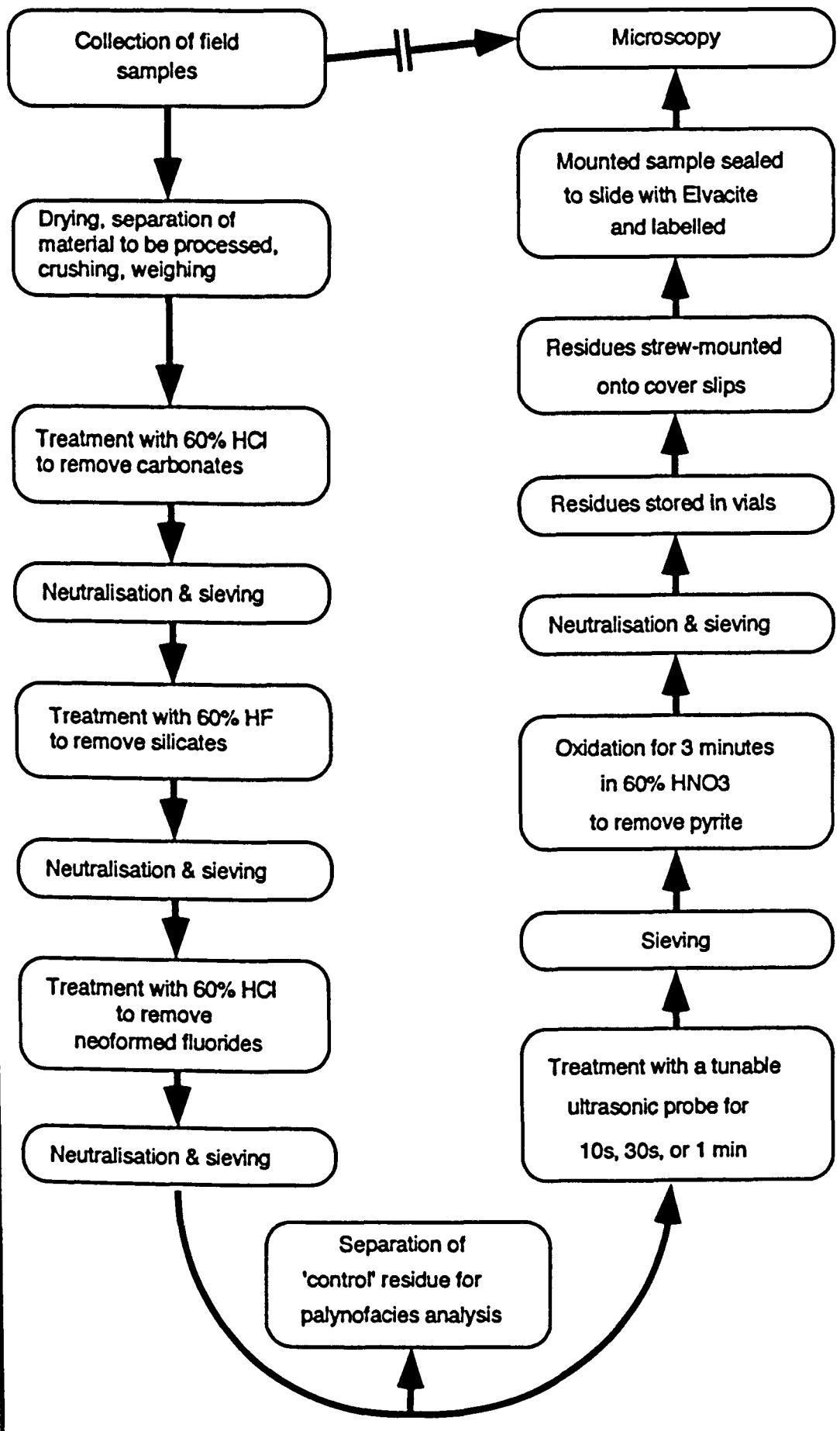
Between 50 and 100 grams were collected from the clayey-mudstone horizons and marls, whereas at least 300 grams were collected from the marly limestones and limestones proper.

3.1.2. Sample processing methods

In the majority of palynological studies the processing techniques employed are listed as being 'standard' or 'standard HCl-HF maceration'. However, review of several publications dealing specifically with this topic (Tyson, 1995; Wood *et al.*, 1996) suggests that although usage of HCl and HF in the removal of inorganic substances is commonplace, variations in the application of these reagents allows only limited value to be attached to the term 'standard'. For this reason the techniques applied in the current study are outlined below. A flow diagram representing the complete process can be seen in Figure 3.1, modified from Wood *et al.* (1996).

Each sample was allowed to dry, and the surfaces thoroughly cleaned, any oxidised 'crusts' (common on the limestones) being removed. The material was then split, and the portion to be used subsequently crushed to 2 - 3 mm sized fragments and weighed. Samples were treated with 58 - 62% hydrochloric acid to remove carbonates, and spiked with tablets containing *Lycopodium clavator* spores. After neutralisation, they were further treated with 58 - 62% hydrofluoric acid to remove silicates and reneutralised. Each was then boiled in 58 - 62% hydrochloric acid for 1 minute to remove neoformed fluorides, and neutralised a third time. Wet strew-mounts of the residues were made to determine whether breakdown of amorphous organic matter (AOM) using a tuneable ultrasonic probe was required, and a small amount of each was separated and kept as a 'control' residue for certain aspects of the palynofacies analysis. Depending on the amount and type of AOM, the residues were variously treated with 10 seconds, 30 seconds or 1 minute's vibration with the probe, and then sieved. In order to remove pyrite and generally 'clean' the residues, each was treated with 60% nitric acid for 3 minutes, and reneutralised for the final time. After each neutralisation stage and following the use of the ultrasonic probe, all residues were sieved using a 20 μm

Figure 3.1: Palynological processing procedure



nylon mesh. Finally each residue was mounted onto two glass slides (hereafter referred to as the 'slide-pair') using Elvacite[®](Dupont), labelled, and subsequently scanned using an Olympus BH-2 stereo-binocular microscope.

3.1.3. Choice of sieve apparatus

A variety of sieving media are available for use in palynological laboratories (Wood *et al.*, 1996). Ediger (1986) noted that of the tools available, the most commonly used and most effective include metal screens with perforations calibrated down to 5 μm (Kidson & Williams 1969); ordinary or borosilicate filter papers; and nylon boulding cloth with mesh size available down to 2 μm (Mid-Anglia Engineering Ltd, 1995: pers. commun.).

Nylon mesh was selected for the current study, since it is relatively inexpensive in comparison to the metal screens, acid resistant, and in contrast to filter papers, does not contaminate the residue with fibres (Ediger 1986). Meshes were mounted in specially tailored pieces of polyethylene guttering or Tupperware[®], which provided robust and acid-resistant frames. The boulding cloth was fixed in place with plastic rings in a manner which provided a water-tight seal, but allowed the mesh to be readily removed between sievings for thorough washing.

A known drawback of boulding cloth is that with extensive use, the mesh distorts and pore sizes can become enlarged or irregular (Ediger 1986). This problem was minimised by replacing the cloth at regular intervals. Both 10 and 20 μm meshes were initially tested, but the former were found to clog up too rapidly when AOM-rich samples were being processed. For the sake of consistency, the 20 μm mesh was used for all samples, with the acknowledgement that finer palynologic matter will have been lost.

3.1.4. The use of *Lycopodium clavator* spore spikes

Methods for determining the absolute abundance of palynologic particles (typically palynomorphs), and statistical considerations accompanying these methods have been presented by numerous authors (see for example, Stockmarr, 1971, 1972; Bonny, 1972; Maher, 1981; de Vernal *et al.*, 1987; White, 1988). In this study, Stockmarr's (1971) method of adding tablets containing exotic *Lycopodium clavator* spores was deemed most suitable. The tablets were supplied by the University of Lund, batch number 124961, containing $12,542 \pm 3.3\%$ spores per tablet (Berglund & Persson, 1994). Once the residues were analysed, the equation in Figure 3.2a was used to calculate the absolute frequency of the various components. The precision by which these abundances can be calculated depends on several factors. Firstly, it assumes that the exotic spores are evenly distributed within the residue: for this reason the tablets are added at the beginning of the processing procedure so that the numerous phases of sieving allow the *Lycopodium* to be uniformly mixed. Secondly, it assumes that the exotic spores counted are in no way confused with specimens of *Lycopodium* native to the residue in question. To prevent this, the exotic spores were acetolysed by the manufacturers during tablet production, giving them a distinctive golden-orange colour. A separate slide was made solely strewn with *Lycopodium clavator* spores so that they could be readily recognised within the residues.

As with any random sample of a population, there are statistical errors associated with absolute analyses, and these typically decrease with increasing count size (including the number of exotic spores as well as of the particles targeted for analysis). This is clearly displayed in Figure 3.2b, redrawn from Stockmarr (1971, p. 620). It is important to note here, that the standard errors generated using exotic spores are always higher than those on the particle counts alone. Moreover, although the total errors decrease with increasing count-size, the proportion of error contributed by the use of *Lycopodium* becomes greater. Clearly, for results with minimum error attached, the counts need to be as large as possible, and ideally the ratio of exotic spores:target

Figure 3.2a: Calculation of absolute particle abundance with the use of exotic *Lycopodium* grains

$$\frac{\text{Number of } Lycopodium \text{ spores in 300 count}}{\text{Number of } Lycopodium \text{ spores added / no. grams sediment}} = X,$$

$$\frac{\text{Count for each category}}{X} = \text{amount/g of sediment.}$$

Figure 3.2b: Estimated error on absolute particle abundance.

(Redrawn from Stockmarr, 1971, p. 620)

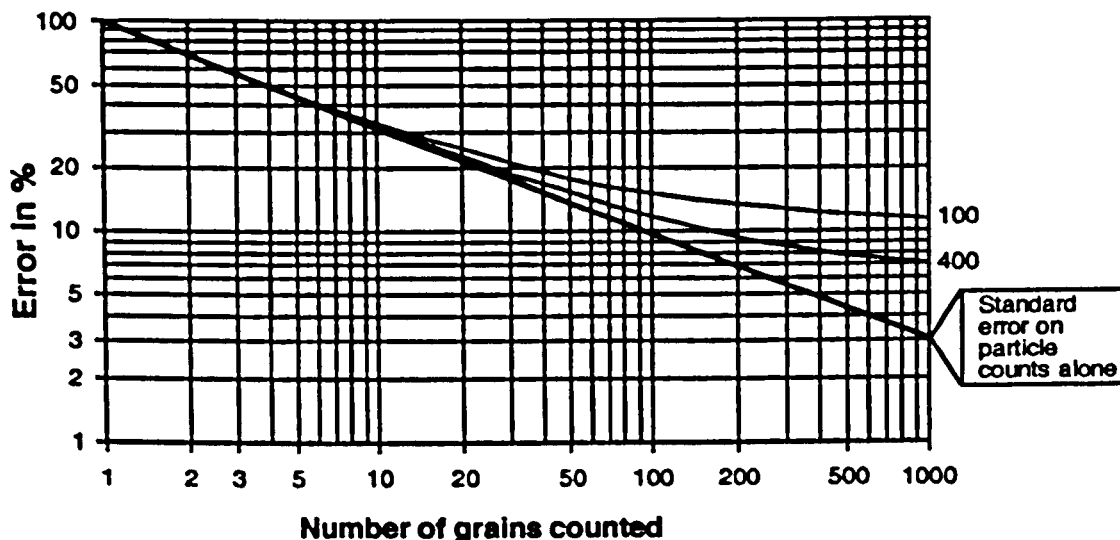


Figure 3.2c: Calculation of estimated error on absolute particle abundance.

$$\text{Estimated error} = 100 \sqrt{\left(\frac{A^1}{A}\right)^2 + \left(\frac{B^1}{B}\right)^2 + \left(\frac{C^1}{C}\right)^2}$$

A = Mean of *Lycopodium* spores in 1 tablet x number of tablets added.

A¹ = Standard error on A.. Given by tablet manufacturers

B = Number of object particles counted

B¹ = Standard error on B. Calculated by B¹ = √B

C = Number of *Lycopodium* spores counted

C¹ = Standard error on C. Calculated by C¹ = √C

particles consistent across the sample suite. In practice the latter is extremely difficult to achieve since the eventual yield of organic matter from each sample is only known when processing is complete. Samples of apparently identical lithology can yield significantly different amounts (and types) of organic matter. To minimise this problem, a small amount of each of the major lithologies was pre-processed to gauge the respective yield, and the number of spore tablets added to the final samples varied accordingly.

The standard error for each absolute abundance can be calculated using the equation in Figure 3.2c, taking into account the error on the number of exotic grains added, the number counted, and the number of target particles counted.

3.2. Analytical methods

3.2.1. Methods employed in the biostratigraphic analysis

In determination of the dinocyst biostratigraphy, all the specimens encountered in the slide-pair were considered. Realistically however, only those specimens representing $\geq 60\%$ of an individual could be identified to species level with any certainty (although operculae can sometimes be useful). In several instances specimens could not be identified from the literature, even when well preserved, and in this event they were assigned to a genus and given an upper-case Roman letter to differentiate the taxon from others of the same genus (for example; *Gonyaulacysta* sp. A). Taxa appearing as 'one-offs' were not used in the formulation of range charts or zonation. Several genera appear to exhibit a large degree of intraspecific morphological variation, and where this is particularly pronounced (but not strong enough to warrant inclusion within a second species), the specimens/taxa were assigned as being of close specific affinity to more standard taxa (for example; *Gochteodinia* cf. *G. villosa*). Several cyst morphologies proved difficult to speculate, typically simple sub-spherical proximate forms, and chorate cysts bearing variable numbers of non-tabular, needle-like processes. These have been assigned into 'groups' with species name being morphologically

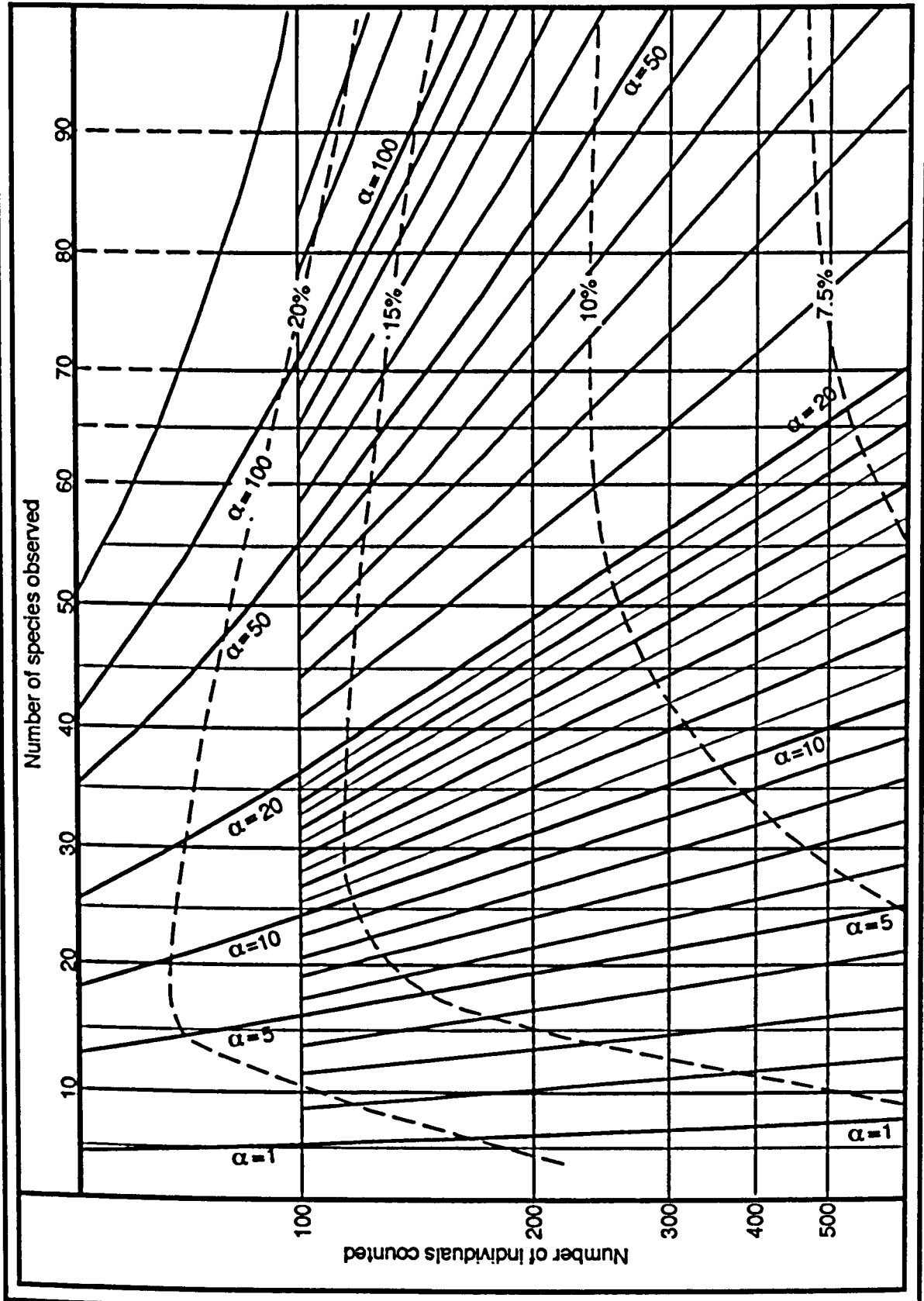
representative. Thus simple unidentified proximate cysts were termed "*Batiacasphaera fenestrata*" or "*Circulodinium ciliatum*", and the chorates were grouped into "*Cleistosphaeridium aciculum*". Since these groups probably contain several different biological taxa, they are not used in construction of the biostratigraphy. The range charts and abundance data are combined, and taxa denoted as '0' (zero) for particular samples were encountered outside the 300 target described below.

3.2.2. Methods used in relative taxonomic abundance, diversity and dominance analyses

The first 300 dinocyst specimens encountered when scanning the slide-pair of each sample were incorporated into this study. A 'constant' target is preferable since Wall *et al.* (1977) note that dinocyst diversity increases with count size. The 300 target was chosen as it has previously been shown to generate statistically significant results. Moreover, Dean (1998) notes that a target of only 200 is standard in pollen analysis, and has previously been shown to include 70% to 85% of the taxa present (Martin, 1963). Where possible, broken and fragmentary specimens were identified: operculae and specimens representing less than 60% of an individual were not included within the 300 count. Frequently, particularly in the AOM-rich residues, some dinoflagellate cyst taxa were too poorly preserved to allow confident identification, and individual specimens then grouped as indeterminate chorate, cavate, or proximate. Acritarch and prasinophyte taxa, as well as forms attributed to the (?multi-taxonomic) grouping 'sacs' were also included in this count. A point-counter was not available for this study, thus the actual count frequently surpassed 300. It is therefore necessary to consider the values in terms of relative percentages.

Similarly, dinocyst diversity cannot here be meaningfully quantified by the number of taxa in the '300' count, although numerous other studies have adopted this approach (Manum, 1976; Goodman, 1979; Mutterlose & Harding, 1987a, b; Habib & Miller, 1989; Dimter & Smelror, 1990; Courtinat *et al.*, 1991; Dodge & Harland, 1991;

Figure 3.3: Fisher α diversity chart; redrawn from Fisher (1943: p. 52)



PAGE
NUMBERING
AS ORIGINAL

Figure 3.4: Calculation of PhytOC and AmexOC values

$$\text{PhytOC} = \left(\frac{\text{Number of phytoclast particles counted}}{\text{Total number of particles counted}} \right) \times \text{TOC}$$

$$\text{AmexOC} = \left(\frac{\left(\text{Number of AOM particles counted} \right) + \left(\text{Number of marine palynomorphs counted} \right)}{\text{Total number of particles counted}} \right) \times \text{TOC}$$

therefore consistent with the counts for other particles, for which the <20 μ m fraction was removed during processing. Such methodology accords with the comments of Tyson (1984) that smaller particles are of little volumetric significance, and is comparable to that author's counting strategy.

It has previously been suggested that mild oxidation of the woody phytoclasts can lead to more accurate distinction between brown and black wood categories (Batten, 1981, 1996). Furthermore, the AOM-rich nature of many of the residues precluded clear observation of the other organic particle categories. For these reasons, analyses of the structured components were undertaken on the portion of the residues subjected to ultrasonic treatment and/or oxidation. All the categories of palynologic matter outlined in Chapter 2.2. were considered within the 500 count. Absolute abundance analysis was undertaken at the same time as the relative analysis, although counting continued until 50 exotic *Lycopodium clavator* spores had been encountered. In some samples this value was exceeded during the relative abundance counts. Occasionally, particularly in the AOM-rich facies, the slide-pair was completely scanned before the 50 target was achieved.

Where possible, 100 particles of brown and black wood were measured from each sample, and for each particle a 'roundness value' attached. The subjective roundness value of a particle is taken as a whole integer range from 1 to 6, where 1 represents very angular, and 6 well rounded, and is separate from assessments of particle geometry. The sum of the value for the two particle types is then divided by the number of particles (of each type) measured, to give the mean roundness, or roundness index (RI) for each sample. For this exercise, tracheids and 'gelified' woody tissues have been combined within the brown wood category (although the two components continued to be distinguished), and both types of 'inertinite' *sensu lato* were included within the black wood category.

3.2.4. Methods employed in the total organic carbon (TOC) analysis

Sample preparation

Approximately two grams of each sample was powdered using an agate pestle and mortar, one half of each being placed into vials ready for total carbon analysis. The remaining halves were transferred into 400ml beakers and immersed in 60% analytical grade HCl for 24 hours in order to remove mineral carbonate. The acid was siphoned-off using a large syringe and the samples passed through a phase of dilution and settling (using MilliQ water) until 'neutral'. Samples were then placed in aluminium foil 'boats' and set on a hot-plate until completely dry (no further weight loss observed). Since this process frequently resulted in the formation of fused fragments, each was again crushed using the pestle & mortar.

TOC content

This part of the analysis was done using the Carlo Erba EA1108 elemental analyser of the School of Ocean & Earth Science, Southampton University. Approximately 3 mg of both acid-treated and untreated samples was placed in 5 by 3.5 mm tin capsules and sealed. These were then set in the elemental analyser, run at 1200 °C, and combusted using flash pyrolysis at 1500 °C. The accuracy of analyses was verified after every six samples by running a capsule containing a Sulphanilamide Standard (41.88 weight % carbon). The machine was recalibrated if the analysis of the standard deviated by more than 0.2%.

Once the samples were run, the analyses gave two values. A total carbon value is returned on the samples which were not acid treated, including a carbon fraction derived from mineral carbonate. The acid-treated samples give adjusted carbon values, since the mineral carbonate has been removed. However, where sediments were originally carbonate-rich, carbonate removal creates a significant sediment weight reduction,

Figure 3.5: Calculation of TOC by combining acid-treated and untreated values

$$\text{TOC} = 100 \left(\frac{\left(\frac{8.3317 \times \text{Total carbon}}{100} \right)^{-1}}{8.3317 - \left(\frac{100}{\text{Acidified carbon}} \right)} \right)$$

artificially inflating the apparent organic carbon content. Both values must therefore be combined using the equation in Figure 3.5 to give the actual TOC content.

3.2.5. Preparation of materials for the scanning electron microscope (SEM)

SEM work undertaken in the current project is limited, and specimens required for examination were individually picked. Wet strews of target residues were made, and specimens isolated using a micropipette (drawn out from a normal glass pipette over a hot Bunsen flame). These were transferred onto squares of developed photographic film which had been scored at millimetre intervals to form a location grid. Each specimen was then oriented using a single eyebrow hair mounted into the end of a micropipette. When complete, the film squares were glued onto SEM stubs, and coated with gold using a Bio-Rad Microscience Division SC650 sputter coater, and subsequently placed in stub-boxes to await analysis.

3.2.6. The use of cluster analysis

Cluster analysis of palynofacies data presented in Chapter 5 was undertaken using MVSP[®] (multi-variate statistical package) version 3.0, run on a Toshiba T1950CS laptop under Windows 3.1.

There are numerous cluster analysis techniques available, each of which uses a different algorithm to produce the clustering. The agglomerative hierarchical clustering technique is used in MVSP[®], and produces a dendrogram where the most similar cases are clustered closely together. There are several methods by which similarity can be calculated, and similarly several parameters which can be used in such measurements. The choice of methods used in the current study was influenced by the investigation of such techniques by Kovach (1989) and Kovach & Batten (1994), who found that both the

unweighted pair group average method (UPGMA) using the Spearman rank-order correlation coefficient, and the minimum variance method (which implicitly uses squared Euclidean distance) were the most effective techniques in discriminating palaeoecological trends.

In UPGMA analysis, the distance between each pair of points in two clusters is measured, and the mean distance is used as the 'similarity' of the clusters. This is demonstrated in Figure 3.6a. The clusters are unweighted, so each set of points is treated equally. This means that no preference is given to sets of data with fewer points, and therefore the clustering is less likely to be affected by variation in the least abundant (and therefore statistically less significant) categories. The Spearman rank-order coefficient was used to measure distance between points and clusters since it is non-metric similarity measure, and therefore not as strongly affected by taphonomically or stochastically induced noise in the data (Kovach, 1989). This coefficient has also been used to good effect in several other studies of plant palaeoecology (Farley & Dilcher, 1986; Kovach, 1988).

Minimum variance cluster analysis takes a different approach to the way in which groups of data are clustered. Here, the within-group variance is calculated by taking the sum of the squared (Euclidean) distances from each point in a cluster to the centroid of that cluster (solid lines in Figure 3.6b). Then, for the most similar pair of clusters (those that will give least increase of within-group variance, usually with the most closely adjacent centroids, a combined centroid is calculated, and the variance (or distance) of each point of the two clusters to this combined centroid is determined (dotted lines, Fig. 3.6c). This is then treated as one cluster, and will appear as the most closely grouped cluster on the resulting dendrogram. The process is repeated until all of the samples/clusters have been grouped (Fig. 3.6d). Minimum variance cluster analysis (otherwise known as Ward's method) has also been used by Kovach (1988) in relation to actual count data (as opposed to percentages) in plant palaeoecology, and by Hunt (1987) on marine palynomorph data. Similarly Kovach & Batten (1994) used this

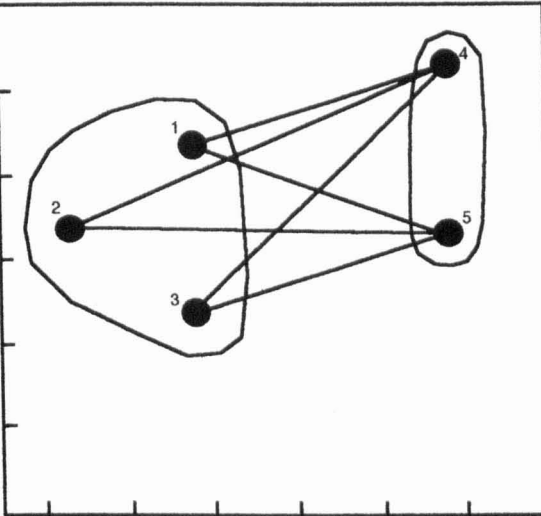


Figure 3.6a: Example of UPGMA cluster analysis. The distance between each pair of points is calculated, followed by the mean distance for each group.

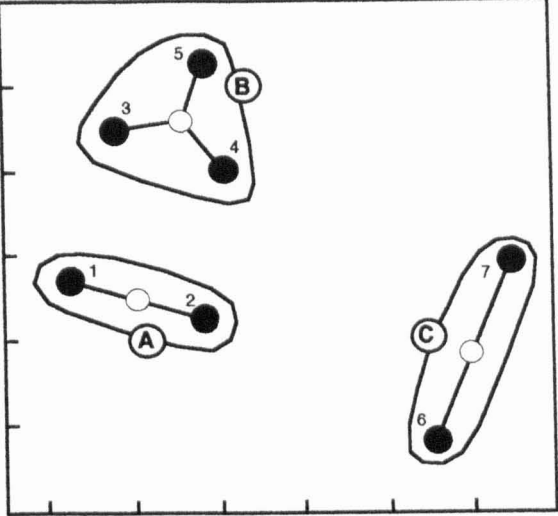


Figure 3.6b: Example of minimum variance cluster analysis. Most closely adjacent points are clustered, and the centroid for each group calculated. The within-group variance is then determined for each cluster.

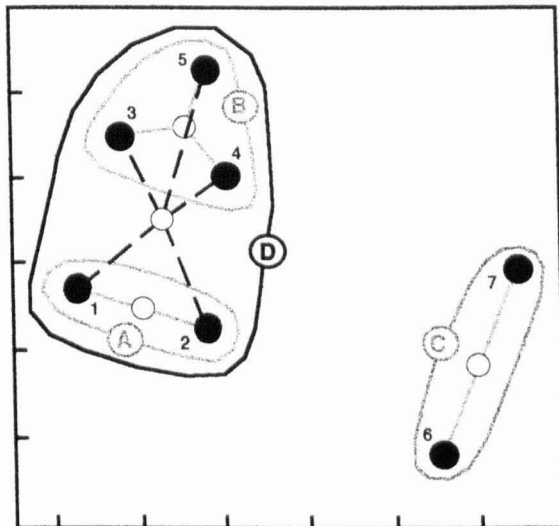


Figure 3.6c: Most closely adjacent clusters are grouped. The centroid, and within-group variance are then calculated for each combined cluster. Clusters combined at this level are thereafter considered as individual clusters (ie A & B are combined in cluster D).

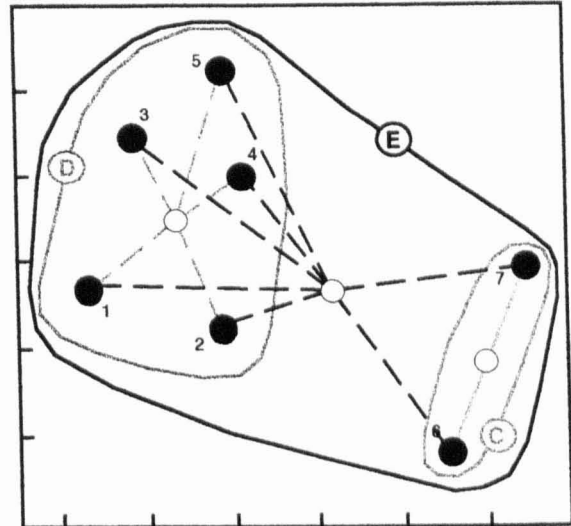


Figure 3.6d: This process is continued until all the clusters and points are combined into a single cluster (E).

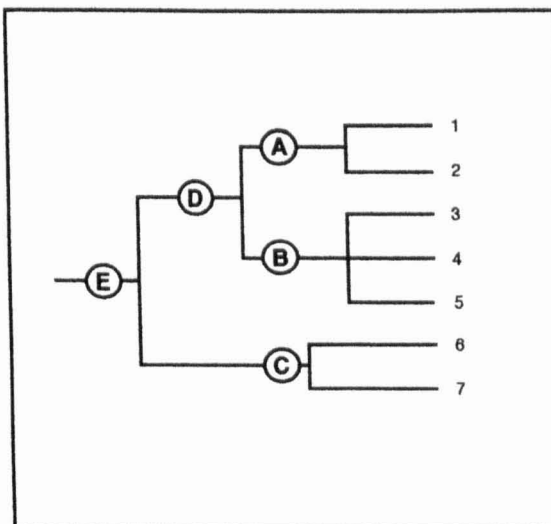


Figure 3.6e: Dendrogram produced by minimum variance cluster analysis of the data distribution presented above.

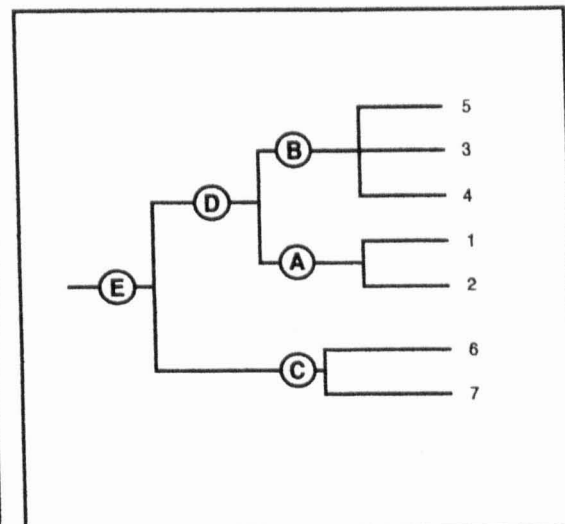


Figure 3.6f: A second dendrogram produced by cluster analysis of the same data distribution as 3.6e. The clustering is identical despite variation in the order of points.

technique to re-analyse various data sets containing a variety of palynological information.

Dendrograms produced from minimum variance cluster analysis of the data point distribution in Figures 3.6b-d are presented in Figures 3.6e & f. For the purposes of cluster analysis, these two dendrograms are identical: only the branching order, and the length of the branches are important, the order of points on the right of the diagram is immaterial. Indeed, the length of the branches is only important when one wishes to compare the level of correspondance of two data sets using the same clustering technique.

3.3. Testing the processing procedure: effects of nitric acid oxidation and ultrasonic vibration on the palynologic matter assemblages.

3.3.1. Rationale and technique

The variable abundance of AOM in the present study forced some degree of flexibility in the length of ultrasonic vibration required to generate sufficiently 'clean' residues for structured particle analysis. In view of the fact that such treatment clearly alters the organic matter assemblage (at least the proportion of AOM), it was deemed appropriate to test its affect on the structured components. As has been pointed out above, there have been suggestions that the nature of woody phytoclast material can be altered during oxidation. Furthermore, Funkhouser & Evitt (1959) suggested that oxidation was particularly damaging to palynomorphs. It was therefore important to assess such effects with regard to the current procedures employed.

Initial review of the palynologic matter assemblages suggested that there were five dominant palynofacies in the Volga Basin material, and one sample from each type was selected for experimental analysis. Residues were processed in the manner described

above up to, but not including the ultrasonic stage. Prior to this, the residues were homogenised by being shaken, and split into three parts. One part was kept as a control, the other two were subjected to either 30 seconds or 1 minute, and three minutes sonification respectively. The decision between 30 seconds and 1 minute was based on the length of time used processing residues for the main analyses, and thereby dependant on the abundance of AOM. Experimental residues U2 and K25 were thus subjected to only 30 seconds of ultrasonic vibration. After treatment the samples were washed through a 20 μ m sieve to remove newly fragmented material.

Next, both the control and the ultrasonic-treated residues were split into three parts after re-homogenisation. The first of these was again kept as a control, the other two subjected to 5 minutes and 10 minutes nitric acid oxidation respectively. The residues were then neutralised and again sieved using a 20 μ m mesh. Finally individual slides were made from each of the experimental preparations, and cover-slips mounted using Elvacite(DuPont).

Counts were performed in the same manner as described above, and AOM was counted alongside the structured particles, not included within the 300 target. The percentage abundances of AOM (shown in Table 3.1 and Figure 3.7) are therefore drawn from the addition of the AOM and structured particle counts.

3.3.2. Effect of processing procedure on the major components of palynologic matter

AOM

Analysis of the data suggests that ultrasonic vibration was a more effective mechanism for disaggregating AOM in AOM-rich sediments than nitric acid oxidation. Diagrammatic representation of the AOM reduction using these methods can be seen in

Figure 12 drawn from the data in Table 3.1 (note that the dinocyst abundance data also shown on these graphs is generated from the 300 structured-grain count, not including AOM). An approximately 10% (U2) to 20% (K25) reduction in the relative abundance of AOM can be seen between the untreated residue and that exposed to 30s of ultrasonic vibration, which equates to an approximate 50% drop in the number of AOM particles observed during the 300 count of structured particles (Table 3.1). The discrepancy between these figures is a reflection of AOM dominance in these particular residues. Surprisingly, there was no such clear-cut reduction between the residues treated with 30s and those with 3 minutes, some values suggesting a slight increase. Such data indicate that AOM reduction took place much more slowly between 30s and 3 minutes than in the first 30 seconds of sonification (Table 3.1). Higher AOM relative abundance in 3-minute treated residues than those treated for 30 seconds appears to be a reflection of decreasing dinocyst abundance.

The effect of oxidation on the AOM content is generally less distinct, although in the unsonified preparations an overall decrease can generally be seen. It would seem that variation in the relative abundance of this material in oxidised residues is a reflection of the changes induced on the structured components.

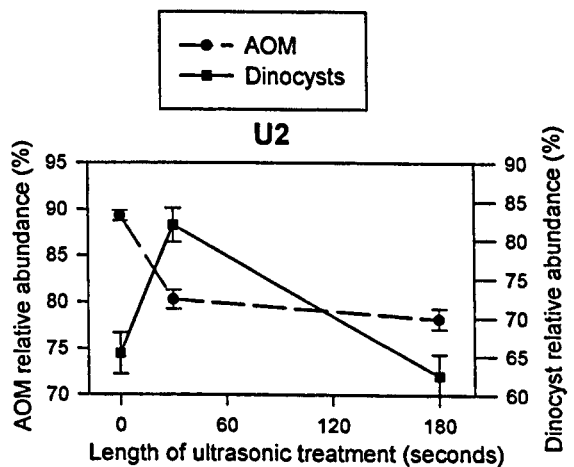
Ultrasonic vibration of extremely AOM-poor residues (K17 & K19) seems to have had little effect when treated for up to 1 minute, but the relative abundance shows a marked increase in those treated for 3 minutes, especially so in residues exposed to maximum oxidation time (Table 3.1). This appears to be the result of significant reduction in the amounts of certain structured particle types. No AOM was observed in any of the experimental preparations from sample K28.

Dinocysts

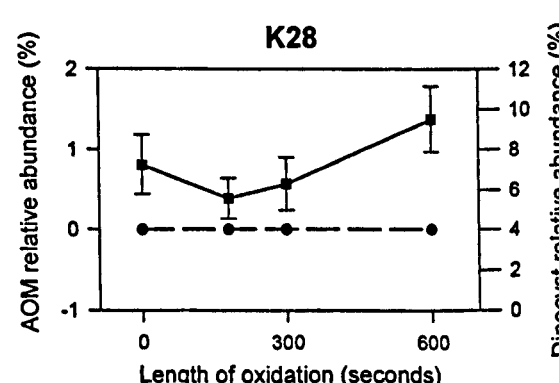
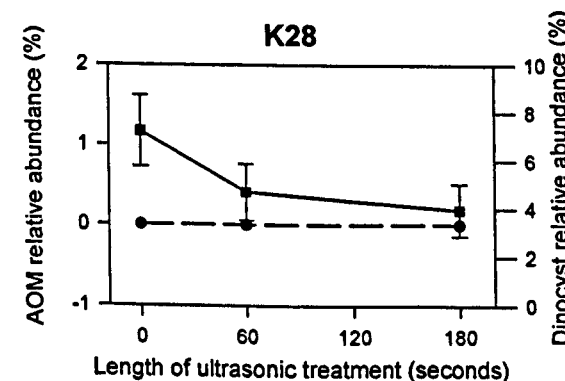
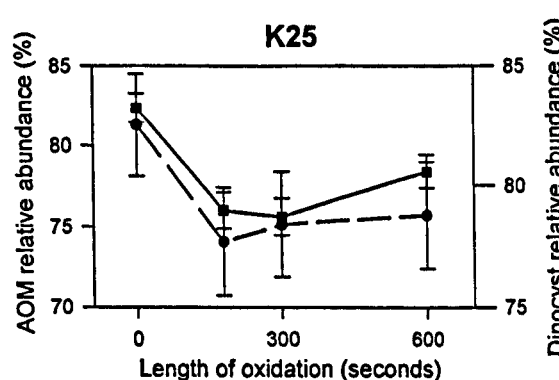
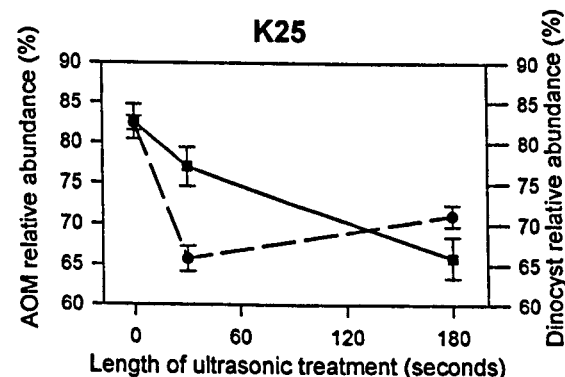
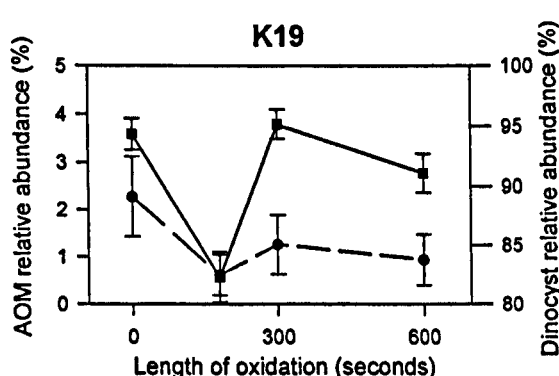
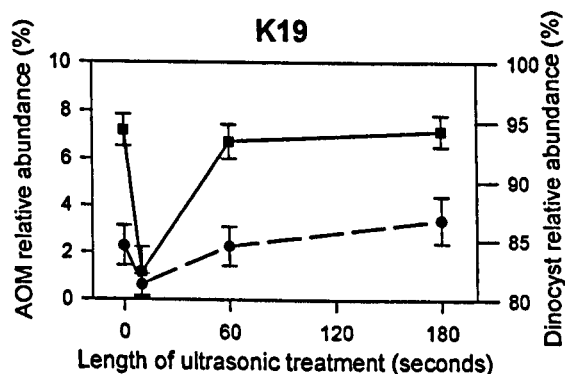
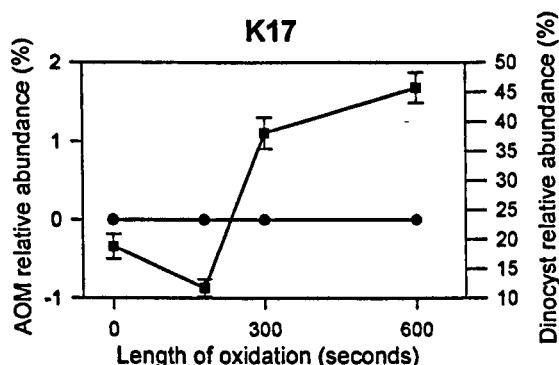
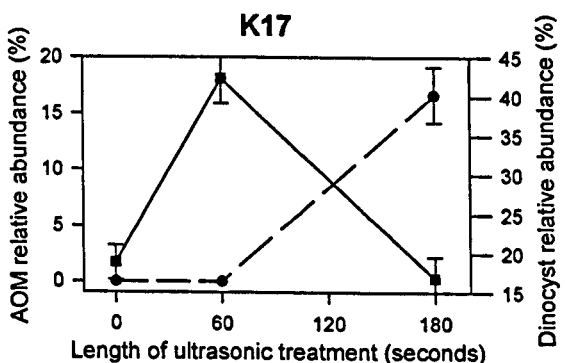
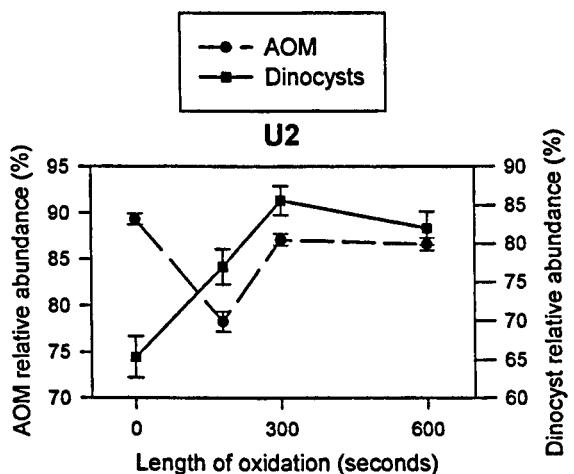
With a couple of exceptions, dinocyst relative abundance in the AOM-rich facies was reduced by increasing the length of ultrasonic treatment (Figure 3.7, Table 3.1).

Figure 3.7: Effects of sonification and oxidation on AOM and dinocyst relative abundance

Effect of ultrasonic treatment (unoxidised residues)



Effect of oxidation (unsonified residues)



This is also the case in experimental preparations of sample K28, although the magnitude of variation was much smaller and possibly insignificant when taking into account standard error. The pronounced peak in dinocyst abundance produced after 60 seconds of ultrasonic treatment on sample K17 is a reflection of the reduction in tracheid abundance. The effects of oxidation are unclear, both decreases and increases in relative abundance can be seen in the samples processed. However, two of the three oxidation series (at 0 and 3 minutes ultrasonic treatment) of sample K17 surprisingly suggest positive correlation between relative abundance of dinocysts and increasing oxidation time. This appears to have been induced by the relative decrease in tracheid abundance, and suggests that in this sample dinocysts were more resistant to oxidation than tracheid material.

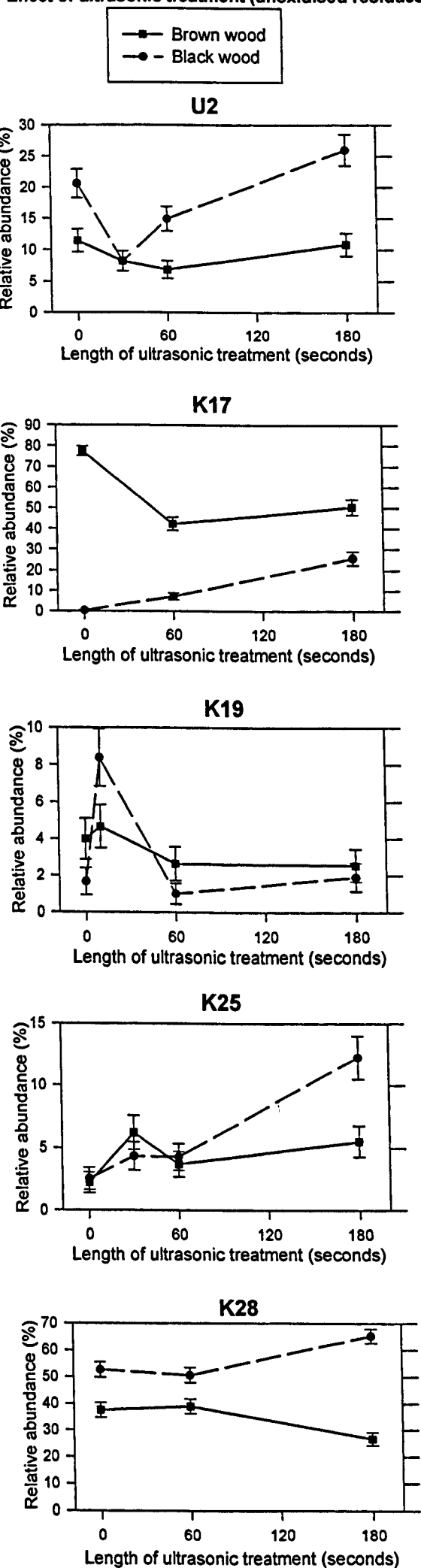
Woody phytoclasts

Only in the residues of sample K17 was there a fundamental change in the proportion of woody components, where the grouped brown wood abundance drops with both increasing sonification and oxidation (Figure 3.8). This trend was created by the strong influence of these procedures on the tracheid material, which dominates the untreated palynofacies in this sample. This was balanced by a dramatic rise in the relative abundance of the black wood component, from 0.3% in the untreated residues to 31.6% in the preparation exposed to maximum sonification and oxidation (Table 3.1). Comparison of the effects of ultrasonic vibration and oxidation suggest that sonification had a much more rapid influence on these components in this residue than did oxidation.

In the other palynofacies investigated, the relative abundances of the woody components show no consistent trends with either increasing oxidation or ultrasonic vibration. Little evidence can be found from these data to support the suggestion that oxidation may convert some material potentially assignable to black wood into brown wood. In several of the residues (K17, K25, K28) the relative abundance of black wood appears to increase with increasing length of ultrasonic vibration. This is presumably a

Figure 3.8: Effects of sonification and oxidation on woody phytoclast relative abundance

Effect of ultrasonic treatment (unoxidised residues)



Effect of oxidation (unsonified residues)

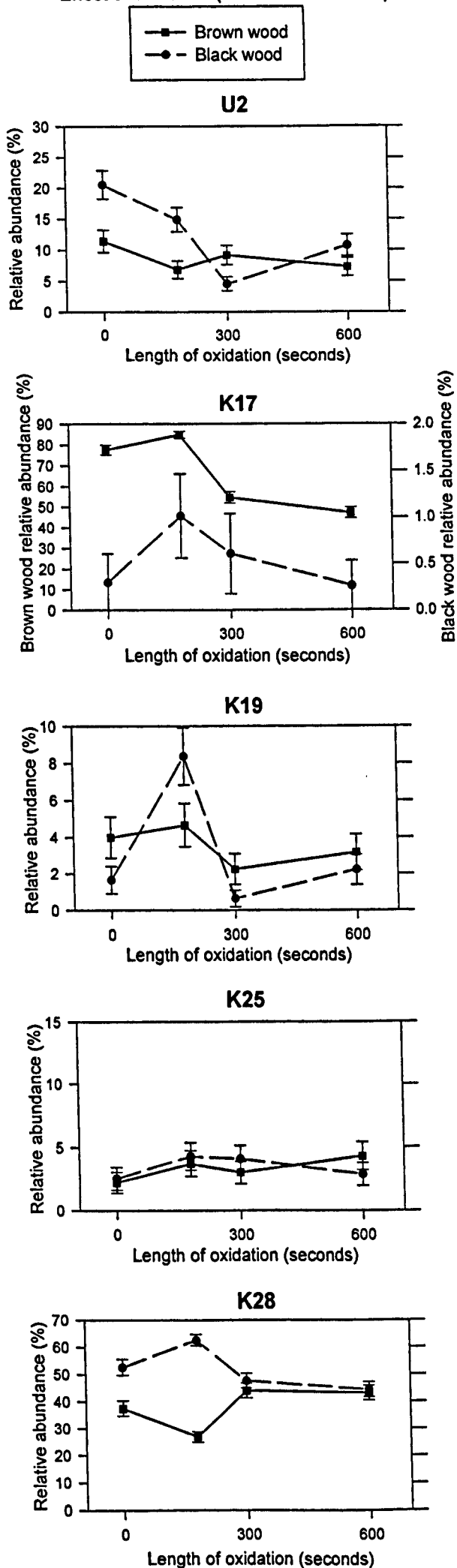
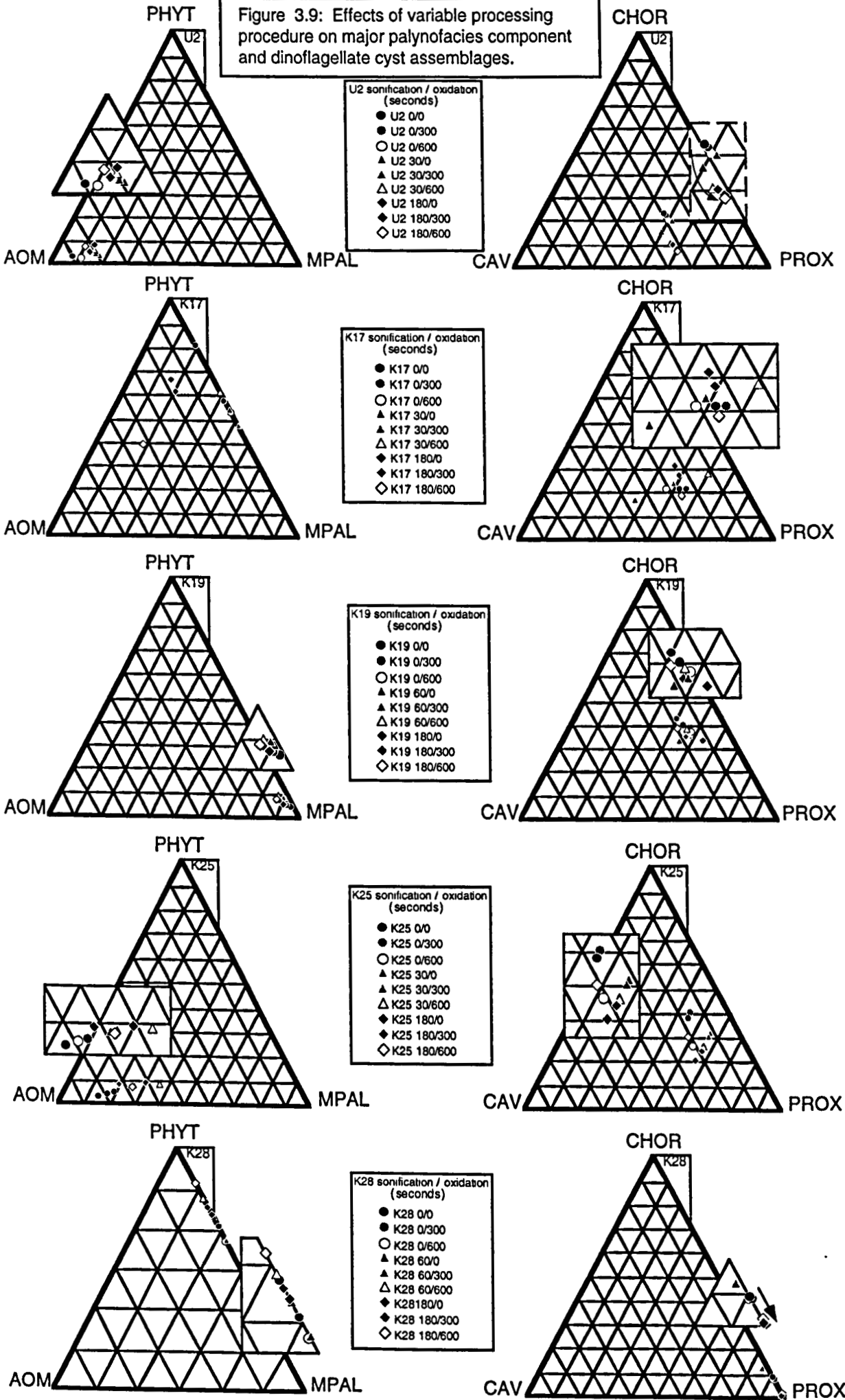


Figure 3.9: Effects of variable processing procedure on major palynofacies component and dinoflagellate cyst assemblages.



reflection of its comparatively robust nature since the absolute abundance of this component shows a decrease after ultrasonic treatment in residue K28. The suggestion that tracheid material is adversely affected by oxidation (K17) contrasts with comments of Batten (1996).

Effects on the major components of palynofacies (AOM, phytoclasts, and marine palynomorphs) can be seen in the ternary plots of Figure 3.9. Generally any significant trends in the responses of individual categories are transferred to the gross components. This is most notably seen in the right-hand shift of AOM rich facies in response to ultrasonic vibration and oxidation. The pronounced increase in AOM within the tracheid-dominated palynofacies of sample K17 is also clearly noticeable. Other trends are difficult to pick out, and the close clustering of all the experimental preparations in samples U2 and K19 suggests that the procedure variation had little significant effect on the relative abundance of bulk components in these samples.

3.3.3. Effects of processing procedure on absolute abundance of palynologic matter

Disappointingly, owing to the inadequate addition of exotic spores, only two of the five experimental samples had small enough standard errors to allow any meaningful remarks to be made. Thus only the data for samples K17 and K28 are displayed in Figures 3.10a & 3.10b, drawn from Table 3.2. In addition, such information needs to be treated with caution, since the precise effects of processing procedure on the exotic *Lycopodium* grains are unknown.

Nevertheless, the effects of ultrasonic vibration seem to be largely intuitive: both samples K17 and K28 showed a marked decrease in dinocyst absolute abundance with increasing ultrasonic treatment. The same trend was also reflected in the abundance of woody phytoclasts, although here the data are less consistent. When the individual

Figure 3.10a: Effects of sonification and oxidation on woody phytoclast and dinocyst absolute abundances

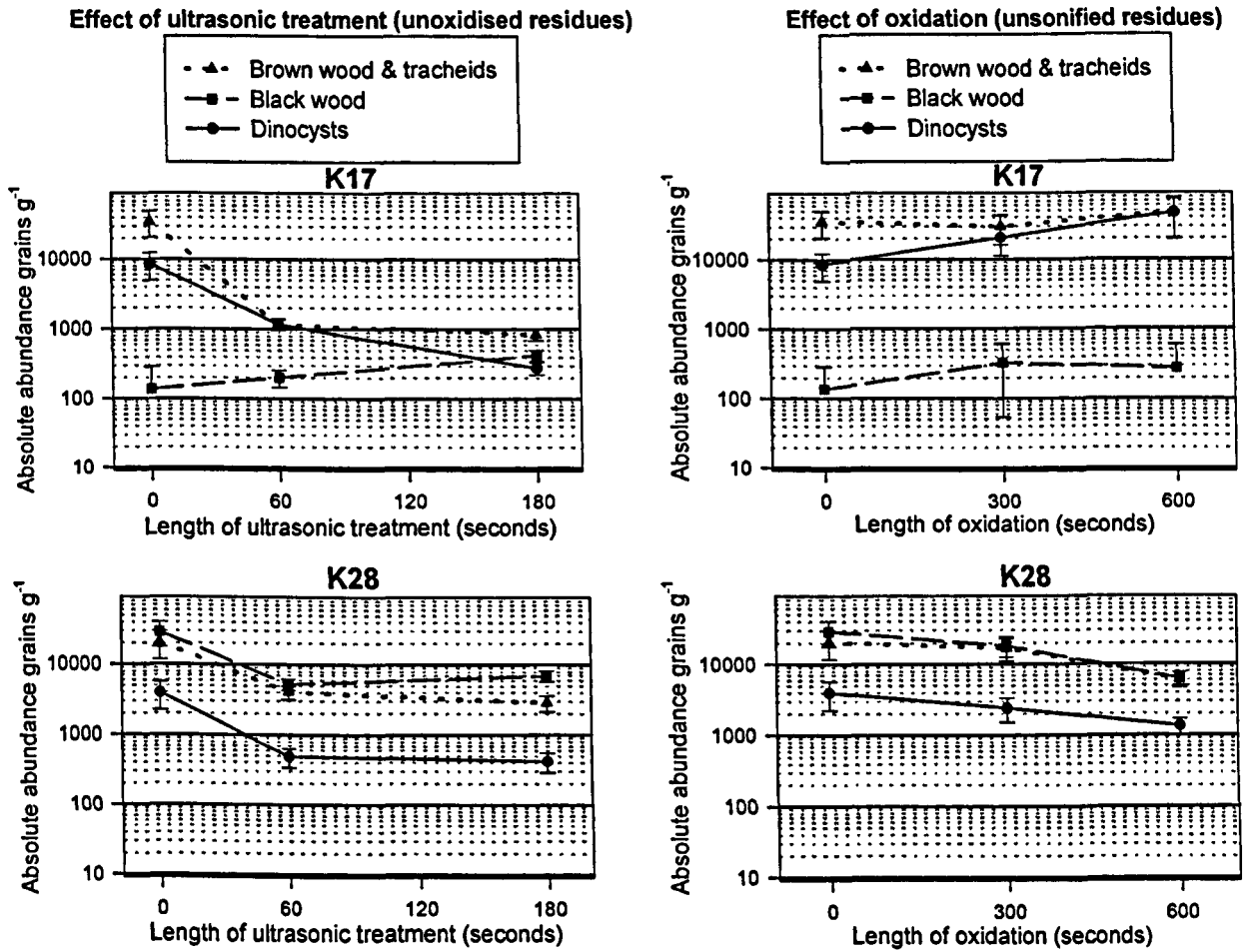
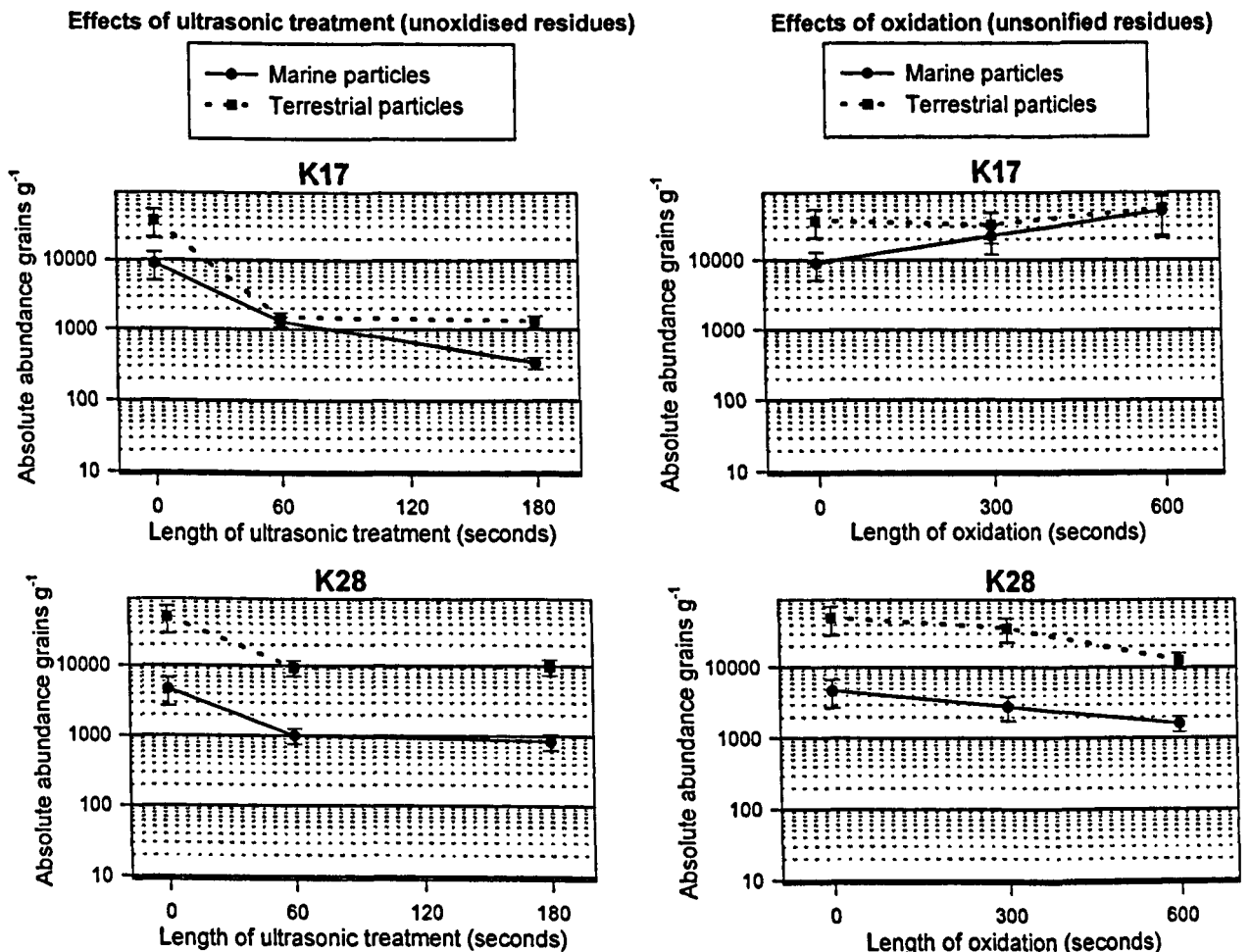


Figure 3.10b: Effects of sonification and oxidation on absolute abundance of marine and terrestrial components



component data are combined into marine- and terrestrially-derived groups (Figure 3.10b), the trends seen are very similar, and both groups show a distinct decrease in abundance with ultrasonic treatment. Data on the effects of oxidation are less consistent. The absolute abundance of dinocysts and both components of woody phytoclasts appears to have increased with oxidation in sample K17. Oxidation seems to have had a more intuitive effect in K28 residues, although maximum oxidation time often shows higher abundances than those exposed to nitric acid for 5 minutes in residues previously subjected to ultrasonic vibration. Since treatment with nitric acid can clearly not create material, some other explanation for absolute abundance increase is necessary. One possibility is that black wood might indeed be converted to brown wood during oxidation, although this cannot be verified here. The most likely cause for apparent increases in absolute data is the decrease in abundance of exotic marker grains, either controlled directly by oxidation, or fractionation during residue splitting.

3.3.4. Effects of processing procedure on the dinocyst assemblages.

Proportions of chorate, cavate and proximate cysts.

Analysis of the data shows that ultrasonic vibration of the residues appears to reduce the abundance of chorate cysts relative to both proximate and cavate morphologies (Figure 3.11, Table 3.3). This is most particularly noticeable in the two AOM-rich samples in which the skolochorate cysts are dominated by forms with long delicate processes (genera like *Systematophora*, *Stiphrosphaeridium*, and the bucket taxon "*Cleistosphaeridium aciculum*") and thin-walled central bodies. Here the chorate abundance values drop by some 15% over the full 3 minutes of sonification. The data also suggest that nearly half of this reduction occurs within the first 30s to 1 minute (Table 3.3). This is particularly important when one considers that a 15% drop represents removal of between 40% and 65% of the chorate cysts in these assemblages.

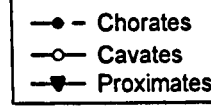
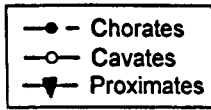
Sample	Chorates count	Chorates %	Standard error of %	Cavates count	Cavates %	Standard error of %	Proximates count	Proximates %	Standard error of %	No. of chorate species	No. of cavate species	No. of proximate species	Total no. of species	Fisher Diversity	Error on Fisher Diversity	Goodman Dominance	Count total	Lycopodium counted
U2 0/0	45	23.4	3.06	56	29.2	3.28	91	47.4	3.6	8	5	19	32	11	1.4	32.3	192	1
U2 0/300	69	22.3	2.36	91	29.4	2.59	150	48.4	2.84	10	5	21	36	10.2	1.1	31.6	310	2
U2 0/600	61	20.2	2.31	88	29.1	2.61	153	50.7	2.88	9	5	20	34	9.6	1	30.7	302	1
U2 30/0	46	15.2	2.06	105	34.7	2.73	152	50.2	2.87	9	4	17	30	8	0.9	41.6	303	4
U2 30/300	56	19.6	2.35	79	27.7	2.65	150	52.6	2.96	10	4	17	31	8.8	1	29.5	285	2
U2 30/600	29	10.1	1.77	97	33.7	2.78	162	56.3	2.92	5	3	17	25	6.5	0.9	42	288	2
U2 60/180	34	12.9	2.07	89	33.8	2.92	140	53.2	3.08	9	4	22	35	10.5	1	40.3	263	2
U2 180/0	24	7.87	1.54	98	32.1	2.67	183	60	2.81	7	4	17	28	7.5	0.9	32.1	305	2
U2 180/300	27	9.31	1.71	95	32.8	2.76	168	57.9	2.9	6	4	16	26	6.8	0.9	37.9	290	3
U2 180/600	20	6.94	1.5	94	32.6	2.76	174	60.4	2.88	6	4	16	26	6.8	0.9	39.6	288	5
K17 0/0	66	21.9	2.38	77	25.6	2.51	158	52.5	2.88	23	9	35	67	26	2.2	26.3	301	35
K17 (0/180)	85	30.7	2.77	59	21.3	2.46	139	50.2	3	24	10	37	71	27	2.3	18.1	277	39
K17 0/300	64	21.4	2.37	69	23.1	2.44	166	55.5	2.87	21	9	35	65	25	2.2	27.1	299	45
K17 0/600	64	21.2	2.35	95	31.5	2.67	143	47.4	2.87	21	10	36	67	26	2.2	25.8	302	16
K17 60/0	18	16.1	3.47	52	46.4	4.71	42	37.5	4.57	9	8	14	31	14.8	2.3	28.6	112	97
K17 60/300	25	23.8	4.16	29	27.6	4.36	51	48.6	4.88	8	6	10	24	9.5	1.5	33.3	105	103
K17 60/600	30	27.8	4.31	12	11.1	3.02	66	61.1	4.69	6	5	12	23	9	1.4	33.3	108	121
K17 180/0	28	26.9	4.35	24	23.1	4.13	52	50	4.9	4	3	5	12	3.3	0.6	30.8	104	355
K17 180/300	30	27.3	4.25	25	22.7	4	55	50	4.77	4	4	7	15	4.4	0.8	30	110	382
K17 180/600	24	18.6	3.43	34	26.4	3.88	71	55	4.38	4	4	6	14	3.8	0.7	27.1	129	390
K19 0/0	119	40.5	2.86	48	16.3	2.16	127	43.2	2.89	23	7	23	53	18.9	1.8	28.2	294	
K19 0/300	129	42.9	2.85	53	17.6	2.2	119	39.5	2.82	22	8	23	53	18.1	1.6	29.9	301	4
K19 0/600	112	37.2	2.79	44	14.6	2.04	145	48.2	2.88	18	7	29	54	18.8	1.7	26.6	301	7
K19 10/180	126	39.7	2.75	48	15.1	2.01	143	45.1	2.79	19	8	26	53	18	1.6	18.9	317	0
K19 60/0	100	33.4	2.73	63	21.1	2.36	136	45.5	2.88	19	9	25	53	18.5	1.7	20.4	299	4
K19 60/300	106	35.3	2.76	48	16	2.12	146	48.7	2.89	14	8	25	47	15.4	1.4	21	300	3
K19 60/600	112	37.3	2.79	45	15	2.06	143	47.7	2.88	14	7	25	46	14.6	1.4	17.3	300	2
K19 180/0	101	33.6	2.72	35	11.6	1.85	165	54.8	2.87	17	7	23	47	15.4	1.4	22.9	301	3
K19 180/300	104	34.9	2.76	51	17.1	2.18	143	48	2.89	18	8	22	48	15.9	1.5	25.5	298	3
K19 180/600	116	38.9	2.82	56	18.8	2.26	126	42.3	2.86	18	7	23	48	15.9	1.5	25.1	298	3
K25 0/0	121	38.1	2.72	54	17	2.11	143	45	2.79	20	11	22	53	17.8	1.6	28.6	318	
K25 0/300	120	39.9	2.82	46	15.3	2.07	135	44.9	2.87	21	11	23	55	19.2	1.7	28.6	301	7
K25 0/600	78	26.1	2.54	63	21.1	2.36	158	52.8	2.89	18	11	21	50	16.7	1.5	28.1	299	5
K25 30/0	94	31.3	2.68	33	11	1.81	173	57.7	2.85	20	6	24	50	16.7	1.5	26	300	4
K25 30/300	90	30.1	2.65	38	12.7	1.93	171	57.2	2.86	18	8	25	51	17.1	1.6	27.4	299	5
K25 30/600	78	25.9	2.53	49	16.3	2.13	174	57.8	2.85	18	8	25	51	17.1	1.6	33.9	301	12
K25 (60/180)	101	37.1	2.93	46	16.9	2.27	125	46	3.02	17	7	19	43	14.3	1.6	24.3	272	
K25 180/0	62	20.7	2.34	67	22.3	2.4	171	57	2.86	18	8	23	49	16.2	1.5	24	300	8
K25 180/300	74	24.4	2.47	54	17.8	2.2	175	57.8	2.84	17	8	24	49	16.1	1.5	23.8	303	8
K25 180/600	90	30.2	2.66	62	20.8	2.35	146	49	2.9	17	7	24	48	16	1.4	22.2	298	8
K28 0/0	24	7.97	1.56	2	0.66	0.47	275	91.4	1.62	10	2	10	22	5.2	0.7	78.4	301	104
K28 (0/180)	26	12.7	2.32	1	0.49	0.49	178	86.8	2.36	11	1	9	21	5.8	0.8	79.5	205	
K28 0/300	23	7.64	1.53	0	0	0	278	92.4	1.53	5	0	7	12	2.3	0.4	92.3	301	190
K28 0/600	18	8.65	1.95	0	0	0	190	91.3	1.95	4	0	5	9	1.8	0.3	86.1	208	290
K28 60/0	0	0	0	0	0	0	72	100	0	0	0	2	2	0.4	0.1	100	72	611
K28 60/300	1	1.2	1.2	0	0	0	82	98.8	1.2	1	0	3	4	0.8	0.2	95.2	83	709
K28 60/600	6	12.2	4.68	1	2.04	2.02	42	85.7	5	2	1	3	6	1.4	0.4	65.3	49	712
K28 180/0	1	1.82	1.8	0	0	0	54	98.2	1.8	1	0	2	3	0.7	0.2	87.3	55	900
K28 180/300	0	0	0	0	0	0	51	100	0	0	0	2	2	0.3	0.1	98.1	51	1212
K28 180/600	0	0	0	0	0	0	43	100	0	0	0	2	2	0.3	0.1	97.7	43	1261

Table 3.3: Dinocyst data generated from the experimental residues.

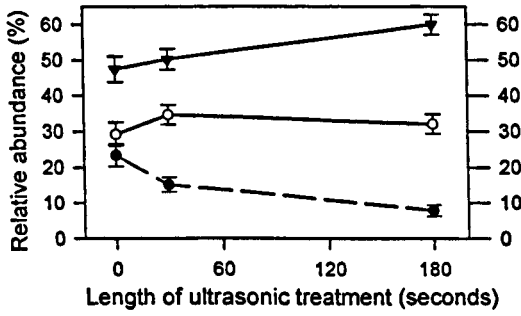
Figure 3.11: Effect of sonification and oxidation on relative abundance of dinocysts per morphological group

Effect of ultrasonic treatment (unoxidised residues)

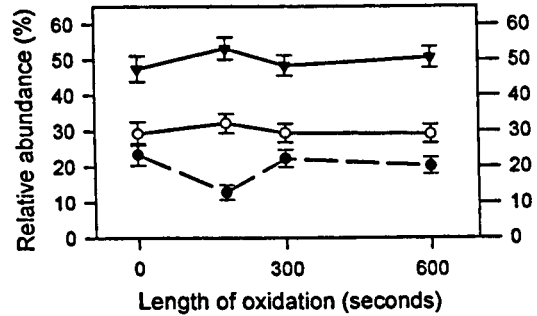
Effect of oxidation (unsonified residues)



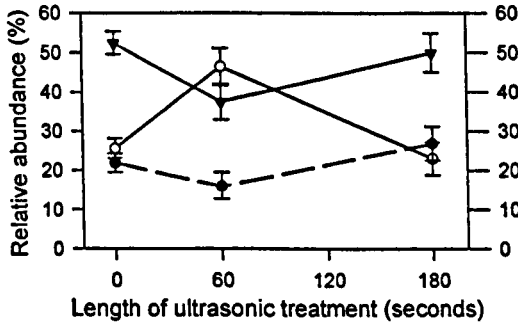
U2



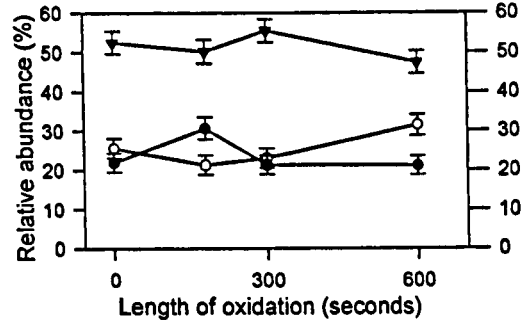
U2



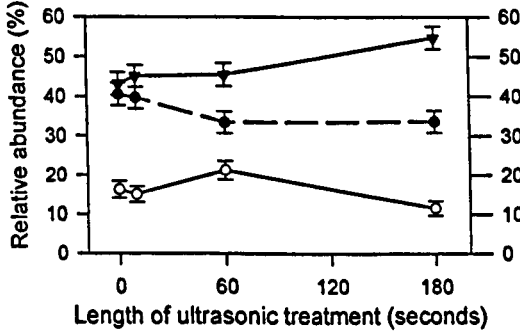
K17



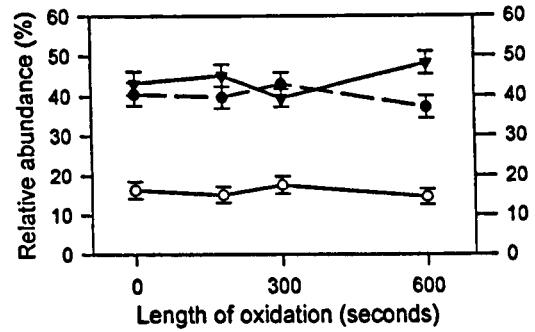
K17



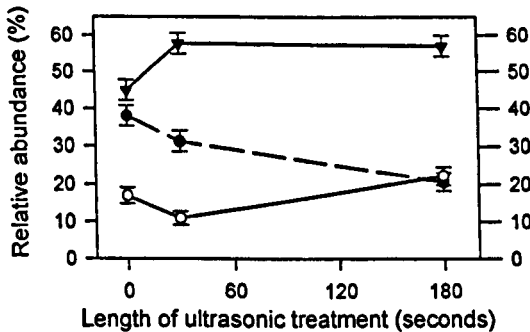
K19



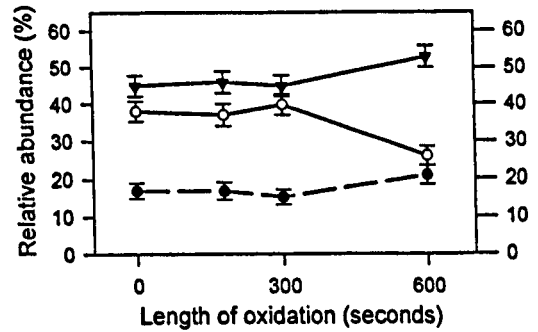
K19



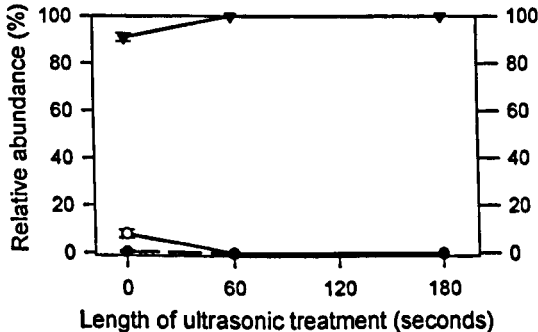
K25



K25



K28



K28

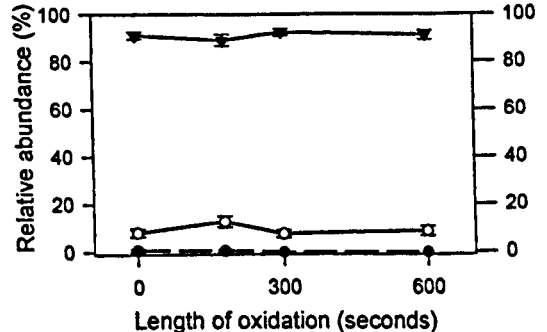
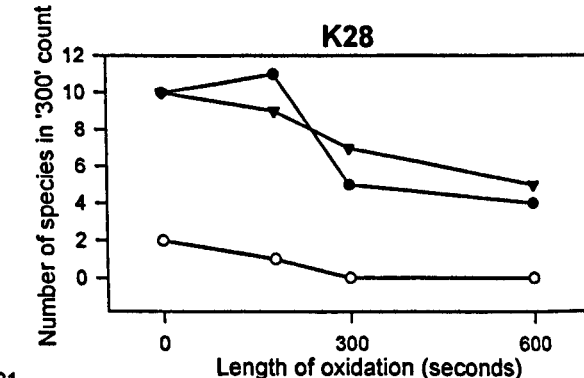
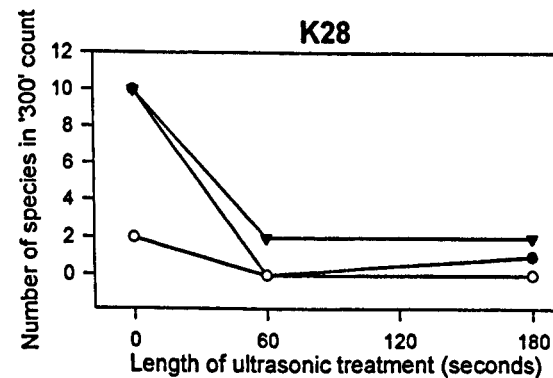
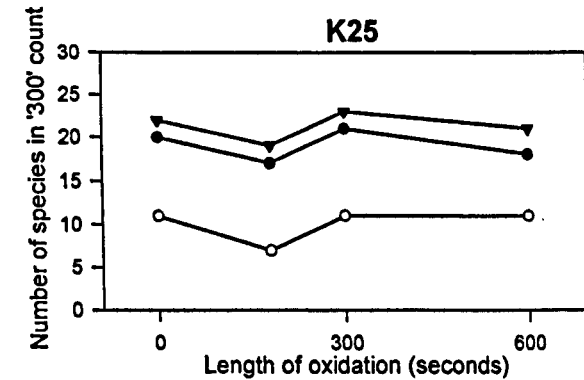
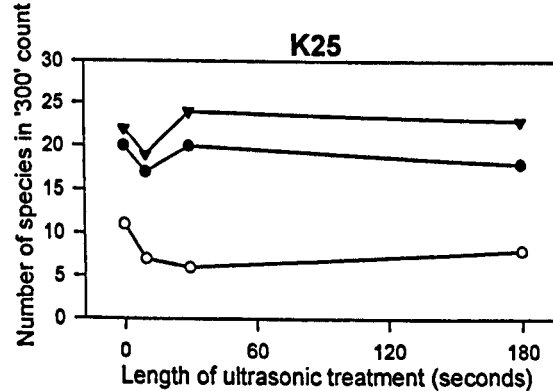
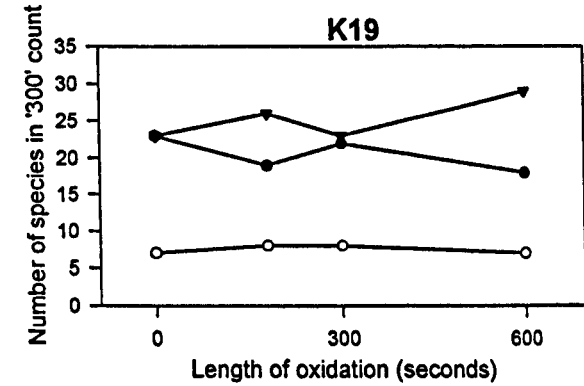
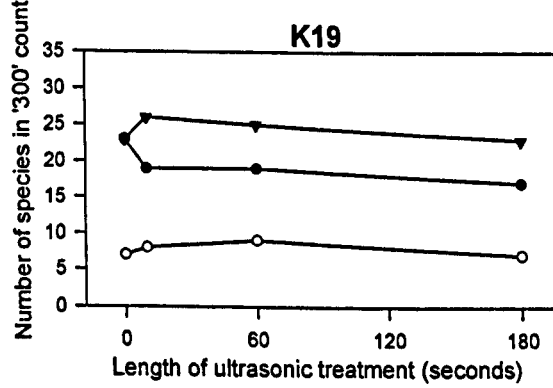
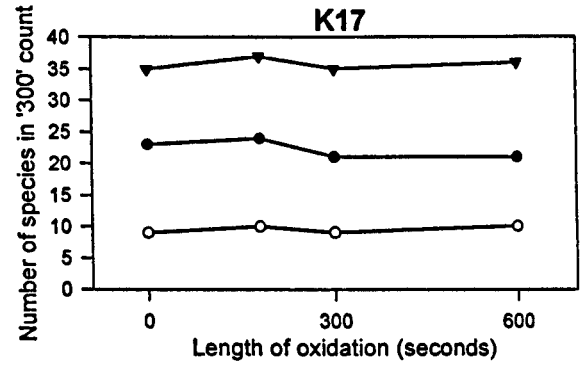
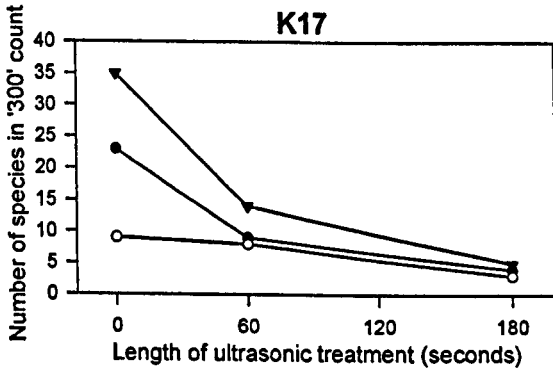
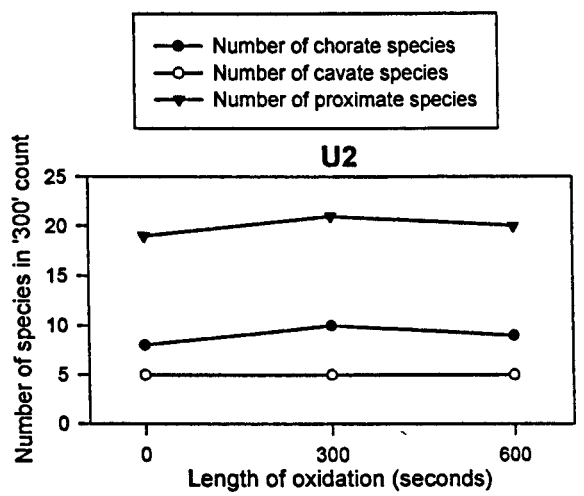
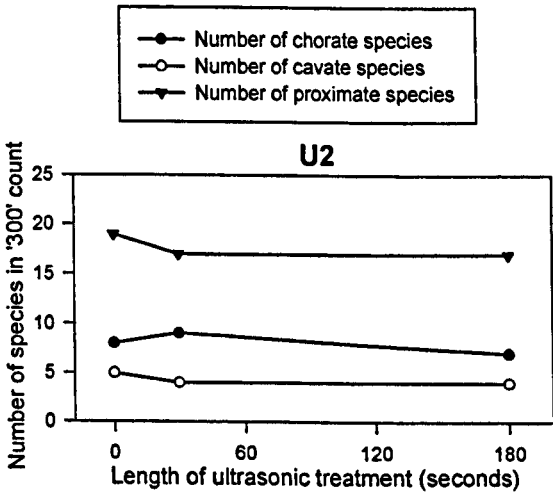


Figure 3.12: Effect of sonification and oxidation on number of dinocyst species per morphological group

Effect of ultrasonic treatment (unoxidised residues)

Effect of oxidation (unsonified residues)



The other samples have chorate assemblages dominated by more robust skolochorates such as *Kleithriasphaeridium* spp. and *Achomosphaera neptuni*, or proximochorates like *Tenua* spp. and *Impletosphaeridium* sp. 1. In these samples the maximum chorate reduction after 3 minutes ultrasonic vibration is approximately 7%. Nitric acid oxidation appears to have had little consistent effect on the relative chorate abundance.

The relative abundance of the cavate group appears to be broadly consistent across the different preparations of each residue. This suggests some loss of cavate cysts, since otherwise the relative abundance of this group would be expected to increase in response to the chorate decline. Comparison of the main taxa involved suggests that a reduction in those morphologies with thin periphragm and generally small size (*Chlamydophorella* spp.) are preferentially removed, although this effect is inconsistently developed. The relative abundance of proximate cysts tends to increase with ultrasonic vibration (as a reflection of the chorate decrease), and oxidation cannot be demonstrated to have had any consistent effect on the group.

When the abundance of these groups is considered in terms of numbers of species (Figure 3.12), it can be seen that although the procedure does not strongly affect the assemblages, there is a general decline in the number of species noted for all groups. The most profound changes occurred in samples K17 and K28, where fewer rare species were encountered with increasing ultrasonic vibration. Oxidation appears to have had little or no affect on the number of species of each morphological group, except in sample K28 where species diversity in each group is reduced.

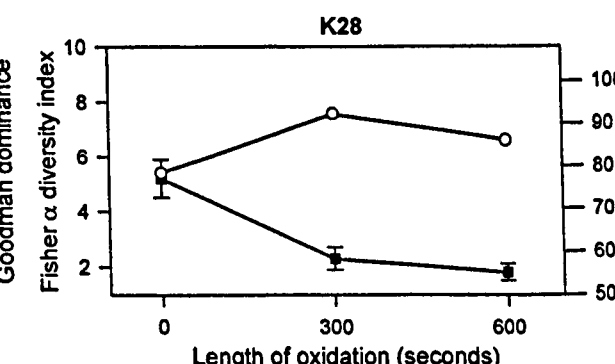
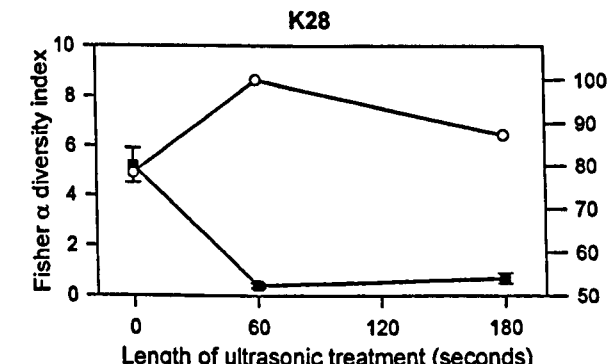
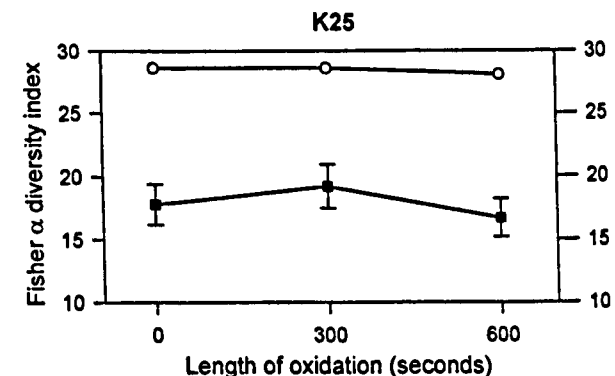
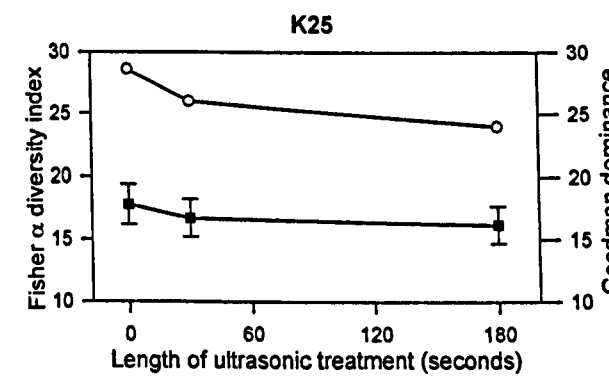
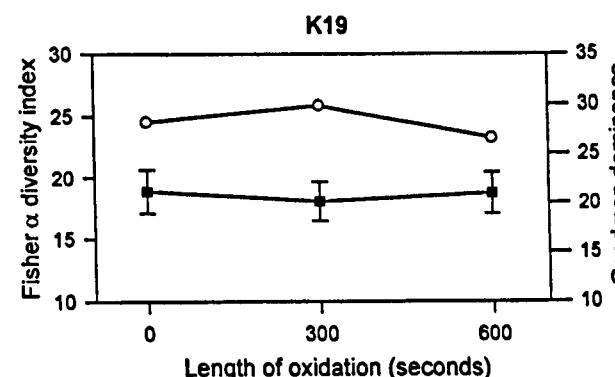
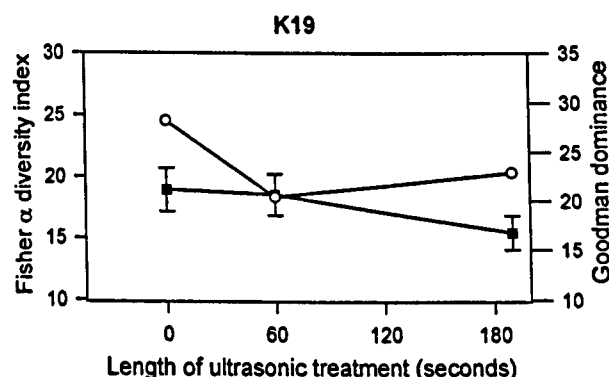
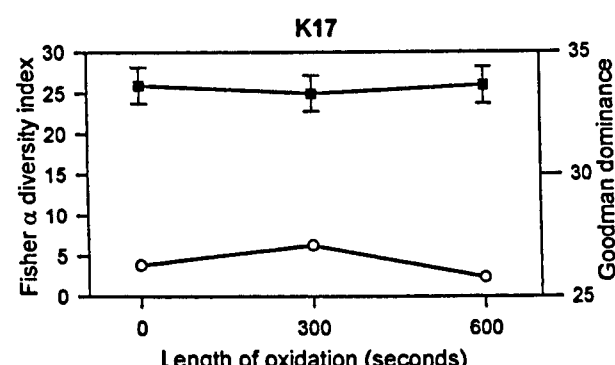
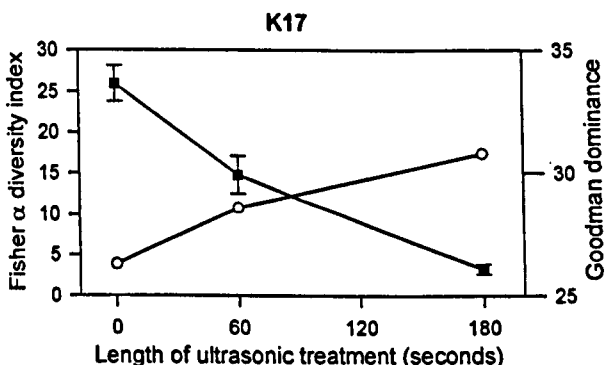
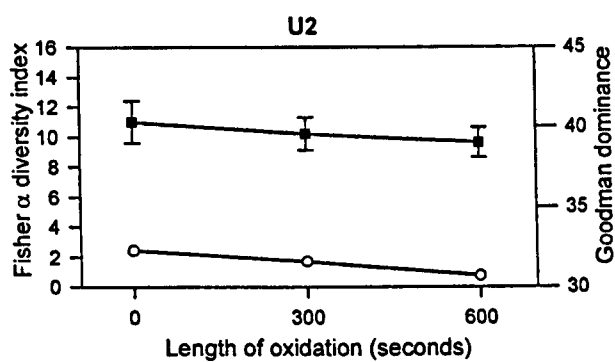
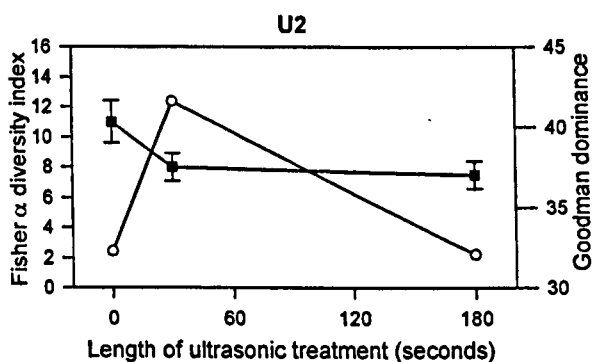
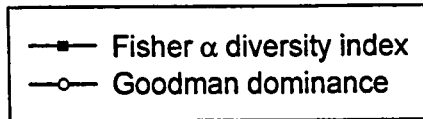
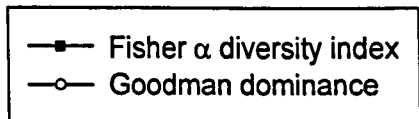
Effects of processing procedure on dinocyst diversity

The effects of processing procedure on dinoflagellate diversity as expressed by the Fisher α index can be seen in Figure 3.13 and Table 3.3. Oxidation has no consistently demonstrable effects on the α values. Conversely ultrasonic vibration is seen to reduce the α value by between 2 and 4, from unsonified residues to those treated for 3 minutes.

Figure 3.13: Effect of sonification and oxidation on Fisher α diversity index and Goodman dominance

Effect of ultrasonic treatment (unoxidised residues)

Effect of oxidation (unsonified residues)



The α values of sample K17 were much more profoundly influenced by ultrasonic vibration, with a drop from 26 in untreated samples to approximately 4 in those exposed to 3 minutes ultrasonic vibration.

Effects of processing procedure on dinocyst dominance.

Neither ultrasonic vibration nor oxidation have consistent effects on dinocyst dominance as measured by Goodman (1987) (Figure 3.13, Table 3.3).

3.3.5. Effects of ultrasonic treatment on woody phytoclast particle size.

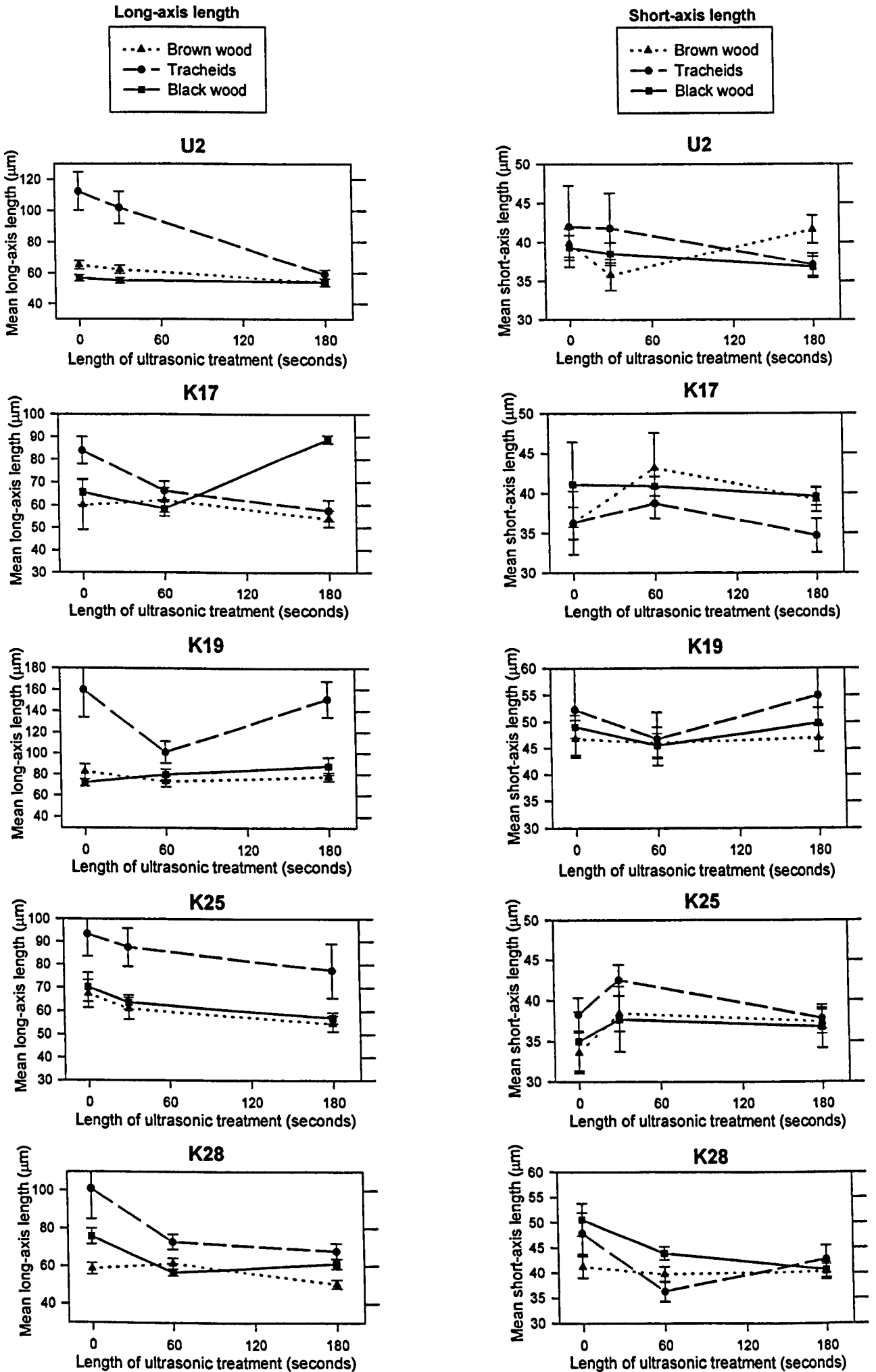
This exercise was performed in a similar manner to that for the main analyses, except that 50 particles each of black and brown wood were counted rather than 100. Tracheid and gelified woody matter are combined to form the brown wood total, although they are clearly separated in Table 3.4 and Figure 3.14 to emphasise any changes taking place.

The most consistent trend revealed is that in each case, increasing the length of exposure to ultrasonic vibration reduces the mean long-axis size. The most notable exception is in the black wood long-axis data of sample K19, which appear to display the reverse trend. Mean short-axis length in all samples is much less strongly affected, few variations being seen to exceed the range of standard error. The affect of ultrasonic vibration on wood particle size is therefore to enhance the equidimensional characteristics of the particle assemblage. Furthermore a concomitant trend to reduced standard deviation of the sample-means with increasing sonification (Table 3.4) portrays increasingly close clustering of the particle sizes. Since in this respect standard deviation might be a useful measurement of the sediment sorting, sonification forces the data to reflect a better sorted assemblage of more equidimensional particles

Sample	Mean brown wood long-axis length	Long-axis standard deviation	Long-axis standard error	Mean brown wood short-axis length	Short-axis standard deviation	Short-axis standard error	Brown wood RI	Mean tracheid long-axis length	Long-axis standard deviation	Long-axis standard error	Mean tracheid short-axis length	Short-axis standard deviation	Short-axis standard error	Tracheid RI	Mean black wood long-axis length	Long-axis standard deviation	Long-axis standard error	Mean black wood short-axis length	Short-axis standard deviation	Short-axis standard error	Black wood RI
U2 0/0	65.2	18.82	2.67	39.9	9.41	1.86	3.14	112	41.51	12.2	42	18.39	5.2	2.99	56.9	13.07	1.98	39.3	11.61	1.59	3.66
U2 30/0	62.3	14.7	2.57	35.8	11.4	1.99	3.15	102	42	10.2	41.8	18.4	4.46	3	55.3	12.5	1.77	38.5	10.4	1.47	3.56
U2 3/0	54.1	13.3	2.47	41.6	9.6	1.78	3.76	59.4	12.2	2.66	37.1	6.67	1.46	3.57	54.2	18.3	2.59	36.8	9.55	1.35	3.84
K17 0/0	60	26.9	11	36.3	9.71	3.97	2.93	84	40	6.02	36.3	13.4	2.02	2.7	65.7	15.3	5.77	41.1	14.1	5.31	2.96
K17 1/0	62.2	21	5.42	43.2	16.9	4.37	3.1	66.4	23.6	3.99	38.8	11.3	1.92	2.73	58.3	22.4	3.16	40.9	8.54	1.21	2.8
K17 3/0	54	19.1	3.6	39.2	7.85	1.48	2.73	57.5	21.9	4.68	34.7	9.89	2.11	2.09	88.9	12.4	1.75	39.6	8.09	1.14	3.46
K19 0/0	82.5	45.2	7.15	46.8	22.5	3.56	3.5	160	81.2	25.7	52.3	27.3	8.62	2.91	72.2	24.4	3.45	49.1	15.2	2.14	2.86
K19 1/0	73	31	4.96	46.1	18.5	2.96	3.47	101	34	10.3	46.8	16.6	5.01	3.17	79.8	36.7	5.2	45.6	16	2.27	2.94
K19 3/0	77.6	24	3.95	47	15.6	2.57	3.79	151	60.7	16.8	55	20.8	5.77	3.5	87.9	59.7	8.44	49.8	19.8	2.8	3.42
K25 0/0	67.3	34.4	5.9	33.6	14.7	2.51	3.26	93.4	39.7	9.93	35	14.6	3.64	2.81	70.2	44.4	6.23	38.3	14.5	2.02	3.18
K25 30/0	61.1	22	4.59	38.4	11.6	2.16	3.28	87.5	38	8.29	37.7	18.3	3.99	3.05	63.7	21.4	2.98	42.5	13.6	1.92	3.22
K25 3/0	54.8	21	3.37	37.4	8.99	1.44	3.44	77.5	39	11.8	36.8	8.74	2.63	3.18	57.2	16.7	2.37	37.8	8.92	1.26	3.48
K28 0/0	58.5	18.5	3.08	41.2	13.2	2.2	3.11	101	60.7	16.2	47.9	15.3	4.08	2.86	75.8	29.3	4.14	50.6	22.6	3.2	3.44
K28 1/0	61.2	16.6	2.93	39.7	8.7	1.54	3.81	72.9	16.9	3.98	36.3	8.76	2.04	3.11	56.5	13	1.84	43.9	12.6	1.28	3.64
K28 3/0	50.3	11.3	2.27	40.3	7.58	1.52	3.68	68	19.8	3.96	42.8	13.4	2.68	3.12	61.1	18.2	2.57	40.7	10.3	1.46	3.78

Table 3.4: Phytoclast size and roundness measurements generated from the experimental residues treated with ultrasonic vibration. Mean data are drawn from the measurements presented in Appendix C.

Figure 3.14: Effect of ultrasonic vibration on woody phytoclast size



than would otherwise have been seen. However the long-axis mean-value difference between untreated preparations and those subjected to 3 minutes of ultrasonic vibration is rarely more than 15 μm .

3.3.6. Effects of processing procedure: summary

The effect of processing procedure on the major palynofacies components has been tested. The experiments indicate the following:

- That ultrasonic vibration was a more destructive part of the procedure on both the AOM and structured particles than oxidation using nitric acid. Oxidation appears to have had few consistently demonstrable effects on the palynologic matter, and the suggestion that this procedure can affect the woody phytoclast composition cannot be substantiated from the limited data available here.
- Review of the data as a whole suggests that the components of palynologic matter most strongly affected by these procedures are AOM, dinoflagellate cysts (most particularly skolochorate varieties), and tracheids.
- The extent to which such treatment can be expected to affect the palynofacies composition is rather unpredictable, and it should not be assumed that the same procedure will have identical effects on different palynofacies. That said, analysis of the bulk component ternary plots suggests that extended exposure to either treatment is necessary for significant palynofacies composition changes to occur. In this respect, the procedures employed in the main analyses can be expected to have had little effect on the bulk components.
- Species diversity as measured by the Fisher α index is reduced by exposure to ultrasonic vibration. Typically, rare forms are lost first, regardless of morphology.

Such changes are likely to have affected the residues prepared for the main analysis, and this must therefore be taken into account.

- Ultrasonic treatment appears to consistently reduce the mean long-axis length of woody phytoclast particles, and artificially enhance the equidimensional nature of the particle assemblages. There is also some evidence to suggest that the angularity index increases (particles become more rounded) after ultrasonic vibration. These effects do take place during the length of treatment used in the main analysis, and must therefore be considered when making interpretations based on such data.

CHAPTER 4. Biostratigraphy of the Volga Basin.

4. Biostratigraphy of the Volga Basin

4.1. Introduction

4.1.1. Location

Both sections studied in this report are located on the western bank of the River Volga in the Ul'yanovsk district of the Russian Platform (Figure 4.1a). Ul'yanovsk itself lies approximately 700 km south-east of Moscow (Figure 4.1a). The local maps of the area are not published with grid-coordinates, and thus locations can only be defined relative to the nearest conurbation. The Gorodische section lies approximately 3.5 km east of the town of Undory, 1km south-east of Gorodische village, and 24 km north of Ul'yanovsk bridge (Fig. 4.1b). The Kashpir section lies approximately 500m east of Kashpir village, and 10km south of the most southerly part of Syzran (Figure 4.1c).

4.1.2. Sedimentology

No formal lithostratigraphy exists for these Volga River sedimentary sequences. However, their sedimentology is discussed below.

Detailed sedimentology of each horizon in the Gorodische section is presented in Table 4.1, and a sedimentary log showing bed numbers, sample positions and ammonite zonation in Enclosure 1.

The panderi Zone, zarajskensis Subzone (beds 1-13) is characterised by an alternation of soft dark grey mudstones and indurated, well-laminated and typically heavily bioturbated micaceous siltstones. The exception to this is the interval from Bed 10 to Bed 12, which is composed of lenticular-bedded siltstones separated by a thin layer of gypsum-rich haematitic sandstone. The virgatus Zone at Gorodische is comprised of coarser-grained sediments. Both the lower and upper boundaries are clearly marked by conglomerates (beds 14 & 16) with predominantly phosphoritic clasts and coarse-grained sandy matrices. These two horizons are separated by a layer of fine

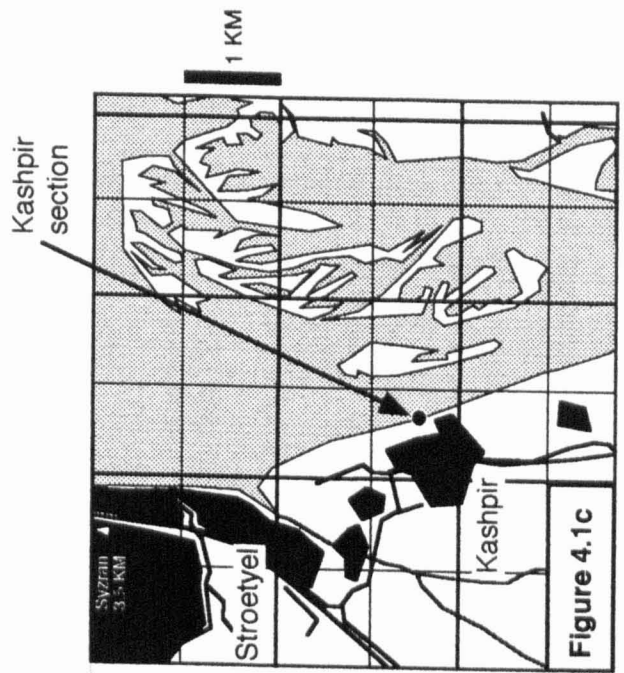
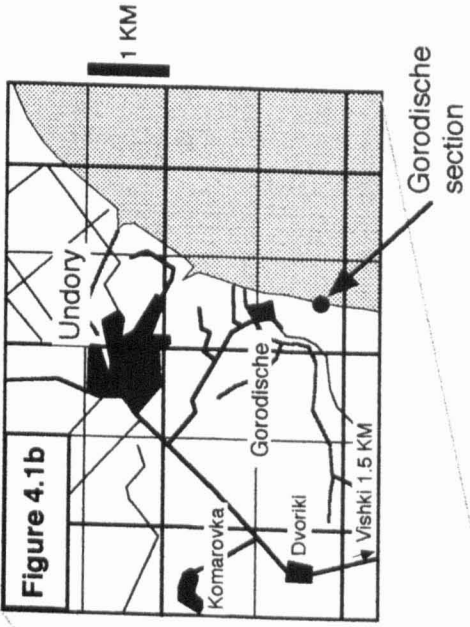
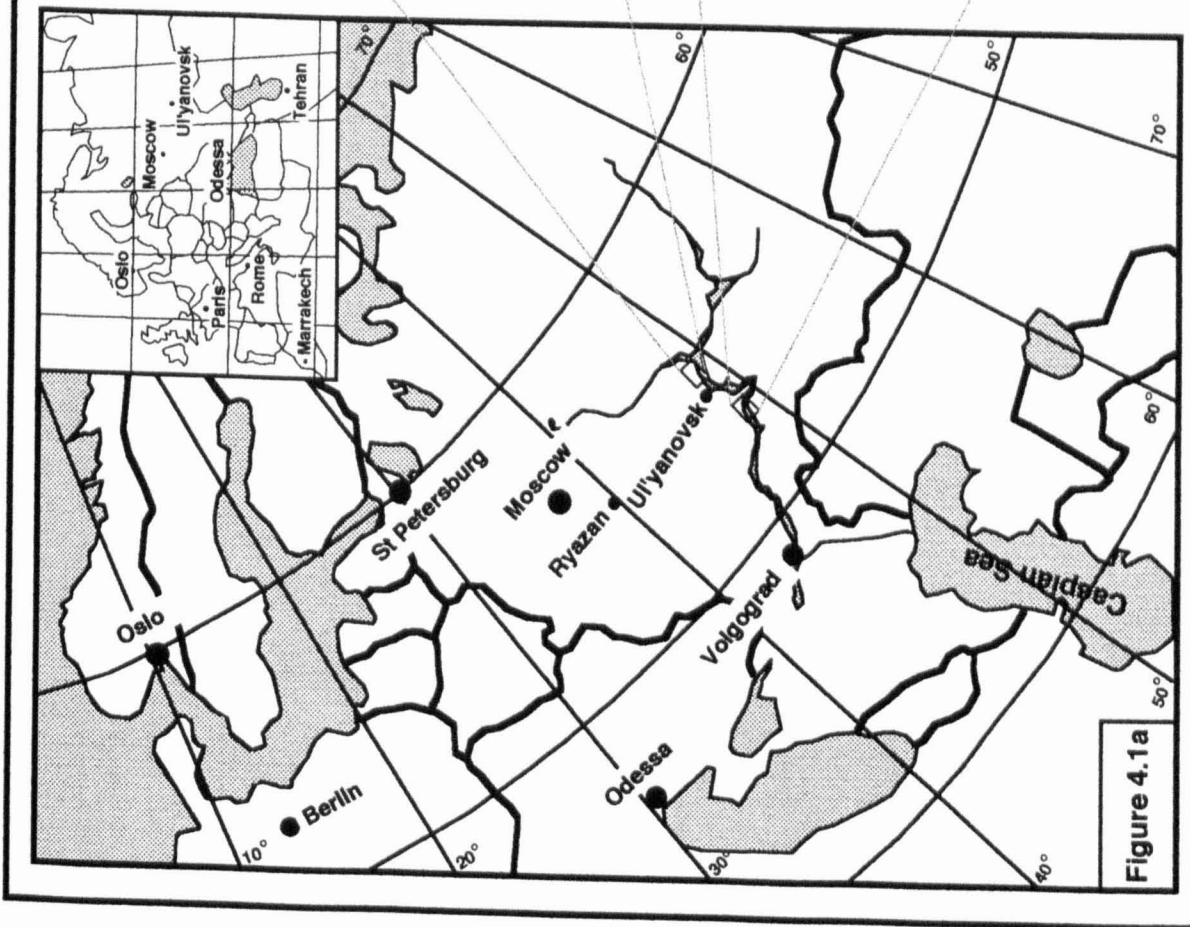


Table 4.1: Gorodische section sedimentology

Bed	Thickness	Ammonite Zone	Sample number	Sedimentological description
1	10cm	panderi	U1	Homogenous light-grey mudstone, with scattered very small bivalves as the only observable macrofauna.
2	65cm	panderi	U2 U3	Soft dark-grey calcareous siltstone with abundant well preserved bivalves, ammonites, and belemnites, as well as a common fragmentary skeletal component.
3	25cm	panderi	U4	Dark-grey siltstone with scattered burrows infilled by cream-coloured skeletal sediment up to fine sand grade. Occasional lamination, well preserved low diversity macrofauna. Occasional pyrite.
4	30cm	panderi	U5 U6	Soft dark-grey calcareous mudstone with increasing proportion of haematite toward the top. Very sparse macrofauna.
5	55cm	panderi	U7 U8	Hard well cemented calcareous brown-grey siltstone. Heavily burrowed, most intensely at top; burrows filled by cream-coloured shelly sediment up to fine-medium sand grade. Cleaves readily, parallel to bedding. Macrofauna abundant, often three-dimensionally preserved, including ammonite aptychi.
6	52cm	panderi	U9 U10 U11	Soft dark-grey calcareous mudstone. Scattered fragmentary shelly material. Very slight normal grading.
7	30cm	panderi	U12 U13	Hard well cemented dark-grey calcareous siltstone. Heavily burrowed throughout, burrows filled by cream-coloured skeletal sediment up to fine sand grade. Abundant macrofauna, occasionally three-dimensionally preserved. Includes ammonite aptichi and echinoid spines.
8	15cm	panderi	U14	Beige calcareous mudstone. Slightly mottled. Macrofauna limited to very small bivalves and rare belemnites. Poor preservation. Upper boundary with Bed 9 is obscured by intense vertical bioturbation.
9	25cm	panderi	U15 U16	Readily cleavable brown-grey calcareous siltstone. Very slightly normally graded. Scattered burrows, infilled by cream-coloured skeletal sediment up to fine sand grade. Some gypsum.
10	30cm	panderi	U17 U18	Dark-grey micaceous mudstone with light-brown siltstone lentices and streaks. Fragmentary skeletal component throughout, concentrated in horizontal burrows. Macrofauna includes belemnites, and occasional three-dimensionally preserved bivalves (dominantly <i>Buchia</i>), as well as rare ammonites and fish scales.
11	3cm	panderi	--	Coarse sand with haematitic matrix. Slightly variable thickness with an irregular, possibly erosional base. Macrofauna absent.

Table 4.1: continued

Bed	Thickness	Ammonite Zone	Sample number	Sedimentological description
12	30cm	panderi	U19	Dark-grey micaceous mudstone with light-brown siltstone lenses and streaks. Fragmentary skeletal component throughout, concentrated in horizontal burrows. Macrofauna includes three-dimensionally preserved belemnites, and occasional bivalves (dominantly <i>Buchia</i>), as well as rare ammonites.
13	20cm	panderi	U20	Light grey to beige claystone/ fine siltstone. Macrofauna absent apart from scattered aptychi.
14	20cm	virgatus	U21 U22	Poorly cemented, poorly sorted matrix-supported conglomerate. Polymodal and polymict, with clast size ranging from 2mm to 10cm. Clasts are of black phosphorite and mudstone, as well as a phosphatised internal moulds of bivalves, gastropods, belemnites, and ammonites. Occasional marine vertebrate fragments. The matrix is well sorted fine beige to greeny-brown (glaucopitic) sandstone. Both the base and the top of this bed are erosional. It can be split into two parts, the lower of which contains the conglomerate, and the upper consists entirely of the well sorted sand. There is no distinct boundary between the two, and no grading: it is drawn at the level where the conglomerate clasts stop. One sample was taken from each part.
15	30cm	virgatus	U23	Green-brown to orange, well sorted, fine grained sandstone. Poorly cemented with a carbonate-rich matrix. The base of the unit is marked by a layer of medium-grained sandstone containing rounded quartz grains and black organic debris which infills pits in the erosional surface on the top of Bed 14. The transition between this fill and the fine sand of Bed 15 is discrete and not graded. Occasional clasts of dark brown coarse sandstone up to 2cm in diameter, and red haematite-stained quartz grains exist at the top of the bed. The macrofauna is composed of bivalves, gastropods and belemnites, where the latter dominate at the top of the bed.
16	20cm	virgatus	U24	Well cemented clast-supported conglomerate with an erosional base. Badly sorted, polymodal and polymict, with clast composition similar to that in the conglomerate of Bed 14. The matrix consists of fine to medium-grained cream-coloured calcareous sandstone bearing glauconite.
17	50cm	nikitini	U25 U26	Light-grey to light-brown fine-grained sandstone. Well cemented with calcareous cement and well sorted. Abundant bivalves

Table 4.1: Continued

Bed	Thickness	Ammonite Zone	Sample number	Sedimentological description
18	100cm	fulgens subditus nodiger	U27 U28 U29 U30 U31 U32	Dark-grey, brown and green very-fine to fine grained calcareous glauconitic sandstone with an erosional base and occasional phosphate nodules. Well sorted but abundantly fossiliferous, the macrofauna being dominated by belemnites and three dimensionally preserved bivalves, which usually have phosphatised internal casts. 20cm above the base, a discrete layer of shelly hash is preserved, with no apparent preferential orientation to the skeletal component (although the shells lie parallel to the bedding), and dominated by a super-abundance of the bivalve <i>Buchia</i> . 25cm from the top of the bed there is a second shelly hash, above which the sediment becomes lenticular, with well spaced lenses of light-grey fine to medium grained sandstone. The shelly component also increases towards the top.
19	30cm	Unzoned	U33	Phosphatised sandstone. Very hard, black, granular (crystalline) matrix with phosphatised or occasionally calcareous reworked skeletal component. Occasional dish-shaped areas of dark-grey muddy sediment, also apparently phosphatised. Erosional base, and irregular top.
20	>>290cm	Unzoned	U34 U35 U36 U37 U38 U39 U40	Dark grey mica-rich mudstone. Heavily fractured, with no apparent bedding or macrofauna. Yellow (secondary) jarosite infills cracks and joints, and transparent gypsum crystals and crystallites can be observed within the sediment.

glaucopit sandstone/siltstone. These deposits are overlain by fine to medium-grained glaucopit sandstones bearing phosphatic internal casts of buchiid bivalves, characteristic of the nikitini to nodiger zone interval. Shelly-hash layers mark the top of the fulgens Zone and the base of the nodiger Zone. The upper part of the nodiger Zone is then marked by increasingly lenticular-bedded sediments, and is abruptly capped by a black, hard, heavily phosphatised sandstone layer (Bed 19). This is immediately superseded by a monotonous sequence of soft, micaceous, strongly fractured siltstones of Valanginian to Barremian age (Blom *et al.*, 1984).

Detailed sedimentology of the section at Kashpir is presented in Table 4.2, and the sedimentary log showing bed numbers, sample positions and ammonite zonation in Enclosure 2.

In common with the section at Gorodische, the zarajskensis Subzone at Kashpir is characterised by an alternation of soft dark grey mudstones and indurated, well-laminated siltstones (beds 1-3). Only the lower 80 cm of exposed sediments at this locality are assigned to this zone. The virgatus Zone is represented by a short (40cm) interval of well cemented and thinly bedded sandstone horizons with numerous erosional surfaces (Bed 4). The superceding nikitini Zone is marked at its base and top by conglomerates which show variability in clast and matrix composition (beds 6, 7, & 10)(see Table 4.2). Between these rudaceous sediments is a 20cm-thick layer of heavily phosphatised blue-green sandstone (bed 8).

Above the nikitini Zone, Bed 11 comprising grey-green siltstones with fine-medium grained sandstone lenses represents part of the fulgens Zone. This zone is capped by a 20cm-thick muddy wackestone with shaley intercalations (Bed 12). This unit shows several stylolitic horizons, suggesting that the shaley layers may be secondary. The basal part of the subditus Zone (Bed 13) is identical in lithology to Bed 11. By contrast, the upper part is comprised of a 20cm-thick unit bearing sandstone-mudstone interbeds of variable thickness (beds 14a-d), and is separated from the

Table 4.2: Kashpir section sedimentology

Bed	Thickness	Ammonite Zone	Sample number	Sedimentological description
1	>10cm	panderi	--	Soft, dark grey calcareous mudstone. Homogeneous. Scattered, poorly preserved macrofauna.
2	8cm	panderi	K1	Dark grey, well cemented coarse-grained calcareous siltstone. Cleaves readily parallel to bedding. Bedding surfaces show horizontal to sub-horizontal burrows where burrow width varies from 0.5 cm to 2 cm. Each burrow is infilled by a lighter, cream coloured, and coarser skeletal sediment, up to fine sand grade. Macrofauna includes the belemnite <i>Cylindroteuthis magnifica</i> , and flattened bivalves of the genera <i>Buchia</i> and <i>Inoceramis</i> . Additionally there are less abundant and completely flattened ammonites, such as <i>Dorsoplanites panderi</i> and <i>Virgatites fallax</i> .
3	55cm	panderi	K2	Massively bedded, dark grey calcareous mudstone. Scattered limestone concretions contain well preserved fossils. Abundant evenly distributed coarse skeletal material, mostly bivalves (<i>Buchia volgensis</i> and smaller unidentifiable fragments), occasional specimens of <i>Dorsoplanites fallax</i> , and rare, poorly preserved belemnites.
4	32cm	virgatus	--	Bed 4a: Four subunits can be recognised in this bed. The basal subunit (4a ¹) rests on Bed 3, and has an irregular base. It is composed of homogeneous, dark brown, medium grained, and unfossiliferous sandstone. Maximum thickness of this subunit is 3cm, varies from 1cm to 3cm with the irregularity of the base. Subunit 4a ² is a 10cm thick layer of dark brown to black well-laminated fine-grained sandstone, well cemented, with an absence of fossils. Subunit 4a ³ is identical to 4a ² in terms of sedimentology, but is separated from the lower subunit by a pronounced erosional contact. 4a ³ contains occasional ?channel infills with planar cross-stratified sandstone of fine to medium grade. 4a ⁴ again has an erosional base, and shows an alternation of fine-grained dark brown sandstone with medium-grained, creamy white sand with a high proportion of skeletal carbonate. It is planar cross stratified, and has occasional concretions of light grey micritic limestone. Very sparsely fossiliferous. All of the sandstone subunits of Bed 4a are well cemented. Bed 4b: Beige-brown medium grained sandstone with calcareous matrix. Occasional planar laminations. Upper part of bed is burrowed predominantly in the horizontal plane, and burrows are infilled by black (organic-rich) sediment.
5	4cm	virgatus	--	Cream to beige-brown coloured, very fine-grained sandstone. Heavily bioturbated with randomly oriented burrows containing dark (organic-rich) infill, or more rarely gypsum crystallites.

Table 4.2: continued

Bed	Thickness	Ammonite Zone	Sample number	Sedimentological description
6	4cm	nikitini	--	Poorly sorted, poorly cemented, clast-supported conglomerate with a clearly erosional base. Clasts are moderately to well rounded, with lithic and skeletal components. Fossil clasts are phosphatised internal casts. Matrix is of dark brown, friable, fine-grained sand.
7	6cm	nikitini	--	Poorly sorted, well cemented, matrix-supported conglomerate with erosional base. Clasts are moderately to well rounded with lithic and skeletal components. Fossil clasts are phosphatised internal casts, often well preserved (bivalves often articulated), with smoothed external surfaces. Matrix is dark grey to black, medium-grained sandstone.
8	20cm	nikitini	--	Massive, internally-structureless, phosphatised sandstone with irregular (erosional?) base. Weathers to turquoise green, but fresh surfaces are dark grey to brown. Medium grained with occasional coarser lithic fragments 2 - 8 cm in length (long axes parallel to bedding). No apparent internal structure.
9	5cm	nikitini	--	Light grey, poorly cemented very fine-grained sandstone. Occasional laminations, and abundant belemnites as only apparent macrofauna.
10	5cm	nikitini	--	Poorly sorted, well cemented, matrix-supported conglomerate with an erosional base. Abundant fossil clasts (phosphatised internal moulds) as well as lithic material. Matrix is medium-grained sandstone and reddened with haematite.
11	52cm	fulgens	K3 K4	Light grey to dark brown siltstone with increasing proportion of cream-coloured skeletal components towards the top of the bed. Similarly, light beige-cream sandy lenses increase in frequency toward the top. Macrofauna predominantly of belemnites, with some rare ammonites and very rare bivalves.
12	10 - 20cm	fulgens	--	Variable thickness skeletal wackestone with irregular and laterally discontinuous siltstone horizons. Fossils often well preserved.
13	100cm	subditus	K5 K6	Grey to dark grey siltstone with cream/beige fine to medium-grained sandstone lenses, and occasional flasers of dark (organic rich) mudstone. Well preserved macrofauna, with abundant belemnites and bivalves (mostly <i>Buchia</i> and <i>Inoceramis</i>), as well as rare specimens of the ammonite <i>Craspedites subditus</i> .

Table 4.2: continued

Bed	Thickness	Ammonite Zone	Sample number	Sedimentological description
14	25cm	subditus	K7 (14a) K8 (14d)	Bed 14a: Grey, fine to medium grained sandstone with delicate, flasers of dark (organic rich) mud. Abundantly fossiliferous with frequent belemnites and ammonites (<i>Craspedites subditus</i>), and common, often well preserved bivalves. Irregular base and top. Bed 14b: Light grey to beige brown calcareous siltstone. Irregular base and top (hence variable thickness). Contains frequent buchiid bivalves. Bed 14c: Same lithology as 14a, but unfossiliferous. Bed 14d: Light grey to beige brown calcareous siltstone. Irregular base and top.
15	43cm	nodiger	--	Grey fine to medium grained sandstone with occasional coarser carbonate-rich skeletal layers and darker, finer grained wavy bedding. Some indication of synsedimentary folding and faulting, as well as some small scale cross laminations. Very sparse macrofauna, limited essentially to bivalves.
16	41cm	nodiger	--	Blue-grey fine to medium grained sandstone with matrix-supported conglomeratic base. Moderately well cemented, with clasts composed of rounded phosphorite and phosphatised internal casts of bivalves and ammonites. The sandstone contains an abundant macrofauna of belemnites and ammonites, including three dimensionally preserved <i>Craspedites kashpuricus</i> still with blue-green nacreous coats, and rarer <i>Craspedites nodiger</i> .
17	55cm	nodiger	K9	Fine grained sandstone. Creamy-beige at base, grades to grey at top, with increasing numbers of grey sand lenses towards the top. Evidence of synsedimentary folding. Sparse macrofauna, limited to occasional specimens of <i>C. kashpuricus</i> and <i>Buchia volgensis</i> .
18	10cm	unzoned	K10	Bituminous shale. Layers of indurated black platy sediment (very organic-rich) are interspersed by laterally discontinuous grey shale horizons.
19	36cm	unzoned	K11 K12	Well laminated, poorly cemented sandstone. Rapidly fining up at base from medium to fine grained. Contains rare small bivalves as only evident macrofauna. Charcoal fragments at the very top of the bed.
20	8cm	unzoned	--	Grey, massively bedded fine-medium grained sandstone. Unfossiliferous.
21	32cm	unzoned	K13	Variably coloured medium grained sandstone with variably coloured, variable grainsize lenses, and fine grained, dark, organic-rich laminae. Glauconitic matrix. Base of the bed is marked by an inconsistently developed string of phosphatic nodules. Unfossiliferous.

Table 4.2: continued

Bed	Thickness	Ammonite Zone	Sample number	Sedimentological description
22	30cm	'Aucella' coquina	--	Fining upwards grey sandstone. Medium grain size at base, fine grained at top. Contains abundant bivalve fossils of the genus <i>Buchia</i> , and rare ammonites of the genus <i>Surites</i> .
23	100cm	spasskensis tzikwinianus	K14(23a) K15(23a) K16 (23b)	23a: Fine-grained, grey-green, unfossiliferous calcareous siltstone at base, grading up to slightly coarser-grained extremely fossiliferous sandstone after the first ten centimetres. Sandstone matrix is glauconitic and contains abundant phosphatic nodules and internal casts of bivalves. Concentration of bivalve shells is such that the sediment is almost clast-supported. The dominant macrofauna are bivalves of the species <i>Buchia surensis</i> and <i>B. volgensis</i> (98% of fauna) and occasional belemnites (<i>Acroteuthis</i>) and rare ammonites (<i>Surites</i> , <i>Riasanites</i>). 23b: Dark grey poorly cemented clayey siltstone with phosphate concretions yielding ? <i>Acroteuthis</i> sp., and <i>Buchia keyserlingi</i> . Some bioturbation.
24	15cm	unzoned	K17	Dark brown medium grained, poorly cemented sandstone. Contains strings of elongate to subround phosphate concretions which hold three dimensionally preserved belemnites and ammonites. Matrix contains abundant belemnites. Erosional base.
25	14cm	unzoned	--	Light grey-brown, medium grained, well laminated and well cemented sandstone. Irregular base, where sandstone laminae 'drape' into pits in the upper surface of Bed 24. Micaceous, well sorted, bimodal.
26	12cm	unzoned	K18	Light grey-beige medium to fine grained sandstone with darker (organic-rich) flasers. Micaceous with ?secondary gypsum. Well cemented, bimodal.
27	175cm	unzoned	K19 K20 K21 K22	Fine dark grey clayey micaceous siltstone. Small scale cross stratification, and minor, inter-lamina erosional surfaces throughout. Cross sets climb at approximately 1.5°. Intensively burrowed. Horizontal burrows are lenticular to subround in cross section, and infilled with cream-white micaceous silt with secondary gypsum. Slightly coarser than host sediment. Vertical burrows tend to be slightly larger (0.5 cm diameter), and are infilled by dark, organic rich sediment. White microcrystals of secondary gypsum are abundant within the sediment laminae, at erosional surfaces, and infilling the burrows. Yellow secondary jarosite is abundant in fractures. Absence of body fossils.
28	15cm	unzoned	K23	Purple-brown clayey siltstone with dwarfed fauna of <i>pecten</i> -like bivalves. No gypsum.
29	260cm	unzoned	K24-K27	Same lithology as Bed 27, but lower intensity of burrowing.
30	120cm	unzoned	K28-K30	Slightly finer than Bed 29, but less burrowing, none at the top. No apparent structure.

underlying lenticular siltstones by a pronounced erosional contact. The nodiger Zone is more thickly developed than at Gorodische, comprising of three sandstone units. The lowermost of the three displays wavy and flaser structures of dark grey, possibly organic-rich sediment within fine-grained glauconitic sandstone. Bed 16 is marked by an irregular base with scattered phosphatic nodules. The upper unit of this zone (Bed 17) is generally finer-grained than the preceding two, and displays lenticular bedding towards the top.

The Jurassic-Cretaceous boundary at Kashpir is marked by a layer of splintery bituminous shale with scattered, laterally discontinuous shale horizons (Bed 18). This is overlain by three layers of finely laminated to lenticular-bedded sandstone (beds 19-21). These units are unzoned but presumably of Early Ryazanian age since they are indirectly overlain by deposits of the spasskensis Zone. Below the base of the spasskensis Zone is a grey-green glauconitic sandstone unit (Bed 22) referred to as the '*Aucella coquina*' by Blom *et al.* (1984). Bed 23a is similar in sedimentology to bed 22, but with a much higher density of shelly material. This bed spans the spasskensis Zone and the lower part of the tzikwinianus Zone. Bed 23b is a unit of grey siltstone bearing phosphatic concretions and internal moulds of *Buchia keyserlingi*. This represents the upper part of the tzikwinianus Zone.

The top of the Ryazanian is marked by an erosional surface above which lies a coarse-grained poorly cemented sandstone bearing strings of phosphatic concretions. This unit (Bed 24) has previously been suggested to be of Valanginian age (Blom *et al.*, 1984). This is overlain by 20cm of unzoned sandstone layers (beds 25 & 26), and a further 6 metres of mica-rich siltstone (beds 27-30). The latter sequence is intensively burrowed at the base with lamina-scale cross stratification and erosional surfaces, but becomes progressively structureless towards the top. The section is capped by a medium-grained grey sandstone with carbonate concretions which frequently contain marine vertebrate remains.

4.1.3. Previous work on the Volga Sections

The Volgian lectostratotype at Gorodishche was discovered in an expedition by Pallas in 1801, and the first descriptions were by Murchison (1845) and Pavlov (1884)(Blom *et al.*, 1984). It has since been redescribed by Russian workers on several occasions. Lord *et al.* (1987) cited a description by Mesezhnikov (1977), an English language copy of which they deposited in the Library of the Geological Society of London (Lord *et al.*, 1987: p. 580). Unfortunately, this copy could not be found by the Geological Society on the present author's request, and the 'classic Russian description' used in this report is therefore the one given by Blom *et al.* (1984).

Correlation of the log provided by Mesezhnikov (in Blom *et al.*, 1984) for the Gorodische section with that of the present study is displayed in Figure 4.2. Low-resolution sedimentological descriptions (recognition of only major units and poorly described sedimentology), and loosely defined bed thicknesses by Blom *et al.* (1984) make such correlations problematic. However, several simple correlations can be made on the basis of key lithologies. Beds 12 and 14 of Blom *et al.* (1984) are described as "phosphorite conglomerates" (p. 121), and clearly correspond to beds 14 and 16 of the present study. Similarly, Bed 20 of Blom *et al.* (1984) is described as "clay...with numerous gypsum crystals" (p. 121), and correlates with Bed 20 of this investigation.

Beds 15-18 of the Russian workers are all described as grey calcareous sandstones containing glauconite, and are divided on the basis of ammonite faunal differences rather than sedimentology. This provides a simple means of correlation of this interval with beds 17 & 18 of the present investigation, and tie-points are indicated in Figure 4.2. Bed 19 of Blom *et al.* (1984) corresponds by default to the phosphorite horizon of the present study since adjacent units have already been correlated. However, the sedimentological description given by the Russian workers ("sandstone, conglomerate-like yellowish-grey, ferruginated, with numerous pebbles from underlying

Figure 4.2: Legend

Key to log 1: Lord *et al.* (1987)



Bituminous shale



Calcareous clay

Key to log 2: Hogg (1994)



(laminated) marl



Bituminous shale



'Shell rock'



Sandstone



Conglomerate
(with glauconite / phosphite)



Phosphoritic clay

Key to log 3: Mesezhnikov in Blom *et al.* (1984)



Pyroschist



Conglomerate



Sandstone



Marl



Lime clay

Key to log 4: present study



Weakly laminated dark grey siltstone



Lenticular bedded mudstone/siltstone



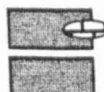
Well-laminated brown calcareous siltstone



Phosphorite deposit



Well-laminated grey calcareous siltstone



Sandstone with calcareous concretions



Sandstone



Light grey calcareous mudstone



Sandstone with shelly hash



Dark grey calcareous siltstone



Mica-rich siltstone



Mottled calcareous claystone



Conglomerate

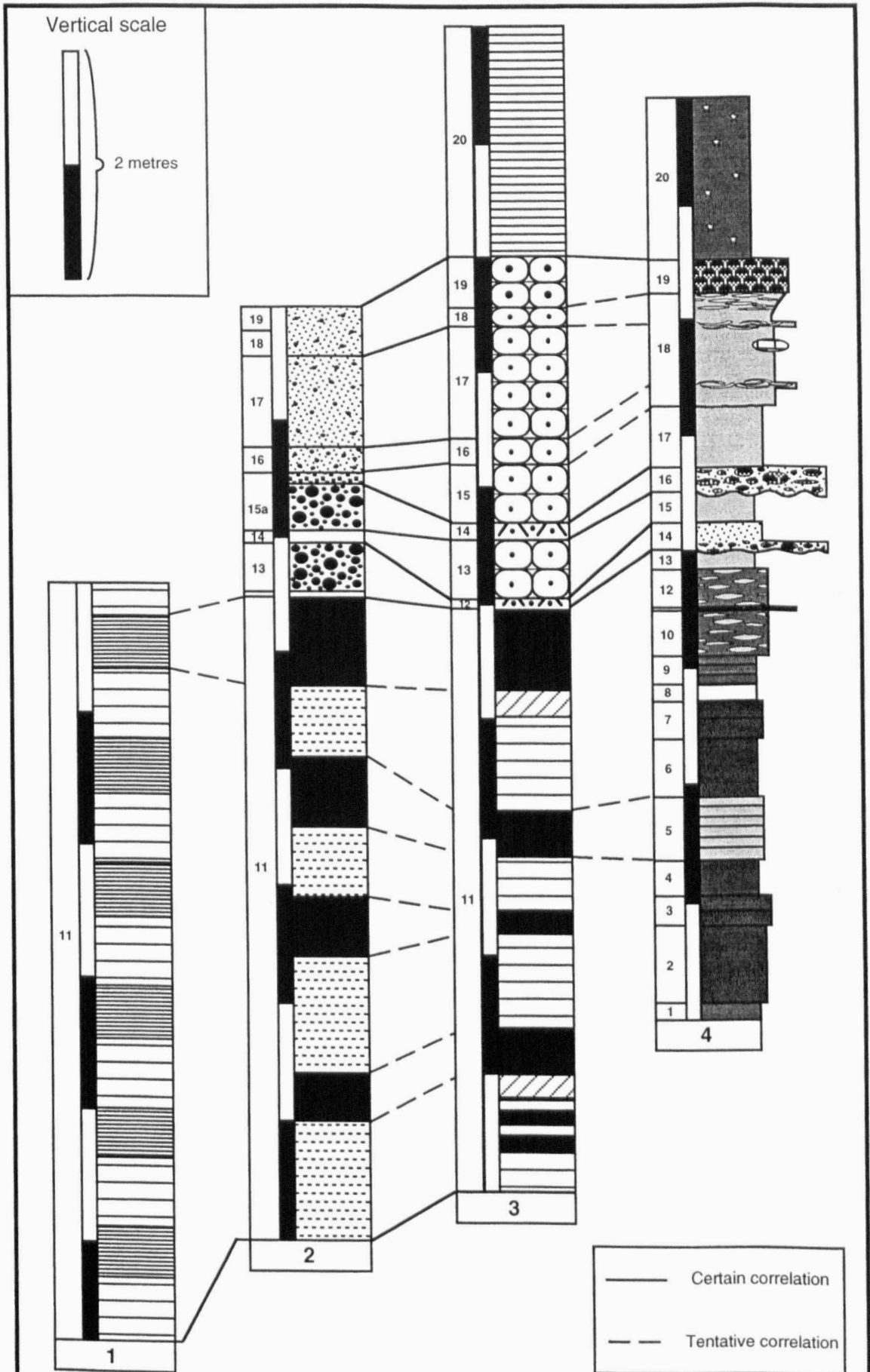


Figure 4.2: Correlation of Gorodische section sedimentary logs: 1; log given by Lord *et al.* (1987), after Mesezhnikov (1977); 2; log given in Hogg (1994), on basis of data supplied by VNIGRI; 3; log prepared by Mesezhnikov *in* Blom *et al.* (1984); 4; present study. Lines of correlation are based on lithology and ammonite zone boundaries indicated in each publication.

sandstone": Blom *et al.*, 1984; p.122) contrasts to that given here. This may suggest lateral variation in this unit, although none was observed in the field by the present author.

Bed 11 of Blom *et al.* (1984) correlates with beds 1-13 of the present study. In the log, black units within Bed 11 of Blom *et al.* (1984)(Fig. 4.2) are described as "pyroschist" in the log key (p. 71), and "bituminous, shaley dark gray brown clay (combustible shale)" in the bed descriptions (p. 121). These probably correlate to the laminated siltstone horizons of the current investigation. The 'laminated' lithology presented in the log is described as "lime clay" by Blom *et al.* (1984; p. 71), and probably corresponds to the calcareous mudstone units (beds 1, 2, 4, & 6) of the current study. The substantial thickness of lenticular siltstones present at the top of the zarajskensis Subzone is not represented in either the log or the sedimentological descriptions given by Blom *et al.* (1984).

The Volgian ammonite zonation of the section was detailed by Mikhailov (1966), Gerasimov & Mikhailov (1966), and Gerasimov (1969). Correlation of the Volgian and English zonations have been proposed by both Russian and English workers, but differ markedly in correlation of the Mid Volgian interval (Lord *et al.*, 1987). Most notable amongst these are the schemes of Kuznetsova (1978: after Gerasimov *et al.*, 1975) and Lord *et al.* (1987), who synthesised data by Casey (1967, 1973), Cope (1967, 1978), Wimbledon & Cope (1978), and Cox & Gallois (1981). The correlation of these two areas has already been presented in Figure 1.1, but comparison of the two main correlations mentioned above are also given in Figure 4.3 in order to emphasise the differences. Kuznetsova's (1978) correlation of the zarajskensis Subzone followed Arkell's (1956) suggestion that *Zaraskaites* and *Progalbanites* are synonymous. Lord *et al.* (1987), however, preferred to correlate the nikitini Zone and Albani Zone after the possible recognition of two specimens of *E. nikitini* in the Albani Zone by Cope (1978). More recently, Riding *et al.* (in press) have adopted the correlation of Kuznetsova (1978), although they did not discuss reasons for this preference in their text.

CHRONO-STRATIGRAPHY		E. England		CHRONO-STRATIGRAPHY		FIGURE 4.3: CORRELATION OF ENGLISH AND VOLGA BASIN AMMONITE ZONES						
						Lord <i>et al.</i> (1987)		Kuznetsova (1978)		Riding <i>et al.</i> (in press)		
RYAZANIAN	LATE	Albidum		RYAZANIAN						tzikwinianus		
		Stenomphalus								spasskensis		
EARLY		Icenii								kochi		
		Kochi								subclypiforme		
PORTLANDIAN		Runctoni								nodiger		
		Lamplughi				nodiger				nodiger		
		Preplicomphalus				subditus				subditus		
		Primitivus				fulgens				fulgens		
		Oppressus										
		Anguiformis										
		Kerberus										
		Okusensis						nikitini		nikitini		
		Glaucolithus						virgatus		virgatus		
		Albani										
VOLGIAN		Fittoni				nikitini				zarajskensis		
		Rotunda				virgatus		panderi		pavlovi		
		Pallasoides				panderi		zarajskensis		panderi		
		Pectinatus				pavlovi		pavlovi		pavlovi		
		Hudlestoni				pseudoscythicus		pseudoscythicus		pseudoscythicus		
		Wheatleyensis				sokolovi		sokolovi		sokolovi		
		Scitulus				klimovi		klimovi		klimovi		
		Elegans										
	KIMMERIDGIAN	EARLY	Autissiodorensis		KIMMERIDGIAN		autissiodorensis				autissiodorensis	
			Eudoxus				eudoxus				eudoxus	
		Mutabilis								acanthicus		
		Cymdoce								Beds with <i>Amoebites</i> and <i>Prorazenia</i>		
		Baylei										
OXF <i>pars</i>		Rosenkrantzi		OXF <i>pars</i>						ravni		

Palynology of the section at Gorodische has been studied by several authors. Lord *et al.* (1987), considered the dinoflagellate cyst biostratigraphy of eight samples spanning the interval from the Late Kimmeridgian Eudoxus Zone to the basal Mid Volgian zarajskensis Subzone. As such, only the uppermost of these samples, taken from Bed 11 of Mesezhnikov (1977) overlaps in age with the interval examined in the present report. The sedimentary log of the section provided by Lord *et al.* (1987) was taken from Mesezhnikov (1977), and is compared with other contributions, including the present study, in Figure 4.2. This log is apparently a generalised representation of Bed 11 as it presents many more 'bituminous shale' horizons than are indicated by Mesezhnikov in Blom *et al.* (1984).

Hogg (1994) studied the section in more detail, having analysed 28 samples from the Eudoxus to nodiger Zones. The log presented by him was based on data provided by VNIGRI, and is compared to other contributions in Figure 4.2. Despite the more detailed sample coverage, Hogg (1994) did not propose any dinocyst zonation for the section, and the taxonomic abundance charts he provided were not discussed in the text. Correlation of the Volgian and English ammonite successions followed Lord *et al.* (1987).

Riding *et al.* (in press) provided the most detailed account of the dinocyst biostratigraphy of the section, and presented a dinocyst zonation for the Bathonian to Ryazanian interval of the Russian Platform. 24 samples spanning the Eudoxus to nodiger Zones were examined, and although each sample is associated with a bed number as proposed by Blom *et al.* (1984), the exact position of the samples is not indicated. Precise comparison of the Riding *et al.* (in press) study with the present work is therefore impossible, but in general terms the uppermost ten samples of their analysis (samples RP56 to RP47) overlap with the interval considered here.

The section at Kashpir has been described by Pavlov (1884), Gerasimov (1969) and Blom *et al.* (1984). Correlation of the log provided by Mesezhnikov (in Blom *et al.*,

1984) and Lord *et al.* (1987) with that of the present study is presented in Figure 4.4. Once again, there are several key lithologies which afford simple horizons for correlation between these two studies. The coarse-grained deposits of the virgatus and nikitini zones are represented by beds 9-12 of Blom *et al.* (1984), and correspond to beds 4-9 of the current investigation. Similarly, bituminous shale Bed 6 of the Russian workers potentially correlates to the laminated siltstone, Bed 2 of the present study. The bituminous shale horizon of Bed 18 (current investigation) corresponds to the "bituminous....combustible shale" unit (Bed 20) of Blom *et al.* (1984). Beds 21-24 of the current investigation are strongly correlated with beds 22-26 of Blom *et al.* (1984) on the basis of the sedimentological descriptions given by them. In particular the Valanginian sandstone bearing phosphatic concretions (Bed 24 of the current report) correlates to Bed 26 of Blom *et al.* (1984), described as "conglomerate...wax-red consists of abundant phosphorite pebbles" (p. 124). The mica-rich siltstones (beds 27-30) of the current investigation are not included in the log given by Blom *et al.* (1984).

Palynology of this section was briefly considered by Lord *et al.* (1987) from two samples taken from the zarajskensis Subzone (beds 5 & 7 of Blom *et al.*; 1984). Recently Riding *et al.* (in press) analysed nine samples from the zarajskensis Subzone (Mid Volgian) to spasskensis Zone (earliest Late Ryazanian) interval. The top five samples correspond to the interval examined in the present report.

Figure 4.4: Legend

Key to log 1: Lord *et al.* (1987)



Bituminous shale



Calcareous clay

Key to log 2: Mesezhnikov in Blom *et al.* (1984)



Pyroschist



Conglomerate



Sandstone



Marl



Aleurolite



Lime clay



Bituminous shale

Key to log 3: present study



Well-laminated grey calcareous siltstone



Lenticular bedded mudstone/siltstone



Light grey calcareous mudstone



Phosphatised sandstone



Sandstone with phosphatic concretions



Sandstone with calcareous concretions



Sandstone



Thinly bedded sandstone



Sandstone with shelly hash



Bituminous shale



Mica-rich siltstones



Conglomerate

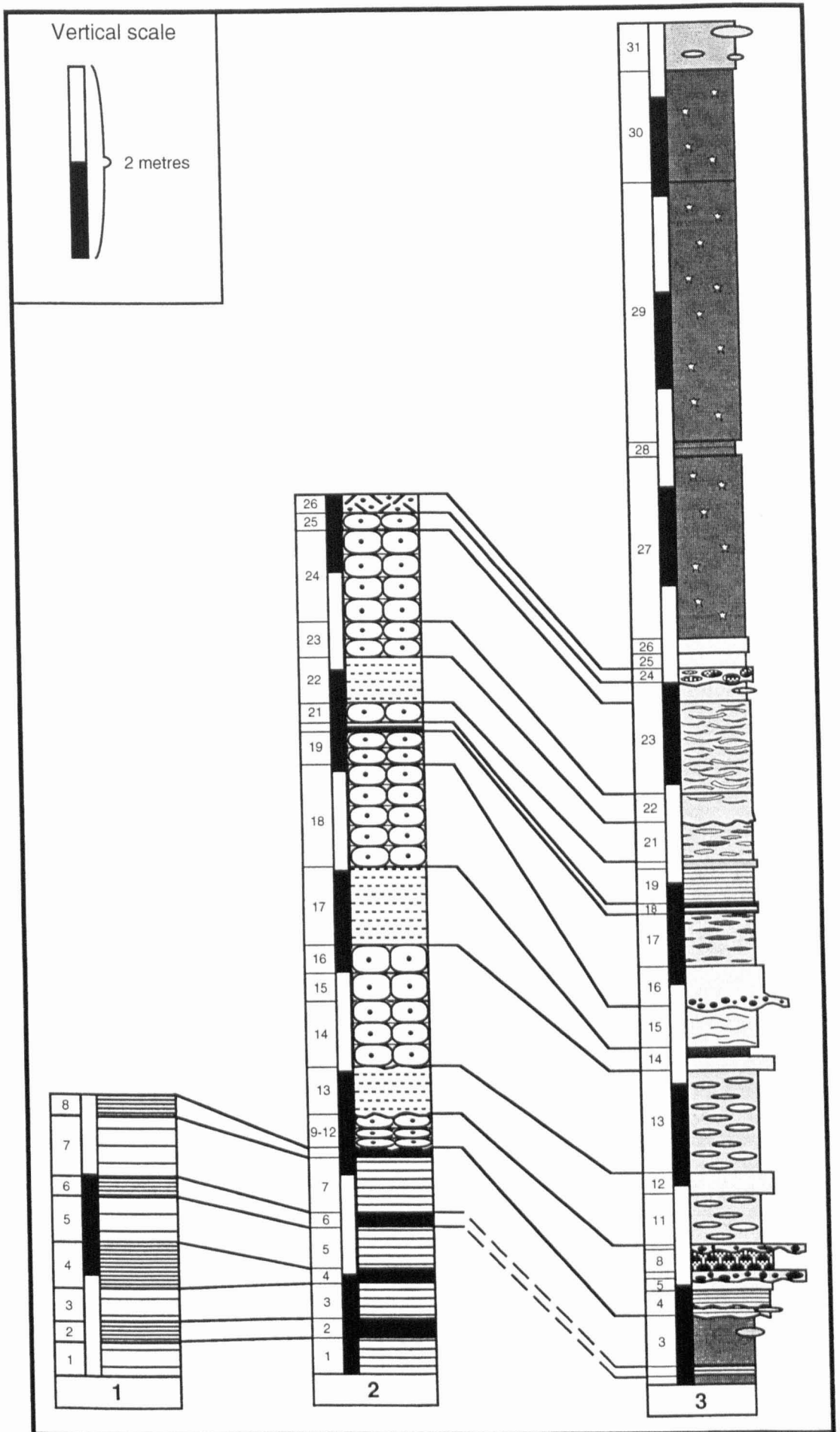


Figure 4.4: Correlation of Kashpir section sedimentary logs.
 1; Lord *et al.* (1987); 2; Mesezhnikov in Blom *et al.* (1984); 3; Present study.

4.2. Dinocyst biostratigraphy and zonation of the Volga Basin.

4.2.1. Introduction.

In the following sections, dinoflagellate cyst biostratigraphy at the two Volga Basin localities is considered. Range tables containing percentage abundance information are presented for Gorodische in Table 4.3 and Kashpir in Table 4.4. Actual count data are provided in Appendices D and E of the floppy disc (back cover). The ranges of stratigraphically useful taxa are plotted in Figures 4.5 (Gorodische) and 4.6 (Kashpir). Dinocyst first appearance data (FADs) and last appearance data (LADs) are indicated for each ammonite zone, along with the typical assemblage compositions. Useful biostratigraphic markers noted in the present study are compared with those elsewhere in the Russian Platform and in NW Europe. Where possible these data are used to correlate ammonite-zoned sequences, or to date Volga Basin sediments which do not have ammonite control. FADs shown to have similar stratigraphic position across the Russian Platform or in NW Europe are used to augment and extend the dinocyst zonation recently proposed by Riding *et al.* (in press). Typical dinocyst assemblages from each zone are described.

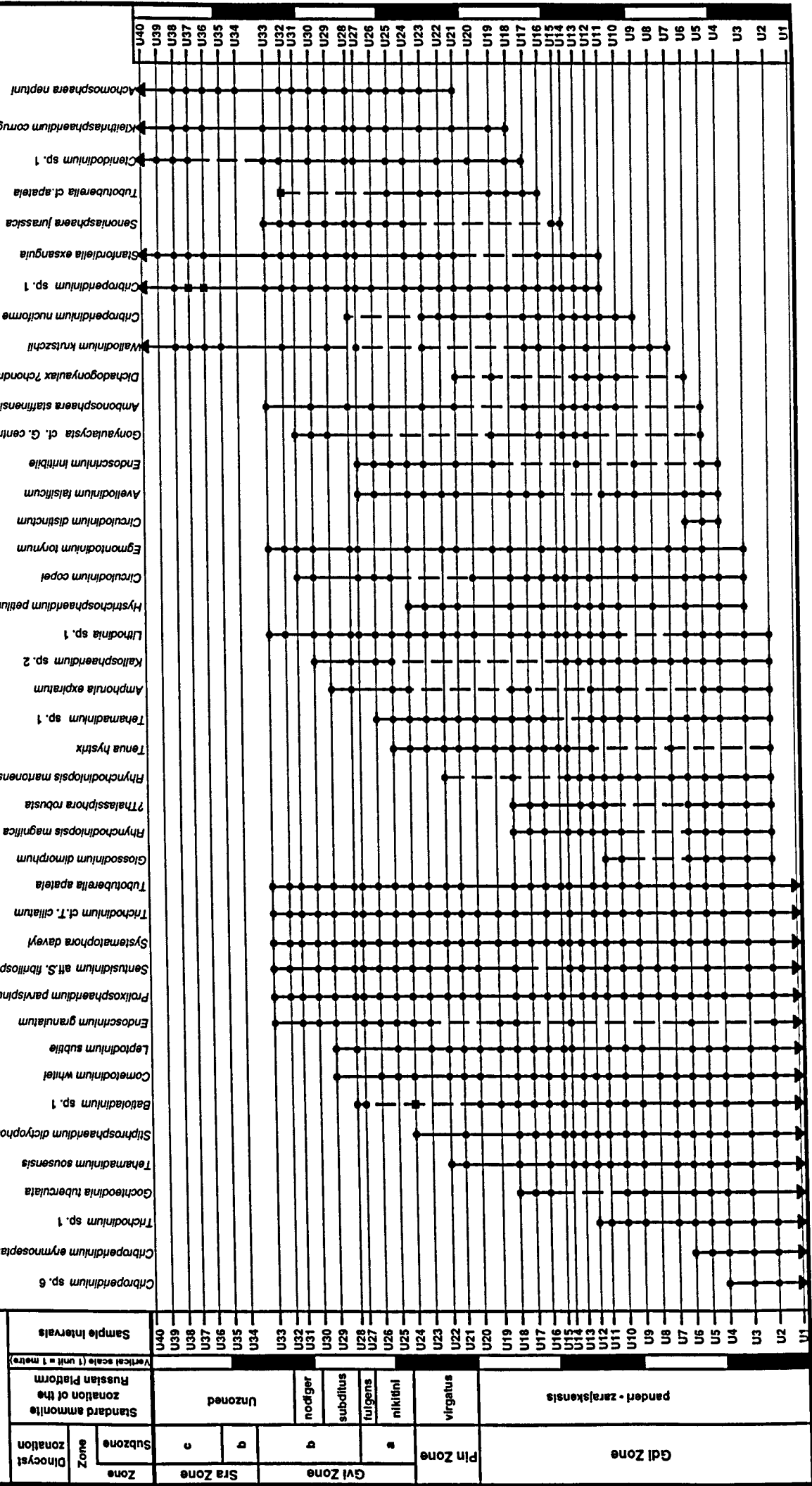
4.2.2. Dinocyst biostratigraphy of the Gorodische section.

Numerous taxa were encountered across the entire stratigraphic interval examined at Gorodische (Table 4.3). These include *Cassiculosphaeridia magna*, *Cassiculosphaeridia reticulata*, *Chlamydochorella nyei*, *Chytroisphaeridia chytroides*, *Dapsilidinium multispinosum*, *Dingodinium tuberosum*, *Gonyaulacysta* spp., *Heslertonia* sp. 1, *Hystrichodinium pulchrum*, *Pareodinia ceratophora*, *Sirmiodinium grossi*, *Tanyosphaeridium magneticum*, and *Wrevittia* spp.

Sample	<i>Stiphosphaeridium anthophorum</i>	<i>Circulidinium compta</i>	<i>Gonyaulacysta speciosa</i>	<i>Tenua cf. T. hystrix</i>	<i>Pseudoceraium pelliciferum</i>	<i>Warrenia brevispinosa</i>	<i>Downlesphaeridium</i> sp. 2	<i>Systematophora</i> sp. 1	<i>Impletosphaeridium lumentum</i>	<i>Muderongia longicoma</i>	<i>Oligosphaeridium complex</i>	<i>Phoberocysta neocomica</i>	<i>Sentusidium</i> sp. 4	<i>Spiriferites ramosus</i>	<i>Baliodinium radiculatum</i>	<i>Nelchtopsia kostromlensis</i>	<i>Sentusidium</i> cf. sp. 3	<i>Baliodinium jaegeri</i>	<i>Aprobolocysta galeata</i>	<i>Gardodinium</i> sp. 1	<i>Baliodinium gochitii</i>	<i>Cometodinium habbilli</i>	<i>Exochosphaeridium phragmites</i>	<i>Endoscrinium campanula</i>	<i>Lithodina bullioidea</i>	<i>Lithodina acranitabulata</i>	<i>Spiriferites primaevus</i>	<i>Phoberocysta tabulata</i>	<i>Spiriferites</i> sp. 2.	<i>Cymosphaeridium validum</i>	dinocest total	
U40	3.31	0.33	0.66						9.27	0	4.97	0.99	2.65	6.95	0.33	3.31	3.31				0.99	4.97	0.66	0	0.66	0	0.33		0.33	0.33	302	
U39		3.5	0	0.7					8.39	0.35	7.34	0.35	2.1	6.99	0.35	2.8	2.45				2.45	0.7	6.99	0	1.4	0.35	0	1.05	0.35	0.7	0.35	286
U38	4.86		0.35						8.33	0	7.29	1.39	2.43	6.6		3.47	2.43	0			1.04	0.35	5.21	0.35	1.04	0.35	0	0.69	1.04	1.39	288	
U37	9.97	0.34	1.37	0					5.5	0	2.75	0.34	4.81	4.47	0.34	3.09	3.44	0.34	1.03	1.72	1.03	2.41	0.69	0	0	0	0	1.03	0		291	
U36	3.72	0.34	0.66						5.5	0	2.75	0.34	4.81	4.47	0.34	3.09	3.44	0.34	1.03	1.72	1.03	2.41	0.69	0	0	0	0	1.03	0		296	
U35	1.79								0.6	0.6	1.19	1.19	0.6	7.14	0.6	29.8	5.36	0.6	0.6													168
U34	0.67								0.67	0.67	13.4	0.67	33.6	0.67																		149
U33	2.81	3.66																														285
U32				4.43																												271
U31	0.74	4.06																														276
U30	0.72	3.62	0.36																													291
U29	0.34	1.72																														290
U28																																277
U27																																291
U26																																295
U25																																273
U24																																291
U23																																284
U22																																287
U21																																140
U20																																301
U19																																297
U18																																307
U17																																191
U16																																269
U15																																269
U14																																268
U13																																268
U12																																279
U11																																309
U10																																289
U9																																290
U8																																265
U7																																263
U6																																307
U5																																275
U4																																287
U3																																305
U2																																275
U1																																275

Table 4.3: Continued.

Figure 4.5a: Dincyst biostratigraphy of the section at Gorodische.



Mid Volgian (panderi Zone, zarajskensis Subzone to nikitini Zone)

Stratigraphically restricted taxa which range and consistently occur through the Mid Volgian interval at Gorodische include; *Cometodinium whitei*, *Hystrichosphaeridium petilum*, *Kleithriasphaeridium fasciatum*, *Lithodinia* sp. 1, *Prolixosphaeridium parvispinum*, *Systematophora daveyi*, *Tehamadinium* sp. 1, *Trichodinium* cf. *ciliatum*, and *Tubotuberella apatela*. In addition *Tenua hystrix* and *Cribroperidinium* sp. 1 appear consistently in the upper part of this interval.

Panderi Zone

Twenty of the samples collected at Gorodische were taken from the panderi Zone, zarajskensis Subzone. The assemblages are typically dominated by *Dingodinium tuberosum* (9.3-36.4%) with abundant *Chytroeisphaeridia chytroeides* (1.7-10.1%) and *Systematophora daveyi* (0.6-18.5%)(Table 4.3). Indeed, *D. tuberosum* and *C. chytroeides* have maximum abundance in the panderi Zone. Also sporadically important in terms of abundance are *Trichodinium* sp. 1 (0-10.6%) and *Sirmiodinium grossi* (0-4.3%). Conversely the occurrence of *C. nyei* is most inconsistently recognised within this zone (Table 4.3).

Common taxa which range through the zarajskensis Subzone include *Batioladinium* sp. 1 (0-2.4%), *Cometodinium whitei* (0-26.4%), *Kleithriasphaeridium fasciatum* (0.3-9.5%), *Leptodinium subtile* (0-4.6%), *Prolixosphaeridium parvispinum* (0-5.6%), *Sentusidinium* sp. 3 (0-4.7%), *Tehamadinium sousense* (0-3.6%), *Trichodinium* cf. *ciliatum* (0-1.8%), and *Tubotuberella apatela* (0-1.1%)(Table 4.3). Of these *C. whitei*, *G. tuberculata*, *B.* sp., and *T. sousense* have maximum abundance and most consistent occurrence within this subzone (Table 4.3). Conversely *T. cf. ciliatum* and *T. apatela* are least consistently observed and show least abundance through this interval.

Taxa with LADs in the panderi Zone, and therefore with range-tops potentially restricted to this zone include *Cribroperidinium erymnoseptatum*, *Cribroperidinium* sp. 6, *Glossodinium dimorphum*, *Gochteodinia tuberculata*, *Rhynchodiniopsis magna* sp. nov., *Stiphrosphaeridium dictyophorum*, ?*Thalassiphora robusta* sp. nov., and *Trichodinium* sp. 1 (Table 4.3, Figure 4.5a).

Taxa which occur in the basal sample from the studied interval (sample U1), and therefore with FADs which probably occur below it include; *Cribroperidinium erymnoseptatum*, *Cribroperidinium* sp. 3, *Cribroperidinium* sp. 6, *Endoscrinium granulatum*, *Gochteodinia tuberculata*, *Stiphrosphaeridium dictyophorum*, *Trichodinium* sp. 1 (Table 4.3, Figure 4.5a), as well as those already mentioned to range through this subzone. Taxa with FADs above the base of the studied interval (in or above sample U2), and therefore with range bases which may occur within the zarajskensis Subzone include; *Ambonosphaera?* *staffinensis*, *Amphorula expiratum*, *Avellodinium falsificum*, *Egmontodinium torynum*, *Endoscrinium inritibile*, *E. pharo*, *Circulodinium distinctum*, *Cribroperidinium* sp. 1, *C. nuciformum*, *Ctenidodinium* sp. 1., *Dichadogonyaulax ?chondrum*, *Glossodinium dimorphum*, *Hystrichosphaeridium petilum*, *Kallosphaeridium* sp. 2, *Kleithriasphaeridium corrugatum*, *Rhynchodiniopsis magna*, *R. martonense*, *Senoniasphaera jurassica*, *Stanfordella exsanguia*, *Tehamadinium* sp. 1, *Tenua hystrix*, ?*Thalassiphora robusta*, and *Wallodinium krutzschii*.

Virgatus Zone

Most abundant within the dinocyst assemblages of this zone are *Chlamydophorella nyei* (1.8-7.2%), *Dingodinium tuberosum* (0.3-4.9%), *Epiplosphaera gochti* (0.4-5.9%), *Systematophora daveyi* (3.5-6.9%), *Tenua hystrix* (1.4-8.8%), and *Trichodinium* cf. *ciliatum* (1.4-7%). Other taxa which range through this zone and are consistently observed within it include *Avellodinium falsificum*, *Cassiculosphaeridia magna*, *Cassiculosphaeridia reticulata*, *Chytroeisphaeridia chytroeides*, *Cribroperidinium* sp. 1, *Gonyaulacysta pectinigera*, *Hystrichodinium pulchrum*,

Hystrichosphaeridium petilum, *Kleithriasphaeridium fasciatum*, *Lithodinia*, sp. 1, *Perisseiasphaeridium ingegerdiae*, *Prolixosphaeridium parvispinum*, *Sentusidinium* sp. 3, *Sirmiodinium grossi*, *Tanyosphaeridium magneticum*, *Tehamadinium* sp. 1, *Tubotuberella apatela*, and *Wrevittia* spp. (Table 4.3, Figure 4.5b).

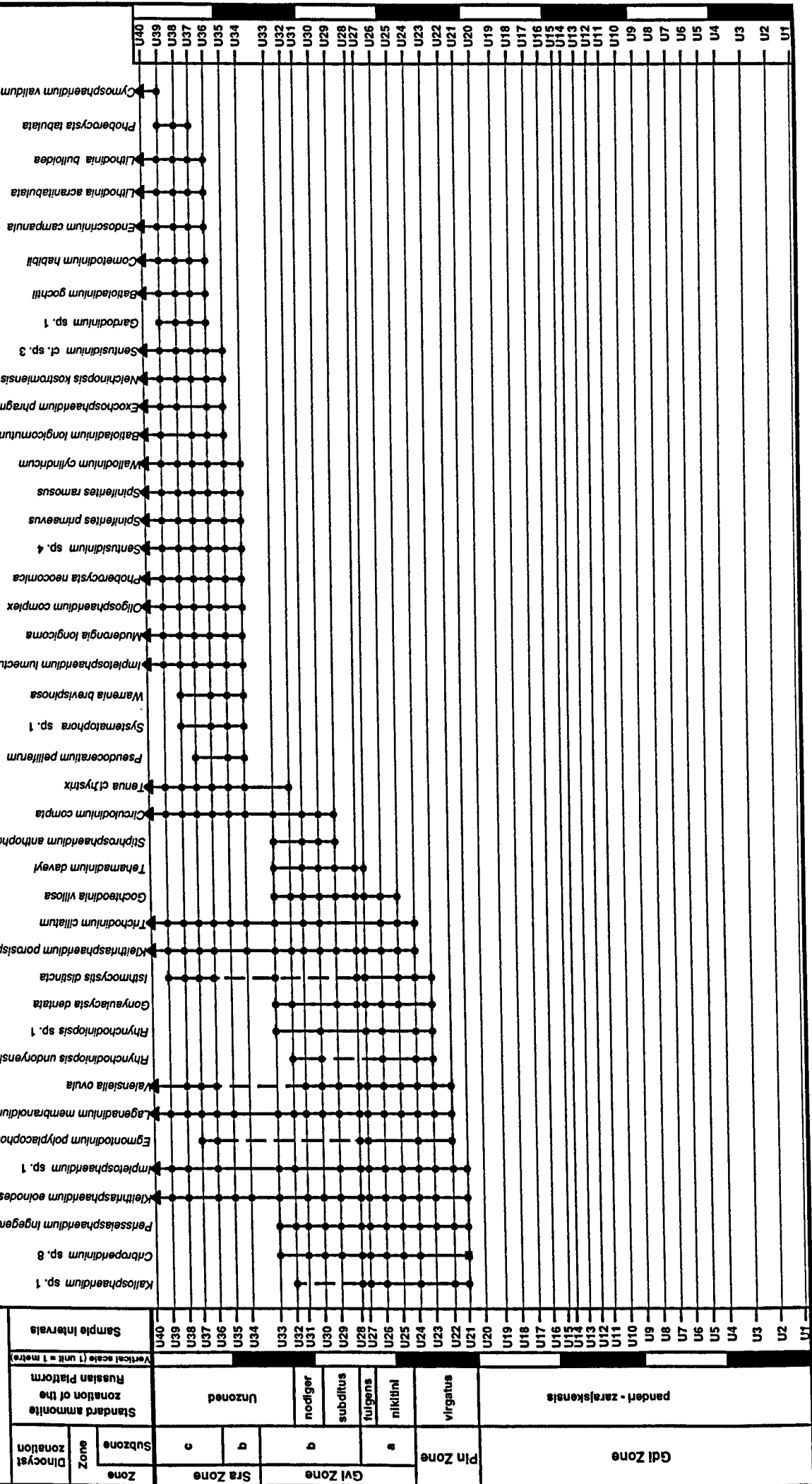
Taxa with LADs in the *virgatus* Zone include *Dichadogonyaulax ?chondrum*, *Hystrichosphaeridium petilum*, and *Tehamadinium sousense*. Taxa with FADs in this zone include *Achomosphaera neptuni*, *Egmontodinium polyplacophorum*, *Gonyaulacysta dentata*, *Impletosphaeridium* sp. 1, *Isthmocystis distincta*, *Kallosphaeridium* sp. 1, *Kleithriasphaeridium eoinodes*, *Kleithriasphaeridium porosispinum*, *Lagenadinium ?membranoidium*, *Cribroperidinium* sp. 8, *Perisseiasphaeridium ingegerdiae*, *Rhynchodiniopsis* sp. 1, *Sentusidinium rioultii*, *Trichodinium ciliatum*, and *Valensiella ovula*.

Nikitini Zone

Most abundant within the dinocyst assemblages of this zone are *Systematophora daveyi* (5.1-7.5%) and *Trichodinium cf. ciliatum* (4.4-5.5%)(Table 4.3). *Achomosphaera neptuni*, *Circulodinium copei*, *Gochteodinia villosa*, *Gonyaulacysta dentata*, *Impletosphaeridium* sp. 2, *Kleithriasphaeridium eoinodes*, *Kleithriasphaeridium porosispinum*, *Lagenadinium ?membranoidium*, *Perisseiasphaeridium ingegerdiae*, *Senoniasphaera jurassica*, *Tehamadinium* sp. 1, *Trichodinium ciliatum*, and *Valensiella ovula* are also commonly observed in both samples.

Tehamadinium sp. 1 and *Tenua hystrix* are the only taxa to have LADs in the *nikitini* Zone. *Gochteodinia villosa* has its first occurrence at the base of this zone (Table 4.3, Figure 4.5b).

Figure 4.5b: Dinocyst biostratigraphy of the section at Gorodische



Late Volgian (fulgens to nodiger zones)

Stratigraphically restricted taxa which range and consistently occur through the Late Volgian interval at Gorodische include; *Achomosphaera neptuni*, *Cribroperidinium* sp. 1, *Cribroperidinium* sp. 2, *Egmontodinium torynum*, *Endoscrinium granulatum*, *Gochteodinia villosa*, *Gonyaulacysta dentata*, *Kleithriasphaeridium corrugatum*, *K. eoinodes*, *K. fasciatum*, *K. porosispinum*, *Lagenadinium ?membranoidium*, *Cribroperidinium* sp. 8, *Lithodinia* sp. 1, *Perisseiasphaeridium ingegerdiae*, *Prolixosphaeridium parvispinum*, *Senoniasphaera jurassica*, *Sentusidinium* aff. *?fibrillospinosum*, *Stanfordella exsanguia*, *Systematophora daveyi*, *Tehamadinium daveyi*, *Trichodinium* cf. *ciliatum*, *Tubotuberella apatela*, *Valensiella ovula*, and *Wrevittia* spp..

Fulgens Zone

Dinocyst assemblages of this zone are dominated by *Systematophora daveyi* (12.6-24.1%). Other common elements include *Cassiculosphaeridia reticulata* (2.9-3.5%), *Chlamydophorella nyei* (2.4-2.5%) *Cribroperidinium* sp. 2 (1.4-2.9%), *Hystrichodinium pulchrum* (2.2-2.8%), *Kleithriasphaeridium corrugatum* (1.4-3.3%), *K. eoinodes* (3.6-3.8%), *K. porosispinum* (2.1-4.5%), *Lagenadinium ?membranoidium* (1-4.3%), *Perisseiasphaeridium ingegerdiae* (2.9-4.1%), *Sentusidinium* sp. 3 (2.5-3.5%), *Trichodinium* cf. *ciliatum* (4.1-4.6%) and *Tubotuberella apatela* (0.3-2.1%)(Table 4.3). Other taxa with stratigraphically restricted ranges which were recognised in both samples are *Batioladinium* sp. 1, *Ctenidodinium* sp. 1, *Egmontodinium torynum*, *Kleithriasphaeridium fasciatum*, *Prolixosphaeridium parvispinum*, and *Senoniasphaera jurassica*.

Taxa with LADs in the fulgens Zone include *Avellodinium falsificum*, *Batioladinium* sp. 1, *Chytroeisphaeridia cerastes*, and *Endoscrinium inritibile*. *Tehamadinium daveyi* has its FAD in this zone at Gorodische (Table 4.3, Figure 4.5b).

Subditus Zone

The two samples from this zone are dominated by *Perisseiasphaeridium ingegerdiae* (8.3-11%), and *Systematophora daveyi* (14.4-16.7%) (Table 4.3). Other common elements include *Chlamydothorella nyei* (1.7-2.2%), *Cribroperidinium* sp. 1 (2.5-4.1%), *Cribroperidinium* sp. 2 (0.7-2.4%), *Gochteodinia villosa* (2.9-3.8%), *Hystriodinium pulchrum* (1.7-4.4%), *Kleithriasphaeridium corrugatum* (0.7-2.9%), *K. eoinodes* (1.5-1.7%), *K. porosispinum* (1.4-2.5%), *Lagenadinium ?membranoidium* (1-1.5%), *Senoniasphaera jurassica* (2.1-5.2%), *Sentusidinium* sp. 3 (2.8-2.9%), *Tehamadinium daveyi* (4.1-4.4%), *Trichodinium* cf. *ciliatum* (3.6-6.2%).

Taxa with LADs in the subditus Zone include *Cometodinium whitei*, *Kallosphaeridium* sp. 2, and *Leptodinium subtile*. *Circulodinium compta* and *Stiphrosphaeridium anthophorum* have FADs in this zone (Figure 4.5b).

Nodlger Zone

Both residues from this zone are dominated by *Systematophora daveyi* (11.4-12.9%), with an acme occurrence of *Trichodinium* cf. *ciliatum* (9.6%) noted in sample U31 (Table 4.3). Other significant taxa recognised in both samples are *Chlamydothorella nyei*, *Cribroperidinium* sp. 1, *Dingodinium tuberosum*, *Egmontodinium torynum*, *Gochteodinia villosa*, *Hystriodinium pulchrum*, *Kleithriasphaeridium fasciatum*, *K. porosispinum*, *Lagenadinium ?membranoidium*, *Perisseiasphaeridium ingegerdiae*, *Prolixosphaeridium parvispinum*, *Senoniasphaera jurassica*, *Sentusidinium* sp. 3, *Stanfordella exsanguia*, and *Tubotuberella apatela*.

Taxa with LADs in this zone, and therefore with range tops restricted to the Volgian at Gorodische include *Circulodinium copei*, and *Kallosphaeridium* sp. 1. No taxa have FADs in the nodiger Zone (Figure 4.5b).

?Lower Cretaceous

Phosphorite horizon

Dinocyst assemblages of this horizon are dominated by long-ranging taxa such as *Chytroeisphaeridia chytrooides* (7%), *Hystriodinium pulchrum* (8.8%), and an abundance of the taxon group "*Cleistosphaeridium aciculum*" (12.3%) (Table 4.3). Of the stratigraphically important taxa with ranges extending both above and below this horizon, *Circulodinium compta*, *Kleithriasphaeridium* spp., *Lagenadinium membranoidium*, *Sirmiodinium grossi*, *Trichodinium ciliatum*, and *Wrevittia* spp. are also numerically important.

Taxa with LADs in sample U33 include; *Egmontodinium torynum*, *Endoscrinium granulatum*, *Gochteodinia villosa*, *Cribroperidinium* sp. 8, *Lithodinia* sp. 1, *Perisseiasphaeridium ingegerdiae*, *Prolixosphaeridium parvispinum*, *Rhynchodiniopsis* sp. 3, *Senoniasphaera jurassica*, *Epiplosphaera gochtii*, *Stiphrosphaeridium anthophorum*, *Systematophora daveyi*, *Tehamadinium daveyi*, *Trichodinium* cf. *ciliatum*, *Tubotuberella apatela*, and *T. dentata*. No taxa have FADs within this horizon (Figure 4.5b).

Lower Cretaceous

Unzoned mica-rich siltstones

Shortly above the phosphorite deposit (particularly from sample U36), the dinocyst assemblages are dominated by the long ranging taxa *Chlamydophorella nyei* (0-12.6%) and *Dingodinium tuberosum* (0-7.3%). *Sentusidinium* sp. 4 is the most abundant taxon in samples U34 & U35 (33.6% and 29.8% respectively)(Table 4.3). Also common

in this interval are *Cassiculosphaeridia reticulata* (0-7.3%), *Circulodinium compta* (0.7-10%), *Cometodinium habibii* (0-7%), *Impletosphaeridium lumectum* (0.7-9.3%), *Lagenadinium ?membranoidium* (0-7.3%), *Nelchinopsis kostromiensis* (0-4.7%), *Oligosphaeridium complex* (1-13.4%), and *Spiniferites ramosus* (0.7-7%).

The LAD of *Endoscrinium pharo* occurs within this interval at Gorodische. Taxa with FADs above the phosphorite deposit include: *Impletosphaeridium lumectum*, *Muderongia longicorna*, *Oligosphaeridium complex*, *Phoberocysta neocomica*, *Pseudoceratium pelliferum*, *Sentusidinium* sp. 4, *Spiniferites ramosus*, and *Warrenia brevispinosa* (all in U34); *Batioladinium longicornutum*, *Nelchinopsis kostromiensis*, and *Sentusidinium* cf. sp. 3, (sample U35); *Aprobolocysta galeata*, *Batioladinium gochtii*, *Cometodinium habibii*, *Endoscrinium campanula*, *Exochosphaeridium phragmites*, *Gardodinium* sp. 1, *Lithodinia acranitabulata*, *Lithodinia bulloidea*, and *Spiniferites primaevus* (all in sample U36). Above this, *Phoberocysta tabulata* has its first occurrence in sample U37, *Spiniferites* sp. 2 in sample U38, and *Cymosphaeridium validum* in sample U39 (Figure 4.5b).

4.2.3. Dinocyst biostratigraphy of the section at Kashpir.

Several taxa span the entire interval examined at Kashpir, or have LADs just before the top of the section. These include *Chytroelsphaeridia chytrooides*, *Dingodinium tuberosum*, *Hystrichodinium pulchrum* and *Kleithriasphaeridium fasciatum*.

Upper Jurassic

Mid Volgian (panderi Zone, zarajskensis Subzone to nikitini Zone)

As indicated in Chapter 4.1., only the very top of the zarajskensis Subzone is exposed at Kashpir, and thus only two samples were collected from this interval. No samples were collected from the virgatus or nikitini zones at Kashpir.

Sample	K30	K29	K28	K27	K26	K25	K24	K23	K22	K21	K20	K19	K18	K17	K16	K15	K14	K13	K12	K11	K10	K9	K8	K7	K6	K5	K4	K3	K2	K1
<i>Gleasonium ditropium</i>																														
<i>Gochliodia tuberculata</i>																														
<i>Rhynchonidopsis marionense</i>																														
<i>Thalassipora? robusta</i>																														
<i>Hyaticosphaeridium petilum</i>																														
<i>Tamadrinum soussense</i>																														
<i>Dichadogonyaulax ?chondrum</i>																														
<i>Leptodinium subtile</i>																														
<i>Aplodinium sp. 3</i>																														
<i>Comatodinium whitei</i>																														
<i>Dingodinium jurassicum</i>																														
<i>Chitropendinium nucleiforme</i>																														
<i>Epiphoesera spp.</i>																														
<i>Systematophora daveyi</i>																														
<i>Amphorula exspiratum</i>																														
<i>Tenua hystrix</i>																														
<i>Libidinia sp. 1</i>																														
<i>Slipthrosphaeridium dictyophorum</i>																														
<i>Tubotuborella epaetia</i>																														
<i>Simiodinium grossi</i>																														
<i>Chitropendinium sp. 3</i>																														
<i>Chitropendinium sp. 1</i>																														
<i>Kallosphaeridium sp. 1</i>																														
<i>Prolixosphaeridium parvispinum</i>																														
<i>Hastieronia sp. 1</i>																														
<i>Paraecodia caratophora</i>																														
<i>Gonyaulacysta pectinifera</i>																														
<i>Sentusidinium sp. 3</i>																														
<i>Steniodella exaerangula</i>																														
<i>Chitropendinium spp.</i>																														
<i>Hysterochordium pulchrum</i>																														
<i>*Chitrosphaeridium aciculium*</i>																														
<i>Chytrosphaeridia chyroides</i>																														
<i>Dingodinium tuberosum</i>																														
<i>Kellichsphaeridium fasciatum</i>																														
<i>Wreavitia fastigiata</i>																														
<i>Trichodinium sp. 1</i>																														
<i>Baurkirchidium spp.</i>																														
<i>Rhynchonidopsis magnifica</i>																														
<i>Warrenia sp. 1</i>																														
<i>Athignaticysta glabra</i>																														
<i>Avellocladum fastidicum</i>																														
<i>Ambrososphaera staliensis</i>																														
<i>Trichodinium cf. T. ciliatum</i>																														
<i>Egmontocidium torynum</i>																														
<i>Endoscrium pharo</i>																														
<i>Chendodinium sp. 1</i>																														
<i>Cassidosphaeridia magna</i>																														
<i>Chlamydomphorella nyel</i>																														
<i>Downiesphaeridium spp.</i>																														
<i>Gonyaulacysta spp.</i>																														
<i>Tanyosphaeridium magnificum</i>																														
<i>Wallicladium kurzschli</i>																														
<i>Chitropendinium sp. 2</i>																														
<i>Gochliadonia cf. villosa</i>																														
<i>Semustidinium aff. ?librilium</i>																														

Table 4.4: Relative abundance and stratigraphic distribution of dinocyst taxa from the section at Kashyk. Values are percentages derived from the count data presented in Appendix E.

Panderi Zone, zarajskensis Subzone

The dinocyst assemblages of this zone are dominated by *Dingodinium tuberosum* (17-34%), with abundant *Cribroperidinium* sp. 1 (0.6-8.4%) and *Systematophora daveyi* (5.1-8%)(Table 4.4). Also numerically important are *Chytroeisphaeridia chytroeides* (0.6-3.9%), *Kleithriasphaeridium fasciatum* (1.8-3%), *Hystrichodinium pulchrum* (1.2-4.4%), and *Sirmiodinium grossi* (1.2-4.4%).

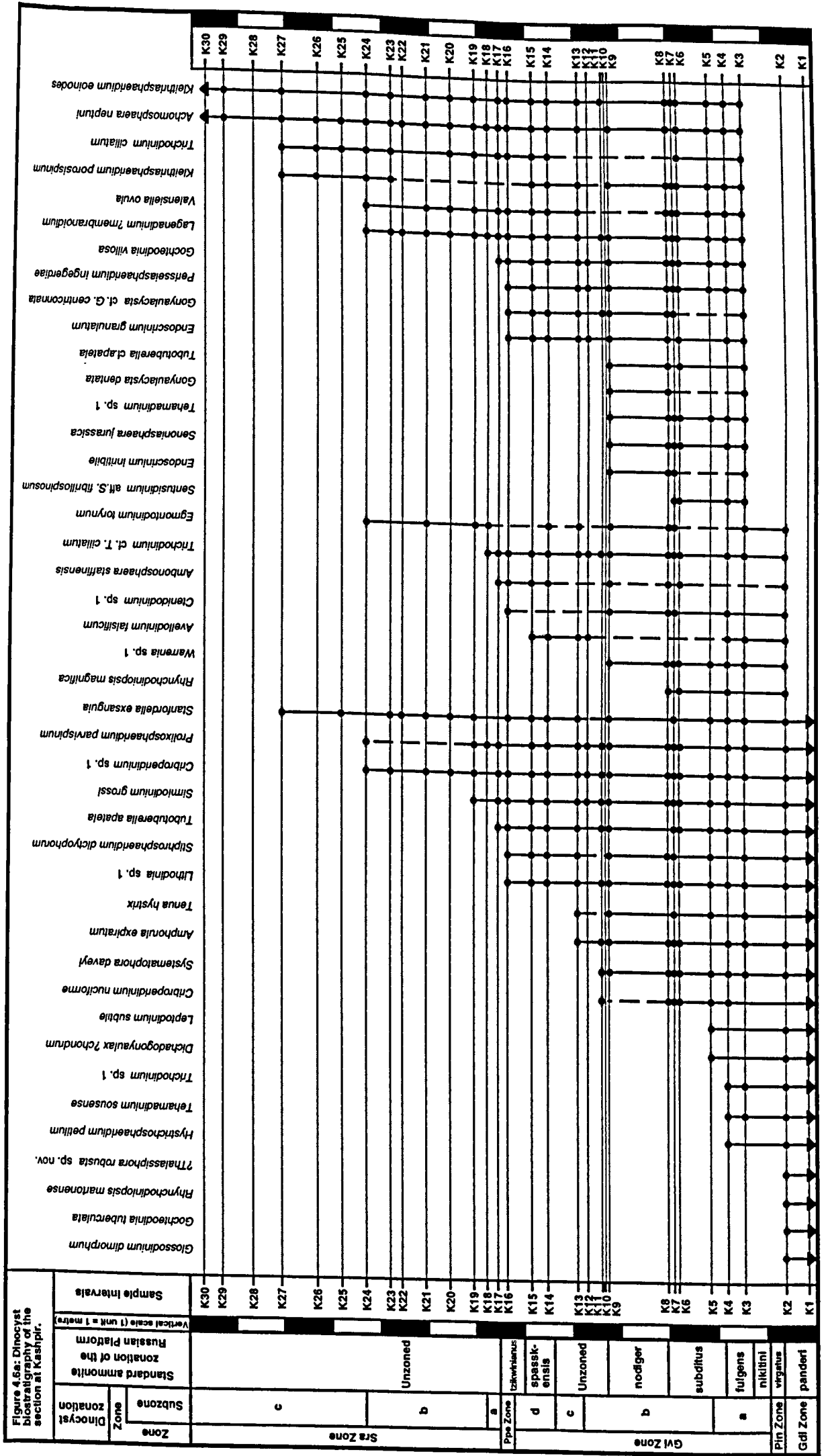
All of the taxa with FADs in the two samples collected from this subzone must be considered to range below the studied section. Stratigraphically useful taxa which thus range through the zarajskensis Subzone at Kashpir include; *Ambonosphaera staffinensis*, *Amphorula expiratum*, *Avellodinium falsificum*, *Cribroperidinium nuciforme*, *Cribroperidinium* sp. 1, *Dichadogonyaulax ?chondrum*, *Egmontodinium torynum*, *Hystrichosphaeridium petilum*, *Leptodinium subtile*, *Lithodinia* sp. 1, *Prolixosphaeridium parvispinum*, *Rhynchodiniopsis magnifica* sp. nov., *Sirmiodinium grossi*, *Stiphrosphaeridium dictyophorum*, *Systematophora daveyi*, *Tehamadinium sousense*, *Tenua hystrix*, *Trichodinium* sp. 1, *T. cf. ciliatum*, and *Tubotuberella apatela*.

Taxa with LADs in the panderi Zone at Kashpir include *Glossodinium dimorphum*, *Gochteodinia tuberculata*, *Rhynchodiniopsis martonense*, and *?Thalassiphora robusta* sp. nov. (Figure 4.6a).

Late Volgian (fulgens to nodiger zones)

Stratigraphically restricted taxa which range and consistently occur through the Late Volgian interval at Kashpir include; *Cribroperidinium* sp. 1, *Cribroperidinium* sp. 2, *Lithodinia* sp. 1, *Pareodinia ceratophora*, *Prolixosphaeridium parvispinum*, *Sentusidinium* sp. 3, *Sirmiodinium grossi*, *Stanfordella exsanguia*, *Stiphrosphaeridium*

Figure 4.6a: Dinocyst biostratigraphy of the section at Kashpir.



dictyophorum, *Systematophora daveyi*, *Trichodinium cf. ciliatum*, *Tubotuberella apatela*, and *Wrevittia* spp..

Fulgens Zone

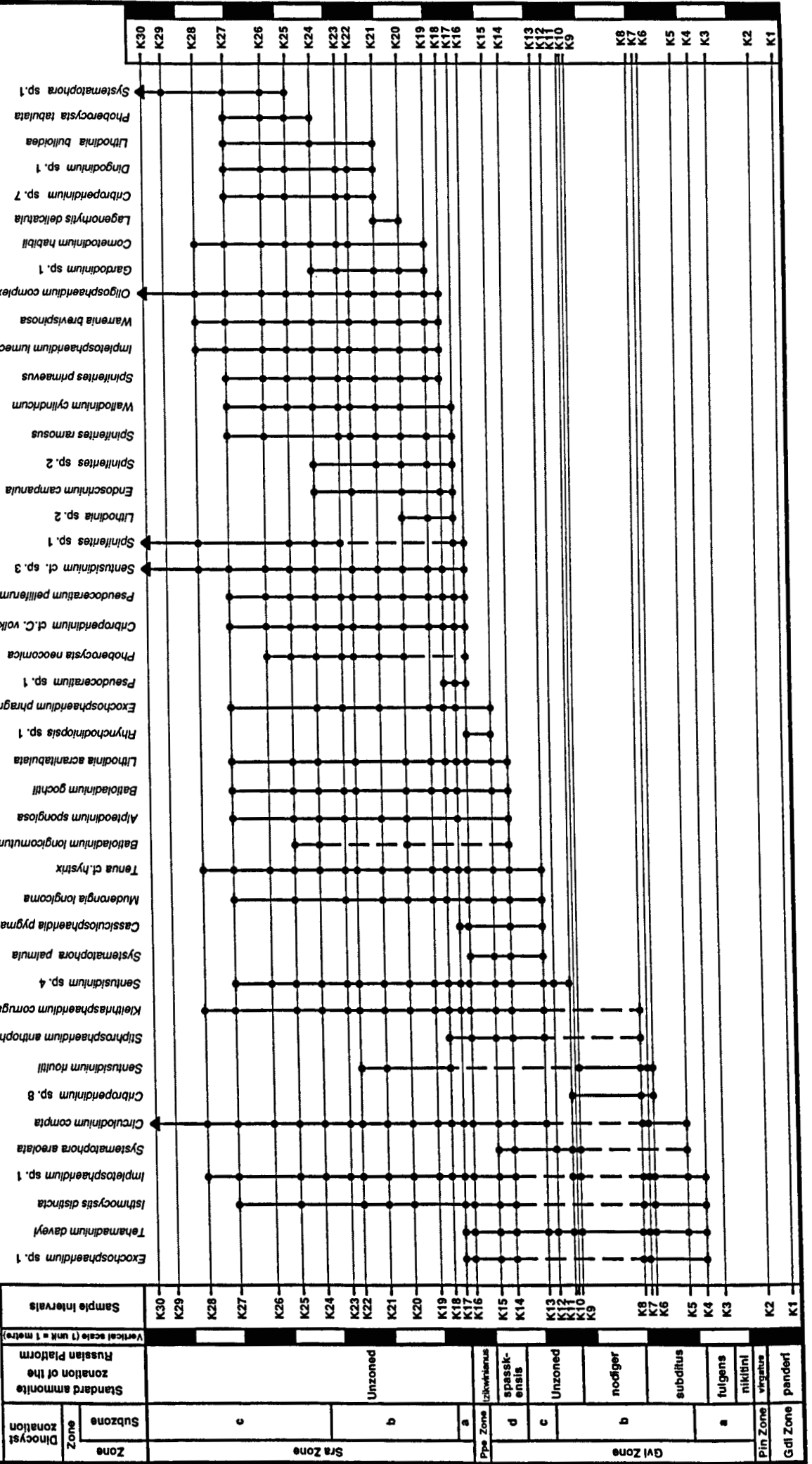
Dinocyst assemblages of the fulgens Zone at Kashpir contain abundant *Hystrichodinium pulchrum* (4.2-9.9%), *Perisseiasphaeridium ingegerdiae* (7.4-9.1%) and *Systematophora daveyi* (7.3-11.3%). Also important numerically are; *Chlamydophorella nyei* (2.5-3.9%), *Downiesphaeridium* spp. (0.7-3.2%), *Gochteodinia villosa* (0.3-1%), *Kleithriasphaeridium porosispinum* (2.2-3.2%), *Lagenadinium ?membranoidium* (2.6-5.8%), *Senoniasphaera jurassica* (1.9-4%), *Sentusidinium* sp. 3 (1.9-3.7%), and *Trichodinium cf. ciliatum* (0-7.3%)(Table 4.4).

Taxa with LADs in the fulgens Zone are *Gochteodinia cf. villosa*, *Tehamadinium sousense*, and *Trichodinium* sp. 1. Taxa with FADs in this zone include; *Achomosphaera neptuni*, *Cassiculosphaeridia reticulata*, *Dapsillidinium multispinosum*, *Endoscrinium granulatum*, *Gochteodinia villosa*, *Gonyaulacysta* sp. 4, *Hystrichodinium voigtii*, *Isthmocystis distincta*, *Kleithriasphaeridium eoinodes*, *K. porosispinum*, *Lagenadinium ?membranoidium*, *Perisseiasphaeridium ingegerdiae*, *Senoniasphaera jurassica*, *Tanyosphaeridium isocalamum*, *Tehamadinium daveyi*, *Tehamadinium* sp. 1 , and *Valensiella ovula* (Figure 4.6b).

Subditus Zone

The dinocyst assemblages contain abundant *Dingodinium tuberosum* (2.4-8.9%), *Gochteodinia villosa* (0.5-4.7%), *Hystrichodinium pulchrum* (2.5-5.6%), *Impletosphaeridium* sp. 1 (1.4-8.8%), *Systematophora daveyi* (2.5-9.1%), and *Trichodinium cf. ciliatum* (0-4.4%). Also important numerically are *Kleithriasphaeridium porosispinum* (1-3.3%), *Perisseiasphaeridium ingegerdiae* (0.3-5.9%), and *Sentusidinium* sp. 3 (1.5-3.8%)(Table 4.4).

Figure 4.6b: Dinocyst biostratigraphy of the section at Kashpir



Epiplosphaera gochti last occurs in the subditus Zone at Kashpir. Taxa with FADs in this zone include; *Egmontodinium polyplacophorum*, *Kleithriasphaeridium corrugatum*, *Sentusidinium rioultii*, *Sentusidinium* sp. 4, and *Systematophora areolata* (Figure 5.6b).

Nodiger Zone

The one dinocyst assemblage from this zone contains common *Dingodinium tuberosum* (4.9%), *Hystrichodinium pulchrum* (5.3%), *Sentusidinium* sp. 3 (10%), and *Systematophora daveyi* (7.9%). Also numerically important are *Gochteodinia villosa* (4.3%), *Epiplosphaera* spp. (3.3%), and *Kleithriasphaeridium porosispinum* (3.3%) (Table 4.4).

Taxa with LADs in the nodiger Zone include *Cometodinium whitei*, *Egmontodinium polyplacophorum*, *Hystrichodinium voigtii*, and *Gonyaulacysta dentata* (Figure 4.6b). No taxa have FADs in this Zone.

Lower Cretaceous

Ryazanian (unzoned interval)

Four samples were collected from this interval. The sample collected from the bituminous shale horizon, thought to mark the Jurassic-Cretaceous boundary is unfortunately barren of identifiable dinocysts (other than 'taxon-groups'). The dinocyst assemblages of the unzoned basal Ryazanian interval contain abundant *Dingodinium tuberosum* (0-17.8%), which dominates the upper sample. Also sporadically important are *Chytroeisphaeridia chytroeides* (0-8%), *Hystrichodinium pulchrum* (0-4%), *Sentusidinium* sp. 3 (0-6.1%), *Trichodinium* cf. *ciliatum* (0-7.6%), with common *Circulodinium compta* (3.6%), *Sentusidinium* sp. 4 (0-4%), and *Tenua* cf. *hystrix* (5.9%) in the uppermost sample (K13)(Table 4.4).

Taxa with LADs in this interval include; *Amphorula expiratum*, *Cribroperidinium nuciforme*, *Cribroperidinium* sp. 8, and *Systematophora daveyi*. Taxa with FADs include; *Cassiculosphaeridia pygmaeus*, *Circulodinium copei*, *Muderongia longicornis*, *Systematophora palmula*, *Tenua* cf. *hystrix* (Figure 5.6b).

Ryazanian (spasskensis Zone)

The dinocyst assemblages contain abundant *Dingodinium albertii* (8-17.2%), *Circulodinium compta* (9.8-16.2%), and *Tenua* cf. *hystrix* (6.1-11.6%). Also numerically important are *Achomosphaera neptuni* (0.3-3.9%), *Cassiculosphaeridia magna* (0.4-3.4%), *Chytroeisphaeridia chytroeides* (0.3-4.6%), *Hystrichodinium pulchrum* (4.2-6.1%), *Impletosphaeridium* sp. 1 (3.2-4.1%), *Kleithriasphaeridium eoinodes* (0.1-4.9%), and *Sirmiodinium grossi* (0-4.4%)(Table 4.4).

Two taxa have LADs in the spasskensis Zone; *Avellodinium falsificum*, and *Systematophora areolata*. Taxa with FADs in this zone include; *Apteodinium spongiosa*, *Gonyaulacysta* sp. 1, *Lithodinia acranitabulata*, and *Tehamadinium evittii* (Figure 4.6b).

Tzikwinianus Zone

The one dinocyst assemblage from this zone contains common *Circulodinium compta* (7%), *Dingodinium tuberosum* (12%), and *Sentusidinium* sp. 4 (7%). Also numerically important are; *Chlamydophorella nyei* (4.9%), *Chytroeisphaeridia chytroeides* (4.9%), *Hystrichodinium pulchrum* (3.8%), *Impletosphaeridium* sp. 1 (3.5%), and *Kleithriasphaeridium corrugatum* (3.5%)(Table 4.4).

Taxa with LADs in this zone include; *Endoscrinium granulatum*, *Gochteodinia villosa*, *Gonyaulacysta* cf. *centriconnata*, *Lithodinia* sp. 1, *Stiphrosphaeridium*

dictyophorum, *Systematophora palmula*, and *Tehamadinium daveyi*. Taxa with FADs in this horizon include; *Cribooperidinium* cf. *volkovae*, *Phoberocysta neocomica*, *Pseudoceratium pelliferum*, *Sentusidinium* sp. cf. 3, and *Spiniferites* sp. 1 (Figure 5.6b).

?Early Valanginian

Sandy horizon with phosphate concretions.

One sample (K17) was collected from this horizon. The assemblage contains abundant specimens of *Circulodinium compta* (7.9%). Also numerically important are; *Chlamydophorella nyei* (4.8%), *Dingodinium cerviculum* (4.1%), *D. tuberosum* (5.5%), *Downiesphaeridium* spp. (3.8%), and *Hystrichodinium pulchrum* (3.8%)(Table 4.4).

Taxa with LADs in this horizon include; *Ambonosphaera staffinensis*, *Perisseiasphaeridium ingegerdiae*, *Tehamadinium evittii*, and *Tubotuberella apatela*. Taxa with FADs in this bed include; *Dingodinium cerviculum*, *Lithodinia distincta* sp. nov., *Muderongia ?australis*, *Spiniferites ramosus*, *Spiniferites* sp. 2, and *Wallodinium cylindricum* (Figure 5.6b).

? Valanginian

Unzoned (samples K18 - K30)

Dinocyst assemblages of this interval usually contain abundant *Achomosphaera neptuni* (0-17.4%), *Circulodinium compta* (0-18.2%), *Dapsillidinium multispinosum* (0-10.1%), *Dingodinium cerviculum* (0-10.3%) *D. tuberosum* (0.4-12.3%), *Kleithriasphaeridium corrugatum* (0-8%), *Impletosphaeridium* sp. 1 (0-11.1%), and *Sentusidinium* sp. 4 (0-11.8%)(Table 4.4). *Chlamydophorella nyei*, *Chytroeisphaeridia chytroeides*, *Dingodinium* sp. 1, *Hystrichodinium pulchrum*, *Impletosphaeridium lumectum*, *Oligosphaeridium complex*, *Phoberocysta neocomica*, *Pseudoceratium pelliferum*, *Sentusidinium* cf. sp. 3, *Tenua* cf. *hystrix*, *Valensiella ovula*, *Warrenia*

brevispinosa are also sporadically important. There appears to be a profound ecological or preservational change at sample K28 (not indicated in the sedimentology) above which the dinocyst floras are impoverished. Most of the stratigraphically useful taxa thus have LADs in sample K27.

Taxa with LADs below sample K27 include; *Batioladinium longicornutum*, *Cribroperidinium* sp. 1, *Gardodinium* sp. 1, *Gonyaulacysta* sp. 1, *Gonyaulacysta* sp. 4, *Isthmocystis distincta*, *Lagenadinium ?membranoidium*, *Lithodinia* sp. 2, *Muderongia ?australis*, *Phoberocysta neocomica*, *Prolixosphaeridium parvispinum*, *Sirmiodinium grossi*, *Spiniferites* sp. 2, *Stiphrosphaeridium anthophorum*, *Trichodinium* cf. *ciliatum*, and *Valensiella ovula*. Taxa with FADs in this interval include; *Cometodinium habibii*, *Cribroperidinium* sp. 7, *Dingodinium* sp. 1, *Gardodinium* sp. 1, *Impletosphaeridium lumectum*, *Lagenorhytis delicatula*, *Lithodinia bulloidea*, *Phoberocysta tabulata*, *Spiniferites primaevus*, and *Warrenia brevispinosa* (Figure 5.6b).

4.2.4. Comparison of the dinocyst biostratigraphy of the two sections.

Zarajskensis Subzone:

Several useful dinocyst data occur in this subzone at both sections. In particular, *Glossodinium dimorphum*, *Gochteodinia tuberculata*, and *Thalassiphora? robusta* are restricted to this subzone in both sections, although the LAD of *G. dimorphum* occurs stratigraphically closer to the base of the *virgatus* Zone at Kashpir than at Gorodische. This may suggest the presence of a short stratigraphic gap beneath the base of the *virgatus* Zone at Kashpir. *Trichodinium* sp. 1 and *Rhynchodiniopsis magna* which both have LADs in this subzone at Gorodische have extended ranges at Kashpir, with last occurrences at the top of the *fulgens*, and the top of the *subditus* zones respectively. Both *Cribroperidinium erymnoseptatum* and *Cribroperidinium* sp. 6 have LADs towards the base of the *zarajskensis* Subzone at Gorodische but do not occur at Kashpir, which corroborates the fact that samples were only taken from the upper part of

this subzone at Kashpir. These two taxa may thus serve to separate the upper and lower parts of this subzone, although samples need to be examined from stratigraphically lower in this subzone at Kashpir in order to verify this.

First appearance data for this subzone are more difficult to compare since only the uppermost part of the subzone was sampled at Kashpir. However, in general all of the taxa with FADs in the *zarajskensis* Subzone at Gorodische also first occur in the same zone at Kashpir. Two notable exceptions are *Kleithriasphaeridium corrugatum* which first appears in the *subditus* Zone at Kashpir, and *Senoniasphaera jurassica*, which appears towards the top of the *zarajskensis* Subzone at Gorodische, but not until the *fulgens* Zone at Kashpir.

Virgatus & nikitini zones.

Since these zones were not sampled at Kashpir, no direct comparisons can be made. However, several of the taxa with LADs in this interval at Gorodische occur in younger deposits at Kashpir. *Dichadogonyaulax? chondrum*, which has last occurrence at Gorodische at the base of the *virgatus* Zone is last found in the *subditus* Zone at Kashpir. *Hystriosphera petilum* and *Tehamadinium sousense*, which both have LADs in the *virgatus* Zone at Gorodische, both extend into the *fulgens* Zone at Kashpir. *Stiphrosphaeridium dictyophorum* and *Tenua hystrix*, which both have LADs in the *virgatus* Zone at Gorodische, last appear in the *Ryazanian* interval at Kashpir. *Tehamadinium* sp. 1, which has its LAD in the *nikitini* Zone at Gorodische last appears at Kashpir within the *nodiger* Zone.

Due to the break in sampling, the following taxa which have FADs in the *virgatus* Zone - *nikitini* Zone interval at Gorodische first appear in the *fulgens* Zone at Kashpir: *Achomosphaera neptuni*, *Gochteodinia villosa*, *Gonyaulacysta dentata*, *Impletosphaeridium* sp. 1, *Isthmocystis distincta*, *Kleithriasphaeridium eoinodes*, *K. porosispinum*, *Lagenadinium ?membranoidium*, *Perisseiasphaeridium ingegerdiae*,

Trichodinium ciliatum, and *Valensiella ovula*. Additionally, *Egmontodinium polyplacophorum* first appears in the virgatus Zone at Gorodische, but has a younger FAD at Kashpir, within the subditus Zone.

Fulgens to nodiger zones

Tehamadinium daveyi has its first occurrence in the fulgens Zone in both sections. In addition to those taxa mentioned above, taxa with FADs in this zone at Kashpir include; *Endoscrinium granulatum*, *Endoscrinium inritibile*, and *Epiplosphaera gochtii* (all of which occur in the zarajskensis Subzone at Gorodische). *Cribroperidinium nuciforme*, which has its LAD in the fulgens Zone at Gorodische last appears in the Early Ryazanian interval at Kashpir.

Circulodinium compta and *Stiphrosphaeridium dictyophorum* have FADs in the subditus Zone of both sections (although the latter taxon appears later, at the top of this zone in Kashpir). In addition to those taxa mentioned above, *Sentusidinium rioultii* and *Endoscrinium campanula* also first appear in this zone at Kashpir. At Gorodische *S. rioultii* has its first occurrence in the virgatus Zone, whilst *E. campanula* was not encountered until the unzoned Valanginian interval. *Leptodinium subtile* has its LAD in the subditus Zone at both localities. *Cometodinium whitei* also last occurs in this zone at Gorodische, but slightly higher, at the base of the nodiger Zone at Kashpir. *Epiplosphaera gochtii* has its FAD in this zone at Kashpir, but last occurs in the phosphorite deposit at Gorodische.

Tenua cf. hystrix is the only taxon to have its FAD in the nodiger Zone at Gorodische, but was first recorded from younger Early Ryazanian deposits at Kashpir. At Gorodische the only notable taxon with its LAD in the nodiger Zone is *Circulodinium copei*. The apparent range of this taxon at Gorodische thus contrasts markedly to that at Kashpir, where its FAD is within the younger Early Ryazanian interval. At Kashpir, *Gonyaulacysta dentata*, and *Senoniasphaera jurassica*, both have LADs in the nodiger

Zone. At Gorodische these taxa all have last occurrences in the unzoned phosphorite deposit.

Ryazanian

The Ryazanian interval is absent at Gorodische, and no comparison with Kashpir can therefore be made. However, the following taxa which appear in the Ryazanian deposits have FADs in the base of the overlying mica-rich facies at Gorodische: *Exochosphaeridium phragmites*, *Muderongia longicornis*, *Pseudoceratium pelliferum*, and *Sentusidinium* sp. 4.

?Valanginian

The Early Cretaceous, post-Ryazanian deposits of the two sections are unzoned by ammonites, hampering accurate comparison of the two sets of dinocyst data. In the Kashpir section, the base of this unzoned sequence is marked by the sandstone horizon bearing phosphatic concretions; the unit which yields the exceptionally well preserved dinocyst assemblage. The dinocyst biostratigraphic evidence does not suggest a significant age separation of this deposit from the overlying strata and they are therefore likely to belong to the same stage.

In both sections *Oligosphaeridium complex*, *Spiniferites ramosus* and *Wallodinium cylindricum* have FADs at the base of this unzoned Early Cretaceous interval. *Impletosphaeridium lumectum*, *Spiniferites primaevus*, and *Warrenia brevispinosa*, have LADs at the very base of the mica-rich siltstone facies in both sections, thus stratigraphically higher in the Valanginian sediments at Kashpir than at Gorodische. This reflects the absence from Gorodische of three sandstone beds (24-26) which are present at Kashpir, including the one bearing phosphatic concretions. The FADs of *Cometodinium habibii*, *Gardodinium* sp. 1, and *Phoberocysta tabulata* then appear in sequence in both sections. Other taxa characteristic of this interval in both

sections include; *Batioladinium longicornutum*, *Lithodinia bulloidea*, and *Systematophora* sp. 1. Neither *Cymosphaeridium validum*, which appears in the uppermost part of the sampled interval at Gorodische, nor *Nelchinopsis kostromiensis* which first appears just above the base of the unzoned interval in that section were encountered at Kashpir.

4.2.5. General comparison of the dinocyst assemblages encountered in the present study with other palynological investigations of the Volga Basin.

Lord et al. (1987) studied the Early to Mid Volgian interval in the Volga Basin, overlapping with the scope of the present investigation in coverage of the panderi Zone, zarajskensis Subzone. At Gorodische they noted an interval of significant floral change between beds 8 and 11 of Mesezhnikov (1977, 1984), with seven new forms appearing in the upper bed. Bed 11 correlates with beds 1 - 13 of the present study, although Lord et al. (1987) took only one sample from this interval. The assemblage recovered by them was similar to that encountered here, if slightly less diverse. Important elements such as *Chytroesphaeridia chytroeides*, *Glossodinium dimorphum*, *Pareodinia ceratophora*, *Systematophora daveyi* (as *Emmetrocysta sarjeantii*), and *Tubotuberella apatela* are common to both studies. Additionally Lord et al. (1987) recorded *Millioudodinium sarjeantii sphaericum* as first appearing in Bed 11 (Mesezhnikov, 1977, 1984) at Gorodische and Bed 7 (below the current interval of study) at Kashpir. This taxon was not noted in the present study, but their photographic example of it (Figure 10, 1-2) bears close morphological similarity to *Cribooperidinium erymnoseptatum* which was recorded in the lower part of the zarajskensis Subzone in the present study.

Hogg (1994) considered the dinocyst floras from 28 samples of Late Kimmeridgian to Late Volgian age, of which the upper 8 overlap with the interval considered here. The assemblages recovered by him were not discussed in detail, but

comparison with his abundance charts shows that they were of similar composition. *Cribroperidinium erymnoseptatum* was recorded by Hogg (1994) in a single sample from the zarajskensis Subzone, possibly comparable to Bed 8 of the current investigation. This level may thus correlate some way above the FAD of this taxon indicated here. *Gochteodinia villosa* was only recorded by Hogg (1994) in the fulgens Zone, and similarly *Kleithriasphaeridium porosispinum* and *Lagenadinium ?membranoidium* was only recorded in the fulgens and subditus zones. The majority of other stratigraphically useful taxa encountered in the present investigation were recorded by Hogg (1994) in similar stratigraphic positions.

The dinocyst floras encountered by Riding *et al.* (in press) from the Volgian deposits of the Russian Platform are broadly comparable to those observed here, although of somewhat lower diversity, particularly in the virgatus and nikitini zones. However, there are significant differences between the two studies. *Cribroperidinium globatum* (considered to be 'prominent' through this interval by Riding *et al.*, in press), *Aldorfia dictyota*, *Dichadogonyaulax? pannea*, and *Tubotuberella rhombiformis* were not encountered in the present study. *T. rhombiformis* has not always been consistently distinguished from *T. apatela* in the literature, and the stratigraphic value of this species is questionable. In the current investigation, all specimens of the *rhombiformis-apatela* plexus lacking paratabular features, or with weakly expressed paracingular ridges restricted to lateral areas were assigned to *T. apatela*. No specimens with well developed paratabulation typical of *T. rhombiformis* were encountered.

Several taxa which were found to be common in the Volgian material examined here were not discussed by Riding *et al.* (in press). These include: *Cribroperidinium erymnoseptatum* from the zarajskensis Subzone, *Perisseiasphaeridium ingegerdiae*, which was found to be common in the nikitini to subditus zones, and the genera *Tehamadinium* and *Tenua*, both found to be common in the Mid to Late Volgian.

The palynological information from the Ryazanian deposits at Kashpir provided by Riding *et al.* (in press) contrasts markedly to that given here in terms of diversity and preservation of the microflora. Riding *et al.* (in press) note the most common elements of this flora (a single sample was examined from this level) are *Cribopteridinium* spp. and *Circulodinium distinctum*, with additional *Cassiculosphaeridia* spp.. Little mention was made of *Chlamydophorella nyei*, *Dingodinium* spp., *Hystriodinium* spp., or *Sentusidinium* sp. 4, which were all found to be common in this interval at Kashpir in the present study. Other Ryazanian material studied by Riding *et al.* (in press) from the Oka Basin appears to bear closer resemblance to the assemblages noted in the present study. In particular, they encountered abundant *Circulodinium compta*, which they note is also common in the Ryazanian of western Europe.

4.2.6. Comparison and correlation of important dinoflagellate cyst ranges and biohorizons in NW Europe and elsewhere in the Russian Platform with those from the Volga Basin.

As indicated in Chapter 1, there is a wealth of information on dinoflagellate cyst data through the Late Jurassic of western Europe. Relatively few of these papers provide detailed correlation of the dinocyst data with the standard ammonite chronozone, making accurate comparison and wider stratigraphic correlations of this nature difficult. However, several of such publications have been used to compare important dinocyst biohorizons common to both the Volga Basin and NW Europe through the Early Volgian to Hauterivian interval (Figures 4.7 & 4.8). Such detailed comparisons are discussed in the text below.

Late Jurassic: Mid Volgian

Most of the taxa present in the zarajskensis Subzone in the Volga Basin have FADs near the base of the studied interval, and are therefore likely to range into older strata. This has largely been verified by comparison with the works of Lord *et al.* (1987), Hogg (1994), and Riding *et al.* (in press). These include the taxa *Tubotuberella apatela*, *Systematophora daveyi*, *Tenua hystrix*, *Glossodinium dimorphum*, *Leptodinium subtile*, *Endoscrinium inritibile*, *Rhynchodiniopsis martonense*, *Senoniasphaera jurassica*, *Sirmiodinium grossi*, *Hystrichodinium pulchrum*, *Egmontodinium torynum*, *Hystrichosphaeridium petilum*, which are known from Kimmeridgian and Volgian deposits in western Europe (Woollam & Riding, 1983; Heilmann-Clausen, 1987; Riding & Thomas, 1992; Poulsen, 1992, 1994, 1996; Bailey *et al.*, 1997)(Figure 4.7). In addition, *Amphorula expiratum* is known to have its range base within the Late Kimmeridgian in western Europe. In particular the FAD of this taxon has been noted at the base of the Wheatleyensis Zone (Riding & Thomas, 1992; Poulsen, 1996), which correlates with the base of the Sokolovi Zone of the Early Volgian in the Russian Platform (Kuznetsova, 1978; Lord *et al.*, 1987).

Riding *et al.* (in press) note the presence of *Perisselasphaeridium pannosum* up to the top of the nikitini Zone in the Russian Platform, and comment that the range top of this species, and of the morphologically related taxon *Oligosphaeridium patulum* are thus younger than the lowermost Mid Volgian last occurrence in England. In the present study *O. patulum* was only noted from a short stratigraphic interval at the base of the zarajskensis Subzone, whilst *P. pannosum* was equally rare, and not recorded above this subzone (Table 4.3).

Kleithriasphaeridium porosispinum, which also has its FAD in the Wheatleyensis Zone in western Europe (Riding & Thomas, 1992; Poulsen, 1996) was not noted below the upper part of the Pavlovi Subzone (panderi Zone) by Riding *et al.* (in press). These authors encountered "significant numbers" of *K. porosispinum* in the

zarajskensis Subzone (Riding *et al.*, in press). This taxon was not encountered below the virgatus Zone in the present study. Thus the range base of this taxon occurs stratigraphically higher in the Russian Platform than in western Europe. *Egmontodinium polyplacophorum* has been reliably recorded in strata below the Late Kimmeridgian Wheatleyensis Zone in western Europe (Riding & Thomas, 1992; Poulsen, 1996)(Figure 4.7). This species was found to be rare in the palynofloras of the Volga Basin with its FAD in the virgatus Zone of the Mid Volgian. Due to the rarity of this species, further work may reveal older specimens from the Russian Platform, but the present study suggests that its range base occurs in stratigraphically younger strata than in western Europe.

Cribroperidinium erymnoseptatum, which is here recorded from the lower part of the zarajskensis Subzone (and which therefore is likely to range below the interval examined here), has previously been recorded from the Kimmeridgian of the North Sea (Bailey, 1993). In this area it was associated with diverse microfloras including taxa such as *Perisselasphaeridium pannosum*, *Endoscrinium inritibile*, *Glossodinium dimorphum*, *Pareodinia ceratophora* and forms of the *Circulodinium distinctum* group. Thus both the range of this taxon and the floral elements associated with it are similar in both areas, perhaps ranging into slightly younger strata in the Volga Basin. Similarly, *Rhynchodiniopsis martonense* has been noted from the zarajskensis Subzone and basal part of the virgatus Zone in the present investigation, and in the zarajskensis Subzone by Riding *et al.* (in press). Bailey *et al.* (1997) described this species from the Hudlestoni to Pectinatus Zones of the Kimmeridge Clay Formation in North Yorkshire, UK. Thus in the Volga Basin the stratigraphic distribution of this taxon is similar, perhaps ranging into slightly younger strata than has previously been recorded in NW Europe.

The range top of *Glossodinium dimorphum* has been demonstrated as being at the top of the Kerberus Zone in north-western Europe (Woollam & Riding, 1983; Riding & Thomas, 1988, 1992)(Figure 4.7), although studies by Haq *et al.* (1987) and Poulsen

(1996) have noted LADs of this taxon at the top of the Okusensis and Fittoni Zones respectively. In the Russian Platform, the LAD of *Glossodinium dimorphum* was noted just below the top of the zarajskensis Subzone by Riding *et al.* (in press). This accords well with the occurrence of *G. dimorphum* noted in the present investigation. Thus the LAD of *G. dimorphum* appears to be reliably established at the top of the zarajskensis Subzone in the Russian Platform, and thus a useful marker in that area. This datum appears to be within the range of possible LADs defined by the data of Poulsen (1996) and Riding & Thomas (1992) for NW Europe.

The LAD of *Leptodinium subtile* has been variously placed between the top of the Albani Zone (Woollam & Riding, 1983; Riding & Thomas, 1988, 1992) and the top of the Okusensis Zone (Davey, 1982) in NW Europe (Figure 4.7). Similarly Riding *et al.* (in press) noted the last occurrence of this taxon from the top of the zarajskensis Subzone at Gorodische, and they suggested that this datum may have stratigraphic significance in the Russian Platform. Contrastingly, Lord *et al.* (1987) recorded the LAD of *Leptodinium subtile* much lower, within the Klimovi Zone at Gorodische. In the present study this taxon has been noted in younger deposits, up to the subditus Zone in both of the studied sections, although it is extremely rare above the virgatus Zone. Thus this species ranges into slightly younger strata in the Volga Basin than has previously been indicated in NW Europe. *Leptodinium deflandrei* recorded by Lord *et al.* (1987) from the zarajskensis Subzone was not encountered in this investigation.

Endoscrinium inritibile has its last occurrence in NW Europe between the top of the Albani Zone (Woollam & Riding, 1983; Riding & Thomas, 1988, 1992; Poulsen, 1996), and the top of the Okusensis Zone (Davey, 1982)(Figure 4.7). Riding *et al.* (in press) noted the LAD of this taxon from the top of the zarajskensis Subzone in the Russian Platform, which would correlate well with the lower of the two possible datums in NW Europe. Specimens of *E. inritibile* have here been recovered from as strata as young as the fulgens Zone at Gorodische and nodiger Zone at Kashpir, although this taxon is rare in the Volga Basin material.

The Albani to Oppressus Zone interval in NW Europe (which corresponds to the Early Volgian interval examined here) embraces the range bases of three stratigraphically useful dinoflagellate cyst taxa. *Endoscrinium pharo* has been demonstrated to have its range base coincident with the base of the Albani Zone (Riding & Thomas, 1992; Poulsen, 1996), although younger FADs have separately been noted by Davey (1982), Heilmann-Clausen (1987), and Costa & Davey (1992)(Figure 4.7). This species was encountered near the base of the zarajskensis Subzone in the present study, suggesting close correlation with the data of Riding & Thomas (1992) and Poulsen(1996), and thus the Russian zarajskensis Subzone with the western European Albani Zone. *Isthmocystis distincta* has been shown to have its range base within the Kerberus Zone (Davey, 1982; Heilmann-Clausen, 1987; Riding & Thomas, 1992) in NW Europe. In the present study, this taxon was recorded from the middle part of the virgatus Zone, which approximately correlates with the base of the Okusensis Zone (using the correlation of Kuztensova, 1978). Thus the FAD of this taxon is approximately one standard ammonite chronozone lower in the Volga Basin than in NW Europe, but remains an approximate tie-point.

The FAD of *Gochteodinia villosa*, which has been described as the "most significant bioevent in the Portlandian" (Stover et al., 1996: p.662) has been proposed to occur at the base of the Anguiformis Zone (Woollam & Riding, 1983; Riding & Thomas, 1988, 1992), but has also been clearly demonstrated from the base of the older Kerberus Zone (Davey, 1982; Heilmann-Clausen, 1987; Poulsen, 1996)(Figure 4.7). The FAD of *Gochteodinia villosa* was not discussed in relation to the Volga Basin sections by Riding et al. (in press), but this datum was suggested as resting at the base of the fulgens Zone in the Oka Basin. In the present investigation, unequivocal *G. villosa* were recorded from the lower part of the nikitini Zone at Gorodische. In addition, a form of close affinity to *G. villosa*, and therefore perhaps the precursor to this species, was recorded in the virgatus and nikitini Zones of the same section. The base of the nikitini Zone correlates to a position approximately midway in the north-west European Okusensis

ammonite Zone according to Kuznetsova (1978). Such precise correlation of this dinocyst bioevent between the two areas is robust independent evidence for the validity of Kuznetsova's (1978) correlation scheme. Indeed, this datum may allow for a slight refinement in her scheme, by equating the base of the nikitini Zone with the base of the Kerberus Zone, thus uniting the FAD of *G. villosa* across the whole of NW Europe and the Russian Platform.

Riding *et al.* (in press) proposed that the LAD of *Prolixosphaeridium parvispinum* was of stratigraphic significance in the Russian Platform, and placed this event at the top of the nikitini Zone (Figure 4.7). In the present study *P. parvispinum* was observed to display some morphological variability (particularly in the number and character of the spines), and specimens of close affinity to the holotype were recorded from the lower part of the mica-rich siltstones (Lower Cretaceous) in both sections. Since such variation appeared to be gradational, all specimens were assigned to *P. parvispinum*, and thus the nikitini Zone LAD biohorizon suggested by Riding *et al.* (in press) cannot be supported here.

Late Jurassic: Late Volgian.

There are relatively few widely recognised dinoflagellate cyst biohorizons in the Late Portlandian of western Europe. The range top of *Egmontodinium polyplacophorum* in this area is between the top of the Okusensis (Poulsen, 1996) and the top of the Primitivus zones, an interval which spans the Mid to Late Volgian of the Russian Platform (Figure 4.7). This taxon was only recorded from the section at Gorodische in the present study, where its LAD is in the fulgens Zone: a level correlated to approximately the middle of the Primitivus Zone in NW Europe. Thus this bioevent in the Russian Platform is within the range of that noted in NW Europe.

Heilmann-Clausen (1987) suggested that the range base of *Avellodinium falsificum* occurs at the base of the Lamplugh Zone. This interval is coincident with an hiatus at the top of the nodiger Zone in the Volga Basin. The range of this taxon in NW Europe thus strongly contrasts with that noted in this report, since *A. falsificum* was encountered in the zarajskensis Subzone, and its LAD occurred within the nodiger Zone, below its apparent range base in NW Europe.

Endoscrinium inritibile, *Senoniasphaera jurassica*, and *Leptodinium subtile*, which have their LADs in the Late Volgian interval in the Volga Basin, all have range tops within older strata in the NW European area (Figure 4.7). *Gonyaulacysta dentata*, which also has its range top in this interval, has not been noted as a significant biostratigraphic marker in NW Europe. The LAD of *Senoniasphaera jurassica* has been variously placed at the top of the Kerberus Zone (Riding & Thomas, 1992) and the Anguiformis Zone (Poulsen, 1996) in western Europe. In the Russian Platform, the LAD of *Senoniasphaera jurassica* was encountered by Riding *et al.* (in press) within the nodiger Zone (text-figure 9), and they suggested that this taxon is a reliable marker for the Mid to Late Volgian in that area. This accords well with the LAD indicated in the present report (Figure 4.7), and thus its marker status can be defended here. *S. jurassica* therefore ranges into stratigraphically younger deposits in this part of Russia than in NW Europe.

Tehamadinium daveyi and *Endoscrinium campanula* which both have FADs in the Late Volgian interval in the Volga Basin have range bases in younger strata in NW Europe (see below). *Circulodinium compta* which has its FAD at the base of the subditus Zone in both sections of the current study is known to range below the Late Kimmeridgian Wheatleyensis Zone in NW Europe (Poulsen, 1996). This datum is therefore only of local significance in the Volga Basin, but may also extend to other areas in the Russian Platform.

Early Cretaceous, Ryazanian.

The LAD of *Amphorula expiratum* is reliably known from the Runctoni Zone of NW Europe (Heilmann-Clausen, 1987; Riding & Thomas, 1992; Poulsen, 1996), although Davey (1982) noted this datum at the top of the younger Icenii Zone (Figure 4.8). A *expiratum* was observed in the unzoned basal Ryazanian interval at Kashpir: an interval which probably corresponds to the subclypieforme and kochi zones of elsewhere in the Russian Platform, and thus by inference to the Runctoni to Kochi chron interval in the NW European area. Thus this datum is broadly comparable in the two areas.

In NW Europe, the range base of *Batioladinium longicornutum* has been reliably established at the base of the Runctoni Zone, and therefore marks the base of the Ryazanian (Davey, 1982; Costa & Davey, 1992; Poulsen, 1996) (Figure 4.8). Indeed, the LAD of this taxon was indicated by Costa & Davey (1992) as being at the top of the Icenii Zone, thus its entire range being encapsulated within the Ryazanian. This contrasts with the Volga Basin material examined here, where the FAD of *B. longicornutum* is in the unzoned mica-rich siltstones which overlie the Ryazanian interval.

The range base of *Systematophora palmula* has been indicated by Davey (1982) at the base of the Runctoni Zone, although FADs of this taxon have also been noted at the base of the Kochi Zone (Heilmann-Clausen, 1987) and within the Stenomphalus Zone (Costa & Davey, 1992)(Figure 4.8). At Kashpir, this datum occurs in the lowest sample collected from the unzoned basal Ryazanian interval. This is therefore a strong tie-point with the data of Davey (1982), and thus, in the absence of *B. longicornutum* from this interval of the Volga Basin, a good marker for the basal Ryazanian.

The FAD of *Batioladinium gochtii* was noted to occur within the lower part of the Ryazanensis (spasskensis) Zone in the Moscow Basin by Iosifova (1996). This correlates well with the FAD of this taxon in the Volga Basin (Kashpir section), which occurs at the

base of the *spasskensis* Zone. Thus the range base of this taxon appears to be a reliable marker for the base of the Late Ryazanian (*spasskensis* Zone) in the Russian Platform.

In north-western Europe *Systematophora daveyi* is reported by Riding & Thomas (1992) to range above the Portlandian, and Poulsen (1996) noted the LAD of this taxon at the top of the Icenii Zone (Figure 4.8). In the Volga sediments, the LAD of *S. daveyi* is found in the unzoned basal Ryazanian sediments, and thus this datum is broadly comparable in both regions.

Species of the genus *Cassiculosphaeridia* from the Middle Volga Basin were not separated by Riding *et al.* (in press), and they commented that although the specimens they encountered of this genus were reminiscent of the earliest Cretaceous, their sample lacked reliable Ryazanian marker species (Riding *et al.*, in press). Numerous species of this genus and its morphological counterpart *Valensiella* were also encountered from the Ryazanian of Kashpir in the present report. *Cassiculosphaeridia pygmaeus* was only recorded in this interval at Kashpir, and thus may be of local stratigraphic significance in marking this stage in the Russian Platform.

The range bases of *Lagenorhytis delicatula* and *Lithodinia bulloidea* have been noted from the *Stenomphalus* Zone in NW Europe (Heilmann-Clausen, 1987; Davey, 1982), although Costa & Davey (1992) noted the FAD of *L. delicatula* in the Albani Zone, and Davey (1982) first encountered this species in the basal Valanginian *Paratollia* Zone (Figure 4.8). These taxa were noted to have FADs in the mica-rich siltstones overlying the Ryazanian strata in the Volga Basin. Thus their first appearances are likely to occur in slightly younger sediments than in NW Europe, although correlation of the FAD of *L. delicatula* between the Volga Basin and Denmark (following Davey, 1982) may be possible.

In NW Europe, the range bases of *Phoberocysta neocomica*, *Phoberocysta tabulata*, and *Pseudoceratium pelliferum* are usually found together. The level of this joint datum

has generally been recognised as marking the base of the Albidum Zone (Davey, 1982; Heilmann-Clausen, 1987; Poulsen, 1996), although Costa & Davey (1992) suggest that it occurs one chronozone lower, at the base of the Stenomphalus Zone (Figure 4.8). Alternatively, Davey (1982) found the FAD of *Phoberocysta* spp. to be at the base of the Polyptychites Zone. In the Volga Basin, these levels correlate to the middle part of the tzikwinianus Zone, and the base of that zone respectively. In the Russian Platform, Riding *et al.* (in press) encountered the FAD of *P. neocomica* within the spasskensis Zone, and the FAD of *P. pelliferum* at the top of the tzikwinianus Zone. They considered this datum to be of stratigraphic importance. The present author found the FAD of *P. pelliferum* at approximately the same level at Kashpir, and therefore this datum is closely comparable to its position at the base of the Albidum Zone in NW Europe. In the present investigation, the FAD of *P. neocomica* was also encountered at the top of the tzikwinianus Zone, thus slightly later than noted by Riding *et al.* (in press). The FAD of *P. tabulata* occurs stratigraphically higher in the Volga Basin sections than in NW Europe, and separate to that of *P. neocomica*. As a separate datum it is likely only to be of local significance in the Volga Basin.

Riding *et al.* (in press) considered the occurrence of *Muderongia simplex* and *Phoberocysta neocomica* to be indicative of Late Ryazanian age. *M. simplex* was not recorded in the present study, since 'simple' specimens of this genus all bear short solid spines on the post-cingular and antapical horns: a feature not characteristic of *M. simplex*. Thus the species *M. longicorna* emended to incorporate the ciliate features of *M. brevispinosa* (Iosifova, 1996) by Monteil (1996) has been adopted in this study. The FAD of *M. longicorna* in the Volga Basin contrasts slightly to that of *M. simplex* noted by Riding *et al.* (in press) since *M. longicorna* was encountered in the unzoned basal Ryazanian interval.

Specimens of *Wallodinium krutzschii* and *W. cylindricum* were also encountered in this interval in the Oka Basin by Riding *et al.* (in press). This contrasts in part with

the present study, since the FAD of *W. cylindricum* was encountered in the Valanginian mica-rich siltstones.

Costa & Davey (1992) note the FAD of *Tehamadinium daveyi* at the base of the Stenomphalus Zone in NW Europe (Figure 4.8). This datum was encountered much lower, within the fulgens Zone of both sections studied from the Volga Basin.

The range bases of *Kleithriasphaeridium corrugatum* and *K. eoinodes* are variously reported to occur either at the base of the Stenomphalus (Costa & Davey, 1992) or at the base of the Albidum (Heilmann-Clausen, 1987) zones in NW Europe (Figure 4.8). These data occur stratigraphically lower in the Volga Basin. *K. corrugatum* was encountered as low as the uppermost part of the zarajskensis Subzone at Gorodische, and *K. eoinodes* from the base of the virgatus Zone.

The range base of *A. neptuni* appears to be reliably reported from the base of the Albidum Zone in NW Europe (Davey, 1982; Heilmann-Clausen, 1987; Costa & Davey, 1992)(Figure 4.8). Riding *et al.* (in press) noted a single questionable specimen of ?*Achomosphaera* sp. from the Ryazanian interval at Kashpir. Unequivocal *A. neptuni* was encountered by the present author from the unzoned basal Ryazanian interval. Moreover, numerous specimens morphologically identical to *A. neptuni*, but with thinner walls than typical of this species, were recovered from the Mid to Late Volgian interval in both sections. Such Mid Volgian occurrences of this taxon are amongst the oldest known examples of the genus *Achomosphaera*. Thus the FAD of *A. neptuni* is much lower in the Volga Basin than in NW Europe.

The short stratigraphic range of *Pseudoceratium* sp. 1 is an excellent tool for correlation with the work of Heilmann-Clausen (1987)(Figure 4.8). This taxon was reported by him to range from the base of the Albidum Zone to the top of the Polyptychites Zone in the Danish Central trough. In the present study it has been recorded from the top of the tzikwinianus Zone to shortly above the base of the mica-rich

siltstones. Its range base in this region is thus a strong independent tie-point of the upper tzikwinianus zone to the Albidum Zone. The range top confirms that at least the base of the mica-rich siltstones is of Valanginian age, and that this interval may correlate with the Paratollia to Polyptychites interval of NW Europe. *Pseudoceratium* sp. 1 is thus a very significant taxon in this part of the column.

Cribroperidinium volkovae was noted by Iosifova (1996) to have its range base in the upper part of the ryazanensis (spasskensis) Zone. *C. cf. volkovae* differs slightly from *C. volkovae* in having intratabular tuberculae (as well as numerous penitabular features), but is otherwise extremely similar. The FAD of *C. cf. volkovae* was noted in the Volga Basin to be within the tzikwinianus Zone, although further sampling between the spasskensis and tzikwinianus zones in this area may reveal earlier specimens of this taxon. The range bases of *C. volkovae* and *C. cf. volkovae* are thus broadly similar across the Russian Platform, affording a reliable marker for the Late Ryazanian in this area.

Early Cretaceous: Valanginian - ?Hauterivian.

The range base of *Spiniferites ramosus* is reliably recorded from shortly above the base of the Early Valanginian Paratollia Zone (Costa & Davey, 1992; Heilmann-Clausen, 1987) in NW Europe, although Davey (1979, 1982) placed this datum slightly higher, in the middle part of this chronozone (Figure 4.8). In the present study the FAD of *S. ramosus* was noted from the base of the mica-rich siltstone at Gorodische, and within the siltstone unit bearing phosphatic concretions (Bed 24) at Kashpir. In NW Europe *Tubotuberella apatela* has not been recorded above the Polyptychites Zone. At Kashpir the LAD of this taxon was noted in Bed 24. Although *S. ramosus* is known to range up into the Hauterivian in NW Europe, the co-occurrence of *S. ramosus*, *Pseudoceratium* sp. 1, and *T. apatela* along with the absence of any reliable Late Valanginian or Hauterivian marker taxa suggests that this unit (Bed 24) is of Early Valanginian age.

In NW Europe, the range top of *Gochteodinia villosa* is known from the lower part of the Early Valanginian Paratollia Zone (Costa & Davey, 1992), although Heilmann-Clausen (1987) did not observe this species above the Albidum Zone (Figure 4.8). Although the LAD of this taxon was noted by Riding *et al.* (in press) to be at the top of the spasskensis Zone in the Russian Platform, in the present investigation this datum has been noted in the tzikwinianus Zone at Kashpir. This is thus comparable to the LAD of this taxon as noted by Heilmann-Clausen (1987). Thus the ranges of *P. pelliferum* and *G. villosa* overlap in the tzikwinianus Zone, in contrast to the findings of Riding *et al.* (in press).

Endoscrinium pharo has a reliably established range top within the Paratollia Zone of NW Europe (Davey, 1982; Heilmann-Clausen, 1987; Costa & Davey, 1992), although Poulsen (1996) noted the LAD of this taxon in the Stenomphalus Zone of Denmark (Figure 4.8). *E. pharo* was last recorded from the lower part of the mica-rich siltstones in both of the Volga sections studied. *Egmontodinium torynum* has its range top in the Paratollia to Polyptychites interval in NW Europe (Davey, 1982; Heilmann-Clausen, 1987; Costa & Davey, 1992). The LAD of this taxon was observed in sample K24 at Kashpir, approximately half way up the studied interval of mica-rich siltstones. In NW Europe, *Circulodinium compta* and *Kleithriasphaeridium porosispinum* have LADs between the top of the Stenomphalus Zone (Poulsen, 1996), and the top of the Polyptychites Zone respectively (Heilmann-Clausen, 1987)(Figure 4.8). In the sections studied from the Volga Basin, both of these taxa have ranges which extend at least to the top of the studied interval. Thus, the combination of last occurrence data for *E. pharo*, *E. torynum*, *C. compta*, and *K. porosispinum* may suggest an Early Valanginian age for the mica-rich siltstones in the Volga Basin, possibly correlatable with the Paratollia to Polyptychites interval of NW Europe.

In the Volga sections *Spiniferites primaevus* has its first occurrence shortly above the base of the mica-rich siltstones. In NW Europe this taxon has its range base in the Paratollia to Polyptychites chron interval (Figure 4.8), and furthermore Costa &

Davey (1992) suggested that the LAD of this taxon occurs at the top of the Polyptychites Zone. By contrast, Davey (1982) noted the FAD of this species from the base of the Hauterivian Amblygonius Zone. Thus the presence of this taxon in sediments from the upper part of the Volga sections may be a further indication of an Early Valanginian age.

The taxa *Cymosphaeridium validum*, *Nelchinopsis kostromiensis*, and *Oligosphaeridium complex* are usually found to have FADs in the Early Hauterivian of NW Europe (see Davey, 1982; Heilmann-Clausen, 1987)(Figure 4.8). However the range bases of *C. validum* and *O. complex* were indicated by Costa & Davey (1992) to be near the base of the Paratollia Zone (Figure 4.8). Similarly, they indicated the range base of *N. kostromiensis* to be at the base of the Polyptychites Zone (Costa & Davey, 1992). In the Volga Basin these taxa were encountered within the ?Lower Valanginian mica-rich siltstones. Although such occurrences are stratigraphically lower than would be common in the NW European area, the data do not conflict with the range bases as indicated by Costa & Davey (1992). The FAD of *Muderongia crucis*, which falls at the base of the Polyptychites Zone in NW Europe (Costa & Davey, 1992), is noted from the upper part of the mica-rich siltstones in the Volga Basin. If these deposits are indeed of Early Valanginian age, this datum is broadly comparable in both areas.

Exochosphaeridium phragmites is another taxon not usually encountered in rocks older than Hauterivian in NW Europe. In the section at Kashpir however, this species was noted to have its FAD in the upper part of the spasskensis Zone, and thereafter to have sporadic occurrence through the mica-rich siltstones. It therefore ranges into much older strata in the Volga Basin than in NW Europe.

Numerous taxa which occur in the Early Cretaceous interval of the Volga Basin have ranges which are known to extend into or above the Late Valanginian in NW Europe. These include: *Achomosphaera neptuni*, *Cymosphaeridium validum*, *Exochosphaeridium phragmites*, *Kleithriasphaeridium eoinodes*, *K. corrugatum*, *Isthmocystis distincta*, *Lithodinia bulloidea*, *Nelchinopsis kostromiensis*, *Phoberocysta neocomica*, *P. tabulata*,

Pseudoceratium pelliferum, *Spiniferites ramosus*, and *Trichodinium ciliatum*. Such taxa clearly range above the studied section, or have LADs near the top of the interval examined, and may thus also range into younger strata. In addition, the mica-rich siltstones yield several taxa noted by Iosifova (1996) to range up into the Hauterivian of the Moscow Basin. These include *Batioladinium gochtii*, *Cribroperidinium cf. volkovae*, *Sentusidinium* sp. 4 (Iosifova), *Spiniferites* sp. 2, and *Warrenia brevispinosa*. Of these, only *W. brevispinosa* was not recorded below the Hauterivian interval in the Moscow Basin. However, since the Valanginian Stage was not sampled at her section, it is not possible to state whether her taxon ranges below the Hauterivian in its type locality.

None of the reliable dinoflagellate markers of the late Late Valanginian or Hauterivian of NW Europe was found to occur in the Volga Basin: *Callaiosphaeridium asymmetricum*, *Discorsia nanna*, *Gardodinium trabeculosum*, *Hystrichodinium furcatum*, *Nematosphaeropsis scala*, *Nexosispinosum vetusculum*, and *Spiniferites dentatus* are all absent in the studied interval at both Gorodische and Kashpir.

4.2.7. Summary of important dinocyst markers.

The following have been found to be useful dinocyst biohorizons, and potential markers for correlation between the Volga Basin and NW European Upper Jurassic to Lower Cretaceous successions:

- FAD of *Gochteodinia villosa*. This occurs at the base of the nikitini Zone in the Volga Basin, and has been previously reported from the base of the Kerberus Zone in NW Europe. Thus this marker is tied to within half an ammonite zone in both regions, and may argue for correlation of the nikitini and Kerberus zone bases.
- The FAD of *Pseudoceratium pelliferum* has been found at a level approximately half way up the tzikwinianus Zone in the Volga Basin in both the present report, and by

Riding *et al.* (press). In NW Europe this datum is most frequently reported to occur at the base of the Albidum Zone (Davey, 1979, 1982; Heilmann-Clausen, 1987; Poulsen, 1992, 1994, 1996). Thus this datum is closely correlatable in both areas.

- The FAD of *Spiniferites ramosus* occurs at the base of the unzoned Valanginian deposits in the Volga Basin, and from a level immediately above the base of the Paratollia Zone in NW Europe. This marker thus supports an Early Valanginian age for these deposits.
- The complete range of *Pseudoceratium* sp. 1, and in particular its FAD are excellent tools for correlation of the latest Ryazanian to Early Valanginian interval in both regions. In the Volga Basin this taxon ranges from the middle part of the tzikwinianus Zone to a short distance above the base of the unzoned Valanginian deposits. In NW Europe Heilmann-Clausen (1987) recorded this species from the Albidum to Polyptychites chron interval. Thus the range base of this taxon is precisely correlatable in both areas, and the restricted range indicates that at least the basal part of the mica-rich siltstones are of Valanginian age.
- The FAD of *Muderongia crucis* occurs approximately half way up the studied mica-rich siltstone interval at Kashpir, and is known from the base of the Polyptychites Zone in NW Europe. This is further evidence for the Valanginian age of these deposits.

In addition, the following have been found to have a similar stratigraphic position across the Russian Platform, and may prove to be useful markers in that area:

- The LAD of *Glossodinium dimorphum* has been reported as marking the top of the zarajskensis Subzone in the Russian Platform by Riding *et al.* (in press). This marker is corroborated here.

- The LAD of *Senoniasphaera jurassica* has been noted from the nodiger Zone in the present report and by Riding *et al.* (in press). The latter authors suggested that this taxon was therefore a good marker of the Late Volgian of the Russian Platform, and this status is defended here.
- The FAD of *Batioladinium gochtii* has been shown to occur within the spasskensis Zone in the Volga and Moscow Basins.
- The FAD of *Cribroperidinium cf. volkovae* has been found to occur within the tzikwinianus Zone in the Volga Basin, whilst the FAD of *C. volkovae* is known from the upper part of the Rjasanensis (spasskensis) Zone in the Moscow Basin. This datum is closely correlatable in both areas, and is thus a useful marker for the Late Ryazanian.

4.2.8. Dinoflagellate cyst age of the unzoned deposits at Gorodische and Kashpir.

Age of the Phosphorite deposit (Bed 19) at Gorodische.

The phosphorite deposit at Gorodische has previously been attributed to the Valanginian Stage by Blom *et al.* (1984). There are indeed several dinocyst taxa which occur in this deposit that may also be found in the Valanginian strata above, but all of these also occur in the underlying Volgian deposits. None of the taxa traditionally used to mark strata of Valanginian age appears in the phosphorite horizon. Moreover, the presence of *Lithodinia* sp. 1, *Perisseiasphaeridium ingegerdiae*, *Cribroperidinium* sp. 8, *Prolixosphaeridium parvispinum*, and *Systematophora daveyi*, is indicative of a Volgian to Ryazanian age by comparison with the occurrence of these taxa in the section at Kashpir, as well as their known ranges in NW Europe. By the same process, the occurrence of *Gonyaulacysta dentata* and *Senoniasphaera jurassica* in this deposit

(which have LADs in the latest Volgian at Kashpir), together with the absence of *Cassiculosphaeridia pygmaeus*, *Muderongia longicornis*, *Sentusidinium* sp. 4, and *Systematophora palmula*, which mark the pre-spasskensis Zone Ryazanian deposits at Kashpir, is suggestive of Late Volgian age. The lack of any profound change in the flora of this deposit compared to that immediately below it suggests that it was deposited at the same time as sediments referable to the nodiger Zone.

Age of the unzoned basal Ryazanian deposits at Kashpir (beds 18-22).

This interval presumably corresponds to the Subclypieforme-Kochi interval of elsewhere in the Russian Platform, although whether it includes an hiatus in the Volga Basin is unclear. The dinoflagellate data offer little evidence to precisely correlate this interval with that of NW Europe. However, the LAD of *Amphorula exspiratum* and the FAD of *Systematophora palmula* both occur in this interval of the Volga Basin, correlatable to the Runctoni to Kochi zones of the Boreal standard in NW Europe.

Age of Bed 24 at Kashpir.

This unit (bearing phosphatic concretions), and the overlying sediments have been assigned to the Hauterivian by Blom *et al.* (1984). However, none of the dinocyst taxa typical of Hauterivian deposits is present in this bed. The co-occurrence of *Egmontodinium torynum*, *Endoscrinium pharo*, *Pseudoceratium* sp. 1, and *Spiniferites ramosus* strongly suggest an Early Valanginian age, most likely correlatable to the lower part of the Paratollia Zone in NW Europe. Using the correlation scheme of Hoedemaeker (1990), this corresponds to the Undulatoplicatilis Zone of elsewhere in the Russian Platform

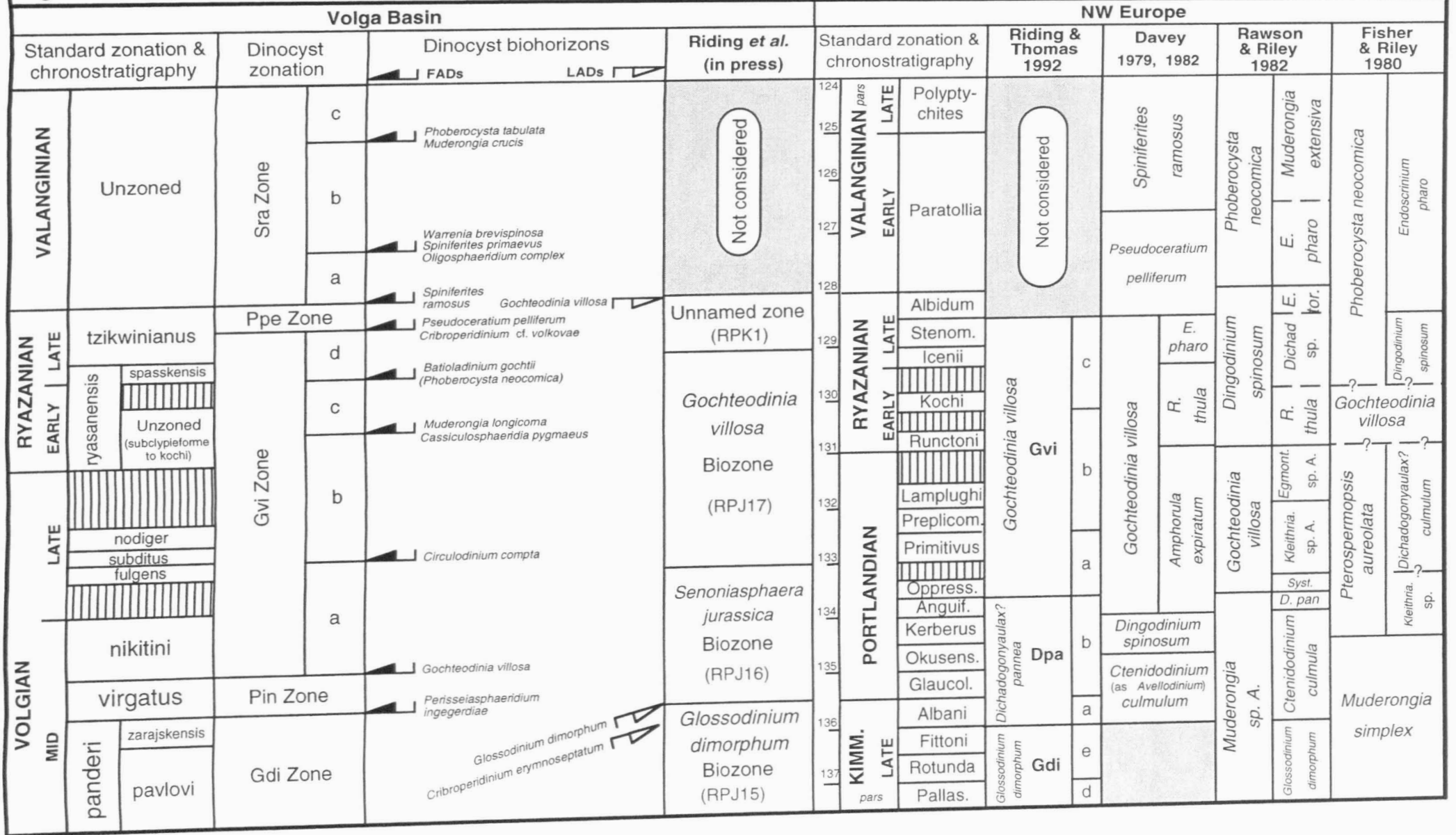
Age of the mica-rich siltstones (Gorodische Bed 20; Kashpir beds 27-30).

These deposits contain dinocyst taxa commonly noted from both the Valanginian and Hauterivian of NW Europe. However, none of the taxa unequivocally associated with the Late Valanginian or Early Hauterivian have been encountered in the present study. By comparison with the known range-tops in NW Europe, the co-occurrence of *Egmontodinium torynum*, *Endoscrinium pharo*, *Pseudoceratium* sp. 1, and *Tubotuberella apatela*, in the lower part of these deposits is strongly indicative of Early Valanginian age. The range-top of *Kleithriasphaeridium porosispinum* is known from the top of the Paratollia Zone in NW Europe, and this taxon ranges above the studied interval in the Volga Basin. The FAD of *Muderongia crucis* may correlate in both areas, and thus be indicative of early Late Valanginian Polyptychites Zone interval.

4.2.9. Dinoflagellate cyst zonation of the Volga Basin

Five dinoflagellate cyst biozones have been constructed, two of which are further divided into subzones. All zones and subzones are interval biozones, as defined by the International Subcommittee on Stratigraphic Classification (Salvador, 1994). Zone and subzone boundaries are thus drawn on the basis of first or last occurrence data for selected dinocyst taxa. Where possible, zonal index, and other important marker taxa from NW Europe have been used in the present scheme. Where possible, first appearance data have been chosen in preference to last occurrence data, due to the potential significance of reworking in such condensed sections as Gorodische and Kashpir. It has proved possible to refine the Russian Platform dinocyst zonation of Riding *et al.* (in press), although the subzones proposed here may only prove to be of local stratigraphic significance. Comparison of the proposed zonation is made with that of Riding *et al.* (in press) for the Russian Platform, and the schemes proposed by various authors for NW Europe in Figure 4.9. Where relevant, these comparisons are discussed in the text.

Figure 4.9: Dinocyst zonation of the Mid Volgian to Valanginian interval in the Volga Basin: comparison to NW Europe



Glossodinium dimorphum (Gdi) Biozone

Definition: The interval from the LAD of *Subtilisphaera? inaffecta*, to the LAD of *Glossodinium dimorphum*, and the FAD of *Perisseiasphaeridium ingegerdiae*.

Notes: This Biozone essentially follows that of Riding *et al.* (in press). The base of the biozone extends below the base of the *zarajskensis* Subzone, and thus below the base of the interval examined here: thus the basal marker of this biozone is not defined here, but follows Riding *et al.* (in press). In the present study, the LAD of *Glossodinium dimorphum* was found to fall below the top of the *zarajskensis* Subzone at Gorodische, but at the top of this subzone at Kashpir. The absence of lenticular-bedded facies at the top of this subzone at Kashpir suggests the presence of a short stratigraphic gap at this level, which may be responsible for this inconsistency. For this reason, the upper limit of the biozone is defined by the last occurrence of *G. dimorphum*, as well as the FAD of *P. ingegerdiae*, which occurs at the base of the *virgatus* Zone.

Age: Late Jurassic, Early to Mid Volgian (*sokolovi* to *panderi* zones)

Reference Sections: Gorodische.

Typical dinocyst assemblages:

The reader is referred to Riding *et al.* (in press) for a description of the Early Volgian Gdi Biozone assemblages. Assemblages from the *zarajskensis* Subzone are characterised by abundant *Batiacasphaera* spp., *Dingodinium* spp., *Impletosphaeridium/Downiesphaeridium* spp., *Systematophora daveyi*, and common *Circulodinium* spp., *Chytroeisphaeridia chytroeides*, *Kleithriasphaeridium fasciatum*, and *Pareodinia* spp.. Sporadically important are *Cometodinium whitei*, *Cribroperidinium* spp., *Lithodinia* sp. 1, *Prolixosphaeridium parvispinum*, *Sentusidinium* sp. 3, *Sirmiodinium grossi*, and *Tehamadinium* sp. 1. Rare, but

characteristic floral elements of this interval include *Glossodinium dimorphum*, *Gochteodinia tuberculata*, *Rhynchodiniopsis martonense*, *Tehamadinium sousense*, and *Thalassiphora robusta* sp. nov.. Additionally, *Cribroperidinium erymnoseptatum* and *Trichodinium* sp. 1 are rare but typical elements of the lower part of the zarajskensis Subzone.

Comparison with other areas:

The upper boundary definition of the Gdi Zone is emended from Riding *et al.* (in press), but remains at the same level across the Russian Platform. This zone corresponds to the Wheatleyensis to Albani Zones of the standard Boreal ammonite scheme. The base of the Gdi Biozone in the Russian Platform is thus drawn slightly higher than in NW Europe, where its base is in the Elegans Zone. Conversely, the top of this biozone in the Russian Platform is stratigraphically lower than in the NW European area. However, the Gdi Biozone in NW Europe is defined on different dinocyst data, and thus the two are only loosely comparable. Riding *et al.* (in press) note that the LAD of *G. dimorphum* in the Russian Platform is stratigraphically lower than in NW Europe. No equivalent interval has been noted in Arctic provinces of the Boreal Realm.

Perisseiasphaeridium ingegerdiae (Pin) Biozone

Definition: The interval from the FAD of *Perisseiasphaeridium ingegerdiae* (and the LAD of *Glossodinium dimorphum*), to the FAD of *Gochteodinia villosa*.

Age: Late Jurassic, Mid Volgian (virgatus Zone)

Reference Section: Gorodische.

Typical dinocyst assemblages:

Assemblages of this biozone contain abundant *Systematophora daveyi* and common *Chlamydophorella nyei*, *Circulodinium* spp., *Cribroperidinium* spp., *Tenua hystrix*, and *Trichodinium* cf. *ciliatum*. Sporadically important are *Dingodinium* spp., *Kleithriasphaeridium fasciatum*, and *Sirmiodinium grossi*. This zone is separable from the underlying zone by the diminished abundance of *Batiacasphaera* spp., and *Dingodinium* spp., and by the increased abundance of *Chlamydophorella nyei*, and *Trichodinium* cf. *ciliatum*, together with the presence of *Achomosphaera neptuni*, *P. ingegerdiae* and *Impletosphaeridium* sp. 1. It is distinguishable from the overlying biozone by the absence of *Gochteodinia villosa*.

Comparison with other areas:

This biozone spans the interval between the Gdi and Gvi biozones, and in this respect is comparable to the *Senoniasphaera jurassica* Biozone of Riding *et al.* (in press). The latter biozone could not be used in the present report since the index taxon was not recovered from the virgatus Zone in the residues studied. *Perisseiasphaeridium ingegerdiae* was not encountered by Riding *et al.* (in press), and has been noted by Poulsen (1996) to range from the Mutabilis to Autissiodorensis zones in NW Europe. Thus the FAD of *P. ingegerdiae* may be only of local significance to the Volga Basin, and does not correlate to areas in NW Europe.

Gochteodinia villosa (Gvi) Biozone

Definition: The interval between the FAD of *Gochteodinia villosa* and the FADs of *Pseudoceratium pelliferum* and *Cribroperidinium* cf. *volkovae*.

Notes: In definition this biozone is close to the original concept of Davey (1979) from NW Europe, except that its upper limit is additionally defined by the FAD of *C.* cf. *volkovae*. The upper limit of this biozone is set at the spasskensis/tzikwinianus zone boundary although only one sample was taken from near the top of the tzikwinianus Zone.

Age: Late Jurassic, Mid Volgian (nikitini Zone) to Early Cretaceous, Late Ryazanian (spasskensis Zone).

Reference section: Gorodische and Kashpir.

Typical dinocyst assemblages:

Late Jurassic assemblages from the Gvi Biozone contain abundant *Systematophora daveyi* and common *Batiacasphaera* spp., "*Cleistosphaeridium aciculum*", *Gochteodinia villosa*, *Perisseiasphaeridium ingegerdiae*, *Tehamadinium daveyi*, and *Trichodinium* cf. *ciliatum*. Also sporadically important are *Dingodinium tuberosum*, *Hystrichodinium pulchrum*, *Impletosphaeridium* sp. 1, *Kleithriasphaeridium porosispinum*, and *Lagenadinium ?membranoidium*. Early Cretaceous assemblages contain common to abundant *Batiacasphaera* spp., *Circulodinium compta*, and *Dingodinium tuberosum*, and common *Chytroeisphaeridia chytroeides*, and *Hystrichodinium pulchrum*. *Tenua* cf. *hystrix* is sporadically important.

Comparison to other areas:

The Gvi Biozone is similar to the same zone of Riding *et al.* (in press), except that the first appearance of the index taxon, and thus the base of the interval is lower than previously noted, in the nikitini Zone. The upper limit of the biozone is slightly higher than that indicated by Riding *et al.* (in press), since *P. pelliferum* was first noted from the upper part of the tzikwinianus Zone. However, precise positioning of this boundary is not possible here, since only one sample was taken from the tzikwinianus Zone. In western Europe, the base of the *Gochteodinia villosa* Zone is drawn either at the base of the Oppressus Zone (Riley, 1977; Riding & Thomas, 1988, 1992), or at the base of the Anguiformis Zone (Davey, 1979, 1982; Poulsen, 1992, 1994), despite the identification of this taxon from the Kerberus Zone (Davey, 1982; Hellmann-Clausen, 1987; Poulsen,

1996). Thus this datum correlates more precisely in the Volga Basin and NW Europe than is indicated from comparison of the dinoflagellate cyst zonation schemes. The top of the Gvi Biozone, as currently drawn, correlates precisely with the top of this zone in NW Europe, since the *tzikwinianus* Zone of the Russian Platform is equivalent to the *Stenomphalus* and *Albidum* ammonite zones of the Boreal standard (Kuznetsova, 1978).

The Gvi Biozone is split into four interval sub-biozones. These are based on dinocyst data of local stratigraphic importance, and are not comparable to the subdivision of this biozone in NW Europe.

Sub-biozone a

Definition: The interval from the FAD of *Gochteodinia villosa* to the FAD of *Circulodinium compta*.

Age: Late Jurassic, Mid to Late Volgian (*nikitini* & *fulgens* zones).

Reference section: Gorodische

Sub-biozone b

Definition: The interval from the FAD of *Circulodinium compta* to the FADs of *Muderongia longicornis* and *Cassiculosphaeridia pygmaeus*.

Age: Late Jurassic, Late Volgian (*subditus* Zone) to Early Cretaceous, Early Ryazanian (lowermost part of the basal Ryazanian unzoned interval, equivalent to the *subclypeiforme-kochi* interval of elsewhere in the Russian Platform, and the *Runctoni-Kochi* interval of the Boreal standard).

Reference section: Kashpir.

Sub-biozone c

Definition: The interval from the FADs of *Muderongia longicorna* and *Cassiculosphaeridia pygmaeus*, to the FAD of *Batioladinium gochtii* (and *Phoberocysta neocomica*).

Note: *Phoberocysta neocomica* is placed in parentheses since although it has been encountered by Riding *et al.* (in press) at this level, it was not recorded in the present investigation lower than the upper part of the tzikwinianus Zone.

Age: Late Early Ryazanian (upper part of the basal Ryazanian unzoned interval).

Reference section: Kashpir.

Sub-biozone d

Definition: The interval from the FAD of *Batioladinium gochtii* (and *Phoberocysta neocomica*) to the FADs of *Pseudoceratium pelliferum* and *Cribroperidinium cf. volkovae*.

Age: Late Ryazanian (spasskensis Zone to the lower part of the tzikwinianus Zone).

Sub-biozones c and d can be distinguished from a and b by the increased abundance of *Achomosphaera neptuni*, *Circulodinium compta*, *Sentusidinium* sp. 4, and *Tenua cf. hystrix*, and by the absence of *Systematophora daveyi*. The FADs of *Batioladinium gochtii* and *Muderongia longicorna* are comparable to those noted by Iosifova (1996) from the Moscow Basin, and are therefore of regional biostratigraphic significance within the Russian Platform. The FADs of *C. compta* and *C. pygmaeus* have been shown to occur at different levels in other parts of the Russian Platform, and are therefore only of local biostratigraphic significance within the Volga Basin.

Pseudoceratium pelliferum (Ppe) Biozone

Definition: The interval from the FADs of *Pseudoceratium pelliferum* and *Cribroperidinium* cf. *volkovae* to the FAD of *Spiniferites ramosus* and the LAD of *Gochteodinia villosa*.

Age: Early Cretaceous, latest Ryazanian (upper part of the tzikwinianus Zone)

Reference section: Kashpir.

Typical dinocyst assemblages:

The residue examined belonging to the Ppe Biozone contains abundant *Dingodinium* spp., and common *Chlamydophorella nyei*, *Chytroeisphaeridia chytroeides*, *Circulodinium compta*, "*Cleistosphaeridium aciculum*", *Impletosphaeridium* sp. 1, *Kleithriasphaeridium corrugatum*, and *Sentusidinium* sp. 4. Rare, but stratigraphically important elements of the flora are *Cribroperidinium* cf. *volkovae*, *Phoberocysta neocomica*, *Pseudoceratium pelliferum*, and *Pseudoceratium* sp. 1.

Comparison to other areas:

The Ppe Biozone corresponds in stratigraphic position to the unnamed zone (RPK1) of Riding *et al.* (in press). RPK1 spanned the interval from the LAD of *G. villosa* to the FAD of *P. pelliferum*. In the present study these two datums have been recorded from the same horizon, eliminating this unnamed zone. The base of the Ppe Biozone as currently defined accurately correlates with the base of this zone in NW Europe, offering independent evidence for the correlation of the upper part of the Russian tzikwinianus Zone with the Albidum Zone of the Boreal standard. The upper boundary of the Ppe Biozone is stratigraphically lower than originally defined in NW Europe, since

Davey (1979, 1982) recorded the FAD of *S. ramosus* from a level approximately half way up the Paratollia Zone. The range base of *S. ramosus* has since been reliably established at the base of the Paratollia Zone (Heilmann-Clausen, 1987; Costa & Davey, 1992), and thus there is strong correlation of this biozone between the NW European and Russian Platform areas.

***Spiniferites ramosus* (Sra) Biozone**

Definition: The interval from the FAD of *Spiniferites ramosus* (and LAD of *Gochteodinia villosa*), to the FAD of *Discorsia nanna*.

Note: This definition uses the upper boundary of the biozone as defined by Davey (1979), since the biozone extends above the interval examined here. The datum of *Gochteodinia villosa* is placed in parentheses since it has been shown to occur slightly higher in the NW European area, and thus may only be of regional stratigraphic significance within the Russian Platform.

Age: Early Cretaceous, Early to Late Valanginian.

Reference sections: Kashpir (and Gorodische) for the Early Valanginian, various sections in NW Europe detailed by Davey (1979) for the Late Valanginian part.

Typical dinocyst assemblages:

Assemblages typical of the Sra Biozone contain common to abundant *Achomosphaera neptuni*, *Chlamydophorella nyei*, *Circulodinium compta*, *Dapsillidium multispinosum*, *Dingodinium* spp., *Impletosphaeridium lumectum*, *Impletosphaeridium* sp. 1, *Kleithriasphaeridium corrugatum*, *Lagenadinium ?membranoidium*, and *Sentusidinium* sp. 4. Sporadically important are *Cassiculosphaeridia reticulata*, *Chytroeisphaeridia chytroeides*, *Circulodinium* spp., "*Cleistosphaeridium aciculum*",

Cometodinium habibii, *Nelchinopsis kostromiensis*, *Oligosphaeridium complex*, *Phoberocysta neocomica*, *Spiniferites ramosus*, *Spiniferites* sp. 2, *Tenua* cf. *hystrix*, and *Warrenia brevispinosa*. Other rare but stratigraphically important elements of the flora are *Cymosphaeridium validum*, *Exochosphaeridium phragmites*, *Lithodinia bulloidea*, *Muderongia crucis*, *Phoberocysta tabulata*, *Spiniferites primaevus*, and *Wallodinium cylindricum*.

Comparison to other areas:

The Sra Biozone is directly comparable to that of NW Europe. The flora however, shows a mix of taxa which are traditionally common in the both the Valanginian and Hauterivian of the latter area. Taxa usually common to the Hauterivian in NW Europe have nevertheless been shown to range down into the Early Valanginian, and are therefore comparable in the two areas. None of the taxa unequivocally associated with the Late Valanginian to Hauterivian interval in NW Europe were encountered in the present study.

The Sra Biozone is subdivided into three interval sub-biozones.

Sub-biozone a

Definition: The interval from the FAD of *Spiniferites ramosus* and LAD of *Gochteodinia villosa* to the FADs of *Oligosphaeridium complex*, *Spiniferites primaevus* and *Warrenia brevispinosa*.

Age: Basal Valanginian (unzoned, possibly equivalent to the undulatoplicatilis Zone of elsewhere in the Russian Platform, and the basal part of the Paratollia Zone of the Boreal standard).

Reference section: Kashpir.

Notes: This sub-biozone encapsulates the sandstone horizon bearing phosphatic concretions (Bed 24) at Kashpir. As such, an exceptionally well preserved microflora has been recovered from this level, including forms apparently exclusive to it. These include *Aprobolocysta pustulosa* sp. nov., *Cyclonephelium? bulbosum* sp. nov., and *Lithodinia distincta* sp. nov..

Sub-biozone b

Definition: The interval from the FADs of *Oligosphaeridium complex*, *Spiniferites primaevus* and *Warrenia brevispinosa*, to the FADs of *Phoberocysta tabulata* and *Muderongia crucis*.

Age: Early Cretaceous, Early Valanginian (unzoned, possibly equivalent to the Hoplitoides Zone of elsewhere in the Russian Platform, and the upper part of the Paratollia Zone of the Boreal standard).

Reference section: Kashpir (and Gorodische)

Notes: *Muderongia crucis* was not encountered at Gorodische. Sub-biozone b is thought to be only of local stratigraphic value within the Volga Basin, although examination of the Valanginian interval in the type-section of *W. brevispinosa* (Tchernaya Retchka, Moscow Basin) may reveal regional stratigraphic significance across the Russian Platform.

Sub-biozone c

Definition: The interval from the FADs of *Phoberocysta tabulata* and *Muderongia crucis* to the top of the studied interval.

Age: Early Cretaceous, Early Valanginian (unzoned, possibly equivalent to the Michalskii Zone of elsewhere in the Russian Platform, and the Polyptychites Zone of the Boreal standard) to the top of the studied interval.

Notes: The top of this sub-biozone cannot be defined in the current investigation. *P. tabulata* is known to range lower in the NW European area, and its FAD in the Volga Basin is therefore only of local stratigraphic significance. In NW Europe, the FAD of *M. crucis* has been noted at the base of the Polyptychites Zone (Costa & Davey, 1992), and thus this datum may be comparable in both areas.

4.2.10. Summary

Dinoflagellate biostratigraphy of the Volga Basin sections at Gorodische and Kashpir has been examined. Comparison of dinocyst markers from this study with known datums from NW Europe has allowed dating of sediments unzoned by ammonites, and several correlation-points between the standard Boreal and Russian Platform ammonite chronologies to be suggested. Such tie-points support the correlation presented by Kuznetsova (1978). Important first appearance data (FADs) have been used in the formulation of a dinoflagellate cyst zonation for the Mid Volgian to Valanginian interval in the Volga Basin. This zonation augments the scheme recently proposed by Riding *et al.* (in press). The scheme proposed here is comparable in parts to the NW European dinocyst zonation most recently proposed by Riding & Thomas (1992), although the ranges of several Jurassic taxa are significantly different in the two areas.

4.3. Dinocyst species list and systematics

4.3.1. Introduction

In the species list given below, dinocyst taxa are classified according to Fensome *et al.* (1993), except for the genera *Stanfordella* and *Wrevittia* which are classified according to Helenes & Lucas-Clark (1997). Species authorship follows Williams *et al.* (1998), except for the taxon *Endoscrinium inritibile* which was omitted from Williams *et al.* (1998), and therefore follows Lentin & Williams (1993). In the systematics section the descriptive terminology largely follows that in Evitt (1985), with paraplate notation following that of Fensome *et al.* (1993) after Kofoid (1909). Six new species are described, but cannot yet be treated as formal taxa until they have been properly published. 60 taxa which have not been found to be conspecific with any previously published species are given brief descriptions, and contrasted with other taxa in the Volga Basin assemblages. Figure 4.10 shows the cyst measurements referred to in the text, and in tables 4.5 - 4.10. Measurement data are provided in the text by a (minimum) mean (maximum) μm format.

4.3.2. Species list

DIVISION Dinoflagellata
SUBDIVISION Dinokaryota
CLASS Dinophyceae
SUBCLASS Peridiniphyceae
ORDER Gonyaulacales
SUBORDER Cladopyxlineae
FAMILY Cladopyxiaceae

Microdinium sp. 1

FAMILY Pareodiniaceae
SUBFAMILY Broomeoideae

Aprobolocysta galeata Backhouse 1987

Aprobolocysta neista Duxbury 1980

Aprobolocysta pustulosa sp. nov.

Batioladinium ?gochtii (Alberti 1961) Lentin & Williams 1977

Batioladinium jaegeri (Alberti 1961) Below 1990

Batioladinium longicornutum (Alberti 1961) Below 1990

Batioladinium varigranosum (Duxbury 1977) Davey 1982

Batioladinium sp. 1

Kalyptea diceras (Cookson & Eisenack 1960) Fisher & Riley 1980

SUBFAMILY Pareodinioideae

Gochteodinia antennata (Gitmez & Sarjeant 1972) Below 1990
Gochteodinia judilentinae McIntyre & Brideaux 1980
Gochteodinia mutabilis (Riley in Fisher & Riley 1980) Fisher & Riley 1982
Gochteodinia tuberculata Below 1990
Gochteodinia villosa (Vozzhennikova 1967) Lentin & Vozzhennikova 1990
Gochteodinia cf. *villosa* (Vozzhennikova 1967) Lentin & Vozzhennikova 1990
Pareodinia ceratophora (Deflandre 1947) Gocht 1970
Pareodinia prolongata Sarjeant 1959
Pareodinia sp. 1

SUBORDER Gonyaulacineae FAMILY Gonyaulacaceae SUBFAMILY Leptodinioideae

Ambonosphaera ?staffinensis (Gitmez 1970) Poulsen & Riding 1992
Amphorula expiratum Davey 1982
Athigmatocysta glabra Duxbury 1977
Ctenidodinium sp. 1
Cymosphaeridium validum Davey 1982
Dichadogonyaulax ?chondra (Drugg 1978) Courtinat 1989
Dichadogonyaulax sp. 1
Egmontodinium polyplacophorum Gitmez & Sarjeant 1972
Egmontodinium torynum (Cookson & Eisenack 1960) Davey 1979
Egmontodinium sp. 1
Endoscinium anceps Raynaud 1978
Endoscrinium granulatum (Raynaud 1978) Lentin & Williams 1981
Endoscrinium inritibile Riley in Fisher & Riley 1980
Endoscrinium pharo Duxbury 1977
Kleithriasphaeridium corrugatum Davey 1974
Kleithriasphaeridium eoinodes (Eisenack 1958) Sarjeant 1985
Kleithriasphaeridium cf. *eoinodes* (Eisenack 1958) Sarjeant 1985
Kleithriasphaeridium fasciatum (Davey & Williams 1966) Davey 1974
Kleithriasphaeridium porosispinum Davey 1982
Leptodinium arcuatum (Klement 1960) Sarjeant 1984
Leptodinium subtile Klement 1960
Lithodinia acranitabulata Brenner 1988
Lithodinia bulloidea (Cookson & Eisenack 1960) Gocht 1976
Lithodinia distincta sp. nov.
Lithodinia sp. 1
Lithodinia sp. 2
Oligosphaeridium complex (White 1842) Davey & Williams 1966
Oligosphaeridium patulum Riding & Thomas 1988
Oligosphaeridium pulcherrimum (Deflandre & Cookson 1955) Davey & Williams 1966
Oligosphaeridium totum Brideaux 1971
Perissiasphaeridium ingegerdiae Nohr-Hansen 1986
Perissiasphaeridium pannosum Davey & Williams 1966
Sirmiodinium grossi (Alberti 1961) Warren 1973
Stanfordella exsanguia (Duxbury 1977) Helenes & Lucas-Clark 1997
Stanfordella fastigiata (Duxbury 1977) Helenes & Lucas-Clark 1997
Stiphrosphaeridium anthophorum (Cookson & Eisenack 1958) Lentin & Williams 1985
Stiphrosphaeridium dictyophorum (Cookson & Eisenack 1958) Lentin & Williams 1985
Systematophora areolata Klement 1960
Systematophora ?daveyi Riding & Thomas 1988
Systematophora palmula Davey 1982
Tehamadinium daveyi Jan du Chene et al. 1986
Tehamadinium evittii (Dodekova 1969) Jan du Chene et al. 1986
Tehamadinium konarae Dodekova 1992

Tehamadinium sousense (Below 1981) Jan du Chene *et al.* 1986
Tehamadinium sp. 1
Wrevittia helicoidea (Eisenack & Cookson 1960) Helenes & Lucas-Clark 1997
Wrevittia cf. *helicoidea* (Eisenack & Cookson 1960) Helenes & Lucas-Clark 1997
Wrevittia ?diutina (Duxbury 1977) Helenes & Lucas-Clark 1997

SUBFAMILY Cribroperidinioideae

Apteodinium daveyi Poulsen 1996
Apteodinium spinosum Jain & Millipied 1975
Apteodinium spongiosum (McIntyre & Brideaux 1980) Davey 1982
Apteodinium sp. 1
Apteodinium sp. 2
Apteodinium sp. 3
Cribroperidinium ?birkelundiae (Fensome 1979) Helenes 1984
Cribroperidinium diaphanum (Cookson & Eisenack 1958) Stover & Evitt 1978
Cribroperidinium erymnoseptatum Bailey 1993
Cribroperidinium nuciforme (Deflandre 1939) Courtinat 1989
Cribroperidinium venustum (Klement 1960) Poulsen 1996
Cribroperidinium cf. *?perforans* (Cookson & Eisenack 1958) Morgan 1980
Cribroperidinium cf. *volkovae* Iosifova 1996
Cribroperidinium sp. 1
Cribroperidinium sp. 2
Cribroperidinium sp. 3
Cribroperidinium sp. 4
Cribroperidinium sp. 5
Cribroperidinium sp. 6
Cribroperidinium sp. 7
Cribroperidinium sp. 8
Kallosphaeridium sp. 1
Kallosphaeridium sp. 2
Rhynchodiniopsis cladophora (Deflandre 1939) Below 1981
Rhynchodiniopsis magnifica sp. nov.
Rhynchodiniopsis martonensis Bailey *et al.* 1997
Rhynchodiniopsis undoryensis sp. nov.
Rhynchodiniopsis sp. 1
?Thalassiphora robusta sp. nov.

SUBFAMILY Gonyaulacoideae

Achomosphaera neptuni (Eisenack 1958) Lister & Batten 1988
Avellodinium falsificum Duxbury 1977
Gonyaulacysta dentata Raynaud 1978
Gonyaulacysta eisenackii (Deflandre 1939) Sarjeant 1982
Gonyaulacysta jurassica (Deflandre 1939) Sarjeant 1982
Gonyaulacysta pectinigera (Gocht 1970) Fensome 1979
Gonyaulacysta cf. *centriconnata* Riding 1983
Gonyaulacysta cf. *speciosa* Harding 1990 ex Harding in Williams *et al.* 1998
Gonyaulacysta sp. 1
Gonyaulacysta sp. 2
Gonyaulacysta sp. 3
Gonyaulacysta sp. 4
Spiniferites primaevus (Duxbury 1977) Monteil 1991
Spiniferites ramosus (Ehrenberg 1838) Mantell 1854
Spiniferites sp. 1
Spiniferites sp. 2
Tubotuberella apatela (Cookson & Eisenack 1960) Sarjeant 1982
Tubotuberella cf. *apatela* (Cookson & Eisenack 1960) Sarjeant 1982

SUBFAMILY Uncertain

Chytroeisphaeridia cerastes Davey 1979
Chytroeisphaeridia chytroeides (Sarjeant 1962) Davey 1979
Cometodinium habibii Monteil 1991
Cometodinium ?whitei (Deflandre & Courteville 1939) Monteil 1991
Escharisphaeridia pocockii (Sarjeant 1968) Erkmen & Sarjeant 1980
Escharisphaeridia spp.
Glossodinium dimorphum Ioannides et al. 1977
Hystrichodinium compactum Alberti 1961
Hystrichodinium pulchrum Deflandre 1935
Hystrichodinium voigtii (Alberti 1961) Sarjeant 1966
Hystrichosphaerina schindewolfii Alberti 1961
Isthmocystis distincta Duxbury 1979
Lagenorhytis delicatula (Duxbury 1977) Piasecki 1984
Nelchinopsis kostromiensis (Vozzhennikova 1967) Harding 1996
Protoellipsodinium sp. 1
Sentusidinium aff. ?*fibrillosum* Backhouse 1988
Sentusidinium rioultii (Sarjeant 1968) Courtinat 1989
Sentusidinium sp. 3 Iosifova 1996
Sentusidinium cf. sp. 3 Iosifova 1996
Sentusidinium sp. 4 Iosifova 1996
Trichodinium ciliatum (Gocht 1959) Eisenack & Klement 1964
Trichodinium cf. *ciliatum* (Gocht 1959) Eisenack & Klement 1964
Trichodinium sp. 1

FAMILY Areoligeraceae

"*Circulodinium ciliatum*" taxon-group
Circulodinium compta (Davey 1982) Helby 1987
Circulodinium copei Bailey et al. 1997
Circulodinium distinctum (Deflandre & Cookson 1955) Jansonius 1986
?Cyclonephelium bulbosum sp. nov
Senoniasphaera jurassica (Gitmez & Sarjeant 1972) Poulsen & Riding 1992
Tenua hystrix (Eisenack 1958) Sarjeant 1985
Tenua cf. *hystrix* (Eisenack 1958) Sarjeant 1985

SUBORDER Ceratlineae

FAMILY Ceratiaceae

Muderongia australis (Helby 1987) Monteil 1991
Muderongia longicorna (Monteil 1991) Monteil 1996
Muderongia crucis (Neale & Sarjeant 1962) Monteil 1991
Phoberocysta neocomica (Gocht 1957) Helby 1987
Phoberocysta tabulata (Raynaud 1978) Monteil 1991
Pseudoceratium pelliferum (Gocht 1957) Dörhöfer & Davies 1980
Pseudoceratium sp. 1

SUBORDER Goniodomineae

FAMILY Goniodomaceae

SUBFAMILY Pyrodinioideae

Hystrichosphaeridium petilum Gitmez 1970

SUBORDER Uncertain
FAMILY Uncertain

"Batiacasphaera fenestrata" taxon-group

Batiacasphaera sp. 1
Batiacasphaera sp. 2
Bourkinidinium sp. 1
Cassiculosphaeridia magna (Davey 1974) Harding 1990
Cassiculosphaeridia pygmaeus Stevens 1987
Cassiculosphaeridia reticulata Davey 1969
Chlamydophorella nyei Cookson & Eisenack 1958
Chlamydophorella wallala Cookson & Eisenack 1960
"Cleistosphaeridium aciculum" taxon-group
Dapsilidinium multispinosum (Davey 1974) Bujak et al. 1980
Dingodinium cerviculum (Cookson & Eisenack 1958) Mehrotra & Sarjeant 1984
Dingodinium jurassicum Cookson & Eisenack 1958
Dingodinium tuberosum (Gitmez 1970) Poulsen 1996
Dingodinium sp. 1
Ellipsoidictyum cinctum Klement 1960
Epiplosphaera gochtii (Fensome 1979) Brenner 1988
Epiplosphaera spp.
Exochosphaeridium phragmites Davey et al. 1966
Exochosphaeridium sp. 1
Gardodinium sp.
Heslertonia ?pellucida Gitmez 1970
Heslertonia sp 1
Impletosphaeridium lumectum (Sarjeant 1960) Islam 1993
Impletosphaeridium sp.1
Mendicodinium reticulatum Morgenroth 1970
Phanerodinium sp. 1
Tanyosphaeridium isocalamum (Deflandre & Cookson 1955) Davey & Williams 1969
Tanyosphaeridium magneticum Davies 1983
Valensiella ovula (Deflandre 1947) Courtinat 1989
Warrenia ?brevispinosa (Iosifova 1992) Iosifova 1996
Warrenia sp. 1

ORDER Uncertain
FAMILY Stephanelytraceae

Lagenadinium ?memranoidium (Vozzhennikova 1976) Lentin & Vozzhennikova 1990

SUBCLASS Uncertain
ORDER Uncertain
FAMILY Uncertain

Prolixosphaeridium mixtispinosum (Klement 1960) Davey et al. 1969
Prolixosphaeridium parvispinum (Deflandre 1937) Davey et al. 1969

Taxa excluded from the Division Dinoflagellata by Fensome et al. 1993:

Wallodinium anglicum (Cookson & Hughes 1964) Lentin & Williams 1973
Wallodinium cylindricum (Habib 1970) Feist-Burkhardt & Monteil 1994
Wallodinium krutzschii (Alberti 1961) Habib 1972
Wallodinium lunum (Cookson & Eisenack 1960) Lentin & Williams 1973

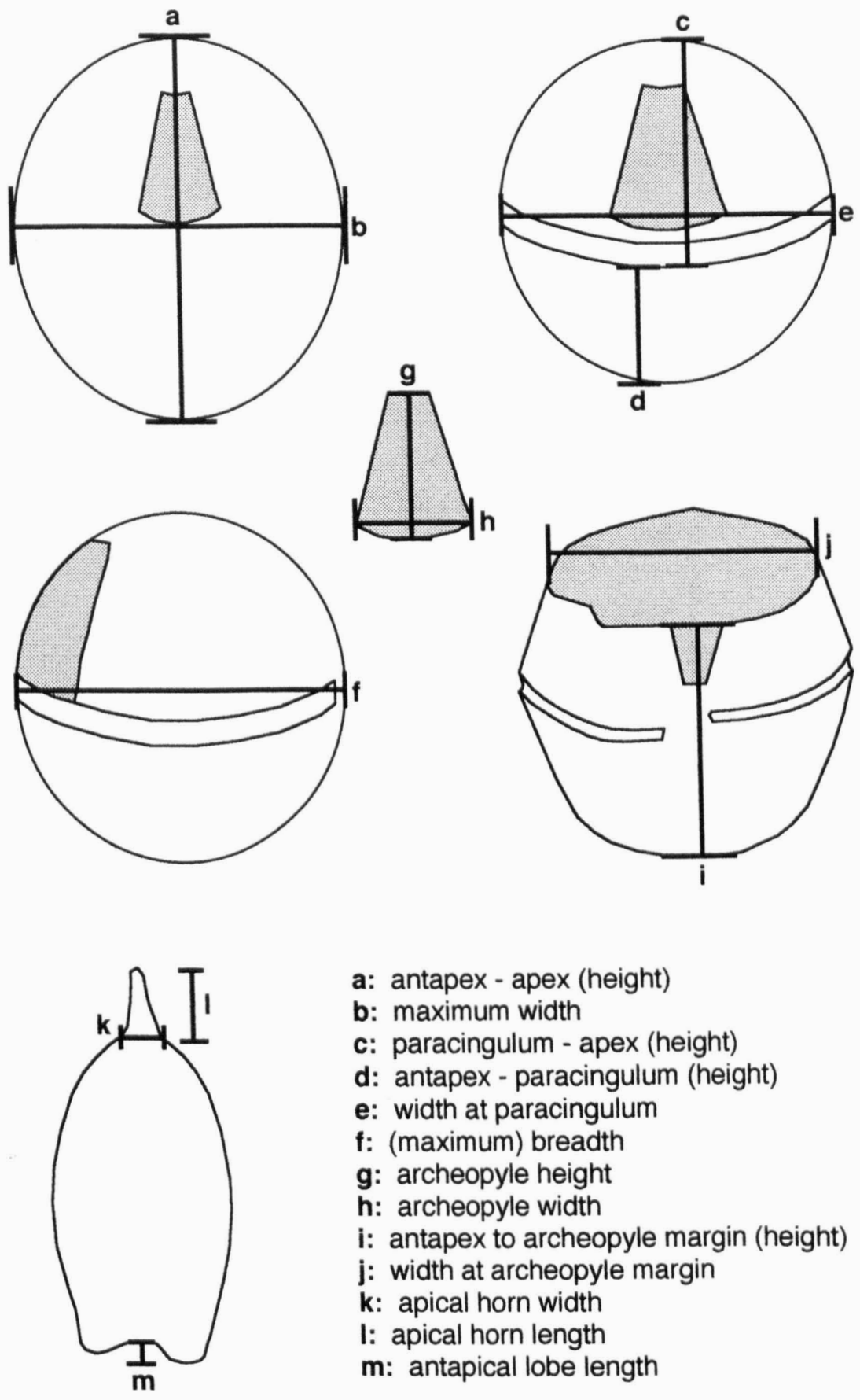


Figure 4.10: Explanation of measurements referred to in the Systematics Section and in Tables 4.5 - 4.10.

4.3.3. Formal description of new taxa

Name: *Aprobolocysta pustulosa* sp. nov.

Holotype: Slide K17/0-5/3, England Finder coordinates O56/1. Plate 1, Figures 1 & 2.

Paratype: Slide K17/0-10, England Finder coordinates Q33. Plate 1, Figures 9-11.

Type locality: Kashpir section, Volga Basin.

Type horizon: Bed 24, sandstone with phosphate concretions, Lower Valanginian, *Spiniferites ramosus* Zone.

Range: Only recorded from the type horizon.

Etymology: After the pustule-like nature of the ornamentation.

Diagnosis: Small elongate ovoidal cysts with apical archeopyle, probably type (2A), the archeopyle margin descending strongly from dorsal to ventral surfaces, with a pronounced sulcal notch on the ventral surface. The periphragm is developed into numerous non-tabular, subspherical to polygonal pustules which frequently deflate to leave concave distal surfaces. Such pustules may be discrete, compound, or be surmounted by one or more micro-pustules. The antapex is rounded to bilobed.

Description: Small, elongate ovoidal cysts, maximum cyst width mid-way between antapex and apex. Apex dome-shaped or slightly conical, antapex rounded to strongly asymmetrically bilobed. Periphragm folded into variable numbers of non-tabular, generally sub-spherical pustules of variable size and position. Between 2-5 pustules have been recorded on the ventral surfaces, and 4-7 on dorsal surfaces of the specimens examined. The pustules may be discrete or fused laterally to form compound clusters, and are restricted basally, close to the endophragm (but never completely closed), so that maximum circumference of the pustule is achieved a short distance from the endophragm. In certain specimens pustules may appear sub-polygonal when densely spaced on the cyst surface. Occasionally smaller subspherical micro-pustules are developed individually or in small clusters on the distal or lateral surfaces of the larger pustules. Endophragm and periphragm are adpressed between pustules. Periphragm is smooth to shagrinate over the pustules, and shagrinate and punctate in adpressed areas. The restricted basal region of many pustules (between the point of maximum

Orientation	Slide	England Finder coords	Antapex-archeopyle margin	Width at archeopyle margin	Maximum width	Antapical lobe length	Minimum pustule diameter	Maximum pustule diameter	Antapical pustule diameter	No. of ventral pustules	No. of dorsal pustules	Length apex-antapex
oblique ventral	K1705/3	O56/1	42	21	27	6.5	5.2	14.3	20	5	6	
oblique ventral	K17010	Q33	39	19	27	5.2	2.6	15.6	10	4	4	
operculum	K17010	R57										
oblique lateral	K17010/2	J43	42	16	27	4.6	5.2	14.3	12	4	6	
oblique ventral	K1705/2	T56/2	39	18	26	3.9	7.8	14.3	n/a	2	4	53
lateral	K17/010	H36	51	20	31	??	3.9	13	??	3	6	
operculum	K17010/2	Q57/4										
ventral	K17/2	S39/2	39	16	25	5.9	6.5	13	n/a	4	5	n/a
oblique lateral	K17010/3	N38/4	39	18	25	n/a	6.5	14.3	14	5	6	
lateral	K17010	J60/4	39	18	21	5.2	6.5	13	n/a	4	5	55
lateral	K17010	L50/4	42	18	25	n/a	5.2	15.6	13	?	5	n/a
lateral	K17010	M40/1	39	18	26	n/a	3.9	15.6	13	4	5	
lateral	K17010	U39/4	43	18	26	n/a	3.9	16.9	n/a	4	5	
ventral	K1705/3	J29/1	42	21	26	5.2	6.5	15.6	10	3	5	
lateral	K1705/3	M30	39	21	26		5.2	14.3	14	5	6	55
		av	41	19	26	5.2	5.3	14.6	13	3.9	5.2	54
		min	39	16	21		2.6	13	10	2	4	64
		max	51	21	31	6.5	7.8	16.9	20	5	6	66

Table 4.5: Measured dimensions of *Aprobolocysta pustulosa* sp. nov. Holotype and paratype are the first two specimens respectively.

circumference and adpression with the endophragm) bears numerous tiny claustra, only visible under the SEM. Pustules frequently deflate (particularly in SEM preparations) to form concave distal surfaces. Endophragm is smooth.

Paratabulation is only indicated at the archeopyle margin which descends strongly from the dorsal to ventral surfaces. Archeopyle is apical, type probably (2A) with a pronounced sulcal notch which is slightly displaced to the right of mid-ventral. The shape of the archeopyle is consistent with the paratabulation of the apical region of this genus as suggested by Fensome *et al.* (1993).

Dimensions: Antapex-archeopyle margin (39)41(51) μm , maximum width (21)26(31) μm . Pustule diameter (2.6)10(16.9) μm . 13 specimens measured. See also Table 4.5.

Remarks: This species differs from other representatives of *Aprobolocysta* by the distinctive subspherical pustules formed from the periphragm. *A. alata* Backhouse 1988 is similar in having an 'inflated' periphragm, with prominent cavation in certain areas of the cyst, but markedly differs in the broad, distinctive paracingular adpression of the wall layers. It differs from *Riasanodinium federovae* Iosifova 1992 in having a strongly developed 'sulcal notch' in the archeopyle margin, by not having plate-centered processes in the periphragm, and by the adpression of the wall layers between pustules.

Name: *Lithodinia distincta* sp. nov.

Holotype: Slide K17/0-10/3, England Finder coordinates N31/4. Plate 4, Figures 1 & 2.

Paratype: Slide K17/0-5/2, England Finder coordinates N61. Plate 4, Figure 3.

Type locality: Kashpir section, Volga Basin.

Type horizon: Bed 24, sandstone with phosphatic concretions.

Range: Only recorded in samples K17 & K18, both from the Early Valanginian *Spiniferites ramosus* Zone.

Etymology: Named after its distinctive appearance in transmitted light.

Diagnosis: Large, subspherical but slightly dorso-ventrally compressed proximate cysts, with a type (tA) archeopyle and a broad sulcal notch. The autophragm is sculpted into narrow muri which form a dense but evenly distributed reticulum with regularly sized and completely formed lumina, and which supports a completely developed ectophragm. No parasutural features are apparent in transmitted light, but a region of reduced height in the reticulum usually indicates the position of the parasulcus.

Description: Large subspherical, but slightly dorso-ventrally compressed proximate cysts, often with a slightly flattened antapex. The autophragm is sculpted into a dense and quite evenly distributed robust reticulation which supports a completely developed ectophragm. Mural height varies from 4.3-6.7 μm between specimens, but is generally markedly reduced at the parasulcus (particularly at the junction of the parasulcus and paracingulum) to between 1.5-5.7 μm . Mural width varies from 0.8-1.4 μm in all specimens measured. In cross section the muri are parallel-sided, but flare slightly at the contacts with the autophragm and ectophragm. Luminal diameter may vary from 2-8 μm in a single specimen. Paratabulation in transmitted light is only indicated by the sculptural restriction at the sulcus, and by the shape of the archeopyle margin. The archeopyle is type (tA), with a free simple polyplacoid operculum involving all four apical paraplate homologues.

SEM examination reveals that the ectophragm is minutely granulate, and most specimens show masses of small circular intratabular depressions on the outer surface formed by 'sagging' of the ectophragm into lumina in the reticulate sculpture. Moreover, the ectophragm is clearly tabulate, although details of sulcal paratabulation are suppressed. The central area of the sulcus bears small flagellar scars.

Paratabulation formula 4', 6'', 6c, xs, 6''', 1p, 1''''', with a leptodinioid arrangement (Figure 4.10). No opercula have been observed under the SEM, and thus the presence/absence of an apical pore complex or an anterior intercalary paraplate cannot be confirmed.

Parasutural areas are broad within the two adcingular series, between the post-cingular and antapical paraplates, within the cingular series, and at the junctions of the

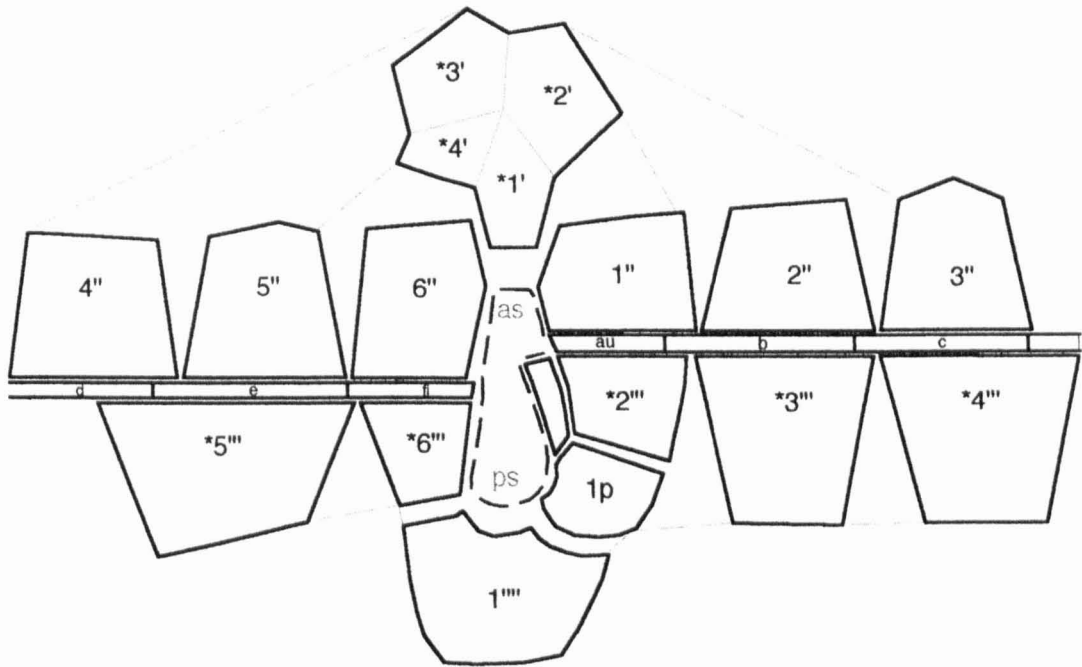


Figure 4.11: Exploded paratabulation of *Lithodinia distincta* sp. nov. Paraplate notation follows the recommendations of Fensome *et al.* (1993) to indicate plate homologues. Details of sulcal paratabulation are largely suppressed. No opercula have been studied under the SEM, so apical series plate boundaries within the operculum are tentative.

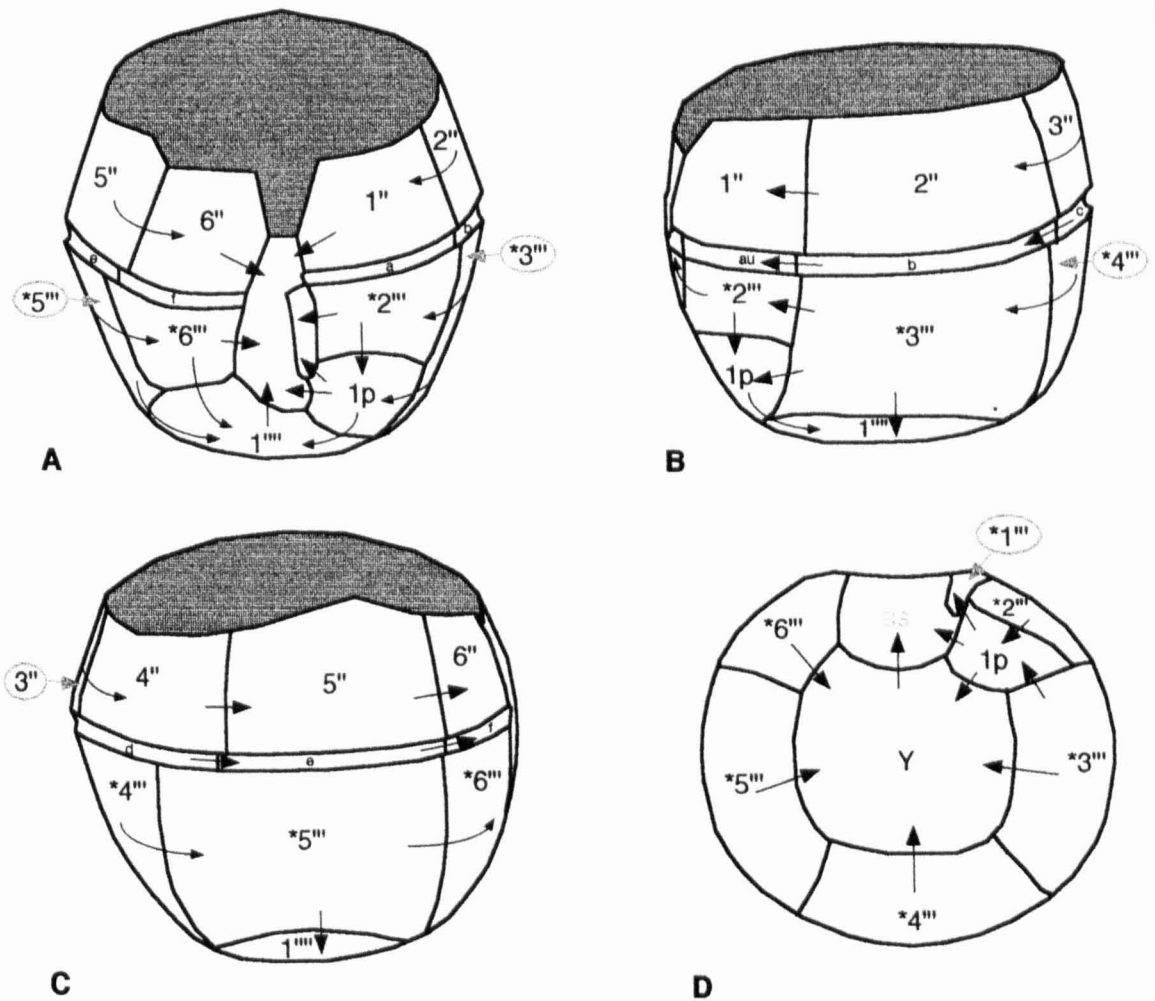


Figure 4.12: Paratabulation of *Lithodinia distincta* sp. nov. showing direction of paraplate overlap. **A:** ventral surface. **B:** Left lateral surface. **C:** Right lateral surface. **D:** Antapical surface. Paratabulation uses the recommendations of Fensome *et al.* (1993), to indicate plate homologues.

posterior intercalary paraplate with adjacent postcingular and antapical paraplates. Conversely, parasutures are narrow between the adcingular and cingular series. Broad parasutural regions appear to represent pandasutural bands, with fine striations on the overlapping plates perpendicular to the plate boundaries. Plates successively overlap from dorsal to ventral surfaces, and from the cingulum to the antapex (Figure 4.11). The posterior intercalary is overlapped by post-cingular paraplate homologues *2''' and *3''', and itself overlaps *1''', 1'''' and the parasulcal region. No un-excysted specimens were studied, so plate overlap of the precingular series with the apical homologues has not been established.

Dimensions: Width (in region of the paracingulum) 80(87)94 μm , height (antapex to archeopyle margin) 50(59)73 μm , breadth 80(86)90 μm (12 specimens measured). See also Table 4.6.

Remarks: In transmitted light, the large cyst size and dense reticulum of narrow muri, and the complete development of an ectophragm rather than a differentiated autophragm make this species quite distinctive from other members of *Lithodinia*. It is not placed in *Cassiculosphaeridia* or *Valensiella* since most examples of these genera not develop such continuous and robust ectophragma, and moreover SEM examination clearly reveals the leptodinioidean paraplate arrangement.

Name: ?*Cyclonephelium bulbosum* sp. nov.

Holotype: Slide K17/0-5, England Finder coordinates K30/3. Plate 4, Figures 6-8.

Paratype: Slide K17/0-10/2, England Finder coordinates N38. Plate 4, Figures 9 & 10.

Type locality: Kashpir section, Volga Basin.

Type horizon: Bed 24, sandstone with phosphate concretions.

Range: Only recorded from the type horizon, *Spiniferites ramosus* Zone..

Etymology: named after the bulbous nature of its processes terminations.

Diagnosis: Proximochorate acavate cyst with a dome-shaped apex, rounded to flattened or bilobed antapex. Hypocyst much longer and wider than epicyst. The autophragm is sculpted into short solid rod-like projections with bulbous terminations, which may be discrete or branching/anastomosing, and are concentrated in marginal and

apical regions. A small process group is usually present at the centre of the antapex, typically between the antapical lobes. The archeopyle is complex, involving all of the apical paraplate homologues as a simple polyplacoid operculum which remains adnate via paraplates 6", as, and 1", and also paraplate 3" which remains adnate via its boundary with the paracingulum. Kofoid archeopyle formula (tA)aP₃"a.

Description: Variable shape, with the apex usually rounded and dome-shaped, the antapex occasionally rounded, but usually flattened to bilobed. The position of the paracingulum is often indicated by a slight or occasionally pronounced restriction of the cyst ambitus (see paratype). Hypocyst is longer and wider than the epicyst. Cyst is proximochorate, acavate, with greatest concentration of processes in marginal and apical regions, and general absence of processes in mid-dorsal, and mid-ventral regions. Processes are short and solid with bulbous terminations, and may be discrete, fused distally, or branching distally to form process-clusters. A small but distinct tuft of slightly longer processes is usually present in the middle of the antapex, between the antapical lobes in bilobed specimens. Autophragm is thin, and smooth in mid-dorsal and mid-ventral areas.

Paratabulation is not expressed by parasutural features on the cyst surface, and is only apparent at the archeopyle margin. However, the dome-shaped nature of the apex often precludes examination of archeopyle character in many specimens, since the operculum is adnate and remains in its original position following excystment. Nevertheless, the apical series clearly forms the majority of the operculum. Both the shape of the operculum and the width of the opercular attachment on the ventral surface suggest that paraplate homologues *4'; *1'; and *2' remain attached at their boundaries with paraplates 6"; 6", as and 1"; and 1" respectively (Figure 4.13). This is supported by the position and number of accessory archeopyle sutures between precingular paraplates. Paraplate 3" is identified in a mid-dorsal position by particularly deep sutures, which probably extend to the paracingulum, and is thus a second adnate part of the operculum. The archeopyle formula is thus (tA)aP₃"a.

Dimensions: Antapex-apex (47)59(66) μm , maximum width (53)59(69) μm (19 specimens measured). See also Table 4.7.

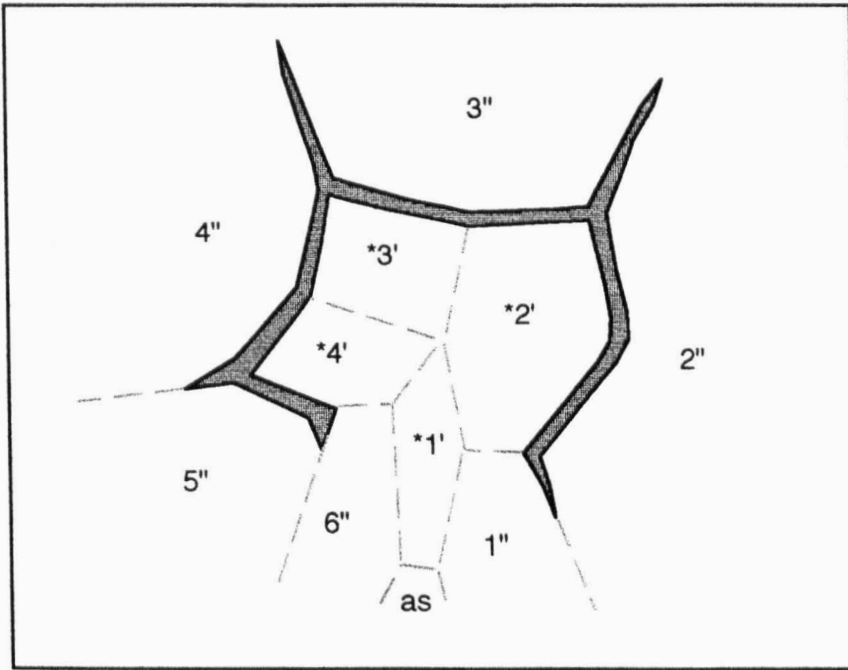


Figure 4.13: Apical view of *Cyclonephelium bulbosum* sp. nov. showing the nature of the archeopyle, with inferred paratabulation following the recommendations of Fensome *et al.* (1993) to indicate plate homology.

Remarks: This species is tentatively placed in *?Cyclonephelium* due to the restriction of processes to marginal and apical regions typical of that genus. However, although the operculum may remain attached in many examples of *Cyclonephelium*, it is not typically adnate, and generally does not have such deep accessory sutures separating paraplate 3". This archeopyle type is thus considered atypical of the genus.

Name: *Rhynchodiniopsis magnifica* sp. nov.

Holotype: Slide U11/2, England Finder coordinates K27/2. Plate 2, Figures 1, 4, 7.

Paratype: SEM stub 11, grid square 2/IV, taken from sample U11. Plate 6, Figure 4.

Type locality: Gorodische section, Volga Basin.

Type horizon: Bed 6 mudstone, zarajskensis Subzone.

Range: Restricted to the zarajskensis Subzone at Gorodische, but extends up into the subditus Zone at Kashpir.

Etymology: Named after its magnificent parasutural septa.

Diagnosis: Slightly elongate oval, proximate, acavate gonyaulacoid cyst with or without a short solid rod-like apical horn. Differentiated autophragm is densely pitted or spongy, and bears high erymnate to fenestrate or perforate parasutural septa which may have smooth to undulose or highly irregular distal margins. Paracingular septa are invariably higher than any others. Possesses a cribroperidinioidean paraplate arrangement, with cingular, sulcal, first postcingular and posterior intercalary paraplates suppressed.

Description: Slightly elongate oval, both epicyst and hypocyst are dome to bell-shaped with rounded apices, and of approximately equal size (the paracingulum descends slightly from dorsal to ventral surfaces, so that the hypocyst is longer than the epicyst on the dorsal surface). Cyst proximate, acavate. Differentiated autophragm appears densely pitted over cyst body in transmitted light, pitted to spongy under the SEM. The apex usually bears a short robust horn, although this is variably developed and may be absent in some specimens. However in most specimens it is present as a solid, short conical, or slightly longer rod-like projection which tapers distally. The autophragm bears erymnate to fenestrate parasutural septa. The height of these septa is

variable, but paracingular septa are always the largest. Height of the pre- and post-cingular septa is greatest adjacent to the paracingulum and in regions close to the apices. Parasutural septa at the antapex tend to be higher (and more elaborate) than those at the apex. Distal margins of parasutural septa tend to be smooth to undulose at the paracingulum, but undulose to highly irregular elsewhere. Spine-like projections are often apparent at gonal areas in transmitted light, typically at junctions of the post-cingular paraplate homologues with paraplate 1''', and pre-cingular series with the apical paraplate homologues. These projections result from the fusion of parasutural septa, the height of which may also be enlarged at such plate junctions.

Paratabulation formula: 4', 6'', 7c, ?s, 5''', 71p, 1''', with a cribroperidinioidean arrangement (Figure 4.14). Elucidation of any anterior intercalary plates has not proved possible due to unfavourable orientation of the specimens.

The first and fourth (*1' and *4') apical paraplate homologues are narrow and elongate: *1' is approximately parallel-sided, *4' is parallel-sided adjacent to paraplate 6'', but broadens towards the apex. Apical plate homologues *2' and *3' are much reduced latitudinally in relation to the other apical homologues. Paraplates 1'' to 5'' are large, extending at least 3/4 of the distance between the paracingulum and apex. Paraplate 6'' is of reduced size in comparison to the other precingular plates, and is trapezoidal to deltoidal in shape. The boundary of this plate with *1' is small and indistinct. The archeopyle is formed from the complete loss of paraplate 3'', and is thus type P. This plate is pentagonal, and is bordered at its anterior by paraplates 2' and 3'. The boundary between paraplates 3'' and 4'' coincides, or is very slightly dextrally offset from the boundary between paraplate homologues *4''' and *5''' on the hypocyst.

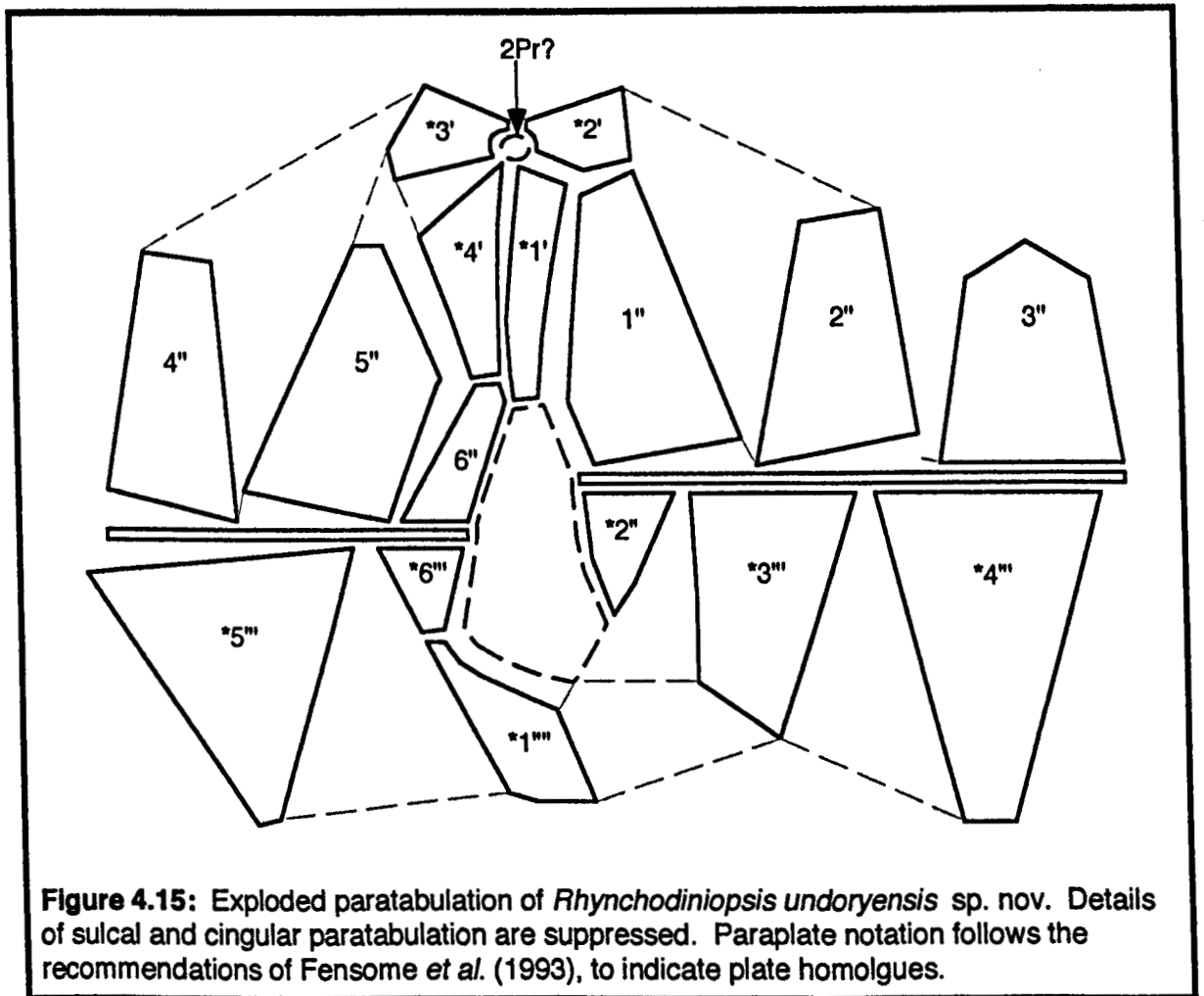
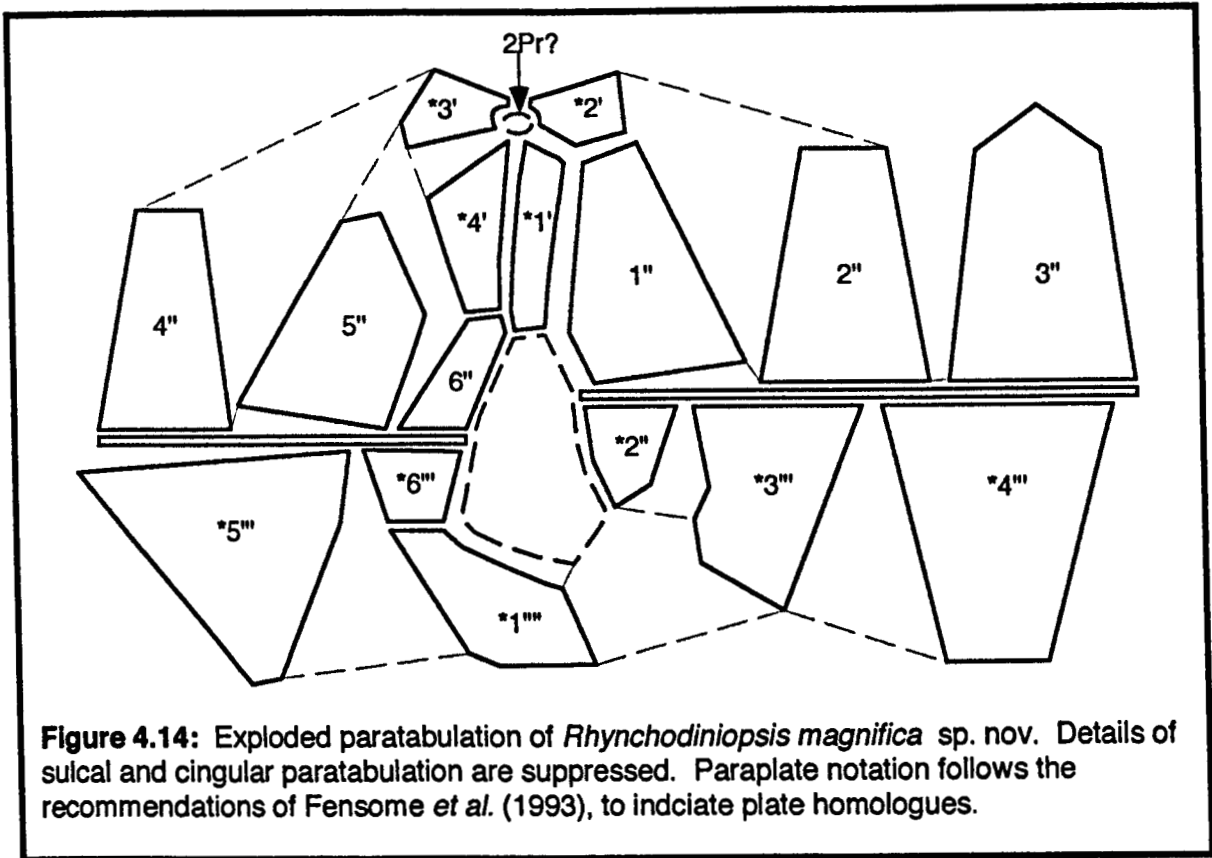
The paracingulum is narrow and helical, descends from posterior to anterior surfaces, and is offset at the parasulcus by 2-4 paracingular widths. Paracingular plates have not been determined. The parasulcal region is deltoidal in shape, being broader at the posterior end than at its anterior. The anterior part extends a short way apically above the paracingular margin. Sulcal, 1st postcingular and posterior intercalary paraplate homologues are suppressed.

Post-cingular paraplate homologues *2''' and *6''' are quadrate, taper towards the antapex, and are of reduced but approximately equal size. By contrast paraplates *3'''- *5''' are large and approximately triangular. *4''' and *5''' are the largest plates on the hypocyst. The antapical paraplate homologue *1''' is displaced ventrally so that only its posterior end is level with the antapex. It is bounded by the parasulcus and post-cingular paraplate homologues *3''' to *6''', and is thus asymmetrical on the ventral surface.

Dimensions: Antapex-apex (base of horn) (60)67(73) μm , width at paracingulum (44)52(60) μm . Length of horn (4)7(12) μm . 21 specimens measured.

Remarks: This taxon differs from most species of *Rhynchodiniopsis* in lacking discrete spines, and is therefore most closely comparable to *R. fimbriata* (Duxbury, 1980) Jan du Chene *et al.* 1985, and *R. pennata* (Riley in Fisher & Riley, 1980) Jan du Chene *et al.* 1985. *R. magnifica* differs from *R. fimbriata* in having an ellipsoidal rather than pentagonal outline, a much less strongly developed apical horn, and suppression of the posterior intercalary paraplate. *R. magnifica* differs from *R. pennata* by having a short solid apical horn rather than a large conical one formed by the entire autophragm, and in having much higher and more elaborate parasutural septa, particularly at the paracingulum. It is also superficially similar to *Leptodinium deflandrei* (Riley in Fisher & Riley, 1980) Lentin & Williams, 1981, but differs by the comparatively short apical horn, lack of apical cavation, the presence of a differentiated autophragm, and by the development of much higher septa.

Fensome *et al.* (1993) placed *Rhynchodiniopsis* in the Family Leptodinioideae. However, specimens of this genus examined in the present report exhibit neutral to dextral torsion of the hypocyst relative to the epicyst, and an elongate or ventrally tapering first antapical homologue, which is usually offset from the antapex. Neutral to dextral torsion is also apparent in most species of this genus figured by Jan du Chêne *et al.* (1986), and in their exploded paratabulation diagram. These characteristics are therefore not consistent with a leptodinioidean arrangement, and *Rhynchodiniopsis* is here moved into the Family Cribroperidinioideae.



projections result from the fusion of parasutural septa, the height of which may also be enlarged at such plate junctions.

Paratabulation formula: 4', 6'', ?c, ?s, 5''', ?1p, 1''''', with a cribroperidinioidean arrangement (Figure 4.15).

The first and fourth (*1' and *4') apical paraplate homologues are narrow and elongate: both are approximately parallel-sided near the parasulcus, but broaden towards the apex. Paraplate 6'' is of reduced size in comparison to the other precingular plates, and is approximately deltoidal in shape with a geniculate anterior margin. The boundary of this plate with *1' is narrow and indistinct. The archeopyle is Type P, formed from the complete loss of paraplate 3''. The archeopyle is pentagonal to ovoidal, generally with a rounded anterior margin. It is of variable size since the position of the paracingulum is variable on the dorsal surface. The 3''/4'' paraplate boundary on the epicyst coincides or is slightly dextrally offset from the *4''''/*5'''' paraplate homologue boundary on the hypocyst.

The paracingulum is narrow and helicoid, descends to a variable extent from posterior to anterior surfaces, and is offset at the parasulcus by 4-5 paracingular widths. Paracingular plates have not been determined. The anterior part of the parasulcal region extends a short way above the apical edge of the paracingulum. Paracingular, sulcal, 1st postcingular and posterior intercalary paratabulation is suppressed.

Post-cingular paraplate homologues *2'''' and *6'''' are quadrate or broadly triangular, taper towards the antapex, and are of reduced but approximately equal size. By contrast paraplate homologues *3'''' to *5'''' are much larger, with *4'''' and *5'''' being the largest plates on the hypocyst. The antapical paraplate is displaced ventrally so that only its boundary with paraplate homologue *4'''' meets the antapex. It is bounded by the parasulcus and post-cingular paraplate homologues *3'''' to *6'''', and is thus asymmetrical on the ventral surface.

Dimensions: Antapex-apex (base of horn) (55)60(70) μm , width at paracingulum (36)40(49) μm . Horn length (5)14(18) μm . 6 specimens measured. See also Table 4.9

Remarks: This taxon is closely comparable to *R. magnifica*. However, it differs in having comparatively linear rather than convex sides in both the epicyst and hypocyst, by the much longer apical horn, and to a lesser extent by the more strongly offset paracingulum. In addition the septa are more 'solid' and fenestrate in appearance rather than truly erymnate. It differs from *R. fimbriata* by having a solid apical horn formed as an extension from the autophragm, rather than a hollow conical horn formed from tapering of the autophragm at the apex. Also by having a more strongly helical paracingulum, and by the suppression of the posterior intercalary plate in *R. undoryensis*. It also contrasts with *R. pennata* in having a much less rounded cyst outline, much longer and more robust apical horn, and in the development of higher, more elaborate parasutural septa, particularly at the paracingulum.

Name: *?Thalassiphora robusta* sp. nov.

Holotype: Slide U3/2, England Finder coordinates J41. Plate 4, Figures 6 & 7.

Type locality: Gorodische section, Volga Basin.

Type horizon: Bed 2 mudstone, zarajskensis Subzone.

Range: Restricted to the zarajskensis Subzone at both Volga Basin localities.

Etymology: Named after the thick & robust nature of the periphragm.

Diagnosis: Large subspherical to ovoidal camocavate cysts. The periphragm is thick and fibrous or spongy, endophragm is smooth and bears a short solid apical horn. Wall layers are adpressed on the dorsal surface, but elsewhere are separated by a significant cavation. The archeopyle is Type P3".

Description: Large subsphaerical to ovoidal cavate cysts. The cysts are always compressed, but with no apparent preferential orientation. The periphragm is thick and fibrous or spongy and adpressed to the endophragm on the dorsal surface. The endophragm is smooth and robust. The apex of the endophragm generally bears a short solid horn, the antapex is always rounded. The archeopyle is located immediately below the apical horn. Although both wall layers lack any indication of paratabulation, and the archeopyle is of slightly variable size and shape, it may well be Type P3".

Dimensions: Periphragm dimensions; height (72)89(153) μm , width (70)93(130) μm .

Endophragm dimensions; (34)50(72) μm , width (38)52(73) μm .

Remarks: This species is only tentatively placed in *Thalassiphora*. However, it lacks the characteristic dorsal 'keel' or periphragmal fold of *Thalassiphora*, and in addition possesses a horn on the endophragm not typically found on the other species of this genus. It cannot be placed in *Membranilarnacia* since it lacks processes supporting the outer wall layer. ?*T. robusta* is superficially similar to *Pareodinia halosa*. However, it clearly possesses two wall layers with a periphragm rather than a kalyptra.

4.3.4. Systematics of selected dinoflagellate cysts

Genus *Apteodinium*

In the present report the distinction between *Cribroridinium* and *Apteodinium* was made on the presence/absence of accessory parasutural ridges. Specimens lacking such features were assigned to *Apteodinium*.

Apteodinium sp. 1

Plate 10, Figure 1.

Dimensions: Antapex-apex (base of horn) (78)81(83) μm , width at paracingulum (76)79(83) μm (3 specimens measured).

Description: Large subspherical to ovoid, thick walled proximate acavate cysts with short broad apical horn (1-2 μm in length). Differentiated autophragm is densely punctate, and appears spongy in transmitted light. Absence of paratabulation except for a faint paracingular trace on some specimens, and a smooth area corresponding to the parasulcus. Archeopyle, type P₃", operculum free.

Remarks: This species differs from the other species attributed to *Apteodinium* in this study by its large size and thick, spongy autophragm.

***Apteodinium* sp. 2**

Plate 10, Figures 2 & 3.

Dimensions: Antapex-apex (base of horn) (63)65(67) μm , width at paracingulum (69)71(72) μm (3 specimens measured).

Description: Subspherical proximate acavate cysts with thin wall. Autophragm smooth, unornamented. Apex bears solid rounded to conical apical horn. Lacks paratabulation apart from low, narrow parasutural ridges which demark the paracingulum. Reduced archeopyle is slightly ovoid, with rounded anterior margin, type P_3'' . Operculum is attached in all specimens observed.

Remarks: This species can be distinguished by its thin, smooth autophragm and by the lack of paratabulation other than at the paracingulum. It is closely comparable to *Apteodinium* sp. 4, but is larger, and lacks the additional tabulation apparent in that species.

***Apteodinium* sp. 3**

Dimensions: Antapex-apex (base of horn) (78)82.5(86) μm , width at paracingulum (63)66(69) μm (3 specimens measured).

Description: Thick-walled robust proximate acavate cysts. Epicyst and hypocyst bell-shaped, maximum width at paracingulum: antapex and apex are rounded. Autophragm scabrate to microgranulate. Apex bears broad conical horn with fine cilia-like projections. Paratabulation is suppressed apart from broad, low parasutural ridges which demark the paracingulum. Archeopyle Type P_3'' . Operculum is free.

Remarks: This species is separable from *Apteodinium* sp. 1 by contrasting wall and apical horn structures, and in having a strongly developed paracingulum.

***Apteodinium* sp. 4**

Dimensions: Antapex-apex (base of horn) (47)53(60) μm , width at paracingulum (47)57(65) μm (4 specimens measured).

Description: Thin-walled subspherical to ovoidal proximate acavate cysts. Autophragm smooth to scabrate. Apex bears broad, solid, conical horn. Paratabulation

Figure 4.7: Comparison of Volga Basin Jurassic dinoflagellate cyst biohorizons with those in western Europe

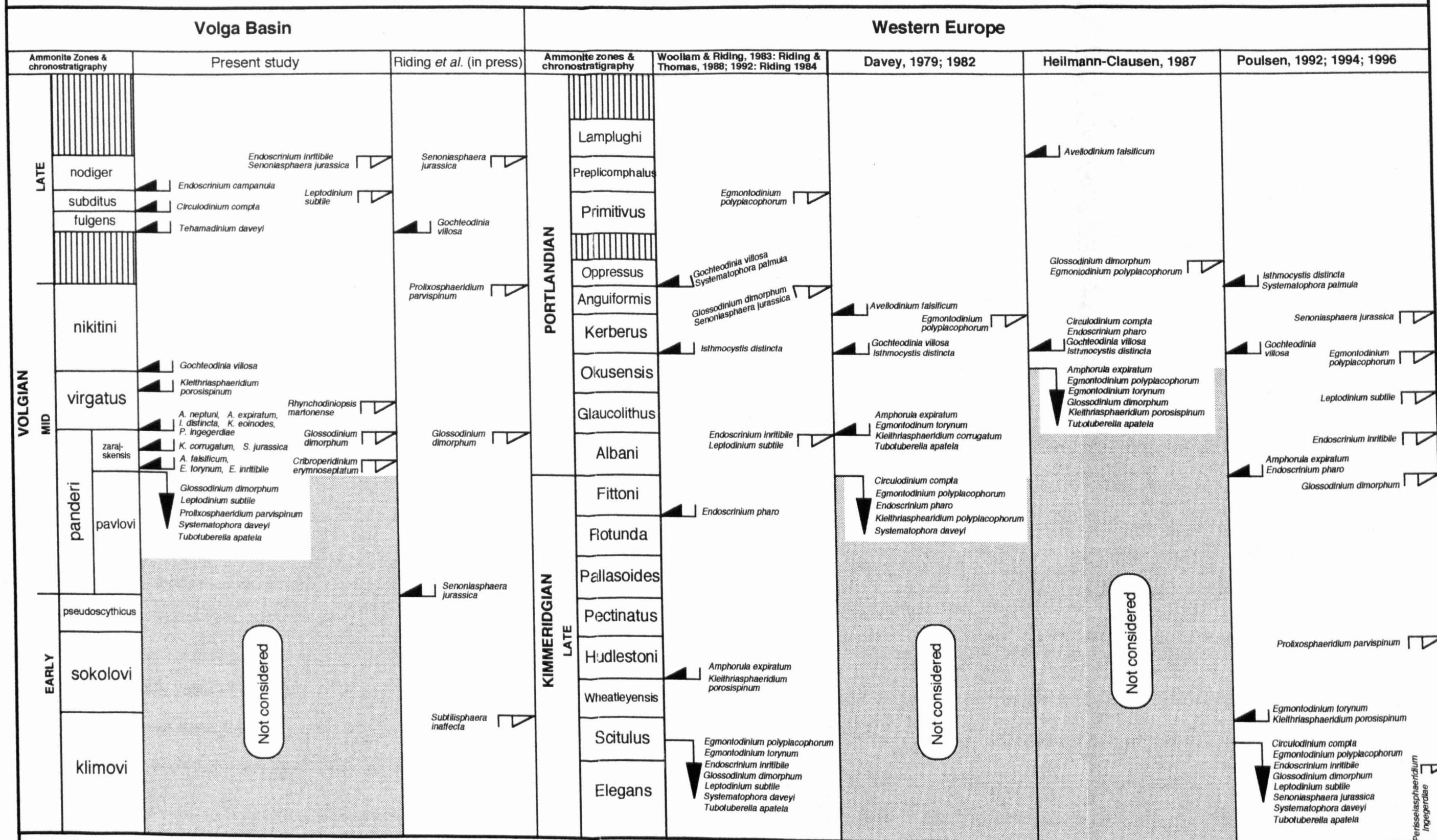
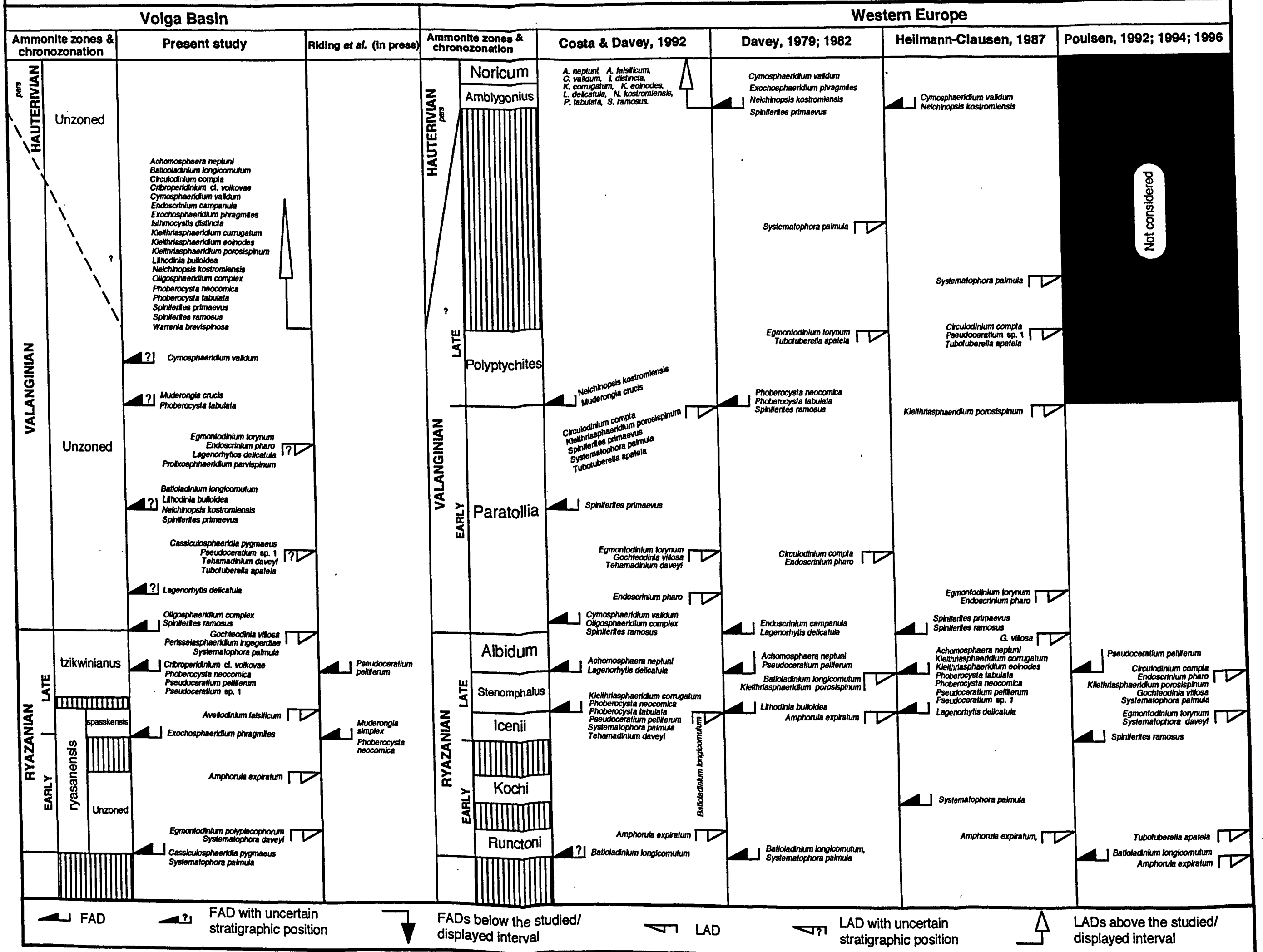


Figure 4.8: Comparison of Volga Basin Cretaceous dinoflagellate cyst biohorizons with those in western Europe



Orientation	Slide	England Finder coordinates	Maximum width	Antapex-paracingulum	Paracingulum-apex	Breadth	Wall thickness	Thickness at sulcus
apical	K17010/3	N31/4	94	?	?	87	5	5
apical	K1705/2	N61	90	?	?	90	6	6
lateral	k1705	M29	89	73	20	?	4.7	?
oblique lateral	K17010/2	K54	80	53	17	80	6.7	6
operculum	K17010/3	E27/4						
ventral	K17010/3	D53	87	57	27	?	4.3	?
oblique lateral	K17010/3	G64	94	57	30	?	5.7	5.7
apical	K17010/3	H48/3	84	?	?	84	5.7	5.7
operculum	K17010/3	L30/1						
oblique apical	K17010/2	Q50/1	90	60	23	90	5.3	5
	K1705/2	E42/3	84	53	20	?	6.7	?
lateral	K1705/2	Q37	84	73	13	?	4.7	?
oblique lateral	K1705/2	T62/3	84	50	33	?	6	?
lateral	K1705	B49/3	?	53	23	87	6.7	6.7
		Average	87	59	23	86	5.6	5.7
		Max.	94	73	33	90	6.7	6.7
		Min.	80	50	13	80	4.3	6

Table 4.6: Dimensions measured from specimens of *Lithodinia distincta* sp. nov. Holotype and paratype are the first two specimens respectively.

Orientation	Slide	England Finder coordinates	Antapex-apex	Antapical lobes-apex	Width at apex	Maximum width	Width at paracingulum	Process-length at antapex	Process length on lobes	Process length at apex
dorso-ventral	K17/05	K30/3	51	52	23	47	42	13	8	2.6
dorso-ventral	K17010/2	N38	49	50	20	48	44	7.9	8	4
dorso-ventral	K17010	G34/3	52	53	22	53	49	6.8	9	??
dorso-ventral	K1705/3	T56/1	46	47	21	48	47	4.6	6	1.3
dorso-ventral	K17010/2	H56/3	43	47	21	44	42	2.6	5	??
dorso-ventral	K17010/2	S31/2	48	49	21	47	43	9.8	7	4.6
dorso-ventral	K1705/2	K42/4	46	48	20	46	40	6.5	6	4.6
dorso-ventral	K1705/2	L58/1	52	53	25	55	49	5.2	5	2.2
dorso-ventral	K17010	D46/4	51	51	23	51	48	4.9	6	1.6
dorso-ventral	K17010	F29/3	52	55	22	46	43	9.1	8	2.6
dorso-ventral	K17010	E53/4	49	50	26	53	52	5.2	4	1.3
dorso-ventral	K17010	J56/1	???	???	21	49	47	7.8	6	???
dorso-ventral	K17010	P39	47	47	21	47	46	4.6	4	1.3
dorso-ventral	K1705	K61/3	55	56	22	51	46	7.8	7	3.6
dorso-ventral	K17010/3	M40/1	39	40	19	46	46	7.2	5	??
dorso-ventral	K17010/3	O51	51	52	23	52	44	7.8	5	3.9
dorso-ventral	K17010/3	P50	49	51	20	47	44	6.5	3	1.3
dorso-ventral	K1705/3	M45/1	47	49	23	57	59	3.3	5	1.3
dorso-ventral	K1705/3	U46/1	51	52	22	48	46	3.3	6	2
		Average	49	50	22	49	46	6.5	5.9	2.5
		Max.	55	56	26	57	59	13	9	4.6
		Min.	39	40	19	44	40	2.6	3	1.3

Table 4.7: Dimensions measured from specimens of *?Cyclonephelium bulbosum* sp. nov. Holotype and paratype are first two specimens respectively.

Name: *Rhynchodiniopsis undoryensis* sp. nov.

Holotype: Slide U24/2, England Finder coordinates J47/1 Plate 3, Figures 1-3.

Paratype: Slide U24/2, England Finder coordinates J40/2 Plate 3, Figures 4-6.

Type locality: Gorodische section, Volga Basin.

Type horizon: Bed 16 conglomerate, virgatus Zone.

Range: Late Volgian.

Etymology: Named after the town of Undory, close to the Gorodische section.

Diagnosis: Elongate, proximate acavate gonyaulacoid cyst with a diamond-shaped ambitus and long robust, distally tapering apical horn. Differentiated autophragm is densely pitted or spongy, and sculpted into high fenestrate parasutural septa which are highest at the paracingulum. Distal edges of the septa are smooth to undulose or occasionally irregular. Paratabulation is cribroperidinioidean, with cingular, sulcal, first postcingular and posterior intercalary paraplates being suppressed.

Description: Elongate diamond-shaped ambitus, both epicyst and hypocyst are conical to bell-shaped with rounded apices, and of approximately equal size (the paracingulum descends from dorsal to ventral surfaces, so that the hypocyst is larger than the epicyst on the dorsal surface). Cyst proximate, acavate. Differentiated autophragm appears densely pitted over cyst body in transmitted light, spongy under the SEM. The apex bears a long robust distally-tapering, solid horn. The autophragm is sculpted into fenestrate parasutural septa. The height of these septa is variable, but paracingular septa are always the highest. Height of the pre- and post-cingular septa is greatest adjacent to the paracingulum and in regions close to the apices. Parasutural septa at the antapex tend to be higher than those at the apex. Distal margins of the parasutural septa are generally smooth to undulose, but may be irregular in poorly preserved specimens. Spine-like projections are often apparent at gonal areas in transmitted light, typically at junctions of the post-cingular paraplate homologues with paraplate *1''', and pre-cingular series with the apical paraplate homologues. These

Orientation	Slide	England Finder coordinates	Antapex-apex	Apical horn length	Apical horn width	Antapex-paracingulum	Paracingulum-apex	Antapical septal height	Paracingular septal height	Width at paracingulum	Av. septal height on hypocyst	Archeopyle height	Archeopyle width
ventral	U24/2	J47/1	61	5.2	2.9	4.4	3.9	7.8	1.3	3.9	6.5	?	?
ventral	U24/2	J40/2	59	1.8	3.9	2.9	2.6	1.2	1.2	3.6	5.2	2.6	1.7
oblique ventral	U21	M50	70	1.6	3.9	2.9	3.1	1.3	1.5	4.9	6.5	3.4	2.1
ventral	U24/3	K36	59	1.0	5.2	3.8	3.6	6.5	1.0	3.9	2.6	1.8	1.7
lateral	U24/3	O51	57	1.8	5.2	3.9	3.4	9.8	9.1	3.9	5.2	2.9	?
oblique apical	U24/3	R37/4	55	?	?	3.9	2.9	1.2	1.2	3.9	6.5	2.5	?
		Average	60	1.4	9.5	3.6	3.3	10	1.2	4.0	5.4	2.6	1.6
		Min.	55	5.2	3.9	2.9	2.6	6.5	9.1	3.6	2.6	1.8	1.7
		Max.	70	1.8	2.9	4.4	3.9	1.3	1.5	4.9	6.5	3.4	2.1

Table 4.9: Dimensions measured from specimens of *Rhynchodiniopsis undoyensis* sp. nov. The first two specimens are the holotype and paratype respectively.

Orientation	Slide	England Finder coordinates.	Antapex-apex (periphragm)	Antapex-apex (endophragm)	Maximum width (periphragm)	Maximum width (endophragm)	Apical horn length	Apical horn width	Archeopyle height	Archeopyle width
dorso-ventral	U3/2	J41	79	38	78	38	2	2.6	1.0	1.6
dorso-ventral	U6/2	P49/2	98	52	111	39	5.2	5.2	1.2	1.7
oblique lateral?	U3/3	M38/4	104	34	111	4.4	?	n/a	n/a	n/a
dorso-ventral	U3/3	M35/1	72	4.6	7.0	4.6	?	?	?	?
dorso-ventral	K14/2	K61/3	111	65	130	68	n/a	n/a	n/a	n/a
oblique ventral	U3old	E33/3	153	72	130	73	n/a	n/a	n/a	n/a
oblique lateral?	U4/2	V33/3	101	57	117	57	2.6	5.2	1.3	?
apical	U3/2	C27/4	?	?	91	5.2	?	?	1.3	1.6
oblique lateral?	U3/2	E44/3	98	65	87	57	3.9	5.2	n/a	n/a
oblique lateral?	U3/2	W46/3	91	59	101	72	n/a	n/a	1.2	n/a
oblique lateral?	U3	B41/3	78	49	91	55	3.9	3.9	n/a	n/a
oblique lateral?	U3	U36/2	85	57	85	72	2.6	3.9	?	?
dorso-ventral	U3	V41/2	85	4.6	81	4.2	3.9	3.9	n/a	n/a
		Average	89	50	93	52	3.2	3.9	9.9	1.1
		Min.	72	3.4	70	3.8	2	2.6	1.0	1.6
		Max.	153	72	130	73	5.2	5.2	1.3	1.7

Table 4.10: Dimensions measured from specimens of *Thalassipora robusta* sp. nov. The first specimen is the holotype.

Description: Thick-walled subcircular, dorso-ventrally compressed, proximate acavate cysts. Autophragm variably granulate, often with particularly large granulae. General absence of granulae from the mid-ventral area marks the position of the parasulcus, and in some specimens a broad mid-dorsal band of finer granulae may demark the paracingulum. Otherwise, paratabulation is only apparent at the archeopyle margin, which indicates an apical archeopyle, type (tA), formed from the loss of 4 apical plate homologues. The operculum frequently remains attached. Deep accessory archeopyle sutures separate 6 precingular paraplates..

Remarks: The dense, coarse granulation together with the presence of deep accessory archeopyle sutures separating all of the precingular paraplates allow this species to be readily distinguished from other species here attributed to *Batiacasphaera*.

Batiacasphaera sp. 2

Plate 15, Figure 6.

Dimensions: Antapex-archeopyle margin (31)34(37) μm , maximum width (just below paracingulum) (37)42(47) μm (3 specimens measured).

Description: Thick-walled ovoidal, dorso-ventrally compressed proximate acavate cysts. Hypocyst much larger than epicyst. Maximum cyst width immediately below paracingulum. Autophragm densely microgranulate. Paratabulation only indicated by pronounced paracingular ridges and at the archeopyle margin. Cyst ambitus restricted between paracingular ridges. Archeopyle apical, type (tA), formed from the loss of 4 apical paraplate homologues. The operculum is attached in two of the three specimens observed. Short accessory archeopyle sutures partially separate 6 precingular paraplates.

Remarks: The pronounced paracingular ridges, thick autophragm, and comparatively inflated hypocyst clearly differentiate this species from the other examples of *Batiacasphaera*.

Genus *Batioladinium*

Batioladinium sp. 1

Dimensions: Antapex-apex (base of horn) (47)51(57) μm , maximum width (46)48(51) μm , 4 specimens measured.

Description: Small ovoidal proximate cysts. Antapex occasionally rounded but usually asymmetrically bilobed, apex bears a broad rounded horn 7-10 μm in length. Autophragm is thick and densely punctate. There is an absence of paratabulation except at the archeopyle margin, which descends strongly from dorsal to ventral surfaces, and is consistent with the apical arrangement proposed by Fensome *et al.* (1993). The operculum remains attached in most specimens.

Remarks: This species is characterised by its thick autophragm with dense distribution of punctae. The bilobed antapex and characteristic apical archeopyle prevent this species from being attributed to *Pareodinia*. It differs from other species of *Batioladinium* by having a densely punctate autophragm.

Genus *Circulodinium*

"*Circulodinium ciliatum*" group

Plate 15, Figure 7.

Dimensions: Antapex-archeopyle margin (43)49(58) μm , maximum width (47)56(67) μm (15 specimens measured).

Description: Thin-walled & delicate, sub-sphaerical to ovoidal proximate acavate cysts. Autophragm smooth but densely covered with short cilia-like hairs 1-2 μm in length. Paratabulation only indicated at the archeopyle margin by variably developed accessory sutures separating 6 precingular paraplates. Archeopyle apical, type (tA), formed from the loss of 4 apical paraplate homologues. Operculum free.

Remarks: Members of this group are distinguishable from *Sentusidinium* sp. 3 Iosifova 1996 by having a much thinner, more delicate autophragm, and significantly shorter, finer ciliate projections.

Genus *Criboperidinium*

Criboperidinium cf. *C. perforans* (Cookson & Eisenack 1958) Morgan 1980.

Plate 11, Figures 3 & 4.

Remarks: The few specimens observed in the Volga residues have generally comparable morphology and shape to *C. perforans*, but possess a larger, more robust apical horn.

Criboperidinium cf. *C. volkova* Iosifova 1996.

Plate 8, Figures 1-3.

Remarks: Encountered specimens differ from the holotype by possessing a variable amount of intratabular sculpture, generally simple conical tuberculae. The holotype is described as having no intratabular ornamentation. The variable abundance of intratabular sculpture observed in the Volga residues suggests that there may be a gradation from specimens comparable to the holotype, and those encountered in the present report.

Criboperidinium sp. 1

Plate 10, Figures 9 & 10.

Dimensions: Antapex-apex (65)67(71) μm , width at paracingulum (58)65(71) μm (8 specimens measured).

Description: Subspherical, proximate acavate cysts. Epicyst and hypocyst approximately equal. Antapex rounded to flattened, apex usually dome-shaped. Apex bears a long, solid, distally tapering horn. Autophragm smooth to scabrate with variable development of intratabular granulae, conical or tuberculae. Incomplete paratabulation indicated by thin parasutural ridges or alignment of tuberculae, with fine secondary parasutural features on some adcingular paraplates. Paracingulum is strongly developed, helicoid with the distal end descending strongly towards the antapex, and is thus offset at the parasulcus by 2-3 paracingular widths. Parasulcus is linear, generally devoid of sculpture (including paratabulation), and bears two small flagellar scars. Paratabulation is consistent with a criboperidinioidean arrangement with

neutral to very slight dextral torsion of the hypocyst relative to the epicyst. The archeopyle is large, occupying approximately 80% of the paracingular-apical distance, formed from the loss of paraplate 3", operculum free.

Remarks: This is a morphologically variable species, some specimens of which may be attributable to *C. globatum*. However the range of sculpture observed here exceeds that characteristic of *C. globatum*, and the gradation between end-members forces the use of a separate species designation.

Cribroperidinium sp. 2

Plate 11, Figures 1 & 2.

Dimensions: Antapex-apex (93)97(105) μm , width at paracingulum (65)71(75) μm (5 specimens measured).

Description: Thin walled, proximate to proximochorate acavate cysts. Epicyst slightly larger than hypocyst. Antapex rounded, dome-shaped, apex roughly conical. Greatest width at paracingulum. Autophragm microgranulate with variable development of conical and capitate spines. Apex bears a solid, robust truncated horn (10-16 μm long) with a terminal spine. Antapex has a robust distally tapering and capitate antapical horn approximately 7-13 μm in length. Incomplete paratabulation indicated by narrow parasutural ridges on the paracingulum, and by low ridges or the alignment of spines in other areas. Paracingulum is strongly developed, linear, with only slight offset at the parasulcus. Autophragm is inwardly folded at the parasulcus, which is also spinate. Paratabulation is consistent with a cribroperidinioidean arrangement. The archeopyle is large, occupying approximately 75% of the paracingular-apical distance. Formed from the loss of paraplate 3", operculum free.

Remarks: This species is separable from the other taxa attributed to *Cribroperidinium* by its large size, its characteristic capitate spines, and robust capitate apical horn.

***Cribroperidinium* sp. 3**

Plate 11, Figures 5 & 6.

Dimensions: Antapex-apex (62)64(67) μm , width at paracingulum (65)65(65) μm (3 specimens measured).

Description: Thin walled, subspherical, proximate acavate cysts. Epicyst and hypocyst approximately equal. Greatest width at paracingulum. Autophragm variably punctate to foveolate giving a pseudo-reticulate to granular appearance. Apex bears a small cluster of thin, delicate processes which often fuse to form a single delicate horn. Antapex occasionally has a sort solid conical antapical horn 2-6 μm in length. Paratabulation indicated by thin parasutural and accessory ridges which are often surmounted by short acuminate spines, particularly in gonal areas. Paracingulum helicoid, offset at the parasulcus by 2 paracingular widths, and is clearly tabulate. Parasulcus is linear, its position is indicated by smooth autophragm, and bears small flagellar scars. Paratabulation is consistent with a cribroperidinioidean arrangement, with strong dextral torsion of the hypocyst relative to the eipcyst. The archeopyle is large, occupying approximately 80% of the paracingular-apical distance, formed from the loss of paraplate 3", operculum free.

Remarks: This species is characterised by the pseudo-reticulate autophragm, the delicate, diaphanous nature of the apical prominence, and by the short acuminate spines which surmount low parasutural ridges.

***Cribroperidinium* sp. 4**

Plate 10, Figure 15.

Dimensions: Antapex-apex (87)88(89) μm , width at paracingulum (77)82(87) μm (3 specimens measured).

Description: Thick-walled, ovoidal, proximate to proximochorate acavate cysts. Epicyst and hypocyst approximately equal in length. Greatest width at paracingulum. Autophragm densely punctate to foveolate. Apex bears a long slender, solid, parallel sided and capitate horn 15-25 μm in length. The antapex is rounded with distinctive echinate parasutural septa. Paratabulation indicated by narrow parasutural and

accessory ridges with gonal spines. Paracingulum is helicoid, offset at the parasulcus by 2 paracingular widths, and paracingular tabulation is not distinct. Parasulcus is linear, indicated by a area of smooth autophragm, occasionally with flagellar scars. Paratabulation is consistent with a cribroperidinioidean arrangement. The archeopyle is large, occupying approximately 75% of the paracingular-apical distance, formed from the loss of paraplate 3", operculum free.

Remarks: This species is identified by its large size, its long slender apical horn, and by the distinctive echinate parasutural septa at the antapex.

Criboperidinium sp. 5

Plate 10, Figures 7 & 8.

Dimensions: Antapex-apex (62)65(67) μm , width at paracingulum (52)57(62) μm (3 specimens measured).

Description: Thick-walled, ovoidal, proximate to proximochorate acavate cysts. Epicyst and hypocyst approximately equal in length. Antapex rounded, dome-shaped. apex rounded to bell-shaped, greatest width at paracingulum. Autophragm smooth, sculpted into intratabular and parasutural spines. Apex bears a short solid conical horn, surmounted by a small group of fused proceses which extend the horn length to between 4 and 15 μm . Paratabulation indicated by narrow paracingular ridges surmounted by spines, and by alignment of spines in other areas. Spines are very variable in length, from 6 to 12 μm . Long parasutural spines are often fused distally to form erymnate septa, particularly at the paracingulum and on the hypocyst. Paracingulum is linear with minimal offset at the parasulcus, and paracingular tabulation is not distinct. Position of the parasulcus is marked by an absence of spines. Paratabulation is generally not fully developed at the apex, but is consistent with a cribroperidinioidean arrangement. The archeopyle is formed from the loss of precingular paraplate 3", the operculum is free.

Remarks: This species is characterised by the long intratabular and parasutural spines which in most specimens fuse distally to form erymnate paracingular septa. Specimens with short spines are superficially similar to specimens of

Cribroperidinium sp. 1 with large elongate conical tuberculae, but can be separated by the more robust and longer apical horn, and the more strongly helical paracingulum in *C.* sp. 1.

Cribroperidinium sp. 6

Plate 10, Figures 13 & 14.

Dimensions: Antapex-apex (55)60(63) μm , width at paracingulum (54)57(61) μm (5 specimens measured).

Description: Thick walled, subspherical to ovoidal, proximate acavate cysts. Epicyst and hypocyst approximately equal in length. Greatest width at paracingulum. Autophragm punctate with occasional small intratabular tuberculae. Apex bears a short solid rod-like horn up to 11 μm in length. Paratabulation indicated by parasutural ridges with smooth distal edges, and by solid acuminate gonal spines 3-5 μm in length. Paracingulum is approximately linear, offset at the parasulcus by a maximum of 1 paracingular width. Paracingular and parasulcal tabulation is suppressed. Paratabulation is consistent with a cribroperidinioidean arrangement. The archeopyle is of type P, formed from the loss of precingular paraplate 3", the operculum is free.

Remarks: This species is characterised by its small size, subspherical shape, and by the presence of solid acuminate gonal spines.

Cribroperidinium sp. 7

Plate 10, Figure 11 & 12.

Dimensions: Antapex-apex (59)62(65) μm , width at paracingulum (65)66(67) μm (4 specimens measured).

Description: Thin-walled, pentagonal, proximate acavate cysts. Epicyst and hypocyst approximately equal in length. Hypocyst rounded to flattened, epicyst triangular. Strongly dorso-ventrally flattened. Greatest width at paracingulum. Autophragm smooth, but densely covered by solid intratabular to penitabular tuberculae. Apex bears a short horn up to 5 μm in length. Paratabulation indicated by parasutural ridges with rounded, entire distal edges. Paracingulum is linear, offset at

the parasulcus by a maximum of 1 paracingular width. The parasulcus is slightly inclined. Otherwise, paratabulation is consistent with a cribroperidinioidean arrangement.

Remarks: This species is characterised by its thin-walled, pentagonal, and dorso-ventrally flattened nature, together with the presence of the large intratabular to penitabular tuberculae.

Criboperidinium sp. 8

Plate 13, Figures 11 & 12.

Dimensions: Antapex-apex (61)71(76) μm , maximum width (61)67(76) μm (3 specimens measured).

Description: Pentagonal proximate acavate cysts. Epicyst and hypocyst approximately equal in length. Antapex occasionally rounded, but usually flattened. Autophragm thin and smooth or variably punctate to granulate, particularly on hypocyst. Apex bears a short solid conical horn. Paratabulation indicated by parasutural alignment of tuberculae or short spines, and by narrow parasutural thickenings in the autophragm. Paracingulum narrow, slightly helicoid, offset at parasulcus by 1-2 paracingular widths. Parasulcus defined by paratabulation of adjoining plates and by an absence of ornamentation. Archeopyle precingular, type P₃", operculum free. Paratabulation is consistent with a cribroperidinioidean arrangement, since there is pronounced dextral torsion of the hypocyst relative to the epicyst.

Remarks: This species is separable from other forms attributed to *Criboperidinium* by the general lack of intratabular ornamentation, the abundance of parasutural tuberculae, and by the pronounced dextral offset of the 3"/4" boundary on the epicyst against the *4"/*5" boundary on the hypocyst.

Genus *Ctenidodinium*

Ctenidodinium sp. 1

Dimensions: Antapex-paracingulum (34)37(41) μm , width at paracingulum (56)62(67) μm (4 specimens measured).

Description: Thin-walled, subspherical, proximate acavate cysts. All specimens encountered were represented by hypocysts, all specimens having excysted. Hypocyst rounded to flattened. Autophragm smooth. Paratabulation indicated by parasutural ridges with dense distribution of acicular spines on distal edges. One rectangular antapical, six paracingular, and six post-cingular paraplate homologues are indentifiable. The archeopyle is of type E (having lost the entire epicyst as the operculum), no opercula were observed.

Remarks: This species is similar to *C. elegantulum* except that the parasutural septa have much more delicate spines, and many more of them.

Genus *Dingodinium*

Dingodinium sp. 1

Plate 14, Figures 8 & 9.

Dimensions: Periphragm diameter (52)54(56) μm , endophragm diameter (40)42(44) μm (4 specimens measured).

Description: Subspherical cavate cyst. Periphragm smooth, robust and entire, endophragm smooth but densely ornamented by large granulae or papillae, which occasionally display a penitabular arrangement. Generally narrow distance between the two wall layers, but adpressed on the dorsal surface. Archeopyle is apical, type (tA), operculum free. Apex of periphragm bears a hollow conical and truncated horn which is distally closed.

Remarks: This species differs from other species encountered by the slightly larger size, small degree of cavation, and by the large and robust nature of the endophragmal granulae.

Genus *Downiesphaeridium*

***Downiesphaeridium* sp. 1**

Plate 17, Figure 9.

Dimensions: Antapex-archeopyle margin (31)35(43) μm , maximum width (34)40(43) μm (7 specimens measured).

Description: Small chorate cyst with subspherical to ovoidal central body. Autophragm thin and delicate, finely granulate. Processes are non-tabular, solid and rod-like, with parallel sides and blunt terminations. Processes are of approximately equal length around the cyst, maximum length observed 11 μm . Archeopyle apical, type (tA), formed from the loss of 4 apical paraplate homologues; operculum free. Accessory sutures partially separate 6 precingular paraplates. Otherwise, paratabulation is suppressed.

Remarks: This species can be separated from the "*Cleistosphaeridium aciculum*" group by having blunt rod-like processes.

***Downiesphaeridium* sp. 2**

Plate 17, Figure 8.

Dimensions: Antapex-archeopyle margin (61)64(67) μm , maximum width (61)72(87) μm (6 specimens measured).

Description: Large proximochorate to chorate cysts with subspherical to ovoidal central body. Autophragm thin, finely granulate. Processes are non-tabular, and bifurcate at their base to form two solid, acicular, and often capitate needles. Processes are of approximately equal length around the cyst, maximum length observed 5 μm . The shape and position of the archeopyle margin indicates an apical archeopyle, type (tA), formed from the loss of 4 apical paraplate homologues; operculum free. Accessory sutures partially separate 6 precingular paraplates. No opercula were observed.

Remarks: This species is characterised by its large size, and by the nature of the bifurcating processes.

Genus *Egmontodinium*

***Egmontodinium* sp. 1**

Plate 19, Figure 18.

Dimensions: Antapex-archeopyle margin (36)40(43) μm , maximum width (34)35(41) μm (3 specimens measured).

Description: Small chorate cysts with ovoidal central body. Autophragm thin & smooth. Processes are long in comparison to cyst diameter (10-15 μm), and have numerous furcations at up to five positions along the process length. Archeopyle apical, type (tA), operculum free, though occasionally 'caught' on processes.

Remarks: This species differs from *Egmontodinium torynum* and *Amphorula expiratum* by its small size, and long, delicate and frequently furcating processes.

Genus *Exochosphaeridium*

***Exochosphaeridium* sp. 1**

Plate 22, Figures 15 & 16.

Dimensions: Antapex-apex (base of horn) (54)54(54) μm , maximum width (48)52(54) μm (4 specimens measured).

Description: Subspherical chorate cysts. Autophragm thick, sculpted into long (12-16 μm in length) slender solid processes which taper distally, often bifurcate, and have pointed terminations. Additionally they appear to be oval to blade-like in cross section. Between processes the autophragm is variably corrugated. The apex bears a distinctive process which is usually thicker than the others, usually spinate, and distally capitate. No paratabulation is apparent other than the archeopyle, which appears to be formed from the loss of precingular paraplate 3", operculum free.

Remarks: This species is closely comparable to *E. phragmites*, but has more commonly furcating, and more flattened processes, and a distinctive apical process not typically present in *E. phragmites*.

Genus *Gonyaulacysta*

Gonyaulacysta sp. 1

Plate 12, Figures 1 & 2; Plate 23, Figure 11.

Dimensions: Antapex-apex (42)43(44) μm , maximum width (32)33(34) μm (5 specimens measured).

Description: Ovoidal to pentagonal proximochorate to chorate acavate cysts. Antapex flattened to rounded, apex dome-shaped, epicyst and hypocyst approximately equal in length. Autophragm smooth. Apex bears a short, solid conical horn. Paratabulation indicated by high parasutural ridges with gonal blade-like to spiniferate processes which taper distally. Paracingulum narrow, helicoid, offset at parasulcus by 2-3 paracingular widths. Parasulcus broad but confined to ventral surface, defined by paratabulation of adjoining plates, sulcal paratabulation suppressed. Paratabulation is consistent with a gonyaulacoidean arrangement, with a L-type to very weakly formed S-type ventral organisation. Archeopyle precingular, type P3", operculum free.

Remarks: This species spans a range of process morphology with end-members in the genera *Gonyaulacysta* and *Spiniferites*. There is a complete gradation from simple blade-like processes to trifurcating spiniferate processes. However, the species is retained in *Gonyaulacysta* due to the prevalence of the L-type sulcal arrangement.

Gonyaulacysta sp. 2

Dimensions: Antapex-apex (46)51(58) μm , maximum width (43)45(46) μm (4 specimens measured).

Description: Subspherical to ovoidal or pentagonal, proximochorate acavate cysts. Antapex flattened to rounded, apex dome-shaped: epicyst and hypocyst approximately equal in length. Autophragm smooth. Paratabulation indicated by parasutural ridges surmounted by short solid processes which bifurcate distally. Bifurcations are parallel to distal edge of septa from which the processes arise. Paracingulum narrow, helicoid, offset at parasulcus by 2-3 paracingular widths. Parasulcus broad, defined by paratabulation of adjoining plates, paratabulation is suppressed. Paratabulation is consistent with a gonyaulacoidean arrangement, with a

significantly reduced fourth apical homologue, although like many members of *Gonyaulacysta* has an L-type ventral organisation. Archeopyle precingular, type P₃", operculum free.

Remarks: This species is distinguished by the nature of the parasutural septa, which are surmounted by bifurcating processes, where the furcated tips are reclined parallel to the distal edges of the host septa.

Gonyaulacysta sp. 3

Plate 12, Figures 16 & 17.

Dimensions: Antapex-apex (36)38(40) μm , width at paracingulum (32)34(36) μm (4 specimens measured).

Description: Small subspherical to ovoidal proximate to proximochorate acavate cysts. Epicyst and hypocyst approximately equal in length. Autophragm punctate and variably tuberculate with small subcircular intratabular tuberculae. In addition, most paraplates (apart from parasulcal series) have numerous intratabular, solid acicular, cilia-like processes (2-5 μm in length), with the density of distribution variable between specimens. Paratabulation indicated by solid parasutural ridges with smooth, serrated or aciculate distal edges. Paracingulum narrow, helicoid, offset at parasulcus by 4-5 paracingular widths. Parasulcus broad. The first postcingular paraplate homologue is partially separable within the sulcal area, and in addition paraplates as, ras, and ps are apparent on some specimens. The paratabulation is consistent with a gonyaulacoidean arrangement, with an L-type to weakly formed S-type ventral organisation. Archeopyle precingular, type P₃", operculum free.

Remarks: This species is separable from other forms attributed to *Gonyaulacysta* by the characteristic intratabular acicular processes, and by the comparative clarity of parasulcal tabulation.

Gonyaulacysta sp. 4

Plate 12, Figures 9-12.

Dimensions: Antapex-apex (40)42(45) μm , width at paracingulum (34)37(40) μm (7 specimens measured).

Description: Small subspherical to ovoidal or pentagonal proximate cysts. Epicyst and hypocyst approximately equal in length. Apex bears a small, hollow truncated-conical horn. Autophragm smooth with variable density of small intratabular granulae to conical tuberculae. Paratabulation indicated by solid parasutural septa with serrated to echinate distal edges. Paracingulum broad, helicoid, offset at parasulcus by 1-2 paracingular widths. Parasulcus broad, paratabulation is suppressed. Paratabulation is consistent with a gonyaulacoidean arrangement, with a strongly developed S-type ventral organisation. Archeopyle precingular, type P₃"', operculum free.

Remarks: This species is characterised by the combination of intratabular tuberculae with a small and poorly developed apical horn, and serrated to echinate parasutural septa.

Genus *Gochteodinia*

Gochteodinia cf. *G. villosa* (Vozzhennikova 1967) Norris 1978.

Plate 7, Figure 6.

Dimensions: Antapex-apex (base of horn) 45(46)49 μm , width 26(28)31 μm . Horn length 12(15)18 μm . 4 specimens measured.

Description: Elongate ovoidal proximochorate acavate cysts. Antapex is rounded, apex is conical and bears a robust apical horn. Autophragm is sculpted into short conical spines (2-4 μm in length) which are evenly distributed over the cyst surface, and non-tabular. Archeopyle is consistent with that proposed by Fensome *et al.* (1993). The operculum is free.

Remarks: This species differs from *G. villosa* in being slightly smaller, and by having spines approximately 1/5th the length of those in *G. villosa*.

Genus *Heslertonia*

Heslertonia sp. 1

Plate 21, Figure 16.

Dimensions: Antapex-apex (42)43(44) μm , width at paracingulum (40)41(43) μm (4 specimens measured).

Description: Spherical to slightly ovoidal, murochorate acavate cysts. Central body occasionally unornamented but usually punctate, giving intratabular areas a pseudo-reticulate appearance. Autophragm thin, and all specimens observed are strongly compressed, though with no apparent preferential orientation. Paratabulation indicated by extremely thin parasutural septa, which are usually notably thickened at gonal intersections. Septa are smooth to very slightly striate, with serrated or undulose distal edges. The delicate nature of the crests is reflected in their generally ragged appearance. Paratabulation is L-type sexiform gonyaulacoid, sulcal paratabulation is suppressed. Archeopyle is of type E, operculum attached, and most specimens additionally show the complete loss of paraplate 3".

Remarks: This species differs from forms of *Ctenidodinium* and *Dichadogonyaulax* by contrasting archeopyle type, and by the nature of the parasutural septa.

Genus *Hystrichodinium*

Hystrichodinium pulchrum Deflandre 1935.

Plate 20, Figures 8-12

Two distinct variants of this species have been noted in the Volga residues. *H. pulchrum* var. 1 has proximally broad, blade-like gonal processes. *H. pulchrum* var. 2 has narrower, much more delicate blade-like processes in both gonal and inter-gonal positions. These variants have not been separated in the stratigraphic or palaeoenvironmental sections since they generally co-occur. SEM examination of *H. pulchrum* var. 1 (Plate 25, Figs 7 & 8) suggests that this species is in fact thecate, rather than being a cyst.

Genus *Impletosphaeridium*

***Impletosphaeridium* sp. 1**

Plate 17, Figures 5-7.

Dimensions: Antapex-archeopyle margin (25)29(33) μm , maximum width (27)29(34) μm (8 specimens measured).

Description: Small sub-spherical to slightly ovoidal, chorate cysts. Autophragm is thick, unornamented, occasionally with slight dorso-ventral compression. Intratabular processes are 5-6 μm in length, parallel-sided, hollow, and distally capitate with closed terminations. Processes are open proximally, so that they have circular ring-like bases in optical sections. Shape of the archeopyle margin suggests an apical archeopyle, type tA, formed from the loss of 4 apical paraplate homologues operculum free, no opercula were observed. Accessory archeopyle sutures partially separate 6 precingular paraplates, which is thus consistent with a gonyaulacoid tabulation.

Remarks: This species is similar to *Chlamydophorella huguoniottii*, except that none of the specimens observed have an ectophragm. It differs from other small chorate forms by the hollow, capitate nature of the processes.

Genus *Kallosphaeridium*

***Kallosphaeridium* sp. 1**

Plate 15, Figure 15.

Dimensions: Antapex-archeopyle margin (27)29(31) μm , maximum width (32)37(44) μm (4 specimens measured).

Description: Ovoidal proximate cysts. Autophragm is thin with small non-tabular tuberculae to small conical spines. Specimens are always strongly flattened, though with no preferential orientation. Archeopyle is apical, type (tA)a, with a simple polyplacoid operculum which remains adnate via the anterior sulcal paraplate. Accessory sutures partially to fully separate 6 precingular paraplates. Compression often fans the cysts out along these accessory sutures so that epicyst is much 'wider' than hypocyst.

PAGE
NUMBERING
AS ORIGINAL

Autophragm is foveolate giving a spongy appearance. A narrow smooth area on the ventral surface indicates the position of the parasulcus, which often possesses flagellar scars. The position of the paracingulum is usually indicated by a slight marginal restriction. Otherwise paratabulation is only apparent at the archeopyle margin, which indicates a type tA apical archeopyle formed from the loss of 4 apical paraplate homologues. No opercula have been observed. Accessory sutures partially separate 6 precingular paraplates as well as paraplate 'as'.

Remarks: This species is separable from other forms here attributed to *Lithodinia* by its small size and spongy autophragm, as well as the general absence of paratabulation. It is closely comparable to *L. acranitabulata* but can be distinguished by the much more poorly developed paracingulum and by the presence of accessory archeopyle sutures which clearly separate sulcal paraplate 'as'.

Lithodinia sp 2

Dimensions: Antapex to archeopyle margin (48)52(57) μm , width at paracingulum (48)54(64) μm . 4 specimens measured.

Description: Thick-walled dorso-ventrally compressed proximate cysts. Antapex flattened. Hypocyst much larger than epicyst. Autophragm spongy, sculpted into parasutural ridges, commonly with accessory ridges and intratabular tuberculae on hypocyst. Paracingulum is broad, tabulate, descends slightly from dorsal to ventral surfaces, and is offset at the parasulcus by up to 1 paracingular width. Parasulcus is smooth, and paratabulation is suppressed. Archeopyle is apical, formed from the loss of 4 apical paraplate homologues. Paratabulation is consistent with a leptodinioidean arrangement, with slight sinistral torsion of the hypocyst relative to the epicyst.

Remarks: This species is characterised by having solid parasutural ridges and intratabular ornamentation, typically solid tuberculae, but occasionally accessory ridges.

Genus *Microdinium*

***Microdinium* sp. 1**

Plate 15, Figures 10 & 11.

Dimensions: Antapex-apex (27)27(27) μm , maximum width (23)25(26) μm (3 specimens measured).

Description: Small ovoidal proximate cysts. Hypocyst much larger than epicyst. Autophragm smooth to finely granulate. Paratabulation indicated by narrow parasutural ridges. The paracingulum is broad, and tabulate, with 76 paracingular plates. Parasulcus is spatulate. There are 6 precingular paraplates, all of which are reduced in height by comparison to the post-cingular paraplates. It has not proved possible to elucidate paratabulation at the apex due to the lack of apical views, but it appears to be complex, and probably has an archeopyle formed from the loss of one or more apical paraplates. However, the observed paratabulation is consistent with a cladopyxiacean arrangement.

Remarks: This species is readily separable in the Volga residues as it is very small, and the only representative of the Cladopyxiinae.

Genus *Protoellipsodinium*

***Protoellipsodinium* sp. 1**

Plate 18, Figures 14 & 15.

Dimensions: Antapex-apex (38)42(45) μm , maximum width (33)34(35) μm (4 specimens measured).

Description: Small ovoidal proximochorate cysts. Autophragm thin, granulate, densely covered by short, fine hair-like processes up to 3 μm in length. No indication of paratabulation apart from the archeopyle, which appears to be formed from the loss of the 3rd precingular paraplate.

Remarks: This species differs from *P. spinosum* in having shorter, finer processes, and a granulate autophragm.

Genus *Rhynchodiniopsis*

Rhynchodiniopsis sp. 1

Dimensions: Antapex-apex (65)69(74) μm , width at paracingulum (58)63(65) μm (5 specimens measured).

Description: Large pentagonal proximate cysts, usually with some element of dorso-ventral compression. Hypocyst and epicyst approximately equal in length or hypocyst slightly larger. Epicyst triangular to dome-shaped with short, broad, conical apical horn. Autophragm smooth, but sculpted into elaborate parasutural septa. Septa are formed from solid parasutural processes which furcate and anastomose to a variable extent, giving the appearance of pseudo-fenestrate crests in particularly elaborate specimens. These septa have distal trabecula linking the processes, which may often be minutely denticulate on the outer edge. The parasutural features are most consistently developed at the paracingulum, surrounding the parasulcal area, and at the antapex, with adcingular and apical paraplate tabulation generally being suppressed. The paracingulum is linear, with little or no offset at the parasulcus. Apparent tabulation is consistent with a cribroperidinioid arrangement. Archeopyle is type P₃", operculum free.

Remarks: This species differs from other forms attributed to *Rhynchodiniopsis* in having the majority of the paratabulation suppressed. Additionally, the parasutural septal structure differs from *R. magnifica* sp. nov. and *R. undoryensis* sp. nov. by having trabecula forming an entire distal edge to the septa.

Genus *Sentusidinium*

Sentusidinium sp. 3 Iosifova

Plate 17, Figures 11 & 12; Plate 25, Figure 2.

Dimensions: Antapex-archeopyle margin (31)35(37) μm , maximum width (34)40(43) μm (6 specimens measured).

Description: Small sub-circular, dorso-ventrally compressed proximochorate cysts. Autophragm thick, sculpted into a dense covering of solid, non-tabular cilia-like acicular processes 2-5 μm in length. Archeopyle is apical, type (tA), formed from the

loss of 4 apical paraplate homologues, with a simple, free, polyplacoid operculum. Accessory archeopyle sutures partially separate 6 precingular paraplates and sulcal paraplate 'as'. The size of either 'as' or the fourth apical homologue is apparently variable, evidenced by specimens exhibiting a pronounced 'sulcal notch'.

Remarks: It is separable from other forms here attributed to *Sentusidinium* by having a thick autophragm and subcircular outline, and densely distributed solid acicular spines.

***Sentusidinium* cf. *S. sp. 3* Iosifova**

Plate 17, Figures 14 & 15.

Dimensions: Antapex-archeopyle margin (31)32(34) μm , maximum width (34)37(40) μm (6 specimens measured).

Remarks: This species differs from *S. sp. 3. Iosifova* in being slightly, but consistently smaller, having less densely distributed and slightly longer processes (4-6 μm), and by having either no, or very poorly developed accessory archeopyle sutures.

***Sentusidinium* sp. 4 Iosifova**

Plate 17, Figures 16-19.

Dimensions: Antapex-archeopyle margin (40)43(49) μm , maximum width (37)42(49) μm (10 specimens measured).

Description: Small sub-spherical, dorso-ventrally compressed proximochorate cysts. Antapex rounded to flattened. Autophragm thin, with solid non-tabular conical tuberculae to very short broad spines evenly distributed over cyst surface. Archeopyle is apical, type (tA), formed from the loss of 4 apical paraplate homologues, with a simple, free, polyplacoid operculum. Accessory archeopyle sutures partially to fully separate 6 precingular paraplates and sulcal paraplate 'as'.

Remarks: It differs from *S. sp. 3 Iosifova* in having a thinner autophragm, with shorter, more robust conical tuberculae, rather than acicular spines.

Genus *Spiniferites*

***Spiniferites* sp. 1**

Plate 12, Figures 23-26.

Dimensions: Antapex-apex (31)33(42) μm , maximum width (31)33(42) μm (4 specimens measured).

Description: Small sub-spherical to ovoidal, proximochorate cysts. Endophragm and periphragm addressed in intratabular areas. Paratabulation indicated by low, suturocavate ridges surmounted by short, thin, distally furcating processes. Gonal processes trifurcate. Furcations are perpendicular to the paraplate boundaries. Paratabulation is consistent with a gonyaulacoidean arrangement, with a strongly developed S-type ventral organisation.

Remarks: This species is characterised by its small size, suturocavation, and short, simply furcating processes.

***Spiniferites* sp. 2**

Plate 12, Figure 22.

Dimensions: Antapex-apex; endophragm (31)31(31) μm . Periphragm; (43)43(43) μm ; width at paracingulum (36)36(36) μm (3 specimens measured).

Description: Small sub-spherical to ovoid, proximochorate cavate cysts. Cavation developed at the antapex and ventral hypocyst, periphragm and endophragm addressed elsewhere. Paratabulation indicated on periphragm by low parasutural ridges surmounted by short delicate, distally furcating processes. Gonal processes trifurcate, inter-gonal processes bifurcate; furcations are perpendicular to the paraplate boundaries. Paratabulation is consistent with a gonyaulacoidean arrangement, with an S-type ventral organisation. Endophragm is thick and smooth, only indication of paratabulation is the archeopyle.

Remarks: This species is characterised by its prominent cavation in the hypocyst, and by the short spiniferate processes which surmount the low parasutural ridges.

Genus *Tehamadinium*

Tehamadinium sp. 1

Plate 18, Figure 10.

Dimensions: Antapex-apex (56)58(62) μm , width at paracingulum (53)55(56) μm (5 specimens measured).

Description: Sub-spherical to ovoid, proximochorate acavate cysts. Apex bears a small cluster of acicular process which coalesce to form a perforate horn in some specimens. Paratabulation indicated either by thin parasutural crests with smooth to undulate distal edges, or by the alignment of short acicular spines. Intratabular areas bear discrete acicular to coniform spines. Paracingulum is slightly helicoid, offset at parasulcus by 1 paracingular width. Parasulcus occasionally bears small flagellar scars, and parasulcal tabulation is well developed. Paratabular arrangement is consistent with a leptodinioidean arrangement. Archeopyle is of type 2P (2" & 3"), operculum free, no opercula have been observed.

Remarks: This species is similar to *T. daveyi* Jan du Chene *et al.* 1986, also encountered in the present report, but differs in having discrete spines in intratabular areas; *T. daveyi* has spines connected by ridges or crests. It is also similar to *T. dodekovi* Jan du Chene *et al.* 1986, but is significantly smaller.

Genus *Tenua*

Tenua hystrix Eisenack 1958

Plate 19, Figures 1-5, 9 & 10; Plate 25, Figures 4 & 5.

Remarks: In these residues a complete gradation exists between specimens with processes restricted to lateral and apical regions, and those with processes evenly distributed over the entire cyst surface. Specimens with processes absent from mid-dorsal and ventral areas are correctly referable to *Tenua*, since this genus is a member of the Areoligeracea, and do not require assignment to *Cyclonephelium*.

Tenua cf. *T. hystrix* Eisenack 1958.

Plate 19, Figures 6-8.

Remarks: *T. cf. hystrix* differs from *T. hystrix* in having significantly longer processes. This variation may be an ecophenotype of *T. hystrix*, although both forms occur in several samples from the unzoned basal Ryazanian deposits at Kashpir.

Genus *Trichodinium*

Trichodinium cf. *T. ciliatum* (Gocht 1959) Eisenack & Klement 1964.

Plate 11, Figures 9 & 10; Plate 24, Figure 12.

This species differs from *T. ciliatum* in having much shorter spines, restricted to conical spinules. In addition, numerous specimens show paracingular and parasulcal regions indicated by the absence of spinules which contrasts to *T. ciliatum*. Specimens with this feature are comparable to *T. discus* Harding 1988, but are generally much larger than that species.

Genus *Tubotuberella*

Tubotuberella cf. *T. apatela*

Plate 14, Figures 15-17.

Remarks: This is identical to *T. apatela* except that numerous specimens have been noted which possess small circular pits on the inner surface of the periphragm (verified under the SEM), inside the antapical projection. The density of pitting is highly variable; all specimens with pitting have been assigned to *T. cf. apatela*, since this is not a typical characteristic of the species.

Genus *Warrenia*

Warrenia sp. 1

Plate 18, Figures 16 & 17; Plate 23, Figure 4.

Dimensions: Antapex-apex (63)68(72) μm , width at paracingulum (62)67(71) μm (5 specimens measured).

Description: Sub-spherical proximochorate acavate cysts. Autophragm thick, sculpted into a dense cover of solid, conical, non-tabular spines 3-5 μm in length, which are often joined at the base into short rows or groups. Apex often bears a small cluster of spines which are slightly longer than on the remainder of the cyst. Paratabulation is suppressed, and is only indicated at the archeopyle margin. Archeopyle type 2P, formed from the removal of either paraplates 2" & 3", or 3" & 4" (both types encountered), although no opercula were observed.

Remarks: This species differs from *Warrenia ?brevispinosa* by having a much thicker, more robust autophragm, and longer, thicker spines joined into small clusters at their base. It differs from species of *Tehamadinium* in lacking any parasutural features. This species is excluded from *Occisucysta* since it lacks any apical cavation.

CHAPTER 5. Volga Basin palynofacies investigation.

5. Volga Basin palynofacies investigation

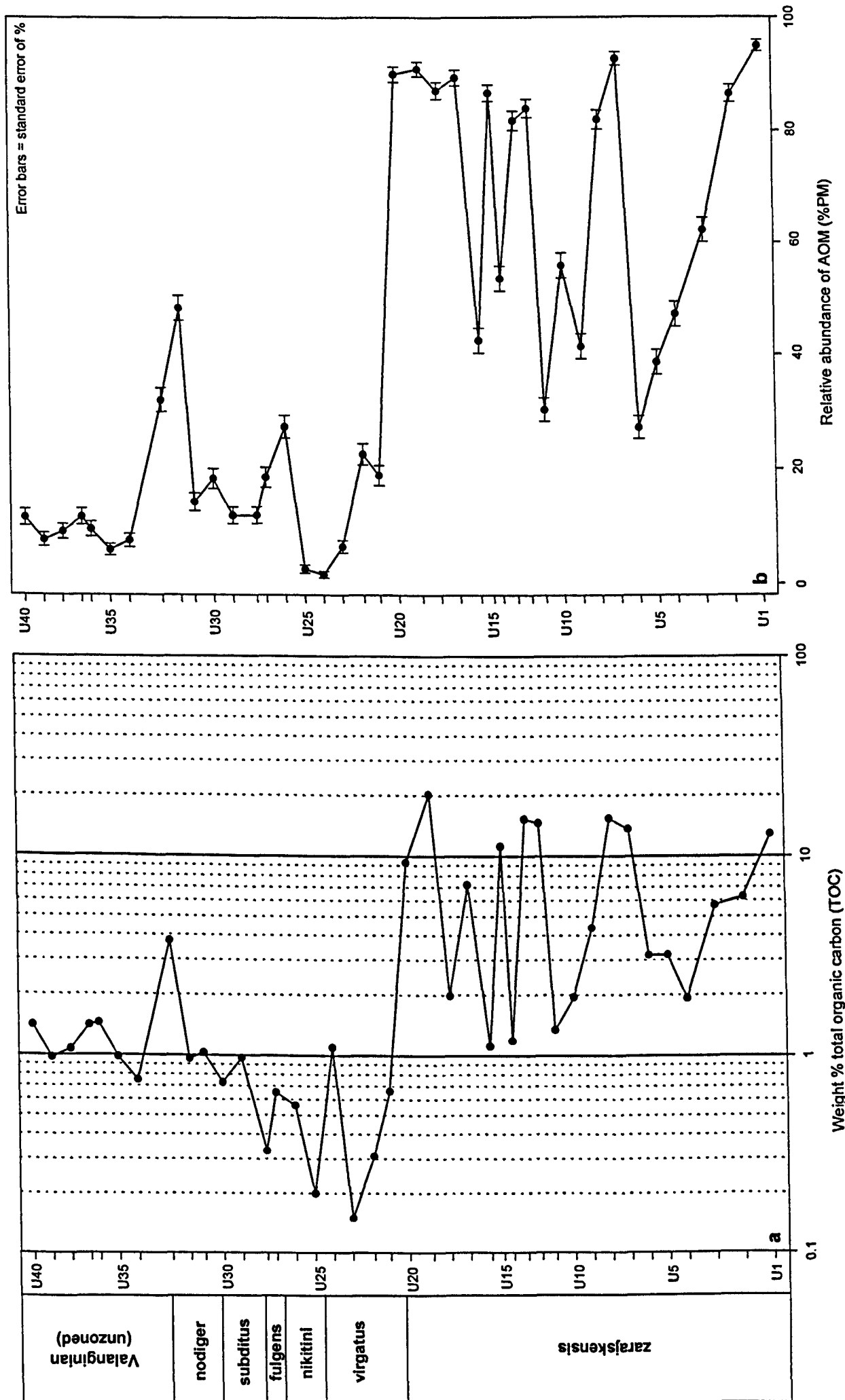
Palynofacies of samples from the two Volga Basin sections have been analysed. Palynologic matter assemblages have also been examined from residues untreated with ultrasonic vibration or oxidation in order to establish the relative abundance of AOM. The relative and absolute abundance of structured materials have also been examined from residues subjected to oxidation and ultrasonic treatment. Data from these analyses have been combined with the sedimentological information presented in Tables 4.1 & 4.2 to make interpretations about depositional environments through the studied interval. Detailed consideration has also been given to the dinoflagellate cyst assemblages, which have been compared to the palynofacies and sedimentological interpretations to see if changes in environment of deposition are consistently reflected in the marine palynomorph data.

5.1. Gorodische palynofacies investigation

5.1.1. Total organic carbon content (TOC)

Samples collected from the Volga Basin localities have been analysed for total organic carbon content (TOC). The raw data for Gorodische can be found in Appendix D, and carbonate-corrected TOC values are additionally presented in Table 5.1 and in Figure 5.1a. It can be seen that TOC is generally high in samples of the zarajskensis subzone (beds 1-13) by comparison with beds 14-20. Three of the four major peaks in TOC within this lower interval correspond to laminated siltstones of beds 5, 7 and 9. The uppermost sample from the lenticular siltstones (Bed 12, sample U19) also shows a marked peak in TOC. The coarse-grained deposits of the virgatus Zone and fine sandstones of the nikitini to nodiger zones generally show low TOC (<1%), although the conglomerate horizon of Bed 16 (sample U24) and the phosphorite deposit (Bed 19, sample U33) both show small peaks in TOC above 1%. Samples taken from the mica-rich siltstones at the top of the section have higher TOC (0.7-1.5 wt%) than sediments of the

Figure 5.1: TOC and AOM at Gorodische



virgatus to fulgens zone interval, though only slightly higher than the fine sandstones of the subditus and nodiger zones.

By comparison with Figure 5.1b it can be seen that there is a strong correlation between high TOC and abundant AOM. This is particularly true of samples taken from the zarajskensis Subzone, where in many cases the palynologic matter assemblages are dominated by this component.

5.1.2. Bulk palynological matter

AOM-phytoclast-marine palynomorph (A-P-D) plots

In the Volga Basin palynofacies, AOM, woody phytoclasts and marine palynomorphs (particularly dinoflagellate cysts) are the three dominant groups of palynological matter. Thus, ternary plots such as the A-P-E diagrams of Tyson (1989, 1993) have particular relevance in presentation of the Volga Basin data. Whilst the general characteristics of the AOM in most samples is consistent with typical autochthonous AOM (derived from the degradation of marine algae) as described by Tyson (1995) and Batten (1996), in the present report it has not been characterised using fluorescence, and therefore must be regarded as being of equivocal provenance. Nevertheless, points clustered at the AOM apex on these ternary diagrams (Figures 5.2a & b) are expected to represent dysoxic to anoxic depositional conditions in the same manner as indicated by Tyson (1993). However, in order to fully represent the terrestrially derived components on one axis, sporomorphs are removed from the 'E' (exinitic) organic matter apex of Tyson (1989, 1993) and included within the phytoclast axis (although such palynomorphs generally comprise an insignificant proportion of the total palynofacies in these residues). Therefore, the 'E' apex retains only marine palynomorphs, a group which is overwhelmingly dominated by dinoflagellate cysts in the residues studied here. Thus the 'A-P-E' plots of Tyson (1989, 1993) have been modified, resulting in an 'A-P-D' plot where apices are labelled by their dominant components (Fig. 5.2a & b). The analyses used to produce the A-P-D plots were

performed on the residues which had not been treated with nitric acid oxidation or ultrasonic vibration.

The proportions of these three components are plotted for each sample at Gorodische in Figure 5.2a, and the data presented in Table 5.1. The concentration of sample points in the lower portion of this diagram clearly shows that AOM and dinocysts are the most abundant components in these palynofacies, and thereby exemplifies the outlying nature of samples U34 and U35. A distinct cluster of samples is notable at the AOM apex of this plot, indicating that such samples were deposited in anoxic conditions, suitable for preservation of this palynological matter component. This is supported by the sedimentology of the samples, which are exclusively dark mudstones and laminated siltstones, known to be common in Jurassic anoxic facies in southern England.

These data have been compared to the sedimentological information, and the samples are clustered according to lithology in Figure 5.2b. Samples from the panderi Zone are grouped within Cluster A at the bottom left of the diagram. This group is further divisible into two sub-clusters, A1 and A2. A1 contains the samples with maximum AOM preservation. This includes samples U1 & U2 (both mudstones), the remainder of points in this cluster being derived from the laminated and lenticular siltstones of the zarajskensis Subzone. The majority of the mudstones from this zone form the larger Sub-cluster A2, ranging between 30% and 60% AOM. The coarse-grained facies of the virgatus Zone are grouped in the crescent-shaped Cluster B. These sediments clearly display low relative abundance of AOM, high relative percentages of dinoflagellate cysts, and generally increased abundance of phytoclasts by comparison with the majority of the other samples examined. Samples from the fine shelly sandstones of the nikitini to nodiger zones (samples U17 - U32), and the phosphorite horizon, sample U33, are grouped in Cluster C at the base of the diagram. The mica-rich siltstones at the top of the section are separable into two distinct clusters, D and E. Cluster D is tightly constrained, indicating little variation in the environment of deposition or degree of preservation between samples U36 and U40. However, samples

Sample	Position	TOC	Brown wood	% brown wood	Standard error of %	Tracheids	% Tracheids	Standard error of %	Black wood	% Black wood	Standard error of %	Total phytoclasts	% Phytoclasts	Standard error of %	Dinocysts	% Dinocysts	Standard error of %	AOM	% AOM	Standard error of %	Count total	PhytOC
U1	5	12.9	4	0.79	0.39	0	0	0	15	2.97	0.76	19	3.76	0.85	6	1.19	0.48	480	95	0.97	505	0.484
U2	35	6.29	7	1.4	0.52	1	0.2	0.2	16	3.19	0.79	24	4.79	0.95	43	8.58	1.25	434	86.6	1.52	501	0.301
U3	65	5.7	17	3.39	0.81	0	0	0	17	3.39	0.81	34	6.79	1.12	155	30.9	2.07	312	62.3	2.17	501	0.387
U4	95	1.93	14	2.79	0.73	1	0.2	0.2	29	5.78	1.04	44	8.76	1.26	221	44	2.22	237	47.2	2.23	502	0.169
U5	115	3.19	17	3.37	0.8	1	0.2	0.2	11	2.18	0.65	29	5.75	1.04	280	55.6	2.21	195	38.7	2.17	504	0.184
U6	135	3.18	26	5.15	0.98	0	0	0	38	7.52	1.17	64	12.7	1.48	303	60	2.18	138	27.3	1.98	505	0.403
U7	155	13.7	16	3.19	0.79	2	0.4	0.28	9	1.8	0.59	27	5.39	1.01	9	1.8	0.59	465	92.8	1.15	501	0.738
U8	175	15.5	17	3.4	0.81	1	0.2	0.2	3	0.6	0.35	21	4.2	0.9	69	13.8	1.54	410	82	1.72	500	0.649
U9	195	4.38	40	7.98	1.21	2	0.4	0.28	33	6.59	1.11	75	15	1.59	218	43.5	2.21	208	41.5	2.2	501	0.656
U10	215	1.96	27	5.4	1.01	1	0.2	0.2	21	4.2	0.9	49	9.8	1.33	171	34.2	2.12	280	56	2.22	500	0.192
U11	235	1.35	34	6.77	1.12	2	0.4	0.28	31	6.18	1.07	67	13.3	1.52	282	56.2	2.21	153	30.5	2.05	502	0.18
U12	250	14.7	9	1.8	0.59	0	0	0	12	2.4	0.68	21	4.19	0.9	59	11.8	1.44	421	84	1.64	501	0.614
U13	265	15.3	10	2	0.63	2	0.4	0.28	13	2.6	0.71	25	5	0.97	66	13.2	1.51	409	81.8	1.73	500	0.765
U14	280	1.19	31	6.16	1.07	0	0	0	19	3.78	0.85	50	9.94	1.33	183	36.4	2.15	270	53.7	2.22	503	0.118
U15	290	11.2	12	2.27	0.65	4	0.76	0.38	6	1.13	0.46	22	4.16	0.87	48	9.07	1.25	459	86.8	1.47	529	0.466
U16	303	1.12	29	5.8	1.05	2	0.4	0.28	9	1.8	0.59	40	8	1.21	247	49.4	2.24	213	42.6	2.21	500	0.09
U17	325	7.21	13	2.59	0.71	0	0	0	9	1.79	0.59	22	4.38	0.91	31	6.18	1.07	449	89.4	1.37	502	0.316
U18	345	1.99	18	3.59	0.83	0	0	0	9	1.8	0.59	27	5.39	1.01	37	7.39	1.17	437	87.2	1.49	501	0.107
U19	365	20.2	12	2.4	0.68	1	0.2	0.2	7	1.4	0.53	20	4	0.88	25	5	0.97	455	91	1.28	500	0.809
U20	390	9.34	17	3.38	0.81	1	0.2	0.2	3	0.6	0.34	21	4.17	0.89	29	5.77	1.04	453	90.1	1.33	503	0.39
U21	410	0.66	60	12	1.45	6	1.2	0.49	82	16.4	1.65	148	29.5	2.04	258	51.5	2.23	95	19	1.75	501	0.195
U22	427	0.31	57	11.3	1.41	8	1.59	0.56	71	14.1	1.55	136	27	1.98	253	50.3	2.23	114	22.7	1.87	503	0.084
U23	450	0.15	67	13.3	1.51	11	2.18	0.65	58	11.5	1.42	136	27	1.98	335	66.5	2.1	33	6.55	1.1	504	0.04
U24	470	1.1	40	7.98	1.21	7	1.4	0.52	29	5.79	1.04	76	15.2	1.6	417	83.2	1.67	8	1.6	0.56	501	0.167
U25	490	0.2	13	2.57	0.7	0	0	0	22	4.35	0.91	35	6.92	1.13	458	90.5	1.3	13	2.57	0.7	506	0.014
U26	510	0.56	3	0.6	0.34	0	0	0	4	0.8	0.4	7	1.39	0.52	358	71.2	2.02	138	27.4	1.99	503	0.008
U27	530	0.65	8	1.6	0.56	1	0.2	0.2	8	1.6	0.56	17	3.4	0.81	390	78	1.85	93	18.6	1.74	500	0.022
U28	540	0.33	22	4.4	0.92	1	0.2	0.2	21	4.2	0.9	44	8.8	1.27	396	79.2	1.82	60	12	1.45	500	0.029
U29	565	0.97	26	5.1	0.97	2	0.39	0.28	11	2.16	0.64	39	7.65	1.18	410	80.4	1.76	61	12	1.44	510	0.074
U30	585	0.73	9	1.78	0.59	0	0	0	4	0.79	0.39	13	2.56	0.7	401	79.1	1.81	93	18.3	1.72	507	0.019
U31	605	1.03	19	3.78	0.85	1	0.2	0.2	14	2.78	0.73	34	6.76	1.12	397	78.9	1.82	72	14.3	1.56	503	0.07
U32	620	0.96	7	1.4	0.52	0	0	0	5	1	0.44	12	2.4	0.68	247	49.3	2.23	242	48.3	2.23	501	0.023
U33	640	3.73	28	5.58	1.02	3	0.6	0.34	22	4.38	0.91	53	10.6	1.37	288	57.4	2.21	161	32.1	2.08	502	0.394
U34	675	0.75	207	41.4	2.2	25	5	0.97	162	32.4	2.09	394	78.8	1.83	68	13.6	1.53	38	7.6	1.19	500	0.591
U35	695	0.98	190	37.6	2.16	27	5.35	1	178	35.2	2.13	395	78.2	1.84	80	15.8	1.62	30	5.94	1.05	505	0.767
U36	715	1.45	40	7.98	1.21	24	4.79	0.95	28	5.59	1.03	92	18.4	1.73	361	72.1	2	48	9.58	1.31	501	0.266
U37	725	1.41	29	5.57	1	14	2.69	0.71	48	9.21	1.27	91	17.5	1.66	369	70.8	1.99	61	11.7	1.41	521	0.246
U38	745	1.07	39	7.75	1.19	19	3.78	0.85	26	5.17	0.99	84	16.7	1.66	373	74.2	1.95	46	9.15	1.29	503	0.179
U39	765	0.97	57	11.3	1.41	16	3.16	0.78	23	4.55	0.93	96	19	1.74	371	73.3	1.97	39	7.71	1.19	506	0.184
U40	785	1.41	29	5.79	1.04	8	1.6	0.56	31	6.19	1.08	68	13.6	1.53	375	74.9	1.94	58	11.6	1.43	501	0.191

Table 5.1: Relative abundance of major palynofacies components from unsonified/unoxidised residues. Gorodische section.

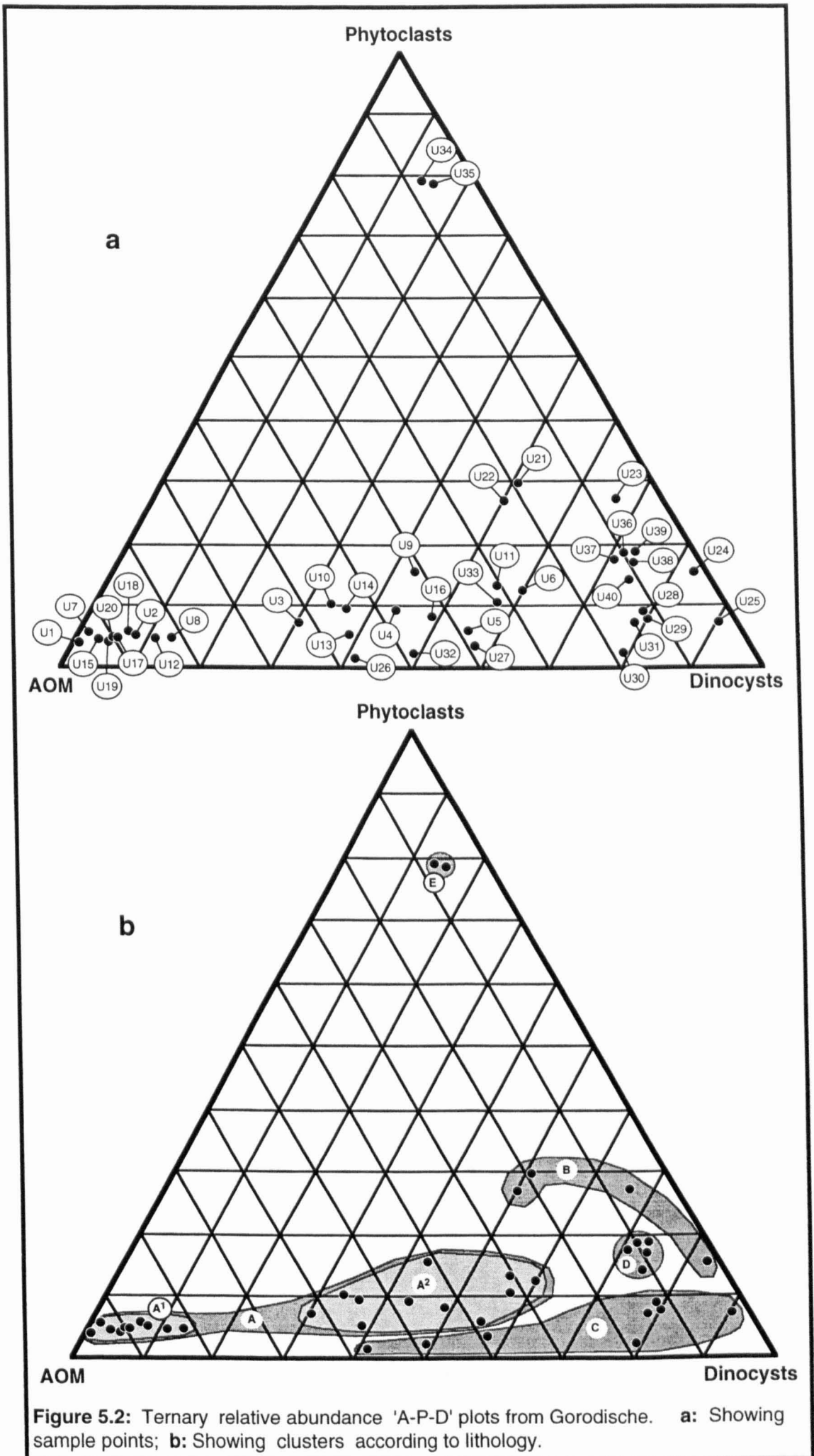


Figure 5.2: Ternary relative abundance 'A-P-D' plots from Gorodische. **a:** Showing sample points; **b:** Showing clusters according to lithology.

U34 & U35 (Cluster E) are derived from essentially identical sediments to those in Cluster D, and therefore must reflect a difference in preservation or depositional environment not apparent in the sedimentology.

The validity of these clusters has been tested by running the same data from the control residues through minimum variance cluster analysis using MVSP[®]. The resulting dendrogram is displayed in Figure 5.3, in which eight clusters can be recognised. To simplify the text, clusters in the dendrogram are referred to as 'branches'. Branch 1 is largely comprised of mudstones and the relatively AOM-poor laminated siltstones from the zarajskensis Subzone, but also includes the phosphorite deposit, Bed 19 (sample U33). This branch is therefore identical to Cluster A2 in Figure 5.2b. Branches 2 & 3 are entirely comprised of samples taken from the fine-grained sandstones of the nikitini to nodiger zone interval, represented on the ternary diagram (Figure 5.2b) by Cluster C. The sensitivity of the cluster analysis technique is demonstrated here, by subdivision of this sedimentary facies into two palynofacies branches, although it is doubtful whether such discrimination has any interpretative value. Branches 4, 5 and 6 correspond to Cluster A1 on Figure 5.2b, representing the AOM-rich sediments. It is interesting that the three samples from the lenticular siltstone facies of Beds 10 and 12 are clearly separable as a sub-branch of Branch 5. Branch 7 combines samples taken from both the mica-rich siltstones and the coarse-grained deposits of the virgatus Zone. although again, some degree of separation is evident. The spatial distribution of these sample points in Figure 5.2b allows the two lithological groups to be clearly separated in clusters D and E. Branch 8 combines samples U34 and U35, also from the mica-rich siltstones, but which are clearly separable from the other samples of this facies in Cluster E on Figure 5.2b. In general it can be seen that minimum variance cluster analysis produced similar clustering of the data to the A-P-D ternary plot.

When this ternary plot is broken down by sequence of deposition, it is possible to detect trends or cycles in the abundance of these components (Figure 5.4). Figures

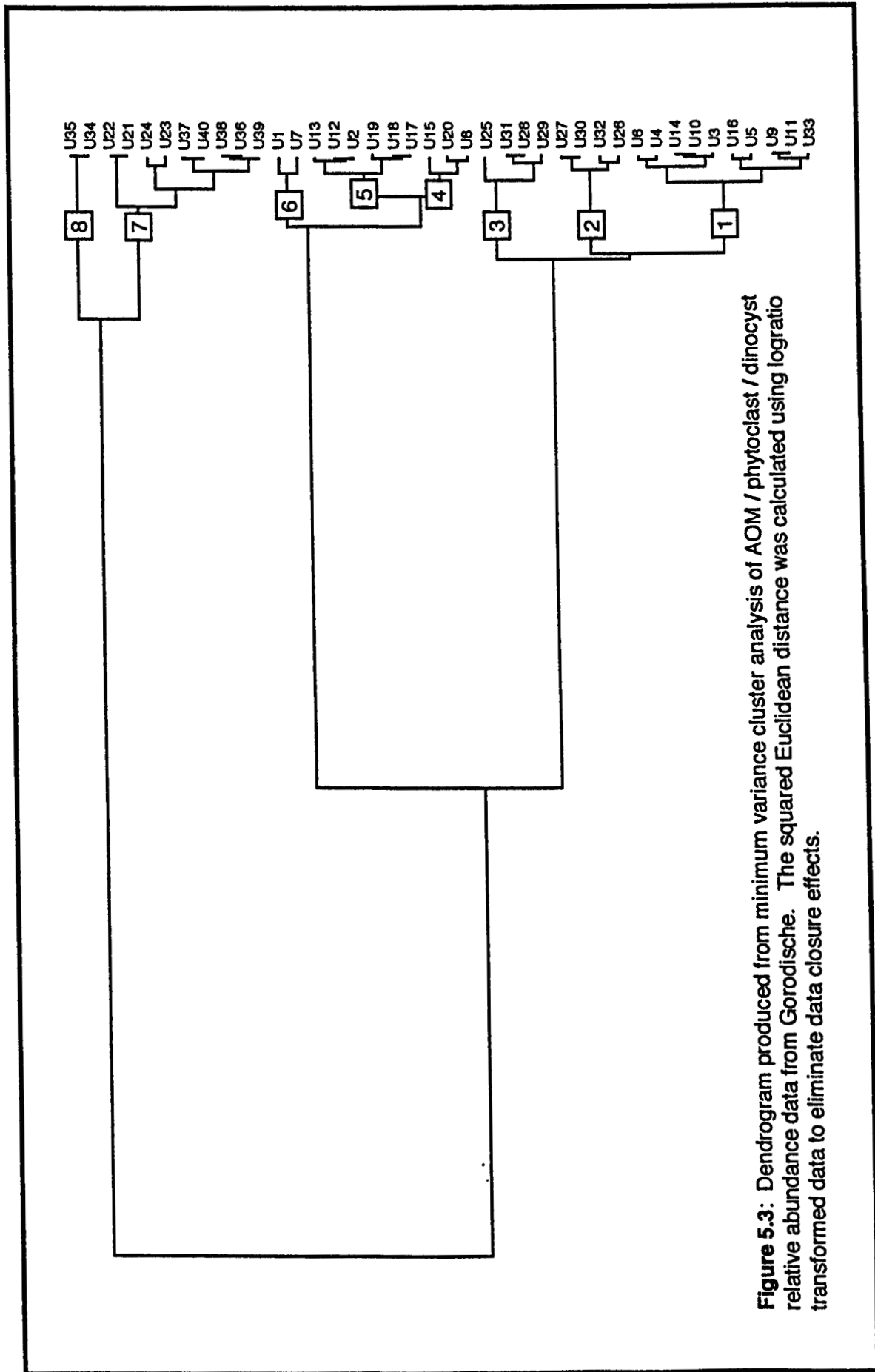


Figure 5.3: Dendrogram produced from minimum variance cluster analysis of AOM / phytoclast / dinocyst relative abundance data from Gorodische. The squared Euclidean distance was calculated using logratio transformed data to eliminate data closure effects.

5.4a, b, c, d and e show significant right-hand shifts in the abundance of AOM, and the repetition in this shift, particularly in the lower part of the section, may be regarded as cyclical. Such right hand shifts are characteristic of either decreasing production or decreasing preservation of AOM, and in the latter case of increasingly oxic conditions at the locus of deposition. Figure 5.4f shows a significant shift towards the dinocyst apex, which may be attributable to either increased productivity of dinoflagellate populations, increased preservation of the dinoflagellate cyst component, or decreased input of phytoclasts. The major trend breaks (the level at which one trend ends and the next begins) all correspond to obvious disconformities or changes in lithology.

Summary

Analysis of the TOC and control residue palynofacies indicates that:

- A strong association exists between high TOC and peak abundance of AOM in the Gorodische assemblages.
- The lower part of the section (zarajskensis Subzone) is composed of comparatively organic- and AOM-rich sediments, which may thus have been deposited in dysoxic to anoxic conditions or in areas of high productivity.
- Several trends towards decreased AOM content may indicate phases or cycles of increasing oxygenation or decreasing productivity at the locus of deposition. This is particularly evident in the zarajskensis Subzone.
- Minimum variance cluster analysis produces very similar results to the A-P-D ternary diagram.

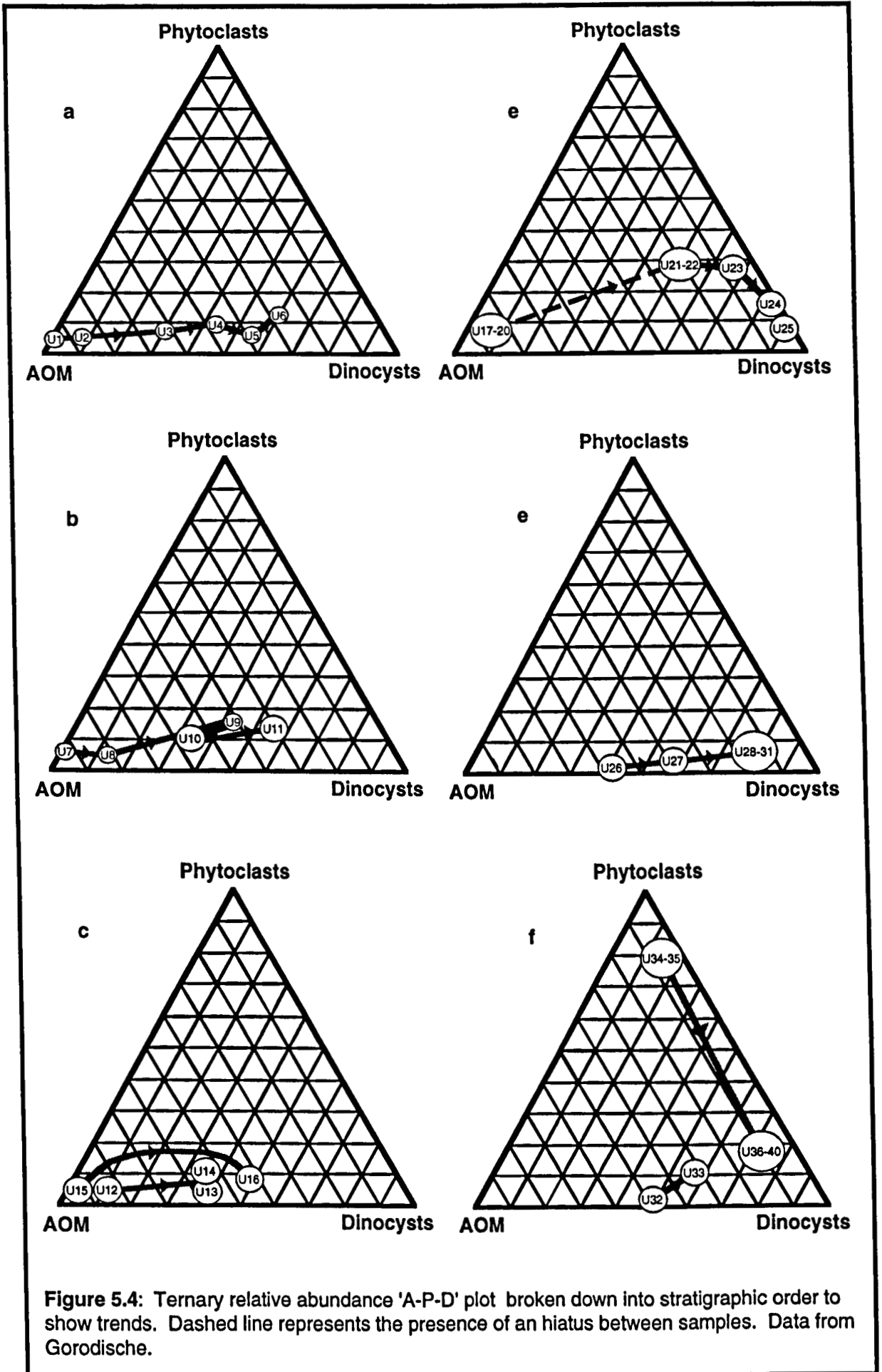


Figure 5.4: Ternary relative abundance 'A-P-D' plot broken down into stratigraphic order to show trends. Dashed line represents the presence of an hiatus between samples. Data from Gorodische.

5.1.3. Analyses of the structured components

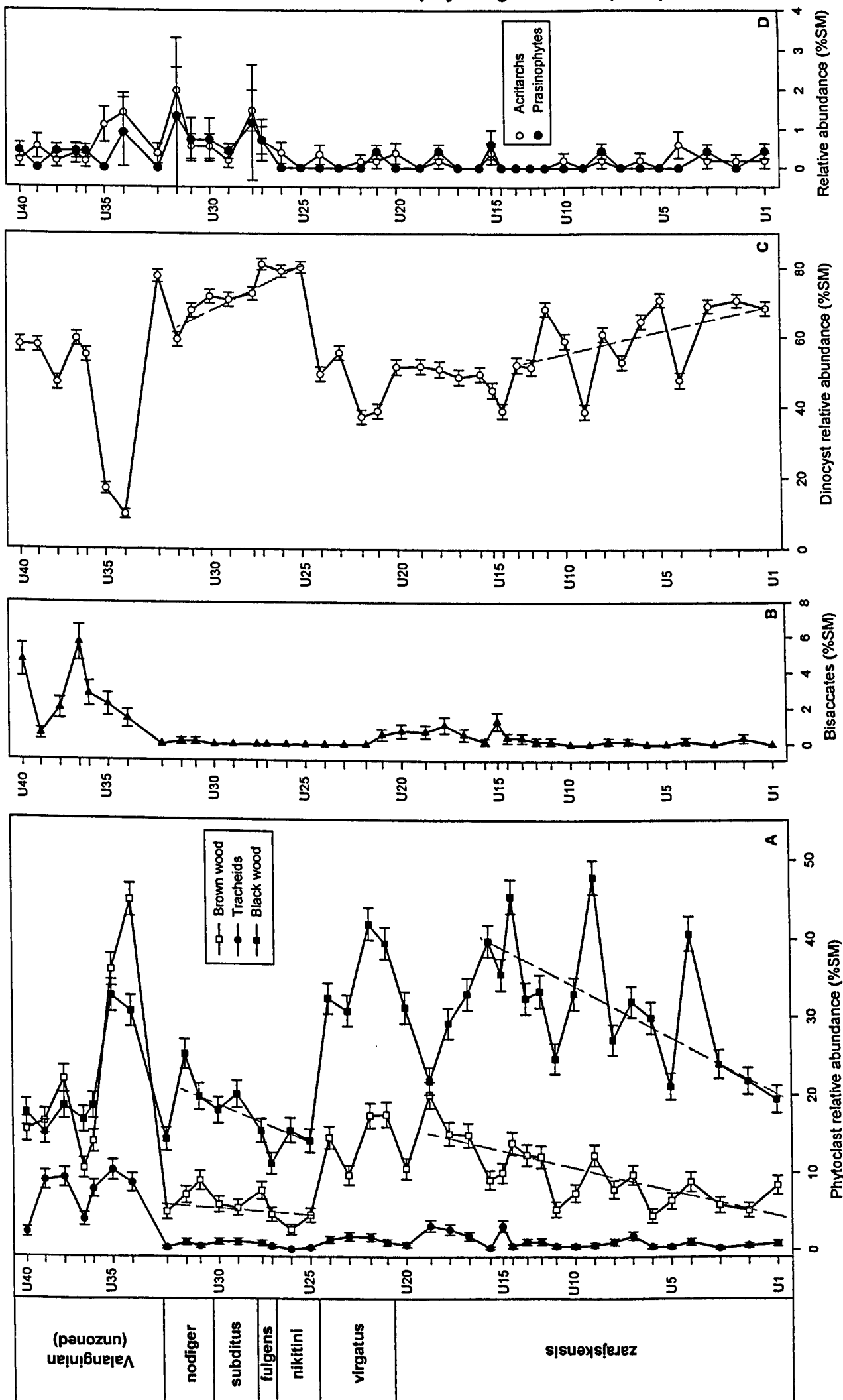
5.1.3.1. Relative abundance data (%SM)

Relative abundance data derived from the structured palynofacies counts (%SM) are presented in Table 5.2 and Figure 5.5. These graphs show that of the structured materials, dinoflagellate cysts and brown & black wood are the three most abundant components. Furthermore, black wood has higher relative abundance than brown wood in the majority of palynofacies, apart from in the mica-rich siltstones at the top of the section.

In the samples from the *zarajskensis* Subzone, 'trend lines' highlight decreasing relative abundance in dinoflagellate cysts up section with concomitant increases in relative abundance of both brown and black wood (Figs. 5.5a & c). It should be noted however that such data are inherently affected by data closure, and it is therefore unclear from this information alone whether such trends reflect absolute increases in the input of phytoclasts, or decreased absolute abundance of dinoflagellate cysts.

Slightly elevated relative abundances of brown wood exist between samples U17 and U24, corresponding to the lenticular siltstones and coarse-grained deposits of the *virgatus* Zone. A peak is also notable in the black wood data corresponding to Beds 14-16 (*virgatus* Zone, samples U21-U24). However, samples taken from the lenticular siltstones show a reduction in black wood relative abundance from sample U16, culminating in a pronounced minimum point in sample U19. This is concomitant with a peak in the relative abundance of brown wood, whilst the dinoflagellate cyst abundance remains comparatively stable. At the *virgatus* - *nikitini* zone transition (samples U24-U25) there is a pronounced drop in the relative abundance of both the major woody phytoclast components (and implicit rise in the dinoflagellate cyst abundance). The fine-grained sandstones of the interval from samples U25-U32 show relatively stable

Figure 5.5: Relative abundance of structured palynological matter (%SM) at Gorodische



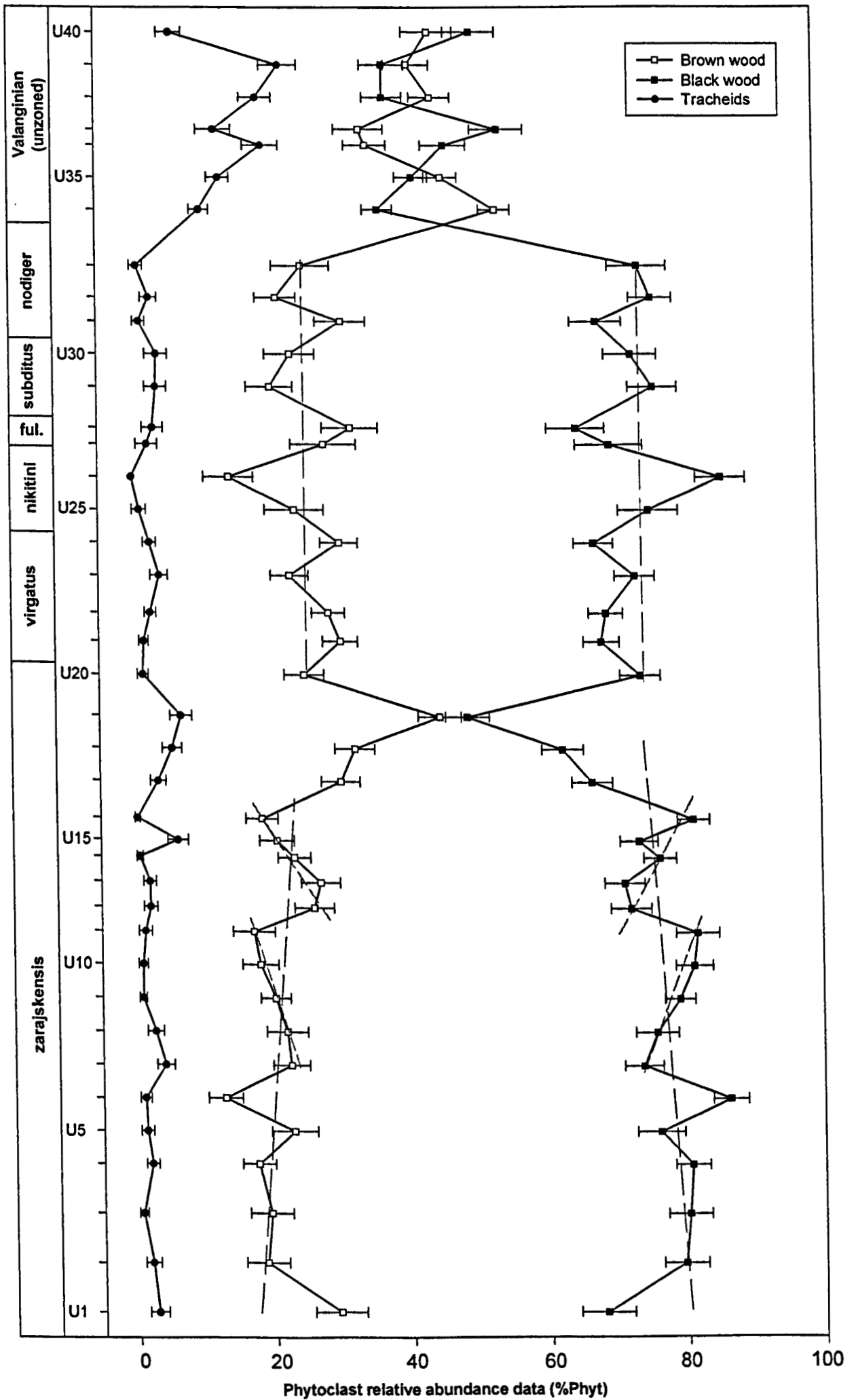
relative proportions of the three major components, with a trend to slightly increased phytoclast abundance (particularly black wood) towards the top of this interval (and associated decrease in the relative abundance of dinoflagellate cysts). Acritarchs and prasinophytes (mostly pterospermellids) reach peak abundance in the upper part of this interval and into the lowermost part of the mica-rich siltstones (however, they never constitute more than 2% of the structured materials and rarely exceed 1%, thus the standard errors of percentage show that even the peaks in these components are of little statistical value)

The phosphorite deposit (sample U33) is marked by slightly increased abundance of dinoflagellate cysts relative to woody phytoclasts. Above this unit, an abrupt change in the palynofacies to markedly increased relative abundance of terrestrially-derived palynologic matter is noted at the base of the mica-rich siltstones. Samples U34 & U35 have the highest relative abundance of terrestrially-derived material, and notable dominance of the brown wood component over black wood. Sporomorphs, particularly bisaccate pollen reach maximum abundance in this part of the section, further indicating strong terrestrial influence.

5.1.3.2. Detailed analysis of the phytoclast assemblages (%Phyt)

Figure 5.6 shows the relative abundance of each of the phytoclast components as a proportion of the total phytoclast population (%Phyt). Cuticle fragments are extremely rare in the Volga Basin sediments (0-1.8%SM), and have not been plotted. As is expected of populations largely comprised of two components, brown wood and black wood %Phyt values closely mirror one-another. Throughout the Jurassic succession both sets of values generally show only minor fluctuations from simplified trend lines, although there appears to be a significant change in slope of this line at sample U20 (Bed 13). Through the zarajskensis Subzone, brown wood %Phyt values generally increase up section (and black wood values decrease)(samples U1-U18), although there appear to be several short reverse trends superimposed on this (sample intervals U7-U11 and U12-

Figure 5.6: Relative abundance within the phytoclast group (%Phyt) at Gorodische



SAMPLE	Brown wood long axis	Standard Deviation (STDEV)	STDEV as % of mean	Standard Error	Brown wood short axis	Standard Deviation (STDEV)	Standard Error	Difference between mean long & short axes	Mean long axis: short axis ratio	% of particles long axis: short axis ratio >3:1	Black wood long axis	Standard Deviation (STDEV)	STDEV as % of mean	Standard Error	Black wood short axis	Standard Deviation (STDEV)	Standard Error	Difference between mean long & short axes	Mean long axis: short axis ratio	% of particles being Type 2	Brown wood FI	Black wood FI
U1	47.3	17.6	37.2	1.76	26.6	6.16	0.62	20.7	1.78	10	40.2	12.3	30.6	1.23	27.5	4.7	0.47	12.7	1.46	3	3.56	3.78
U2	48.1	15.3	31.8	1.53	29.6	7.81	0.78	18.4	1.62	4	39.4	9.16	23.2	0.92	28.4	4.69	0.47	11	1.39	0	3.58	3.8
U3	49.1	16.2	33	1.62	30.6	5.96	0.6	18.5	1.61	4	41.2	10.9	26.5	1.09	29.9	5.18	0.52	11.3	1.38	1	3.36	3.7
U4	49.4	14.4	29.1	1.44	31.8	6.36	0.64	17.7	1.56	4	40.6	9.63	23.7	0.96	29.9	5.33	0.53	11.4	1.39	0	3.43	3.93
U5	47.8	16	33.5	1.6	29.5	6.42	0.64	18.3	1.62	5	40.3	10.2	25.3	1.02	27.4	4.85	0.49	12.9	1.47	3	3.37	3.83
U6	49.8	19.6	39.4	1.96	32	8.83	0.88	17.8	1.56	4	41.1	9.42	22.9	0.94	29.6	5.65	0.57	11.6	1.39	0	3.41	3.91
U7	48	15.2	31.7	1.52	30.6	7.45	0.75	17.4	1.57	5	41.3	9.88	23.9	0.99	29.2	6.67	0.67	12.1	1.41	0	3.61	3.83
U8	42.6	12.3	28.9	1.23	28.7	6.75	0.68	13.9	1.48	6	40.2	9.82	24.4	0.98	27.8	4.8	0.48	12.4	1.45	2	3.49	3.82
U9	45.9	11.3	24.6	1.13	30.3	6.24	0.62	15.6	1.52	3	38	8.42	22.2	0.84	27.5	5.58	0.56	10.5	1.38	1	3.31	3.94
U10	45.3	11.7	25.8	1.17	30.8	5.4	0.54	14.5	1.47	1	39.3	9.4	23.9	0.94	27.6	5.59	0.56	11.9	1.43	4	3.38	3.88
U11	44.7	13.2	29.5	1.32	30.3	6.78	0.68	14.3	1.47	1	40.1	12	29.9	1.2	27.2	4.54	0.45	13	1.48	4	3.32	3.8
U12	49.3	15.7	31.8	1.57	29.9	6.96	0.7	19.9	1.68	7	40.2	12.6	31.3	1.26	27.2	4.19	0.42	12.9	1.47	3	3.44	3.91
U13	49.5	15.9	32.1	1.59	29.6	6.91	0.69	20.1	1.67	6	40.4	12.8	31.7	1.28	27.4	4.27	0.43	13	1.47	2	3.46	3.88
U14	45.4	11.8	26	1.18	29.3	5.91	0.59	16.1	1.55	4	38.3	9.25	24.2	0.93	28	6.68	0.68	10.3	1.37	0	3.2	3.79
U15	42.1	11	26.1	1.1	27.4	5.88	0.59	14.7	1.53	1	40.9	11	26.9	1.1	27.1	4.04	0.4	13.8	1.51	3	3.64	3.75
U16	43.9	11.5	26.2	1.15	28.7	5.3	0.53	15.3	1.53	4	39.3	9.53	24.2	0.95	27.5	5.05	0.51	11.7	1.43	0	3.61	3.87
U17	49.2	17.4	35.4	1.74	28.9	6.96	0.7	20.3	1.7	6	39.2	9.58	24.4	0.96	28.9	4.94	0.49	10.3	1.35	0	3.47	3.29
U18	42.5	13.1	30.8	1.31	26.7	8.51	0.85	15.8	1.59	8	37	11.4	30.8	1.14	25.6	6.77	0.68	11.4	1.44	2	3.53	3.62
U19	49.6	17.7	35.7	1.77	30.3	7.91	0.79	19.3	1.64	8	43	12	27.9	1.2	29.3	4.8	0.48	13.7	1.47	4	3.61	3.75
U20	44.7	13.9	31.1	1.39	28.9	6.86	0.69	15.7	1.54	1	38.8	11	28.5	1.1	28.6	5.79	0.57	12	1.45	3	3.54	3.85
U21	53.6	23.5	43.8	2.35	30.9	8.32	0.83	22.7	1.73	8	40.1	10.4	25.9	1.04	27.6	5.64	0.56	12.5	1.45	2	3.28	3.82
U22	50.9	22	43.2	2.2	33.6	19.5	1.95	17.3	1.51	3	45	18.8	41.8	1.88	31.5	13.6	1.36	13.5	1.43	0	3.31	3.79
U23	45.4	20.8	45.8	2.08	27.4	8.19	0.82	18	1.65	8	39.8	11.5	28.9	1.15	27.8	5.65	0.57	12	1.43	0	3.38	3.68
U24	58.9	28.5	48.4	2.85	34.5	12.2	1.22	24.5	1.71	10	42.3	13.6	32.2	1.36	30.3	8.03	0.8	12	1.39	0	3.34	3.72
U25	48.7	15.4	31.6	1.54	29.3	7.01	0.7	19.3	1.66	3	43.1	15.7	36.4	1.57	32.1	10.9	1.09	11	1.34	0	3.35	3.7
U26	45.7	16.2	35.4	1.62	29.7	8.73	0.87	16	1.54	4	43.1	15.6	36.2	1.56	29.1	6.35	0.64	14	1.48	1	3.41	3.72
U27	48.7	16.9	34.7	1.69	30.8	7.86	0.79	17.9	1.58	3	42.1	14.4	34.2	1.44	28	6.43	0.64	14.1	1.5	2	3.41	3.93
U28	47.1	15.9	33.8	1.59	30.7	7.93	0.79	16.4	1.53	1	41.6	14.7	35.3	1.47	30.2	11.1	1.11	11.5	1.38	1	3.37	3.79
U29	47.4	14.9	31.4	1.49	29.7	6.34	0.63	17.7	1.59	6	38.4	12.3	32	1.23	28.9	10.4	1.04	9.56	1.33	0	3.39	3.85
U30	47.8	14.4	30.1	1.44	30	7.29	0.73	17.8	1.59	3	39.8	13	32.7	1.3	28.8	6.77	0.68	11	1.38	1	3.19	3.78
U31	50.7	16.8	33.1	1.68	30.4	6.86	0.69	20.3	1.61	3	40.9	12.8	31.3	1.28	28.6	6.13	0.61	12.2	1.43	1	3.1	3.73
U32	51	19.4	38	1.94	31.3	11.5	1.15	19.1	1.63	6	44.5	15.4	34.6	1.54	31.2	10.8	1.08	13.3	1.43	1	3.19	3.57
U33	51.5	28.3	55	2.83	30	8.68	0.87	21.5	1.72	9	47.9	20.1	42	2.01	30.8	8.98	0.9	17.1	1.56	3	3.49	3.62
U34	50.6	22.1	43.7	2.21	29.6	7.09	0.71	21	1.71	5	41.9	14.1	33.7	1.41	29.1	7.95	0.8	12.8	1.44	1	3.34	3.51
U35	49.9	27.3	54.7	2.73	29	7.86	0.79	20.9	1.72	8	40.9	12.9	31.5	1.29	28	6.5	0.65	12.8	1.46	2	3.19	3.53
U36	54.2	28.9	53.3	2.89	30.5	8.73	0.87	23.7	1.78	6	43.1	17.6	40.8	1.76	29.7	6.78	0.68	13.4	1.45	1	3.18	3.53
U37	57.1	33.9	59.4	3.39	30.6	8.8	0.88	26.5	1.87	11	42.6	15.8	37.1	1.58	28.9	7.09	0.71	13.7	1.47	5	2.99	3.46
U38	48.6	18.4	37.9	1.84	31.5	9.52	0.95	17.1	1.54	5	42.2	14.8	35.1	1.48	28.9	8.54	0.85	13.2	1.46	3	3.07	3.62
U39	51.7	24.1	46.6	2.41	31.5	12.6	1.26	20.2	1.64	10	44	16.2	36.8	1.62	28.9	6.66	0.67	15.1	1.52	4	3.03	3.46
U40	57.9	26	44.9	2.6	32.7	11.8	1.18	25.2	1.77	12	43.1	20.2	46.9	2.02	28.2	6.53	0.65	14.9	1.53	4	2.94	3.6

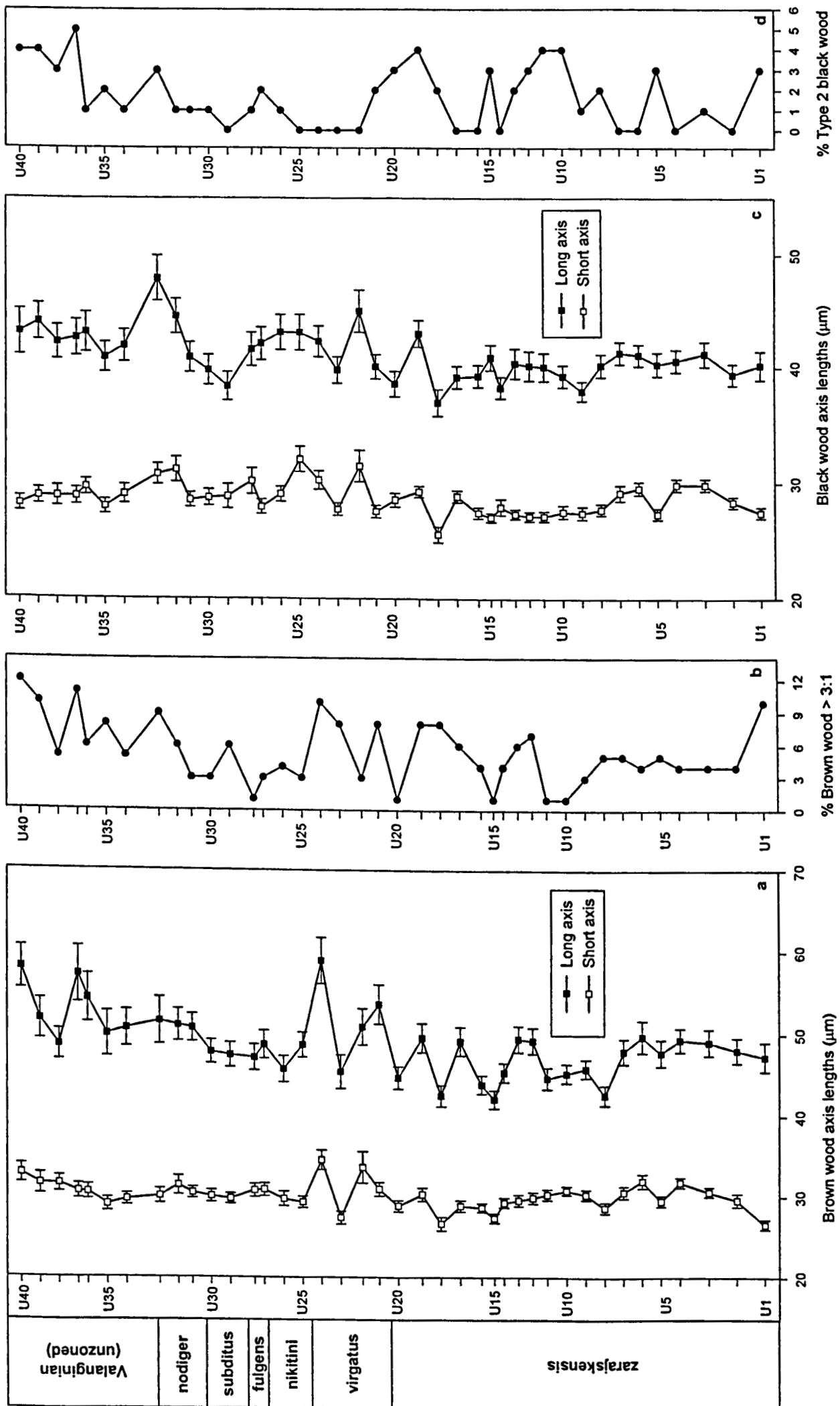
Table 5.3: Mean phytoclast particle size data from Gorodische.

U16). This lower trend is capped by an increase in both brown wood and tracheids relative to black wood at sample U19, as also reflected in the %SM data. From sample U21 to U33 the %Phyt data of both brown wood and black wood are quite consistent with respect to their trend lines, which remain horizontal through this interval. Most of the abrupt changes in %Phyt data through the Jurassic succession coincide with lithological changes from mudstone to laminated siltstone, or otherwise to erosional contacts evident in the sedimentary log (Enclosure 1). In a similar manner to the data presented in Figure 5.5, the %Phyt data (Fig. 5.6) pick out a significant change in the phytoclast population above sample U33: the relative abundance of brown wood and black wood components become closely comparable, with brown wood often dominating the phytoclast assemblage. Furthermore tracheids reach maximum relative importance in these mica-rich siltstones.

Quantitative assessment of the phytoclast size distribution in the present study only takes into account the >20 μm size fraction because all residues were sieved. Nevertheless, analysis of such data (Table 5.3, Figure 5.7) reveals several correlations between the relative abundance data and mean particle size for each sample. For example, mean brown wood long-axis data show generally high values in the mica-rich siltstones at the top of the section, correlated with elevated levels in relative abundance of this component (Fig. 5.6). However, samples U34 and U35 which show peak relative abundance of brown wood do not show a corresponding peak in mean long-axis size for this phytoclast type. Brown wood long-axis peaks in samples U21 and U24 correspond to the two conglomerate horizons from the *virgatus* Zone, and to similar peaks in the %Phyt and %SM data.

Black wood mean long-axis data is generally more consistent between samples than that of brown wood, although there are conspicuous peaks at samples U19, U22 and U33. These do not correlate with peaks in the black wood %Phyt values; indeed U19 displays a pronounced minimum in the relative abundance of this component. Analysis of the type of black wood in these assemblages is potentially of interest. Figure 5.7d

Figure 5.7: Brown & black wood phytoclast size (Gorodische)



shows that Type 2 black wood (long axis: short axis ratio >3:1, equivalent to material interpreted by Batten (1973b, 1981, 1996), as burnt tracheidal matter) never constitutes more than 5 % of the total black wood population. It has previously been shown that black wood, particularly the equant material (=Type 1 of the current investigation), is common in reworked deposits, and may be derived from heavily carbonised brown wood, commonly during extended periods of transport (Smythe *et al.*, 1992). In this report particles suggested to be reworked are considered to be locally reworked, or reworked into distal sediments from proximal deposits, thus both within the sedimentary system, not redeposited from the erosion of older rocks. Thus the Type 1 black wood in these deposits has three possible origins: 1) It is derived from extended periods of transport, 2) by distal deposition of reworked proximal sediments, or 3) by extended sediment-surface residence times due to low sediment supply, probably combined with localised reworking. It seems unlikely that a simple relationship exists, and therefore it is difficult to make interpretations on the basis of black wood abundance alone. However, reduced black wood relative abundance in samples U18 & U19, and in the mica-rich siltstone interval contrasts with both increased relative abundance of brown wood and tracheids and peaks in the abundance of both Type 2 black wood fragments and elongate brown wood. This is therefore indicative of either decreased input of reworked materials or increased influx of 'fresh' phytoclasts.

Whether the measurement of grain roundness/angularity used in the study of clastic sediment grains (Powers, 1953) can be meaningfully applied to the microscopic examination of woody phytoclasts is uncertain. The physics governing the abrasion of small, 'buoyant', comparatively soft phytoclasts is not necessarily comparable with hard, dense, macroscopic (or even microscopic) mineral/lithic grains. Furthermore, we cannot necessarily expect 'proximal' phytoclasts to be particularly angular: indeed newly formed charcoal fragments are often blocky rather than angular *per se*. Thus the interpretative value of the Roundness Index (RI) (see Chapter 3) used in the present report is unclear.

However, the values collected have been plotted for brown and black wood in Figure 5.8a. High values might be expected to reflect extended periods of particle abrasion, either during transport or by reworking. It is clear from this diagram that in general (Type 1) black wood particles appear more rounded than brown wood, lending further support to their reworked status. The RI of brown wood is markedly lower in the uppermost part of the section possibly indicating decreased duration of particle transport, and a similar trend is seen in the black wood component. The change from lenticular siltstones at the top of the *zarajskensis* Subzone to the coarser conglomerates and sandstones of the *virgatus* to *nodiger* zones is reflected in a pronounced reduction in brown wood RI at sample U21. The brown wood RI increases slightly from sample U21 to U29, but a marked reduction in RI values in samples immediately below the phosphorite deposit once again suggests decreased duration of particle abrasion.

Size-sorting of a particle assemblage can be analysed in two ways: it can be considered as the 'absolute' variation in μms , either using maximum-minimum spread or variation from mean (=standard deviation), or as a relative property of each assemblage, in this case percentage variation from mean. Two assemblages with identical 'absolute' sorting (STDEV) can have very different relative values depending on mean particle size. Thus both approaches are used in the present report. However, it is important to remember that such values are properties of the 'adjusted' assemblages, since all residues were sieved using a 20 μm mesh.

Standard deviation of the mean phytoclast long axis data is presented as the absolute sorting measure in Figure 5.8b, and as percentage of mean in 5.8c. The standard deviation of black wood long axis data is consistently lower than that of brown wood, indicating that the black wood component is better sorted. This is consistent with reworking. Significant peaks in the brown wood standard deviation are notable in samples U21 to U24 and within and above the phosphorite horizon (sample U33). The black wood standard deviation gives a similar but much less pronounced signal. The same situation is seen in the relative sorting plot (5.8c). Clearly, phytoclast

Increasing duration of particle abrasion (transport / reworking)

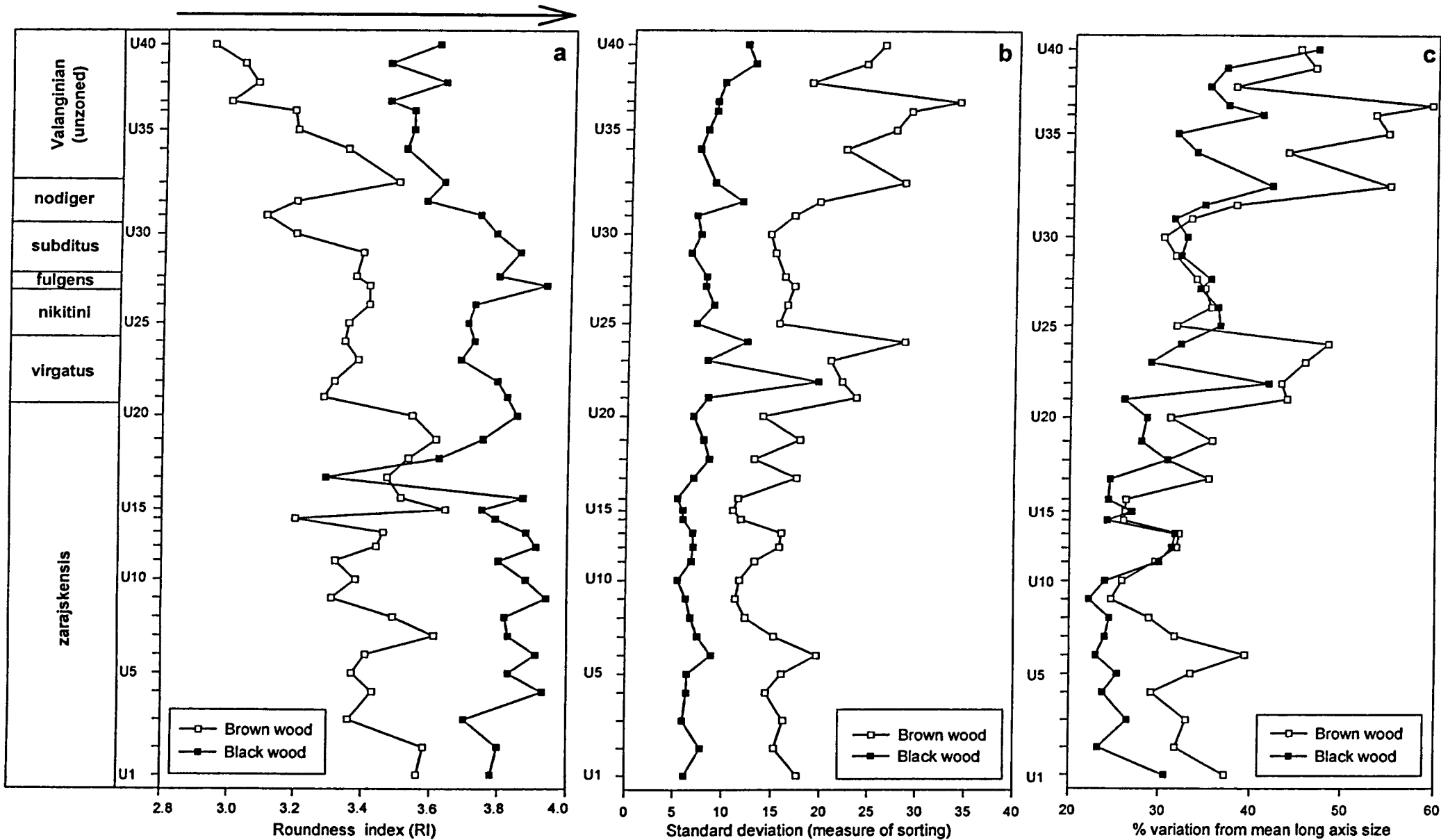


Figure 5.8: Phytoclast roundness and and sorting at Gorodische

assemblages (particularly brown wood) are least well sorted in the coarse-grained deposits and in the mica-rich siltstones.

A ternary plot showing the relative abundance of the three phytoclast types (tracheids are combined with sporomorphs) reveals that certain lithological types can be grouped on the basis of this data (Figure 5.9a). The mica-rich siltstones are clearly distinguishable from the remaining samples in Cluster C. Cluster B partially separates the lenticular bedded siltstones of beds 10 and 12 (Enclosure 1) from the remaining rock types in Cluster A. From the latter, Sub-cluster A1 is further separable, representing the coarse-grained sandstone and conglomerate horizons of the virgatus Zone. Considering the pronounced lithological variety enclosed within Cluster A, it is perhaps surprising that further differentiation is not evident.

Much of the brown wood examined from these residues was heavily carbonised, often black with brown rims, but since a complete gradation exists between 'fresh' brown and heavily oxidised material, it is impossible to objectively separate the two extremes. For this reason plots of marine palynomorphs versus terrestrially-derived materials must be generated twice, in each case separately combining brown wood with 'oxidised' or 'fresh' materials. These are presented in Figures 5.9b and 5.10. In these graphs 'marine palynomorphs' are taken as dinoflagellate cysts plus prasinophytes, omitting acritarchs which have been shown to have some affinity with inner neritic or restricted marine conditions. Thus in Figure 5.9b, the axis labelled 'tracheids and sporomorphs' is intended to represent the input of fresh terrestrially-derived material. The combined brown wood-black wood axis represents the sum of reworked phytoclasts, or those which have undergone extended periods of transport. As can be seen, the sample points are clustered along the right-hand edge of the diagram, since the structured palynological matter in these residues is dominated by dinoflagellate cysts plus brown and black wood. Nevertheless, they can be grouped into several loose clusters according to lithology. The mica-rich siltstone palynofacies are most clearly separable, and confined to Cluster E. Clusters A and B represent the majority of sample points: A combines the

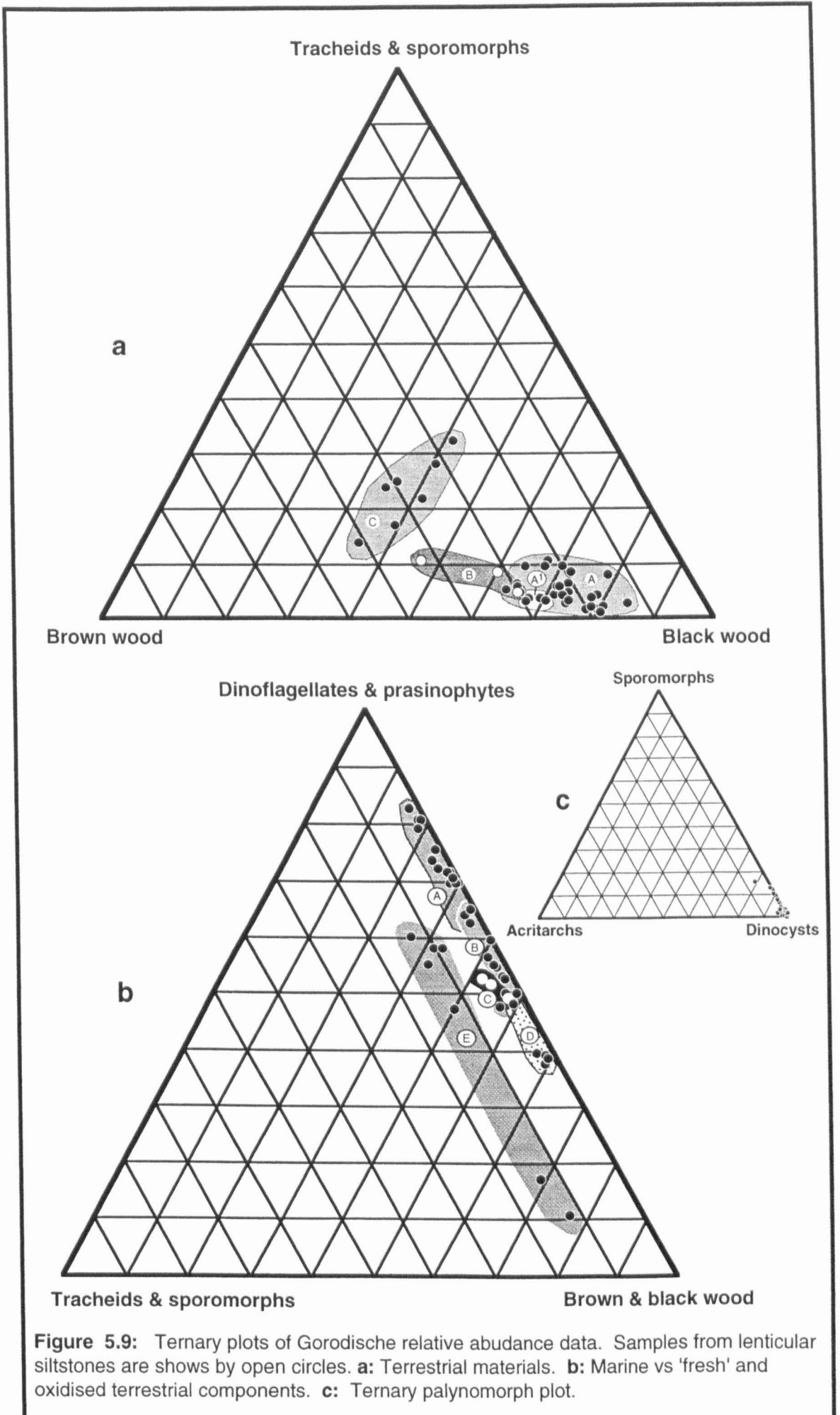


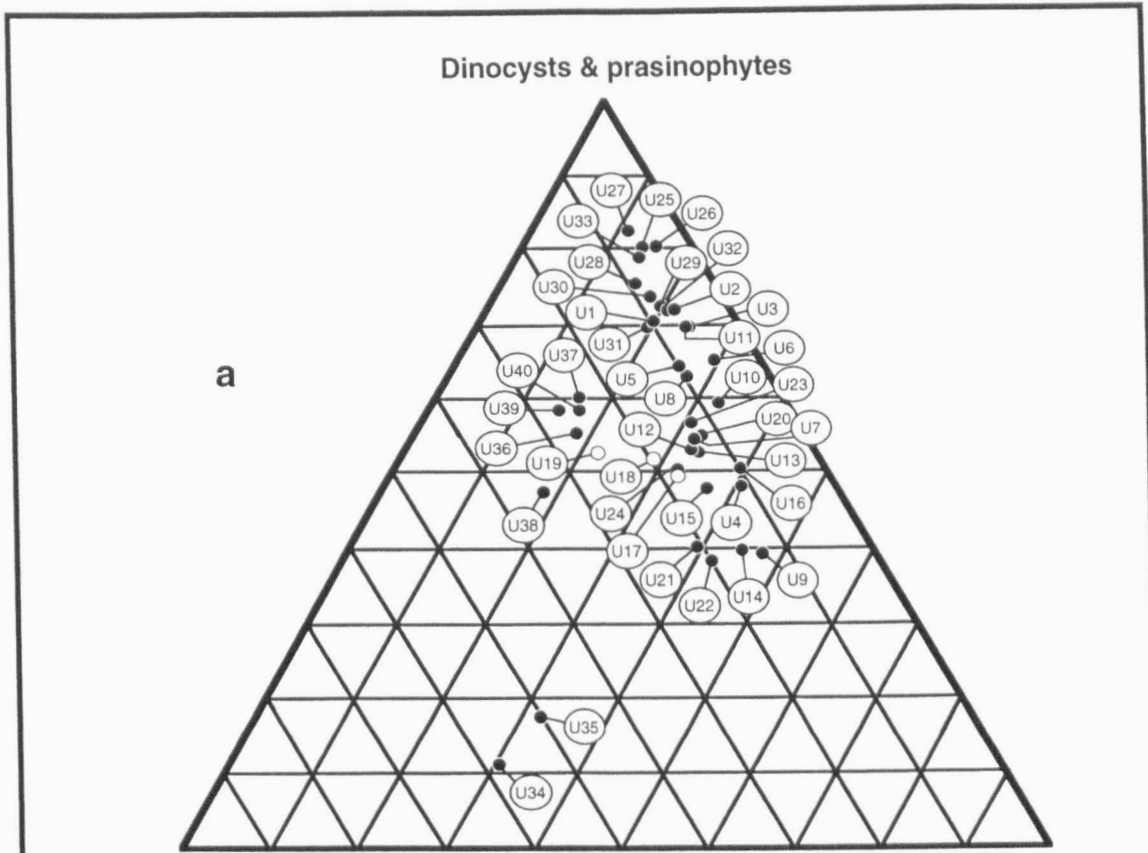
Figure 5.9: Ternary plots of Gorodische relative abundance data. Samples from lenticular siltstones are shown by open circles. **a:** Terrestrial materials. **b:** Marine vs 'fresh' and oxidised terrestrial components. **c:** Ternary palynomorph plot.

fine sandstones from the nikitini to nodiger zones plus the dark mudstones from the lowest part of the zarajskensis Subzone. Cluster B contains the mudstones from the upper part of the zarajskensis Subzone plus the laminated siltstones from this subzone. Clusters C and D encompass the lenticular siltstones of the zarajskensis Subzone and the coarse sandstones/conglomerates of the virgatus Zone respectively.

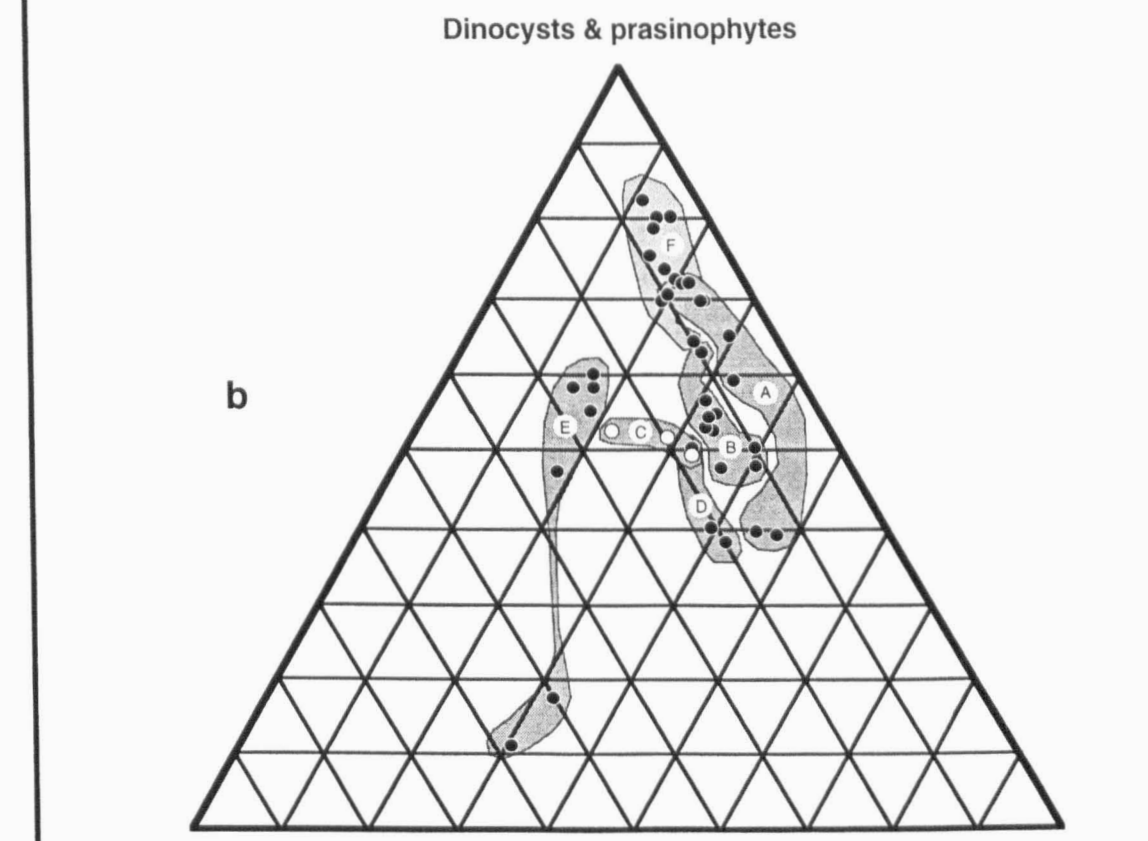
This plot is expanded in Figure 5.10, where the tracheid and sporomorph components are combined with brown wood. Most of the clusters from Figure 5.10b can still be recognised, although more clearly so when brown wood is associated with 'fresh' components. In this plot the mudstones of the zarajskensis Subzone are grouped into one cluster (Cluster A), whilst the laminated siltstones from the interval of samples U12 to U16 are constrained within Cluster B. Clusters C, D and E are similarly recognisable, and using this plot, the fine sandstones from the nikitini to nodiger zone interval can be differentiated in Cluster F near the marine palynomorph apex.

Minimum variance cluster analysis has not proved as effective as the ternary plots in lithological discrimination using relative abundance palynofacies data from Gorodische. Figure 5.11 shows a dendrogram separable into 4 main branches. Branch 4 comprises samples from the mica-rich siltstones, which are clearly distinguishable from the remainder of the sample set. This branch is thus comparable to Cluster E on both of the ternary plots. Branch 1 is broadly comparable to clusters A and E in Figure 5.10 although not all sample points contained within these clusters are held within this branch. Branch 3 is partly comparable to clusters B, C & D, but the lithologies are not as well separated as in the ternary diagram of Figure 5.10. Branch 2 is most poorly differentiated, including elements from most of the lithological groups.

Figure 5.9c shows a ternary palynomorph plot from the Gorodische residues. As can be seen, little information can be gleaned from this diagram as the sample points are tightly clustered at the dinocyst and prasinophyte apex. Ternary plots or ratios



Tracheids + Brown wood + sporomorphs Black wood



Tracheids + Brown wood + sporomorphs Black wood

Figure 5.10: Ternary plots of marine vs 'fresh' & oxidised terrestrial components at Gorodische. **a:** Showing sample points; **b:** Showing clusters according to lithology. Samples from the lenticular siltstones shown by open circles

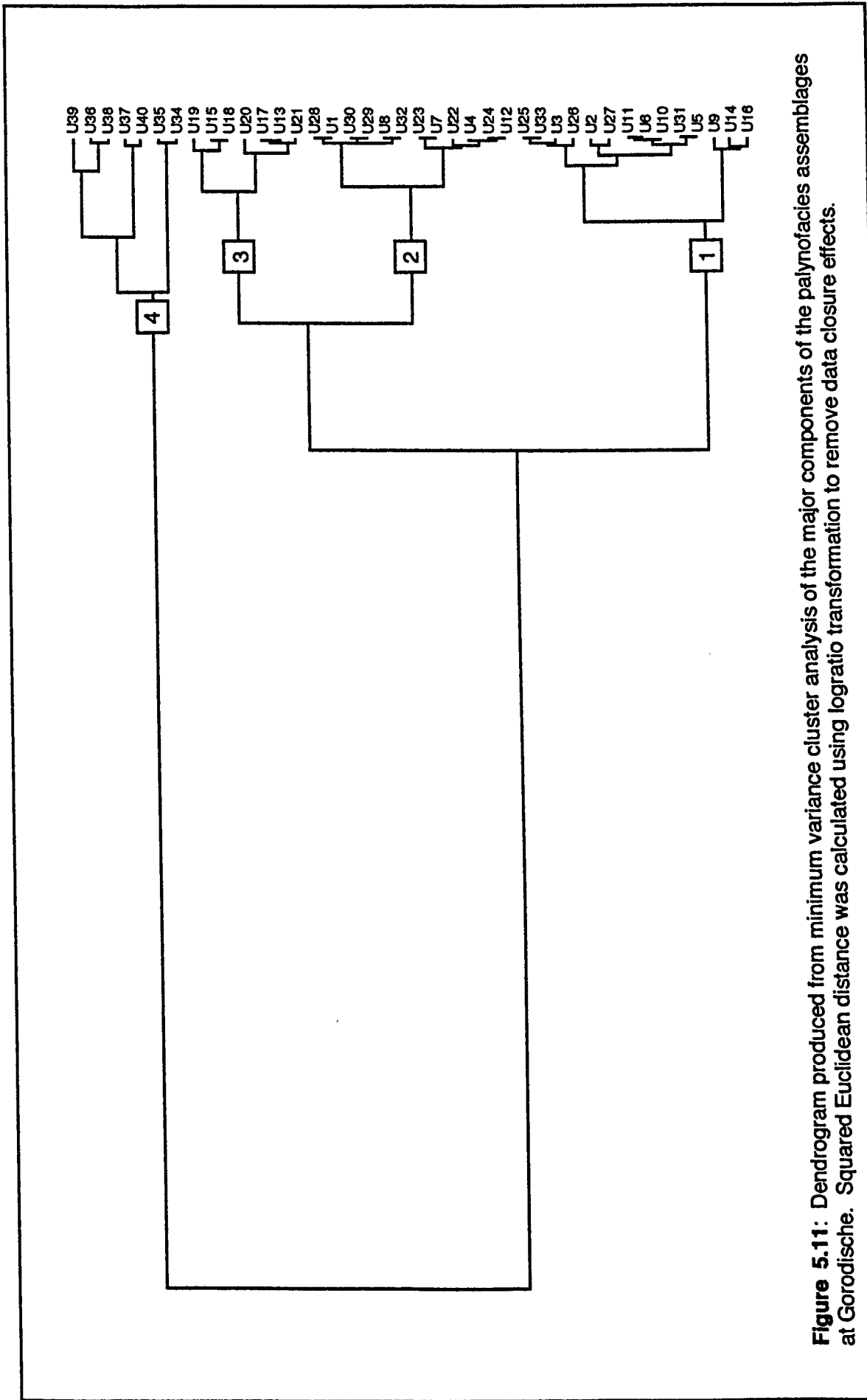


Figure 5.11: Dendrogram produced from minimum variance cluster analysis of the major components of the palynofacies assemblages at Gorodische. Squared Euclidean distance was calculated using logratio transformation to remove data closure effects.

showing the various sporomorph elements were not generated since these components were not counted in statistically significant numbers to allow separate analysis.

5.1.3.3. Absolute abundance analyses.

Absolute abundance with *Lycopodium* spores

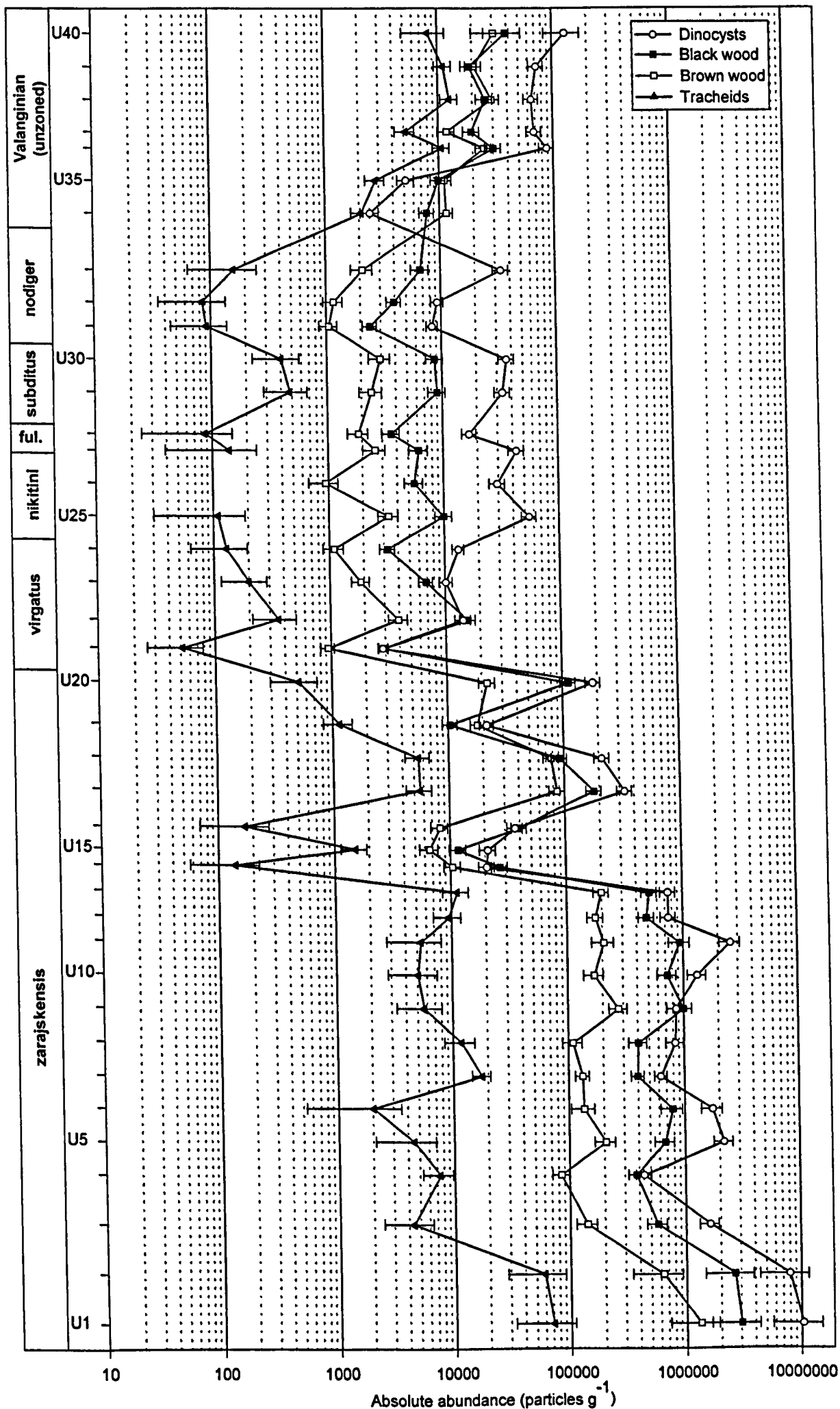
Absolute abundance data of the major structured components of the palynofacies are displayed in Table 5.4 and Figure 5.12. AOM cannot be considered in terms of absolute abundance. Whilst counts of AOM can be used to gauge its abundance relative to other types of palynological matter, it is important to recall that particles of AOM in a palynological slide do not relate to sedimentary grains in the same way as, for example, phytoclasts. In many cases AOM may form at the sediment surface (or within the sediment) as breakdown products of other sedimentary organic matter, and not be deposited *per se*. Furthermore AOM is known to disaggregate during processing of palynological residues. Therefore this component has not been examined in this study of absolute abundances.

The first striking aspect of the absolute abundance data (Figure 5.12) is that the trends and patterns observed across the sample suite are remarkably similar in the three main structured components. This is most particularly evident in the interval from samples U13 to U21, where similarities are accentuated by closely comparable abundance values of the three components, but is also notable from samples U22 to U33. Throughout the section dinoflagellate cysts can be seen to be the most abundant structured component, with black wood generally more abundant than brown wood. Since both marine and terrestrial particles are included within this plot (dinoflagellate cysts, brown & black wood & tracheids), such a phenomenon cannot simply be the result of proximal - distal relationships.

Sample	% error	total error (acriarchs)	Prasinophyte count	Absolute abundance	% error	total error	Microforam count	Absolute abundance	% error	total error	Others	Absolute abundance	% error	total error	Total marine particles	Absolute abundance	% error	total error	Total terrestrial particles	Absolute abundance	% error	total error	Lycopodium counted	Sample weight	No. of L. tablets added
U1	73.105	13036	3	17832	73.105	13036	2	11888	83.732	9954.2	51	303147.9	47	142417.905	1809	10752833.2	44.9	4828656.72	740	4398616.11	44.995	1979145.39	5	2.11	5
U2	73.105	9356	0	0	0	0	0	0	0	0	33	140777.6	48.1	67720.3296	1907	8135236.05	44.9	3652943.79	780	3327469.39	44.987	1496929.56	5	2.94	5
U3	73.105	1080	3	2216	60.844	1343.8	0	0	0	0	0	0	0	0	2208	1629425.91	18.7	304348.905	973	718690.577	18.831	135339.747	30	2.83	5
U4	33.468	1722.9	0	0	0	0	0	0	0	0	5	2339.925	47	1100.26568	959	448797.687	14.9	66784.9019	1013	474068.881	14.862	70456.8722	50	2.68	5
U5	73.105	1652	0	0	0	0	2	2260	73.105	1652	16	18078.56	31.1	5628.635	1961	2215753.33	18.7	414200.629	796	899408.288	18.892	169916.355	30	1.85	5
U6	102.12	1038.2	0	0	0	0	0	0	0	0	0	0	0	0	1722	1750755.84	20.8	364513.074	918	933329.767	20.942	195458.958	24	2.57	5
U7	0	0	0	0	0	0	3	939.6	59.036	554.71	85	26622.47	18.4	4370.49945	2089	654286.235	12.5	81888.8719	1691	529630.456	12.561	66525.2204	71	2.82	5
U8	101.47	670.89	2	1322	72.779	962.35	1	661.1	101.47	670.89	30	19834.48	25.1	4978.64983	1300	859493.938	17.4	149961.054	792	523630.153	17.588	92098.2915	35	2.71	5
U9	72.672	1178.7	0	0	0	0	1	810.9	101.4	822.27	12	9731.282	33.4	3248.87212	1074	870949.696	17	148469.047	1582	1282907.28	16.959	217566.662	37	2.09	5
U10	53.137	1803.1	0	0	0	0	1	848.3	101.6	861.96	6	5090.097	44.6	2270.76472	1568	1328515.42	17.2	241299.44	1065	903492.289	18.246	164847.555	32	2.31	5
U11	0	0	0	0	0	0	0	0	0	0	41	44329.48	25.6	11344.4902	2440	2638144.83	20.4	537502.487	1064	1150404.14	20.504	235877.908	25	2.32	5
U12	0	0	0	0	0	0	3	1420	59.534	845.3	46	21771.02	20.7	4506.14556	1834	773344.453	14.7	113955.411	1416	670168.755	14.787	98966.0819	50	2.65	5
U13	0	0	0	0	0	0	6	2818	43.332	1221.3	47	22077.68	20.6	4544.8822	1644	772248.989	14.7	113784.235	1539	722926.517	14.748	106618.755	50	2.67	5
U14	101.05	47.26	1	46.77	101.05	47.26	1	46.77	101.05	47.26	6	280.8165	43.3	121.597292	452	21139.7787	15.3	3227.78881	805	37649.3847	14.948	5627.72634	50	16.09	3
U15	59.534	118	3	198.2	59.534	118	1	68.07	101.05	66.762	26	1717.781	24.4	419.232593	354	23388.2423	15.5	3617.70598	291	19225.928	15.664	3011.64434	50	11.39	3
U16	101.05	57.739	0	0	0	0	0	0	0	0	11	628.5285	33.5	210.355534	652	37254.5968	15	5604.92325	846	48339.5535	14.928	7215.92223	50	13.17	3
U17	59.534	372.1	0	0	0	0	2	416.7	72.187	300.79	28	5833.488	23.8	1390.47038	1624	338342.326	14.7	49860.4268	1300	270840.532	14.789	40053.6811	50	6.02	5
U18	47.021	414.73	2	352.8	72.187	254.68	7	1235	40.492	499.99	9	1587.595	36.4	577.265592	1231	217147.707	14.8	32144.8723	992	174988.242	14.869	26019.3309	50	7.11	5
U19	0	0	0	0	0	0	0	0	0	0	3	215.5806	59.1	127.30582	306	21989.2208	13.7	3003.3524	407	29247.1008	13.358	3908.86182	70	7.48	3
U20	30.419	367.51	0	0	0	0	2	172.6	72.187	124.59	101	8716.115	17.6	1534.68483	2249	194084.573	14.7	28488.7153	1601	138163.362	14.74	20364.8394	50	8.72	3
U21	100.22	13.009	1	12.98	100.22	13.009	1	12.98	100.22	13.009	5	64.90643	45.2	29.337876	227	2946.75209	9.33	275.038317	303	3933.32988	8.7216	343.05017	312	9.29	3
U22	101.05	51.589	0	0	0	0	0	0	0	0	7	357.3704	40.5	144.705613	287	14652.1872	15.7	2297.42986	389	19859.5848	15.386	3055.53154	50	14.74	3
U23	0	0	0	0	0	0	0	0	0	0	5	168.6608	46.3	77.1133818	311	10366.2993	13.2	1363.61794	265	8833.02032	13.365	1180.5162	77	14.66	3
U24	71.506	46.063	0	0	0	0	0	0	0	0	3	96.62889	58.7	56.7268868	414	13334.7863	11.7	1561.97836	143	4605.97692	13.527	623.056061	98	11.92	3
U25	101.05	55.343	0	0	0	0	0	0	0	0	1	54.76856	101	55.3433839	1002	54878.0961	14.9	8158.0706	256	14020.7511	15.814	2217.20618	50	13.74	3
U26	72.187	79.769	0	0	0	0	0	0	0	0	3	165.7533	59.5	98.6802442	536	29614.5903	15.2	4488.04037	126	6961.63877	17.04	1186.29509	50	13.62	3
U27	43.332	181.66	3	209.6	59.534	124.79	0	0	0	0	3	209.6156	59.5	124.793401	628	43879.532	15.1	6610.18138	136	9502.57382	16.868	1602.92823	50	10.77	3
U28	37.785	130.82	8	346.2	37.785	130.82	0	0	0	0	0	0	0	0	410	17744.0304	14.2	2522.33137	129	5582.87785	15.975	891.860423	60	14.49	3
U29	52.067	141.45	2	135.8	72.187	98.055	0	0	0	0	5	339.5848	47	159.677547	501	34026.4007	15.2	5171.25387	178	12089.2202	16.346	1976.10456	50	11.08	3
U30	52.067	139.07	5	333.9	47.021	156.99	2	133.5	72.187	96.402	4	267.0878	52.1	139.065644	559	37325.5262	15.1	5647.15843	187	12486.3567	16.263	2030.68724	50	11.27	3
U31	58.604	40.051	3	68.34	58.604	40.051	0	0	0	0	0	0	0	0	372	8474.32432	11.3	958.700131	160	3644.87068	12.791	466.20475	111	14.86	3
U32	32.172	99.774	11	310.1	32.172	99.774	0	0	0	0	2	56.38628	71.6	40.3701919	353	9952.17821	12.4	1236.16811	187	5272.11707	13.395	708.209036	87	15.34	3
U33	47.021	123.55	1	52.55	101.05	53.102	4	210.2	52.067	109.45	0	0	0	0	645	33894.9302	15.1	5101.33886	187	9826.90223	16.263	1598.1578	50	14.32	3
U34	37.317	135.35	5	226.7	46.288	104.93	0	0	0	0	4	181.3476	51.4	93.223798	72	3264.2568	16.8	547.656248	448	20310.9312	12.842	2608.29437	76	10.92	3
U35	42.717	143.69	0	0	0	0	0	0	0	0	1	56.06115	101	56.5024925	99	5550.05364	16.1	893.336322	397	22256.2757	13.537	3012.90999	68	9.87	3
U36	52.067	147.44	2	141.6	72.187	102.21	0	0	0	0	1	70.7921	101	71.5350982	1248	88348.5381	14.8	13075.1339	880	62297.0461	14.912	9289.90268	50	10.63	3
U37	47.021	199.01	3	253.9	59.534	151.18	0	0	0	0	0	0	0	0	812	68734.1102	14.9	10271.7231	487	41223.5366	15.217	6272.83524	50	8.89	3
U38	59.534	178.02	2	199.3	72.187	143.9	0	0	0	0	0	0	0	0	655	65284.8477	15	9820.52702	593	59105.2132	15.098	8922.25481	50	7.55	3
U39	36.361	247.5	0	0	0	0	0	0	0	0	0	0	0	0	981	72680.5749	14.9	10814.9559	548	41445.3226	15.141	6275.3787	50	9.95	3
U40	105.46	455.95	1	432.3	105.46	455.95	0	0	0	0	0	0	0	0	299	129267.77	34	43942.8294	196	84737.4009	34.251	29023.5634	9	9.67	3

Table 5.4: Continued.

Figure 5.12: Major structured component absolute abundance (Gorodische)

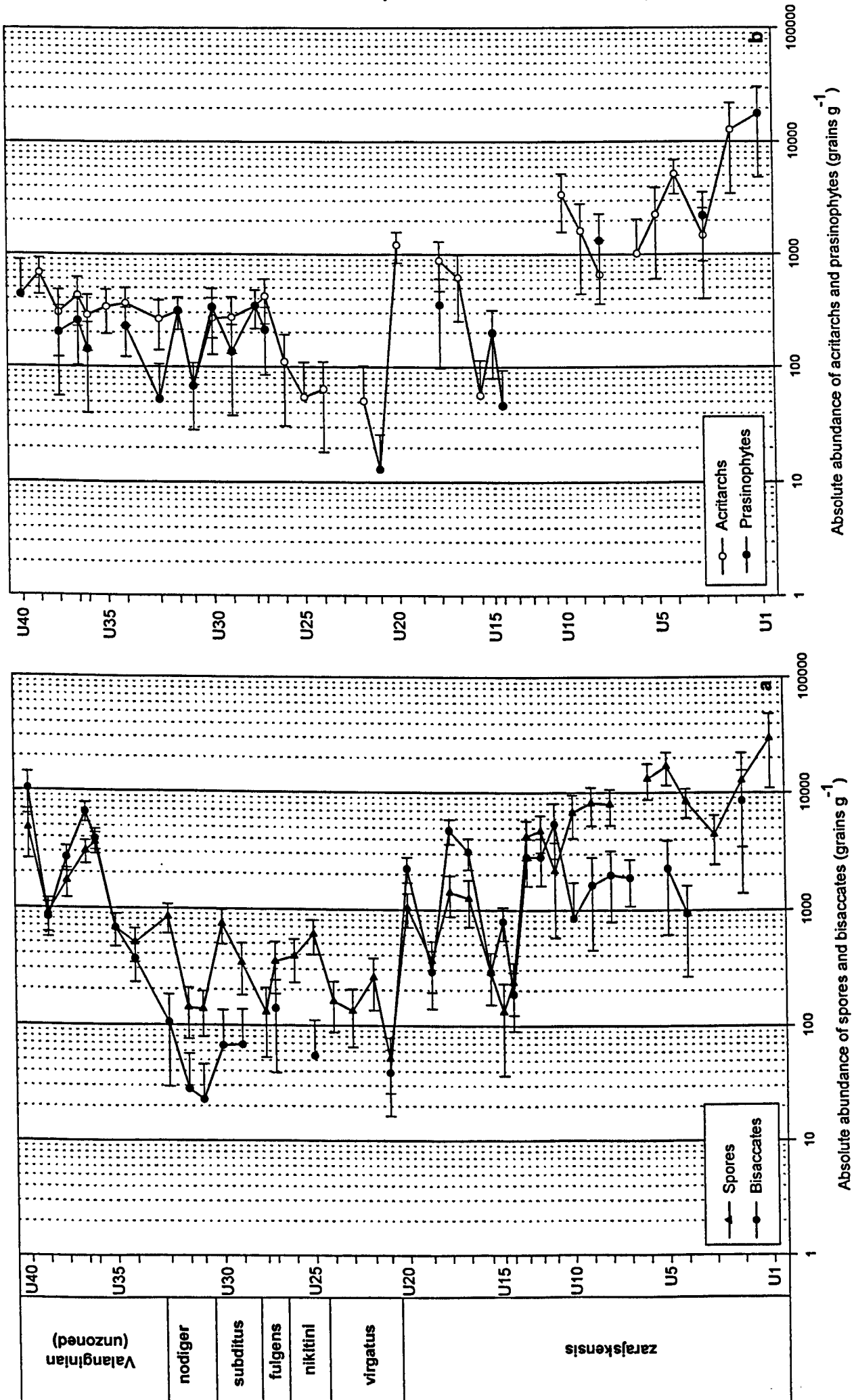


The absolute abundance of these components is highest in the lower part of the *zarajskensis* Subzone (samples U1-U13, Beds 1-7). Within this sample interval, reduced absolute abundance of black wood and (to a lesser extent) dinocysts in samples U4, U7 & U8 and U12 & U13, corresponds to the laminated siltstone horizons of beds 3, 5 and 7. These minima are weakly reflected in the brown wood absolute data, and correspond to peaks in the tracheid abundance. A pronounced drop in the absolute abundance of the major structured components is notable from samples U14 (Bed 8) to U16 (Bed 9), and again at the top of the lenticular siltstone in sample U19 (Bed 12). A significant drop in absolute abundance of these components occurs at sample U21 (conglomerate horizon, Bed 14), and the interval from this sample to U33 displays the lowest phytoclast absolute abundance values of the section. A further drop occurs in the dinocyst absolute abundance in samples U34 and U35, which coincides with a pronounced increase in the abundance of brown wood and tracheids. Brown wood absolute abundance is comparable with or exceeds black wood abundance in the interval from sample U34 to the top of the section.

Consideration of the minor component absolute abundance is more complicated than that of the main components partly because zero values cannot be plotted on logarithmic curves. 'Missing' data values in these plots (Figure 5.13) thus correspond to zero values. Moreover, the small number of specimens counted in each of these lesser categories renders a high degree of error on the absolute values. However, in general the trends seen in both sporomorph and marine palynomorph (acritarchs and prasinophytes) abundance strongly echoes the patterns seen in the major components. In addition, bisaccate pollen grains are most abundant in the interval from samples U15-U19, and in the mica-rich siltstones. Other pollen grains are extremely rare in these residues and have not been plotted.

The absolute abundance data has been subjected to minimum variance cluster analysis at two levels: once using only the three major components (dinocysts and brown & black wood) and again having added data on tracheids, bisaccate pollen and spores.

Figure 5.13: Minor structured component absolute abundance (Gorodische)



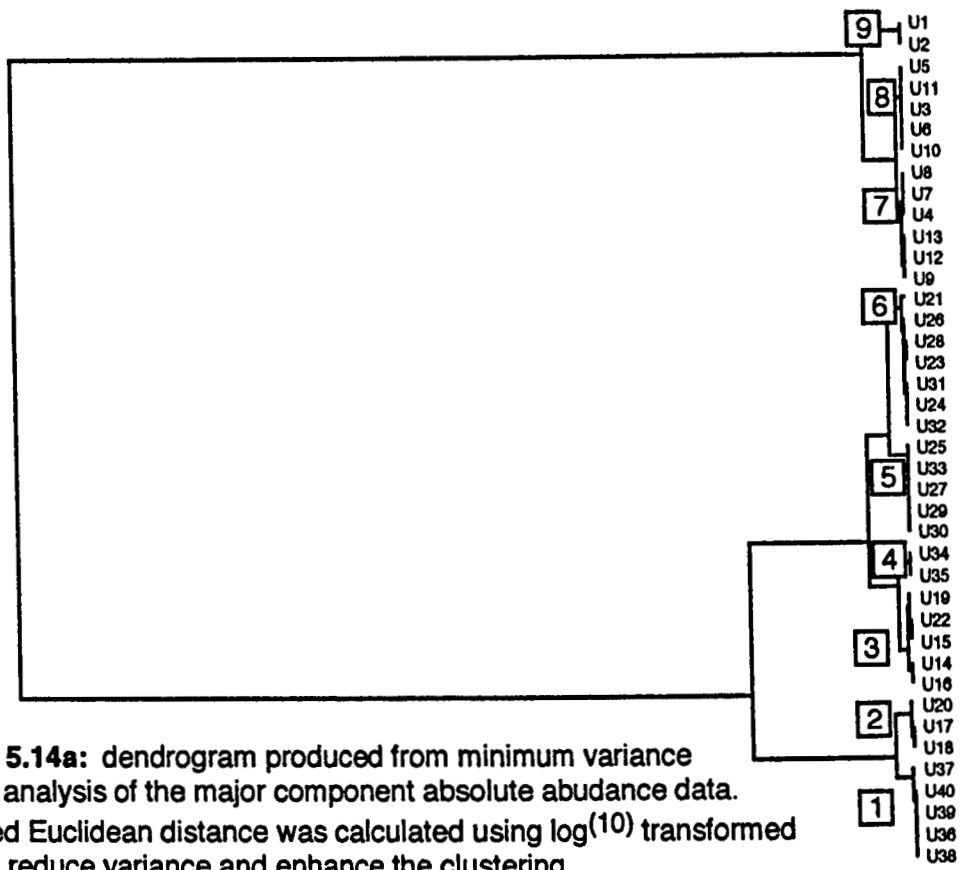


Figure 5.14a: dendrogram produced from minimum variance cluster analysis of the major component absolute abundance data. Squared Euclidean distance was calculated using $\log^{(10)}$ transformed data to reduce variance and enhance the clustering.

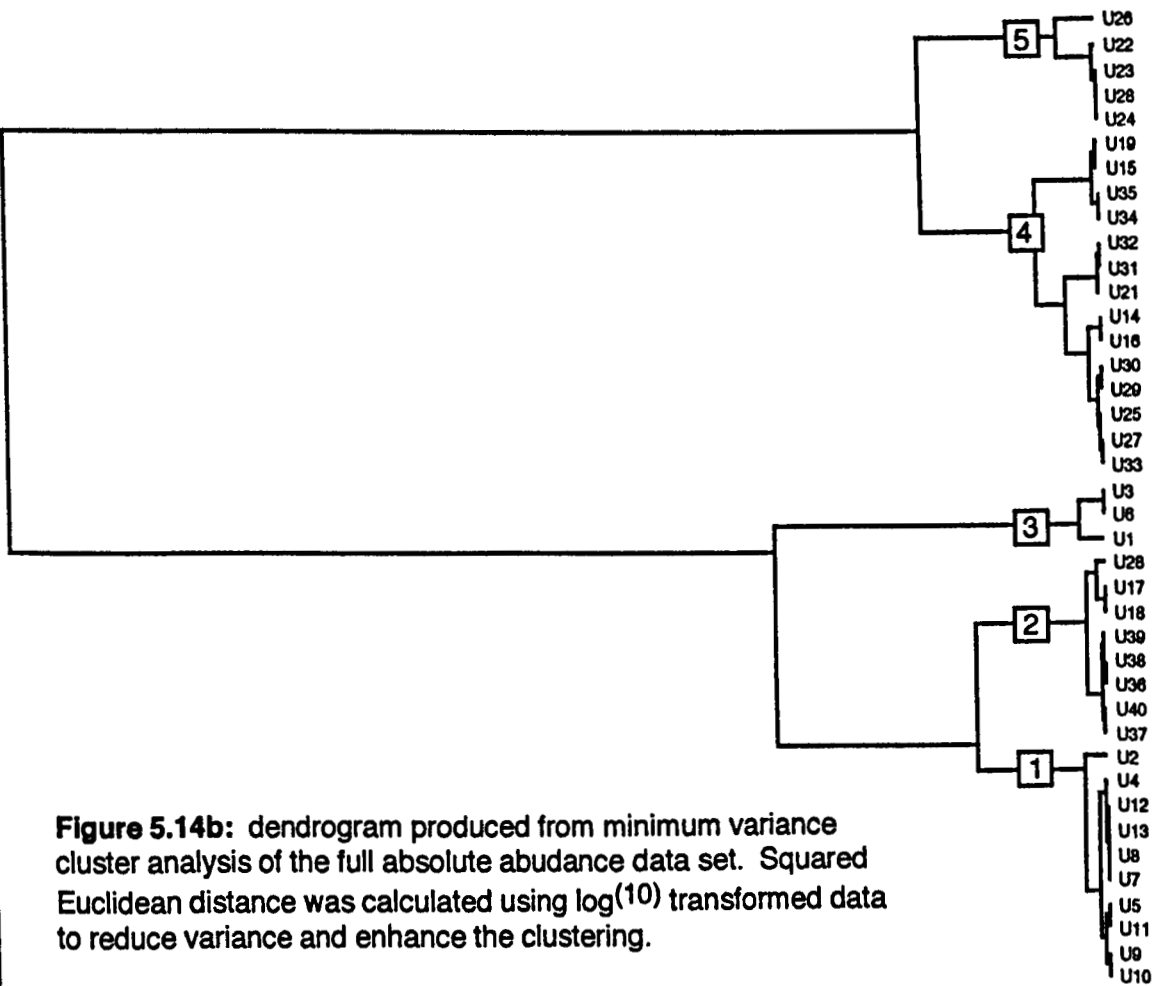


Figure 5.14b: dendrogram produced from minimum variance cluster analysis of the full absolute abundance data set. Squared Euclidean distance was calculated using $\log^{(10)}$ transformed data to reduce variance and enhance the clustering.

The resulting dendrograms are displayed in Figure 5.14. The first dendrogram (Fig. 5.14a) shows strong clustering of the data into lithologically-similar groups using only the three major structured components. Branch 1 is exclusively comprised of samples from the mica-rich siltstones. Samples U34 and U35, also from this lithology are clustered separately in Branch 4. Branches 2, 3, 5, and 6 contain the remainder of proximally deposited (neritic) sediments, including the coarse-grained deposits of the *virgatus* Zone, fine-grained sandstones of the *nikitini* to *nodiger* zones and the lenticular bedded siltstones from the upper part of the *zarajskensis* Subzone. Branch 7 is largely comprised of laminated siltstones from the *zarajskensis* Subzone, whilst branches 8 and 9 cluster the remaining mudstones from this subzone. Thus the main lithological groups are remarkably well separated using cluster analysis of the major structured component absolute abundance.

This clustering is much less well developed when minor components are included in the analysis (Fig 5.14b). Branch 1 combines both laminated siltstone and mudstone samples from the *zarajskensis* Subzone, with the remainder of samples from these deposits in branches 3 & 4. Branch 2 combines samples from the mica-rich siltstones with other sediments, with samples U34 & U35 included in Branch 4. Branches 4 & 5 mostly contain the coarse-grained deposits and fine sandstones of the *virgatus* to *nodiger* zone interval.

PhytOC ranking

The PhytOC and AmexOC parameters have been developed by Tyson (1989, 1993) as an alternative absolute measurement to the use of exotic spikes. Whilst they have been used successfully by the latter author in determination of North Sea palynofacies, their application to the Volga Basin material is problematic. AmexOC simply cannot be calculated for the present data set since identification of AOM provenance is equivocal without extensive examination under UV light. In addition, there are several problems

with this approach in relation to the data collection methods utilised here. These are outlined below:

1: The most significant problem is that the counting approach used here does not take account of particle size. For example a phytoclast 20 μm in diameter is given the same 'ranking' as a particle 100 μm in diameter despite the fact that the latter clearly has a larger volume/area and therefore will contribute a larger amount of organic carbon to the TOC value. Thus a proximal palynofacies with relatively large mean phytoclast size will have an artificially low PhytOC in comparison to a more distal palynofacies with small mean phytoclast size. This will have the effect of reducing variation between proximal and distal PhytOC values, and exaggerating the apparent dilution of organic matter by increased influx of siliciclastic material, particularly in coarse grained sediments.

2: Since the residues used in the present analyses have been sieved, the $\leq 20\mu\text{m}$ size fraction has here been lost. Tyson (1989) stated that such particles are volumetrically insignificant. Whilst this may be true for individual particles, in reality it is unclear what proportion of the total organic matter volume is represented by this size category, and thereby how accurate the remaining PhytOC values are.

3: The approach used by Tyson (1993) assumes dinoflagellate cysts and other particles are volumetrically equal, despite the fact that such marine palynomorphs are effectively hollow sacs. Whilst Tyson (1993) notes that such treatment will tend to exaggerate the AmexOC value, due to data closure it will also cause the PhytOC to be underestimated whether or not AmexOC is calculated. Such an effect on the PhytOC will be minimised as relative abundance of marine palynomorphs decreases, but is clearly a problem in most of the Volga Basin palynological matter assemblages.

4: It is important to consider the phytoclast counts with TOC values which have been calculated using carbonate-corrected data.

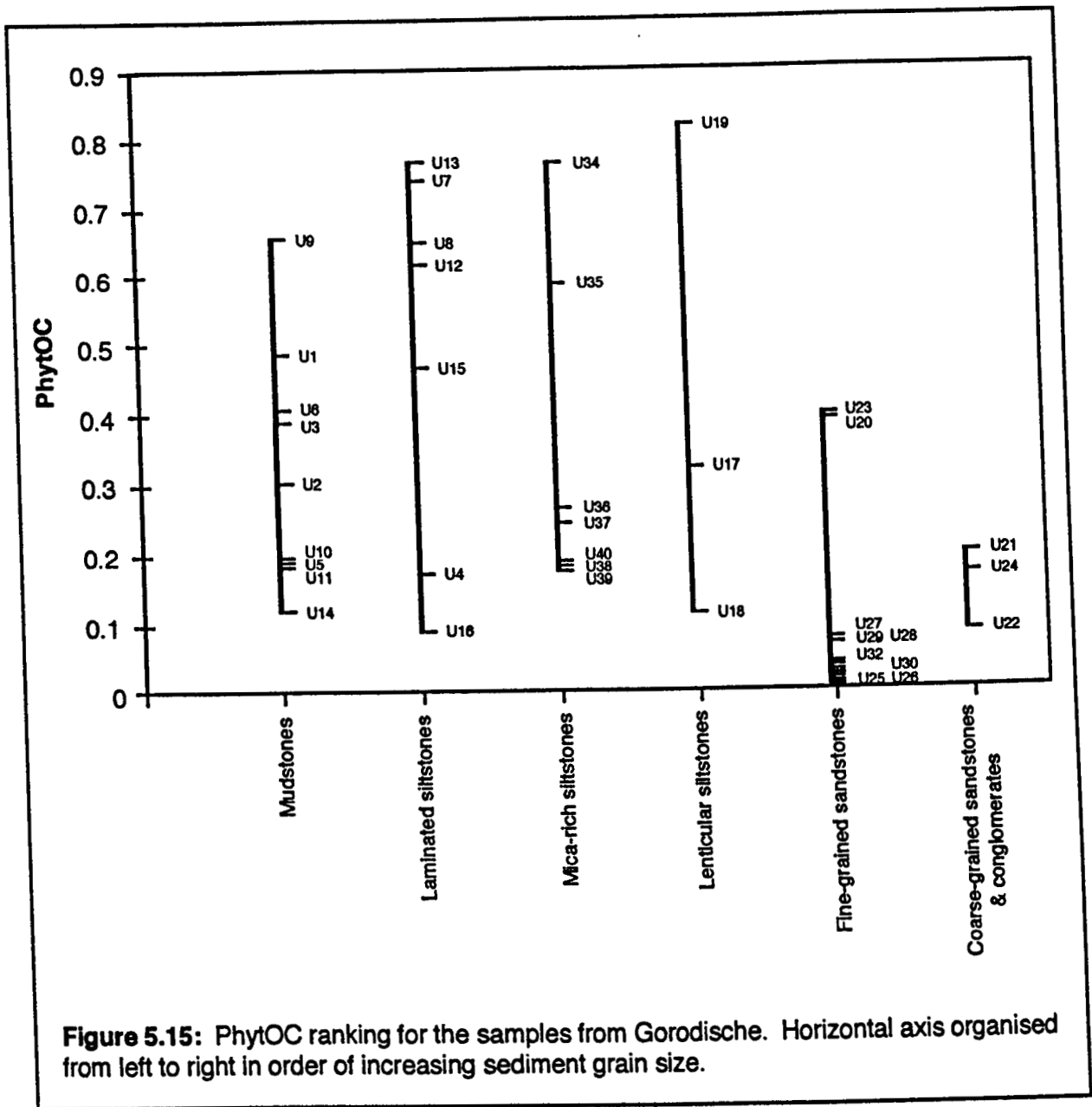


Figure 5.15: PhytOC ranking for the samples from Gorodische. Horizontal axis organised from left to right in order of increasing sediment grain size.

With these problems in mind it is clear that such parameters as PhytOC and AmexOC are mainly useful as comparative measures within sample suites, and that the 'absolute' values themselves must be treated with caution. Taking this into account, Figure 5.15 shows the PhytOC ranking of the 6 main lithological groups from the section at Gorodische. The groups have been arranged from left to right in order of increasing sediment grain size. It can be seen that the PhytOC values pick out few significant differences between the mudstone to siltstone groups despite the different environments in which they were deposited. It is unclear to what extent the factors of sediment dilution and particle size bias mask the data. However, both the fine sandstone and coarse sandstone/conglomerate groups to the right of the diagram show comparatively tightly clustered, low PhytOC values. This contrasts to more intuitive high PhytOC values expected for comparatively proximal sediments, and is undoubtedly strongly influenced by clastic sediment dilution in a similar manner to that described by Tyson (1989, 1993). It is interesting that the two conglomerate horizons have closely comparable PhytOC values despite the significant difference in bulk palynological matter assessments.

5.1.4. Interpretation of depositional environments for the Gorodische section based on palynofacies and sedimentological data

The alternation of organic-rich laminated siltstones and dark mudstones of the lower part of the zarajskensis Subzone at Gorodische is comparable to analogous sediments from the Eudoxus Zone of the Kimmeridge Clay Formation in Dorset described by Wignall (1991). Such sediments are intuitively associated with basinal facies, and Wignall (1991) interprets the Kimmeridge deposits as indicative of maximum coastal onlap. The distal nature of these sediments is supported by the palynofacies data on the following grounds:

- Both relative and absolute abundance of 'fresh' terrestrial components (brown wood, tracheids and sporomorphs) are low in comparison to black wood and dinoflagellate cysts. Brown wood and tracheid particles are usually darkened or heavily carbonised suggesting extended periods of transport and/or reworking from adjacent areas.
- Analysis of the phytoclast particle characteristics shows that mean long axis data in these samples is generally small, the standard deviation from mean is generally low (hence the assemblages are comparatively well sorted), and that the populations consist of well rounded particles. These aspects indicate a phytoclast assemblage that has undergone extensive particle abrasion, either by extended periods of transport or reworking.

The presence of the coarser-grained, organic-rich, laminated siltstones within a mudstone-dominated sequence suggests either short-lived periods of increased fluvial output into the basin, or phases of regression/uplift within the basin generated the source of this siliciclastic sediment. The association of laminated shales and abundant organic matter has also been noted in analogous sequences from the UK Lias by Ebukansson & Kinghorn (1985) and Waterhouse (1999). In the Volga Basin however, these units are associated with decreased absolute abundance of structured organic matter grains, presumably as a response to increased sedimentation rate and siliciclastic dilution. Variation in the input of organic matter to siliciclastic material is reflected in the wide spread of PhytOC values noted from these laminated sediments (Fig. 5.15).

High relative abundance of AOM is often taken as indicative of stagnant or stratified basins where dysoxic to anoxic conditions suitable for the preservation of this material prevail at the sediment/water interface (Dow & Pedersen, 1975; Venkatachala, 1981a; Bellet *et al.*, 1982). Such environmental interpretation for the lower part of the zarajskensis Subzone explains the abundance of AOM in the majority of these residues,

and the abundance of AOM in beds 5 & 7 suggests that the basin remained dysoxic throughout the phases of regression or uplift. Indeed, the data collected from the unsonified/unoxidised residues indicates that AOM production/preservation was increased during deposition of the laminated siltstones despite the presence of extensive horizontal bioturbation at these horizons. Thus the slightly increased burial rate may have actually enhanced AOM preservation at these levels.

The cause of such dysoxia cannot be identified using these palynofacies data. Hallam (1986b) suggested that increased fluvial output might lead to bottom-water anoxia by the development of a salinity stratified (and therefore non-mixing) water column. Waterhouse (1999) noted that any such change in fluvial output would be identifiable in the phytoclast assemblages, particularly in aspects of the size and shape of phytoclast grains. One might also expect to see a shift in the ratio of 'fresh' vs. degraded terrestrially-derived materials reflecting this change in the mechanism of transport. Such fluctuations are not apparent in the Volga Basin data, and therefore the development of a halocline cannot be supported for this particular sequence.

Numerous authors have commented on the condensed nature of the Volgian lectostratotype at Gorodische (Arkell, 1956; Ager, 1968; Casey, 1968; Hogg, 1994) which has been attributed to the tectonic stability of the Russian Platform (Arkell, 1956; Lord *et al.*, 1987; Hogg, 1994). The relatively high TOC values of the zarajskensis Subzone in comparison to the superceding sediments, combined with notably higher absolute abundance of structured particles despite apparently distal deposition is indeed indicative of an extremely low overall sedimentary rate. Moreover, the relative thickness of the zarajskensis Zone in comparison to overlying units suggests relatively continuous sedimentation albeit at a slow rate. This of course, is also consistent with a structurally stable basin.

The distal sediments from the lower part of the zarajskensis Subzone are abruptly capped by proximal lenticular bedded siltstones. Such transition can only be

explained by rapid regression/uplift and/or by the presence of a significant hiatus at the base of Bed 10. The onset of regression is however noticeable in the palynofacies data where 'trend lines' in the abundance of both brown and black wood increase relative to dinoflagellate cysts (%SM data, Figure 5.5), and where brown wood increases relative to black wood (%Phyt data, Figure 5.6). Moreover there is a profound drop in absolute abundance of structured materials in the interval from samples U14 to U16, and accompanying fall in the abundance of AOM and thereby TOC. Such changes are consistent with both an increase in the levels of bottom-water oxygenation as well as significantly increased (but still slow) rate of siliciclastic input. The abundance of AOM in sample U15 at the base of Bed 9 (Figure 5.1) and concomitant peak in TOC is suggestive of a brief return to anoxic conditions.

Lenticular bedding is known to occur in environments affected by alternating energy levels, and typically from intertidal zones. As such, wave generated ripples and other structures are preserved as sandy or silty lenses within more cohesive muddy sediment. It is difficult to characterise a 'typical palynofacies' for the lenticular bedded siltstones of beds 10 and 12 since the amount of silt versus mud in each sample was not quantified (samples were homogenised prior to maceration), although the three samples taken from this sedimentary facies are distinguishable in the ternary plots of Figures 5.9b & 5.10. There is a significant increase in the relative abundance of 'fresh' phytoclasts (brown wood and tracheids) relative to reworked black wood through this interval as well as slightly increased abundance of bisaccate pollen (Figure 5.5b). High relative abundance of AOM in these samples is possibly related to the development of algal mats across the sediment/water interface of the mudstone component rather than a return to anoxia (which is difficult to reconcile in a Jurassic intertidal environment). Peak TOC is established in sample U19 (Fig. 5.1a), correlated with a marked drop in the absolute abundance of structured palynologic matter (Fig. 5.12). This is difficult to explain simply by clastic sediment dilution, and may point to extensive algal mat growth upon the notably more mud-rich sediment of Bed 12. Despite an increased sedimentary rate by comparison with the underlying basinal deposits, a generally low rate of

siliciclastic influx is still indicated by the phosphorite and glauconite rich nature of these sediments, which is typical of sediment-starved basins. The absence of labile terrestrial materials such as leaf cuticle suggests either extremely low productivity or selective destruction of such tissues during extended reworking/oxidation/biodegradation at the sediment surface.

The final bed of the *zarajskensis* Subzone (Bed 13) is a fine-grained sandstone, presumably deposited below the intertidal zone as it lacks characteristic sedimentary structures. The reduced abundance of 'fresh' phytoclasts relative to black wood together with a slight decrease in the mean long axis data indicate more distal deposition/greater degree of reworking. Maintenance of high relative abundance of AOM and TOC together with a slight peak in the absolute abundance of structured materials suggests that conditions at the locus of deposition were suitable for the preservation of organic matter, and the abundance of phosphorite grains again indicates low input of siliciclastic sediment.

The coarse-grained sediments of the *virgatus* Zone overlie this fine sandstone deposit, the basal conglomerate horizon (Bed 14) having a scoured and clearly erosional base. Bed 14 is apparently normally graded, with large phosphorite clasts at the base and a rapid transition to coarse sandstone at the top. It is therefore likely to be the product of rapid deposition and waning energy conditions such as a debris flow or storm deposit, although it is not possible to identify the exact nature of this unit (or Bed 16) without comparison with the same bed at other localities. The low relative abundance of AOM and thereby low TOC, and low absolute abundances of the structured organic matter components support this genesis. The grain size of the sediment, the relatively increased mean long axis data and standard deviation (poor sorting) of the phytoclasts, together with a notable increase in woody phytoclasts relative to dinoflagellate cysts all point to the reworking of rather proximal sediments, and that the debris flow itself is likely to be proximal to its source. Bed 16 is similar to the conglomeratic part of Bed 14, again with a scoured and clearly erosional base. However the unit is clast-

supported, contains a much greater proportion of phosphorite clasts, and shows no evidence of grading. The palynofacies of this horizon are similar to that of Bed 14, although a higher TOC is noted, possibly as a result of the higher proportion of comparatively organic-rich phosphorite clasts. A similar origin for Bed 16 is therefore likely, although the greater mean brown wood long-axis size together with peak standard deviation of particle size (most poorly sorted assemblage), greater proportion of conglomerate clasts and the absence of grading point to relatively more proximal deposition. PhytOC values of samples U21, U22 and U24 are tightly clustered and comparatively low despite apparently proximal deposition (Figure 5.15), reflecting significant dilution of terrestrially-derived organic matter by siliciclastic material.

The fine-grained phosphoritic and glauconitic sandstones of the *nikitini* to *nodiger* zones (samples U25 to U32 plus U23) are indicative of proximal sediment-starved deposition. Hogg (1994) compared these to the Spilsby Sandstone and Sandringham Sands lithologies of Eastern England, which Ruffell & Rawson (1994) believe to be the result of low clastic input during arid low sea-level phases. Low absolute abundance of phytoclasts, low PhytOC, low input of sporomorphs and relative dominance of dinoflagellate cysts over these components indicate low input of terrestrial materials. In addition, analysis of the phytoclast characteristics reveals a well sorted, well rounded and generally small-sized assemblage in comparison to the *virgatus* Zone sediments, suggesting extended periods of particle abrasion. However, interpretation of these data is equivocal as such patterns could be generated either by more distal deposition, or by proximal deposition with low sediment input and corresponding extended organic matter residence times at the sediment/water interface. The latter is clearly more consistent with the sedimentological data. Extended sediment surface residence times effectively expose organic matter particles to additional reworking, and mechanical, chemical and biological degradation, particularly in well-oxygenated conditions. Thus the phytoclast assemblage is abraded, dominated by reworked black wood and carbonised brown wood, and any cuticle fragments are rapidly degraded so do not appear in the palynofacies. Similarly, the low absolute abundances of dinoflagellate

cysts, AOM, and therefore TOC through this interval is consistent with a low degree of preservation of these materials under the conditions described above. The shelly-hash horizons present in this interval are also consistent with low influx of siliciclastic sediment: they probably represent winnowed horizons and/or the accumulation of bivalve shells in the absence of other sediment. The drop in both absolute abundance of structured organic matter components and TOC in sample U28 reflects the greater weight-proportion of shelly debris.

The upper part of Bed 18 (samples U31 and U32) represents a return to intertidal conditions with lenticular bedding, although with significantly lower mud deposition than in Beds 10 and 12. This transition is gradual, with sample U32 being taken from a more densely lenticular interval than sample U31. A gradual palynofacies change throughout the nikitini to nodiger interval is also reflected in the relative abundance data, which show increasing importance of woody phytoclasts in comparison to dinoflagellate cysts. The absolute abundance of structured components drops markedly in the upper two samples of this interval, possibly suggesting increased sediment dilution in this more proximal environment, although no such change is notable in the TOC.

The phosphorite deposit (Bed 19) is difficult to separate from the underlying sandstones on palynological grounds, although the slightly elevated PhytOC and TOC levels (and AOM abundance) may reflect increased preservation of organic matter, perhaps by rapid phosphatisation. It seems likely that the sediment was deposited in shallow shelf starved of sediment as phosphorites are known to occur in these environments (Leeder, 1982), although the cause and mechanism of such pervasive phosphatisation are unclear.

Samples U33 and U34 are separated by the most significant hiatus/unconformity within the succession at Gorodische, spanning the entire Ryazanian interval (see Chapter 4). This is reflected in the abrupt change in both sedimentology and palynofacies. The Valanginian sediments of the sample interval U34 to U40 are grey micaceous siltstones with an abundance of secondary gypsum and jarosite. The palynofacies clearly suggests a shift to increased influx of terrestrial components. Particularly revealing are analyses of the phytoclast assemblages, which show significantly increased input of 'fresh' phytoclasts relative to black wood, comparatively large mean long-axis of brown and black wood, together with peak abundance in elongate components, high standard deviation (poorly sorted assemblage), and maximum angularity. Sporomorphs (particularly bisaccate pollen) reach maximum abundance in this part of the column, and absolute abundance of structured organic matter grains are higher in these sediments than in the underlying Volgian sandstones. Continued dominance of dinoflagellate cysts through this interval (apart from samples U34 and U35) suggests the maintenance of normal marine salinity, apart from samples U34 & U35, which indicate either much more restricted conditions (less marine influence) or poorer preservation potential of dinocysts. In this case, the presence of gypsum, and in particular jarosite, point to chemical weathering of pyrite within the sequence, and the subsequent removal of carbonate minerals. This is in part supported by the absence of body fossils, and by the identification of framboidal (sedimentary) pyrite in some of the unoxidised residues from these deposits. The quantity of sulphate minerals in the sequence suggests similarly abundant pyrite, which may have been generated from biological degradation of the copious plant matter encountered in these sediments. The different character of the mica-rich siltstones is such that they can be readily separated from other palynofacies using ternary plots such as those of Figs. 5.2, 5.9b & 5.10.

5.2. Kashpir palynofacies investigation

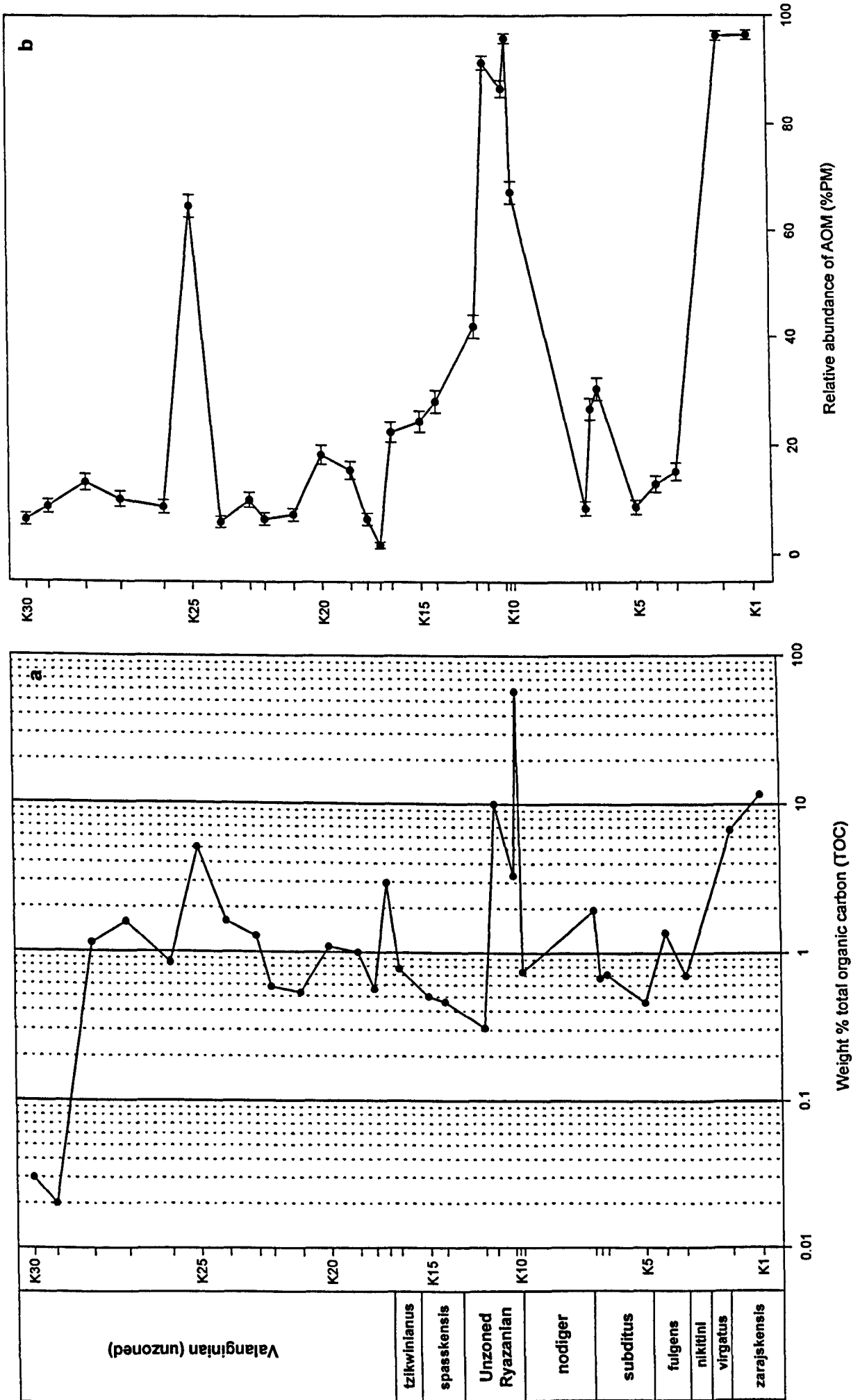
5.2.1. Total organic carbon content (TOC)

The raw TOC data for Kashpir can be found in Appendix E, and carbonate-corrected TOC values are additionally presented in Table 5.5 and in Figure 5.16a. Both samples from the *zarajskensis* Subzone have high TOC (7-10wt%) in comparison to the samples from the *fulgens* and *nodiger* zones, which have between 0.5-2wt% TOC. The bituminous shale horizon (Bed 18, sample K10) has peak TOC, at 58wt%, and the two samples taken from the laminated sandstone of Bed 19 (K11 and K12) are also comparatively organic rich at approximately 3wt% and 10wt% TOC. The remainder of the samples taken from Ryazanian deposits are organic poor (0.3 - 0.7wt%). Samples from the mica-rich siltstones are variable in terms of TOC, although they generally contain between 0.5 and 2wt%. The uppermost two samples from the section have extremely low organic carbon content. In a similar manner to the data collected from Gorodische, there is a strong correlation between relative abundance of AOM and TOC content. Thus the high TOC in both samples from the *zarajskensis* Subzone, in the sample interval K10 - K12, and the peak at sample K25 are all correlated with similar peaks in the relative abundance of AOM (Figure 5.16a & 5.16b). A small peak in TOC corresponds to the basal Ryazanian sandstone with phosphatic concretions (Bed 24, sample K17). This is not generated by increased abundance of AOM, and must therefore be due either to increased input or to increased preservation of the structured components.

5.2.2. Bulk palynological matter: A-P-D plots

Proportions of the three main components of the palynological matter assemblages at Kashpir are presented in Figure 5.17a and in Table 5.5. The sample points largely fall in the lower quarter of the ternary plot emphasising the dominance of AOM and dinoflagellate cysts in these residues. However several samples (K17, K28 - K30) are clustered at the phytoclast apex suggesting either drastically increased input,

Figure 5.16: TOC and AOM at Kashpir



Sample	Sample position (cm)	TOC	Brown wood count	% brown wood	Standard error of %	Tracheid count	% tracheids	Standard error of %	Black wood count	% black wood	Standard error of %	Total phytoclasts	% Phytoclasts	Standard error of %	Dinocyst count	% dinocysts	Standard error of %	AOM count	% AOM	Standard error of %	Total count	PhyOC
K1	13.5	11.70	3	0.6	0.35	0	0	0	11	2.2	0.66	14	2.8	0.74	4	0.8	0.4	482	96.4	0.83	500	0.328
K2	66	6.70	5	0.99	0.44	1	0.2	0.2	7	1.39	0.52	13	2.57	0.7	6	1.19	0.48	486	96.2	0.85	505	0.172
K3	145	0.70	5	0.99	0.44	1	0.2	0.2	25	4.96	0.97	31	6.15	1.07	396	78.6	1.83	77	15.3	1.6	504	0.043
K4	180	1.37	13	2.59	0.71	1	0.2	0.2	42	8.38	1.24	56	11.2	1.41	380	75.8	1.91	65	13	1.5	501	0.153
K5	215	0.46	25	4.99	0.97	0	0	0	77	15.4	1.61	102	20.4	1.8	355	70.9	2.03	44	8.78	1.26	501	0.094
K6	280	0.71	3	0.6	0.35	0	0	0	6	1.2	0.49	9	1.8	0.59	339	67.8	2.09	152	30.4	2.06	500	0.013
K7	292	0.67	2	0.4	0.28	0	0	0	13	2.59	0.71	15	2.99	0.76	352	70.3	2.04	134	26.7	1.98	501	0.02
K8	302	1.94	4	0.8	0.4	1	0.2	0.2	8	1.6	0.56	13	2.6	0.71	444	88.8	1.41	43	8.6	1.25	500	0.05
K9	425	0.74	8	1.59	0.56	3	0.6	0.34	13	2.58	0.71	24	4.77	0.95	141	28	2	338	67.2	2.09	503	0.035
K10	432	58.09	15	2.96	0.75	0	0	0	3	0.59	0.34	18	3.55	0.82	3	0.59	0.34	486	95.9	0.88	507	2.062
K11	439	3.34	14	2.8	0.74	5	1	0.44	13	2.6	0.71	32	6.4	1.09	35	7	1.14	433	86.6	1.52	500	0.214
K12	470	10.01	17	3.4	0.81	0	0	0	4	0.8	0.4	21	4.2	0.9	22	4.4	0.92	457	91.4	1.25	500	0.42
K13	490	0.31	32	6.4	1.09	3	0.6	0.35	54	10.8	1.39	89	17.8	1.71	201	40.2	2.19	210	42	2.21	500	0.055
K14	557	0.46	29	5.79	1.04	4	0.8	0.4	28	5.59	1.03	61	12.2	1.46	299	59.7	2.19	141	28.1	2.01	501	0.056
K15	585	0.5	36	7.17	1.15	5	1	0.44	29	5.78	1.04	70	13.9	1.55	309	61.6	2.17	123	24.5	1.92	502	0.07
K16	635	0.77	23	4.55	0.93	2	0.4	0.28	4	0.79	0.39	29	5.74	1.04	362	71.7	2	114	22.6	1.86	505	0.044
K17	655	2.96	37	7.37	1.17	378	75.3	1.92	3	0.6	0.34	418	83.3	1.67	75	14.9	1.59	9	1.79	0.59	502	2.465
K18	677	0.56	10	2	0.62	1	0.2	0.2	3	0.6	0.34	14	2.79	0.74	454	90.6	1.3	33	6.59	1.11	501	0.016
K19	705	1	15	2.99	0.76	2	0.4	0.28	17	3.39	0.81	34	6.79	1.12	389	77.6	1.86	78	15.6	1.62	501	0.068
K20	755	1.09	14	2.8	0.74	1	0.2	0.2	23	4.6	0.94	38	7.6	1.19	370	74	1.96	92	18.4	1.73	500	0.083
K21	805	0.53	11	2.2	0.66	3	0.6	0.35	25	5	0.97	39	7.8	1.2	424	84.8	1.61	37	7.4	1.17	500	0.041
K22	855	0.58	10	1.99	0.62	1	0.2	0.2	26	5.18	0.99	37	7.37	1.17	432	86.1	1.55	33	6.57	1.11	502	0.043
K23	880	1.29	16	3.17	0.78	4	0.79	0.39	33	6.53	1.1	53	10.5	1.36	401	79.4	1.8	51	10.1	1.34	505	0.135
K24	930	1.62	10	2	0.63	3	0.6	0.35	16	3.2	0.79	29	5.8	1.05	441	88.2	1.44	30	6	1.06	500	0.094
K25	980	5.04	5	0.97	0.43	0	0	0	24	4.66	0.93	29	5.63	1.02	153	29.7	2.01	333	64.7	2.11	515	0.284
K26	1030	0.84	16	3.2	0.79	3	0.6	0.35	15	3	0.76	34	6.8	1.13	422	84.4	1.62	44	8.8	1.27	500	0.057
K27	1105	1.58	9	1.8	0.59	2	0.4	0.28	9	1.8	0.59	20	4	0.88	429	85.8	1.56	51	10.2	1.35	500	0.063
K28	1165	1.14	73	14.6	1.58	22	4.4	0.92	311	62.2	2.17	406	81.2	1.75	28	5.6	1.03	66	13.2	1.51	500	0.926
K29	1230	0.02	81	16.2	1.65	31	6.2	1.08	327	65.4	2.13	439	87.8	1.46	17	3.4	0.81	44	8.8	1.27	500	0.018
K30	1270	0.03	80	16	1.64	36	7.19	1.15	335	66.9	2.1	451	90	1.34	18	3.59	0.83	32	6.39	1.09	501	0.027

Table 5.5: Relative abundance of palynologic matter components from the unsonified/unoxidised residues. Kashpir section.

PAGE
NUMBERING
AS ORIGINAL

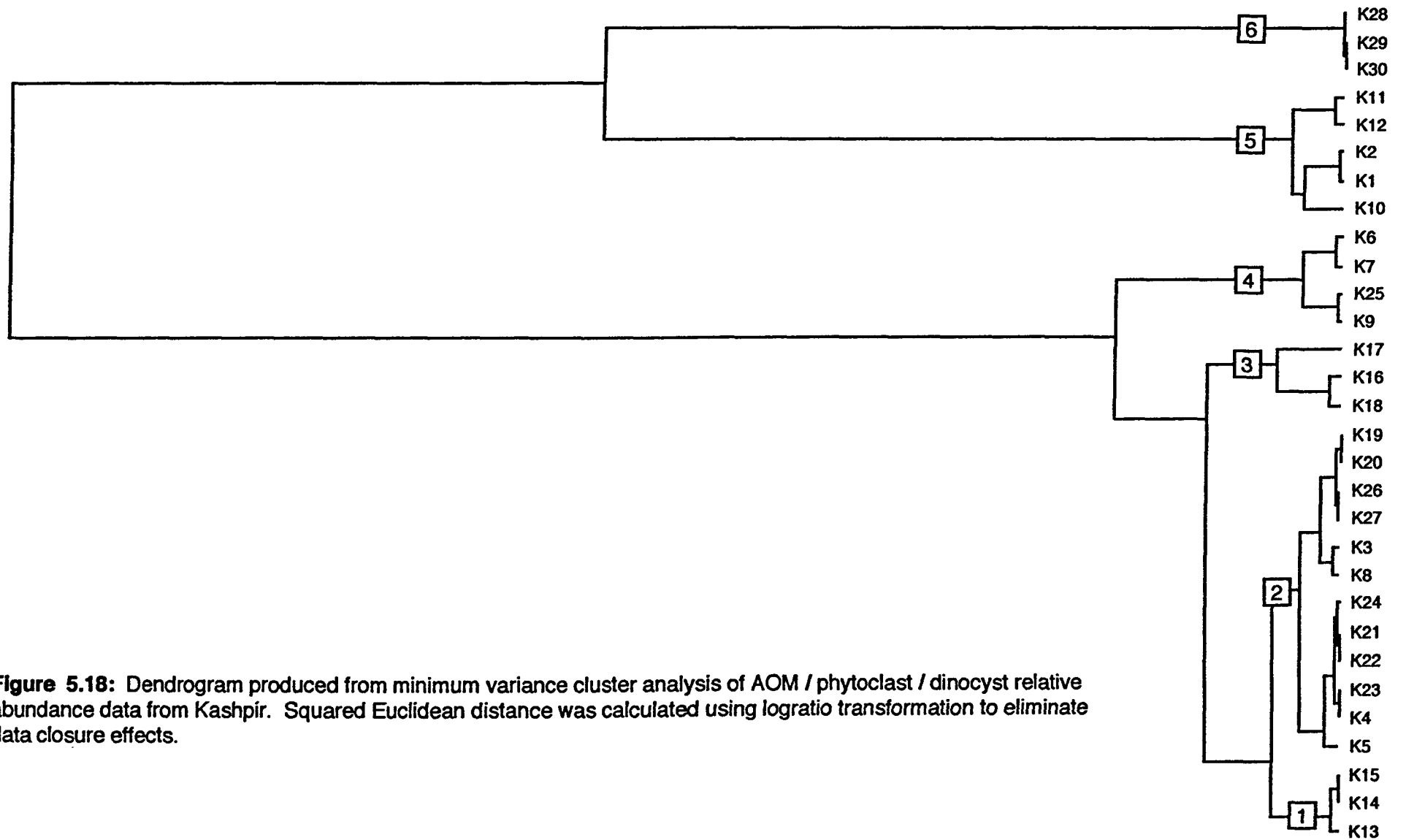


Figure 5.18: Dendrogram produced from minimum variance cluster analysis of AOM / phytoclast / dinocyst relative abundance data from Kashpir. Squared Euclidean distance was calculated using logratio transformation to eliminate data closure effects.

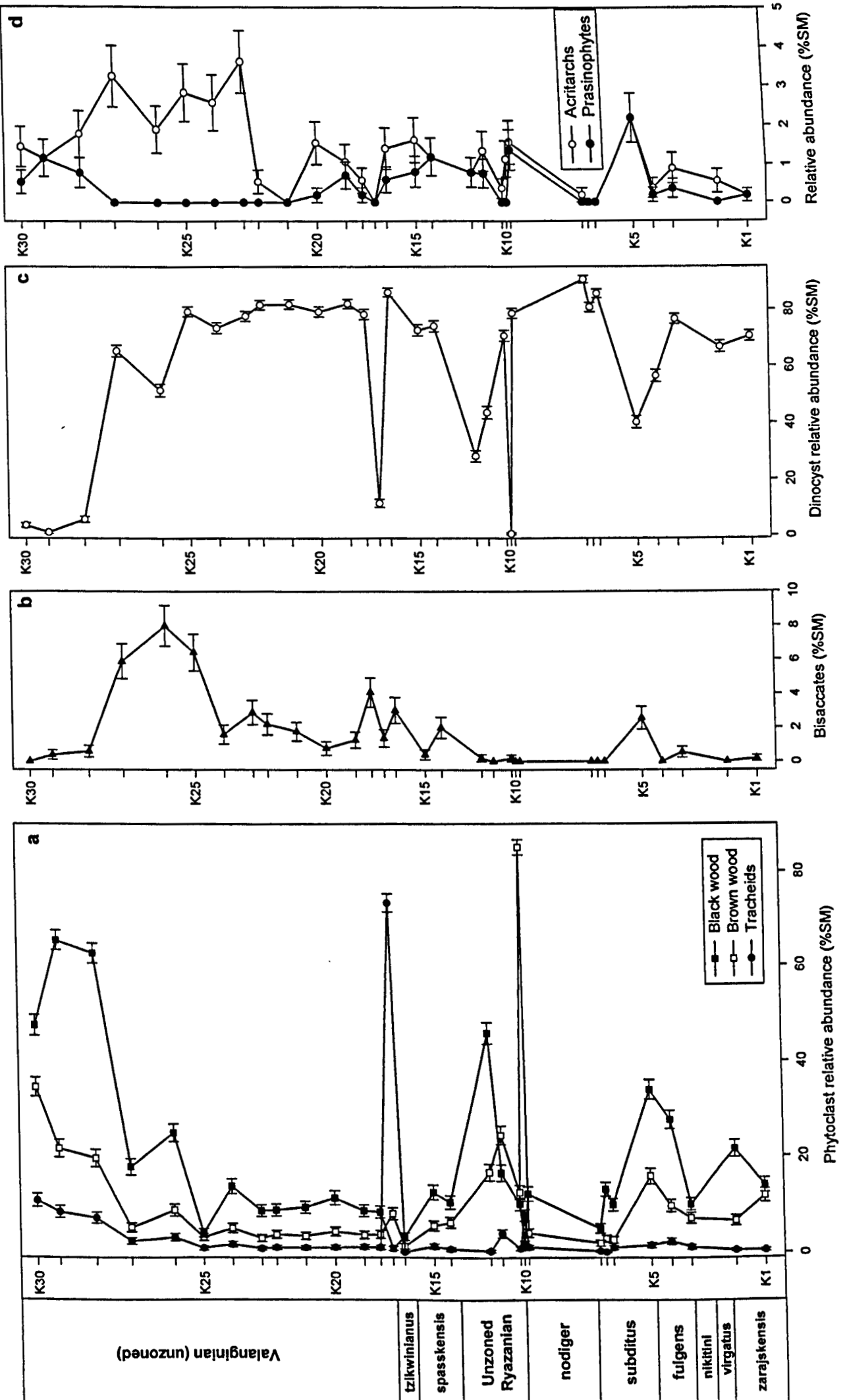
5.2.3. Analysis of the structured components

5.2.3.1. Relative abundance data (%SM)

Data on relative abundance of structured components (%SM) in the palynological matter assemblages from Kashpir are presented in Table 5.6 and in Figure 5.19. Figure 5.19 clearly shows that dinoflagellate cysts are by far the most abundant element of the structured components, with brown and black wood also generally important, and dominant in some assemblages. The number of hiatuses through this section in relation to the sampling interval used prevent any trend-lines from being drawn on these curves below the mica-rich siltstones.

In the two assemblages from the *zarajskensis* Subzone dinocysts comprise between 65 and 70% of the structured components, and black wood is dominant over brown wood, significantly so in sample K2. Relative abundance of these elements is somewhat variable in the lenticular sandstones of Beds 11 & 13. Due to the nature of this lithology it is difficult to interpret whether such variation corresponds to true changes in ecological conditions or is the result of inconsistent proportions of lens to host sediment in the samples (samples were homogenised prior to maceration). However samples K4 and K5 (particularly the latter) show considerably lower dinoflagellate cyst relative abundance than the other two samples from this lithology, with correspondingly higher abundance of both brown and black wood components. The %SM abundance of dinoflagellate cysts is comparatively high (79 - 91%) between samples K6 and K9, and remarkably consistent considering the variation in lithology. The greatest abundance of this component within the assemblages from Kashpir is in sample K8, which shows a concomitant drop in the relative abundance of black wood in comparison to adjacent samples. Sample K10, taken from the bituminous shale horizon, has peak relative abundance of brown wood and concomitant minimum in the %SM abundance of dinoflagellate cysts. Brown wood relative abundance exceeds that of black wood in samples K10 - K12, and remains comparatively high in sample K13, despite the notable peak in black wood abundance in this sample.

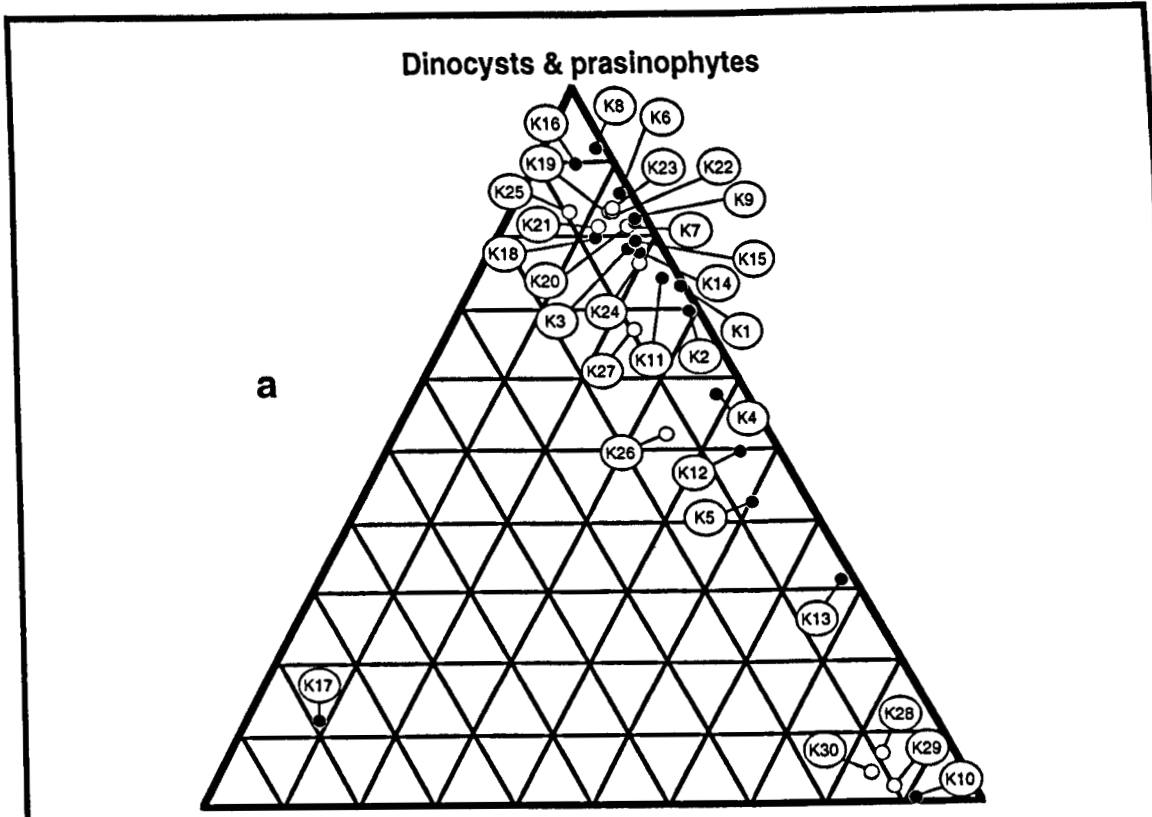
Figure 5.19: Relative abundance of structured palynological matter (%SM) from Kashpir



The two samples from the spasskensis Zone (Bed 23a, samples K14 & K15) have closely comparable palynofacies, with 72-74%SM dinoflagellate cysts and a dominance of black wood (10 - 12%SM) over brown wood (6-7%SM). Sample K16, taken from Bed 23b is of identical sedimentary nature to 23a but without the abundance of the shelly component. Nevertheless, the relative abundance of dinoflagellate cysts is notably higher in this sample than in the preceding two (at 86%SM), with both brown and most notably black wood abundance being lower. Sample K17 taken from Bed 24 with phosphate concretions shows an enormous comparative increase in the relative abundance of tracheids from a general abundance of 1 or 2 %SM in most of the samples to 75%SM, and a minor increase in the relative abundance of brown wood. The relative abundance of dinoflagellate cysts in this sample is reduced accordingly.

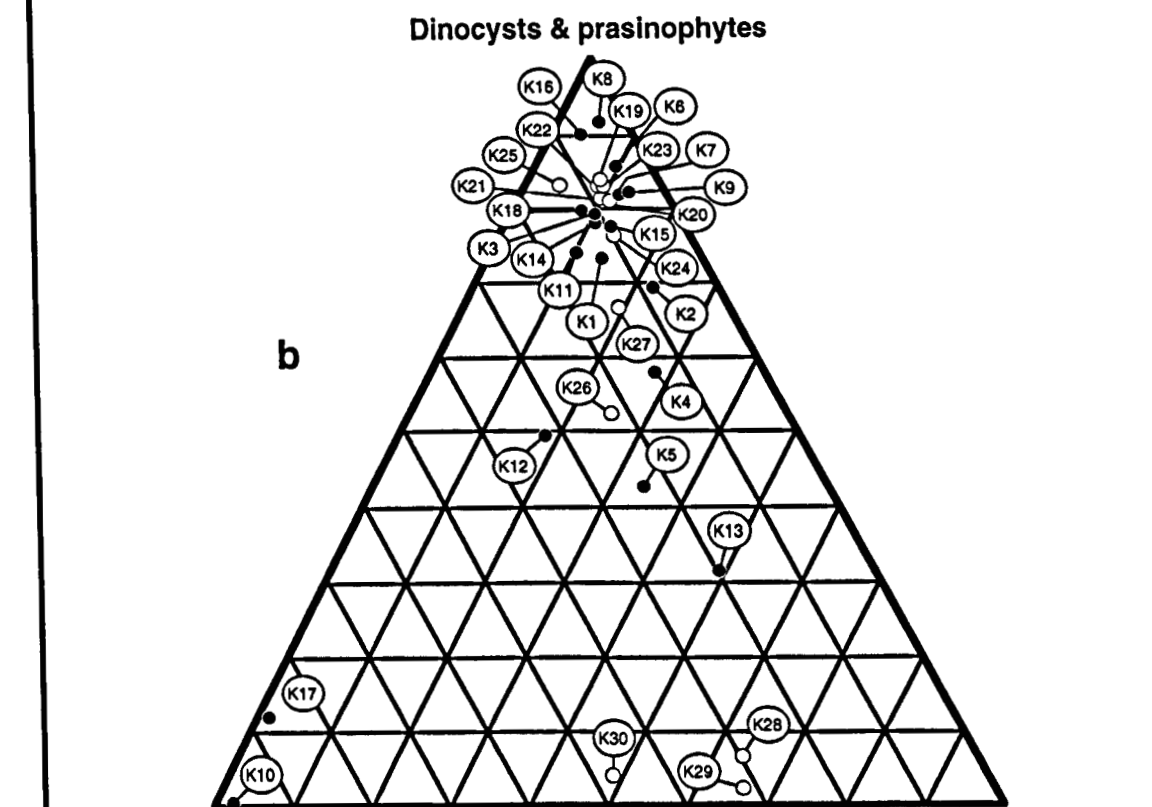
The palynofacies of the mica-rich siltstones (Beds 27 - 30) is remarkably consistent from samples K19 to K24, and comparable to that of the flaser bedded sandstone of Bed 26 (sample K18). Through this interval the relative abundance of dinoflagellate cysts is stable at approximately 80%SM; this stability is also reflected in the woody phytoclast components. In the uppermost part of this sample interval (K26-K30) there is a marked increase in the relative abundance of all three woody phytoclast components, and corresponding decrease in the abundance of dinoflagellate cysts. This trend is interrupted in sample K25 by a marked low point in the relative abundance of black wood, although the other woody phytoclasts are not significantly affected. A similar reduction in this component is seen in sample K30. Here the reduction is only significantly reflected in a rapid increase in the abundance of brown wood, although black wood still remains more important in this assemblage than in any sample prior to K28.

The relative abundance (%SM) data for the major components has been plotted on Ternary diagrams in Figure 5.20. Brown wood is combined with black wood in 5.20a and with tracheids & sporomorphs in 5.20b. The diagrams show that little differentiation of each lithology is possible on the basis of such palynofacies data. The majority of



Tracheids & sporomorphs

Brown & black wood



Tracheids + brown wood + sporomorphs

Black wood

Figure 5.20: Ternary plots of marine vs 'fresh' and oxidised terrestrial components from Kashpir. **a:** Brown & black wood combined. **b:** Brown wood & tracheids combined. Samples from mica-rich siltstones are shown by open circles.

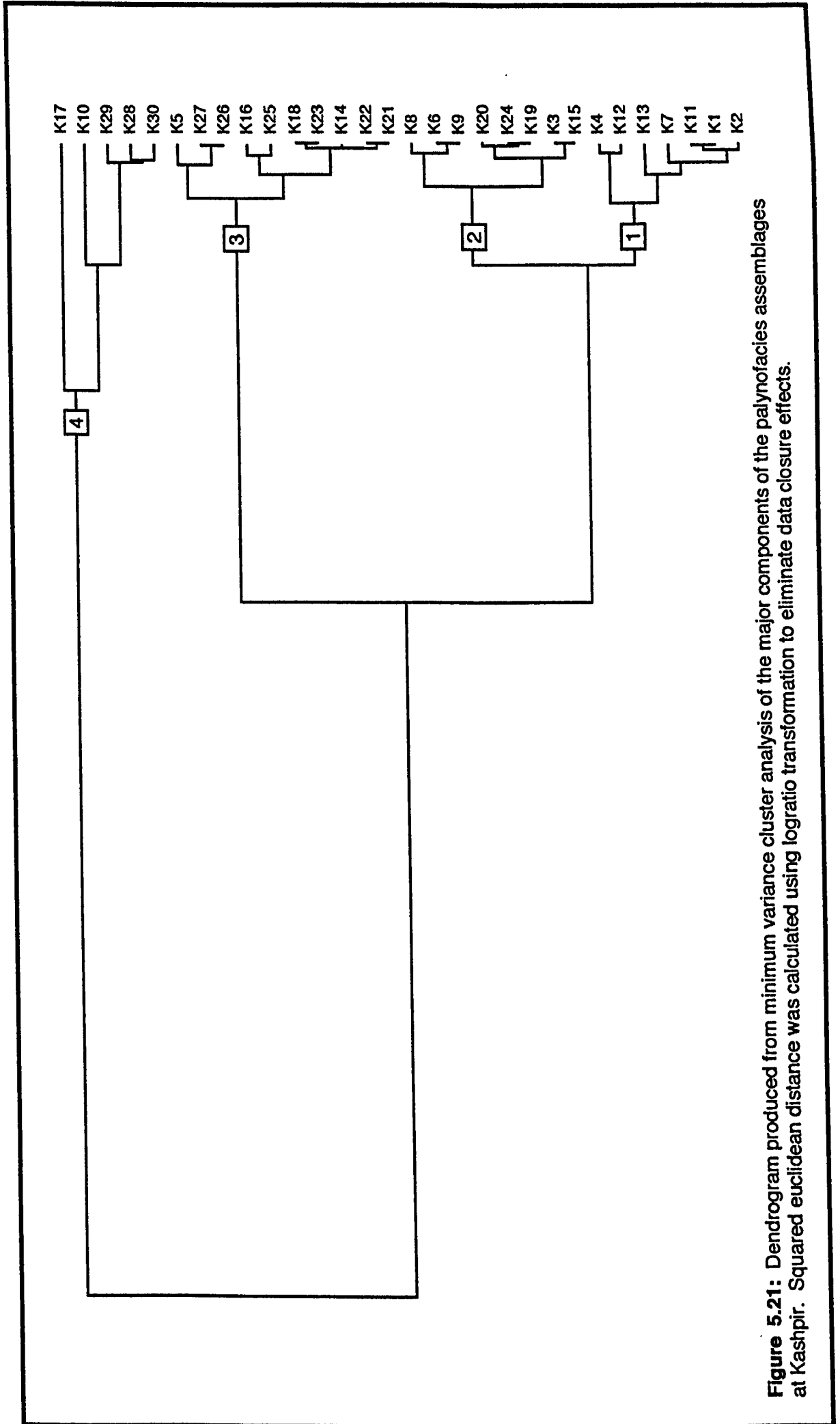


Figure 5.21: Dendrogram produced from minimum variance cluster analysis of the major components of the palynofacies assemblages at Kashpir. Squared euclidean distance was calculated using logratio transformation to eliminate data closure effects.

samples fall within the cluster at the dinoflagellate & prasinophyte apex, with outlying samples from various lithologies scattered over the remainder of the diagram.

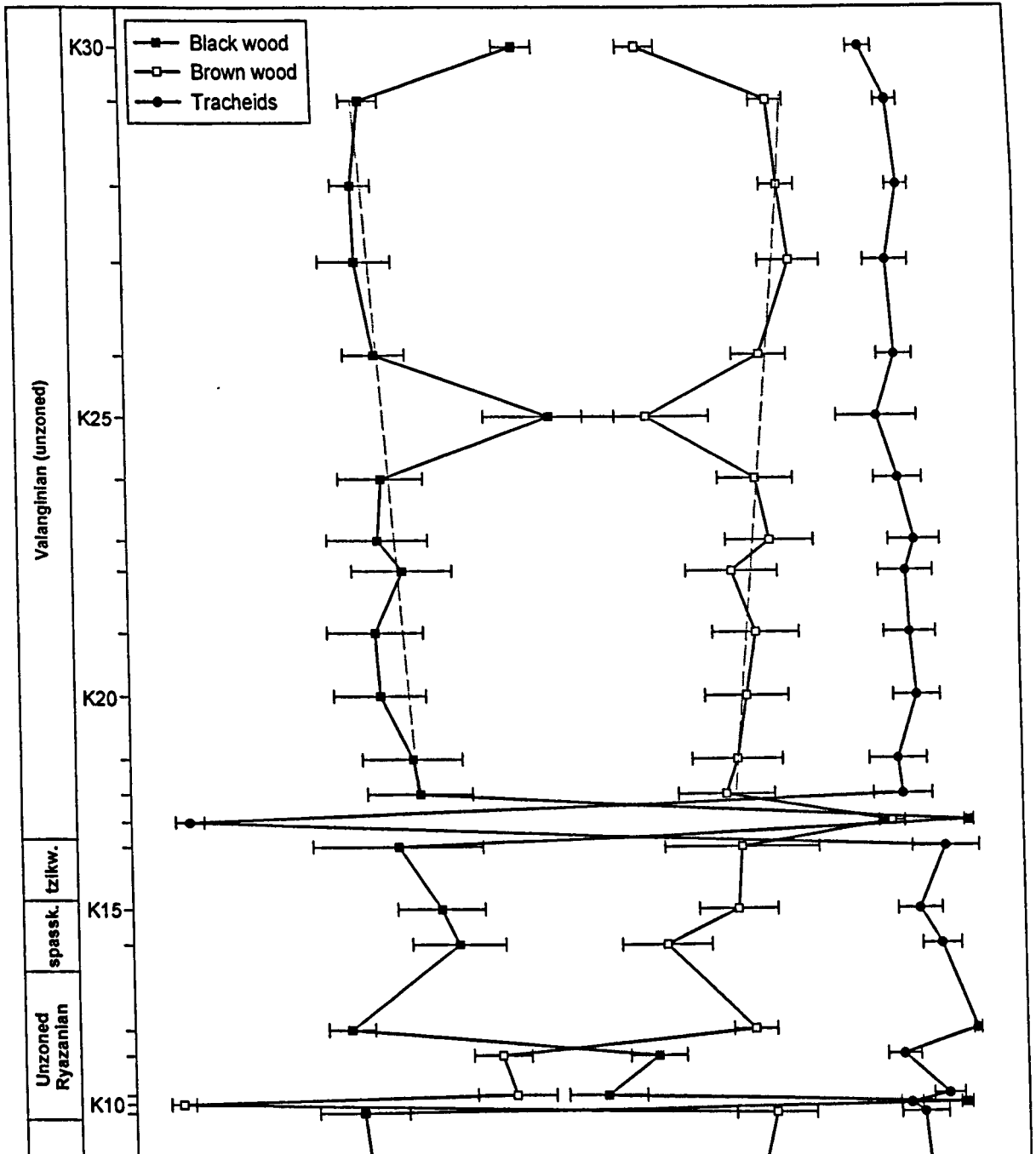
Minimum variance cluster analysis is similarly ineffective in distinguishing the various lithologies on the basis of these palynofacies data (Figure 5.21). Generally organic- and dinoflagellate-rich samples are clustered in Branch 1, including both samples from the zarajskensis Subzone. Dinoflagellate-poor samples are similarly grouped in Branch 4. Branches 2 & 3 group the remaining samples, with no apparent clustering according to lithology.

5.2.3.2. Detailed analyses of the phytoclast assemblages (%Phyt)

Relative abundance of the phytoclast components is displayed in Figure 5.22. Cuticle fragment abundance is not displayed as this component is extremely rare in the Volga Basin palynofacies investigated. The two samples from the zarajskensis Subzone show consistent relative proportions of tracheids at between 2 - 5%Phyt, whereas there is significant difference between the two samples in terms of black & brown wood %Phyt. The laminated siltstone (sample K1) has approximately 44% brown wood in the phytoclast assemblage and 53%Phyt black wood, whereas sample K2 has only 22%Phyt brown wood and 76%Phyt black wood.

The lenticular siltstones are again variable in terms of phytoclast proportions, but generally reflect a decrease in brown wood relative abundance from 39%Phyt in sample K3 to 18%Phyt in K6, with a concomitant increase in black wood. This trend is continued into the sandstone of sample K7. Tracheid abundance is comparatively stable through this interval and slightly higher than that in the zarajskensis Subzone, although the relative abundance of this component is significantly lower in sample K7 than in the underlying sediments. Samples K8 & K9 have similar phytoclast assemblage composition despite the difference in lithology between the two, with 66 - 69%Phyt

Figure 5.22: Relative abundance within the phytoclast group (%Phyt) at Kashpir



black wood, 25 - 28%Phyt brown wood and 5 - 7%Phyt tracheids. As indicated in the %SM data, there is a significant change in the phytoclast assemblage in the interval from sample K10 - K12, where brown wood becomes dominant over black wood, particularly so in sample K10 where brown wood reaches 88% of the phytoclast assemblage. This trend is rapidly reversed in sample K13 where black wood returns to 69% of the phytoclast assemblage, and remains at between 57 and 65% up to and including sample K16.

In sample K17 (sandstone with phosphatic concretions) tracheid abundance reaches 89%Phyt, with corresponding reduction in the abundance of the other woody phytoclast components. In the mica-rich siltstones, the composition of the phytoclast assemblage is for the most part remarkably consistent. Trend-lines drawn on the black and brown wood curves show a general increase in the relative %Phyt abundance of black wood towards the top of the section at the expense of brown wood. Significant deviation from these trends occurs at samples K25 and K30 where brown wood %Phyt abundance is higher and black wood abundance correspondingly lower. Tracheid abundance is also consistent through this interval, and consistently higher than in the lower part of the section, at approximately 10% Phyt. Slight peaks in the %Phyt of tracheids correspond to the two peaks in brown wood abundance in this interval.

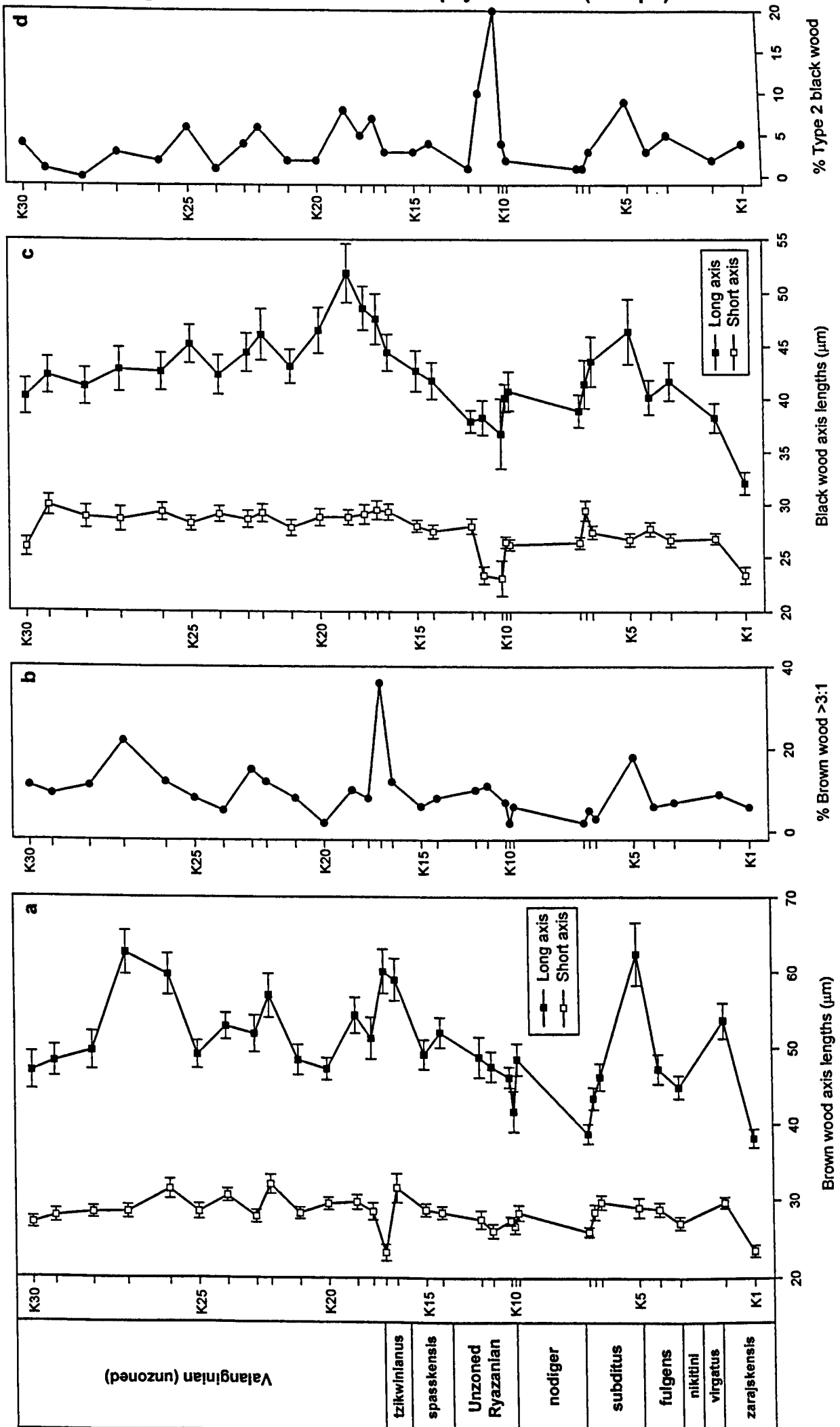
5.2.3.3. Analysis of the particle size data

Table 5.7 & Figure 5.23 show brown and black wood particle size data for the section at Kashpir. Comparison of the data for both components shows that brown wood mean long axis data are generally higher than that of black wood, although in many samples the difference is not pronounced. This suggests that in comparison to Gorodische much more of the black wood component is comprised of Type 2 material. This is not supported by the data displayed in Figure 5.23d which only shows elevated percentages of Type 2 material in a few samples. Alternatively more of the brown wood assemblage may represent reworked material.

SAMPLE	Brown wood long axis	Standard deviation (STDEV)	STDEV as % of mean	Standard error (STER)	Brown wood short axis	Standard deviation (STDEV)	Standard error (STER)	Difference between mean long & short axes	Mean long axis: short axis ratio	% particles with long axis: short axis ratio >3:1	Black wood long axis	Standard deviation (STDEV)	STDEV as % of mean	Standard error (STER)	Black wood short axis	Standard deviation (STDEV)	Standard error (STER)	Difference between mean long & short axes	Mean long axis: short axis ratio	% particles of Type 2	Brown wood RI	Black wood RI
K1	38.2	12.1	31.7	1.21	23.5	7.74	0.77	15.8	1.62	6	32.1	10.6	33	1.06	23.4	7.58	0.76	9.34	1.37	4	3.68	3.56
K2	53.6	23.1	43.1	2.31	29.7	7.24	0.72	25.86	1.81	9	38.3	13.8	35.5	1.36	26.8	5.26	0.53	12.39	1.43	2	3.15	3.79
K3	44.93	15.25	33.9	1.53	27.1	8.24	0.82	19.25	1.66	7	41.7	18	43.1	1.8	26.65	6.43	0.64	16.25	1.56	5	3.92	3.63
K4	47.28	19.12	40.4	1.91	28.85	8.69	0.87	19.9	1.63	6	40.2	16.1	40.1	1.61	27.73	6.62	0.66	13.47	1.45	3	3.14	3.48
K5	62.45	41.7	66.8	4.17	29.08	12.3	1.23	36	2.15	18	48.43	30.7	66.2	3.07	26.7	6.23	0.62	21.3	1.74	9	3.08	3.59
K6	46.25	17.36	37.5	1.74	29.75	9.06	0.91	17.8	1.55	3	43.6	23.5	53.9	2.35	27.4	6.19	0.62	17.5	1.59	3	3.31	3.58
K7	43.43	14.65	33.7	1.47	28.5	9.41	0.94	16.1	1.52	5	41.45	22.7	54.7	2.27	29.48	9.53	0.95	12.9	1.41	1	3.37	3.58
K8	38.79	12.87	33.2	1.29	25.96	6.1	0.61	12.6	1.49	2	38.95	15.2	39.1	1.52	26.4	5.57	0.56	13.6	1.48	1	3.14	3.74
K9	48.53	20.55	42.3	2.06	28.4	9.53	0.95	21.7	1.71	6	40.78	18.3	44.6	1.83	26.2	4.98	0.5	15.7	1.56	2	3.3	3.48
K10	41.73	26.7	64	2.67	26.7	9.19	0.92	16.2	1.56	2	40.15	12.9	32	1.29	26.45	5.32	0.53	14.8	1.52	4	3.68	3.4
K11	46.2	13.8	29.4	1.36	27.4	5.53	0.55	20.3	1.69	7	36.8	16.4	44.6	3.29	23.1	8.24	1.65	20.6	1.59	20	3.62	3.48
K12	47.6	19.4	40.8	1.94	26.1	8.84	0.88	23.2	1.82	11	38.3	16.1	42	1.61	23.4	7.99	0.8	16.1	1.64	10	3.56	3.49
K13	48.83	26.42	54.1	2.64	27.58	11.3	1.13	23	1.77	10	37.95	10.2	28.9	1.02	27.95	7.24	0.72	10.8	1.36	1	3.2	3.56
K14	52.03	19.51	37.5	1.95	28.45	7.96	0.8	25.5	1.83	8	41.75	17.1	40.9	1.71	27.45	6.36	0.64	15.4	1.52	4	3.16	3.68
K15	49.18	19.21	39.1	1.92	28.78	8.04	0.8	22	1.71	6	42.68	19.1	44.7	1.91	27.98	5.67	0.57	15.9	1.53	3	3.36	3.87
K16	58.98	28.14	47.7	2.81	31.6	19	1.9	29.6	1.87	12	44.43	17.3	38.9	1.73	29.33	7.44	0.74	16.3	1.51	3	3.28	3.66
K17	60.1	29.6	49.3	2.96	23.3	10.7	1.07	39.7	2.58	36	47.6	23.9	50.2	2.39	29.5	8.77	0.88	19.5	1.61	7	3.12	3.54
K18	51.3	27.1	52.8	2.71	28.6	10.7	1.07	24.6	1.8	8	48.6	20.7	42.8	2.07	29.1	9.15	0.92	21.1	1.67	5	3.38	3.49
K19	54.3	23.2	42.7	2.32	29.8	9.13	0.91	26.5	1.83	10	51.9	27.5	53	2.75	28.8	7.2	0.72	25	1.81	8	3.43	3.52
K20	47.3	14.5	30.7	1.45	29.6	7.83	0.78	19.1	1.6	2	46.5	21.6	46.5	2.16	28.8	8.04	0.8	19.1	1.61	2	3.23	3.58
K21	48.5	19.7	40.8	1.97	28.4	7.33	0.73	21.7	1.71	8	43.1	15.9	36.9	1.59	27.8	7.5	0.75	18.6	1.55	2	3.12	3.71
K22	56.9	28.7	50.4	2.87	32.1	12.3	1.23	26.8	1.77	12	46.1	24.3	52.7	2.43	29.2	8.45	0.85	18.2	1.58	6	3.14	3.48
K23	51.9	23.9	46.1	2.39	28	8.32	0.83	25.8	1.85	15	44.4	18.1	40.8	1.81	28.6	8	0.8	17.1	1.55	4	3.32	3.53
K24	52.9	17.1	32.3	1.71	30.7	8.24	0.82	23.9	1.72	5	42.3	18.4	43.5	1.84	29.1	7.48	0.75	14.3	1.45	1	3.07	3.82
K25	49.2	17.9	36.4	1.79	28.6	9.89	0.99	22.2	1.72	8	45.2	18.1	40	1.81	28.2	7.13	0.71	18.4	1.6	6	3.61	3.45
K26	59.7	27.5	46.1	2.75	31.5	12.2	1.22	30.5	1.9	12	42.8	17.5	41.1	1.75	29.3	8.29	0.83	14.4	1.46	2	2.84	3.54
K27	62.6	29.2	46.6	2.92	28.6	8.77	0.88	36.7	2.19	22	42.8	20.7	46.4	2.07	28.6	11.7	1.17	15.3	1.5	3	3.25	3.66
K28	49.7	24.7	49.7	2.47	28.5	7.57	0.76	22.9	1.74	11	41.2	17.3	42	1.73	28.8	10.8	1.08	13.4	1.43	0	3.09	3.42
K29	48.3	20.1	41.6	2.01	28	8.74	0.87	21.9	1.72	9	42.2	17.2	40.8	1.72	29.9	9.79	0.98	13.3	1.41	1	3.25	3.61
K30	47	24.4	51.9	2.44	27.1	7.78	0.78	21.5	1.73	11	40.2	16.8	41.8	1.68	25.9	8.7	0.87	15.4	1.55	4	3.02	3.47

Table 5.7: Mean phytoclast particle size data from Kashpir.

Figure 5.23: Brown & black wood phytoclast size (Kashpir)

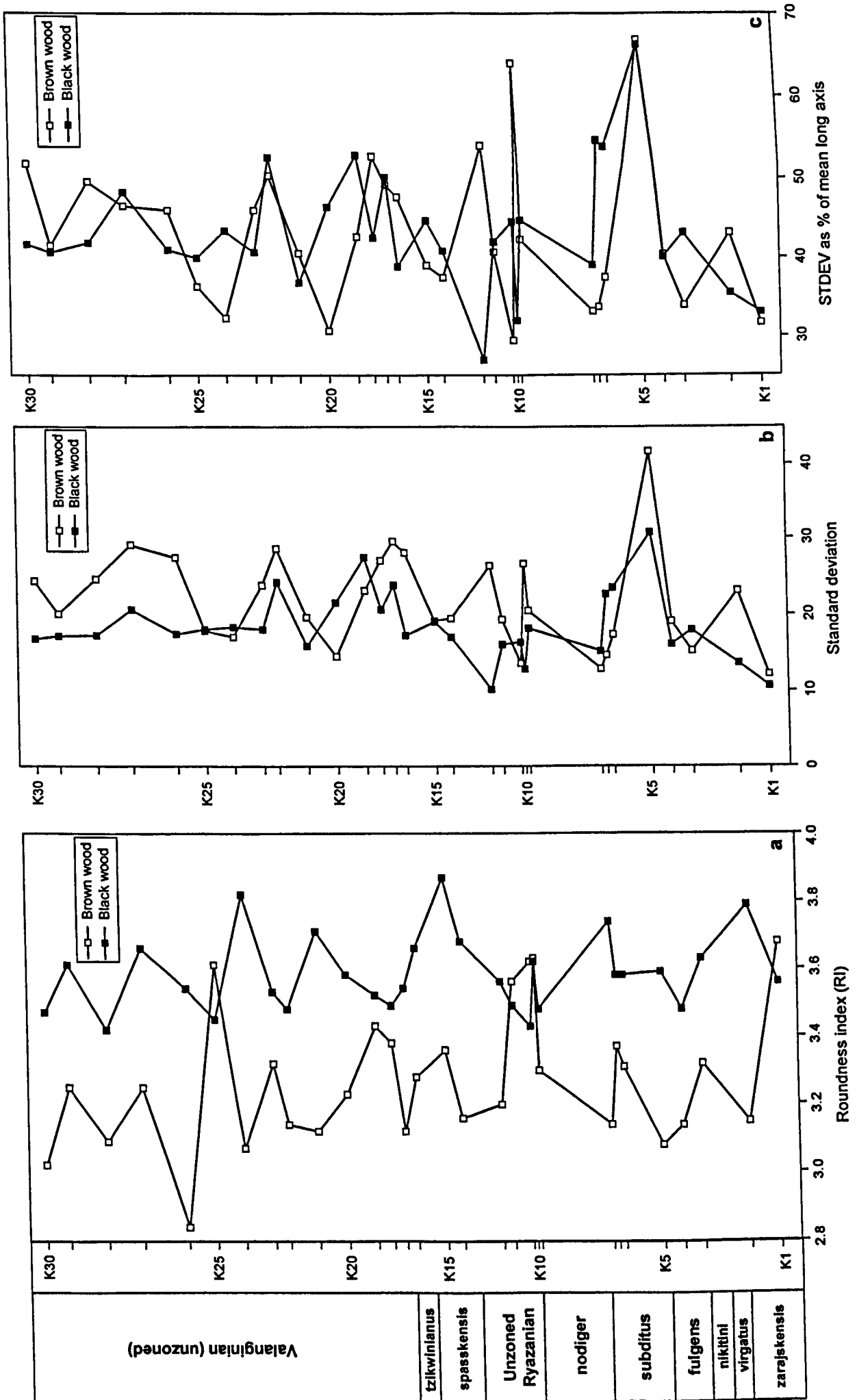


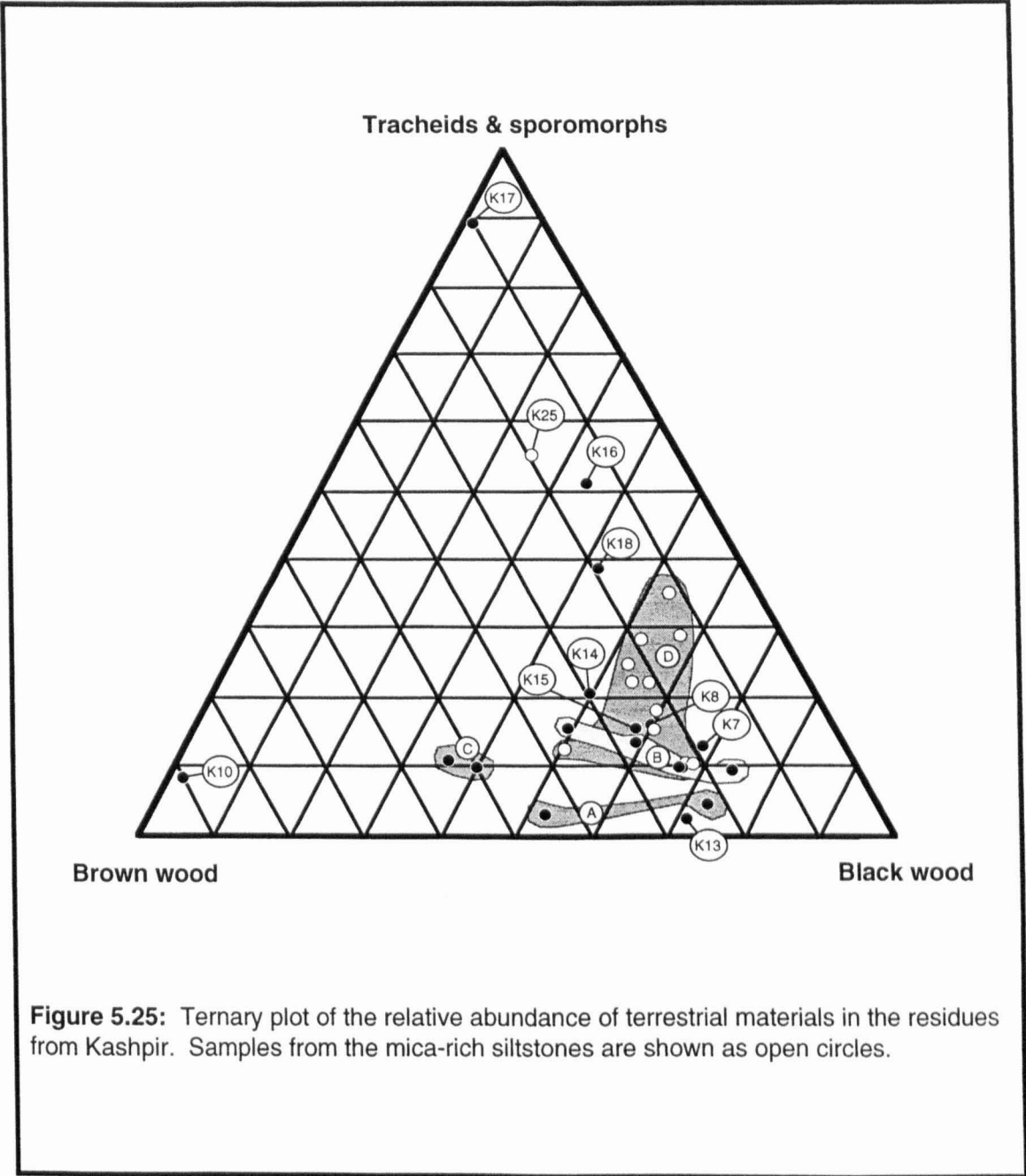
The data on mean long axis size show little correlation with the %Phyt data for either component. However peaks in the brown wood long axis data at sample K5 and K16 correlate to similar peak in the %SM. Many of the samples from the mica-rich siltstones have higher mean long axis data for brown wood than samples earlier in the section, although this is not true of the uppermost three samples from the section, which the %SM data indicate possess heightened abundance of woody phytoclasts. There is less spread in the black wood long axis data, and apart from a peak in long axis size at sample K5 which corresponds to a peak in this component in the %SM data, little comparison can be made. However, the mean long axis data are lower in the basal part of the section, notably so in the samples from the *zarajskensis* Subzone.

The RI and sorting parameters for this data are equally inconclusive (Figure 5.24). Black wood generally shows a higher RI values than brown wood, indicating a better rounded assemblage, although inversions in this pattern are evident at several sample levels (K1, K10 - K12, K25) possibly reflecting the highly degraded nature of the brown wood assemblage in these samples. Standard deviation is here quite strongly correlated with mean particle size of each sample, and in this respect is difficult to interpret. The standard deviation is closely comparable for both components, as is the percentage variation from mean.

A Ternary plot of the phytoclast assemblages from Kashpir is presented in Figure 5.25 which shows clustering of these sample points according to lithology. Due to the variety of lithologies present in this section, many of the samples have proved impossible to cluster on the basis of the phytoclast assemblage. However, where sufficient samples from each lithology were taken, clustering has been attempted. Cluster A at the base of the ternary diagram groups both samples from the *zarajskensis* Subzone. The wide spread for such a small sample set reflects the two distinct lithologies. Cluster B groups all samples taken from lenticular sandstone facies of beds 11, 13, and 21. These generally have low abundance of 'fresh' terrestrial material, and a dominance of black wood over brown. Cluster C groups the two samples from the

Figure 5.24: Phytoclast roundness and sorting (Kashpir)





laminated organic-rich sandstone of Bed 19. Cluster D includes all samples from the mica-rich siltstones, excluding sample K25 which is left as an outlier. This cluster covers a broad range of phytoclast compositions, and overlaps with several other lithologies on this basis, including Cluster B. Thus clustering of the data using ternary plots is difficult. Most of the samples have low abundance of 'fresh' components (and moderate to low abundance of brown wood) despite the apparent proximal nature of the deposits as indicated by the sedimentology, particularly in the lenticular bedded sandstones.

5.2.3.4. Absolute abundance of the structured components

Absolute abundance with *Lycopodium* spores

Absolute abundance of the main structured components is presented in Table 5.8 and Figure 5.26, and of the minor components in Figure 5.27. Figure 5.26 shows that of the structured components, dinoflagellate cysts dominate the majority of assemblages, black wood is generally the most abundant phytoclast, and tracheids the least abundant. Absolute abundance of each component is highest in the sample from the zarajskensis Subzone; dinoflagellate cysts reach nearly 3×10^6 grains per gram⁻¹ in sample K1. Samples K3, K4 and K6 are approximately equivalent in terms of absolute abundance of the three main structured components, with considerably lower values than in the first two samples. There is a significant drop in absolute abundance of all components in sample K5.

The remainder of the section up to the mica-rich siltstones is composed of numerous different lithologies, making inter-sample comparison difficult. There are significant peaks in the abundance of all the major components at samples K8 and K12, and significant minima at samples K9 and K13. Samples K13 to K16 show comparatively low absolute abundance of tracheids and to a lesser extent dinoflagellate cysts than most of the preceding samples. K17 however has remarkably increased input of tracheids and

Sample	Position	Brown wood count	Absolute abundance	Standard error	Total error	Tracheid count	Absolute abundance	Standard error	Total error	Black wood count	Absolute abundance	Standard error	Total error	Dinocyst count	Absolute abundance	Standard error	Total error	Spore count	Absolute abundance	Standard error	Total error	Pollen count	Absolute abundance	Standard error	Total error	Bisaccate count	Absolute abundance	Standard error	Total error
K1	13.5	212	143880	19.8	28469	9	6108.1	38.2	2330.3	798	541586	18.9	102312	3912	2654995	18.6	494501	1	678.7	102	690.3	0	0	0	0	12	8144	34.3	2795
K2	66	149	68755	17.3	11916	11	5075.9	33.8	1715.6	465	214571	16	34247	1421	655709	15.5	101640	11	5076	33.8	1716	3	1384	59.7	827	7	3230	40.8	1317
K3	145	62	4158.3	19.3	802.35	11	737.76	33.5	246.91	86	5768	18.1	1043.5	639	42857.4	15.1	6452.3	9	603.6	36.4	219.5	0	0	0	0	5	335	47	158
K4	180	195	10422	16.2	1687.9	48	2565.4	20.5	525.34	811	43345	14.9	6477.7	1501	80222.5	14.8	11836	39	2084	21.6	450.6	0	0	0	0	0	0	0	0
K5	215	86	840.06	12.5	104.71	9	87.913	33.9	29.816	187	1826.6	9.62	175.75	221	2158.75	9.18	198.27	17	166.1	25	41.59	1	9.77	100	9.79	14	137	27.4	37.5
K6	280	48	2683.6	20.5	549.54	19	1062.2	27.2	288.44	221	12356	16	1977.9	1804	100858	14.7	14842	12	670.9	32.3	216.8	0	0	0	0	0	0	0	0
K7	292	35	1912.7	22.3	426.3	4	218.6	52.1	113.82	172	9399.7	16.4	1542.1	1049	57327.1	14.9	8513.5	15	819.7	29.6	242.9	0	0	0	0	0	0	0	0
K8	302	176	9433.3	16.4	1543.8	38	2036.7	21.8	443.51	448	24012	15.3	3667.9	8003	428947	14.6	62494	75	4020	18.6	745.9	0	0	0	0	0	0	0	0
K9	425	36	1735.5	22.1	383.69	10	482.08	34.8	167.76	107	5158.2	17.4	900.06	682	32877.6	15	4939	4	192.8	52.1	100.4	2	96.4	72.2	69.6	0	0	0	0
K10	439	442	56590	14	7900.9	44	5633.4	20	1126.1	10	1280.3	34.2	438.37	3	384.096	59.2	227.42	0	0.1	0	0	0	0	0	0	0	0	0	0
K11	432	430	20441	15.3	3128.7	30	1426.1	23.3	332.73	327	15545	15.5	2416.2	2250	106960	14.7	15700	25	1188	24.7	293.8	12	570	32.3	184	5	238	47	112
K12	470	789	316155	15	47285	108	43276	17.4	7540.5	516	206763	15.2	31384	1371	549364	14.8	81169	15	6011	29.6	1781	5	2004	47	942	3	1202	59.5	716
K13	490	79	1288.5	14.4	185.18	7	114.17	38.8	44.343	231	3767.6	11.1	418.3	142	2316	12.3	284.03	5	81.55	45.6	37.19	0	0	0	0	1	16.3	100	16.4
K14	557	45	2098.1	20.8	436.71	4	186.5	52.1	97.105	73	3403.6	18.7	634.93	492	22939.3	15.2	3489	12	559.5	32.3	180.8	0	0	0	0	14	653	30.4	199
K15	585	38	1831.9	21.8	398.9	8	385.66	38.2	147.41	81	3904.8	18.3	714.13	471	22705.8	15.2	3460.3	9	433.9	36.4	157.8	0	0	0	0	3	145	59.5	86.1
K16	635	11	311.85	32.4	100.89	4	113.4	51.4	58.239	46	1304.1	18.8	245.71	1121	31780.2	12.1	3846.8	15	425.2	28.4	120.6	4	113	51.4	58.2	34	964	20.8	200
K17	655	201	11347	16.1	1832.3	1808	102067	14.7	15020	26	1467.8	24.4	358.22	379	21395.7	15.4	3296.6	9	508.1	36.4	184.7	1	56.5	101	57	35	1976	22.3	440
K18	677	29	1617.7	23.6	381.4	8	446.27	38.2	170.58	66	3681.7	19	701	579	32298.7	15.1	4880	13	725.2	31.3	227	5	279	47	131	29	1618	23.6	381
K19	705	50	3007.7	20.3	609.76	13	782	31.3	244.83	107	6436.4	17.4	1123.1	999	60093.3	14.9	8934	14	842.1	30.4	256.2	0	0	0	0	14	842	30.4	256
K20	755	71	4329.7	18.8	812.17	18	1097.7	27.7	303.91	198	12074	16.2	1952.6	1221	74459.2	14.8	11024	12	731.8	32.3	236.5	3	183	59.5	109	11	671	33.5	225
K21	805	38	1983.1	21.8	431.82	13	678.42	31.3	212.4	109	5688.3	17.4	989.75	931	48585	14.9	7235	0	0	0	0	11	574	33.5	192	20	1044	26.7	278
K22	855	42	2218	21.2	470.03	12	633.7	32.3	204.79	102	5386.5	17.6	946.93	896	47316.3	14.9	7052.7	7	369.7	40.5	149.7	1	52.8	101	53.4	27	1426	24.1	344
K23	880	33	2215.3	22.7	502.26	14	939.81	30.4	285.88	146	9800.9	16.7	1638.6	1167	78340	14.8	11609	31	2081	23.1	480.7	1	67.1	101	67.8	44	2954	20.9	618
K24	930	78	5171.5	18.4	952.48	27	1790.1	24.1	431.64	217	14387	16	2306.9	1130	74920.5	14.8	11109	16	1061	28.9	306.7	1	66.3	101	67	19	1260	27.2	342
K25	980	165	24665	16.5	4065.1	49	7324.9	20.4	1492.4	231	34532	15.9	5506.7	3998	597651	14.6	87329	87	13005	18.1	2348	0	0	0	0	311	0	15.6	0
K26	1030	136	8033.2	16.9	1355.1	51	3012.4	20.2	607.81	393	23214	15.4	3569.6	819	48376.3	14.9	7227.7	32	1890	22.9	432.5	0	0	0	0	128	7561	17	1286
K27	1105	65	3777.1	19.1	721.48	36	2091.9	22.1	462.5	279	16213	15.7	2547.3	998	57993.4	14.9	8622	11	639.2	33.5	213.9	0	0	0	0	91	5288	17.9	947
K28	1165	99	3045.8	14.6	443.49	37	1138.3	19.5	222.27	315	9691.1	11.9	1157.9	28	861.429	21.6	186.39	6	184.6	42.2	77.83	1	30.8	101	30.9	3	92.3	58.7	54.2
K29	1230	112	3813.3	14.7	561.19	43	1464	19	277.73	335	11406	12.5	1429.8	5	170.238	46.1	78.518	4	136.2	51.3	69.81	0	0	0	0	2	68.1	71.6	48.8
K30	1270	190	6052.8	13.6	821.33	60	1911.4	17.3	330.05	261	8314.7	13	1083.5	19	605.283	25.6	155.24	2	63.71	71.6	45.64	2	63.7	71.6	45.6	0	0	0	0

Table 5.8: Absolute abundance of structured palynologic matter components at Kashpir.

Sample	Acritarch count	Absolute abundance	Standard error	Total error	Prasinophyte count	Absolute abundance	Standard error	Total error	Microforam count	Absolute abundance	Standard error	Total error	Others	Absolute abundance	Standard error	Total error	Total marine particles	Absolute abundance	Standard error	Total error	Total terrestrial particles	Absolute abundance	Standard error	Total error	No. of Lycopodium counted	Sample weight	Tablets added
K1	9	6108	38.2	2330	11	7465	35.4	2643	18	12216	30	3665	123	83478	20.6	17222	4073	3E+06	18.6	514777	1023	694289	18.8	130652	30	3.08	5
K2	12	5537	32.7	1808	3	1384	59.7	827	17	7845	28.7	2248	53	24456	20.5	5023	1506	694932	15.5	107630	635	293016	15.8	46235	45	3.02	5
K3	7	469.5	40.5	190	2	134	72.2	96.8	0	0	0	0	6	402.4	43.3	174.4	654	43863	15	6598.5	162	10865	16.5	1794.4	50	11.22	3
K4	9	481	36.4	175	7	374	40.5	151	8	427.6	38.2	163.4	22	1176	25.8	303.3	1547	82681	14.7	12193	1045	55851	14.9	8295	50	14.08	3
K5	12	117.2	29.5	34.6	12	117	29.5	34.6	7	68.38	38.3	26.2	6	58.61	41.3	24.21	258	2520.2	8.82	222.38	305	2979.3	8.48	252.6	356	10.82	3
K6	0	0	0	0	0	0	0	0	0	0	0	0	0	0	0	0	1804	100858	14.7	14842	281	15710	15.7	2467	50	13.46	3
K7	0	0	0	0	0	0	0	0	0	0	0	0	3	163.9	59.5	97.61	1052	57491	14.8	8537.3	222	12132	16	1941.4	50	13.77	3
K8	15	804	29.6	238	0	0	0	0	12	643.2	32.3	207.9	47	2519	20.6	518.6	8077	432913	14.6	63070	699	37465	15	5623.8	50	14.04	3
K9	14	674.9	30.4	205	12	578	32.3	187	3	144.6	59.5	86.1	3	144.6	59.5	86.1	714	34420	15	5163.2	149	7182.9	16.7	1197.9	50	15.61	3
K10	6	768.2	42.9	329	0	0	0	0	20	2561	25.9	663.9	0	0	0	0	29	3712.9	22.7	844.34	452	57870	13.9	8069.3	62	4.74	3
K11	9	427.8	36.4	156	0	0	0	0	5	237.7	47	111.8	102	4849	17.6	852.4	2366	112474	14.7	16501	799	37983	15	5678.7	50	15.83	3
K12	44	17631	20.9	3691	21	8415	26.2	2206	258	1E+05	15.8	16222	11	4408	33.5	1475	1703	682397	14.7	100497	1328	532133	14.8	78666	50	3.13	5
K13	4	65.24	50.8	33.1	4	65.2	50.8	33.1	0	0	0	0	8	130.5	36.5	47.58	158	2577	12	308.45	316	5153.9	10.6	544.52	145	15.91	3
K14	7	326.4	40.5	132	7	326	40.5	132	2	93.25	72.2	67.31	15	699.4	29.6	207.2	523	24385	15.2	3699.2	144	6713.9	16.7	1124.4	50	16.14	3
K15	9	433.9	36.4	158	6	289	43.3	125	8	385.7	38.2	147.4	5	241	47	113.3	499	24056	15.2	3656.5	131	6315.2	17	1070.5	50	15.61	3
K16	16	453.6	27.6	125	6	170	42.5	72.3	6	170.1	42.5	72.25	9	255.1	35.3	90.16	1158	32829	12.1	3969.9	110	3118.5	15.1	471.4	79	16.8	3
K17	0	0	0	0	0	0	0	0	9	508.1	36.4	184.7	0	0	0	0	388	21904	15.4	3370.5	272	15355	15.7	2417.1	50	13.33	3
K18	4	223.1	52.1	116	1	55.8	101	56.4	0	0	0	0	6	334.7	43.3	145	590	32912	15.1	4969.2	142	7921.3	16.8	1328.9	50	13.49	3
K19	14	842.1	30.4	256	8	481	38.2	184	1	60.15	101	60.78	4	240.6	52.1	125.3	1026	61717	14.9	9170	185	11128	16.3	1811.8	50	12.51	3
K20	25	1525	24.7	377	1	61	101	61.6	0	0	0	0	4	243.9	52.1	127	1251	76289	14.8	11290	295	17990	15.6	2815.3	50	12.34	3
K21	0	0	0	0	1	52.2	101	52.7	1	52.19	101	52.73	9	469.7	36.4	170.8	942	49159	14.9	7318.4	178	9289.1	16.3	1518.4	50	14.42	3
K22	8	422.5	38.2	161	0	0	0	0	0	0	0	0	2	105.6	72.2	76.24	906	47844	14.9	7129.5	179	9452.7	16.3	1544.2	50	14.25	3
K23	58	3894	19.6	762	0	0	0	0	1	67.13	101	67.83	3	201.4	59.5	119.9	1229	82502	14.8	12213	255	17118	15.8	2707.8	50	11.21	3
K24	36	2387	22.1	528	0	0	0	0	1	66.3	101	67	1	66.3	101	67	1168	77440	14.8	11475	331	21946	15.5	3408.5	50	11.35	3
K25	134	20031	16.9	3385	2	299	72.2	216	2	299	72.2	215.8	26	3887	24.4	948.6	4162	622167	14.6	90891	794	118693	15	17749	50	8.39	5
K26	41	2422	21.3	517	0	0	0	0	1	59.07	101	59.69	0	0	0	0	861	50857	14.9	7588.2	689	40698	15	6111.8	50	12.74	3
K27	44	2557	20.9	535	0	0	0	0	0	0	0	0	1	58.11	101	58.72	1043	60608	14.9	9001.9	446	25917	15.3	3959.7	50	12.95	3
K28	9	276.9	35	96.8	4	123	51.1	62.9	0	0	0	0	0	0	0	0	41	1261.4	18.8	237.63	424	13045	11.6	1513.4	100	12.23	3
K29	6	204.3	42.4	86.5	6	204	42.4	86.5	0	0	0	0	2	68.1	71.6	48.76	19	646.9	25.6	165.39	453	15424	12.2	1885	86	12.85	3
K30	8	254.9	37.2	94.7	3	95.6	58.9	56.3	0	0	0	0	2	63.71	71.6	45.64	32	1019.4	21.1	214.8	455	14495	12.4	1795.7	83	14.23	3

Table 5.8: Continued.

Figure 5.26: Major structured component absolute abundance (Kashpir)

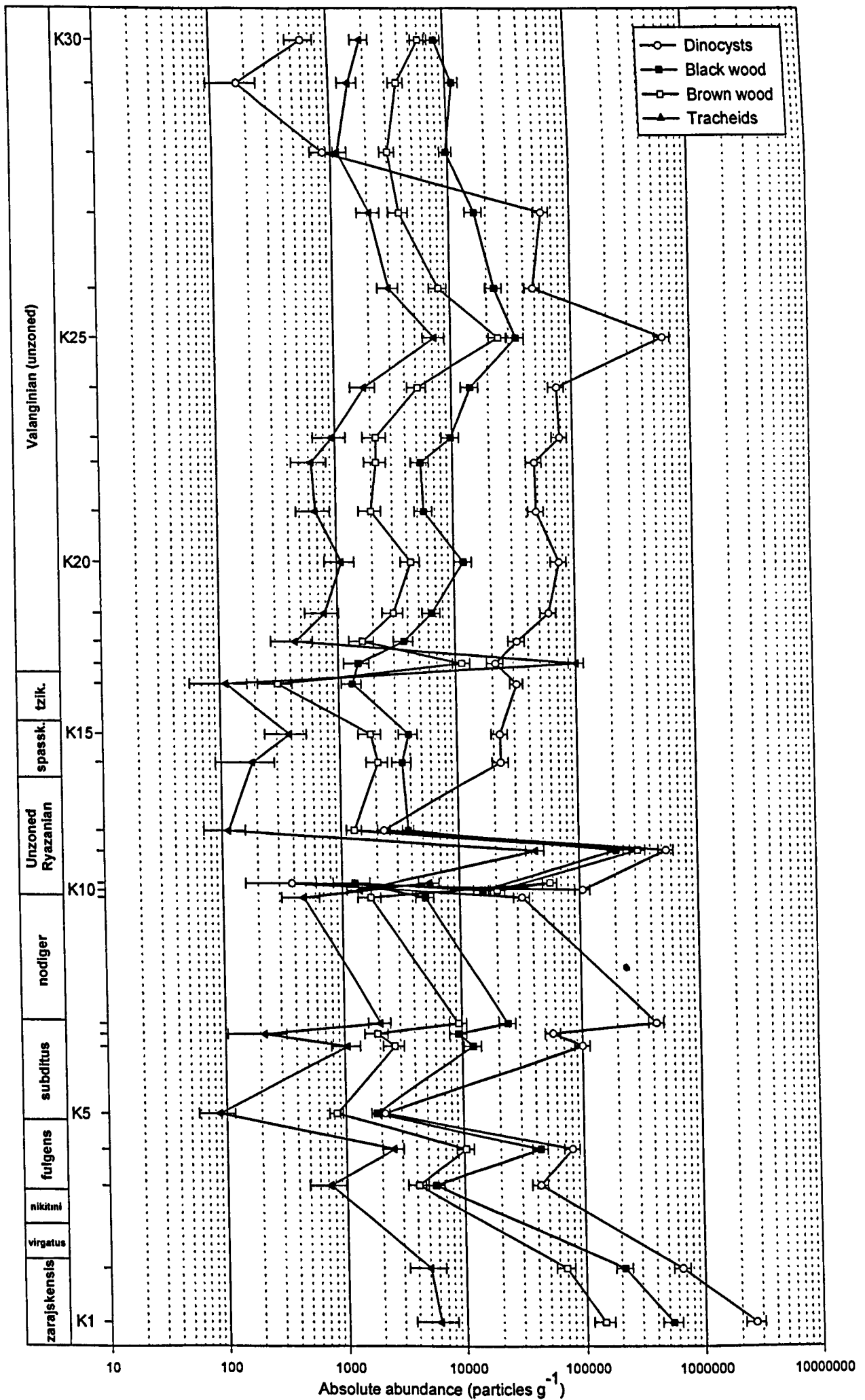
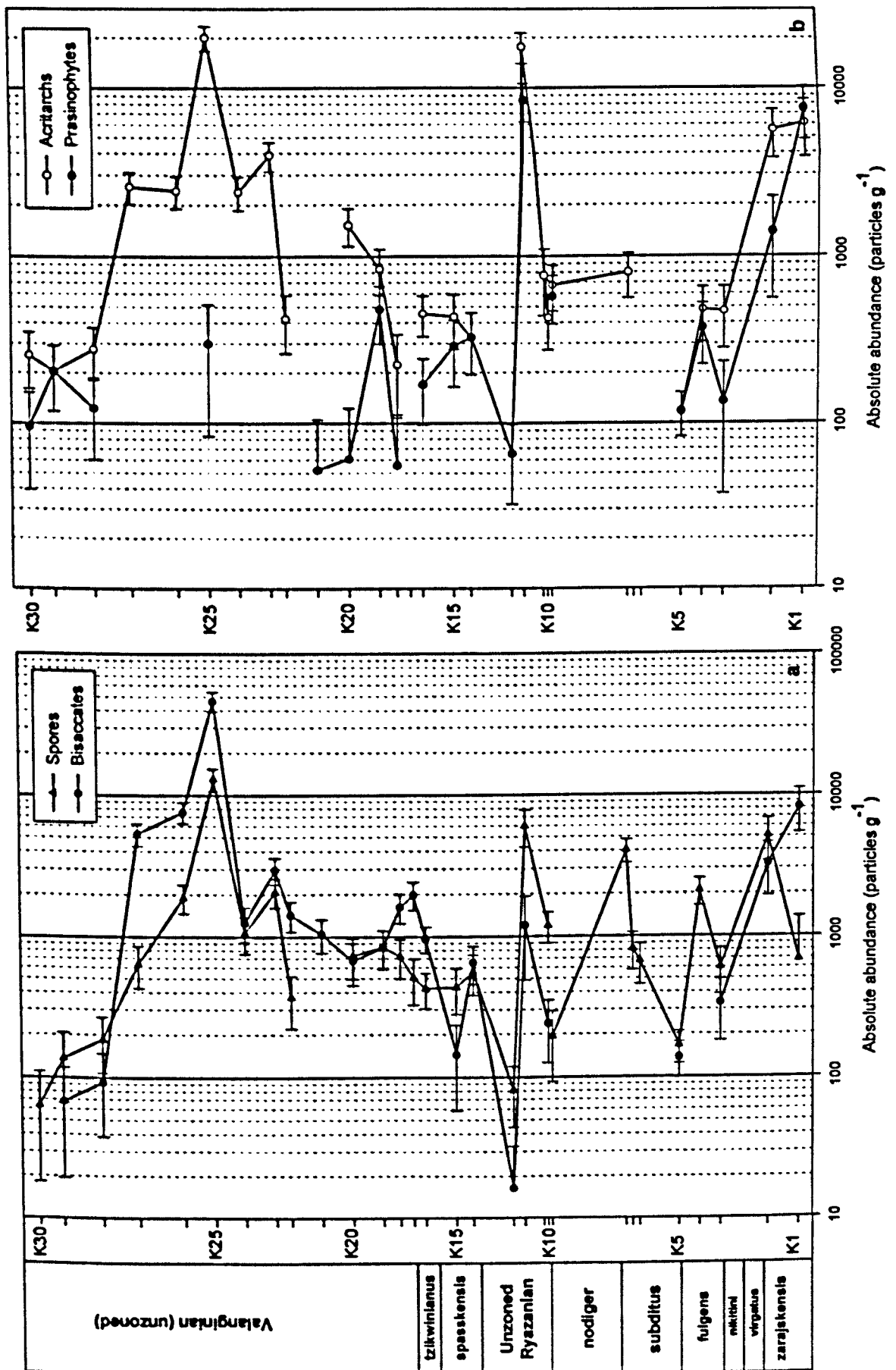


Figure 5.27: Minor structured component absolute abundance (Kashpir)



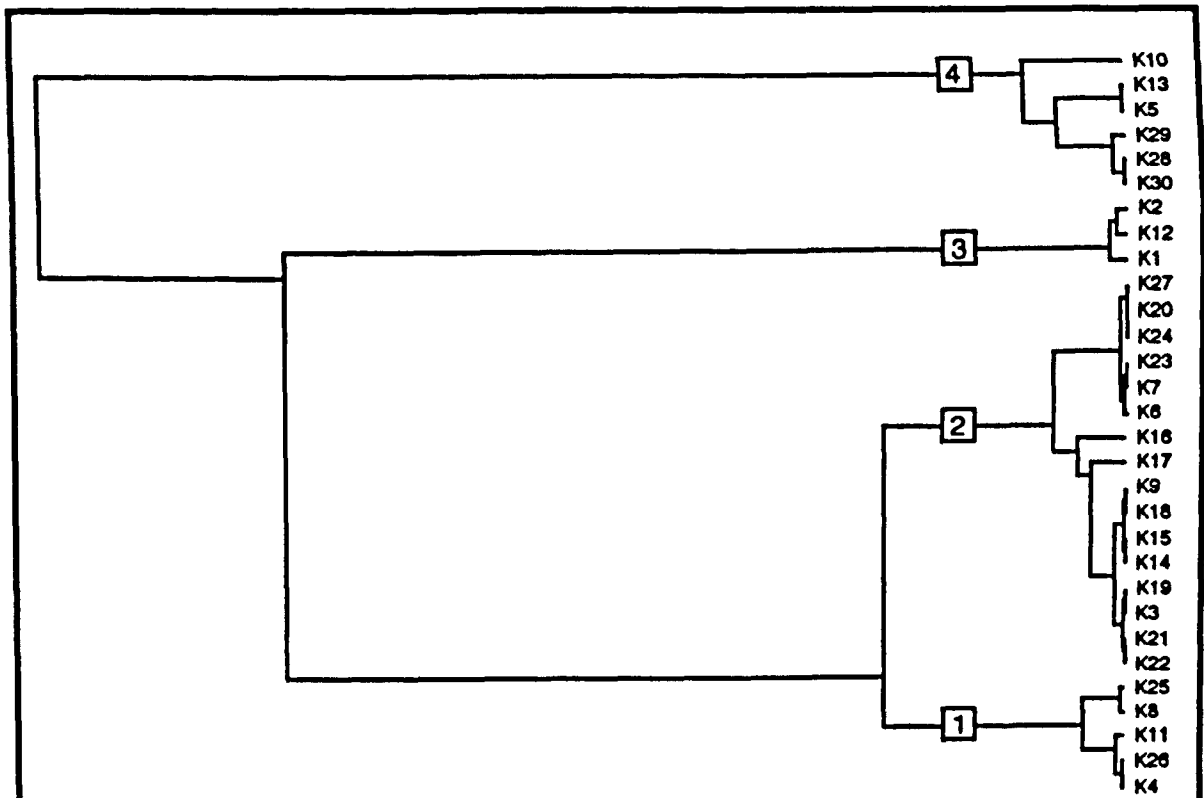


Figure 5.28a: Dendrogram produced from minimum variance cluster analysis of the major component absolute abundance data. Squared Euclidean distance was calculated using \log_{10} transformed data to reduce variance and enhance clustering

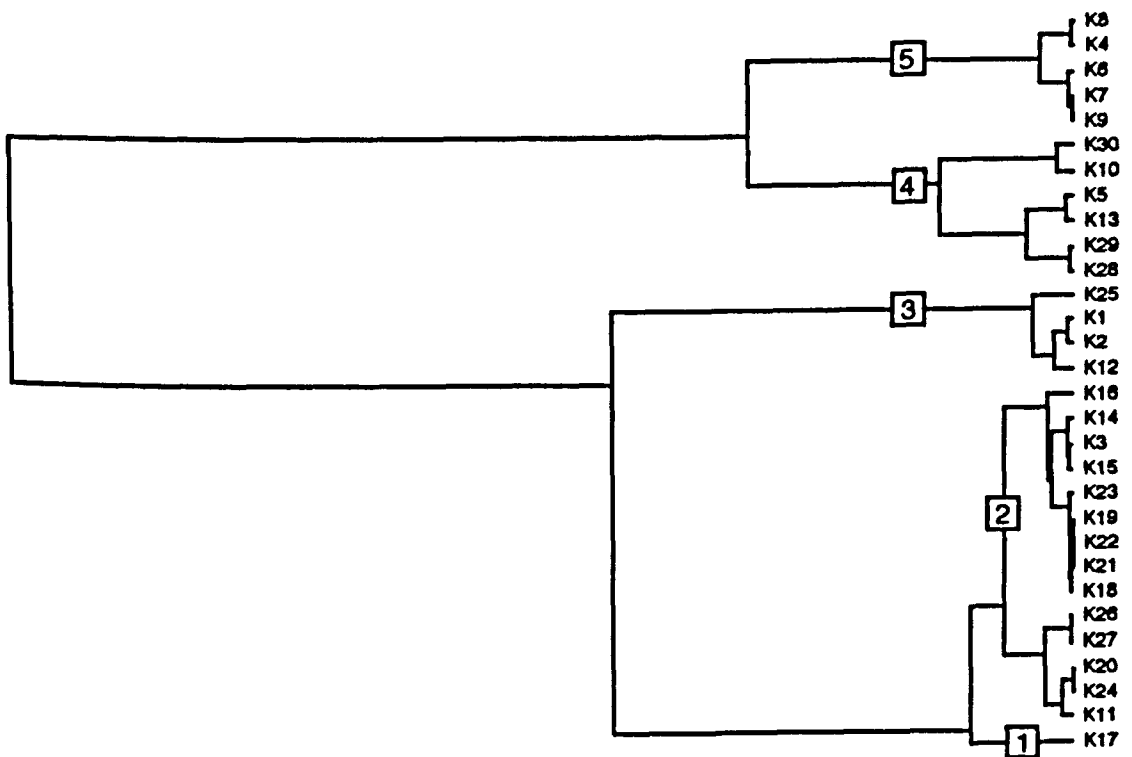


Figure 5.28b: Dendrogram produced from minimum variance cluster analysis of the full absolute abundance data set. Squared Euclidean distance was calculated using \log_{10} transformed data to reduce variance and enhance clustering

also a significant peak in brown wood. Absolute abundance of these components is generally consistent through the samples of the mica-rich siltstones. However there is a significant peak in absolute abundance of all these components in sample K25, and there appears to be a broad 'bulge' in the abundance of the phytoclast components between samples K22 and K28, peaking at K25. Above this bulge, there is a profound drop in the absolute abundance of dinoflagellate cysts in samples K28 - K30 which is not reflected in the phytoclast curves.

Once again, the absolute abundance data has been subjected to minimum variance cluster analysis. Only the major components were run in the first analysis, and the dendrogram produced is shown in Figure 5.28a. Clustering of this data is poorly developed according to lithology, and in this case not even the mica-rich siltstones have been clearly separated. The 'full' absolute abundance data set achieved more refined clustering according to lithology (Figure 5.29b). Branch 1 on Figure 5.28b interestingly separates K17 (phosphate concretions) from all other samples. Branch 2 includes all of the samples from the mica-rich siltstones, plus all the samples from the shelly sandstones of Bed 23. Branch 3 groups most of the organic-rich sediments (bar sample K10). Branch 4 includes all the dinoflagellate-poor sediments, regardless of lithology. Branch 5 comprises most of the samples from the interval from beds 11 - 14, which clearly do have similar palynofacies in terms of absolute abundance (Figure 5.26) regardless of lithology. This contrasts to the heightened detail apparent using the major components rather than the full data set seen in analysis of the section at Gorodische.

PhytOC ranking

PhytOC for the section at Kashpir is plotted in Figure 5.29, with increasing grain size of the sediments from left to right. Unfortunately, there are not enough samples in each lithology for any statements about the PhytOC values to be definitive. However, most of the samples from the mica-rich siltstones and those from the lenticular sandstones are tightly clustered, with generally low PhytOC despite apparent proximity

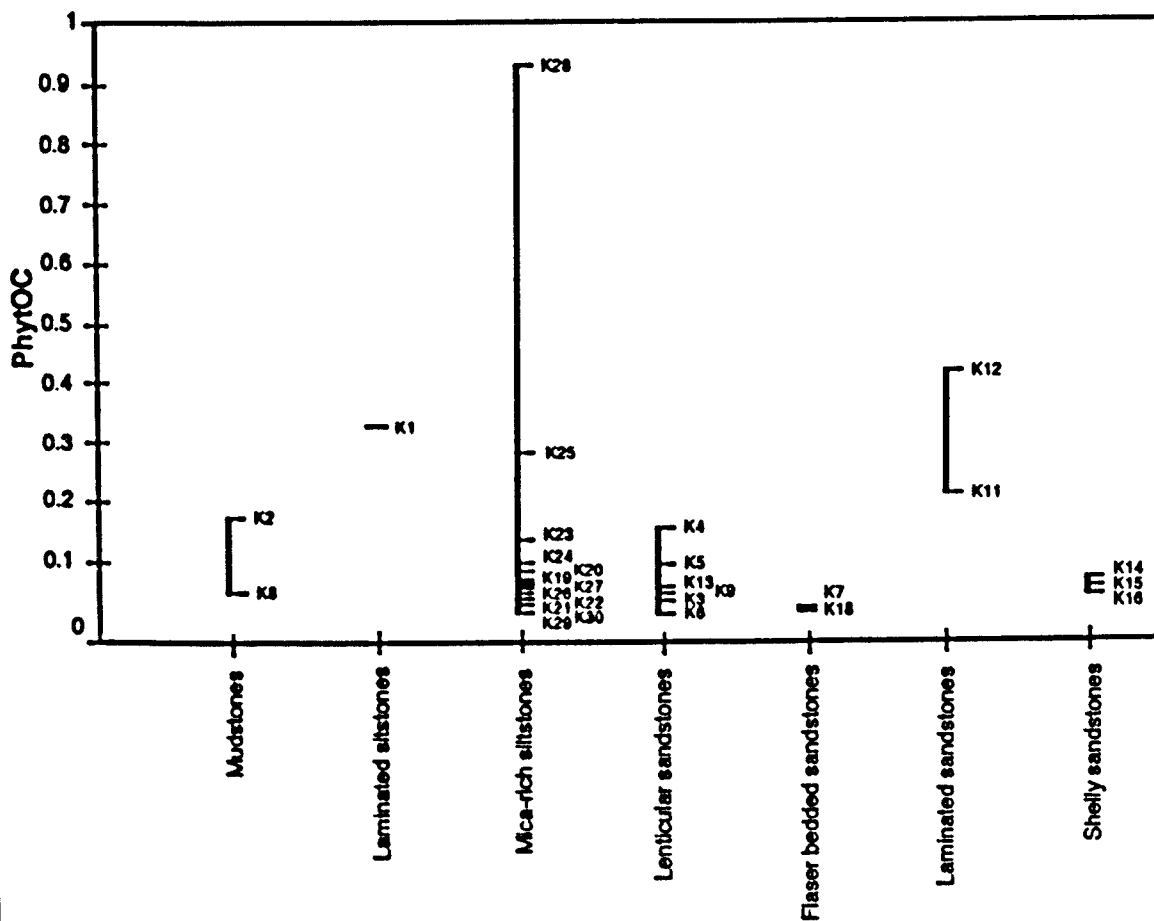


Figure 5.29: PhytoC ranking for the samples at Kashpir. Horizontal axis organised from left to right in order of increasing sediment grain size.

of these sediments. Plausible explanations for this include sediment dilution and/or breakdown of phytoclasts (particularly cuticle) during extended periods of reworking/residence time at the sediment/water interface, or simply extremely low input of terrestrial materials.

5.2.4. Interpretation of depositional environments for the Kashpir section based on palynofacies and sedimentological data.

The two samples from the *zarajskensis* Subzone are directly comparable to those taken from the mudstone and laminated siltstone lithologies of this subzone at Gorodische. All aspects of the palynofacies in samples K1 & K2 are also consistent with the analogous deposits at Gorodische, and therefore a similar interpretation is proposed: these sediments were deposited in an anoxic, probably restricted basin, with periodic short-lived phases of uplift or increasing proximity creating a source for the laminated siltstones. The high TOC and high absolute abundance of the structured components suggests extremely low rate of siliciclastic sediment input.

No samples were taken from the coarse-grained deposits of the *virgatus* and *nikitini* zones at Kashpir. The sediments of both zones however reflect much more proximal deposition than those of the *zarajskensis* Subzone, and are separated from the underlying deposits by a pronounced erosional contact. Indeed, proximal deposits of the uppermost *zarajskensis* Subzone analogous to the lenticular siltstones (beds 10 & 12) at Gorodische are absent at Kashpir, suggesting the presence of a significant unconformity/hiatu at this level. Bed 4 at Kashpir has tightly packed units of planar cross-stratified sandstone with trough-shaped erosional surfaces and sediment infill characteristic of channel deposits (Table 4.2). Beds 6, 7, and 10 of the *nikitini* zone are thin but laterally continuous conglomerates with coarse grained matrices (with haematite in the case of Bed 10) and a variety of lithic, phosphatic, and skeletal clasts.

Bed 8 is a glauconitic phosphatised sandstone, quite typical of sediments which form in shallow neritic, sediment-starved environments (after Leeder, 1982).

These proximal conditions are continued, if not intensified in the lenticular sediments of beds 11 & 13. As explained in Section 5.4, lenticular sediments are indicative of alternating energy conditions, typically intertidal areas. Beds 11 and 13 are slightly unusual in having medium-grained sandstone lenses set within fine-grained sandstone rather than more cohesive muddy material. Such sediment perhaps suggests higher input of sandy material, or generally higher energy conditions than the lenticular siltstone deposits at Gorodische. The comparative lack of glauconite and phosphate in these units is consistent with a higher rate of deposition. The palynofacies data are equivocal, but do not contradict such conclusions: both abundance of AOM and TOC content are generally low suggesting well oxygenated conditions unsuitable for the preservation of this material and/or enhanced sediment dilution. The reduced absolute abundance of structured components is consistent with either increased sediment dilution, sediment-starved conditions where much of the organic matter is degraded during extended periods of reworking, or low primary productivity. The pronounced drop in absolute abundance of all the main components at sample K5, together with slightly increased relative abundance of brown and black wood and increased mean long axes of these components is most consistent with increased sedimentation rate, at least in this sample.

The wackestone of Bed 12 suggests a significant change in depositional environment from an otherwise siliciclastic depositional regime. Such a change probably in part represents a distal shift into the zone of carbonate sedimentation. The wackestone texture indicates continued neritic conditions rather than a drastic shift to basin sedimentation. The discontinuous silty horizons are almost certainly secondary and of stylolitic origin, but are testament to continued input of fine siliciclastic material, albeit at an extremely low sedimentary rate.

Beds 15 and 16 were not sampled, but continue to represent proximal conditions. Bed 15 is predominantly fine to medium-grained sandstone with thin, wavy mud layers. In a similar manner to lenticular bedding, wavy laminations suggest intertidal deposition, and the predominance of sand over mud indicates heightened input of siliciclastic sediment. Bed 16 shows rapid normal grading from a conglomeratic base to a medium-grained sandstone which contains a mass-accumulation of ammonites still bearing blue-green nacreous shells. This bed is here suggested to be a storm deposit, with rapid sedimentation, and thus reduced length of abrasion to the ammonite shells. Bed 17 becomes increasingly lenticular towards the top, consistent with either increasing proximity and influence of intertidal conditions. Sample K9 was taken from the upper part of this interval, and the palynological matter assemblage observed is consistent with the other lenticular-bedded sandstones from beds 11 and 13. Comparatively high relative abundance of AOM but low TOC content and low absolute abundance of structured components probably reflects higher sedimentation rate than in the underlying lenticular sediments.

Bed 18 is predominantly bituminous shale (in excess of 55% TOC) intercalated with laterally discontinuous shale horizons. From the sedimentology alone, it is difficult to interpret the environment in which this sediment may have formed, although such an organic accumulation would require extremely low sedimentary input. The markedly reduced absolute abundance of both marine palynomorphs and black wood, together with peaks in brown wood and tracheid abundance is more consistent with deposition in a proximal environment. A significant proportion of the brown wood component is degraded, and it is often difficult to distinguish between a gellified phytoclast and an amorphous particle. Fluorescence shows that a significant proportion of the 'AOM' in this deposit is of degraded algal origin, and is, in fact bitumen. Thus the deposit is clearly marine, but further examination is needed both in the field and in polished section before more concrete conclusions can be drawn about this unit.

The finely laminated sandstones of Bed 19 probably represent low-energy proximal deposition, possibly from suspension: there is no evidence of cross-lamination on oblique faces, or to flow-parallel striations typical of upper-phase flow. The sediments continue to be organic-rich (between 3 and 10% TOC), and the AOM of Type 3 nature. However, the renewed presence of dinoflagellate cysts indicates increased marine influence, although the comparable absolute abundance of woody phytoclasts and these marine palynomorphs, together with dominance of brown wood over reworked black wood suggests strong terrestrial input. This is supported by the abundance of macroscopic woody plant fragments at the top of this unit.

Bed 21 is a unit of glauconitic lenticular and wavy bedded sandstone, with a phosphoritic lag at the base indicating the presence of an hiatus. The combination of wavy and lenticular bedding suggests variable conditions, most likely variations in rate of sedimentation, whilst the variable nature of the lenses in this unit (including mudstone, glauconitic siltstones and sandstones, and cream-coloured sandstones) suggests fluctuating source materials. The overall fabric of this deposit is indicative of sediment starved deposition over an extended period of time, sufficient for fluctuation of source materials to be reflected in the sedimentology. The low TOC, low absolute abundance of structured components, low relative and absolute abundance of marine palynomorphs in relation to phytoclasts, low absolute abundance of tracheids in relation to brown and black wood, and increased relative abundance of black wood all point to proximal deposition with extended residence times of organic matter at the sediment/water interface (slow rate of deposition). The palynofacies data from sample K13 is thus entirely consistent with the interpretation of this deposit based on sedimentological grounds.

Beds 22 and 23a are fine-grained glauconitic sandstones with mass accumulations of bivalve shells, typically with phosphatic internal casts. The sedimentology thus indicates a neritic marine environment, with sufficiently low siliciclastic sediment accumulation rate to allow the build-up of such mass

accumulations, and the deposition of both phosphate and glauconite. Samples K14 and K15 were taken from Bed 23a, and have almost identical palynofacies. The low absolute and relative abundance of tracheids in comparison to other phytoclasts, the low TOC, the low absolute abundance of terrestrial components in comparison to dinoflagellate cysts suggests low input of 'fresh' terrestrial components, and low sedimentation rate in general forcing extended periods of organic matter degradation. Moreover, the increased absolute and relative abundance of dinoflagellate cysts indicates more distal deposition than does the palynofacies of sample K13. Bed 23b is much less abundantly fossiliferous and less glauconitic than 23a, with occasional phosphatic concretions. The palynofacies are similar in this deposit (sample K16) to those of Bed 23a, suggesting similar conditions, but the increase in mean brown wood long axis size, increase in angularity and decreased sorting (standard deviation) of both brown and black wood indicate less particle abrasion, and therefore either less reworking or an increase in proximity (decreased distance of transport). The decrease in absolute abundance of these phytoclast components therefore probably reflects increased sediment dilution.

Bed 24 is a poorly cemented, medium-grained sandstone with strings of phosphate concretions which often (but not exclusively) appear to have nucleated around macrofossils. The palynofacies show hugely increased absolute and relative abundance of 'fresh' phytoclasts, in particular tracheids, combined with increased mean brown wood long axis, decreased sorting and a generally angular phytoclast assemblage, and comparatively high TOC despite the virtual absence of AOM. Such attributes of the phytoclast assemblages are consistent with deposition proximal to the terrestrial source. Preservation of the dinoflagellate cysts is split between exceptionally well preserved 3-dimensional specimens and a much more poorly preserved component. It seems unlikely that such specimens could have been so beautifully preserved in the poorly cemented sandstone matrix, and may thus have been preserved within the phosphatic concretions. If this is the case, phosphatisation must have occurred at an early stage in diagenesis, prior to significant compaction. The poorly preserved portion of the assemblage may thus have been sourced from the sandstone matrix.

It is unclear whether the significant peak in 'fresh' phytoclasts is the result of enhanced preservation within these concretions, or whether the nucleation of the concretions was a result of enhanced input of organic material. Indeed, our knowledge of how and why such types of phosphate deposits form is somewhat limited. It is clear that large quantities of phosphorous are required, either by precipitation from dissolved mineral phosphates, or from the breakdown of abundant organic matter. Several studies have shown an association between phosphate sedimentation and abundance of marine phytoplankton, including dinoflagellate cysts (Fauconnier & Slansky, 1978; Slansky 1986), particularly during 'red-tide' events and/or in upwelling systems. However, neither the dinocyst assemblage recovered from this deposit, nor from Bed 19 (sample U33) at Gorodische, exhibit features characteristic of upwelling-driven bloom production, such as high dominance (Davey & Rogers, 1975; Fauconnier & Slansky, 1980; Honigstein *et al.*, 1989), the prevalence of peridinioid cysts (Wall *et al.*, 1977; Fauconnier & Slansky, 1980; Bujak, 1984; Rauscher *et al.*, 1986, 1990; Powell *et al.*, 1990; Powell *et al.*, 1992), or an abundance of cysts with a cavate morphology (Courinat *et al.* 1993).

It seems possible then, that in Bed 24 at Kashpir there is causal relationship between the super-abundance of plant material and the nucleation of these phosphatic nodules. This becomes increasingly plausible when one considers the role of bacteria in the degradation of organic matter. Although the importance of bacteria in phosphate precipitation has yet to be clearly demonstrated, evidence of bacterial action on organic substance within phosphate rocks has been identified (Belayouni, 1984). Furthermore, accumulations of bacteria have been suggested as a rich source of phosphate (Slansky, 1986).

Beds 25 and 26 above the phosphatised sandstone are closely comparable in terms of sediment grain size, but have contrasting structure, with the lower unit being planar laminated (no apparent cross bedding) and the upper being wavy bedded with

mudstone drapes. The sedimentology of Bed 26 indicates intertidal deposition, although the palynofacies of sample K18 taken from this horizon is difficult to distinguish from that of the overlying mica-rich siltstones. The latter contain mm-scale cross laminae with an extremely low angle of climb between sets (approximately 1.5°, Bed 27), and are clearly bioturbated with both horizontal and vertical burrows. The intensity of burrowing drops rapidly above Bed 27, and is virtually absent in Bed 30. It is unclear whether the absence of cross-lamination in the upper part is due to primary absence of structure, or due to the homogenisation of the sediment by intense bioturbation: the presence of fewer obvious burrows above Bed 27 cannot be taken to mean that there was less faunal activity. However the presence of preserved cross-lamination in these siltstones suggests net deposition (albeit at a slow rate of sediment influx) under non-turbulent conditions.

In common with analogous deposits at Gorodische, these siltstones are rich in secondary gypsum and jarosite, which are again interpreted as the chemical weathering products of pyrite and subsequently carbonate materials. Similarly, the development of disseminated pyrite in this part of the sequence is expected to have been caused by the degradation of abundant plant matter. The abundance of well-preserved AOM at sample horizon K25 suggests that this process may have contributed to the development of bottom-water or pore-water anoxia. However, the continued abundance of dinoflagellate cysts in most of these deposits is testament to the maintenance of 'normal' marine conditions, at least in the surface waters.

There is a significant change in the palynofacies from sample K27 to sample K28, with a dramatic drop in the relative and absolute abundance of dinoflagellate cysts, although the absolute abundance of the three main phytoclast components remains unaffected. This is combined with an increase in relative abundance of the brown wood component at the expense of black wood (or *visa-versa*). Such changes could be the result of a change in preservation, leaving only the most robust particles, but the

continued levels of tracheid fragments suggests increased proximity to the terrestrial source.

The section at Kashpir is capped by a medium to coarse-grained sandstone horizon with carbonate concretions which yield marine vertebrate and ammonite fragments. This unit was not sampled and will not be discussed further.

5.3. Assessment of the dinoflagellate cyst assemblages

This section focuses exclusively on the dinoflagellate cyst assemblages recovered from the Volga Basin samples. The data are examined at four levels: diversity and dominance of the assemblages as a whole; bulk proximate/chorate/cavate abundance; relative abundance of more tightly defined morphological groups; and detailed analysis of the generic abundance taking into account the distribution of key species. Each aspect is assessed to establish whether relationships exist between the dinocyst data and the palaeoenvironmental conditions inferred from the sedimentology and palynofacies.

5.3.1. Diversity & dominance

Diversity and dominance within the dinoflagellate cyst assemblages is plotted for both sections in Figure 5.30 from data in Tables 5.9. & 5.10. Diversity has been calculated using the Fisher α diversity index (Fisher, 1949) which allows for disparity in count size between samples, and dominance using the technique developed by Goodman (1987). In both of these measures the 'taxon-groups' were counted as single species. This means that diversity will have been consistently underestimated, and dominance overestimated in those samples in which a 'taxon-group' was a dominant species. The dominance therefore is shown by two curves, one which includes taxon-

groups (where appropriate), and one which does not. The real dominance is therefore expected to fall between these two curves.

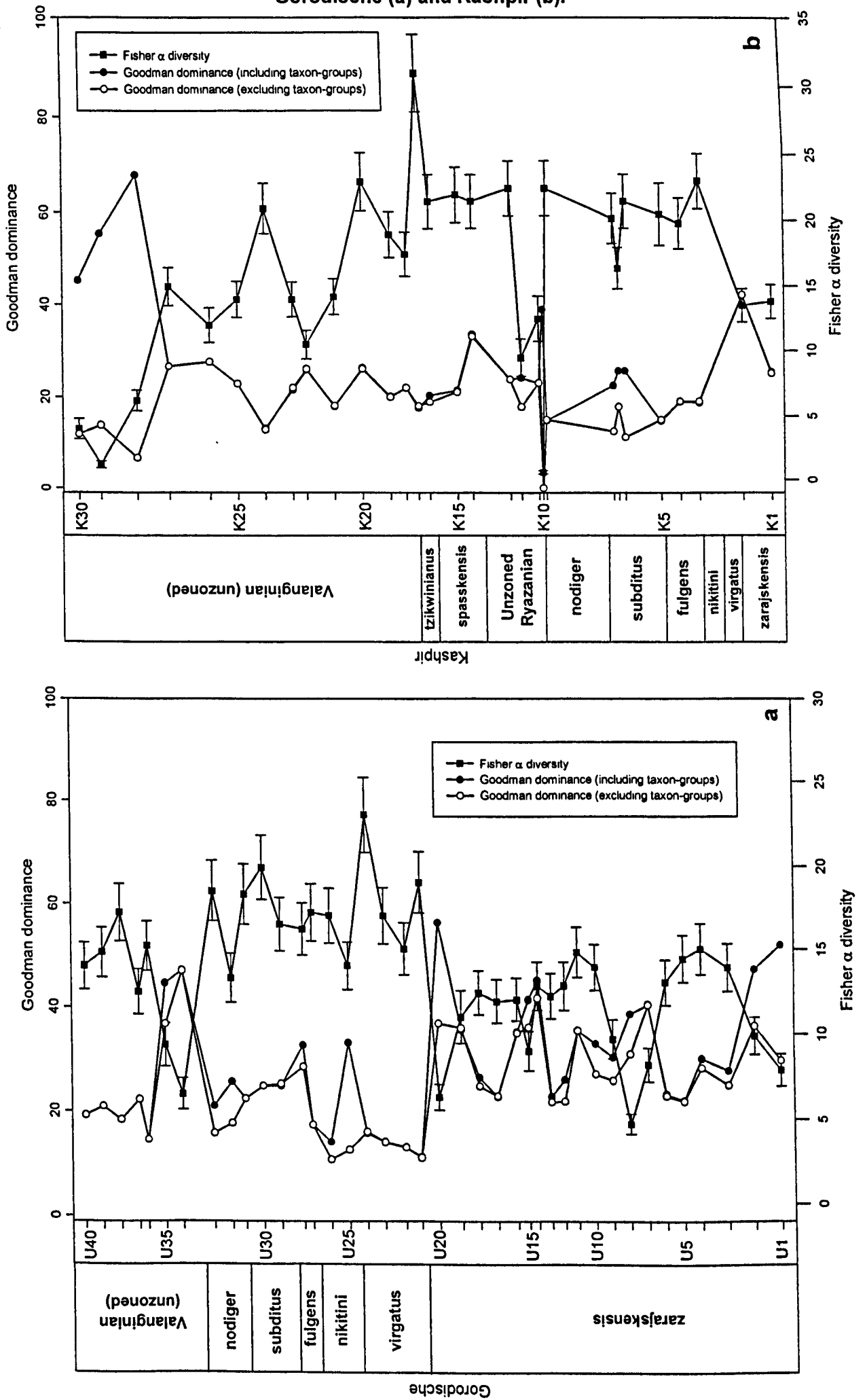
5.3.1.1. Gorodische

At Gorodische, dinocyst diversity appears fairly consistent about a trend line in the zarajskensis Subzone, which shows slightly decreasing diversity from samples U3 to U19. A major drop in diversity is apparent between samples U7-U9, corresponding to a peak in dominance. Dominance is rather variable through this part of the section (using either curve), and major changes in the values correspond to changes in lithology, although there is no consistent relationship between dominance and either sediment grain size, or inferred palaeoenvironment. There is a significant increase in diversity at the base of the virgatus Zone, with two peaks in this zone (samples U21 & U24) corresponding to the two conglomerate horizons. This presumably reflects the combination of reworked and autochthonous assemblages. Diversity varies between $\alpha=15$ and $\alpha=20$ in the sample interval U22-U33. Dominance is generally much lower through this interval than in the zarajskensis Subzone, with significant peaks only notable when the taxon-groups are included. Dominance is lowest and most consistent between samples in the virgatus Zone (samples U21 - U24). Diversity drops to between $\alpha=7-9$ at the base of the mica-rich siltstones (samples U34 & U35), but varies between $\alpha=12-16$ in the remainder of samples from this unit. A significant peak in dominance corresponds to the drop in diversity at the base of this Valanginian interval, with dominance between 37% and 47% of the assemblages. However, dominance is quite low, between 15% and 22% in the remaining samples from this unit.

5.3.1.2. Kashpir

At Kashpir diversity is comparatively low ($\alpha=15$) and dominance high (25-43%) in the two samples from the zarajskensis Subzone (Figure 5.31b). Diversity is then

Figure 5.30: Fisher α diversity and Goodman dominance for the sections at Gorodische (a) and Kashpir (b).



fairly consistent through the Middle to Upper Volgian (sample interval U3-U9), and higher than in the underlying deposits. Conversely dominance is lower than in the zarajskensis Subzone (13-25%). Sample K10 from the bituminous shale horizon has very low diversity, most of the encountered dinoflagellate cysts belonging to taxon-groups. This explains the disparity between the two dominance curves at this sample, but is unclear whether this is biological or preservational phenomenon. Diversity remains low in samples K11 & K12 ($\alpha=12-14$), but higher, and very consistent between samples K13 to K16 ($\alpha=21-22$). Dominance is moderately high in the Ryazanian interval (20-23%), and quite consistent apart from a peak at sample K14 (33%). Diversity is low and quite variable in the mica-rich siltstones, and varies between $\alpha=2-6$ in the uppermost three samples from this section. Dominance is also variable, but has comparable values to the Ryazanian deposits. Samples K28-K30 are dominated by taxon-groups, with few other species recorded.

5.3.1.3. Summary

Diversity is generally lower in samples from basinal deposits (zarajskensis Subzone) than from the (open marine) neritic sediments. This accords with previous observations (Wall, 1971; Dale, 1976, 1983; Tyson, 1995). However, there appears to be little consistent difference in dinocyst diversity between samples from intertidal deposits and those thought to represent open marine neritic conditions, although the few phytoclast-dominated assemblages which possibly reflect reduced marine influence do have notably lower diversity. Samples from the mica-rich siltstones generally have lower and more highly variable diversity than the open marine neritic deposits. Such variable diversity possibly reflects fluctuations in fluvial output.

Dominance is generally higher, and most variable in the basinal deposits than in the neritic sediments. This probably reflects the low number of pelagic species and development of water column stratification. Dominance is comparatively low in all of the

neritic sediments (apart from those with phytoclast-dominated assemblages), including samples taken from intertidal deposits, and those with otherwise strong terrestrial influence (mic-rich siltstones). Since these deposits must have been brackish to some extent, this contrasts with numerous other studies (Wall *et al.*, 1977; Morzadec-Kerfourn, 1977; May, 1980; Piasecki, 1986; Goodman, 1987; Hunt, 1987; Lister & Batten, 1988; Andrews & Walton, 1990; Courtinat *et al.* 1991; Harding & Allen, 1995).

5.3.2: Chorate/Cavate/proximate groups

Previous studies of the distribution of chorate, cavate, and proximate dinoflagellate cysts have shown that there is a general gradation between proximate or cavate-dominated assemblages in inner neritic settings and chorate-dominated floras in open marine sediments (Vozzhennikova, 1965; Scull *et al.*, 1966; Davey, 1970; Riley, 1974; Davey & Rogers, 1975; Morzadec-Kerfourn, 1983; Sarjeant *et al.*, 1987; Tyson, 1985, 1989; Courtinat *et al.*, 1991; Tribovillard & Gorin, 1991; Hssaïda & Morzadec-Kerfourn, 1993; Sittler & Olivier-Pierre, 1994; Al-Ameri & Batten, 1997). To test whether this relationship exists in the Volga Basin assemblages, the data on the relative and absolute abundance of these groups has been compared with the palaeoecological interpretations presented earlier. The relative abundance data are presented as both binary and ternary plots to ensure that any relationships are identified. In this exercise skolochorate and proximochorate cysts are combined to form the chorate group.

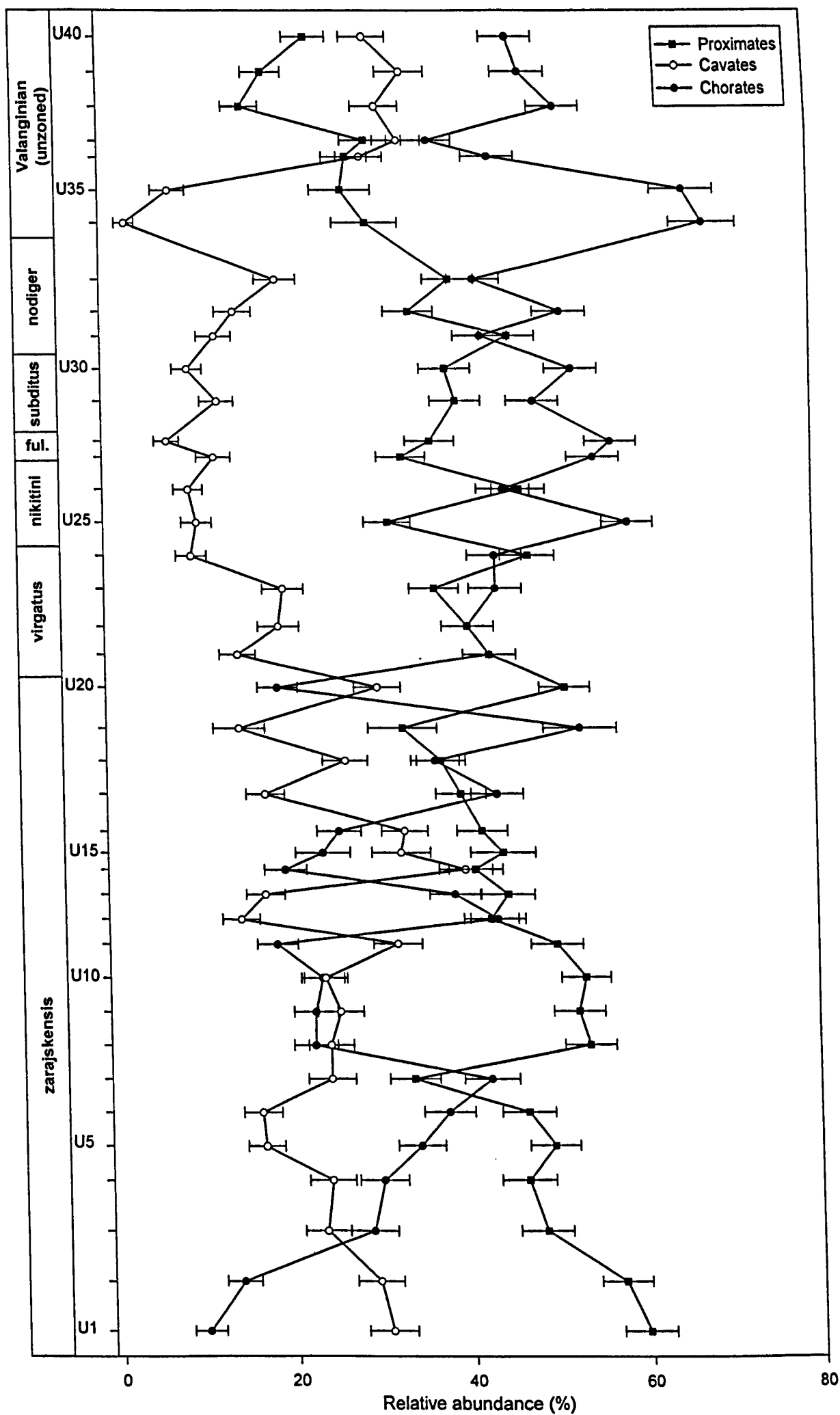
5.3.2.1. Gorodische

The data for Gorodische are presented in Table 5.9, and Figures 5.31 & 5.32. Figure 5.31 shows a general reduction in the abundance of proximate cysts through the zarajskensis Subzone (samples U1-U20) which is perhaps separable into two cycles about sample U7. Proximate relative abundance is variable through the virgatus to

Sample	Fisher Diversity	% error on Fisher diversity	Total error in Fisher Diversity	Goodman dominance (incl. bucket taxa)	Goodman dominance (excl. bucket taxa)	Total sklochorates	% Sklochorates	Standard error of %	Total proximochorates	% proximochorates	Standard error of %	Total chorates	% chorates	Standard error of %	Total cavates	% cavates	Standard error of %	Total proximates	% proximates	Standard error of %	Total delicate cysts	% delicate cysts	Standard error of %	Total robust cysts	% robust cysts	Standard error of %	log ratio
U40	14	9.8	1.37	19.2	19.2	84	27.8	2.58	55	18.2	2.22	139	47.2	2.95	90	29.8	2.63	70	23.2	2.43	189	112	0.59	-0.2			
U39	14.8	10	1.48	21	21	88	30.8	2.73	47	16.4	2.19	135	47.2	2.95	97	33.9	2.8	52	18.2	2.28	198	85	0.43	-0.4			
U38	17.2	10	1.72	18.4	18.4	93	32.3	2.76	54	18.8	2.3	147	51	2.95	89	30.9	2.72	45	15.6	2.14	183	99	0.54	-0.3			
U37	12.5	10.5	1.31	22.3	22.3	58	19.9	2.34	49	16.8	2.19	107	36.8	2.83	97	33.3	2.76	86	29.6	2.67	180	99	0.55	-0.3			
U36	15.2	9.7	1.47	14.5	14.5	89	30.1	2.87	40	13.5	1.99	129	43.6	2.88	86	29.1	2.64	81	27.4	2.59	169	106	0.63	-0.2			
U35	9.4	13.5	1.27	44.6	36.9	48	28.6	3.49	62	36.9	3.72	110	65.5	3.87	12	7.14	1.99	45	26.8	3.42	47	91	1.94	0.29			
U34	6.5	14.5	0.94	47	47	46	30.9	3.78	55	36.9	3.95	101	67.8	3.83	3	2.01	1.15	44	29.5	3.74	54	72	1.33	0.12			
U33	18.5	9.8	1.81	21.1	15.8	106	37.2	2.86	13	4.56	1.24	119	41.8	2.92	55	19.3	2.34	111	38.9	2.89	67	184	2.11	0.33			
U32	13.3	10.8	1.44	25.8	17.7	106	39.1	2.96	33	12.2	1.99	139	51.3	3.04	39	14.4	2.13	93	34.3	2.88	121	126	1.04	0.02			
U31	18.3	9.9	1.81	22.5	22.5	94	34.7	2.89	21	7.75	1.62	115	42.4	3	33	12.2	1.99	123	45.4	3.02	89	157	1.76	0.25			
U30	19.9	9.6	1.91	25	25	126	45.7	3	19	6.88	1.52	145	52.5	3.01	25	9.06	1.73	106	38.4	2.93	115	151	1.31	0.12			
U29	16.5	9.8	1.62	25	25.4	107	38.8	2.93	33	11.3	1.86	140	48.1	2.93	36	12.4	1.93	115	39.5	2.87	114	184	1.44	0.16			
U28	16.2	9.7	1.57	32.8	28.6	147	50.7	2.94	18	6.21	1.42	165	56.9	2.91	33	11.9	1.95	92	33.2	2.83	86	139	1.62	0.21			
U27	17.2	10	1.72	17.3	17.3	125	45.1	2.99	27	9.75	1.78	152	54.9	2.99	26	8.93	1.67	135	46.4	2.92	67	173	2.58	0.41			
U26	17	9.7	1.65	14.1	10.7	103	35.4	2.8	27	9.28	1.7	130	44.7	2.91	29	9.83	1.73	93	31.5	2.71	80	183	2.29	0.36			
U25	14	10	1.4	33.2	12.5	154	52.2	2.91	19	6.44	1.43	173	58.6	2.87	25	9.16	1.75	129	47.3	3.02	83	139	1.67	0.22			
U24	23	9.6	2.21	15.8	16	73	26.7	2.68	46	16.8	2.27	119	43.6	3	57	19.6	2.33	107	36.8	2.83	92	150	1.63	0.21			
U23	17	10	1.74	14.1	14	98	33.7	2.77	29	9.97	1.76	127	43.6	2.91	54	19	2.33	115	40.5	2.91	116	148	1.28	0.11			
U22	15	10.4	1.56	13	13	69	24.3	2.54	46	16.2	2.19	115	40.5	2.91	41	14.3	2.07	123	42.9	2.92	75	138	1.84	0.26			
U21	19	9.7	1.84	11.1	11	80	27.9	2.65	43	15	2.11	123	42.9	2.92	88	30	2.68	150	51.2	2.92	134	120	0.9	0			
U20	6.3	12.2	0.77	56.3	36.9	43	14.7	2.07	12	4.1	1.16	55	18.8	2.82	20	14.3	2.96	46	32.9	3.97	70	53	0.76	-0.1			
U19	11	14	1.54	35.7	36	68	48.6	4.22	6	4.29	1.71	74	52.9	4.22	79	26.2	2.54	112	37.2	2.79	155	111	0.72	-0.1			
U18	12.4	10.2	1.26	26.6	24.9	98	32.6	2.7	12	3.99	1.13	110	36.5	2.78	79	26.2	2.54	112	37.2	2.79	155	111	0.72	-0.1			
U17	11.9	10.5	1.25	22.9	23	107	36	2.79	22	7.41	1.52	129	43.4	2.88	51	17.2	2.19	117	39.4	2.84	120	116	0.97	0			
U16	12	10.3	1.24	35.2	35	60	19.5	2.26	18	5.86	1.34	78	25.4	2.48	101	32.9	2.68	128	41.7	2.81	169	90	0.53	-0.3			
U15	9	12.8	1.15	41.4	36.1	33	17.3	2.74	12	6.28	1.76	45	23.6	3.07	62	32.5	3.39	84	44	3.59	92	56	0.61	-0.2			
U14	12.8	11	1.41	45	41.6	35	13	2.05	107	63.2	1.48	52	19.3	2.41	107	39.8	2.98	110	40.9	3	151	87	0.58	-0.2			
U13	12.2	10.8	1.32	22.9	21.9	104	36.1	2.83	7	2.43	0.91	111	38.5	2.87	49	17	2.21	128	44.4	2.93	127	91	0.72	-0.1			
U12	12.8	11	1.41	26.1	22	104	38.8	2.98	12	4.48	1.26	116	43.3	3.03	38	14.2	2.13	114	42.5	3.02	134	92	0.69	-0.2			
U11	14.8	10.2	1.51	35.5	35.5	41	14.7	2.12	10	3.58	1.11	51	18.3	2.31	89	31.9	2.79	139	49.8	2.99	172	81	0.47	-0.3			
U10	13.9	9.8	1.36	33	27.2	61	19.7	2.26	11	3.56	1.05	72	23.3	2.4	73	23.6	2.42	164	53.1	2.84	218	83	0.38	-0.4			
U9	9.7	11.6	1.13	30.4	26	46	15.9	2.15	19	6.57	1.46	65	22.5	2.46	73	25.3	2.56	151	52.2	2.94	106	86	0.81	-0.1			
U8	4.7	13	0.61	38.6	31	60	20.7	2.38	5	1.72	0.76	65	22.4	2.45	70	24.1	2.51	155	53.4	2.93	108	63	0.58	-0.2			
U7	8.2	12	0.99	40.4	40.4	105	39.6	3	7	2.64	0.99	112	42.3	3.03	64	24.2	2.63	89	33.6	2.9	133	77	0.58	-0.2			
U6	13	10.3	1.34	23.3	23	85	30	2.72	21	7.42	1.56	106	37.5	2.88	46	16.3	2.19	131	46.3	2.96	160	111	0.69	-0.2			
U5	14.4	9.8	1.41	22.1	22	80	26.1	2.51	25	8.14	1.56	105	34.2	2.71	51	16.6	2.12	151	49.2	2.85	166	114	0.69	-0.2			
U4	15	10.3	1.55	30.2	28.4	69	25.1	2.61	13	4.73	1.28	82	29.8	2.76	66	24	2.58	127	46.2	3.01	165	81	0.49	-0.3			
U3	13.9	10.2	1.42	27.9	25.1	69	24	2.52	13	4.53	1.23	82	28.6	2.67	67	23.3	2.5	138	48.1	2.95	173	104	0.6	-0.2			
U2	9.9	11	1.09	47.2	36.4	32	10.5	1.75	10	3.28	1.02	42	13.6	1.97	89	29.2	2.6	174	57	2.83	160	100	0.63	-0.2			
U1	7.9	12	0.95	52	29.8	23	8.36	1.67	4	1.45	0.72	27	9.82	1.79	84	30.5	2.78	164	59.6	2.96	111	89	0.8	-0.1			

Table 5.9: Dinoocyst data from Gerodische.

Figure 5.31: Relative abundance of chorate, cavate, and proximate cyst morphologies at Gorodische.



nodiger zone interval (31 - 47%)(samples U21-U33), and significantly lower in the mica-rich siltstones than in samples from any of the other lithologies. The relative abundance of chorate cysts broadly shows an opposing trend with major deviations from this caused by data closure against the cavate group. Thus chorate relative abundance increases through the lower part of the zarajskensis Subzone (samples U1-U7), and is highly variable in the upper part. The abundance of this group is quite consistent (42 - 44%) through the coarse-grained deposits of the virgatus Zone (U21-U24), and variable, with decreasing abundance (58-42%) through the fine-grained sandstones of the nikitini - nodiger zone interval (samples U25-U33). The abundance of this group peaks in the phytoclast-dominated samples at the base of the mica-rich siltstones (66-68%) (samples U34 & U35) and thereafter is of comparable abundance to the nodiger Zone. The abundance of cavate cysts is inconsistent and largely independent of lithology in the zarajskensis Subzone and virgatus Zone (U1-U24), but more consistent, and generally lower in the nikitini to nodiger zones (U25-U33). Minimum abundance of this group occurs in the basal samples from the mica-rich siltstones, and thereafter higher values are maintained until the top of the section.

This information is plotted on a ternary diagram in Figure 5.32a, and the sample points are clustered according to lithology in Figure 5.32b. Despite the fact that many of the clusters overlap, some lithological discrimination is possible. The mica-rich siltstone samples fall in two sub-clusters, both with low proximate abundance, but one with particularly low cavate abundance (containing samples U34 & U35, Sub-cluster F2). The sediments with coarsest grain size, or those considered to have been deposited most proximally to the terrestrial source are located closest to the centre of the diagram (clusters C, D, & F). The transition from low chorate abundance in the mudstones to higher values in the proximal deposits contrasts to the expected trend as discussed above.

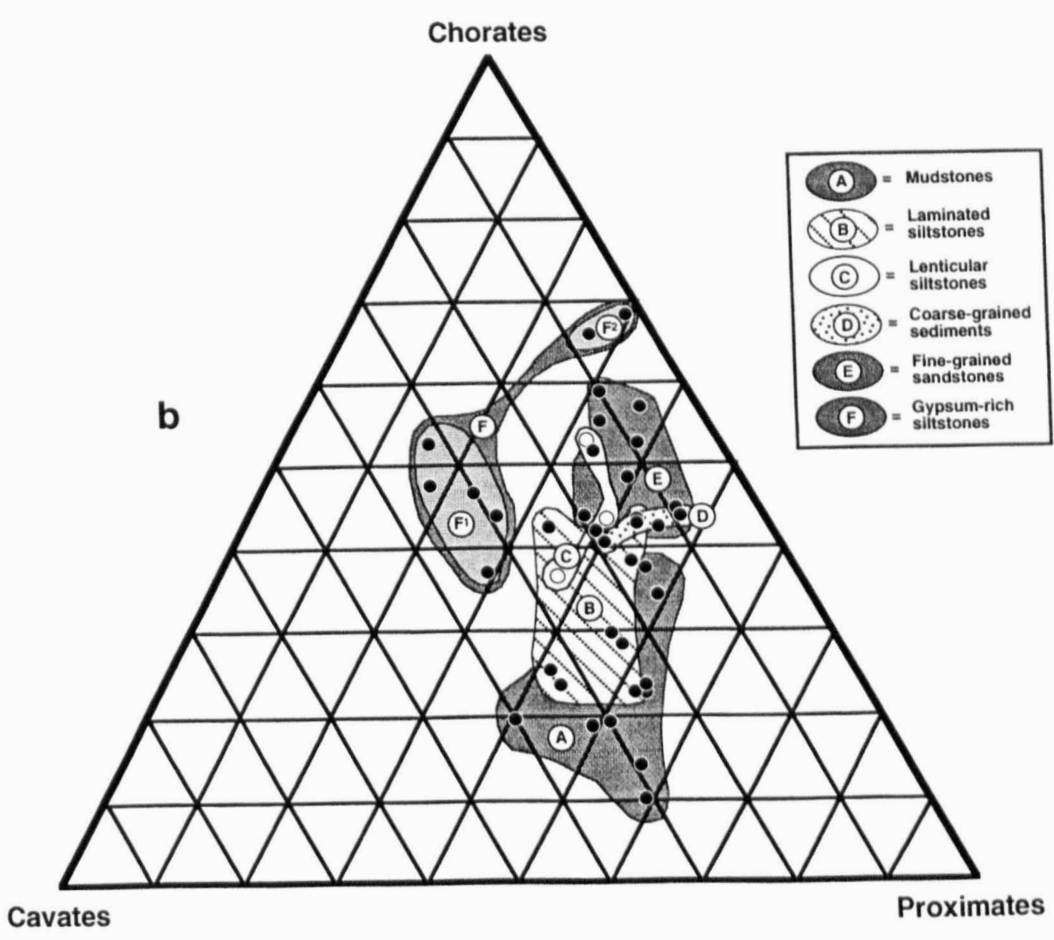
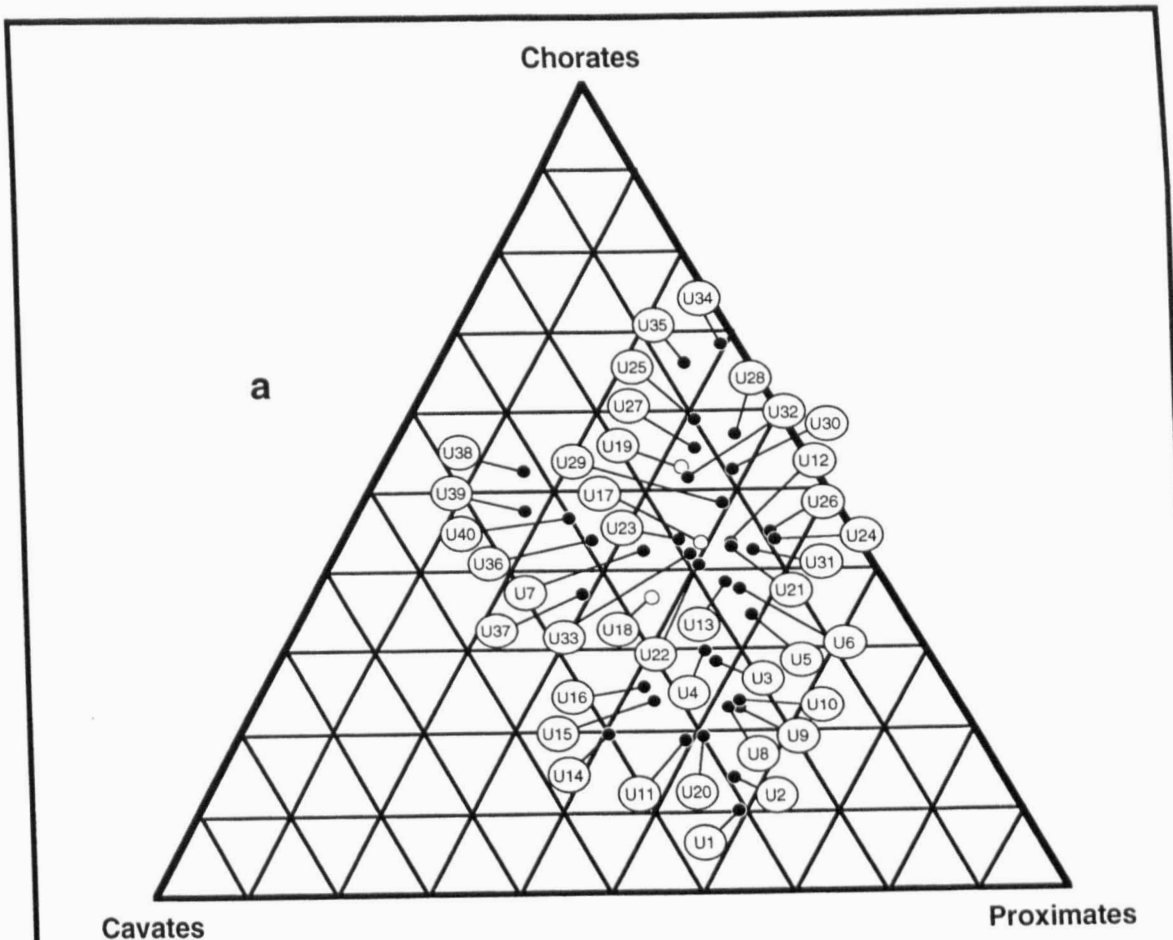


Figure 5.32: Ternary plots of chorate / cavate/ and proximate dinocyst relative abundance at Gorodische. Samples from the lenticular siltstones shown by open circles. **a:** Showing sample points. **b:** Showing clusters according to lithology.

5.3.2.2. Kashpir

Data for Kashpir is presented in Table 5.10, and Figures 5.33 & 5.34. Figure 5.33 shows that there is considerable variation in the relative abundance of these groups at Kashpir, and that very few consistent trends can be isolated. Generally low chorate abundance occurs in the two samples taken from the *zarajskensis* Subzone, and in the samples taken from phytoclast-dominated palynofacies (K10, K28-K30). Proximate abundance is similar in the majority of samples examined, but is significantly higher, and higher than chorate relative abundance in the phytoclast-dominated assemblages. Cavate abundance is variable, and highest in the sample taken from the mudstone lithology at the base of the *zarajskensis* Subzone (K2).

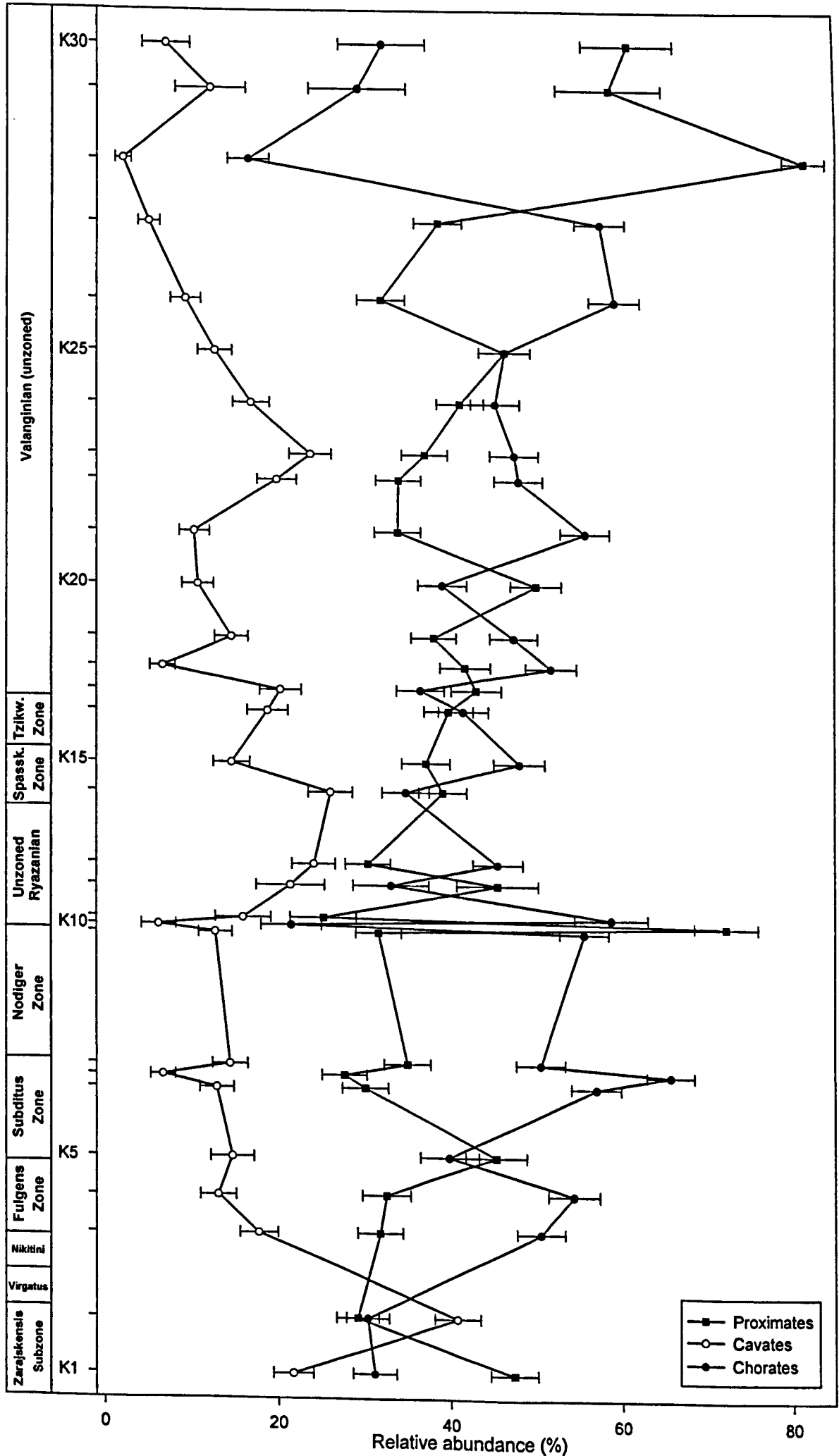
As a result of the lack of consistent trends in this data, the majority of samples fall within a single area when plotted on a ternary diagram (Figure 5.34). The two samples from the *zarajskensis* Subzone are separable into Cluster A, which is approximately comparable to the position of samples from similar sediments at Gorodische. Cluster B, containing the samples from the mica-rich siltstones falls on the right hand-side of the diagram (low relative abundance of cavate cysts), in contrast to the position of the corresponding cluster from Gorodische.

As mentioned earlier, the 'model' distribution of cysts is such that delicate chorate types are associated with open marine conditions, whilst robust proximate or cavate form are most common in inner neritic environments. Thus far, the data have not supported a chorate to proximate/cavate transition. This raises the question of whether the distribution of cysts is controlled by their durability rather than length of processes. Unfortunately, in the absence of experimental data on dinocyst abrasion, there is no objective or rigorous way to test this. However, from the available data, the majority of species encountered have been split into 'delicate' and 'robust' categories according to their appearance under the transmitted light microscope. Species with thick walls and/or simple, thick processes were considered more robust than species

Sample	dinocyst total	Fisher Diversity	% Error on Fisher Diversity	Total Error on Fisher Diversity	Goodman Dominance (incl. bucket taxa)	Goodman Dominance (excl. bucket taxa)	Total skolochores	% skolochores	Standard error of %	Total proximochores	% proximochores	Standard error of %	Total chorates	%chorates	Standard error of %	Total cavates	%cavates	Standard error of %	Total proximates	%proximates	Standard error of %	Total robust cysts	Total delicate cysts	ratio delicate:robust	log of ratio
K30	84	4	20	0.8	45.2	11.9	24	28.6	4.93	3	3.57	2.02	27	32.1	5.1	6	7.14	2.81	51	60.7	5.33	11	49	0.22	-0.6
K29	65	1.2	23	0.28	55.4	13.8	19	29.2	5.64	0	0	0	19	29.2	5.64	8	12.3	4.07	38	58.5	6.11	9	38	0.24	-0.6
K28	240	6.2	13	0.81	67.9	6.67	26	10.8	2.01	14	5.83	1.51	40	16.7	2.41	5	2.08	0.92	195	81.3	2.52	25	180	0.14	-0.9
K27	293	15	9.8	1.47	26.6	26.6	93	31.7	2.72	75	25.6	2.55	168	57.3	2.89	15	5.12	1.29	113	38.6	2.84	126	152	0.83	-0.1
K26	276	12	11.2	1.34	27.5	27.5	115	41.7	2.97	48	17.4	2.28	163	59.1	2.96	26	9.42	1.76	88	31.9	2.81	123	146	0.84	-0.1
K25	289	14	10	1.4	22.8	22.8	81	28	2.64	53	18.3	2.28	134	46.4	2.93	37	12.8	1.97	134	46.4	2.93	110	148	0.74	-0.1
K24	318	21	9.1	1.91	13.2	12.9	86	27	2.49	58	18.2	2.17	144	45.3	2.79	54	17	2.11	131	41.2	2.76	171	129	1.33	0.12
K23	316	14	9.7	1.36	21.5	22	77	24.4	2.41	73	23.1	2.37	150	47.5	2.81	75	23.7	2.39	117	37	2.72	121	179	0.68	-0.2
K22	321	10.5	10.5	1.1	25.9	26	74	23.1	2.35	80	24.9	2.41	154	48	2.79	64	19.9	2.23	109	34	2.64	161	150	1.07	0.03
K21	307	14.2	9.8	1.39	17.9	18	80	26.1	2.51	91	29.6	2.61	171	55.7	2.84	32	10.4	1.74	104	33.9	2.7	160	140	1.14	0.06
K20	286	23	9.5	2.19	26.2	26	59	20.6	2.39	53	18.5	2.3	112	39.2	2.89	31	10.8	1.84	143	50	2.96	129	150	0.86	-0.1
K19	333	19	9.2	1.75	20.1	20	82	24.6	2.36	76	22.8	2.3	158	47.4	2.74	49	14.7	1.94	127	38.1	2.66	146	187	0.87	-0.1
K18	282	17.5	9.7	1.7	22	22	69	24.5	2.56	77	27.3	2.65	146	51.8	2.98	19	6.74	1.49	118	41.8	2.94	135	134	1.01	0
K17	290	31	9	2.79	17.6	18	63	21.7	2.42	43	14.8	2.09	106	36.6	2.83	59	20.3	2.36	125	43.1	2.91	153	102	1.5	0.18
K16	286	21.5	9.5	2.04	20.3	18.9	74	25.9	2.59	45	15.7	2.15	119	41.6	2.91	54	18.9	2.31	114	39.9	2.9	165	111	1.49	0.17
K15	285	22	9.5	2.09	21.4	21	74	26	2.6	63	22.1	2.46	137	48.1	2.96	42	14.7	2.1	106	37.2	2.86	173	100	1.73	0.24
K14	296	21.5	9.4	2.02	33.4	33	49	16.6	2.16	54	18.2	2.24	103	34.8	2.77	77	26	2.55	116	39.2	2.84	154	135	1.14	0.06
K13	303	22.5	9.2	2.07	23.8	23.8	89	29.4	2.62	49	16.2	2.12	138	45.5	2.86	73	24.1	2.46	92	30.4	2.64	145	136	1.07	0.03
K12	112	9.5	15.1	1.43	24.1	17.9	32	28.6	4.27	5	4.46	1.95	37	33	4.44	24	21.4	3.88	51	45.5	4.71	42	42	1	0
K11	131	12.5	14	1.75	22.9	23	44	33.6	4.13	33	25.2	3.79	77	58.8	4.3	21	16	3.21	33	25.2	3.79	85	46	1.85	0.27
K10	144	0.6	22	0.13	38.9	0	31	21.5	3.43	0	0	0	31	21.5	3.43	9	6.25	2.02	104	72.2	3.73	44	20	2.2	0.34
K9	304	22.5	9.2	2.07	14.8	15	103	33.9	2.71	66	21.7	2.36	169	55.6	2.85	39	12.8	1.92	96	31.6	2.67	175	103	1.7	0.23
K8	303	20.2	9.4	1.9	22.4	12.5	102	33.7	2.71	51	16.8	2.15	153	50.5	2.87	44	14.5	2.02	106	35	2.74	210	81	2.59	0.41
K7	297	16.4	9.7	1.59	25.6	17.8	128	43.1	2.87	67	22.6	2.43	195	65.7	2.76	20	6.73	1.45	82	27.6	2.59	203	86	2.36	0.37
K6	293	21.5	9.5	2.04	25.6	11.3	125	42.7	2.89	42	14.3	2.05	167	57	2.89	38	13	1.96	88	30	2.68	196	76	2.58	0.41
K5	203	20.5	11.5	2.36	14.8	15	60	29.6	3.2	21	10.3	2.14	81	39.9	3.44	30	14.8	2.49	92	45.3	3.49	75	64	1.17	0.07
K4	274	19.8	9.7	1.92	19	19	119	43.4	2.99	30	10.9	1.89	149	54.4	3.01	36	13.1	2.04	89	32.5	2.83	144	100	1.44	0.16
K3	309	23	9.1	2.09	18.8	19	117	37.9	2.76	39	12.6	1.89	156	50.5	2.84	55	17.8	2.18	98	31.7	2.65	132	149	0.89	-0.1
K2	341	13.5	9.5	1.28	41.9	42	95	27.9	2.43	8	2.35	0.82	103	30.2	2.49	139	40.8	2.66	99	29	2.46	80	198	0.4	-0.4
K1	332	13.8	9.5	1.31	25.3	25	91	27.4	2.45	12	3.61	1.02	103	31	2.54	72	21.7	2.26	157	47.3	2.74	111	156	0.71	-0.1

Table 5.10: Dinocyst data from Kashpir.

Figure 5.33: Relative abundance of chorate, cavate, and proximate cyst morphologies at Kashpir.



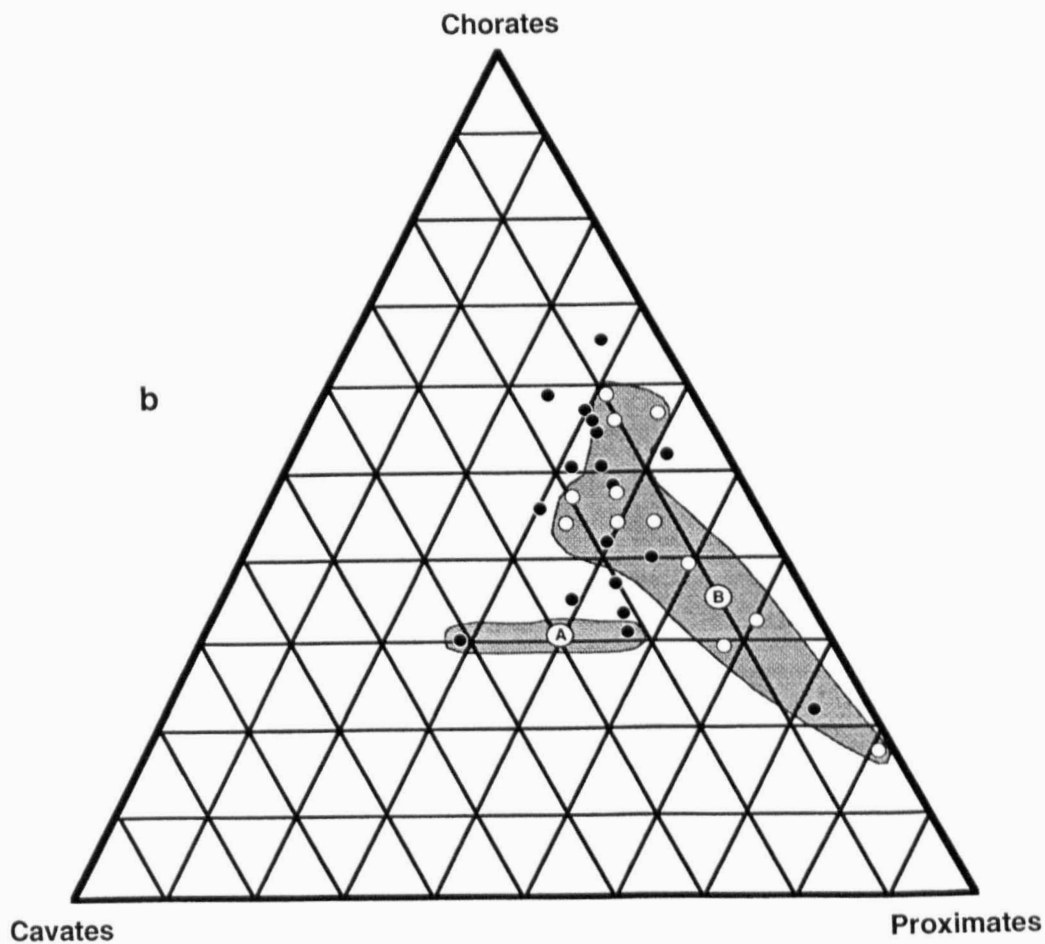
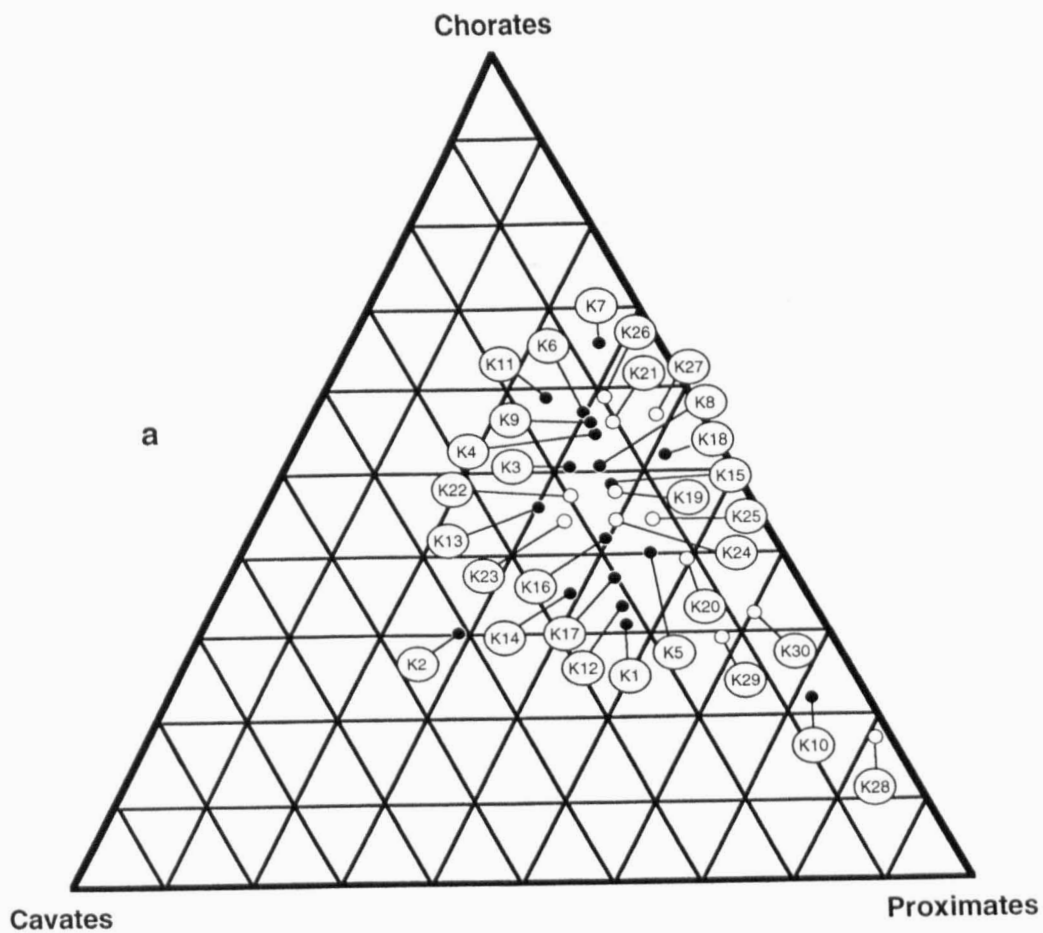


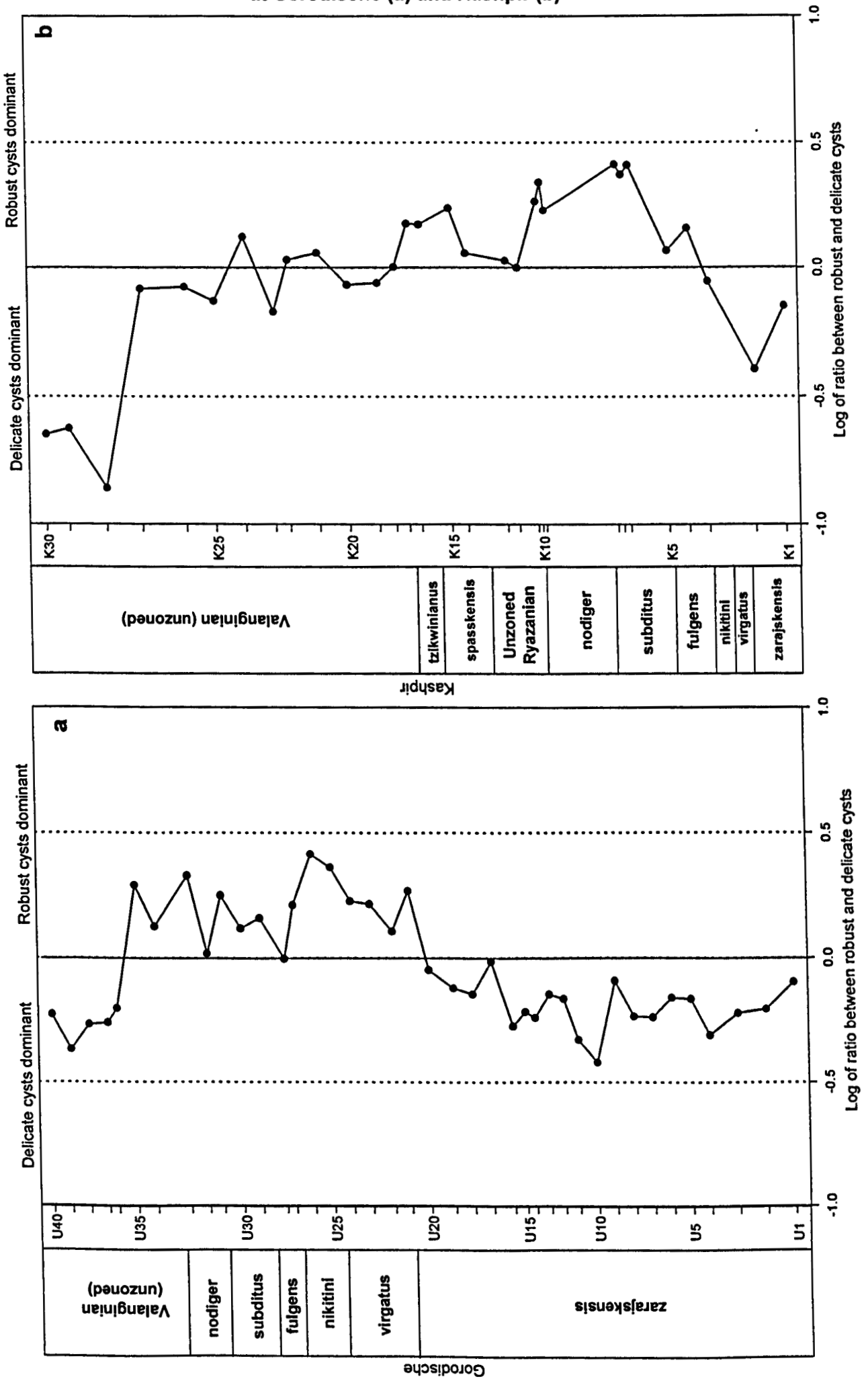
Figure 5.34: Ternary plots of chorate / cavate / and proximate dinocyst relative abundance at Kashpir. Samples from mica-rich siltstones shown by open circles. **a:** Showing sample points. **b:** Showing limited clustering according to lithology.

Table 5.11.

Robust cysts	Delicate cysts
<i>Achomosphaera neptuni</i>	<i>Aprobolocysta pustulosa</i>
<i>Ambonosphaera staffinensis</i>	<i>Avellodinium falsificum</i>
<i>Aprobolocysta galeata</i>	" <i>Batiacasphaera fenestrata</i> "
<i>Apteodinium spinosum</i>	<i>Cassiculosphaeridia reticulata</i>
<i>Batiacasphaera</i> sp. 2	<i>Chlamydophorella nyei</i>
<i>Batioladinium gochtii</i>	<i>Chytroeisphaeridia cerastes</i>
<i>Batioladinium longicornutum</i>	<i>Chytroeisphaeridia chytroeides</i>
<i>Batioladinium</i> sp. 1	" <i>Circulodinium ciliatum</i> "
<i>Cassiculosphaeridia magna</i>	<i>Circulodinium compta</i>
<i>Circulodinium copei</i>	" <i>Circulodinium granulatum</i> "
<i>Cometodinium habibii</i>	<i>Cometodinium whiteii</i>
<i>Cribroperidinium nuciforme</i>	<i>Cribroperidinium erymnoseptatum</i>
<i>Cribroperidinium</i> sp. 1	<i>Cribroperidinium</i> sp. 7
<i>Cribroperidinium</i> sp. 2	<i>Cymosphaeridium validum</i>
<i>Cribroperidinium</i> sp. 3	<i>Dapsilidinium multispinosum</i>
<i>Cribroperidinium</i> sp. 8	<i>Dichadogonyaulax chondrum</i>
<i>Ctenidodinium</i> sp. 1	<i>Dingodinium cerviculum</i>
<i>Egmontodinium polyplacophorum</i>	<i>Dingodinium jurassicum</i>
<i>Endoscrinium campanula</i>	<i>Dingodinium tuberosum</i>
<i>Endoscrinium granulatum</i>	<i>Downiesphaeridium</i> sp. 2
<i>Endoscrinium inritibile</i>	<i>Egmontodinium</i> sp. 1
<i>Endoscrinium pharo</i>	<i>Egmontodinium torynum</i>
<i>Exochosphaeridium phragmites</i>	<i>Gardodinium</i> sp.
<i>Gochteodinia villosa</i>	<i>Glossodinium dimorphum</i>
<i>Gonyaulacysta</i> sp. 4	<i>Gochteodinia tuberculata</i>
<i>Gonyaulacysta</i> aff. <i>centriconnata</i>	<i>Gonyaulacysta dentata</i>
<i>Gonyaulacysta pectiniger</i>	<i>Heslertonia</i> sp. 1
<i>Impletosphaeridium</i> sp. 1	<i>Hystrichosphaeridium petilum</i>
<i>Impletosphaeridium polytrichum</i>	<i>Hystrichodinium pulchrum</i>
<i>Isthmocystis distincta</i>	<i>Impletosphaeridium lumectum</i>
<i>Kleithriasphaeridium corrugatum</i>	<i>Kallosphaeridium</i> sp. 2
<i>Kleithriasphaeridium eoinodes</i>	<i>Lagenadinium membranoideum</i>
<i>Kleithriasphaeridium fasciatum</i>	<i>Lithodinia bulloidea</i>
<i>Kleithriasphaeridium porosispinum</i>	<i>Muderongia longicorna</i>
<i>Leptodinium subtile</i>	<i>Oligosphaeridium complex</i>
<i>Lithodinia acranitabulata</i>	<i>Oligosphaeridium pulcherrimum</i>
<i>Lithodinia</i> sp. 1	<i>Perisseiasphaeridium ingegerdiae</i>
<i>Nelchinopsis kostromiensis</i>	<i>Phoberocysta neocomica</i>
<i>Pereodinia ceratophora</i>	<i>Prolixosphaeridium parvispinum</i>
<i>Phoberocysta tabulata</i>	<i>Pseudoceratium pelliferum</i>
<i>Pseudoceratium</i> sp. 1	<i>Rhynchodiniopsis magna</i>
<i>Senoniasphaera jurassica</i>	<i>Rhynchodiniopsis martonense</i>
<i>Sentusidinium</i> cf. sp. 1	<i>Spiniferites primaevus</i>
<i>Sentusidinium fibrillospinosum</i>	<i>Spiniferites</i> sp. 2
<i>Sentusidinium rioultii</i>	<i>Stanfordella exanguia</i>
<i>Sentusidinium</i> sp. 1	<i>Stiphrosphaeridium anthophorum</i>
<i>Sentusidinium</i> sp. 2	<i>Stiphrosphaeridium dictyophorum</i>
<i>Stanfordella fastigiata</i>	<i>Systematophora daveyi</i>
<i>Sirmiodinium grossi</i>	<i>Systematophora</i> sp. 1

<i>Spiniferites ramosus</i>	<i>Tanyosphaeridium magneticum</i>
<i>Tehamadinium daveyi</i>	<i>Tehamadinium sousense</i>
<i>Tehamadinium</i> sp. 1	<i>Trichodinium</i> sp. 1
<i>Tenua hystrix</i>	<i>Walloodium krutzschii</i>
<i>Tenua</i> cf. <i>hystrix</i>	<i>Warrenia brevispinosa</i>
<i>Trichodinium</i> cf. <i>ciliatum</i>	
<i>Trichodinium ciliatum</i>	
<i>Tubotuberella apatela</i>	
<i>Tubotuberella</i> cf. <i>apatela</i>	
<i>Valensiella ovula</i>	
<i>Wrevittia</i> cf. <i>helicoidea</i>	

Figure 5.35: Log of ratio between robust and delicate cysts at Gorodische (a) and Kashpir (b)



with thin, delicate walls, and thin or intricate processes. The groups into which each of the taxa have been placed are displayed in Table 5.11. The log of the ratio between robust and delicate cysts is plotted from both sections in Figure 5.35. Points plotted to the right of the 'zero' line represent assemblages dominated by robust cyst taxa. Thus, robust cysts dominate the assemblages in the sample interval U21-U34 at Gorodische, and K4-K18 at Kashpir. These intervals correspond to the coarsest-grained open marine neritic sediments. Conversely, delicate cysts are most abundant in the finer-grained sediments deposited under lower energy conditions. Thus, there is a strong correlation between the sediment grain size, and the nature of the dinocyst assemblages. However, it remains unclear whether such a relationship is a result of preferential preservation of cysts with robust morphology in higher energy sediments, or whether more cysts with robust morphology are produced in response to higher energy conditions.

5.3.2.3. Absolute abundance data

The data on absolute abundance for these sections are presented in Tables 5.12 & 5.13, and Figure 5.36. Both of the abundance plots show that the trends of each group are closely comparable, and minor variation in the ratios between these groups are largely masked by some overriding signal. Moreover the trends displayed are quite similar to the plots generated from the palynofacies data (Figs. 5.12 & 5.26). This suggests that the controls acting on the dinoflagellate cyst population are the same as those on the other structured elements of the palynofacies. One possible explanation for this is that productivity of dinoflagellate population changed with supply of terrestrial organic nutrients. However, such a phenomenon is usually associated with peridinioid-dominated assemblages unlike those encountered in this study. The interaction of clastic sediment dilution rate and level of sea-water oxygenation was used to explain this pattern in the palynofacies data, and it is therefore inferred to be the dominant control on the absolute abundance of the three cyst morphologies.

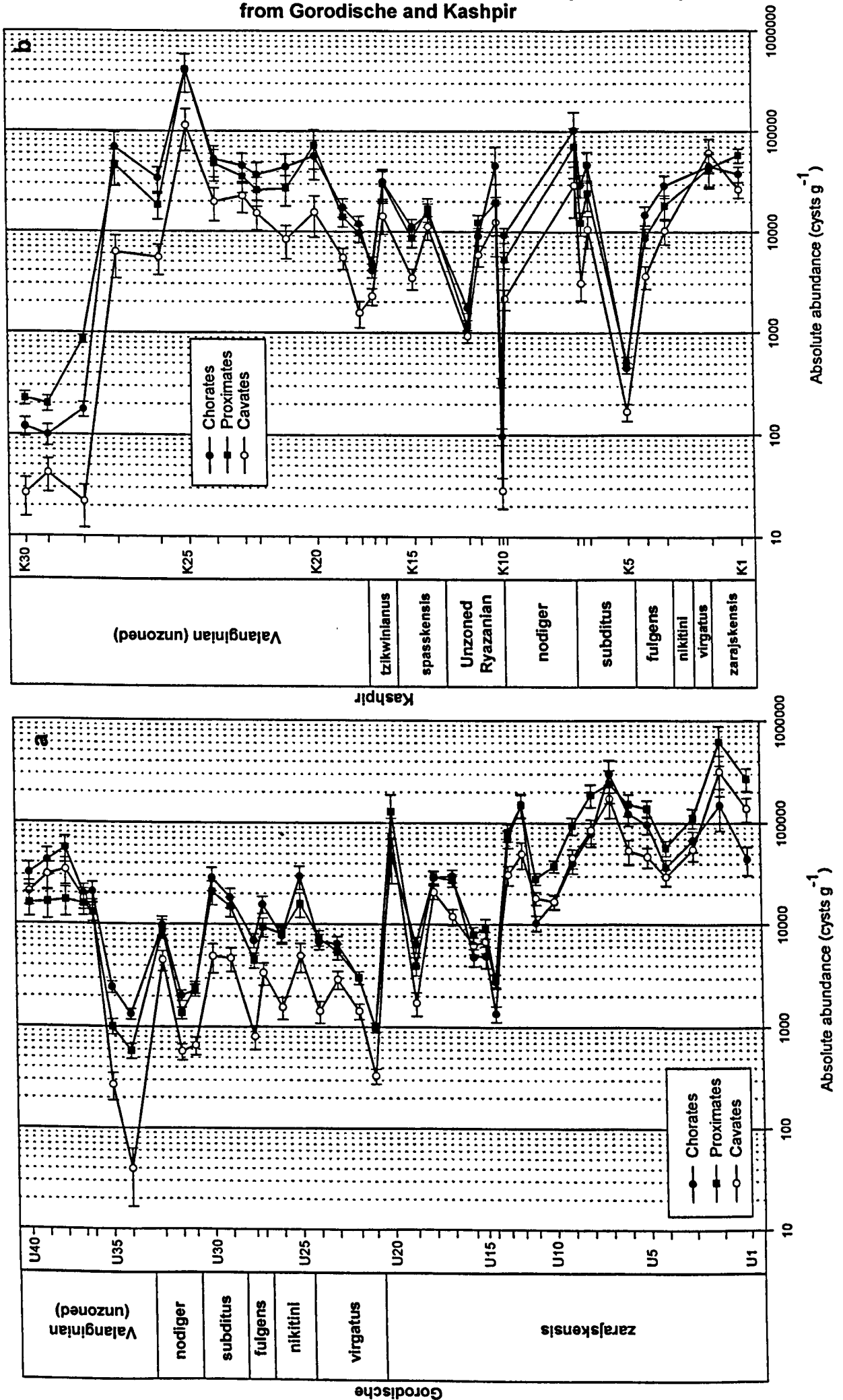
Sample	Total skolochorates	Absolute abundance	% error on absolute abundance	Error on absolute abundance	Total proximochorates	Absolute abundance	% error on absolute abundance	Error on absolute abundance	Total chorates	Absolute abundance	% error on absolute abundance	Error on absolute abundance	Total cavates	Absolute abundance	% error on absolute abundance	Error on absolute abundance	Total proximates	Absolute abundance	% error on absolute abundance	Error on absolute abundance
U40	84	19226	26.8	5152.8	55	12589	27.9	3518.2	139	31815	25.9	8242.3	90	20599	26.7	5490.3	70	16022	27.2	4364.6
U39	88	27731	31	8583.1	47	14811	32.5	4815.5	135	42542	30.3	12893	97	30567	30.8	9408.7	52	16387	32.2	5276
U38	93	35652	29.8	10623	54	20701	31.1	6432.1	147	56353	29.1	16413	89	34118	29.9	10193	45	17251	31.7	5461.9
U37	58	10673	24.9	2653.7	49	9018.8	25.5	2298.6	107	19690	23.2	4572.3	97	17850	23.4	4181.9	86	15825	23.7	3751.9
U36	89	14319	24	3442.3	40	6435.6	26.7	1721.5	129	20755	23.3	4836.7	86	13837	24.1	3337.6	81	13032	24.3	3162.9
U35	48	1070.1	16.7	178.36	62	1382.2	15.2	209.97	110	2452.3	12.7	310.58	12	267.52	30	80.382	45	1003.2	17.1	171.34
U34	46	607.27	16.3	99.176	55	728.09	15.2	110.39	101	1333.4	12.2	162.39	3	39.605	58.2	23.034	44	580.87	16.6	96.606
U33	106	8703.6	20.4	1779.1	13	1067.4	33.1	352.86	119	9771.1	20.2	1972.6	55	4516	22.5	1015.2	111	9114.2	20.3	1853.6
U32	106	1556.9	12.9	200.12	33	484.69	19.3	93.724	139	2041.6	12	243.99	39	572.81	18.1	103.63	93	1365.9	13.4	182.45
U31	94	1871.8	14	262.11	21	418.12	23.8	99.469	115	2289.7	13.3	304.37	33	657.05	19.8	130.22	123	2449	13.1	320.3
U30	126	24745	26.1	6446.1	19	3731.4	33.5	1251.9	145	28476	25.8	7361.1	25	4909.7	31.6	1552	106	20817	26.3	5482.4
U29	107	13975	22.1	3090.7	33	4310.1	26.4	1139.3	140	18285	21.6	3951.7	36	4701.9	26	1220.2	115	15020	22	3299.6
U28	147	6257.6	15.6	975.41	18	766.24	27	207.1	165	7023.8	15.3	1078	19	808.8	26.5	214.18	106	4512.3	16.4	740.46
U27	125	12844	19.6	2520.6	27	2774.3	26	721.06	152	15618	19.3	3008	33	3390.8	24.7	836.21	92	9453.3	20.3	1923
U26	103	6185.7	18	1116	27	1621.5	24.5	396.78	130	7807.2	17.5	1364.2	26	1561.4	24.8	386.6	135	8107.5	17.4	1410
U25	154	26357	26.5	6978.2	19	3251.9	34.1	1108.7	173	29609	26.3	7799.2	29	4963.4	31.3	1554.5	93	15917	27.3	4340.3
U24	73	4189.6	18.2	760.87	46	2640	20.3	534.71	119	6829.6	16.6	1136.4	25	1434.8	24.3	349.34	129	7403.5	18.4	1217.3
U23	98	5030.5	17.7	890.06	29	1488.6	23.6	350.96	127	6519.1	17	1109.7	57	2925.9	19.7	575.18	107	5492.5	17.4	958.39
U22	69	1834.7	16.1	295.9	46	1223.1	18.2	223.06	115	3057.9	14.2	434.75	54	1435.9	17.3	248.85	115	3057.9	14.2	434.75
U21	80	644.16	12.5	80.428	43	346.24	16.2	56.198	123	990.4	10.6	104.9	41	330.13	16.6	54.726	123	990.4	10.6	104.9
U20	43	37108	47.4	17577	12	10356	53.3	5523	55	47464	46.8	22226	88	75942	46.1	35005	150	129447	45.8	59004
U19	68	5897.5	18.2	1072.1	6	520.37	43	223.82	74	6417.9	17.8	1145.5	20	1734.6	26.1	453.45	46	3989.5	20	798.71
U18	98	25876	14.8	3823.3	12	3168.5	30.8	976.4	110	29045	14.4	4180.7	79	20859	15.6	3250.7	112	29573	14.3	4240
U17	107	25041	14.8	3709.2	22	5148.6	24.1	1240.5	129	30190	14.3	4306.4	51	11935	17.9	2141.8	117	27381	14.5	3981.4
U16	60	3726.5	19.9	740.68	18	1117.9	28	313.01	78	4844.4	18.9	914.82	101	6272.9	18.1	1135	128	7949.8	17.5	1391.8
U15	33	3633.8	25.4	924.56	12	1321.4	34.3	453.46	45	4955.1	23.8	1179.5	62	6827.1	22.5	1535.2	84	9249.6	21.5	1991.1
U14	35	919.62	20.2	186	17	446.87	26.7	119.15	52	1366.3	17.8	242.76	107	2811.4	14.7	413.99	110	2890.2	14.6	423.08
U13	104	66017	19.4	12826	7	4443.5	41.4	1837.4	111	70461	19.3	13578	49	31104	22	6852.6	128	81252	19	15404
U12	104	136726	25.7	35198	12	15776	37.4	5902.7	116	152502	25.5	38964	38	49958	28.8	14390	114	149873	25.6	38336
U11	41	8342.3	18.5	1542.5	10	2034.7	33.1	674.22	51	10377	17.1	1779.4	89	18109	14.5	2626.3	139	28283	13	3686.6
U10	61	14064	16.6	2332	11	2536.1	31.9	810	72	16600	15.8	2624.1	73	16830	15.7	2650.4	164	37810	13.1	4958.6
U9	46	28818	22.7	6534.2	19	11903	28.7	3414.8	65	40721	21.2	8643.7	73	45733	20.8	8524.2	151	94598	19.1	18022
U8	60	73074	26.5	19389	5	6089.5	50.4	3067.4	65	79164	26.3	20812	70	85253	26.1	22234	155	188775	24.5	46311
U7	105	283572	34.9	98940	7	18905	50.5	9547.8	112	302477	34.8	105278	64	172844	35.8	61799	89	240361	35.1	84451
U6	85	98765	24.6	24290	21	24401	31	7573.7	106	123166	24.1	29702	46	53449	26.5	14188	131	152214	23.7	36134
U5	80	73291	20.2	14773	25	22904	26.1	5978.2	105	96195	19.4	18666	51	46723	21.8	10208	151	138338	18.6	25788
U4	69	31049	18.7	5794.2	13	5849.8	31.2	1824.3	82	36899	18	6654.8	66	29699	18.8	5594.4	127	57148	16.8	9597.8
U3	69	56629	22.9	12991	13	10869	33.9	3619.1	82	67298	22.4	15098	67	54987	23	12667	138	113257	21.3	24128
U2	32	113760	44.6	50750	10	35550	51.7	18396	42	149310	43.8	65352	89	316394	42.3	133863	174	618568	41.7	257665
U1	23	37976	31.6	12017	4	6604.5	55.4	3657.4	27	44581	30.6	13646	84	138695	26.2	36316	184	270786	25.1	67834

Table 5.12: Absolute abundance of major dinocyst morphological groups at Gorodische.

Sample	Total skolochorates	Absolute abundance	% error on absolute abundance	Error on absolute abundance	Total proximochorates	Absolute abundance	% error on absolute abundance	Error on absolute abundance	Total chorates	Absolute abundance	% error on absolute abundance	Error on absolute abundance	Total cavates	Absolute abundance	% error on absolute abundance	Error on absolute abundance	Total proximates	Absolute abundance	% error on absolute abundance	Error on absolute abundance
K30	24	105.77	21.1	22.295	3	13.221	58	7.6646	27	118.99	20	23.739	6	26.441	41.2	10.884	51	224.75	15	33.619
K29	19	99.702	23.6	23.494	0	0	0	0	19	99.702	23.6	23.494	8	41.98	35.8	15.013	38	199.4	17.1	34.08
K28	26	114.27	20.2	23.136	14	61.531	27.2	16.733	40	175.8	16.6	29.169	5	21.975	45	9.8896	195	857.03	8.75	74.999
K27	93	38601	39.3	15183	75	31130	39.7	12346	168	69732	38.7	26999	15	6226	45.9	2857.4	113	46903	39.1	18335
K26	115	24260	28.5	6914.1	48	10126	30.6	3094	163	34386	28	9644.2	26	5484.8	33.3	1827.3	88	18564	29	5377
K25	81	249730	42.4	105985	53	163404	43.2	70593	134	413134	41.9	172940	37	114074	44.1	50347	134	413134	41.9	172940
K24	86	31677	35.2	11148	58	21364	36	7686.6	144	53041	34.5	18309	54	19890	36.2	7191.7	131	48253	34.6	16704
K23	77	23495	32.4	7613.2	73	22275	32.5	7242.2	150	45770	31.4	14378	75	22885	32.5	7427.7	117	35701	31.7	11321
K22	74	17763	32.5	5770.2	80	19203	32.3	6208	154	36966	31.4	11602	64	15362	32.8	5040.1	109	26164	31.8	8322.7
K21	80	20874	33.7	7035.7	91	23745	33.5	7949.7	171	44619	32.7	14592	32	8349.7	36.4	3037.6	104	27137	33.3	9029.5
K20	59	29983	43	12886	53	26934	43.2	11636	112	56917	42	23925	31	15754	44.7	7045.7	143	72670	41.8	30379
K19	82	9134.4	22.4	2049.3	76	8466	22.6	1917.4	158	17600	21.1	3711.5	49	5458.4	24.2	1320.7	127	14147	21.5	3034.6
K18	69	5660.4	21.2	1200.8	77	6316.7	20.9	1317.4	146	11977	19.3	2315.1	19	1558.7	28.8	449.44	118	9680.1	19.7	1911.4
K17	63	2418.3	18	435.02	43	1650.6	19.9	329.05	106	4068.9	16.1	655.08	59	2264.8	18.3	414.12	125	4798.3	15.6	750.83
K16	74	19608	33.9	6638.2	45	11924	35.1	4187.3	119	31532	33.1	10434	54	14308	34.6	4948.7	114	30207	33.1	10013
K15	74	6017	21	1262.5	63	5122.6	21.5	1103.3	137	11140	19.4	2166.1	42	3415.1	23.3	795.96	106	8619	20	1722.7
K14	49	7163.2	28.3	2030.3	54	7894.2	28	2211	103	15057	26.4	3973.4	77	11257	27	3039.5	116	16958	26.2	4439.8
K13	89	1127.8	12.9	145.68	49	620.91	16.1	99.844	138	1748.7	11.3	197.03	73	925.03	13.8	128	92	1165.8	12.8	148.92
K12	32	7818.6	21.1	1650.2	5	1221.7	46.2	564.21	37	9040.2	20.1	1815.3	24	5863.9	23.4	1374.8	51	12461	18.1	2260.3
K11	44	26146	52.3	13682	33	19609	53	10402	77	45755	51.4	23513	21	12479	54.7	6820.2	33	19609	53	10402
K10	31	97.418	18.4	17.898	0	0	0	0	31	97.418	18.4	17.898	9	28.283	33.6	9.4908	104	326.82	10.5	34.452
K9	103	5642.5	18.3	1033.3	66	3615.6	19.7	713.83	169	92507	17.2	1596.7	39	2136.5	22.2	475.19	96	5259	18.5	973.2
K8	102	68338	51.1	34906	51	34169	52	17778	153	102507	50.8	26030	44	29479	52.3	15426	106	71018	51	36249
K7	128	19431	25.4	4933.6	67	10171	26.8	2721.2	195	29602	24.9	7358	20	3036.1	32.7	991.53	82	12448	26.2	3266.3
K6	125	34942	33	11542	42	11741	35.3	4149.5	167	46683	32.7	15277	38	10622	35.7	3791.8	88	24599	33.5	8249.6
K5	60	338.91	14.1	47.74	21	118.62	22.5	26.734	81	457.53	12.5	57.001	30	169.45	19.1	32.378	92	519.66	11.9	61.587
K4	119	11778	21.6	2540.9	30	2969.2	26.7	793.8	149	14747	21.2	3123.1	36	3563.1	25.7	914.79	89	8808.7	22.2	1957.3
K3	117	21798	25.5	5566	39	7265.9	28.7	2084.4	156	29063	25.1	7298.7	55	10247	27.4	2803.2	98	18258	25.9	4721
K2	95	41680	37	15406	8	3509.9	50.1	1758.8	103	45190	36.9	16654	139	60984	36.5	22265	99	43435	36.9	16030
K1	91	33687	17.4	5861.2	12	4442.3	32	1423	103	38129	17	6492.3	72	26654	18.2	4854.5	157	58120	16	9308.7

Table 5.13: Absolute abundance of major dinocyst morphological groups at Kashpir.

Figure 5.36: Absolute abundance of chorate, cavate, and proximate cysts from Gorodische and Kashpir



5.3.2.4. Summary

This analysis has produced little consistent information. However, inner neritic deposits from these sections do not appear to have fewer chorate cysts than outer neritic or basinal facies. Indeed, the trends apparent at Gorodische suggests that chorate abundance increased with increasing proximity. This information contrasts with the expected distribution, and that noted in numerous other studies (Vozzhennikova, 1965; Scull *et al.*, 1966; Davey, 1970; Riley, 1974; Davey & Rogers, 1975; Morzadec-Kerfourn, 1983; Sarjeant *et al.*, 1987; Tyson, 1985, 1989; Courtinat *et al.*, 1991; Tribollivard & Gorin, 1991; Hssaïda & Morzadec-Kerfourn, 1993; Sittler & Olivier-Pierre, 1994; Al-Ameri & Batten, 1997). Such paradox may be due to the combination of skolochorate and proximochorate groups in the present report. To more closely analyse whether the abundance of each morphology is linked to proximal-distal relationships, finer subdivision of the dinocyst assemblage is necessary.

5.3.3. Detailed morphological subdivision

Analyses of dinocyst data based on the occurrence of individual taxa may allow much more detailed observations on the changes within the recovered assemblages. However, when such data are considered in relation to geological sections, it is important isolate stratigraphic trends from those controlled by ecological variation (Dimter & Smelror, 1990). In this respect, numerous workers have found it useful to combine taxa with like morphology into more detailed morphological groups than those described in previous sections, typically naming each group after a characteristic or dominant element (see Downie *et al.*, 1971; Brinkhuis & Zachariasse, 1988; Courtinat *et al.*, 1991; Courtinat, 1993; Brinkhuis, 1994; Wilpshaar & Leereveld, 1994; Li & Habib, 1996; Lamolda & Mao, 1999). The majority of these studies have made inferences about each group based on comparison with previously reported occurrences, or to the distribution of analogous morphologies from Recent sediments, and then applied them to specific

palaeoecological problems. Typically, sea-level change has been the target of such techniques (Brinkhuis & Zachariasse, 1988; Brinkhuis, 1994; Wilpshaar & Leereveld, 1994; Li & Habib, 1996; Lamolda & Mao, 1999), with complex proximal-distal and regressive-transgressive interactions being proposed on the basis of these data.

However, despite a significant volume of research, the study of ancient dinocyst assemblages and their palaeoecology is still in its infancy. It remains unclear whether trends in the distribution of dinocysts are related to passive sorting of the thanatocoenosis or to ecologically controlled distribution of the living thecae. Thus sediment sorting (fractionation of larger cysts into coarser sediment), transportation (of cysts away from locus of production), palaeoproductivity, (related to salinity, temperature, upwelling, run-off, oxygenation and seasonal stability), inter- and intra-specific variation in the ratio of thecae: cysts, lateral changes in hydrographic conditions, and taphonomy (mechanical and biological degradation, preferential preservation of robust cyst morphologies) must all be considered as possible factors affecting the distribution of cysts in sediments. Thus using the relative abundance of different cyst morphologies to make direct deductions about sea-level probably represents an overly simplistic approach.

Nevertheless, analysis of variation in such groups is potentially of interest, and focused investigations are required to examine the importance of each factor in the observed distribution of dinoflagellate cysts. Therefore, in the present report 12 dinocyst groups have been developed by combining cyst taxa with comparable morphologies. Data on the abundance of these groups are then compared to the sedimentological and bulk palynofacies data to see if any relationships exist between cyst morphology and either sediment grain size or the inferred proximal-distal trends. In this respect possible hydrodynamic relationships are being explored. Since the groups are based on the characteristics deemed most likely to have a bearing on hydrodynamic properties (process length/structure, cyst size, presence/absence of cavation), and in some cases contain taxa from contrasting taxonomic groups, this

analysis is expected to provide a rigorous test of apparent cyst sorting in relation to morphology.

The relative abundance data for each group are generated from the total number of specimens in all twelve groups, rather than the total number of specimens counted in each sample, since not all taxa were allocated into groups. However, between 97-100% of the total dinocyst count was used within these groups at Gorodische, and between 78-100% at Kashpir. Although taxa with restricted stratigraphic ranges have been included in this study, there are only one or two groups for which the dominant taxon has a clearly stratigraphically-controlled distribution. Most groups encompass sufficient taxa for potential ecological or hydrodynamic trends to be apparent beyond stratigraphic influences. The morphological groups are as follows:

1: *Systematophora* Group: large skolochorates with long delicate processes (>1/3 cyst diameter). Includes all specimens of the genera *Cymosphaeridium*, *Hystrichodinium*, *Hystrichosphaeridium*, *Stiphrosphaeridium*, *Systematophora*, and of the species *Impletosphaeridium lumectum*.

2: *Kleithriasphaeridium* Group: large skolochorates with long (robust) tubular processes (>1/3 cyst diameter). Includes all specimens of the genera *Kleithriasphaeridium*, *Oligosphaeridium*, and *Perissiasphaeridium*.

3: *Achomosphaera* Group: large skolochorates with spiniferate, and *Spiniferites*-like processes (>1/3 cyst diameter). Includes *Achomosphaera neptuni*, *Avellodinium falsificum*, *Egmontodinium torynum*, *E. sp. 1.* *Exochosphaeridium* spp., and *Spiniferites primaevus*.

4: *Downiesphaeridium* Group: small chorates with long, delicate, needle-like (solid or tubular) processes (>1/5 cyst diameter). Includes all specimens of the genera *Bourkinidinium*, *Cometodinium*, *Downiesphaeridium*, *Prolixosphaeridium*,

Protoellipsodinium, *Tanyosphaeridium*, and of the species "*Cleistosphaeridium aciculum*", and *Gochteodinia villosa*.

5: *Sentusidinium* Group: proximochores with short needle-like processes (< 1/5 cyst diameter). Includes all specimens of the genus *Sentusidinium* and of the species *Apteodinium spinosum*, *?Cyclonephelium bulbosum*, *Gochteodinia* cf. *villosa*, *Kallosphaeridium aptense*, and *Tehamadinium* sp. 1.

6: *Spiniferites* Group: proximochores with short spiniferate processes (<1/3 cyst diameter). Includes all remaining specimens of the genus *Spiniferites* (not included in Group 3).

7: *Tenua* Group: proximochores with short robust, often capitate, non-tabular or penitabular processes or short paratabular or gonal spines (<1/3 cyst diameter). Includes all specimens of the genera *Ctenidodinium*, *Epiplosphaera*, and *Tenua*, and of the species *Amphorula expiratum*, *Cribroperidinium* sp. 2., *Impletosphaeridium* sp. 1., *Rhyncodiniopsis martonensis*, *Pseudoceratium* sp. 1, and *Warrenia* sp. 1.

8: *Endoscrinium* Group: large cavates. Includes all specimens of the genera *Endoscrinium*, *Muderongia* and *Phoberocysta*, and the species *Dingodinium* sp. 1, *Senoniasphaera jurassica*, *Sirmiodinium grossi* and *Thalassiphora? robusta*.

9: *Dingodinium* Group: small cavates. Includes all specimens of the genera *Athigmatocysta*, *Chlamydophorella*, *Gardodinium*, *Lagenadinium*, *Nelchinopsis*, *Tubotuberella*, *Wallodinium*, and of the species *Ambonosphaera staffinensis*, *Dingodinium cerviculum*, *D. tuberosum*, *D. jurassicum*, *Gonyaulacysta dentata*, and *Gonyaulacysta eisenackii*.

10: *Cribroperidinium* Group: large proximates. Includes all specimens of the genera *Lithodinia*, *Isthmocystis*, *Leptodinium*, *Trichodinium*, the remaining specimens of

Apteodinium, *Cribroperidinium*, *Tehamadinium*, *Warrenia*, and the species *Cassiculosphaeridia magna*, *C. reticulata*, and *Valensiella ovula*.

11: *Batiacasphaera* Group: small proximates. Includes all specimens of the genera *Batiacasphaera*, *Chytroeisphaeridia*, *Circulodinium*, *Mendicodinium*, *Microdinium*, *Stanfordella*, *Wrevittia*, the species *Cassiculosphaeridia pygmaeus*, *Dichadogonyaulax pannea*, *Egmontodinium polyplacophorum*, *Ellipsoidictyum cinctum* *Gochteodinia tuberculata*, and the remaining species of the genus *Gonyaulacysta*.

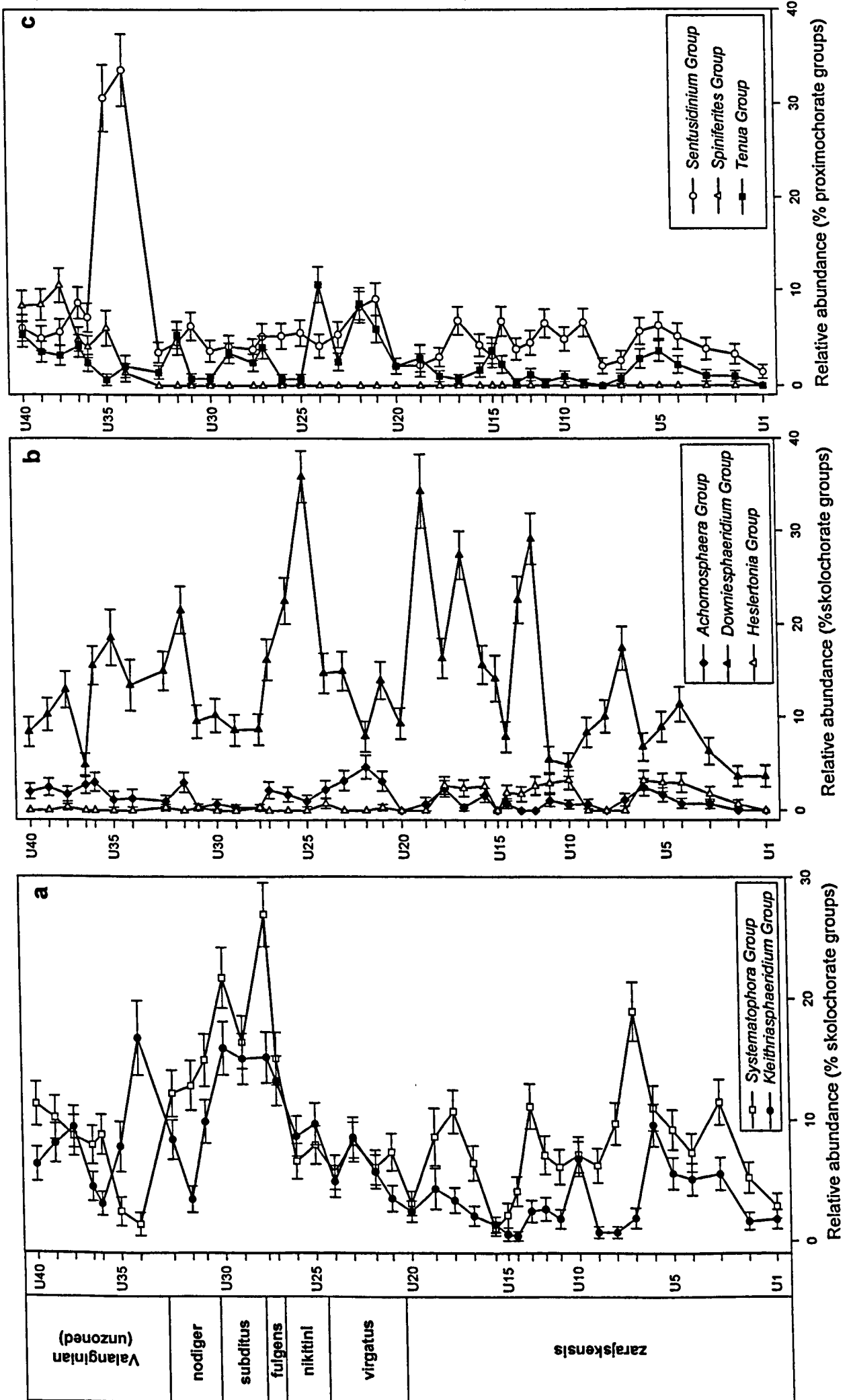
12: *Heslertonia* Group: murochorates with septa/murae $>1/5$ cyst diameter. Includes all specimens of the genus *Heslertonia*, and of the species *Glossodinium dimorphum*, and *Rhynchodiniopsis magnifica*.

The data on dinocyst occurrence are re-arranged into these groups and presented in Table 5.14 (Gorodische) and Table 5.15 (Kashpir). This information is considered in terms of relative abundance of each group. For clarity in the abundance plots certain groups have been combined into larger sets: for example, groups 1 - 4 have been combined into skolochorate plots in Figure 5.37a & b. This enables direct comparison of the various components of the skolochorate group.

5.3.3.1. Gorodische

Figures 5.37a & b show relative abundance of the skolochorate groups. There appears to be some similarity between the trends in the *Downiesphaeridium* and *Systematophora* groups in samples from the zarajskensis Subzone, markedly so up to sample U11 where the two groups have similar relative abundance values. In this subzone, peaks in the relative abundance of these two groups (most notably the *Downiesphaeridium* Group since it generally has higher relative abundance) correspond to laminated siltstone beds 5 (sample U7), and 7 (samples U12 & U13) and to the

Figure 5.37: Relative abundance of skolochorate and proximochorate groups at Gorodische



lenticular siltstone interval of beds 10 & 12 (samples U17, U18 & U19). The *Downiesphaeridium* Group shows a marked drop in relative abundance in the uppermost sample from the *zarajskensis* Subzone (U20), and through the coarse-grained deposits of the *virgatus* Zone (samples U21 - U24). This is not reflected in the other skolochorate groups. This group peaks again in the *nikitini* Zone (sample U25 & U26), has low relative abundance in the *fulgens* & *subditus* zones (samples U28 - U31), and is variable between the *nodiger* Zone and the lower part of the mica-rich siltstones. The *Systematophora* Group shows an opposing trend through the *nikitini* to *nodiger* interval, with peak values of this group in the *fulgens* to *subditus* zones. A marked drop in this group at the base of the mica-rich siltstones corresponds to the disappearance of the taxon *S. daveyi* which is a major constituent of this group, and therefore this phenomenon is largely stratigraphically imposed.

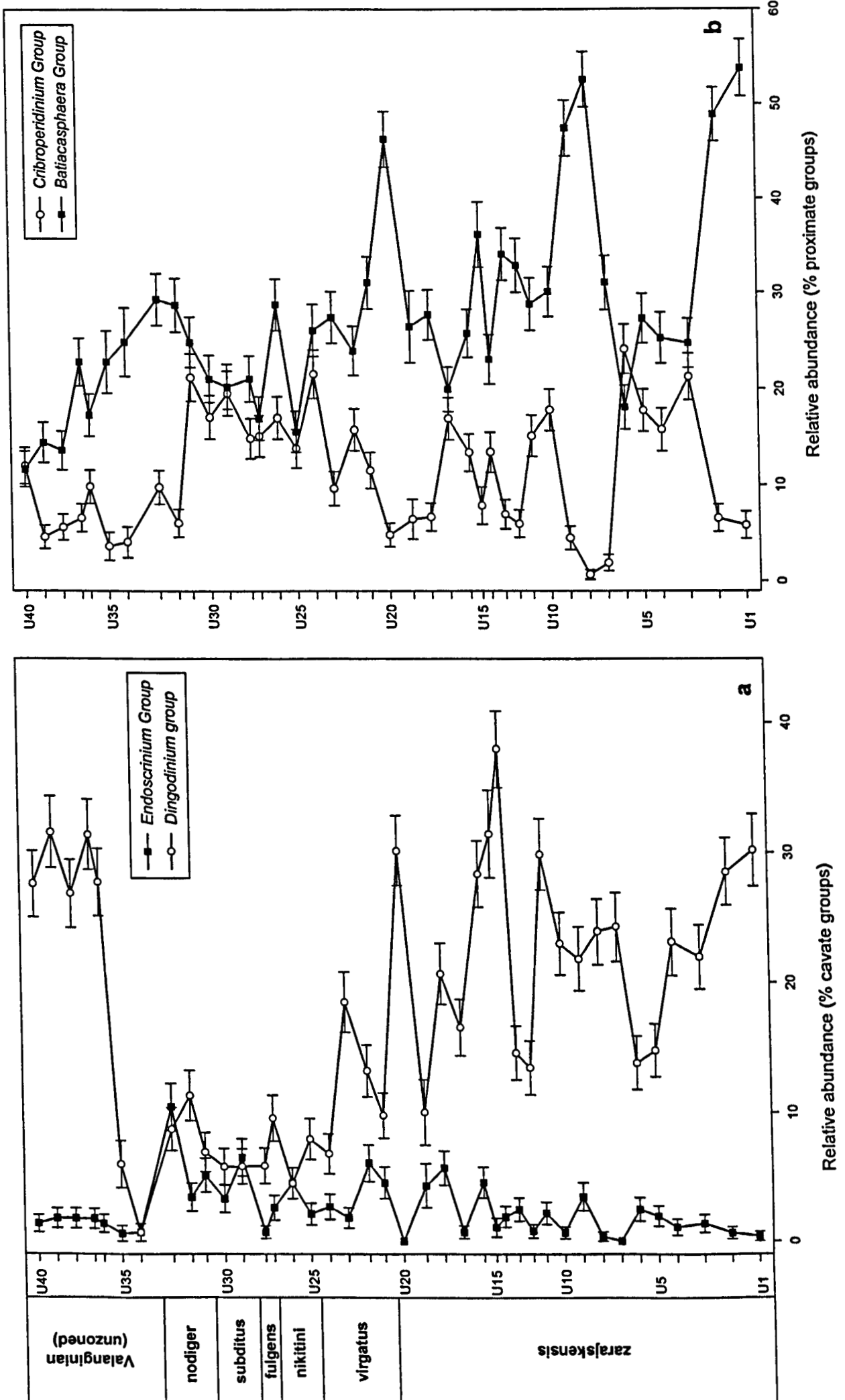
The relative abundance of the *Kleithriasphaeridium* Group is much more consistent between samples than in other groups, and the maxima/minima apparent in the *Systematophora* and *Downiesphaeridium* groups are generally not observed in the *Kleithriasphaeridium* Group. However in comparison to the rest of the samples, the relative abundance of this group is high in the *fulgens* to *subditus* zone interval, which coincides with a peak in the *Systematophora* Group. The relative abundance of these three groups is comparatively low in the uppermost part of the section. The curve for the *Achomosphaera* Group appears to be largely stratigraphically controlled, with highest values in the upper half of the section after the appearance of the nominative genus, and in the mica-rich siltstones where it is combined with *Spiniferites primaevus*. Moreover the low values of this group produce comparatively large standard errors, and must be treated with caution.

Relative abundance of the proximochorate groups are presented in Figure 5.37c. The curves for both the *Sentusidinium* and *Tenua* groups are quite comparable in the Jurassic part of the section. Slight minima in the *Sentusidinium* Group correspond to the laminated siltstone horizons in the *zarajskensis* Subzone (beds 5 & 7), and both

groups show slight peaks which correspond to the coarse-grained deposits of the virgatus Zone. The two curves significantly diverge in samples U34 & U35, where the abundance of the *Sentusidinium* Group peaks at between 30 and 35% in comparison to between 2 and 10% in the majority of the other samples from Gorodische. This peak corresponds to the FAD of *Sentusidinium* sp. 4 Iosifova, and may therefore be largely stratigraphically imposed. The *Spiniferites* Group is absent from the Jurassic part of the section, only appearing in the mica-rich siltstones. This is also a stratigraphically imposed phenomenon since the group only contains the nominative genus, which has its FAD in sample U34. The curves for the proximochorate groups can be seen to be quite different in both value and general trends to the skolochorate groups. Whilst the affect of data closure on these data can by no means be underestimated, such disparity between the two general morphologies suggests that significant information may be lost if these two groups were combined into a united chorate group.

Analysis of the cavate groups (Figure 5.38a) reveals significant difference in relative abundance between the *Dingodinium* (small cavates) Group and the *Endoscrinium* (large cavates) Group. There appears to be a long term trend towards decreased relative abundance of the *Dingodinium* Group through the Jurassic part of the section, although there are significant deviations from this. Such deviations appear to be largely independent of lithology and the result of data closure effects against other groups, most notably the *Downiesphaeridium* Group (Figure 5.38b). The *Dingodinium* Group is remarkably abundant in the mica-rich siltstones (not so in samples U34 & U35 from the phytoclast-dominated palynofacies). This may either be a cumulative data closure effect, since the majority of other groups are of low abundance through this interval, or a real reflection of the heightened abundance of this group. It does not appear to be stratigraphically imposed as the major constituents of this group are present in the majority of samples from the Gorodische section. The *Endoscrinium* Group becomes important in the upper part of the zarajskensis Subzone and reaches a peak in the phosphorite horizon at the top of the nodiger Zone. This may suggest either the increased passive sorting of larger cavates into such coarser-grained deposits, or the

Figure 5.38: Relative abundance of cavate and proximate groups at Gorodische



increased abundance of these cysts in neritic sediments by comparison with basinal sediments from the lower part of the section. The virtual absence of large cavates from the mica-rich siltstones is perhaps more consistent with the sorting hypothesis, although the terrestrial influence apparent in these deposits may also have influenced the abundance of these cysts and the distribution of the parent dinoflagellates.

The *Batiacasphaera* Group generally has higher relative abundance than the *Cribroperidinium* Group, and there appears to be significant interaction between these two groups, the abundance of one increasing at the expense of the other (Figure 5.38b). Such a relationship exists in the samples taken from the *zarajskensis* Subzone (and possibly the *virgatus* Zone), and the degree of correspondence between the two curves suggests real relationships exist between these two rather than the action of data closure from the other groups. From the base of the *nikitini* Zone to the base of the *nodiger* Zone the relative abundance values of these groups is closely comparable, but a drop in the abundance of the *Cribroperidinium* Group occurs within the *nodiger* Zone, and values for this group remain low through the mica-rich siltstones. By contrast the abundance of the *Batiacasphaera* Group reaches a slight peak at the top of the *nodiger* Zone (samples U32 & U33), and thereafter decreases through the sampled interval of the mica-rich siltstones to the top of the section.

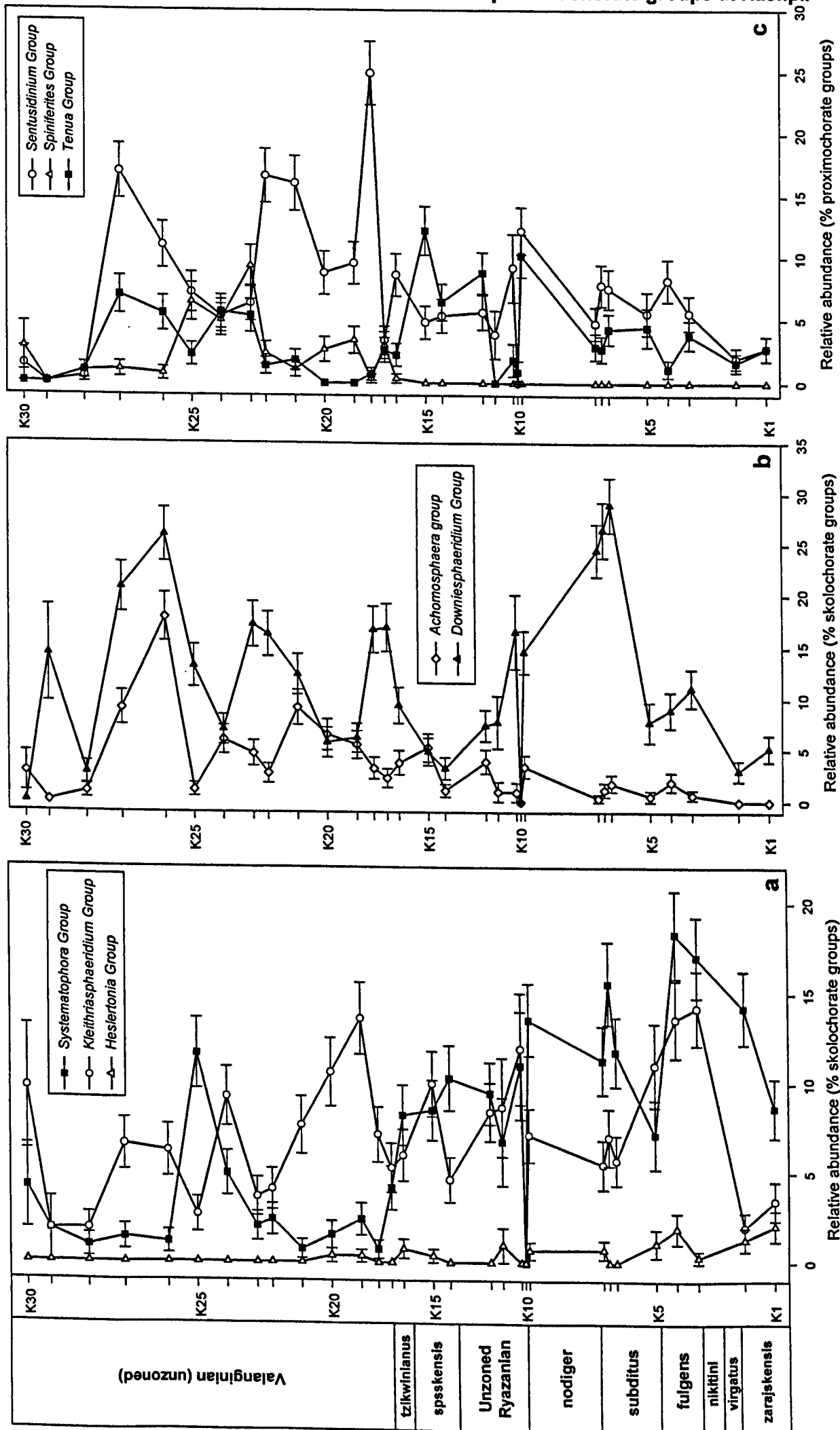
5.3.3.2. Kashpir

The lithological variety and the nature of the sampling interval at Kashpir make observations of any consistent behaviour of the dinocyst groups difficult. Relative abundance of the skolochorate groups has been plotted in Figures 5.39a & b. None of the four skolochorate groups appears to show consistent abundance variation correlatable with either sediment grain-size or with proximal-distal relationships inferred from the sedimentology and bulk palynofacies data. The rapid increase in relative abundance of the *Kleithriasphaeridium* and *Downiesphaeridium* groups between sample K2 and K3 is a

Sample	Total Systematophora group	% Systematophora group	Standard error of %	Total Kleithriasphaeridium Group	% Kleithriasphaeridium Group	Standard error of %	Total Achomosphaera group	% Achomosphaera group	Standard error of %	Total Downiesphaeridium Group	% Downiesphaeridium group	Standard error of %	Total Sentusidinim Group	% Sentusidinim Group	Standard error of %	Total Spiniferites group	% Spiniferites Group	Standard error of %	Total Tenua Group	% Tenua group	Standard error of %	Total Endoscirium Group	% Endoscirium group	Standard error of %	Total Dingodinium group	% Dingodinium Group	Standard error of %	Total Cribrerpidinium Group	% Cribrerpidinium Group	Standard error of %	Total Batiacasphaera group	% Batiacasphaera Group	Standard error of %	Total Heslertonia group	% Heslertonia Group	Standard error of %	Group total	Percent used of dinocyst total
K30	3	4.17	2.4	7	9.72	3.5	2	2.78	1.9	0	0	0	1	1.39	1.4	2	2.78	1.9	0	0	0	0	0	0	6	8.33	3.3	1	1.39	1.4	50	69.4	5.4	0	0	0	72	85.7
K29	1	1.79	1.8	1	1.79	1.8	0	0	0	8	14.3	4.7	0	0	0	0	0	0	0	0	0	0	0	0	8	14.3	4.7	0	0	0	38	67.9	6.2	0	0	0	56	86.2
K28	2	0.91	0.6	4	1.83	0.9	2	0.91	0.6	6	2.74	1.1	1	0.46	0.5	2	0.91	0.6	2	0.91	0.6	0	0	0	5	2.28	1	11	5.02	1.5	184	84	2.5	0	0	0	219	91.3
K27	4	1.38	0.7	19	6.57	1.5	26	9	1.7	60	20.8	2.4	49	17	2.2	3	1.04	0.6	20	6.92	1.5	5	1.73	0.8	8	2.77	1	27	9.34	1.7	68	23.5	2.5	0	0	0	289	98.6
K26	3	1.09	0.6	17	6.2	1.5	49	17.9	2.3	71	25.9	2.6	30	10.9	1.9	2	0.73	0.5	15	5.47	1.4	4	1.46	0.7	23	8.39	1.7	36	13.1	2	24	8.76	1.7	0	0	0	274	99.3
K25	31	11.7	2	7	2.63	1	3	1.13	0.6	35	13.2	2.1	19	7.14	1.6	17	6.39	1.5	6	2.26	0.9	10	3.76	1.2	20	7.52	1.6	19	7.14	1.6	99	37.2	3	0	0	0	266	92
K24	15	4.95	1.2	28	9.24	1.7	18	5.94	1.4	21	6.93	1.5	16	5.28	1.3	15	4.95	1.2	17	5.61	1.3	4	1.32	0.7	39	12.9	1.9	32	10.6	1.8	98	32.3	2.7	0	0	0	303	95.3
K23	6	1.99	0.8	11	3.64	1.1	14	4.64	1.2	52	17.2	2.2	19	6.29	1.4	28	9.27	1.7	16	5.3	1.3	10	3.31	1	47	15.6	2.1	19	6.29	1.4	80	26.5	2.5	0	0	0	302	95.6
K22	7	2.37	0.9	12	4.07	1.2	8	2.71	0.9	48	16.3	2.1	49	16.6	2.2	7	2.37	0.9	4	1.36	0.7	31	10.5	1.8	57	19.3	2.3	11	3.73	1.1	61	20.7	2.4	0	0	0	295	91.9
K21	2	0.73	0.5	21	7.64	1.6	25	9.09	1.7	34	12.4	2	44	16	2.2	3	1.09	0.6	5	1.82	0.8	7	2.55	0.9	31	11.3	1.9	35	12.7	2	68	24.7	2.6	0	0	0	275	89.6
K20	4	1.52	0.8	28	10.6	1.9	17	6.44	1.5	15	5.68	1.4	23	8.71	1.7	7	2.65	1	0	0	0	2	0.76	0.5	29	11	1.9	42	15.9	2.3	96	36.4	3	1	0.38	0.4	264	92.3
K19	7	2.38	0.9	40	13.6	2	16	5.44	1.3	18	6.12	1.4	28	9.52	1.7	10	3.4	1.1	0	0	0	5	1.7	0.8	43	14.6	2.1	35	11.9	1.9	91	31	2.7	1	0.34	0.3	294	88.3
K18	2	0.71	0.5	20	7.12	1.5	9	3.2	1.1	47	16.7	2.2	70	24.9	2.6	1	0.36	0.4	2	0.71	0.5	3	1.07	0.6	15	5.34	1.3	38	13.5	2	74	26.3	2.6	0	0	0	281	99.6
K17	11	4.14	1.2	14	5.26	1.4	6	2.26	0.9	45	16.9	2.3	9	3.38	1.1	8	3.01	1	7	2.63	1	7	2.63	1	52	19.5	2.4	21	7.89	1.7	86	32.3	2.9	0	0	0	266	91.7
K16	22	8.21	1.7	16	5.97	1.4	10	3.73	1.2	25	9.33	1.8	23	8.58	1.7	1	0.37	0.4	6	2.24	0.9	3	1.12	0.6	50	18.7	2.4	38	14.2	2.1	72	26.9	2.7	2	0.75	0.5	268	93.7
K15	23	8.49	1.7	27	9.96	1.8	14	5.17	1.3	13	4.8	1.3	13	4.8	1.3	0	0	0	33	12.2	2	6	2.21	0.9	36	13.3	2.1	26	9.59	1.8	79	29.2	2.8	1	0.37	0.4	271	95.1
K14	29	10.3	1.8	13	4.61	1.2	3	1.06	0.6	9	3.19	1	15	5.32	1.3	0	0	0	18	6.38	1.5	15	5.32	1.3	62	22	2.5	32	11.3	1.9	86	30.5	2.7	0	0	0	282	95.3
K13	27	9.44	1.7	24	8.39	1.6	11	3.85	1.1	21	7.34	1.5	16	5.59	1.4	0	0	0	25	8.74	1.7	5	1.75	0.8	68	23.8	2.5	11	3.85	1.1	78	27.3	2.6	0	0	0	286	94.4
K12	7	6.73	2.5	9	8.65	2.8	1	0.96	1	8	7.69	2.6	4	3.85	1.9	0	0	0	0	0	0	2	1.92	1.3	22	21.2	4	6	5.77	2.3	44	42.3	4.8	1	0.96	1	104	92.9
K11	12	11	3	13	11.9	3.1	1	0.92	0.9	18	16.5	3.6	10	9.17	2.8	0	0	0	2	1.83	1.3	0	0	0	21	19.3	3.8	20	18.3	3.7	12	11	3	0	0	0	109	83.2
K10	0	0	0	0	0	0	0	0	0	0	0	0	0	0	0	0	0	0	1	0.88	0.9	0	0	0	9	7.96	2.5	0	0	0	103	91.2	2.7	0	0	0	113	78.5
K9	40	13.6	2	21	7.12	1.5	10	3.39	1.1	43	14.6	2.1	36	12.2	1.9	0	0	0	30	10.2	1.8	4	1.36	0.7	35	11.9	1.9	29	9.83	1.7	45	15.3	2.1	2	0.68	0.5	295	97
K8	31	11.3	1.9	15	5.47	1.4	1	0.36	0.4	67	24.5	2.6	13	4.74	1.3	0	0	0	8	2.92	1	10	3.65	1.1	34	12.4	2	39	14.2	2.1	54	19.7	2.4	2	0.73	0.5	274	90.4
K7	40	15.6	2.3	18	7	1.6	3	1.17	0.7	68	26.5	2.8	20	7.78	1.7	0	0	0	7	2.72	1	6	2.33	0.9	14	5.45	1.4	34	13.2	2.1	47	18.3	2.4	0	0	0	257	86.5
K6	33	11.8	1.9	16	5.71	1.4	5	1.79	0.8	81	28.9	2.7	21	7.5	1.6	0	0	0	12	4.29	1.2	17	6.07	1.4	21	7.5	1.6	27	9.64	1.8	47	16.8	2.2	0	0	0	280	95.6
K5	13	7.18	1.9	20	11	2.3	1	0.55	0.6	14	7.73	2	10	5.52	1.7	0	0	0	8	4.42	1.5	7	3.87	1.4	23	12.7	2.5	11	6.08	1.8	72	39.8	3.6	2	1.1	0.8	181	89.2
K4	47	18.3	2.4	35	13.6	2.1	5	1.95	0.9	23	8.95	1.8	21	8.17	1.7	0	0	0	3	1.17	0.7	15	5.84	1.5	21	8.17	1.7	38	14.8	2.2	44	17.1	2.3	5	1.95	0.9	257	93.8
K3	49	17	2.2	41	14.2	2.1	2	0.69	0.5	32	11.1	1.9	16	5.56	1.3	0	0	0	11	3.82	1.1	11	3.82	1.1	44	15.3	2.1	28	9.72	1.7	53	18.4	2.3	1	0.35	0.3	288	93.2
K2	43	14.2	2	6	1.99	0.8	0	0	0	9	2.98	1	6	1.99	0.8	0	0	0	5	1.66	0.7	17	5.63	1.3	122	40.4	2.8	18	5.96	1.4	72	23.8	2.5	4	1.32	0.7	302	88.6
K1	25	8.65	1.7	10	3.46	1.1	0	0	0	15	5.19	1.3	8	2.77	1	0	0	0	8	2.77	1	5	1.73	0.8	67	23.2	2.5	56	19.4	2.3	89	30.8	2.7	6	2.08	0.8	289	87

Table 5.15: Relative abundance of detailed dinocyst morphological groups at Kashpir.

Figure 5.39: Relative abundance of skolochorate and proximochorate groups at Kashpir



stratigraphically imposed phenomenon, with the FADs of *Gochteodinia villosa* and *Kleithriasphaeridium porosispinum* occurring in K3. The significant peak in abundance of the *Downiesphaeridium* Group in the sample interval K6 - K9 is a result of the dramatically increased relative abundance of "*Cleistosphaeridium aciculum*", but since these samples are taken from three different lithologies, and therefore three different environments it is difficult to make any interpretation of such a peak. All the chorate groups are absent from sample K10 (bituminous shale horizon), which can be attributed to either real negative ecological selection or to preservational bias. The remainder of the peaks in each group seem to be attributable to more stochastic processes, and are the result of abundance peaks in particular taxa rather than of the groups as a whole. The *Downiesphaeridium*, *Achomosphaera* and *Kleithriasphaeridium* groups show a marked decrease in relative abundance between sample U27 and U28, once again due either to real ecological selection or preservational bias.

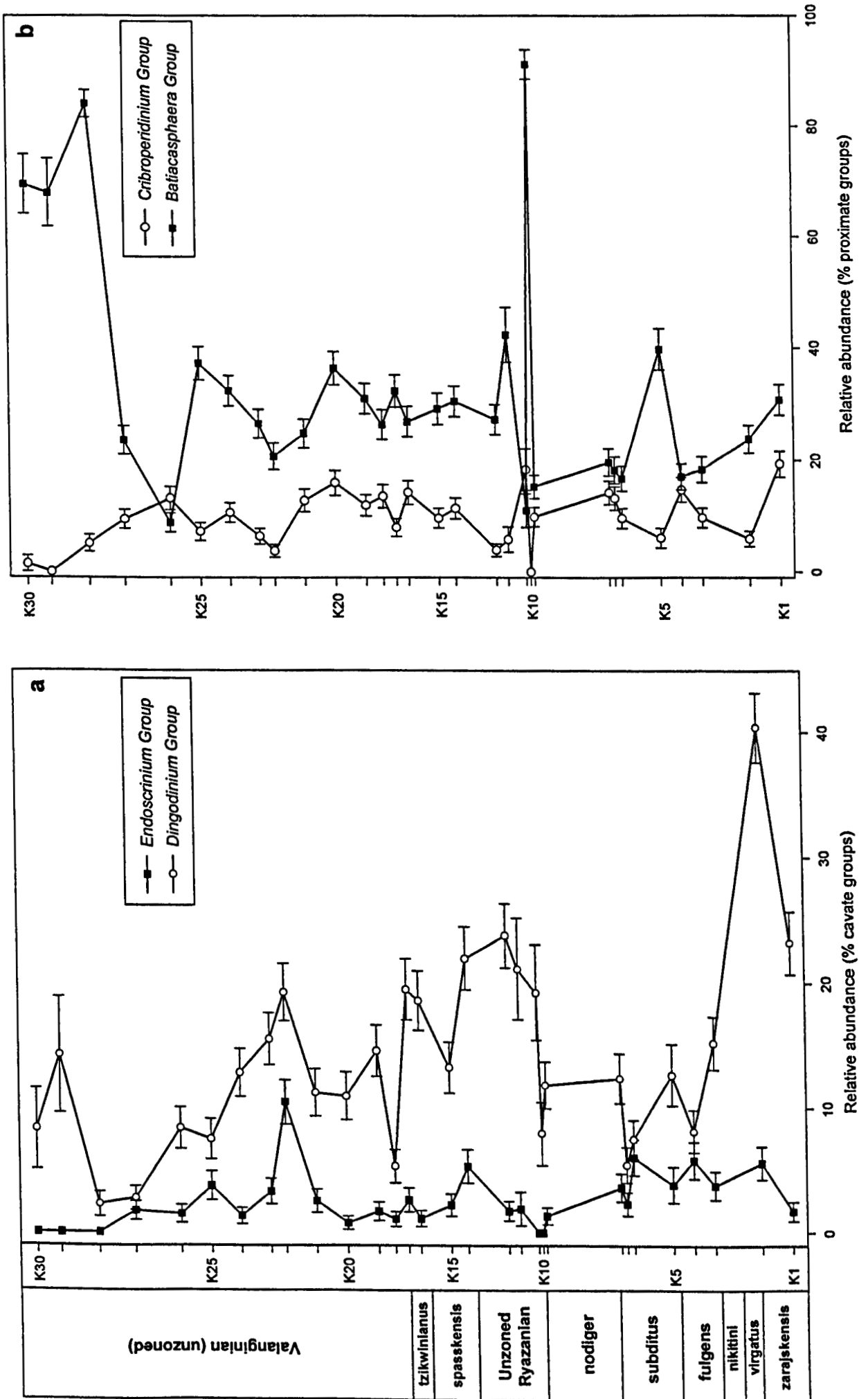
Examination of the data on the proximochorate groups reveals similar complexity and again is difficult to correlate with sedimentological information (Figure 5.39c). The relative abundance of the *Sentusidinium* and *Tenua* groups generally shows a positive trend up to the top of the nodiger Zone (sample interval K1 - K9) despite the presence of several significant hiatuses. Indeed the two curves are closely comparable through this interval. Similarly, both groups are virtually absent from K10. Peaks in the relative abundance of the *Sentusidinium* Group in samples K11, K18, K22, and K27 correspond to similar peaks in the *Downiesphaeridium* Group, although this may simply be a data closure effect. The variation seen within the mica-rich siltstones appears not to be stratigraphically imposed, but the interpretations made on the basis of sedimentology and bulk palynofacies are not detailed enough to allow evaluation of the dinocyst groups through this interval. All three proximochorate groups have extremely low relative abundance in samples K28 - K30, reflecting either true ecological variation (possibly data closure against another group) or preservational bias. The curve for the *Spiniferites* Group is stratigraphically controlled in a similar manner as in the section at Gorodische, although there is a notable peak in this group in the sample interval K23

- K25. In comparison to the sedimentological and palynofacies data, this may correspond to a phase of increased preservation due to the development of bottom-water anoxia.

Relative abundance of the *Dingodinium* Group is significantly higher than of the *Endoscrinium* Group (Figure 5.40a). At Kashpir the relative abundance of the *Dingodinium* Group appears to be higher in the distal sediments of the zarajskensis Subzone than in any other samples from this section. Abundance values are comparatively low (and quite consistent) in the sample interval K3 - K10 independent of lithology. The presence of this group in sample K10, albeit at a low level of abundance may be significant, since most other groups are absent from this sample. Slightly elevated relative abundance of this group exists in the interval from samples K11 to K17, again apparently independent of lithology. The pronounced minimum at sample K18 is apparently the result of data closure effects against peaks in the *Sentusidinium* and *Downiesphaeridium* groups. The abundance of the *Dingodinium* Group appears to decline between sample K22 and K28 in the mica-rich siltstones. The abundance of this group is generally not as high in this lithology at Kashpir as it is at Gorodische.

Analysis of the proximate groups (Fig. 5.40b) shows that the *Batiacasphaera* group (small proximates) are more abundant than the *Cribroperidinium* Group, that both have fairly consistent values across the majority of the samples from Kashpir independent of lithology, and that any major changes in the abundance of the *Batiacasphaera* Group are reflected by opposite changes in the *Cribroperidinium* Group, largely due to data closure. Dominance of the *Batiacasphaera* Group at samples K10, and K28 - K30 may be significant. These horizons represent phytoclast-dominated palynofacies, and are interpreted as having the most terrestrial influence. It is unclear however, whether this abundance in these samples is due to preferential preservation or some real affect of ecological selection.

Figure 5.40: Relative abundance of cavate and proximate groups from Kashpir



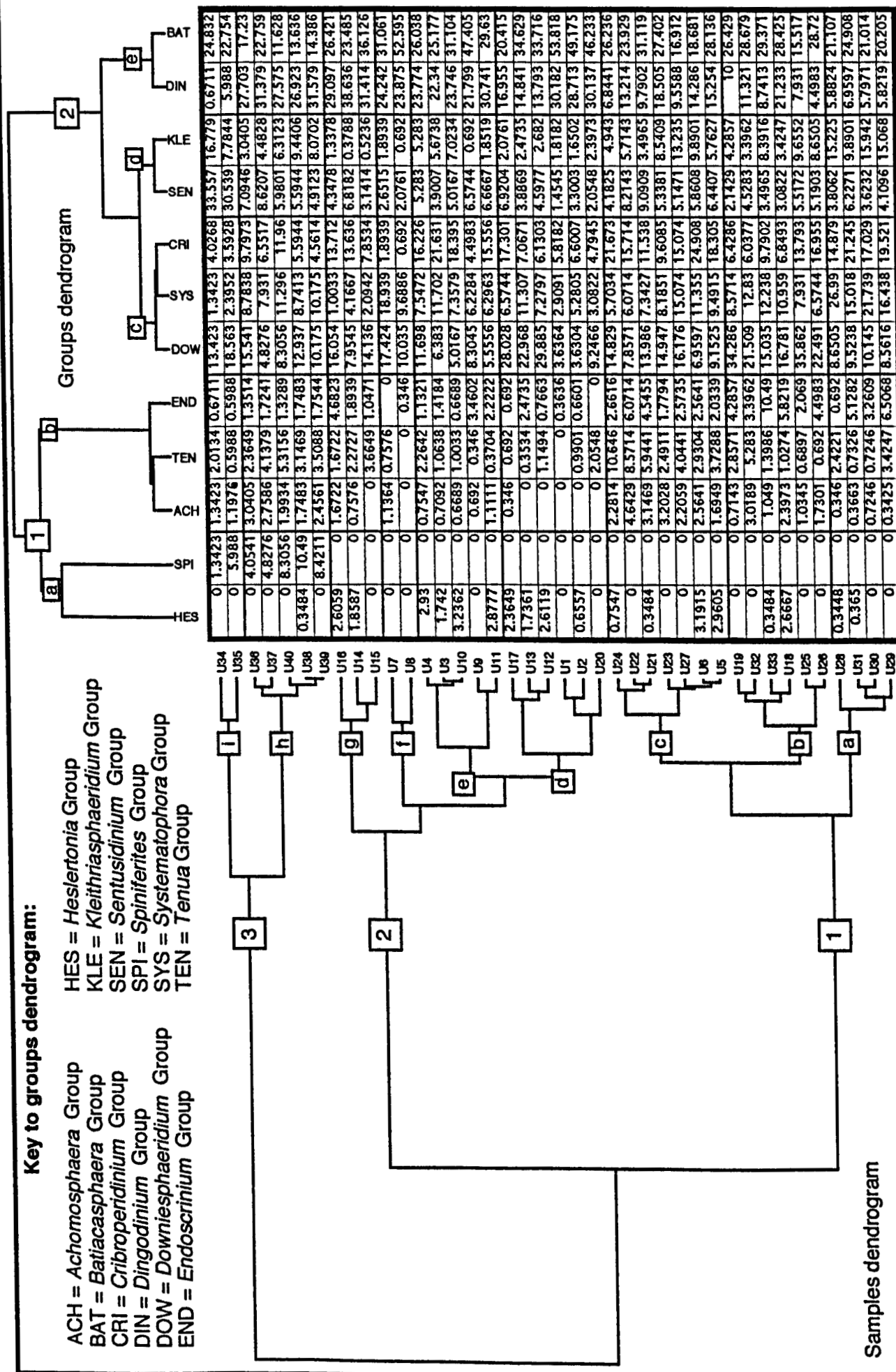
5.3.3.3. Discussion

Evaluation of the relative abundance data for the morphological groups used here does not reveal any significant correlation with proximal-distal relationships inferred from the sedimentology or palynofacies data, or with the sediment granulometry. Abundance of each group in the Kashpir section appears to be largely stochastic, and related to either data closure effects against other groups, isolated peaks in individual taxa rather than multiple taxa within each group, or to environmental factors which are untestable in the palaeontological data collected here. It is unclear whether relative abundance increases in the *Dingodinium* or *Batiacasphaera* Group in sediments interpreted as having most terrestrial influence represents true ecological variation or preservational bias.

To further test if there are any relationships between cyst morphological groups and sedimentology, the relative abundance data have been subjected to cluster analysis. Both the groups and the samples have been clustered, and are presented adjacent to the data matrix so that relationships with the original data can be analysed. The relative percentage data were log-ratio transformed during the analyses in order to eliminate data closure effects. Both minimum variance and the unweighted pair-group average method (UPGMA) were used in separate analyses (for discussion on the use of these methods see Chapter 3). However, the UPGMA clustering did not produce good results with these data, and are not discussed.

Minimum variance cluster analysis of the data from Gorodische reveals 3 main branches and 9 sub-branches in the samples dendrogram, and 2 main branches with 5 sub-branches in the groups dendrogram (Figure 5.41). As is expected of this approach, the dinocyst groups are clustered together according to the general abundance of each: the *Batiacasphaera* and *Dingodinium* groups are clustered together in Branch 2c as they are most abundant, whilst the generally least abundant *Achomosphaera*, *Tenua* and *Endoscrinium* groups are clustered in Branch 1b. The distinct branches of the sample

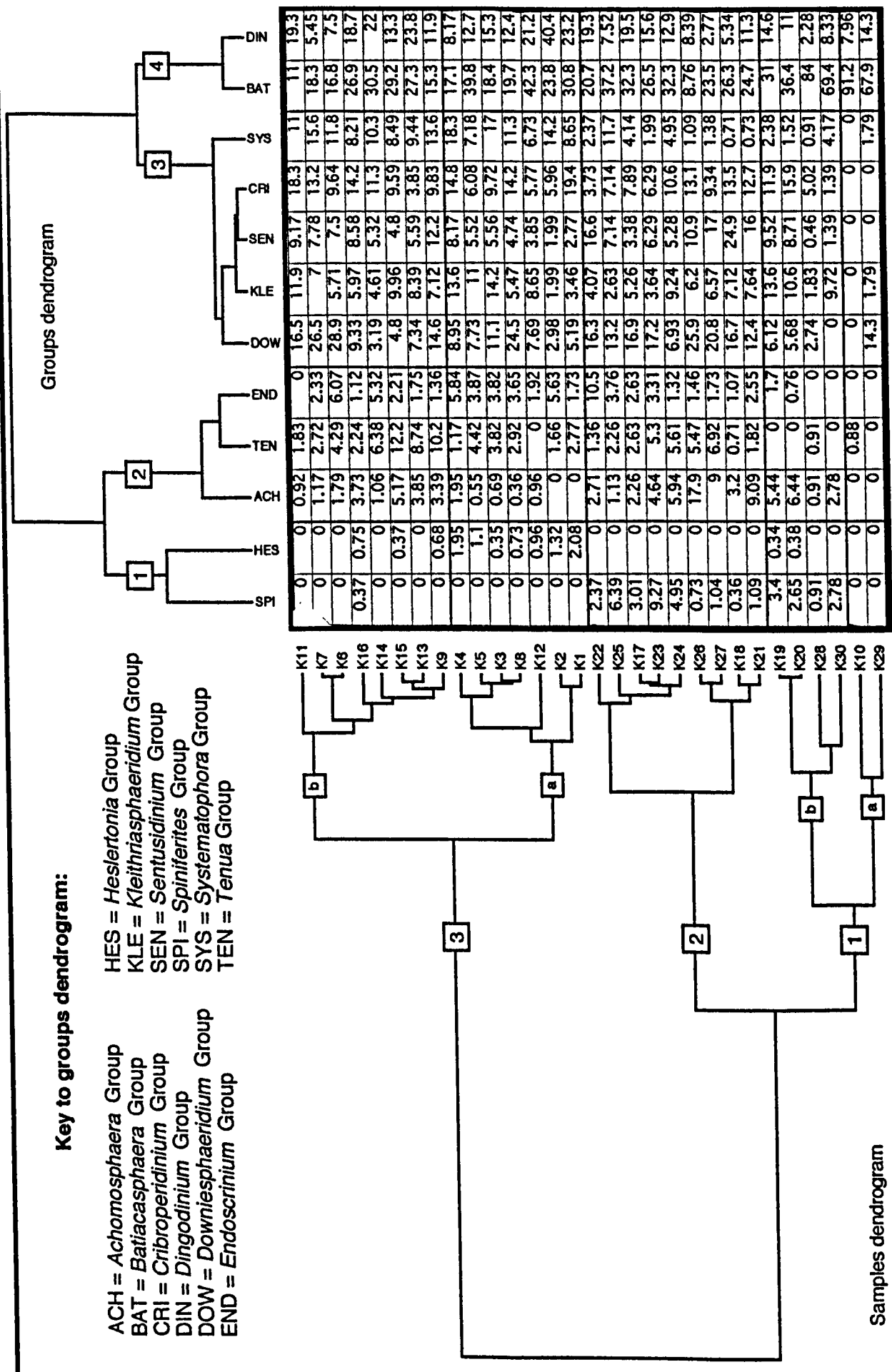
Figure 5.41: Minimum variance cluster analysis of the dinocyst morphological groups from Gorodische. Squared Euclidean distance was calculated using logratio transformation to eliminate data closure effects.



dendrogram separate the samples taken from the Jurassic deposits (branches 1 & 2) from those of the mica-rich siltstones (Branch 3). It is apparent from the data matrix that this was performed on the presence or absence of the *Spiniferites* Group, and is therefore a stratigraphically imposed separation. Branches 1 and 2 are separable on the higher relative abundance of the *Dingodinium* Group in Branch 2, which exclusively includes samples (but not all samples) from the zarajskensis Subzone. The decreased abundance of this group in the Late Volgian deposits was also evident in the relative abundance plot (Figure 5.38a). The remaining sub-branches combine samples from varying lithologies and proximities to source or shore-line on the basis of this dinocyst group data set, although interestingly the coarse-grained virgatus Zone deposits are grouped together in Branch 1c. Similarly most of the samples taken from the fine-grained sandstones of the nikitini to nodiger zones are grouped in branches 1a & 1b. Samples U34 and U35 (from the phytoclast-dominated palynofacies) are also separable from the remainder of the samples from the mica-rich siltstones on the basis of these dinocyst groups (Branch 3b).

Minimum variance cluster analysis of the Kashpir data reveals almost identical clustering of the dinocyst groups as in the Gorodische section, although the *Systematophora* Group is more clearly separable from the remainder of the groups in Branch 3 (Figure 5.42). This procedure performed on the samples shows distinct separation of the mica-rich siltstone facies from the majority of the Volgian and Ryazanian samples. Branches 1a and 1b closely group the phytoclast-dominated palynofacies from this section, identifiable in this data set by the super-abundance of the *Batiacasphaera* Group. This similarity is also notable from the relative abundance plots. The remaining samples from the mica-rich siltstones are tightly clustered in Branch 1c, which also included sample K17 from the sandstone with phosphatic concretions. Thus despite the significant difference in sedimentology of this sample, it is inseparable from the other Valanginian deposits on the basis of these dinocyst groups. Branch 3 is separable into 3a, which largely contains samples from the Volgian strata, and 3b which is mainly comprised of Ryazanian samples. This distinction appears to have been developed on the abundance of the murochorate Group, and in particular of the

Figure 5.42: Minimum variance cluster analysis of the dinocyst morphological groups from Kashpir. Squared Euclidean distance was calculated using logratio transformation to eliminate data closure effects.



taxa *Heslertonia* sp. 1 and *Rhynchodiniopsis magnifica* which are both restricted to the Volgian deposits. This is therefore a stratigraphically imposed subdivision.

5.3.3.4. Summary

Analysis at this level on the Volga Basin samples is unable to consistently separate environmental from stratigraphic trends. Certainly there are no trends in the abundance of these groups correlated to sediment grain size. The mica-rich siltstones are usually differentiated from other samples, although this is probably a stratigraphic phenomenon. In an attempt to further isolate stratigraphic and ecological trends, the taxonomic abundance is considered.

5.3.4. Taxonomic abundance

Many studies on the distribution of dinoflagellate cysts have noted an association between the environment of deposition (typically proximity to shoreline) and the abundance of certain key genera. For example, it has been suggested that an abundance of the genus *Oligosphaeridium* is typical of open marine neritic environments (May, 1980; Hunt, 1987; Lister & Batten, 1988; Smelror & Leereveld, 1989; Wilpshaar & Leereveld, 1994), whilst *Cyclonephelium* and *Muderongia* are indicative of inner neritic to restricted marine conditions (Brinkhuis & Zachariasse, 1988; Lister & Batten, 1988; Brinkhuis, 1994). To establish whether any such relationships exist in the Volga Basin data, the relative abundance of the 50 most common genera is examined below (data presented in Tables 5.16 & 5.17). Absolute abundance has not been considered here since the low number of specimens counted for each genus render values with high percentage errors, and are generally not statistically significant. Since in general many of the genera considered are comprised of more than one species in these residues, this approach also has a certain element of 'stratigraphic smoothing' not available in the

assessment of individual taxa. Nevertheless it has also proved useful to consider the distribution of individual taxa in order to isolate possible environmental influence from stratigraphic information.

When considering the generic abundance, the closely related genera *Gonyaulacysta*, *Stanfordella*, *Wrevittia*, and *Cassiculosphaeridia* & *Valensiella* have been combined into a *Gonyaulacysta* group and a *Cassiculosphaeridia* group respectively. Due to the amount of data available in the set of ~50 genera, minimum variance cluster analysis was performed first to see whether any salient trends could be distinguished, and to aid the elimination of stratigraphically or stochastically distributed taxa from further consideration. UPGMA cluster analysis was also attempted, but did not produce clear results.

5.3.4.1. Gorodische

The dendrograms and ordered data matrix from Gorodische are presented in Figure 5.43. Branches 1 & 2 on the samples dendrogram (left) are entirely comprised of samples from the mica-rich siltstones. On the basis of the dinocyst assemblage, these are distinguishable from all the other samples by the abundance of the taxa in Branch 3a (in particular *Spiniferites*, *Oligosphaeridium* and *Nelchinopsis* which first occur in these sediments), and the virtual absence of taxa from branches 2 and 4b of the genera dendrogram (top). Branch 1 containing samples U34 and U35 is further separable from the other samples of mica-rich siltstone by the high abundance of *Circulodinium* and *Sentusidinium* in Branch 5, and by the general low abundance or absence of the taxa in branches 4a, 4c & 6 on the genera dendrogram.

The samples taken from the fine-grained siltstones of the nikitini-nodiger zones are entirely and exclusively combined in Branch 3 of the samples dendrogram, and are characterised by the combination and abundance of taxa in Branch 2 of the genera

dendrogram, and by the comparatively high abundance of *Systematophora* (Branch 6). The coarse-grained deposits of the *virgatus* Zone are clustered in Branch 4 of the samples dendrogram, and are separable from the underlying deposits on the the presence of *Perisselasphaeridium*, *Achomosphaera*, *Impletosphaeridium*, and *Lagenadinium*, which first occur in this zone, and on the comparatively high abundance of *Tenua*. Branch 5 of the samples dendrogram contains all the samples from the *zarajskensis* Subzone, and typically all three contain abundant *Dingodinium*. This branch is further divisible into three sub-branches, although these are not correlatable with separate lithologies. However, Branch 5a is distinguished from other branches by the absence of *Tenua*, and by the generally high abundance of *Leptodinium*, *Tehamadinium*, and *Kleithriasphaeridium*. Sub-branch 5b has heightened (maximum) abundance of *Dingodinium* and *Batiacasphaera*, whilst 5a has slightly elevated abundance of *Cribroperidium*, but is otherwise indistinct from 5b.

On the genera dendrogram, Branch 1 is comprised of rare taxa or those with generally low abundance which occur sporadically throughout the section. The occurrence of these is thus stochastic, and they can be eliminated from further consideration. Branch 2 contains the taxa which characterise the fine-grained siltstones of the *nikitini* - *nodiger* zones, although these taxa are not exclusive to this interval. Thus, although there is a strong element of stratigraphic control on these taxa, they should continue to be considered. Branch 3a contains taxa which are either most abundant in the mica-rich siltstones, or confined to them. Since these sediments were clearly deposited in different conditions to the underlying material, such taxa cannot yet be eliminated despite the potential for stratigraphic influence. Branch 4a combines rare to common taxa which are sporadically present throughout most of the section. Most of these are therefore either cosmopolitan or controlled by stochastic mechanisms. *Tenua* is the most significant exception from this group, with peak abundance in the coarse-grained deposits, and will thus be given further consideration. Branch 5b contains taxa which are generally common elements throughout the Jurassic deposits at Gorodiche, and their abundance is generally inconsistent with either sediment grain-

size or inferred proximity to shoreline. These will not be considered further. Similarly, Branch 5c contains genera which are rare to common throughout the section, and in general are given no further attention. However, on close examination *Cometodinium* potentially appears to have an association with inner neritic or restricted marine conditions (as indicated by heightened abundance in some samples from the lenticular and mica-rich siltstones), and will be considered further. Branches 5 & 6 contain taxa which are generally common to abundant throughout the section, with the most abundant taxa in Branch 6. Whether or not these genera have apparent association with prevailing palaeoecological conditions is unclear, but their generally high abundance warrants further investigation.

5.3.4.2. Kashpir

The dendrograms and ordered data matrix from Kashpir are presented in Figure 5.44. Branch 1 of the sample dendrogram exclusively, but not completely combines samples from the mica-rich siltstones. These are separated from other deposits on the presence and/or comparatively greater abundance of the majority of taxa in Branch 3 of the genera dendrogram, on the comparatively low abundance of *Systematophora* and *Batiacasphaera*, and on the absence from these deposits of some 13 genera recorded in the underlying strata. Therefore, this may largely be a stratigraphically controlled cluster. This branch is further divisible on the abundance of *Warrenia* (within the cluster), with this genus virtually absent from Branch 1b.

Branches 2 and 3 of the samples dendrogram combine samples from the Ryazanian and Volgian deposits and the clustering does not correspond to lithology (although interestingly most of the samples from Branch 2 come from sediments with high TOC: Figure 5.16). The two branches are comparable on the basis of the comparatively high abundance of *Dingodinium*, but Branch 2 differs from 3 in having comparatively high abundance of *Tenua*, *Achomosphaera*, *Hystrichodinium*, *Gonyaulacysta*, and

Impletosphaeridium. Branch 4 exclusively contains samples taken from Volgian deposits, and is separable from branches 2 & 3 by the comparatively high abundance of *Egmontodinium*, *Endoscrinium*, *Gochteodinia*, *Senoniasphaera*, *Perisseiasphaeridium*, and *Cleistodphaeridium*. It is comparable to Branch 3 in the abundance of *Prolixosphaeridium* and *Systematophora*, which reach peak abundance in both these branches. Branch 5 groups three of the four samples from sediments with phytoclast-dominated assemblages. These samples have low abundance of most of the genera considered, but peak abundance of *Circulodinium*. Sample K10 is separable from K29 & K30 by the peak abundance of *Batiacasphaera* in this sample.

Branch 1 on the genera dendrogram is generally comprised of rare taxa with sporadic abundance throughout most of the section, most likely controlled by stochastic mechanisms. These are eliminated from further investigation. Branch 2a contains genera which are rare to common throughout the section. *Lagenadinium* is given further consideration so that comparison can be made with its abundance at Gorodische. Branch 2b contains genera which are rare to common in Branches 2-4 of the samples dendrogram. These are apparently stochastically controlled and not given further consideration. Branch 2c contains *Senoniasphaera* and *Perisseiasphaeridium* which are characteristic elements of Branch 4 on the samples dendrogram. This is considered to be a largely stratigraphically controlled grouping, and is not considered further. Branch 3 contains taxa which are most abundant or exclusive to the mica-rich siltstones. As already suggested, this is probably a stratigraphically controlled grouping, but owing to the different nature of these deposits, an element of environmental control cannot easily be ruled out. *Downiesphaeridium* and *Warrenia* are not given further consideration since they are least abundant elements of this group. Branch 4 contains taxa which are common to abundant in the majority of samples studied apart from those in Branch 5 of the samples dendrogram. The abundance of these taxa warrants their continued consideration.

It is quite apparent from the cluster analysis of data from both sections that whilst some interesting observations on the relationship of certain taxa to palaeoenvironmental conditions may be possible, stratigraphic influence on many taxa is also problematic. In an attempt to further isolate stratigraphic and ecological influences, the genera selected from the cluster analysis are plotted for each section, and compared to the lithological information from both.

The abundance of taxa which appear to be dominantly controlled by stratigraphic influence is presented in in Figures 5.45 (Gorodische), and 5.46 (Kashpir). These include *Gochteodinia*, *Oligosphaeridium*, *Pseudoceratium*, *Senoniasphaera*, and *Spiniferites*. The dominance of stratigraphic over ecological control on these genera supports their value as biostratigraphic markers as used in Chapter 4. It interesting to note the much greater abundance of *Gochteodinia villosa* in the Volgian deposits than in Ryazanian samples.

Despite the fact that the almost complete restriction of the genus *Spiniferites* to the mica-rich siltstone interval is attributed to stratigraphic control, the abundance of this taxon accords well with the suggested distribution of extant representatives of *S. ramosus*. Brinkhuis (1994) noted that that although this species has a somewhat cosmopolitan distribution, the motile stage is largely restricted to estuarine and neritic waters, and thus the corresponding cysts are expected to be abundant in these settings (see also Davey, 1971; Wall *et al.*, 1977; Davies *et al.*, 1982; Hultberg & Malmgren, 1987). Paradoxically, this genus has also been used as an open marine indicator in a number of investigations (Davey & Rogers, 1975; Wilpshaar & Leereveld, 1994; Li & Habib, 1996; Lamolda & Mao, 1999), although Brinkhuis (1994) notes that high abundance of *S. ramosus* may occur in more distal deposits due to offshore transport.

In addition, although the stratigraphic distribution of *Muderongia* and *Phoberocysta* does not permit examination of their abundance in basin deposits, these taxa are found to be common in neritic conditions, and most abundant in an inner neritic

Figure 5.45: Relative abundance of selected taxa with stratigraphically controlled distribution (Gorodische)

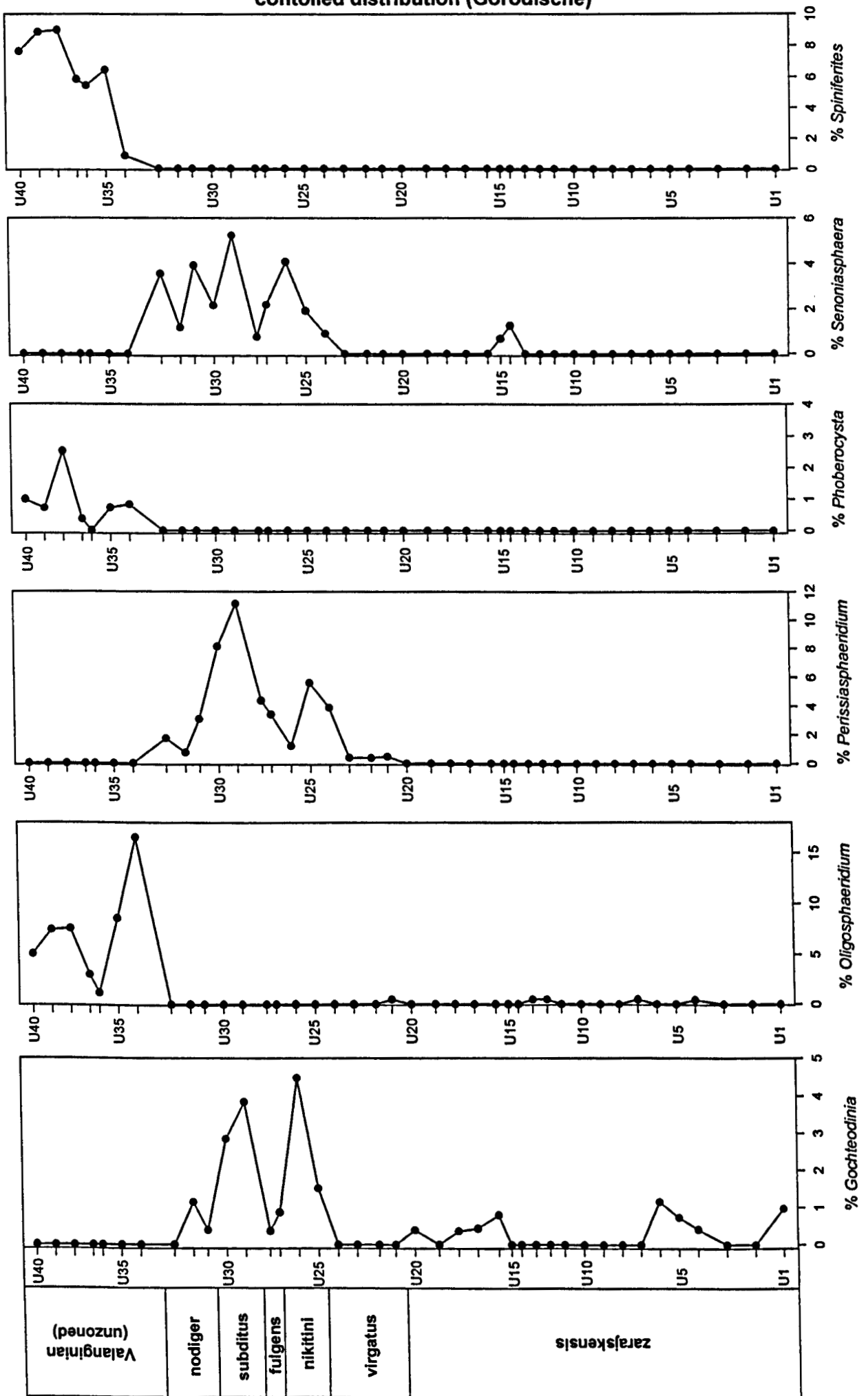
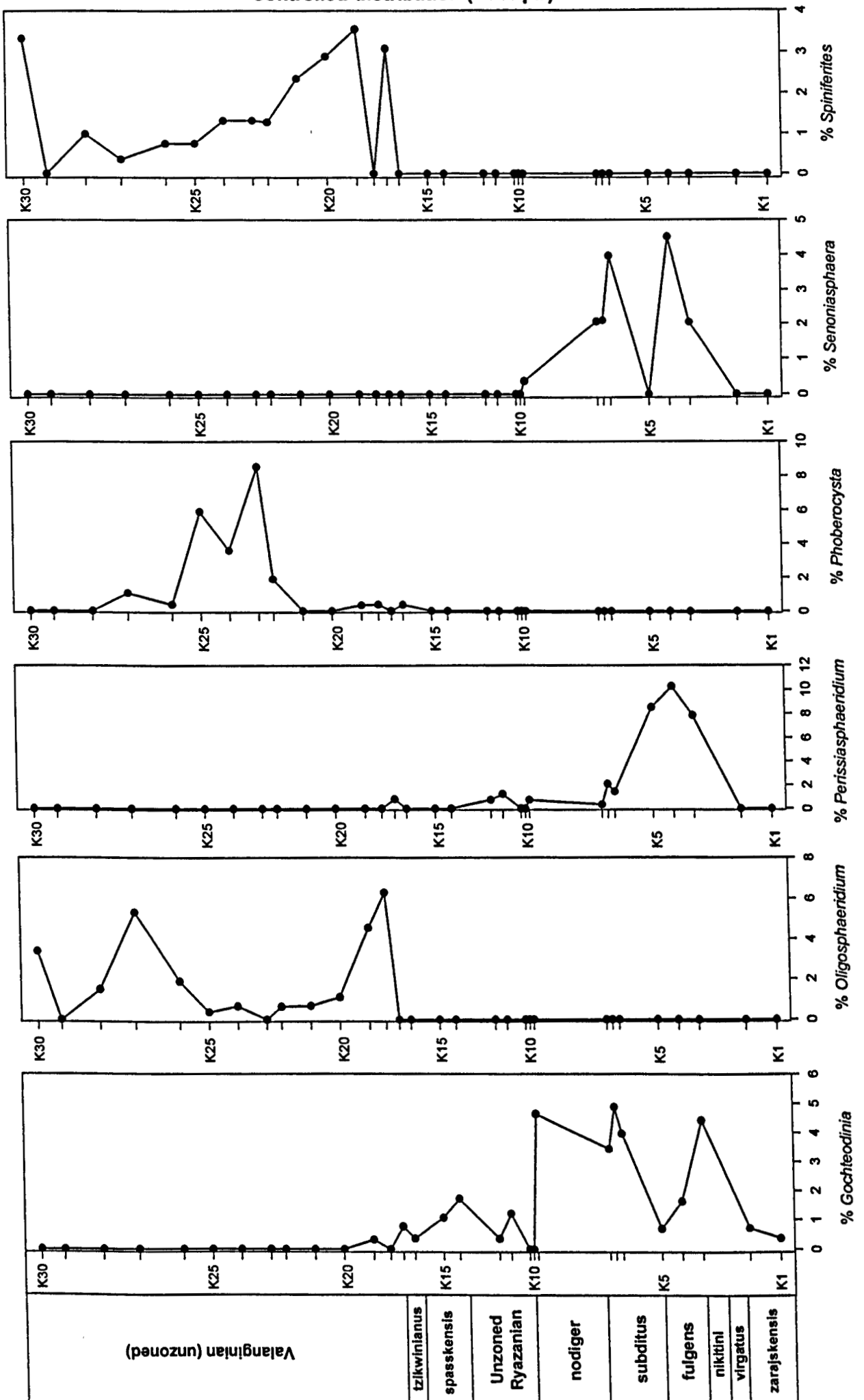


Figure 5.46: Relative abundance of selected taxa with stratigraphically controlled distribution (Kashpir)



PAGE
NUMBERING
AS ORIGINAL

Figure 5.47a: Relative abundance of selected taxa at Gorodische

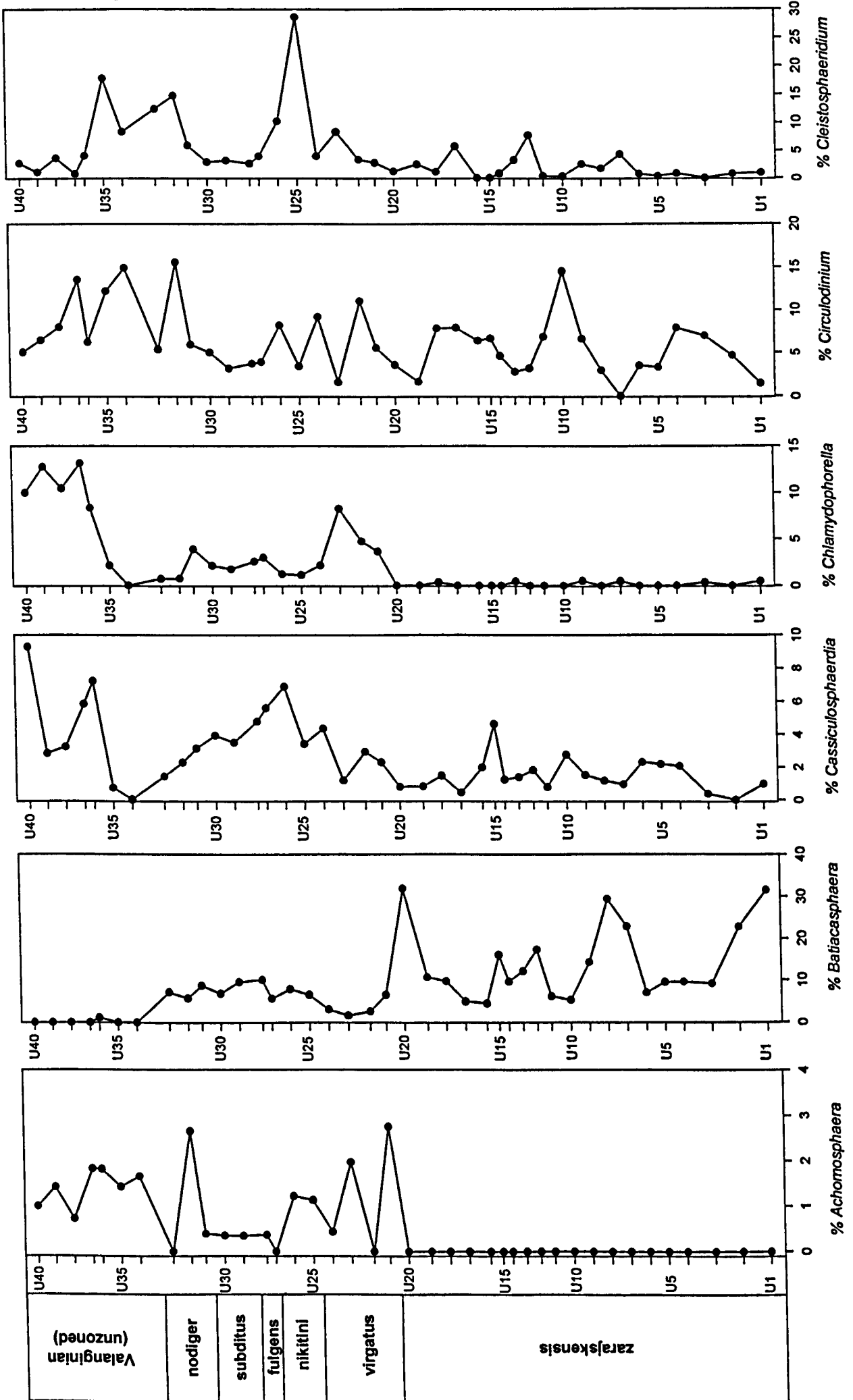


Figure 5.47b: Relative abundance of selected taxa at Gorodische

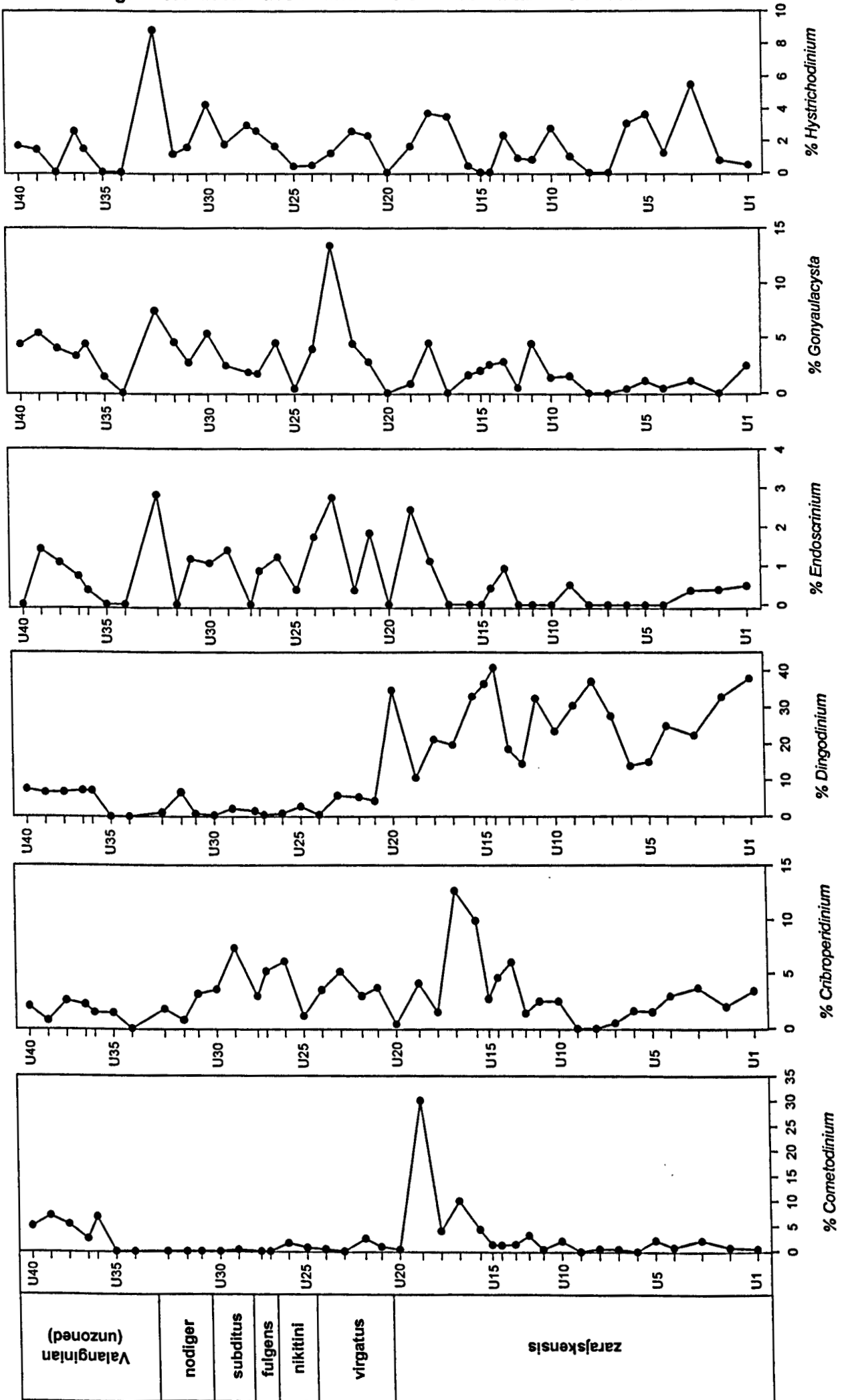


Figure 5.47c: Relative abundance of selected taxa at Gorodische

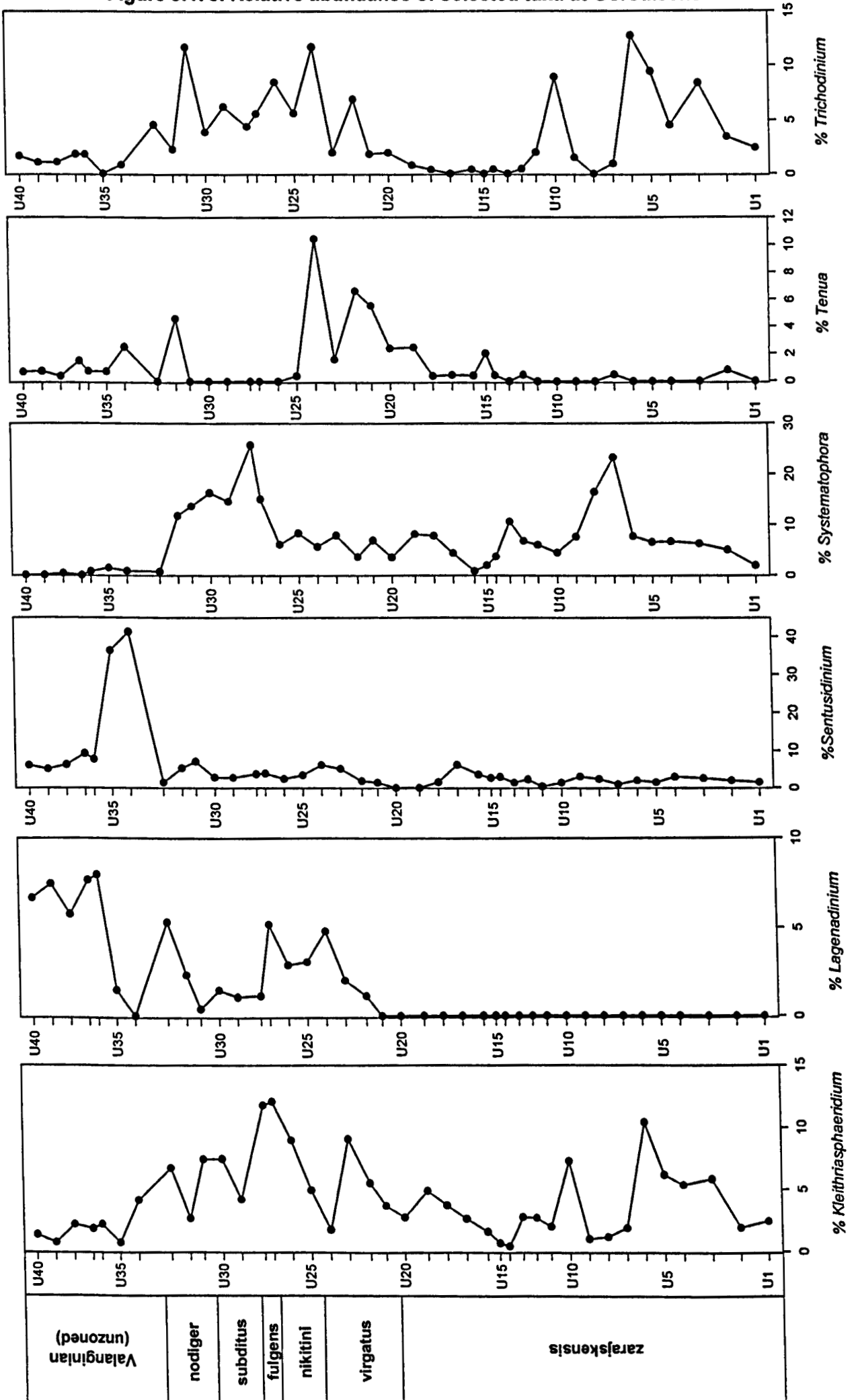


Figure 5.48a: Relative abundance of selected genera at Kashpir

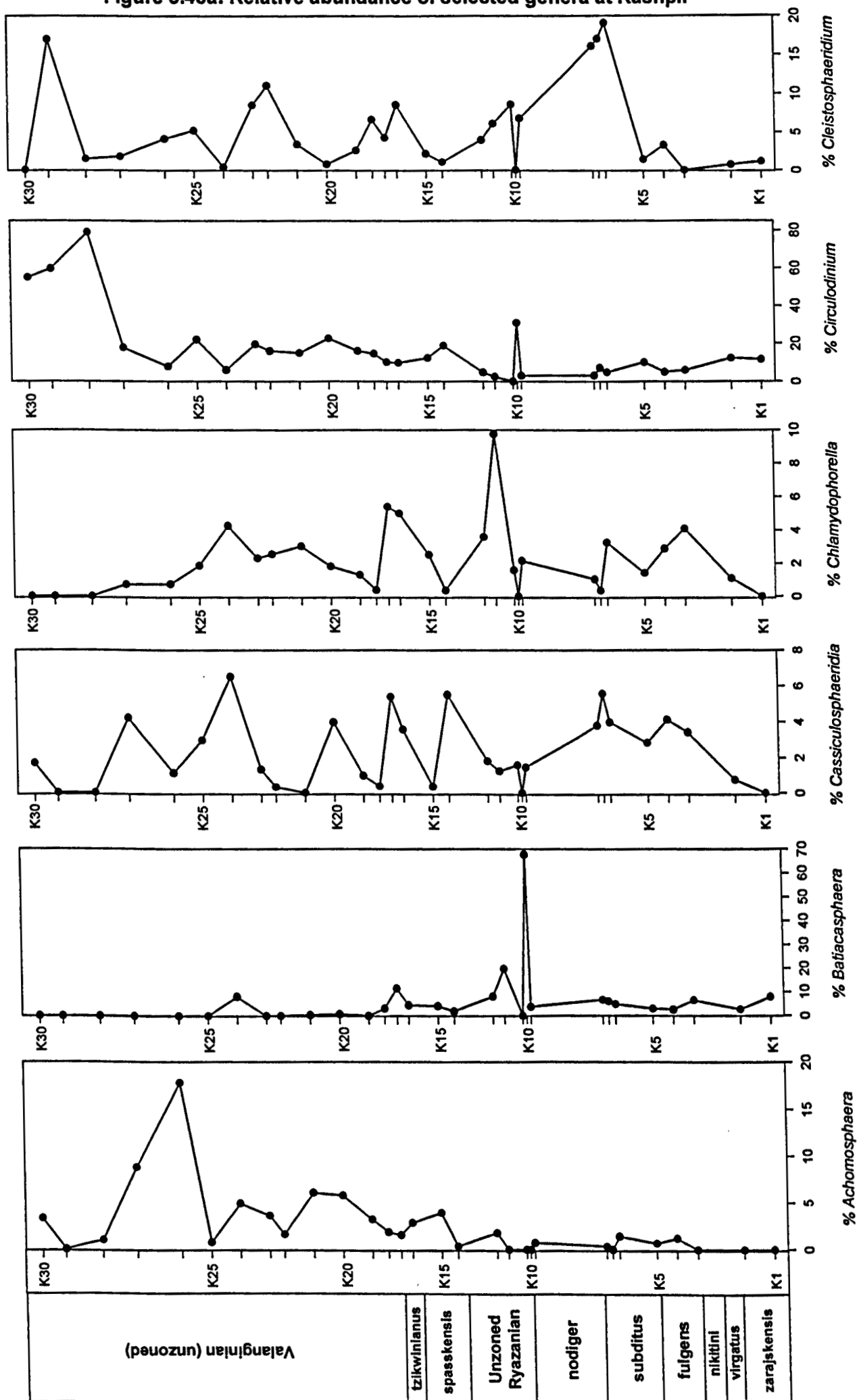


Figure 5.48b: Relative abundance of selected genera at Kashpir

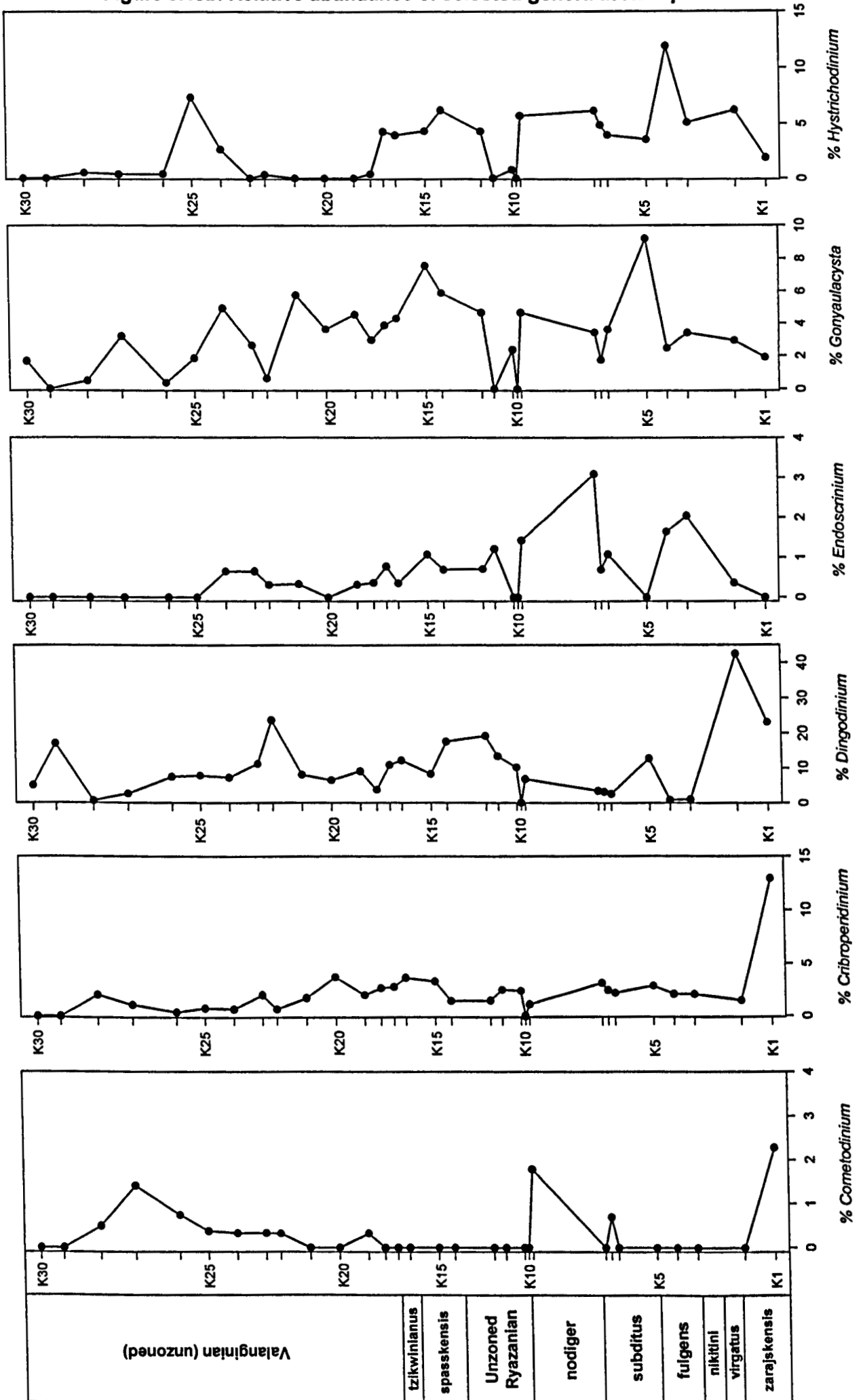
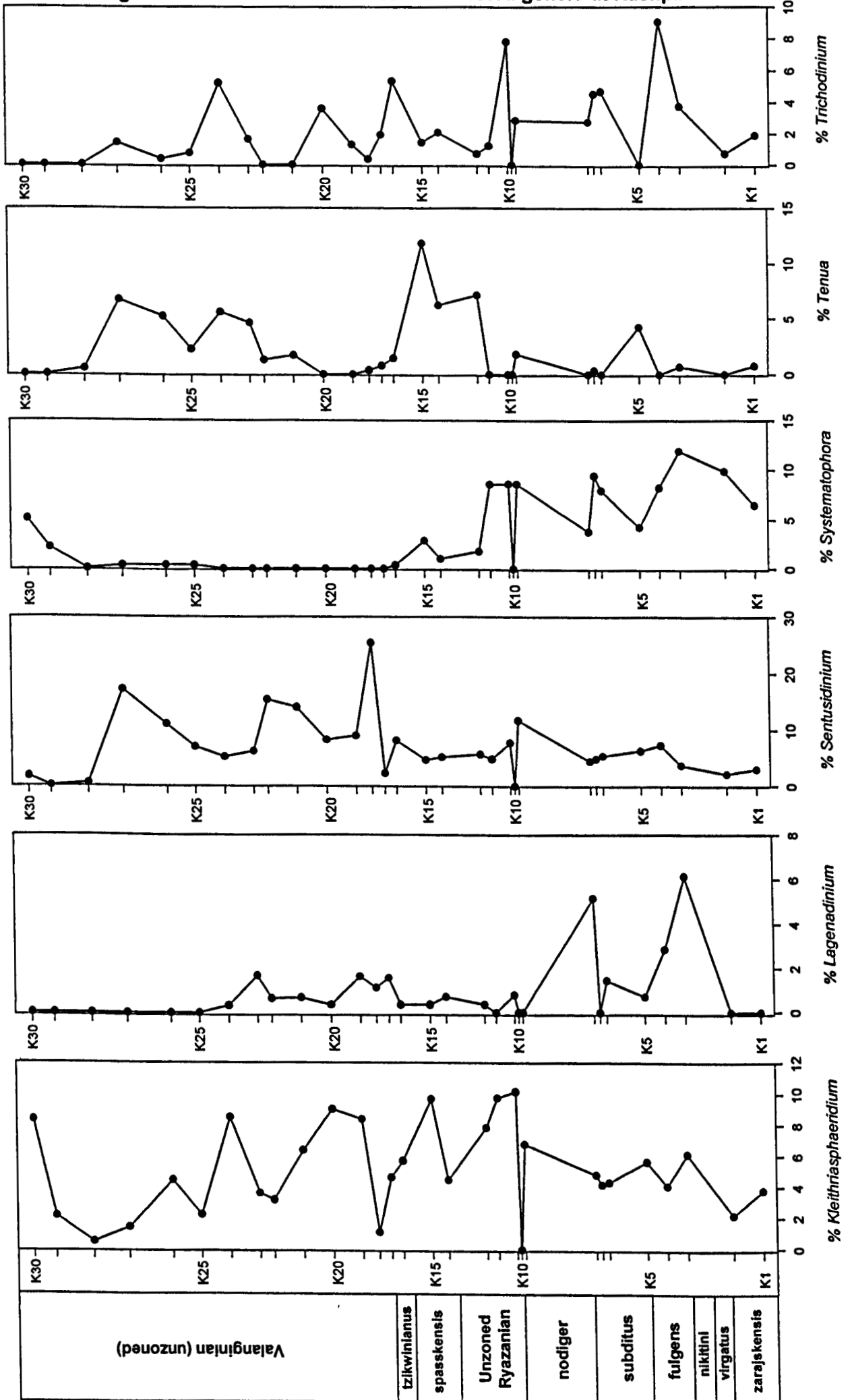


Figure 5.48c: Relative abundance of selected genera at Kashpir



Zachariasse, 1988; Brinkhuis, 1994; Li & Habib, 1996; Lamolda & Mao, 1999). Similarly, species of *Cassiculosphaeridia* have been shown to occur in alternations of restricted marine to freshwater sediments in the Lower Cretaceous Vectis Formation of the English Wealden (Batten & Lister, 1988). The abundance of *Achomosphaera* and *Cometodinium* is difficult to separate from stratigraphic controls, but these genera are also most abundant in samples from inner neritic sediments. *Sentusidinium* is generally cosmopolitan, but a strong association between comparatively high abundance of *S.* sp. 4 and restricted marine sediments (mica-rich siltstone facies) has been noted.

The genus *Trichodinium* is cosmopolitan, but analysis of the three species encountered reveals more detailed associations. *Trichodinium* sp. 1 is generally most consistently observed and most abundant in basinal deposits. *T.* cf. *ciliatum* and *T. ciliatum* are typically found in neritic deposits, with *T. ciliatum* most abundant in inner neritic sediments (particularly the mica-rich siltstones) from which *T.* cf. *ciliatum* is absent. However, it is unclear to what extent stratigraphy influences the distribution of these taxa.

No such association could be found with *Chytroeisphaeridia*, *Cleistosphaeridium*, *Cribroperidinium* or *Gonyaulacysta*, and these appear to be truly cosmopolitan in their distribution. The distribution of *Cribroperidinium* has previously been suggested as typically inner neritic (Brinkhuis & Zachariasse, 1988; Lister & Batten, 1988; Wilpshaar & Leereveld, 1994), which is thus more specific than the observations made here.

Table 5.18. Summary of dinocyst distribution

Genus	Gorodische	Kashpir	Interpretation
<i>Achomosphaera</i>	FAD of <i>A. neptuni</i> in virgatus Zone enforces stratigraphic control. Otherwise, this taxon is rare to common in coarse-grained deposits and the mica-rich siltstone facies.	Rare in the Volgian deposits, common in open marine deposits of Ryazanian, most abundant in mica-rich siltstone facies.	Stratigraphic occurrence does not coincide with oceanic/basinal deposits. Appears to be most common in inner neritic or coarse-grained deposits.
<i>Batiacasphaera</i>	Most abundant in the open marine to basinal deposits of the zarajskensis Subzone. Also common in Volgian neritic sediments	Rare to common in neritic and basin sediments. Peak relative abundance in bituminous shale horizon where the abundance of other taxa is reduced.	Typical of open marine conditions, most abundant in basin deposits.
<i>Cassiculosphaeridia</i>	Most abundant in inner neritic deposits.	Most abundant in inner neritic deposits.	Cosmopolitan, but most abundant in inner neritic deposits.
<i>Chlamydophorella</i>	Most abundant in coarse-grained and mica-rich siltstone facies. Very low abundance in zarajskensis Subzone. Abundance closely related to that of <i>Lagenadinium</i> .	Common in neritic deposits, rare to common in the mica-rich siltstone facies. Abundance closely related to that of <i>Lagenadinium</i> .	Typically abundant in neritic deposits.
<i>Chytroeisphaeridia</i>	Rare to common element in all samples. Most abundant in basin deposits of zarajskensis Subzone.	Rare to common element of most samples.	Cosmopolitan, most common in basin deposits.
<i>Circulodinium</i>	<i>C. ciliatum</i> bucket taxon most abundant in the mica-rich siltstone facies, particularly the phytoclast-dominated palynofacies..	<i>C. ciliatum</i> bucket taxon most abundant in the mica-rich siltstone facies, particularly the phytoclast dominated palynofacies..	Cosmopolitan. Generally most abundant where other taxa are not. <i>C. ciliatum</i> appears to be most abundant in samples with least marine influence.
<i>Cleistosphaeridium</i>	Abundance highly variable and apparently stochastic.	Cosmopolitan. Abundance highly variable but apparently stochastic.	Cosmopolitan.
<i>Cometodinium</i>	<i>C. whitei</i> cosmopolitan within stratigraphic range, but peak abundance in intertidal sediments. <i>C. habibii</i> only present in mica-rich siltstones with FAD in the Early Valanginian.	<i>C. whitei</i> only present in two samples from sediments with tidal influence. <i>C. habibii</i> stratigraphically restricted to mica-rich siltstone deposits.	Difficult to separate from stratigraphic controls. However maximum abundance of this genus occurs within inner neritic conditions.
<i>Criproperidinium</i>	Rare to common in all samples	Rare to common in all samples	Cosmopolitan.
<i>Dingodinium</i>	Maximum abundance in the zarajskensis Subzone, and in open marine to basin sediments.	Maximum abundance in basin sediments, but also common in neritic sediments.	Cosmopolitan, but must abundant in basin sediments.
<i>Endoscrinium</i>	Rare, but most consistently observed in neritic sediments. Least abundant in deep-water sediments.	Rare, but most consistently observed in neritic sediments. Generally low abundance in mica-rich siltstone facies.	Most consistently observed in neritic sediments.
<i>Gonyaulacysta</i>	Rare to common throughout.	Rare to common throughout.	Cosmopolitan.

Table 5.18. Continued.

Genus	Gorodische	Kashpir	Interpretation
<i>Hystrichodinium</i>	Rare to common throughout.	Rare to common in neritic sediments, rare in mica-rich siltstone facies except in zone of increased marine influence (samples K24 & K25).	Cosmopolitan, but least abundant in inner neritic conditions.
<i>Lagenadinium</i>	FAD of <i>L. membranoideum</i> in virgatus Zone thus stratigraphically restricted. Most abundant in the mica-rich siltstone facies.	Most abundant in intertidal deposits. Rare in gypsum-rich siltstones.	Neritic?
<i>Sentusidinium</i>	Rare to common throughout. <i>S. sp. 2</i> restricted to mica-rich siltstone facies, but has peak abundance in the phytoclast-dominated palynofacies.	Rare to common throughout. <i>S. sp. 2</i> occurs in Ryazanian deposits, but most abundant in mica-rich siltstone facies.	Cosmopolitan. <i>S. sp. 2</i> is most abundant in inner neritic sediments.
<i>Systematophora</i>	<i>S. daveyi</i> common throughout Volgian deposits, most abundant in outer neritic sandstones of nikitini to nodiger zones.	<i>S. daveyi</i> common in all Volgian deposits, <i>S. palmula</i> & <i>S. areolata</i> most common in inner neritic deposits, and restricted to Ryazanian.	Common in open marine, neritic to basin deposits.
<i>Tehamadinium</i>	<i>T. sousense</i> & <i>T. sp. 1</i> most common in basin deposits. Other species common in both basin and neritic sediments. Rare or absent in mica-rich siltstone facies.	Rare to common in basin and neritic sediments. Absent from mica-rich siltstone facies.	Common element of basinal and open marine neritic sediments.
<i>Tenua</i>	<i>T. hystrix</i> most abundant in coarse-grained deposits, possibly due to its robust nature. Rare in basin deposits. <i>T. cf. hystrix</i> restricted to mica-rich siltstones.	<i>T. hystrix</i> generally rare. <i>T. cf. hystrix</i> common in Ryazanian open marine neritic deposits, and in mica-rich siltstone facies.	Common in neritic deposits. Possibly enhanced relative abundance in coarse-grained deposits due to the robust nature of these cysts.
<i>Trichodinium</i>	<i>T. sp. 1</i> restricted to basin deposits, possibly with stratigraphic control. <i>T. cf. ciliatum</i> common in neritic sediments. <i>T. ciliatum</i> restricted to mica-rich siltstone facies.	<i>T. cf. ciliatum</i> rare to common in neritic sediments, absent from mica-rich siltstone facies. <i>T. ciliatum</i> most abundant in the latter deposits.	<i>T. sp. 1</i> most common in basin deposits. <i>T. cf. ciliatum</i> common in basin to neritic sediments, <i>T. ciliatum</i> in inner neritic deposits.
<i>Tubotuberella</i>	Rare in basin deposits, rare to common in neritic deposits. Absent from the mica-rich siltstones.	Rare in basin deposits, rare to common in neritic deposits. Absent from the mica-rich siltstones.	Rare in basin deposits, rare to common in neritic deposits. Absent from the mica-rich siltstones.

5.3.5. Summary of the dinocyst investigation

Analysis of the dinoflagellate cyst diversity shows that in general the most diverse assemblages occur in samples taken from open marine neritic sediments. Both basinal deposits and those with strong terrestrial influence have lower diversity. The dominance of certain taxa in these assemblages was often higher in the anoxic basinal sediments than in the neritic facies. Assessment of chorate cavate and proximate cyst abundance has not revealed a trend of increasing proximate cyst abundance in an onshore direction. However, there is a strong association between assemblages with dominantly robust cysts and coarse-grained neritic sediments. It is unclear whether such a relationship represents passive preservational bias of the robust morphologies, or increased production of cysts with robust walls in higher energy conditions.

Detailed morphological subdivision of these cyst assemblages has not produced comparable results to similar arrangements proposed by previous authors (Brinkhuis & Zachariasse, 1988; Courtinat *et al.*, 1991; Courtinat, 1993; Brinkhuis, 1994; Wilpshaar & Leereveld, 1994; Li & Habib, 1996; Lamolda & Mao, 1999). This is largely because both sections have strong stratigraphic influence, with basinal, open marine neritic, and inner neritic (strongly terrestrially influenced) facies being of Mid Volgian, Late Volgian to Ryazanian, and Valanginian age respectively. In addition, the extremely low sedimentary rate causing extended sediment-surface residence times of organic matter have clearly had some influence on the palynofacies assemblages, and it is unclear how such factors have affected the dinocyst assemblages.

Analysis of the dinocyst generic abundance has allowed greater separation of stratigraphic from ecological trends. Most taxa appear to be cosmopolitan in their distribution, having been recovered from most of the sedimentary facies sampled. However, *Tenua* and *Cassiculosphaeridia* (and *Valensiella*) appear to be most abundant in inner neritic sediments. *Dingodinium* and *Tehamadinium* reached highest abundance in the basinal deposits.

CHAPTER 6. Summary and conclusions.

6. Summary and conclusions

6.1. Biostratigraphy - summary

Previous work on the Late Jurassic-Early Cretaceous dinocyst floras of both the Boreal and Tethyan realms has been summarised, and the biostratigraphic zonations proposed for this interval by various authors have been graphically compared.

Biostratigraphic assessment of the two key Jurassic/Cretaceous boundary sections in the Volga Basin has been undertaken, and is the finest-scale appraisal of the dinoflagellate cyst floras yet completed. These sections are located close to the towns of Gorodische and Kashpir, the former being the lectostratotype of the Volgian Stage. In total 202 dinocyst taxa have been recovered from these deposits, of which 6 species are formally described as new taxa. Dinocyst assemblages recovered from each ammonite zone at both localities have been described in detail, and compared between sections. From this comparison, dinocyst taxa of potential stratigraphic utility have been identified. Where appropriate, the ranges of such taxa are compared with published data on their occurrences within the Russian Platform, and from NW Europe.

6.2. Biostratigraphy - conclusions

The biostratigraphic work has led to the following taxa and biohorizons being identified as having local stratigraphic significance across the Russian Platform:

- The LAD of *Glossodinium dimorphum*, which marks the top of the zarajskensis Subzone.
- The LAD of *Senoniasphaera jurassica*, which occurs at the top of the nodiger Zone. This corroborates previous work, identifying this taxon as an excellent marker for the Late Volgian in this area.

- The FAD of *Batioladinium gochtii*, which occurs in the spasskensis Zone across the Russian Platform.
- The FAD of *Cribroperidinium cf. volkovae*, which occurs in the tzikwinianus Zone.

Similarly, numerous dinocyst tie-points between the Volga ammonite succession and the Boreal Standard sequence have been identified. These include:

- The FAD of *Gochteodinia villosa*, which occurs at the base of the nikitini Zone in the Volga Basin, and within the Kerberus Zone in NW Europe. This tie-point supports the validity of Kuznetsova's (1978) correlation.
- The FAD of *Pseudoceratium pelliferum*, which has now been reliably recorded from a level mid-way up the tzikwinianus ammonite Zone across the Russian Platform, and from the Base of the Albidum Zone in NW Europe.
- The complete range (and in particular the FAD) of *Pseudoceratium* sp. 1, which was recorded from the tzikwinianus Zone to the lower part of the unzoned mica-rich siltstones in the Volga Basin, and from the closely comparable Albidum to Polyptychites Zone interval of NW Europe.
- In addition, the FADs of *Spiniferites ramosus* and *Muderongia crucis*, which are known from the Paratollia and Polyptychites zones (respectively) in NW Europe, also occur sequentially in the mica-rich siltstones which cap the two studied sections.

Identification of these tie points (and comparable ranges of several other taxa between these two regions) has allowed Volga Basin deposits previously of uncertain age, to be dated by dinoflagellate cysts. At Gorodische, the phosphorite bed (Bed 19) which marks the Jurassic/Cretaceous boundary has previously been attributed to the Valanginian Stage. However, the presence of several taxa which are characteristic of Upper Volgian strata, together with the absence of any taxa which are unequivocally

associated with Ryazanian or Valanginian deposits elsewhere, force the inclusion of this deposit within the Upper Jurassic. The lack of any profound change in the flora of this deposit compared to underlying sediments warrants its inclusion within the nodiger Zone. Dinoflagellate cyst evidence corroborates the absence of Ryazanian deposits from this section.

At Kashpir the unzoned basal Ryazanian deposits are comparable with the Runctoni to Kochi zone interval from NW Europe, by encompassing the LAD of *Amphorula exspiratum* and the FAD of *Systematophora palmula*. The unzoned sandstone deposit with phosphate concretions (Bed 24) has previously been attributed to the Hauterivian by Blom *et al.* (1984), but the association of dinoflagellate cysts recovered from this deposit in the present investigation strongly indicate an Early Valanginian age. Similarly, the mica-rich siltstones which cap both sections, have also been attributed to the Hauterivian Stage by Blom *et al.* (1984). Assemblages recovered from this interval contain abundant taxa which are associated with the Valanginian to Hauterivian interval in NW Europe. However, no taxa unequivocally assignable to the Late Valanginian or Early Hauterivian in Europe have been recorded from these deposits. Furthermore the association of *Egmontodinium torynum*, *Endoscrinium pharo*, *Kleithriasphaeridium porosispinum*, *Pseudoceratium* sp. 1, and *Tubotuberella apatela*, recorded from these deposits is indicative of an Early Valanginian age by comparison with their known range-tops in NW Europe.

From both localities, first appearance data shown to be of either local or regional significance have been used to construct a dinocyst zonation for the Late Volgian to Early Valanginian interval of the Volga Basin. This zonation extends and revises the zonation recently proposed by Riding *et al.* (in press). Five interval biozones are formally proposed. The *Glossodinium dimorphum* biozone (Gdi) spans the interval from the base of the section to the top of the zarajskensis Subzone. The *Perisseiasphaeridium ingegerdiae* (Pin) biozone is restricted to the virgatus Zone. The *Gochteodinia villosa* (Gvi) Biozone spans the nikitini to spasskensis Zone interval, and thus incorporates the

(Gvi) Biozone spans the niktini to spasskensis Zone interval, and thus incorporates the Jurassic/Cretaceous boundary. It is further divided into four sub-biozones, one which is restricted to the Late Volgian, one which spans the Volgian/Ryazanian boundary, and two which are restricted to the Ryazanian. The *Pseudoceratium pelliferum* Biozone (Ppe) is confined to the upper part of the tzikwinianus Zone. The *Spiniferites ramosus* (Sra) Biozone encompasses all of the unzoned Valanginian deposits, and extends to the top of the studied interval. It is further divided into three sub-biozones by the successive FADs of key taxa.

6.3. Sedimentological and palynofacies analysis - summary

The sedimentological information provided for these sections in the current report is by far the most comprehensive so far available, and the accompanying sedimentary logs the most representative of the exposed successions. These logs have been correlated in detail with those provided by previous authors (Casey, 1967; Lord *et al.*, 1987; Hogg, 1994, unpublished) which were drawn exclusively from the work of Russian authors.

The main classification schemes aimed at palaeoenvironmental interpretation of palynological matter have been reviewed and compared. Terminology and identification of palynological matter used in the present report has been described in detail, and correlated with previously proposed schemes. This project reports the first palynofacies investigation to be completed from sections in the Volga Basin. Bulk palynological matter components, structured particle relative and absolute abundance, PhytOC, and detailed assessment of the phytoclast assemblages (including composition, mean long axis length, and roundness index) have been examined from both sections. In addition, standard deviation of the mean phytoclast size has been devised as both an absolute and relative sorting parameter in measurements of the particle assemblages. Cluster analysis has been used extensively to test the strength of patterns emerging

from binary and ternary plots, and to further probe the data where these more traditional analyses have not produced sufficiently clear results.

The effects of processing procedure used to generate these palynological residues has been tested. Ultrasonic vibration and nitric acid oxidation were both found to adversely affect the palynologic matter assemblages, but only significantly so when treated for more extended periods than those used here. Ultrasonic vibration is more effective in the removal of AOM than nitric acid oxidation, and in AOM-dominated palynofacies, the effects of even extended exposure to these techniques on the remaining organic matter components is negligible.

6.4. Sedimentological and palynofacies analysis - conclusions

Results from the integration of sedimentological and palynofacies data indicate that the lower part of the zarajskensis Subzone was deposited in a basinal environment, probably with a stratified water column and the development of bottom-water anoxia. This is indicated by the AOM-rich nature of both the mudstone and laminated siltstones from this part of the sequence, and there is a strong association between AOM-dominated assemblages and those with high TOC. Both palynofacies and sedimentology indicate an extremely slow rate of siliciclastic input. The thickness of these deposits in relation to overlying strata thus indicates that the basin maintained a high degree of structural stability throughout this interval. However, regression is indicated at the top of the zarajskensis Subzone at Gorodische by the presence of intertidal sediments. Analogous deposits are absent from Kashpir suggesting the presence of a previously unrecognised hiatus or disconformity at this level, and this is supported by a distinct erosional contact at the zarajskensis/virgatus zone boundary.

Both coarse grained sedimentation through the virgatus Zone at both localities, and the character of palynological assemblages recovered from this interval, point to neritic deposition. The abundance of phosphorite and glauconite grains indicate a

sediment-starved regime. At Gorodische the nikitini to nodiger zone interval is characterised by fine glauconitic sands interpreted as representing outer neritic deposition. The palynofacies characteristics of the phosphorite deposit at the top of the Jurassic succession at Gorodische are indistinguishable from those of the underlying sediments, adding weight to the inclusion of this deposit within the nodiger Zone. At Kashpir, the nikitini to nodiger zones are characterised by abundant lenticular-bedded sediments, suggesting more proximal deposition by comparison with contemporaneous deposits at Gorodische. Available data suggests that the overlying Ryazanlan sediments were deposited in an open marine, probably outer neritic environment, once again with a low rate of sediment input.

The base of the Valanginian interval at Kashpir is marked by set of sandstone layers indicative of proximal conditions. The basal unit of this set contains phosphatic concretions with an exceptionally well preserved dinocyst assemblage. The remainder of the Valanginian sediments at both Gorodische and Kashpir consist of mica-rich siltstones, which the palynofacies evidence shows were deposited under strong terrestrial influence. The abundant weathering products of pyrite, and the abundant AOM in certain samples suggests the possible development of bottom- or pore-water anoxia resulting from the biological degradation of the large quantities of plant matter present in these sediments.

6.5. Assessment of the dinocyst assemblages - summary & conclusions

Detailed analyses have been completed on the dinocyst assemblages. Dinocyst diversity is lower in the sediments deposited in a basinal environment than in the neritic sediments. Similarly, dominance is greater in basinal deposits than in the remaining sediments, apart from those with phytoclast-dominated palynofacies. Such low-diversity high-dominance characteristics of the deep basin sediments probably reflects the low number of more oceanic dinocyst species, as well as the development of water-column stratification.

Analysis of the chorate/cavate/proximate cyst abundance has not shown the previously documented trend of increasing chorate abundance towards open marine conditions. Indeed, evidence from Gorodische points to increasing chorate abundance with increasing proximity to the terrestrial source. This apparent paradox may in part be due to the combination of proximochorate and skolochorate groups in the present study, but suggests that the abundance of these groups cannot necessarily be taken as a direct indicator of proximal-distal interactions. Moreover, simple division of the encountered taxa into delicate and robust groups reveals a strong correlation between the abundance of thick-walled and generally robust cyst morphology, and coarse-grained sediments deposited under higher energy conditions. However, it remains unclear whether such a relationship is a result of preferential preservation of robust cysts, or the higher production of cysts with robust morphology in response to higher energy conditions.

The potential relationship of hydrodynamic sorting and cyst morphology has been tested by constructing 12 dinocyst groups based on morphological features most likely to have a bearing on hydrodynamic properties. Disparity in the patterns of abundance displayed by these groups indicates that their combination into the broad groupings outlined in the paragraph above may cause potentially useful information to be lost. Furthermore, although potential ecological trends in the Volga Basin assemblages are difficult to separate from stratigraphic control, analysis of the distribution of these groups has not revealed a consistent association between their relative abundance, and either proximity to terrestrial source or sediment granulometry. Thus the controls on the distribution of these groups are more complex than simply hydrodynamic sorting (whether biologically or passively induced), and their abundance cannot automatically be taken as a direct parameter for measuring sea-level. Clearly, further work needs to be aimed specifically at the distribution of cysts (and their morphological groups) in sediments before they can be used confidently as palaeoecological indicators.

The relationships of individual taxa to inferred environmental conditions have also been examined. Taxa with a dominance of stratigraphic over ecological control were eliminated from this investigation with the use of cluster analysis. This exercise proved the validity of using *Glossodinium dimorphum*, *Gochteodinia villosa*, *Pseudoceratium pelliferum*, *Pseudoceratium* sp. 1, *Senoniasphaera jurassica*, and *Spiniferites ramosus* as major zonal indices. Within the range of facies represented by these sections, the majority of taxa were revealed to have a cosmopolitan distribution controlled by largely stochastic processes. However, *Dingodinium* and *Tehamadinium* were found to be most abundant in basinal deposits, whilst *Cassiculosphaeridia*, *Tenua*, and *Valensiella* are most abundant in sediments attributed to an inner neritic regime.

6.5. Suggestions for further research

- Finer scale sampling of both sections would allow the precise positions of the dinocyst zones within the ammonite framework to be identified, and lead to closer correlation with other sequences in the future. This would also permit an extremely comprehensive assessment of the palynofacies assemblages, which could be used to refine the palaeoenvironmental deductions made here, and pinpoint any hiatuses overlooked as a result of the current sampling strategy.
- The examination of the sediments from the area could be extended into a petrological study, which would be particularly useful in making further interpretations about the mechanisms of formation and environment of deposition of both the phosphorite horizons and the basal Ryazanian bituminous shale. Wider geographic examination of the lithologies encountered, particularly of units like the phosphatic conglomerates, should allow a better understanding of the lateral facies variations in the area, and how contemporaneous deposits from the two localities relate to one another.

- Further palynological analysis of the exceptionally well preserved dinocyst assemblage recovered from the phosphorite horizon at Kashpir, may allow further new species to be identified, or additional characteristics to be defined for existing taxa. Separate study of phosphate concretions and sandy matrix should prove that the well preserved fraction is sourced from the concretions.
- Much further study needs to be directed at the passive mechanisms controlling the distribution of dinoflagellate cysts in sediments. In particular, the relationships of specific cyst morphology to hydrodynamic properties, sediment granulometry (by sediment grain-size calibration in the lab) and the preferential preservation of robust versus delicate cysts, both require detailed examination.

REFERENCES

- Ager, D. 1968. Discussion. (of the article by Casey, R.; 1968) *Proceedings of the Geological Society of London*. Vol. 1648. p. 75.
- Al-Ameri, T.K., & Batten, D.J. 1997. Palynomorph and palynofacies indications of age, depositional environments and source potential for hydrocarbons: Lower Cretaceous Zubair Formation, southern Iraq. *Cretaceous Research*. Vol. 18. pp. 789 - 797.
- Alberti, G. 1961. Zur kenntis mesozoischer und altertiärer dinoflagellaten und hystrichosphaerideen van nord- und mitteldeutschland sowie einigen anderen europäischen gebieten. *Palaeontographica Abt. A*. Vol. 116. pp. 1 - 58.
- Allemann, F., Grün, W., & Wiedmann, J. 1975. The Berriasian of Caravaca (Prov. of Murcia) in the subbetic zone of Spain and its importance for defining this stage and the Jurassic - Cretaceous boundary. *Memoires de la Bureau de Recherches Geologiques et Minières*. Vol. 86. pp. 14 - 22.
- Allen, P., & Wimbledon, W.A. 1991. Correlation of NW European Purbeck - Wealden (nonmarine Lower Cretaceous) as seen from the English type-areas. *Cretaceous Research*. Vol. 12. pp. 511 - 526.
- Andrews, J.E., & Walton, W. 1990. Depositional environments within Middle Jurassic oyster-dominated lagoons: an integrated litho-, bio-, and palynofacies study of the Duntulum Formation (Great Estuarine Group, Inner Hebrides). *Transactions of the Royal Society of Edinburgh, Earth Sciences*. Vol. 81. pp. 1 - 22.
- Antonescu, E., & Avram, E. 1980. Corrélation des dinoflagellés avec les zones d'ammonites et de calpionelles du Crétacé inférieur de Svinita - Banat. *Annuaire de l'Institut de Géologie et de Géophysique*. Vol 56. pp. 97 - 132.
- Arkell, W.J. 1956. *The Jurassic Geology of the World*. London.
- Ascoli, P., Poag, C.W., & Remane, J. 1984. Microfossil zonation across the Jurassic/Cretaceous boundary on the Atlantic margin of North America. In: Westermann G. E. G. (Ed.). *Jurassic - Cretaceous Biochronology and Paleogeography of North America*. Geological Association of Canada, Special Paper 27. pp. 31 - 48.
- Ashraf, A.R. 1979. Die Räto-Jurassischen floren des Iran und Afghanistans. 6. Jurassische und unterkretazische dinoflagellaten und acritarchen aus Nordafghanistan *Palaeontographica Abt. B*. Vol. 169. pp. 122 - 158.
- Århus, N. 1992. Some dinoflagellate cysts from the Lower Cretaceous of Spitzbergen. *Grana*. Vol. 31. pp. 305 - 314.
- Århus, N., Kelly, S.R.A., Collins, J.S.H., & Sandy, M.R. 1990. Systematic palaeontology and biostratigraphy of two Early Cretaceous condensed sections from the Barents Sea. *Polar Research*. Vol. 8. pp. 165 - 194.
- Århus, N., Verdenius, J., & Birkelund, T. 1986. Biostratigraphy of a Lower Cretaceous section from Sklinnabanken, Norway, with some comments on the Andøya exposure. *Norsk Geologisk Tidsskrift*. Vol. 66. pp. 17 - 43.
- Bailey, D. 1993. Selected *Cribroperidinium* species (Dinophyceae) from the Kimmeridgian and Volgian of northwest Europe. *Journal of Micropalaeontology*. Vol. 12. pp. 219 - 226.
- Bailey, D., Milner, P., & Varney, T. 1997. Some dinoflagellate cysts from the Kimmeridge Clay Formation in North Yorkshire and Dorset, UK. *Proceedings of the Yorkshire Geological Society*. Vol. 51. pp. 235 - 243.

- Baird, J.G. 1992. Palynofacies of the eastern margin of the Gippsland Basin. In: *Energy, Economics, and Environment, Proceedings of the Gippsland Basin Symposium, Melbourne June 1992. Australian Institute of Mining and Metallurgy.* pp. 25 - 42.
- Baltes, N. 1959. Observatii palinologice asupra mezozoicului din Cîmpia Româna. *Petrol si Gaze.* Vol. 10. pp. 93 - 96.
- Baltes, N. 1963. Dinoflagellate si Hystrichosphaeride cretacice din Platforma Moesica. *Petrol si Gaze.* Vol. 14. pp. 581 - 589.
- Baltes, N. 1966. Cretaceous microfloristic complexes from the Moesic Platform, Romania. *Pollen et Spores.* Vol. 8. pp. 565 - 571.
- Barron, H.F. 1989. Dinoflagellate cyst biostratigraphy and palaeoenvironments of the Upper Jurassic (Kimmeridgian to basal Portlandian) of the Helmsdale region, east Sutherland, Scotland. In: Batten D. J., & Keen, M.C. (Eds.). *Northwest European Micropalaeontology and Palynology.* Micropalaeontological Society Publication Series. Ellis Horwood, Chichester. pp. 193 - 213.
- Barss, M.S. et. a.l. 1979. Palynological Zonation and correlation of sixty-seven wells, eastern Canada. *Geological Survey of Canada.* Paper 78-24. pp. 118 pp.
- Batten, D.J. 1973a. Palynology of Early Cretaceous soil beds and associated strata. *Palaeontology.* Vol. 16. pp. 399 - 424.
- Batten, D.J. 1973b. Use of palynologic assemblage types in Wealden correlation. *Palaeontology.* Vol. 16. pp. 1 - 40.
- Batten, D.J. 1974. Wealden palaeoecology from the distribution of plant fossils. *Proceedings of the Geologist's Association.* Vol. 85. pp. 433 - 458.
- Batten, D.J. 1978. Early Cretaceous to Middle Jurassic Miospores and palynofacies of the northwest European Continental Shelf. In: Thusu, B. (Ed.). *Distribution of biostratigraphically diagnostic dinoflagellate cysts and miospores from the northwest European continental shelf and adjacent areas.* Continental Shelf Institute, Publication 100. pp. 97 - 101.
- Batten, D.J. 1981. Palynofacies, organic maturation and source rock potential for petroleum. In: Brooks, J. (Ed.). *Organic Maturation Studies and Fossil Fuel Exploration.* Academic Press. pp. 201 - 223.
- Batten, D.J. 1982. Palynofacies and salinity of the Purbeck and Wealden of southern England. In: Banner, F. T. & Lord, A.R. (Eds.). *Aspects of Micropalaeontology.* Allen & Unwin, London. pp. 278 - 308.
- Batten, D.J. 1996. Chapter 26: Palynofacies. In: Jansonius, J. & McGregor, D.C. (Eds.). *Palynology: Principles and Applications.* American Association of Stratigraphic Palynologists Foundation. pp. 1011 - 1085.
- Batten, D.J., & Lister, J.K. 1988. Evidence of freshwater dinoflagellates and other algae in the English Wealden (Early Cretaceous). *Cretaceous Research.* Vol. 9. pp. 171 - 179.
- Baumgartner, P.O. 1983. Summary of Middle Jurassic-Early Cretaceous radiolarian biostratigraphy of site 534 (Blake-Bahama Basin) and correlation to Tethyan sections. *Initial Reports of the Deep Sea Drilling Project.* Vol. 76. pp. 569 - 571.
- Beju, D. 1971. Jurassic microplankton from the Carpathian Foreland of Romania. *Annales Institutii Geologice Publici Hungarici.* Vol. 54. pp. 275 - 302.

- Belayouni, H. 1984. Etude de la matière organique dans la série phosphatée du Bassin Gafsa. Metlaoui (Tunisie). Application à la compréhension des mécanismes de la phosphatogenèse. *Bureau du Recherches Geologique et Minières, Documents*. No. 77. 240 pp.
- Bellet, J., Oudin, J.L., Favero, V., & Passega, R. 1982. Analyse optique de la matière organique du Quaternaire: sondage CNR VE-1 Venise. *Revue de l'Institut Français du Pétrol*. Vol. 37. pp. 587 - 598.
- Below, R. 1981a. Dinoflagellate-Zysten aus dem oberen Hauterivien bis unteren Cenoman süd West Morokkos. *Palaeontographica Abt. B*. Vol. 176. pp. 1 - 145.
- Below, R. 1981b. Dinoflagellaten-zysten aus den Platylenticeras-Schichten (unteres Mittel-Valendis) der Ziegeleitongrube Schnepfer in Suddendorf/ Nordwest Deutschland. *Newsletters on Stratigraphy*. Vol 10. pp. 115 - 125.
- Below, R. 1982a. Dinoflagellate cysts from the Valanginian to Lower Hauterivian sections near Alt Hamouch, Morocco. *Revista Española de Micropaleontología*. Vol. 14. pp. 23 - 52.
- Below, R. 1982b. Skolochorate Zysten der Gonyaulacaceae (Dinophyceae) aus der Unterkreide Marokkos. *Palaeontographica Abt. B*. Vol. 182. pp. 1 - 51.
- Benninghoff, W.S. 1962. Calculation of pollen and spores density in sediments by addition of exotic pollen in known quantities. *Pollen et Spores*. Vol. 4. pp. 332 - 333.
- Benson, D.G.J. 1985. Observations and recommendations on the fossil dinocyst genera *Ctenidodinium*, *Dichadogonyaulax*, and *Korystocysta*. *Tulane Studies in Geology and Palaeontology*. Vol. 18. pp. 145 - 155.
- Benson, J.M. 1990. Palynofacies characteristics and palynological source rock assessment of the Cretaceous sediments of the northern Orange Basin (Kudu 9a-2 and 9A-3 boreholes). *Communications of the Geological Survey of Namibia*. Vol. 6. pp. 31 - 39.
- Benton, M.J. 1995. Diversification and extinction in the history of life. *Science*. Vol. 268. pp. 52 - 58.
- Benzaggagh, M., & Atrops, F. 1996. Répartition stratigraphiques des principales espèces de <microproblématiques> dans le Malm supérieur-Berriasien du Prérif interne et du Mésorif (Maroc). Biozonation et corrélation avec les zones d'ammonites et de calpionelles. *Comptes Rendus de la Academie des Sciences, Paris, Séries 2*. t. 322. pp. 661 - 668.
- Berglund, B., & Persson, T. 1994. Information on spore tablets. Report distributed with *Lycopodium* tablets batch 124961. Published by the University of Lund. 2 pp.
- Berthau, P.Y., & Leerveld, H. 1990. Stratigraphic implications of palynological studies on Berriasian to Albian deposits from western and southern Portugal. *Review of Palaeobotany and Palynology*. Vol. 66. pp. 313 - 344.
- Bint, A.N., & Helby, R. 1988. Upper Triassic palynofacies and environmental interpretations for the Rankin Trend, northern Carnarvon Basin, Western Australia. In: Purcell, P. G. & Purcell, R.R. (Eds.). *The North West Shelf, Australia, Proceedings, North West Shelf Symposium, Perth*. Petroleum Exploration Society of Australia. pp. 591 - 598.
- Birkelund, T., & Håkansson, E. 1983. The Cretaceous of North Greenland - a stratigraphic and biogeographical analysis. *Zitteliana*. Vol. 10. pp. 7 - 25.

- Birkelund, T., Thusu, B., & Vigran, J. 1978. Jurassic-Cretaceous biostratigraphy of Norway, with comments on the British *Rasenia cymodoce* Zone. *Palaeontology*. Vol. 21. pp. 31 - 63.
- Bjærke, T. 1977. Mesozoic palynology of Svalbard-2. Palynomorphs from the Mesozoic sequece of Kong Karls Land. *Norsk Polarinstitutt Årbok*. Vol. 1976. pp. 83 - 120.
- Bjærke, T. 1980. Mesozoic palynology of Svalbard V. Dinoflagellates from the Agardhfjellet Member (Middle and Upper Jurassic) in Spitzbergen. *Norsk Polarinstitutt Skrifter*. Vol. 172. pp. 145 - 167.
- Bjærke, T., Edwards, M.B., & Thusu, B. 1976. Microplankton from the Janusfjellet Subgroup (Jurassic-Lower Cretaceous) at Agardhfjellet, Spitzbergen. A preliminary report. *Norsk Polarinstitutt Årbok*. Vol. 1974. pp. 63 - 88.
- Bjærke, T., & Thusu, B. 1976. Cretaceous palynomorphs from Spitzbergenbanken, NW Barents Shelf. *Norsk Polarinstitutt Årbok*. Vol. 1974. pp. 258 - 262.
- Blanco, J. 1995. The distribution of dinoflagellate cysts along the Galician (NW Spain) coast. *Journal Of Plankton Research*. Vol. 17. pp. 283 - 302.
- Blom, G.I., Kuznetsova, K.I., & Mesezhnikov, M.S. 1984. Cretaceous boundary beds in the Middle Volga River area and Ryasan District. Guide to Excursion 060. In: Blom, G. I., Breslav, S.L., Gerasimov, P.A., Golivkin, N.I., Demchenko, D.M., Dmitriev, V.P., Zolotariov, G.S., Kononov, N.D., Korobeinikov, V.N., Kuznetsova, K.I., Kuzmenko, Yu.T., Lazarenko, M.T., Lifits, Ya.G., Mesezhnikov, M.S., & Orlov, V. *27th International Geological Congress, USSR. Central Regions of the European part of the RSFSR; Moscow syncline, Voronezh and Volgo-Ural anticlines. Guidebook for excursions 059, 060, 066*. Moscow., pp. 113 - 124 & Figs 11 & 12 (pp 71 - 72).
- Blondel, T., Gorin, G.E., & Jan du Chên, R. 1993. Sequence stratigraphy in coastal environment: sedimentology and palynofacies of the Miocene in Central Tunisia. In: Posamentier, H. W., Summerhayes, C.P., Haq, B.U., & Allen, G.P. (Eds.). *Sequence Stratigraphy and Facies Association*. Special Publication Number 18 of the International Association of Sedimentologists. Published by Blackwell Scientific. pp. 161 - 179.
- Bolli, H.M. 1980. Calcisphaerulidae and Calpionellidae from the Upper Jurassic and Lower Cretaceous of Deep Sea Drilling Project Hole 416A, Moroccan Basin. *Initial Reports of the Deep Sea Drilling Project*. Vol. 50. pp. 525 - 543.
- Bonny, A.P. 1972. A method for determining absolute pollen frequencies in lake sediments. *New Phytologist*. Vol. 71. pp. 393 - 405.
- Borza, V., & Petercáková, M. 1994. The Jurassic/Cretaceous boundary beds in the Strázovce section (Strázovské vrchy Mts., Western Carpathians). *Palaeopelagos Special Publication*. Vol. 1. pp. 7 - 15.
- Botz, R., Hiltmann, W., Schoell, M., Teschner, M., & Wehner, H. 1981. Kriterien und Bewertung des Zechstein-Stinkschiefers im Hinblick auf sein Erdöl und Erdgaspotential. *Geologisches Jahrbuch*. Vol. 47. pp. 113 - 132.
- Boulter, M.C., & Riddick, A. 1986. Classification and analysis of palynodebris from the Palaeocene sediments of the Forties Field. *Sedimentology*. Vol. 33. pp. 871 - 886.
- Boulter, M.C. 1994. An approach to a standard terminology for palynodebris. In: Traverse, A. (Ed.). *Sedimentology of Organic Particles*. Cambridge University Press. pp. 199 - 216.

- Bralower, T.J., Monechi, S., & Thierstein, H.R. 1989. Calcareous nannofossil zonation of the Jurassic/Cretaceous boundary interval and correlations with the geomagnetic polarity timescale. *Marine Micropaleontology*. Vol. 14. pp. 153 - 235.
- Brideaux, W.W. 1977. Taxonomy of Upper Jurassic - Lower Cretaceous microplankton from the Richardson Mountains, District of MacKenzie, Canada. *Geological Survey of Canada Bulletin*. 281. 89 pp.
- Brideaux, W.W., & Fisher, M.J. 1976. Upper Jurassic-Lower Cretaceous dinoflagellate assemblages from Arctic Canada. *Geological Survey of Canada Bulletin*. Vol. 259. pp. 1 - 53.
- Brideaux, W.W., & Myhr, D.W. 1976. Lithostratigraphy and dinoflagellate cyst succession in the Gulf Mobil Parsons N-10 Well, District of Mackenzie. (Projects 710019 and 710036). *Geological Survey of Canada*. Paper 76-1B. pp. 235 - 249.
- Brinkhuis, H. 1994. Late Eocene to Early Oligocene dinoflagellate cysts from the Priabonian type area (northeast Italy): biostratigraphy and paleoenvironmental interpretation. *Palaeogeography, Palaeoclimatology, Palaeoecology*. Vol. 107. pp. 121 - 163.
- Brinkhuis, H., & Zachariasse, W.J. 1988. Dinoflagellate cysts, sea level changes and planktonic foraminifers across the Cretaceous/Tertiary boundary at El Haria, northwest Tunisia. *Marine Micropaleontology*. Vol. 13. pp. 153 - 191.
- Bryant, I.D., Kantorowitz, J.D., & Love, C.F. 1988. The origin and recognition of laterally continuous carbonate-cemented horizons in the Upper Lias Sands of southern England. *Marine & Petroleum Geology*. Vol. 5. pp. 108 - 133.
- Bujak, J.P., Barss, M.S., & Williams, G.L. 1977. Offshore East Canada's organic type and color and hydrocarbon potential. *Oil and Gas Journal*. Vol. 75. pp. 96 - 100.
- Bujak, J.P., & Williams, G.L. 1977. Jurassic Palynostratigraphy of Offshore Eastern Canada. In: Swain, F. M. (Ed.). *Stratigraphic Micropalaeontology of the Atlantic Basin and Borderlands*. Dev. Palaeontol. Strat. Elsevier. pp. 321 - 339.
- Bujak, J.P., & Williams, G.L. 1978. Cretaceous palynostratigraphy of offshore southeastern Canada. *Geological Survey of Canada*. Bulletin 297. pp. 1 - 19.
- Burger, D. 1966. Palynology of the uppermost Jurassic and lowermost Cretaceous strata in the eastern Netherlands. *Leidse Geologische Mededelingen*. Vol. 35. pp. 211 - 276.
- Burger, D. 1980. Early Cretaceous (Neocomian) microplankton from the Carpentaria Basin, northern Queensland. *Alcheringa* Vol. 4. pp. 263 - 279.
- Burgess, J.D. 1974. Microscopic examination of kerogen (dispersed organic matter) in petroleum exploration. *Geological Society of America, Special Paper, 153*. pp. 19 - 30.
- Busnardo, R., Donze, P., Le Hégarat, G., Memmi, L., & M'Rabet, A. 1976. Précisions Biostratigraphiques nouvelles sur le Berriasien des Djebel Nara et Sidi Kralif (Tunisie Central). *Géobios*. No. 9. pp. 231 - 250.
- Bustin, R.M. 1988. Sedimentology and characteristics of dispersed organic matter in Tertiary Niger Delta: origin of source rocks in the deltaic environment. *Bulletin of the American Association of Petroleum Geologists*. Vol. 72. pp. 277 - 298.

- Bustin, R.M. 1991. Quantifying macerals: some statistical and practical considerations. *International Journal of Coal Geology*. Vol. 17. pp. 213 - 238.
- Calloman, J.H. 1984. Biostratigraphy, chronostratigraphy and all that - again! In: Michelson, O. & Zeiss, A. (Eds.). *International Symposium on Jurassic Stratigraphy*. Geological Survey of Denmark, Copenhagen. pp. 612 - 624.
- Calvert, S.E., & Pedersen, T.F. 1992. Organic carbon accumulation and preservation in marine sediments: How important is anoxia? In: Whelan, J. K., & Farrington, J.W. (Eds.). *Organic matter: productivity, accumulation, and preservation in recent and ancient sediments*. pp. 231 - 263.
- Casey, R. 1967. The position of the Middle Volgian in the English Jurassic. *Proceedings of the Geological Society of London*. Vol. 1640. pp. 128 - 133.
- Casey, R. 1968. The type section of the Volgian stage (Upper Jurassic) at Gorodische, near Ulyanovsk, U.S.S.R.. *Proceedings of the Geological Society of London*. Vol. 1648. pp. 74 - 75.
- Casey, R. 1973. The ammonite succession at the Jurassic - Cretaceous boundary in eastern England. In: Casey, R. & Rawson, P.F. (Eds.). *The Boreal Lower Cretaceous*. Geological Journal Special Issue No. 5. pp. 193 - 266.
- Casey, R., Mesezhnikov, M.S, & Shulgina, N.I. 1977. Sopostavlenie pogranychikh otlozhenij Yury i Mela Anglii, Russkoj platformy, pripolyarnogo Urala i Sibiri. *Izvestia Akademiya Nauk SSSR, Series Geology*. Vol. 7. pp. 14 - 33.
- Casey, R., & Rawson, P.F. 1973. A review of the Boreal Lower Cretaceous. In: Casey, R. & Rawson, P.F. (Eds.). *The Boreal Lower Cretaceous*. Geological Journal Special Issue No. 5. pp. 415 - 430.
- Ceratini, C. 1994. Palynofacies of some Recent marine sediments: the role of transportation. In: Traverse, A. *Sedimentology of Organic Particles*. Cambridge University Press. pp. 129 - 139.
- Ceratini, C., Bellet, J., & Tissot, C. 1979. Étude microscopique de la matière organique: Palynologie et palynofaciès. In: *Géochimie des Sédiments Marins Profonds. ORGON III: Mauritaine-Sénégal-Isles du Cap-Vert*. Éditions du Centre National de la Recherche Scientifique, Paris. pp. 215 - 265.
- Ceratini, C., Bellet, J., & Tissot, C. 1983. Les Palynofacies: représentations graphique, interpret de leur étude pour les reconstitutions paléogéographiques. In: *Géochimie organique des sédiments marins d'Orgon a Misedor*. pp. 327 - 352.
- Chen, Y.Y. 1978. Jurassic and Cretaceous palynostratigraphy of a Madagascar well. Unpublished PhD thesis, University of Arizona, Tucson.
- Chen, Y.Y. 1982. Recognition of the dinocyst genus *Komewuia* with assignable species from Madagascar. *Micropalaeontology*. Vol. 28. pp. 31 - 42.
- Claret, J., Jardine, S., & Robert, P. 1981. La diversité des roches mères pétrolières: aspects géologiques et implications économiques à partir de quatre exemples. *Bulletin des Centres Recherche Exploration-Production Elf-Aquitaine*. Vol. 5. pp. 383 - 417.
- Clark, R. L. 1986. Pollen as a chronometer and sediment tracer, Burrinjack Reservoir, Australia. *Hydrobiologia*. Vol. 143. pp. 63 - 69.
- Clarke, R.F.A. 1967. Dinoflagellates and their stratigraphic use. *Geologie en Mijnbouw*. Vol. 46. pp. 206 - 207.

- Cole, D.C., & Harding, I.C. 1998. Use of palynofacies analysis to define Lower Jurassic (Sinemurian to Pleinsbachian) genetic stratigraphic sequences in the Wessex Basin, England. In: Underhill, J. R. (Ed.). *Development, Evolution, and Petroleum Geology of the Wessex Basin*. Geological Society Special Publication. pp. 165 - 185.
- Colin, J.-P., Ioannides, N.S., & Vining, B. 1992. Mesozoic stratigraphy of the Goban Spur, offshore south-west Ireland. *Marine and Petroleum Geology*. Vol. 9. pp. 527 - 541.
- Combaz, A. 1964. Les Palynofaciès. *Review de Micropalaeontologie*. Vol. 7. pp. 205 - 218.
- Combaz, A. 1967. Leiosphaeridiacea Eisenack 1954, et Protoleiosphaeridae Timofeev 1959 - leurs affinités, leur rôle sédimentologique et géologique. *Review of Palaeobotany and Palynology*. Vol. 1. pp. 309 - 321.
- Combaz, A. 1980. Les kérogènes vus au microscope. In: Durand, B. (Ed.). *Kerogen: Insoluble Organic Matter from Sedimentary Rocks*. Paris. pp. 55 - 111.
- Conway, B.H. 1990. Paleozoic-Mesozoic palynology of Israel II. Palynostratigraphy of the Jurassic succession in the subsurface of Israel. *Geological Survey of Israel, Bulletin*. Vol. 82. pp. 1 - 18.
- Conway, B.H. 1996. A palynological investigation across the Jurassic/Cretaceous boundary on the south-east flanks of Mount-Hermon, Israel. *Cretaceous Research*. Vol. 17. pp. 197 - 214.
- Cope, J.C.W. 1967. The palaeontology and stratigraphy of the lower part of the Upper Kimmeridge Clay of Dorset. *Bulletin of the British Museum (Natural History) Geology*. Vol. 15. pp. 1 - 79.
- Cope, J.C.W. 1978. The ammonite faunas and stratigraphy of the upper part of the Upper Kimmeridge Clay of Dorset. *Palaeontology*. Vol. 21. pp. 469 - 533.
- Cope, J.C.W. 1993. The Bolonian Stage: an old answer to an old problem. *Newsletters on Stratigraphy*. Vol. 28. pp. 151 - 156.
- Cope, J.C.W., Duff, K.L., Parsons, C.F., Torrens, H.S., Wimbledon, W.A., & Wright, J.K. 1980. A correlation of Jurassic rocks in the British Isles. Part Two: Middle and Upper Jurassic. *Geological Society of London. Special Report No. 15*. 109pp.
- Cope, M.J. 1981. Products of natural burning as a component of the dispersed organic matter of sedimentary rocks. In: Brooks, J. (Ed.). *Organic Maturation Studies and Fossil Fuel Exploration*. Academic Press. pp. 89 - 109.
- Costa, L.I., & Davey, R.J. 1992. Dinoflagellate cysts of the Cretaceous System. In: Powell, A. J. (Ed.). *A Stratigraphic Index of Dinoflagellate Cysts*. Micropalaeontological Society Publications Series. Chapman & Hall, London. pp. 99 - 153.
- Courtinat, B. 1989. Les organoclastes des formations lithologiques du Malm dans le Jura méridional, biostratigraphie et éléments d'interprétation paléoécologiques. *Laboratoires de Géologie de la Faculté des Sciences de Lyon, Documents*. 105. pp. 1 - 361.
- Courtinat, B. 1993. The significance of palynofacies fluctuations in the Greenhorn Formation (Cenomanian-Turonian) of the Western Interior Basin, U.S.A.. *Marine Micropalaeontology*. Vol. 21. pp. 249 - 257.

- Courtinat, B., Crumière, J.-P., Méon, H., & Schaaf, A. 1991. Les associations de kystes de dinoflagellés du Cénomanién-Turonien de Vergons (Bassin Vocontien France). *Geobios*. Vol. 24. pp. 649 - 666.
- Cox, B.M., & Gallois, R.W. 1981. The stratigraphy of the Kimmeridge Clay of the Dorset type area and its correlation with some other Kimmeridgian sequences. *Institute of Geology Scientific Reports*. 80/4. pp. 1 - 44.
- Cox, B.M., Lott, G.K., Thomas, J.E., & Wilkinson, I.P. 1987. Upper Jurassic stratigraphy of four shallow cored boreholes in the U.K. sector of the southern North Sea. *Proceedings of the Yorkshire Geological Society*. Vol. 46. pp. 97 - 109.
- Cross, A.T., Thompson, G.G., & Zaitzeff, J.B. 1966. Source and distribution of palynomorphs in bottom sediments, southern part of Gulf of California. *Marine Geology*. Vol. 4. pp. 467 - 524.
- Dale, B. 1976. Cyst formation, sedimentation, and preservation: Factors affecting dinoflagellate assemblages in Recent sediments from Trondheimsfjord, Norway. *Review of Palaeobotany and Palynology*. Vol. 22. pp. 39 - 60.
- Dale, B. 1983. Dinoflagellate resting cysts: "benthic plankton". In: Fryxell, G. A. (Ed.). *Survival strategies of the algae*. Cambridge University Press. pp. 69 - 136.
- Darby, J., & Hart, G.F. 1994. Organic sedimentation in a carbonate environment. In: Traverse, A. (Ed.). *Sedimentation of Organic Particles*. Cambridge University Press. pp. 177 - 197.
- Darrell, J.H., & Hart, G.F. 1970. Environmental determinations using absolute miospore frequency, Mississippi River delta. *Geological Society of America Bulletin*. Vol. 81. pp. 2513 - 2518.
- Davey, R.J. 1970. Non-calcareous microplankton from the Cenomanian of England, northern France and North America, part 2. *Bulletin of the British Museum (Natural History) Geology*. Vol. 18. pp. 333 - 397.
- Davey, R.J. 1974. Dinoflagellate cysts from the Barremian of the Speeton Clay, England. *Symposium on stratigraphic palynology, Birbal Sahni Institute of Palaeobotany, Special publication*. Vol. 3. pp. 41 - 75.
- Davey, R.J. 1979. The stratigraphic distribution of dinocysts in the Portlandian (latest Jurassic) to Barremian (Early Cretaceous) of northwest Europe. *American Association of Stratigraphic Palynologists, Contributions Series 5B*. pp. 48 - 81.
- Davey, R.J. 1982. Dinocyst stratigraphy of the latest Jurassic to Early Cretaceous of the Haldager No. 1 borehole, Denmark. *Geological Survey of Denmark, Series B*. No. 6. pp. 1 - 57.
- Davey, R.J., Downie, C., Sarjeant, W.A.S., & Williams, G.L. 1966. Studies on Mesozoic and Cainozoic dinoflagellate cysts. *Bulletin of the British Museum of Natural History (Geology), London*. Vol. 17. pp. 1 - 26.
- Davey, R.J., & Riley, L.A. 1978. Late and Middle Jurassic Dinoflagellate Cysts. In: Thusu, B. (Ed.). *Distribution of biostratigraphically diagnostic dinoflagellate cysts and miospores from the northwest European continental shelf and adjacent areas*. Continental Shelf Institute, Publication 100. pp. 31 - 45.
- Davey, R.J., & Rogers, J. 1975. Palynomorph distribution in Recent offshore sediments along two traverses off south west Africa. *Marine Geology*. Vol. 18. pp. 213 - 225.

- Davies, E.H. 1983. The dinoflagellate Opperl-zonation of the Jurassic-Lower Cretaceous sequence in the Sverdrup Basin, Arctic Canada. *Geological Survey of Canada. Bulletin* 359. pp. 1 - 59.
- Davies, E.H., & Norris, G. 1980. Latitudinal variations in encystment modes and species diversity in Jurassic dinoflagellates. In: Strangway, D. W. (Ed.). *The Continental Crust and its Mineral Deposits. Geological Association of Canada, Special Paper* 20. pp. 361 -373.
- Davies, E.H., & Poulton, T.P. 1986. Upper Jurassic dinoflagellate cysts from strata of north-eastern British Columbia. *Geological Survey of Canada. Paper* 86-1B. pp. 519 - 537.
- Davies, J. R., McNestry, A., & Walters, R.A. 1991. Palaeoenvironments and palynofacies of a pulsed transgression: the late Devonian and early Dinantian (Lower Carboniferous) rocks of southeast Wales. *Geological Magazine. Vol.* 28. pp. 355 - 380.
- Davis, R.B. 1967. Pollen studies of near-surface sediments in Maine lakes. In: Cushing, E. J. & Wright, H.E., Jr. (Eds.). *Quaternary Palaeoecology. Yale University Press, New Haven.* pp. 143 - 173.
- Dean, G. 1998. Finding a needle in a palynological haystack: comparison of methods. In: Bryant, V. M. & Wrenn, J.H. (Eds.). *New Developments in Palynomorph Sampling, Extraction, and Analysis. American Association of Stratigraphic Palynologists Foundation. Contributions Series Number* 33. pp. 53 - 59.
- Deroo, G., de Graciansky, P., Habib, D., & Herbin, J.P. 1978. L'origine de la matière organique dans les sédiments crétacés du site I.P.O.D. 398 (haut-fond de Vigo): corrélations entre les données de la sédimentologie, de la géochimie organique et de la palynologie. *Bulletins Société Géologiques de la France. Vol.* 7. pp. 465 - 469.
- de Vernal, A., Bilodeau, G., Hillaire-Marcel, C., & Kassou, N. 1992. Quantitative assessment of carbonate dissolution in marine sediments from foraminifer linings vs. shell ratios: Davis Strait, northwest North Atlantic. *Geology. Vol.* 20. pp. 527 - 530.
- de Vernal, A., & Giroux, L. 1991. Distribution of organic-walled microfossils in Recent sediments from the Estuary and Gulf of St Lawrence: some aspects of the organic matter fluxes. *Special Publication of Canadian Fisheries and Aquatic Sciences. Vol.* 113. pp. 189 - 199.
- de Vernal, A., Larouche, A., & Richard, P.J.H. 1987. Evaluation of palynomorph concentrations: do the aliquot and the marker-grain methods yield comparable results? *Pollen et Spores. Vol.* 29. pp. 291 - 303.
- Deflandre, G. 1938. Microplankton des mers jurassiques conservé dans les marnes de Villers-sur-Mer (Calvados). Étude liminaire et considérations générales. *Travaux Station Zoologique, Wimereux. Vol.* 13. pp. 147 - 200.
- Deflandre, G. 1941. Le microplankton kimméridgien d'Orbagnoux et l'origine des huiles sulfurées naturelles. *Mémoires de l'Académie des Sciences. Vol.* 65. pp. 1 - 32.
- Dennison, C.N., & Fowler, R.M. 1980. Palynological identification of facies in a deltaic environment. In: *The Sedimentation of North Sea Reservoir Rocks. Norwegian Petroleum Society.* pp. 1 - 22.
- Détraz, H., & Mojon, P.-O. 1989. Évolution paléogéographique de la marge jurassienne de la Téthys du Tithonique-Portlandien au Valanginien: corrélations biostratigraphique et séquentielle des faciès marins à continentaux. *Eclogae Geologicae Helveticae. Vol.* 82. pp. 37 - 112.

- Dimter, A., & Smelror, M. 1990. Callovian (Middle Jurassic) marine microplankton from southwest Germany: biostratigraphy and palaeoenvironmental interpretations. *Palaeogeography, Palaeoclimatology, Palaeoecology*. Vol. 80. pp. 173 - 195.
- Dodekova, L. 1967. Les dinoflagellés et acritarchs de l'Oxfordien-Kimmeridgien de la Bulgarie du Nord-est. *Annales University Sofia*. Vol. 60. pp. 9 - 29.
- Dodekova, L. 1969. Dinoflagellés et acritarches du Tithonique aux environs de Pleven, Bulgarie Centrale du Nord. *Bulletin, Geological Institute of Sofia* Vol. 18. pp. 13 - 24.
- Dodekova, L. 1992. Dinoflagellate cysts from the Bathonian - Tithonian (Jurassic) of north Bulgaria. II. Taxonomy of Oxfordian and Kimmeridgian dinoflagellate cysts. *Geologica Balcanica*. Vol. 22. pp. 33 - 69.
- Dodekova, L. 1994. Dinoflagellate cysts from the Bathonian - Tithonian (Jurassic) of North Bulgaria. III. Tithonian dinoflagellate cysts. *Geologica Balcanica*. Vol. 22. pp. 11 - 46.
- Dodge, J.D., & Harland, R. 1991. The distribution of planktonic dinoflagellates and their cysts in the eastern and northeastern Atlantic Ocean. *New Phytologist*. Vol. 118. pp. 593 - 603.
- Dörhöfer, G., & Norris, G. 1977. Discrimination and correlation of highest Jurassic and lowest Cretaceous terrestrial palynofloras in north-west Europe. *Palynology*. Vol. 1. pp. 79 - 93.
- Dörhöfer, G. 1977. Palynologie und Stratigraphie der Bückenberg-Formation (Berriasium-Valanginium) in der Hilsmulde (NW-Deutschland) *Geologische Jahrbuch Series A*. Vol. 42. pp. 3 - 122.
- Döring, H. 1965. Die sporenpaläontologische Gliederung des Wealden in Westmecklenburg (Struktur Werle). *Geologie Jahrg.* Vol. 14. pp. 1 - 118.
- Dow, W.G., & Pederson, D.B. 1975. Organic matter in Gulf Coast sediments. In: *Offshore Technology Conference Proceedings*. Dallas, Texas. Vol. 3. Paper 2343, 10pp.
- Downie, C. 1956. Microplankton from the Kimmeridge Clay. *Quarterly Journal of the Geological Society of London*. Vol. 112. pp. 413 - 434.
- Downie, C., Hussain, M.A., & Williams, G.L. 1971. Dinoflagellate cyst and acritarch associations in the Paleogene of southeast England. *Geoscience and Man*. Vol. 3. pp. 29 - 35.
- Downie, C., & Sarjeant, W.A.S. 1966. The morphology, terminology and classification of fossil dinoflagellates. In: Davey, R. J., Downie, C., Sarjeant, W.A.S., Williams, G.L. *Studies on Mesozoic and Cainozoic dinoflagellate cysts*. Bulletin of the British Museum Natural History (Geology), Supplement 3, pp. 10 - 17.
- Drugg, W.S. 1978. Some Jurassic dinoflagellate cysts from England, France and Germany. *Palaeontographica Abt. B*. Vol 168. pp. 61 - 79.
- Dürr, G. 1987. Dinoflagellate-Zysten aus dem Weißjura δ (Mittelkimmergien) der westlichen schwäbischen Alb (Süddeutschland). *Neues Jahrbuch für Geologie und Paläontologie, Abhandlungen*. Vol. 176. pp. 67 - 80.

- Dürr, G. 1988. Palynostratigraphie des Kimmeridgium und Tithonium von Süddeutschland und Korrelation mit borealen Floren. *Tübinger Mikropaläontologische Mitteilungen*. Vol. 5. pp. 1 - 159.
- Dürr, G. 1989. Palynostratigraphische Untersuchungen im Oxfordium und Kimmeridgium der Goethermiebohrung Saulgau GB3. *Geologische Abhandlungen*. Vol. 13. pp. 23 - 51.
- Duxbury, S. 1977. A palynostratigraphy of the Berriasian to Barremian of the Speeton Clay of Speeton, England. *Palaeontographica Abt. B*. Vol. 160. pp. 17 - 67.
- Duxbury, S. 1978. Early Cretaceous Dinoflagellate Cysts. In: Thusu, B. (Ed.). *Distribution of biostratigraphically diagnostic dinoflagellate cysts and miospores from the northwest European continental shelf and adjacent areas*. Continental Shelf Institute, Publication 100. pp. 19 - 29.
- Duxbury, S. 1979. Three new genera of dinoflagellate cyts from the Speeton Clay (Early Cretaceous) of Speeton, England. *Micropalaeontology*. Vol. 25. pp. 198 - 205.
- Dybkjær, K. 1991. Palynological zonation and palynofacies investigation of the Fjerritslev Formation (lower Jurassic - basal Middle Jurassic) in the Danish subbasin. *Danmarks Geologiske Undersøgelse, Serie A*. Vol. 30. pp. 1 - 150.;
- Ebukanson, E.J., & Kinghorn, R.R.F. 1985. Kerogen facies in the major Jurassic mudrock formations of southern England, and implications on the depositional environments of their precursors. *Journal of Petroleum Geology*. Vol. 8. pp. 435 - 462.
- Ediger, V.S. 1986. Sieving techniques in palynological sample processing with special reference to the MRA system. *Micropalaeontology*. Vol. 32. pp. 256 - 270.
- Edwards, L.E. 1989. Dinoflagellate cysts from the Lower Tertiary Formations, Haynesville cores, Richmond County, Virginia. *United States Geological Survey Professional Paper, 1489-C*. pp. 1 - 12.
- Erkman, U., & Sarjeant, W.A.S. 1980. Dinoflagellate cysts, acritarchs and tasmanitids from the uppermost Callovian of England and Scotland: with a reconsideration of the "*Xanthidium pilosum*" problem. *Geobios*. Vol. 13. pp. 45 - 99.
- Evitt, W.R. 1985. *Sporopollenin dinoflagellate cysts: Their morphology and interpretation*. American Association of Stratigraphic Palynologists Foundation. 333pp.
- Farley, M.B., & Dilcher, D.L. 1986. Correlation between miospores and depositional environments of the Dakota Formation (mid-Cretaceous) of north-central Kansas and adjacent Nebraska, USA. *Palynology*. Vol. 10. pp. 117 - 133.
- Farr, K.M. 1989. Palynomorph and palynodebris distributions in modern British and Irish estuarine sediments. In: Batten, D. J. & Keen, M.C. (Eds.). *Northwest European Micropalaeontology and Palynology*. British Micropalaeontology and Palynology Series. Ellis Horwood. pp. 265 - 285.
- Fauconnier, D. 1989. Palynology du stratotype historique de L'Hauterive. *Mémoires de la Societe Neuchâteloise des Sciences Naturelles*, Vol. 11. pp. 233 - 255.
- Fauconnier, D., & Slansky, M. 1978. Role possible des dinoflagelles dans la sédimentation phosphatée. *Bulletines de la Bureau Recherches Geologiques et Minières*. Vol. 4. pp. 191 - 200.
- Fauconnier, D., & Slansky, M. 1980. Relations entre le développement des Dinoflagellés et la sédimentation phosphatée du Bassin de Gafsa (Tunisie). *Documents de Bureau du Recherche Géologique et Minières*. Vol. 24. pp. 185 - 204.

- Federova, V.A., Bystrova, V.V., & Kolpenskaya, N.N. 1993. Detailed microbiostratigraphy of the Boreal Berriasian reference sections of the Russian territory (Izhma, Yatriya, and Boyarka Rivers). In: *Stratigraphiya phanarozoya neftegazonosnih regionov rossiy. Goskomgeologiya rossiskoi federatsii. Vserossiskii ordina Troodovoga Krasnoga Zrameni. Neftryanoi nauchna-isseldovatelskii geologorazvedochnie institut (VNIGRI)*. (in Russian). pp. 172 - 188.
- Fensome, R.A. 1979. Dinoflagellate cysts and acritarchs from the Middle and Upper Jurassic of Jameson Land, East Greenland. *Grønlands Geologiske Undersøgelse Bulletin*. Vol. 132. pp. 1 - 96.
- Fensome, R.A., Taylor, F.J.R., Norris, G., Sarjeant, W.A.S., Wharton, D.I., & Williams, G.L. 1993. A classification of living and fossil dinoflagellates. *Micropaleontology Special Publication no. 7*. 351 pp.
- Firth, J.V. 1993. Palynofacies and thermal maturation analysis of sediments from the Nankai Trough. *Initial Reports of the Deep Sea Drilling Project*. Vol. 131. pp. 57 - 69.
- Fisher, M.J. 1980. Kerogen distribution and depositional environments in the middle Jurassic of Yorkshire, U.K. In: *4th International Palynological conference, Lucknow, 1976-1977*. Vol. 2. pp. 574 - 580.
- Fisher, M.J., & Riley, L.A. 1980. The stratigraphic distribution of dinoflagellate cysts at the Boreal Jurassic-Cretaceous boundary. In: *Fourth International Palynological conference, 1976-1977*. Lucknow. Vol. 2. pp. 313 - 329.
- Fisher, R.A., Corbet, A.S., & Williams, C.B. 1943. The relation between the number of species and the number of individuals in a random sample of an animal population. *Journal of Animal Ecology*. Vol. 12. pp. 42 - 58.
- Frank, M.C., & Tyson, R.V. 1995. Parasequence-scale organic facies variations through an Early Carboniferous Yoredale cyclothem, Middle Limestone Group, Scremerston, Northumberland. *Journal of the Geological Society of London*. Vol. 152. pp. 41 - 50.
- Funkhouser, J.W., & Evitt, W.R. 1959. Preparation techniques for acid insoluble microfossils. *Micropalaeontology*. Vol. 5. pp. 369 - 375.
- Funkhouser, J.W. 1969. Factors that affect sample reliability. In: Tschudy, R. & Scott, R.T. (Eds.). *Aspects of Palynology*. Wiley Interscience. pp. 97 - 102.
- Garg, R., Ateequzzaman, K., & Jain, K.P. 1987. Jurassic and Lower Cretaceous dinoflagellate cysts from India with some remarks on the concept of upper Gondwana. *The Palaeobotanist*. Vol. 36. pp. 254 - 267.
- Gerasimov, P.A. 1969. *The upper substage of the Volgian Stage of the central part of the Russian Platform: a palaeontological - stratigraphical - lithological study*. Moscow. 144 pp.
- Gerasimov, P.A., Kuznetsova, K., Mikchailov, N.P., & Uspenskaya, E.A. 1975. Correlation of the Volgian, Portlandian and Tithonian stages. *Bureau de Recherches Geologiques et Minières: Memoirs*. Vol. 86. pp. 117 - 121.
- Gerasimov, P.A., & Mikhailov, N.P. 1966. Volgian Stage and the geostratigraphical scale for the upper series of the Jurassic System. *Izvestia Akademii Nauk SSSR Series Geology*. 1977/7. pp. 14 - 33.

- Geysant, J. 1997. Chapitre 1.11: Tithonien. In: Cariou, E., & Hantzpergue, P. (Eds.). *Biostratigraphie Jurassique Ouest-Européen et Méditerranéen. Zonations parallèles et distributions des invertébrés et microfossiles*. Groupe Français Etude Jurassique Memoire 17. pp. 97 - 103.
- Gitmez, G.U. 1970. Dinoflagellate cysts and acritarchs from the Basal Kimmeridgian (Upper Jurassic) of England, Scotland and France. *Bulletin of the British Museum (Natural History)-Geology*. Vol. 18. pp. 233 - 331.
- Gitmez, G.U., & Sarjeant, W.A.S. 1972. Dinoflagellate cysts and acritarchs from the Kimmeridgian (Upper Jurassic) of England, Scotland and France. *Bulletin of the British Museum (Natural History): Geology*. Vol. 21. pp. 171 - 257.
- Goodman, D.K. 1979. Dinoflagellate 'communities' from the Lower Eocene Nanjemoy Formation of Maryland, USA. *Palynology*. Vol. 3. pp. 169 - 190.
- Goodman, D.K. 1987. Dinoflagellate cysts in Ancient and Modern Sediments. In: Taylor, F. J. R. (Ed.). *The Biology of Dinoflagellates*. Botanical Monographs. pp. 649 - 722.
- Gorin, G., Gülçar, F., & Cornioley, Y. 1989. Organic geochemistry, maturity, palynofacies and palaeoenvironment of Upper Kimmeridgian and Lower Tertiary organic-rich samples in the southern Jura (Ain, France) and subalpine massifs (Haute-Savoie, France). *Eclogae Geologicae Helveticae*. Vol. 82. pp. 491 - 515.
- Gorin, G., & Monteil, E. 1990. Preliminary note on the organic facies, thermal maturity, and dinoflagellate cysts of the Upper Maastrichtian Wang Formation in the northern Subalpine Massifs (western Alps, France). *Eclogae Geologicae Helveticae*. Vol. 83. pp. 265 - 285.
- Gorin, G., & Steffen, D. 1991. Organic facies as a tool for recording eustatic variations in marine fine-grained carbonates: example of the Berriasian stratotype at Berrias (Ardèche, SE France). *Palaeogeography, Palaeoclimatology, Palaeoecology*. Vol. 85. pp. 303 - 320.
- Górka, H. 1965. Les microfossiles du Jurassique supérieur de Magnuszew (Pologne). *Acta Palaeontologica Polonica*. Vol. 10. pp. 291 - 334.
- Gradstein, F.M., Huang, Z., Merret, D., & Ogg, J.G. 1992. Probabilistic zonation of early Cretaceous microfossil sequences, Atlantic and Indian Oceans, with special reference to Leg 123. *Proceedings of the Ocean Drilling Program, Scientific Results*. Vol. 123. pp. 759 - 773.
- Gregory, W.A., & Hart, G.F. 1992. Towards a predictive model for the palynologic response to sea-level changes. *Palaios*. Vol. 7. pp. 3 - 33.
- Groot, J.J., Groot, C.R., Ewing, M., Burckle, L., & Conolly, J.R. 1967. Spores, pollen, diatoms and provenance of the Argentine Basin sediments. *Progress in Oceanography*. Vol. 4. pp. 179 - 217.
- Gross, M.G., Carey, A.G. Jr., Fowler, G.A., & Kulm, L.D. 1972. Distribution of organic carbon in surface sediment, northeast Pacific Ocean. In: Pruter, A. T., & Alverson, D. (Eds.). *The Columbia River Estuary and Adjacent Ocean Waters - Bioenvironmental Studies*. University of Washington Press. pp. 254 - 264.
- Gübeli, A., Hochuli, P.A., & Wildi, W. 1984. Lower Cretaceous turbiditic sediments from the Rif chain (northern Morocco)- palynology, stratigraphy and palaeogeographic setting. *Geologische Rundschau*. Vol. 73. pp. 1081 - 1114.

- Habib, D. 1972. Dinoflagellate Stratigraphy Leg 11, Deep Sea Drilling Project. *Initial Reports of the Deep Sea Drilling Project*. Vol. 11. pp. 367 - 425.
- Habib, D. 1976. Neocomian dinoflagellate zonation in the western North Atlantic. *Micropalaeontology*. Vol. 21. pp. 373 - 392.
- Habib, D. 1977. Comparison of Lower and Middle Cretaceous palynostratigraphic zonation in the western North Atlantic. In: Swain, F. M. (Ed.). *Stratigraphic Micropalaeontology of the Atlantic Basin and Borderlands*. Elsevier. pp. 341 - 367.
- Habib, D. 1978. Palynostratigraphy of the Lower Cretaceous section at Deep Sea Drilling Project Site 391, Blake-Bahama basin, and its correlation in the North Atlantic. *Initial Reports of the Deep Sea Drilling Project*. Vol. 44. pp. 887 - 897.
- Habib, D. 1979a. Sedimentary origin of North Atlantic Cretaceous paynofacies. In: Talwani, M., Hay, W., & Ryan, W.B.F. (Eds.). *Deep Drilling Results in the Atlantic Ocean: Continental Margins and Palaeoenvironment*. American Geophysical Union, Maurice Ewing Series 3. pp. 420 - 437.
- Habib, D. 1979b. Sedimentology of palynomorphs and palynodebris in Cretaceous carbonaceous facies south of Vigo Seamount. *Initial Reports of the Deep Sea Drilling Project*. Vol. 47. pp. 451 - 465.
- Habib, D. 1982. Sedimentary supply origin of Cretaceous Black Shales. In: Schlanger, S. O., & Cita, M.B. *Nature and Origin of Cretaceous Carbon-Rich facies*. Academic Press. pp. 113 - 127.
- Habib, D. 1983. Sedimentation-rate dependant distribution of organic matter in the North Atlantic Jurassic-Cretaceous. *Initial Reports of the Deep Sea Drilling Project*. Vol. 76. pp. 781 - 794.
- Habib, D., & Drugg, W.S. 1983. Dinoflagellate age of Middle Jurassic to Early Cretaceous sediments in the Blake-Bahama basin. *Initial Reports of the Deep Sea Drilling Project*. Vol. 76. pp. 623 - 638.
- Habib, D., & Drugg, W.S. 1987. Palynology of Sites 603 and 605, Leg 93, Deep Sea Drilling Project. *Initial Reports of the Deep Sea Drilling Project*. Vol. 92. pp. 751 - 775.
- Habib, D., Eshet, Y., & van Pelt, R. 1994. Application of data on palynosedimentation to solution of geological problems. Palynology of sedimentary cycles. In: Traverse, A. (Ed.). *Sedimentology of Organic Particles*. Cambridge University Press. pp. 311 - 335.
- Habib, D., & Miller, J.A. 1989. Dinoflagellate species and organic facies evidence of marine transgression and regression in the Atlantic coastal plain. *Palaeogeography, Palaeoclimatology, Palaeoecology*. Vol. 74. pp. 23 - 47.
- Habib, D., Moshkowitz, S., & Kramer, C. 1992. Dinoflagellate and calcareous nannofossil response to sea-level change in Cretaceous/Tertiary boundary sections. *Geology*. Vol. 20. pp. 165 - 168.
- Habib, D., & Warren, J.S. 1973. Dinoflagellates near the Cretaceous/Jurassic Boundary. *Nature*. Vol. 241. pp. 217 - 218.
- Hallam, A. 1986a. The Pleinsbachian and Tithonian extinction events. *Nature*. Vol. 319. pp. 765 - 768.
- Hallam, A. 1986b. Origin of minor limestone-shale sequences: climatically induced or diagenetic? *Geology*. Vol. 14. pp. 609 - 612.

- Hancock, J.M. 1991. Ammonite scales for the Cretaceous System. *Cretaceous Research*. Vol. 12. pp. 259 - 291.
- Hantzpergue, P., Atrops, F., & Enay, R. 1997. Chapitre 1.10: Kimmerdigien. In: Cariou, E. & Hantzpergue, P. (Eds.). *Biostratigraphie Jurassique Ouest-Européen et Méditerranéen. Zonations parallèles et distributions des invertébrés et microfossiles*. Groupe Français Etude Jurassique Memoire 17. pp. 87 - 96.
- Haq, B.U., Hardenbol, J., & Vail, P.R. 1987. Chronology of fluctuating sea levels since the Triassic. *Science*. Vol. 235. pp. 1156 - 1167.
- Harding, I.C. 1990. A dinocyst calibration of the European Boreal Barremian. *Palaeontographica Abt. B*. Vol. 218. pp. 1 - 76.
- Harding, I.C., Allen, R.M. 1995. Dinocysts and the palaeoenvironmental interpretation of non-marine sediments: an example from the Wealden of the Isle of Wight. *Cretaceous Research*. Vol. 16. pp. 727 - 743.
- Harland, R. 1973. Dinoflagellate cysts and acritarchs from the Bearpaw Formation, (Upper Campanian) of southern Alberta, Canada. *Palaeontology*. Vol. 16. pp. 665 - 706.
- Harland, R. 1983. Distribution maps of Recent dinoflagellate cysts in bottom sediments from the North Atlantic Ocean and adjacent seas. *Palaeontology*. Vol. 26. pp. 321 - 387.
- Hart, G.F. 1986. Origin and classification of organic matter in clastic systems. *Palynology*. Vol. 10. pp. 1 - 23.
- Hart, G.F., Pasley, M.A., & Gregory, W.A. 1994. Sequence stratigraphy and sedimentation of organic particles. Particulate organic matter, maceral facies models, and applications to sequence stratigraphy. In: Traverse, A. (Ed.). *Sedimentology of Organic Particles*. Cambridge University Press. pp. 337 - 390.
- Håkansson, E., Birkelund, T., Piasecki, S., & Zakharov, V. 1981. Jurassic-Cretaceous boundary strata of the extreme Arctic (Peary Land, North Greenland). *Bulletin of the Geological Society of Denmark*. Vol. 30. pp. 11 - 42.
- Heilmann-Clausen, C. 1987. Lower Cretaceous dinoflagellate biostratigraphy in the Danish Central Trough. *Geological Survey of Denmark, Series A*. Vol. 17. pp. 1 - 89.
- Helenes, J. 1984. Morphological analysis of Mesozoic-Cenozoic *Cribroperidinium* (Dinophyceae) and taxonomic implications. *Palynology*. Vol. 8. pp. 107 - 117.
- Helenes, J., & Lucas-Clarke, J. 1997. Morphological variations among species of the fossil dinoflagellate genus *Gonyaulacysta*. *Palynology*. Vol. 21. pp. 173 - 196.
- Hellem, T., Kjemperud, A., & Øverbo, O.K. 1986. The Troll Field; a geological/geophysical model established by the PLO85 Group. In: Spencer, A. M. (Ed.) *Habitat of Hydrocarbons on the Norwegian Continental Shelf*. Graham & Trotman, London. pp. 217 - 238.
- Hergreen, G.F.W., Van Hoeken-Klinkenberg, P.M.J., & De Boer, K.F. 1980. Some remarks on selected palynomorphs near the Jurassic/Cretaceous boundary in the Netherlands. In: *4th International Palynological conference, Lucknow*. Vol. 2. pp. 357 - 367.

- Herring, J.R. 1985. Charcoal fluxes into sediments of the North Pacific Ocean: the Cenozoic record of burning. In: Sundquist, E. T. & Broecker, W.S. (Eds.). *The Carbon Cycle and Atmospheric CO₂: Natural Variations Archean to Present*. *Geophysical Monographs*. pp. 419 - 442.
- Heusser, L.E. 1983. Pollen distribution in the bottom sediments of the western North Atlantic Ocean. *Marine Micropalaeontology*. Vol. 8. pp. 77 - 88.
- Heusser, L.E., & Balsam, W.L. 1977. Pollen distribution in marine sediments on the continental margin off northern California. *Marine Geology*. Vol. 80. pp. 131 - 147.
- Highton, P.J.C., Pearson, A., & Scott, A.C. 1991. Palynofacies and palynodebris and their use in Coal Measure palaeoecology and palaeoenvironmental analysis. *Neues Jahrbuch für Geologie und Paläontologie, Abhandlungen*. Vol. 183. p. 135 - 169.
- Hoedemaeker, P.J. 1987. Correlation possibilities around the Jurassic/Cretaceous boundary. *Scripta Geologica*. Vol. 84. pp. 1 - 64.
- Hoedemaeker, P.J. 1991. Tethyan-Boreal correlations and the Jurassic/Cretaceous boundary. *Newsletters on Stratigraphy*. Vol. 25. pp. 37 - 60.
- Hoedemaeker, P.J. 1999. A Tethyan-Boreal correlation of pre-Aptian Cretaceous strata: correlating the uncorrelatables. *Geologica Carpathica*. Vol. 50. pp. 101 - 124.
- Hoedemaeker, P.J., Company, M., (reporters) and Aguirre-Urreta, M.B., Avram, E., Bogdanova, T.N., Bujtor, L., Bulot, L., Cecca, F., Delanoy, G., Ettachfini, M., Memmi, L., Owen, H.G., Rawson, P.F., Sandoval, J., Tavera, J.M., Thieuloy, J.P., Tovbina, S.Z., & Vasicek, Z. 1993. Ammonite Zonation for the Lower Cretaceous of the Mediterranean region; basis for the stratigraphic correlations within IGCP-Project 262. *Revista Española de Paleontología*. Vol. 8. pp. 117 - 120.
- Hoedemaeker, P.J., & Leereveld, H. 1995. Biostratigraphy and sequence stratigraphy of the Berriasian- lowest Aptian succession, Caravaca, SE Spain. *Cretaceous Research*. Vol. 16. pp. 195 - 230.
- Hoelstad, T. 1986. Palynology of the Middle Jurassic Lower Graben Sand Formation of the U1 well, Danish Central Trough. *Danmarks Geologiske Undersøgelse*. A 14. 25 pp.
- Hogg, N.M. 1994. A research study into the Boreal Late Jurassic: Direct calibration of palynostratigraphy to ammonite zones of the type Volgian of the Russian Platform. *Report for Shell UK Exploration and Production by University College London*.
- Holland, C.H., Audley-Charles, M.G., Bassett, M.G. et al. 1978. A guide to stratigraphic procedure. *Geological Society of London Special Report*, 11.
- Honigstein, A., Lipson-Benitah, S., Conway, B., Flexer, A., & Rosenfeld, A. 1989. Mid Turonian anoxic event in Israel - a multidisciplinary approach. *Palaeogeography, Palaeoclimatology, Palaeoecology*. Vol. 69. pp. 103 - 112.
- Hopkins, J.S. 1950. Differential flotation and deposition of coniferous and deciduous tree pollen. *Ecology*. Vol. 31. pp. 633 - 641.
- Housa, V., Krs, M., Krsová, M., & Pruner, P. 1996. Magnetostratigraphic and micropaleontological investigations along the Jurassic/Cretaceous boundary strata, Brodno near Zilina (western Slovakia). *Geologica Carpathica*. Vol. 47. pp. 135 - 151.

- Hssaïda, T., & Morzadec-Kerfourn, M.-T. 1993. Kystes de dinoflagellés et palynofaciès: indicateurs des variations bathymétriques dans le bassin de Guercif (Maroc) au Jurassique (Bathonien terminal-Oxfordien basal). *Review of Palaeobotany and Palynology*. Vol. 77. pp. 97 - 106.
- Hughes, N.F., & Croxton, C.A. 1973. Palynologic correlation of the Dorset "Wealden". *Palaeontology*. Vol. 16. pp. 66 - 77.
- Hughes, N.F., & Moody-Stuart, J.C. 1967. Palynological facies and correlation in the English Wealden. *Review of Palaeobotany and Palynology*. Vol. 1. pp. 259 - 268.
- Hughes, N.F., & Moody-Stuart, J.C. 1969. A method of stratigraphic correlation using early Cretaceous miospores. *Palaeontology*. Vol. 12. pp. 84 - 111.
- Hughes, N.F., & Norris, G. 1974. Palynologic taxa stratigraphically important for recognising the Jurassic/Cretaceous boundary in Britain. *American Association of Stratigraphic Palynologists, 7th Annual Meeting Abstracts*.
- Hughes, N.F., & Norris, G. 1975. Palynologic correlations in north-west Europe for the Jurassic-Cretaceous boundary. *Meeting of the European Geological Society: Abstracts*.
- Hunt, C.O. 1987. Dinoflagellate cyst and acritarch assemblages in shallow-marine and marginal-marine carbonates; the Portland Sand, Portland Stone, and Purbeck Formations (Upper Jurassic - Lower Cretaceous) of southern England and northern France. In: Hart, M. B. (Ed.). *Micropalaeontology of Carbonate Environments*. Ellis-Harwood. pp. 208 - 225.
- Hunt, J.M. 1979. *Petroleum Geochemistry and Geology*. Freeman., San Fransisco. 617 pp.
- Ilyina, V.I. 1986. Subdivision and correlation of the marine and non-marine Jurassic sediments in Siberia based on palynological evidence. *Review of Palaeobotany and Palynology*. Vol. 46. pp. 357 - 364.
- Ioannides, N.S., Stavrinou, G.N., & Downie, C. 1976. Kimmeridgian microplankton from Clavell's Hard, Dorset, England. *Micropalaeontology*. Vol. 22. pp. 443 - 478.
- Iosifova, E.K. 1996. Dinocysts from Tchernaya Retchka (Ryazanian-Aptian, Lower Cretaceous) of the Moscow Basin, Russia. *Review of Palaeobotany and Palynology*. Vol. 91. pp. 187 - 240.
- Jain, K.P., Garg, R., Kumar, S., & Singh, I.B. 1978. Dinoflagellates and radiolarians from the Tethyan sediments, Malla Johar area, Kumoan Hamalaya. A preliminary report. *Journal of the Palaeontological Society of India*. Vol. 21. pp. 116 - 119.
- Jain, K.P., Garg, R., Kumar, S., & Singh, I.B. 1984. Upper Jurassic dinoflagellate biostratigraphy of the Spiti Shale (Formation), Malla Johar area, Tethys Himalaya, India. *Journal of the Palaeontological Society of India*. Vol. 29. pp. 67 - 83.
- Jain, K.P., Jana, B.N., & Maheshwari, H.K. 1986. Fossil floras of Kutchch, part IV. Jurassic dinoflagellates. *The Palaeobotanist*. Vol. 35. pp. 73 - 84.
- Jaing, Q., Mungai, M.W., Downie, C., & Neves, R. 1992. Late Jurassic dinoflagellate assemblages of the Mto Panga quarry, Mombassa, Kenya. *Review of Palaeobotany and Palynology*. Vol. 74. pp. 77 - 100.

- Jan du Chêne, R., Busnardo, R., Charollais, J., Clavel, B., Deconinck, J-F., Emmanuel, L., Gardin, S., Gorin, G., Manivit, H., Monteil, E., Raynaud, J-F., Renard, M., Steffen, D., Steinhäuser, N., Strasser, A., Strohmenger, C., & Vail, P.R. 1993. Sequence stratigraphic interpretation of Upper Tithonian-Berriasian reference sections in south-east France: a multidisciplinary approach. *Bulletin des Centres Recherches Exploration-Production Elf Aquitaine*. Vol. 17. pp. 151 - 181.
- Jansonius, J. 1986. Re-examination of Mesozoic Canadian dinoflagellate cysts published by S.A.J. Pocock (1962, 1972). *Palynology*. Vol. 10. pp. 210 - 223.
- Jardiné, S., Raynaud, J.-F., & de Reneville, P. 1984. Dinoflagellés, spores et pollens. In: Debrand-Passard, J., Courboulex, S., & Lienhardt, M.J. (Eds.). *Synthèse Géologique sud-est de la France*. Bureau de Recherches Géologique et Minières, Memoire 125. pp. 300 - 303.
- Jeletzky, J.A. 1971. Marine Cretaceous biotic provinces, and palaeogeography of western and Arctic Canada. *Geological Survey of Canada*. Paper 70-22.
- Jeletzky, J.A. 1973. Biochronology of the marine Boreal latest Jurassic, Berriasian and Valanginian in Canada. In: Casey, R., & Rawson, P.F. (Eds.). *The Boreal Lower Cretaceous*. Geological Journal Special Issue No. 5. pp. 41 - 80.
- Jeletzky, J.A. 1984. Jurassic/Cretaceous boundary beds of western and Arctic Canada and the problem of the Tithonian in the Boreal Realm. In: Westermann, G.E.G. (Ed.). *Jurassic - Cretaceous Biochronology and Paleogeography of North America*. Geological Association of Canada. Special Paper 27. pp. 175 - 255.
- Jingxian, Y. 1982. Late Jurassic to Early Cretaceous dinoflagellate assemblages of eastern Heilongjiang Province, China. *Bulletin, Shenyang Institute of Geological and Mineralogical Research*. Chinese Academy of Sciences. Vol. 5. pp. 1 - 8.
- Johnson, C.D., & Hills, L.V. 1973. Microplankton zones of the Savik Formation, (Jurassic), Axel Heiberg and Ellesmere Islands, District of Franklin. *Bulletin of Canadian Petroleum Geology*. Vol. 21. pp. 178 - 218.
- Kemper, E., Rawson, P.F., & Thieuloy, J.-P. 1981. Ammonites of Tethyan ancestry in the early Lower Cretaceous of north-west Europe. *Palaeontology*. Vol. 24. pp. 251 - 311.
- Kidson, E.J., & Williams, G.L. 1969. Concentration of palynomorphs by the use of sieves. *Oklahoma Geology Notes*. Vol. 29. pp. 117 - 119.
- Klement, K.W. 1960. Dinoflagellaten und Hystrichosphaerideen aus dem unteren und mittleren Malm südwestdeutschlands. *Palaeontographica Abt. A*. Vol. 114. pp. 1 - 104.
- Kofoid, C.A. 1909. On *Peridinium steini* Jörgensen, with a note on the nomenclature of the skeleton of the Peridinidae. *Archiv für Protistenkunde*. Vol. 16. pp. 25 - 47.
- Kovach, W.L. 1988. Quantitative palaeoecology of megaspores and other dispersed plant remains from the Cenomanian of Kansas, USA. *Cretaceous Research*. Vol. 9. pp. 265 - 283.
- Kovach, W.L. 1989. Comparisons of multivariate analytical techniques for use in pre-Quaternary plant palaeoecology. *Review of Palaeobotany and Palynology*. Vol. 60. pp. 255 - 282.
- Kovach, W.L., & Batten, D.J. 1994. Association of palynomorphs and palynodebris with depositional environments. In: Traverse, A. (Ed). *Sedimentation of Organic Particles*. pp. 391 - 407.

- Krimgolts, G.Y., Mesezhnikov, M.S., & Westermann, G.E.G. 1988. The Jurassic ammonite zones of the Soviet Union. *Geological Society of America. Special Paper* 223. 116 pp.
- Kumar, A. 1986. A dinocyst assemblage from the middle member (Lower Kimmeridgian-Tithonian) of the Jhuran Formation, Kachchh, India. *Review of Palaeobotany and Palynology*. Vol. 48. pp. 377 - 407.
- Kumar, A. 1987a. Additional dinocysts and acritarchs from the Middle Member (Lower Kimmeridgian to Tithonian) of the Jhuran Formation, Kachchh, India. *Revista Española de Micropaleontología*. Vol. 19. pp. 239 - 249.
- Kumar, A. 1987b. Distribution of dinocysts in the Jurassic rocks of Kachchh, India. *Journal of the Geological Society of India*. Vol. 29. pp. 594 - 602.
- Kunz, R. 1990. Phytoplankton und Palynofazies im Malm NW-Deutschlands Hannoversches Bergland. *Palaeontographica Abt. B*. Vol. 216. pp. 1 - 105.
- Kuttek, J., & Zeiss, A. 1975. A contribution to the correlation of the Tithonian and Volgian stages: the ammonite fauna from Brzostowska near Tomaszow Mazowiecki, central Poland. *Memoires de la Bureau de Recherches Geologiques et Minieres*. Vol. 86. pp. 123 - 128.
- Kuznetsova, K.I. 1978. Correlation of zonal subdivisions in stratotypes of the Volgian and Kimmeridgian stages. *Bulletin of the Academy of Sciences of the USSR*. Vol. 21. pp. 24 - 36.
- Lam, K., & Porter, R. 1977. The distribution of palynomorphs in the Jurassic rocks of the Brora Outlier, N.E Scotland. *Journal of the Geological Society of London*. Vol. 134. p. 45 - 55.
- Lamolda, M.A., & Mao, S. 1999. The Cenomanian-Turonian boundary event and dinocyst record at Ganuza (northern Spain). *Palaeogeography, Palaeoclimatology, Palaeoecology*. Vol. 150. pp. 65 - 82.
- Lantz, J. 1958. Étude palynologique de quelques échantillons Mésozoïques du Dorset (Grande Bretagne). *Revue de L'Institut Français du Pétrole*. Vol. 13. 917 - 943.
- Le Hégarat, G., & Remane, J. 1968. Tithonique supérieur et Berriasien de l'Ardèche et de l'Hérault. Correlation des ammonites et des calpionelles. Vol. 16. pp. 7 - 70.
- Leckie, D.A., Singh, C., Goodarzi, F., & Wall, J.H. 1990. Organic-rich, radioactive marine shale: a case study of a shallow-water condensed section, Cretaceous Shaftesbury Formation, Alberta, Canada. *Journal of Sedimentary Petrology*. Vol. 60. pp. 101 - 117.
- Leeder, M.R. 1991. *Sedimentology. Processes and Product*. Harper Collins. 6th Edition. 344 pp.
- Leereveld, H. 1989. Dinoflagellate cysts from the Río Argos section (Lower Cretaceous), southern Spain. In: *Abstracts, 1st Meeting Working Group 2 ('Pelagic Facies') of the IGCP-Project 262 ('Tethyan Cretaceous Correlation')*, Urbano, Italy. pp. 58 - 69.
- Leereveld, H. 1995. Dinoflagellate cysts from the Lower Cretaceous Río Argos succession (Se Spain). *LPP contributions series; No. 2.*, Universiteit Utrecht.

- Leereveld, H. 1997. Upper Tithonian-Valanginian (Upper Jurassic-Lower Cretaceous) dinoflagellate cyst stratigraphy of the western Mediterranean. *Cretaceous Research*. Vol. 18. pp. 385 - 420.
- Lenoir, E.A., & Hart, G.F. 1988. Palynofacies of some Miocene sands from the Gulf of Mexico, offshore Louisiana, U.S.A. *Palynology*. Vol. 12. pp. 151 - 165.
- Lentin, J.K., & Vozzhennikova, T.F. 1990. Fossil dinoflagellates from the Jurassic, Cretaceous and Paleogene deposits of the USSR - a re-study. *American Association of Stratigraphic Palynologists Contributions Series*. Number 23. 221 pp.
- Lentin, J.K., & Williams, G.L. 1993. Fossil Dinoflagellates: index to genera and species. 1993 edition. *American Association of Stratigraphic Palynologists Contributions Series*, Number 28. 826 pp.
- Li, H., & Habib, D. 1996. Dinoflagellate stratigraphy and its response to sea-level change in Cenomanian-Turonian sections of the Western Interior of the United States. *Palaios*. Vol. 11. pp. 15 - 30.
- Lister, J.K., & Batten, D.J. 1988. Stratigraphic and palaeoenvironmental distribution of Early Cretaceous dinoflagellate cysts in the Hurlands Farm Borehole, West Sussex, England. *Palaeonographica Abt. B*. Vol. 210. pp. 9 - 89.
- Loh, H., Prauss, M., & Riegel, W. 1986. Primary production, maceral formation and carbonate species in the Posidonia Shale of NW Germany. *Mitteilungen der Geologische Paläontologischen Institut der Universität Hamburg*. Vol. 60. pp. 397 - 421.
- Lord, A.R., Cooper, M.K.E., Corbett, P.W.M., Fuller, N.G., Rawson, P.F., & Rees, A.J.J. 1987. Microbiostratigraphy of the Volgian Stage (Upper Jurassic), Volga River, USSR. *Neues Jahrbuch für Geologie und Paläontologie. Monatshefte*. Vol. 10. pp. 577 - 605.
- Løfaldli, M., & Thusu, B. 1979. Micropalaeontological studies of the Upper Jurassic and Lower Cretaceous of Andøya, northern Norway. *Palaeontology*. Vol. 22. pp. 413 - 425.
- Lund, J.J., & Ecke, H.H. 1988. Dinoflagellate cyst stratigraphy applied to the Middle to Late Jurassic of the Regensburg-Passau area, Bavaria. *Bulletines des Centres de Recherches Exploration-Production Elf-Aquitaine*. Vol. 12. pp. 345 - 359.
- Lund, J.J., & Pedersen, K.R. 1985. Palynology of the marine Jurassic formations in the Vardekløft ravine, Jameson Land, East Greenland. *Bulletin of the Geological Society of Denmark*. Vol. 33. pp. 371 - 399.
- Luppov, N.P., Bogdanova, T.N., & Lobatcheva, S.V. 1979. Paleontologicheskoe obosnovanie sopostlaveniya Berriasa i Valanzhina Mangyshlaka, yugovostochnoj Frantsil, severa FRG i Russkoj platformy. *Institut Geologich i Geofizika, Akademiya Nauk SSSR. Sib. otdel.* pp. 159 - 168.
- Magniez-Jannin, F., & Dommergues, J-L. 1994. Foraminifères vs. ammonites en fosse vocontienne vers la limite Valanginien - Hauteriviien. *Comptes Rendus de la Academie des Sciences Paris, Série II*. Vol. 319. p. 957 - 962.
- Maher, L.J., Jr. 1981. Statistics for microfossil concentration measurements employing samples spiked with marker grains. *Review of Palaeobotany and Palynology*. Vol. 32. pp. 247 - 249.
- Mantou, A.A. 1966. Some current trends in palynology. *Earth Science Reviews*. Vol. 2. pp. 317 - 343.

- Manum, S.B. 1976. Dinocysts in Tertiary Norwegian-Greenland Sea sediments (Deep Sea Drilling Project Leg 38), with observations on palynomorphs and palynodebris in relation to environment. *Initial Reports of the Deep Sea Drilling Project*. Vol. 38. pp. 877 - 919.
- Manum, S.B., & Thronsen, T. 1978. Dispersed organic matter (kerogen) in the Spitzbergen Tertiary. *Norsk Polarinstitut Årbok*, 1977. pp. 179 - 187.
- Marret, F. 1994. Distribution of dinoflagellate cysts in Recent marine sediments from the east equatorial Atlantic (Gulf of Guinea). *Review of Palaeobotany and Palynology*. Vol. 84. pp. 1 - 22.
- Martin, P.S. 1963. *The Last 10,000 Years*. University of Arizona Press. 87 pp.
- Marzi, R., & Rullkötter, J. 1986. Organic matter accumulation and migrated hydrocarbons in deep-sea sediments of the Mississippi Fan and adjacent intraslope basins, northern Gulf of Mexico. *Mitteilungen Geologische Paläontologisches Institut Universität Hamburg*. Vol. 60. pp. 359 - 379.
- Masran, T.C. 1984. Sedimentary organic matter of Jurassic and Cretaceous samples from North Atlantic deep-sea drilling sites. *Bulletin of Canadian Petroleum Geology*. Vol. 32. pp. 52 - 73.
- Masran, T.C., & Pocock, S.A.J. 1981. The classification of plant-derived particulate organic matter in sedimentary rocks. In: Brooks, J. (Ed.). *Organic Maturation Studies and Fossil Fuel Exploration*. Academic Press. pp. 145 - 175.
- Massoud, M.S., & Kinghorn, R.R.F. 1985. A new classification for the organic components of kerogen. *Journal of Petroleum Geology*. Vol. 8. pp. 85 - 100.
- Masure, E. 1984. L'Indice de diversité et les dominances de << communautés >> de kystes de Dinoflagellés: marqueurs bathymétriques; forage 398D, croisière 47 B. *Bulletin de la Société Géologique de France*. Vol. 26. pp. 93 - 111.
- Masure, E. 1988. Berriasian to Aptian dinoflagellate cysts from the Galicia margin, offshore Spain, Sites 638 and 639, ODP Leg 103. *Proceedings of the Ocean Drilling Project: Scientific Results*. Vol. 103. pp. 433 - 444.
- May, F.E. 1980. Dinoflagellate cysts of the Gymnodiniaceae, Peridiniaceae, and Gonyaulacaceae from the Upper Cretaceous Monmouth Group, Atlantic Highlands, New Jersey. *Palaeontographica Abt. B*. Vol. 172. pp. 10 - 116.
- Mebradu, S. 1978. Stratigraphic palynology of the Upper Jurassic of the Dorset Coast, England. Part 1: statistical variables. *Palinologia, numero extraordinario*. 1. pp. 327 - 333.
- Memmi, L., & Salaj, J. 1975. Le Berriasien de Tunisie. Succession de Faunes d'ammonites, de foraminifères et de Tintinnoidiens. *Memoires de la Bureau de Recherches Géologiques et Minières*. Vol. 86. pp. 58 - 67.
- Mesezhnikov, M. S. 1977. *Jurassic/Cretaceous boundary beds in the middle Volga area*. Ministry of Geology of the USSR, VNIGRI, Leningrad. (Field guide in Russian and English). pp. 1 - 33.
- McIntyre, D.J., & Brideaux, W.W. 1980. Valanginian miospore and microplankton assemblages from the northern Richardson Mountains, district of MacKenzie, Canada. *Canada Geological Survey Bulletin*. Vol. 320. pp. 1 - 57.

- Mikhailov, N.P. 1966. Boreal Jurassic ammonites (Dorsoplanitidae) and zonal subdivision of the Volgian Stage. *Trudy Geologicheskogo Instituta. Akademiya Nauk SSSR (Leningrad)*. Vol. 151. pp. 1 - 116.
- Millioud, M.E. 1967. Palynological study of the type localities at Valangin and Hauterive. *Review of Palaeobotany and Palynology*. Vol. 5. pp. 155 - 167.
- Millioud, M.E. 1969. Dinoflagellates and acritarchs from some western european Lower Cretaceous type localities. In: *Proceedings of the First International Conference on Planktonic Microfossils, Genève*. pp. 420 - 434.
- Monteil, E. 1990. Revision and emendation of the dinocyst genus *Amphorula* Dodekova 1969. The concept of morphostratigraphy. *Bulletin des centres des Recherches Exploration-Production Elf Aquitaines*. Vol. 14. pp. 587 - 609.
- Monteil, E. 1992. Kystes de dinoflagelles index (Tithonique-Valanginien) du sud-est de la France. Proposition d'une nouvelle zonation palynologique. *Revue de Paléobiologie*. Vol. 11. pp. 299 - 306.
- Monteil, E. 1993. Dinoflagellate cyst biozonation of the Tithonian and berriasian of south-east France. Correlation with sequence stratigraphy. *Bulletin des Centres de Recherch Exploration - Production Elf Aquitaine*. Vol. 17. pp. 249 - 273.
- Monteil, E. 1996. *Daveya boresphaera* gen. et sp. nov., a valid name for the dinoflagellate cysts *Gonyaulacysta* sp. a Davey 1979 and sp. b Davey 1982, and some remarks regarding the formal status of *Muderongia brevispinosa* Iosifova 1996. *Bulletin des Centres de Recherches Exploration-Production Elf Aquitaine*. Vol. 20. pp. 37 - 59.
- Morter, A.A. 1984. Purbeck - Wealden Beds Mollusca and their relationship to ostracod biostratigraphy, stratigraphical correlation and palaeoecology in the Weald and adjacent areas. *Proceedings of the Geologists' Association* Vol. 95. pp. 217 - 234.
- Morzadec-Kerfourn, M.T. 1977. Les kystes de dinoflagellés dans les sédiments Recents le long de Côtes Bretonnes. *Revue de Micropaléontologie*. Vol. 20. pp. 157 - 166.
- Morzadec-Kerfourn, M.T. 1983. Intérprêt des kystes de dinoflagellés pour l'établissement de reconstitutions paléogéographiques: exemple du Golfe de Gabès (Tunisie). *Cahiers du Micropaléontologie*. Vol. 4. pp. 15 - 22.
- Moshkovitz, S., & Habib, D. 1993. Calcareous nannofossil and dinoflagellate stratigraphy of the Cretaceous-Tertiary boundary, Alabama and Georgia. *Micropalaeontology*. Vol. 39. pp. 167 - 191.
- Mudie, P.J. 1982. Pollen distribution in modern marine sediments, eastern Canada. *Canadian Journal of Earth Sciences*. Vol. 19. pp. 729 - 747.
- Muir, M.D. 1964. The palaeoecology of the Small Spores of the Middle Jurassic of Yorkshire. Unpublished Ph.D. thesis, University of London. 234 pp.
- Muir, M.D., & Sarjeant, W.A.S. 1978. The palynology of the Langdale Beds (Middle Jurassic) of Yorkshire and its stratigraphical implications. *Review of Palaeobotany and Palynology*. Vol. 25. pp. 193 - 239.
- Mukherjee, J., & Chopra, A.S. 1987. Study of organic matter types in relation to the depositional environments in the well of Bengal Basin. *Bulletin of the Oil and Natural Gas Commission*. Vol. 24. pp. 81 - 99.

- Mukhopadhyay, P.K., Hagemann, H.W., & Gormley, J.R. 1985. Characterisation of kerogens as seen under the aspect of maturation and hydrocarbon generation. *Erdöl und Kohle-Erdgas-Petrochemievereinigt mit Brennstoff-Chemie*. Vol. 38. pp. 7 - 18.
- Muller, J. 1959. Palynology of the Recent Orinoco Delta and shelf sediments: reports of the Orinoco Shelf expedition. *Micropalaeontology*. Vol. 5. pp. 1 - 32.
- Mussard, J.M., Gerard, J., Ducazeaux, J., & Begouen, V. 1994. Quantitative palynology: A tool for the recognition of genetic depositional sequences. Application to the Brent Group. *Bulletins des Centres de Recherches Exploration-Production Elf Aquitaine*. Vol. 18. pp. 463-474.
- Mutterlose, J., & Harding, I.C. 1987a. The Barremian Blätterton: an anoxic warm water sediment of the Lower Saxony Basin. *Geologische Jahrbuch*. Vol. 96. pp. 187 - 207.
- Mutterlose, J., & Harding, I.C. 1987b. Phytoplankton from the anoxic sediments of the Barremian (Lower Cretaceous) of North-West Germany. *Abhandlungen Geologischen Bundesanstalt, Wien*. Vol. 39. pp. 177 - 215.
- Nagy, J., Dypvik, H., & Bjaerke, T. 1984. Sedimentological and paleontological analyses of Jurassic North Sea deposits from deltaic environments. *Journal of Petroleum Geology*. Vol. 7. pp. 169 - 188.
- Neale, J.W., & Sarjeant, W.A.S. 1962. Microplankton from the Speeton Clay of Yorkshire. *Geological Magazine*. Vol. 99. pp. 439 - 458.
- Norris, G. 1963. Upper Jurassic and Lower Cretaceous miospores and microplankton from southern England. Unpublished PhD thesis, University of Cambridge.
- Norris, G. 1969. Miospores from the Purbeck Beds and marine Upper Jurassic of southern England. *Palaeontology*. Vol. 12. pp. 574 - 620.
- Norris, G. 1970. Palynology of the Jurassic/Cretaceous boundary in southern England. *Geoscience and Man*. Vol. 1. pp. 56 - 65.
- Norris, G. 1978. Phylogeny and a revised supra-generic classification for the Triassic-Quaternary organic-walled dinoflagellate cysts (Pyrrophyta). Part II. Families and sub-orders of fossil dinoflagellates. *Neues Jahrbuch für Geologie und Paläontologie Abhandlungen*. Vol. 156. pp. 1 - 30.
- Nøhr-Hansen, H. 1986. Dinocyst stratigraphy of the Lower Kimmeridge Clay, Westbury, England. *Bulletin of the Geological Society of Denmark*. Vol. 35. pp. 31 - 51.
- Nøhr-Hansen, H. 1989. Palynological studies of the organic matter. In: Christiansen, F. G. (Ed.). *Petroleum Geology of North Greenland. Grønlands Geologiske Undersøgelse, Bulletin*. pp. 27 - 31.
- Nwachukwu, J.I., & Barker, C. 1985. Organic Matter: size fraction relationships for Recent sediments from the Orinoco delta, Venezuela. *Marine and Petroleum Geology*. Vol. 2. pp. 202 - 209.
- Oboh-Ikuenobe, F.E. 1992. Middle Miocene palaeoenvironments of the Niger Delta. *Palaeogeography, Palaeoclimatology, Palaeoecology*. Vol. 92. pp. 55 - 84.
- Oboh-Ikuenobe, F.E. 1996. Correlating palynofacies assemblages with sequence stratigraphy in Upper Cretaceous (Campanian) sedimentary-rocks of the Book Cliffs, east-central Utah. *Geological Society of America Bulletin*. Vol. 108. pp. 1275 -1294.

- Oboh-Ikuenobe, F.E., Yepes, O., Mascle, J., Lohmann, G.P., Clift, P., Allerton, S., Ask, M., Barrera, E., Barton, E., Basile, C., Bellier, J.P., Benkhellil, J., Brantuoh, E., Edwards, R., Ewert, E., Goncalves, C., Janik, A.G., & Holmes, M.A., 1997. Palynofacies analysis of sediments from the Côte d'Ivoire Ghana transform margin: Preliminary correlation with some regional events in the Equatorial Atlantic. *Palaeogeography Palaeoclimatology Palaeoecology*. Vol. 129. pp. 291 - 314.
- Ogg, G. 1992. Early Cretaceous palynomorphs of the western Pacific Ocean. *Proceedings of the Ocean Drilling Program, Scientific Results*. Vol. 129. pp. 221 - 228.
- Ogg, G. 1994. Dinoflagellate cysts of the Early Cretaceous North Atlantic Ocean. *Marine Micropalaeontology*. Vol. 23. pp. 241 - 263.
- Ogg, J.G., Hasenyager, R.W., Wimbledon, W.A., Channell, J.E.T., & Bralower, T.J. 1991. Magnetostratigraphy of the Jurassic/Cretaceous boundary interval- Tethyan and English faunal realms. *Cretaceous Research*. Vol. 12. pp. 455 - 482..
- Olóriz, F., & Tavera, J.M. 1989. The significance of Mediterranean ammonites with regard to the traditional Jurassic/Cretaceous boundary. *Cretaceous Research*. Vol. 10. pp. 221 - 237.
- Oppel, A. 1865. Die tithonische etage. *Zeitschripte deutschlands geologische ges*. Vol. 17. pp. 535 - 558.
- Paproth, E., & Streel, M. 1970. Corrélations biostratigraphiques près de la limite Dévonien/Carbonifère entre les faciés littoraux ardennais et les faciés bathyaux rhénans. In: *Colloque sur la Stratigraphie du Carbonifère, Liège, Avril, 1969. Les Congrès et Colloques de l'Université de Liège*. Vol. 55. pp. 365 - 398.
- Parry, C.C., Whitely, P.K.J., & Simpson, R.D.H. 1981. Integration of palynological and sedimentological methods in facies analysis of the Brent Formation. In: Illing, L. V., & Hobson, G.D. (Eds.). *Petroleum Geology of the Continental Shelf of North-West Europe*. Heyden & Son Ltd. pp. 205 - 215.
- Partington, M.A., Copestake, P., Mitchener, B.C., & Underhill, J.R. 1993. Biostratigraphic calibration of genetic stratigraphic sequences in the Jurassic - lowermost Cretaceous (Hettangian to Ryazanian) of the North Sea and adjacent areas. In: Parker, J. R. (Ed.). *Petroleum Geology of Northwest Europe: Proceedings of the 4th Conference*. pp. 371 - 386.
- Pasley, M.A., Gregory, W.A., & Hart, G.F. 1991. Organic matter variations in transgressive and regressive shales. *Organic Geochemistry*. Vol. 17. pp. 483 - 509.
- Peniguel, G., Courderc, R., & Seyve, C. 1989. Les microalgues actuelles et fossiles. Intéret stratigraphique et pétrolière. *Bulletin des Centres Recherches Exploration-Production Elf-Aquitaine*. Vol. 13. pp. 455 - 482.
- Piasecki, S. 1984. Dinoflagellate cyst stratigraphy of the Lower Cretaceous Jydegård Formation, Bornholm, Denmark. *Bulletin of the Geological Society of Denmark*. Vol. 32. pp. 145 - 161.
- Piasecki, S. 1986. Palynological analysis of organic debris in the Lower Cretaceous Jydegård Formation, Bornholm, Denmark. *Grana*. Vol. 25. pp. 119 - 129.

- Pocknall, D.T., & Beggs, J.M. 1990. Palynofacies as a tool for the interpretation of depositional environments in the Waikato and Taranaki Basins, New Zealand. In: *Proceedings, 1989 New Zealand Oil Exploration Conference*. Petroleum and Geothermal Unit, Energy and Resource Division, Ministry of Commerce (New Zealand). pp. 250 - 258.
- Pocock, S.A.J. 1962. Microfloral analysis and age determinations of strata at the Jurassic-Cretaceous boundary in the western Canada plains. *Palaeontographica Abt. B*. Vol. 111. pp. 1 - 95.
- Pocock, S.A.J. 1967. The Jurassic/Cretaceous boundary in northern Canada. *Review of Palaeobotany and Palynology*. Vol. 5. pp. 129 - 136.
- Pocock, S.A.J. 1972. Palynology of the Jurassic sediments of western Canada. Part 2. Marine species. *Palaeontographica Abt. B*. Vol 137. pp. 85 - 153.
- Pocock, S.A.J. 1976. A preliminary donoflagellate zonation of the uppermost Jurassic and lower part of the Cretaceous, Canadian Arctic, and possible correlation with the western Canada Basin. *Geoscience and Man*. Vol. 15. pp. 101 - 114.
- Pocock, S.A.J. 1980. Palynology at the Jurassic/Cretaceous boundary in North America. In: *4th International Palynological conference, Lucknow*. Vol. 2. pp. 377 - 385.
- Pocock, S.A.J. 1982. Identification and recording of particulate sedimentary organic matter. In: Staplin, F. L., Dow, W.G., Milner, C.W.D., O'Connor, D.I., Pocock, S.A.J., Van Gijzel, P., Welte, D.H., & Jilke, M.A. *How to assess maturation and paleotemperatures*. Society of Economic Paleontologists and Mineralogists, Short Course, 7. pp. 13 - 133.
- Pocock, S.A.J., Vasanthi, G., & Venkatachala, B.S. 1988. Introduction to the study of particulate organic materials and ecological perspectives. *Journal of Palynology*. Vol. 23 - 24. pp. 167 - 188.
- Poulsen, N.E. 1986. Callovian - Volgian dinocyst stratigraphy of the Central Trough in the Danish North Sea area. *Bulletin of the Geological Society of Denmark*. Vol. 35. pp. 1 - 10.
- Poulsen, N.E. 1991. Upper Jurassic dinocyst stratigraphy of the Danish Central Trough. In: Michelson, O. & Fransen, N. (Eds.). *The Jurassic in the Southern Central Trough*. Danmarks Geologiske Undersøgelse, Serie B. pp. 7 - 15.
- Poulsen, N.E. 1992. Jurassic dinoflagellate cyst biostratigraphy of the Danish Subbasin in relation to sequences in England and Poland: a preliminary review. *Review of Palaeobotany and Palynology*. Vol. 75. pp. 33 - 52.
- Poulsen, N.E. 1993. Dinoflagellate cyst biostratigraphy of the Oxfordian and Kimmeridgian of Poland. *Acta Geologica Polonica*. Vol. 43. pp. 251 - 272.
- Poulsen, N.E. 1994. Dinoflagellate cyst biostratigraphy of Rhaetian-Ryazanian (Uppermost Triassic-Lowermost Cretaceous) deposits from the Danish subbasin. *Geobios M.S.* Vol 17. pp. 409 - 414.
- Poulsen, N.E. 1996. Dinoflagellate cysts from marine Jurassic deposits of Denmark and Poland. *American Association of Stratigraphic Palynologists Contributions Series Number 31*. 227 pp.
- Powell, A.J., Dodge, J.D., & Lewis, J. 1990. Late Neogene to Pleistocene palynological facies of the Peruvian continental margin upwelling, leg 112. *Proceedings of the Ocean Drilling Program, Scientific Results*. Vol. 112. pp. 297 - 321.

- Powell, A.J., Lewis, J., & Dodge, J.D. 1992. The palynological expression of post-Palaeogene upwelling: a review. In: Summerhayes, C. P., Prell, W.L., & Emeis, K.C. (Eds.). *Upwelling Systems; Evolution since the Early Miocene*. Geological Society of London Special Publication. pp. 215 - 226.
- Powell, T.G., Greaney, S., & Snowdon, L.R. 1982. Limitations of use of organic petrographic techniques for identification of petroleum source rocks. *American Association of Petroleum Geologists Bulletin*. Vol. 66. pp. 430 - 435.
- Powers, M.C. 1953. A new roundness scale for sedimentary particles. *Journal of Sedimentary Petrology*. Vol. 23. pp. 117 - 119.
- Prauss, M. 1989. Dinozysten-stratigraphie und palynofazies im oberen Lias und Dogger von NW-Deutschland. *Palaeontographica Abt. B*. Vol. 214. pp. 1 - 124.
- Prauss, M., Ligouis, B., & Luterbacher, H. 1991. Organic matter and palynomorphs in the 'Posidonienschiefer' (Toarcian, Lower Jurassic) of southern Germany. In: Tyson, R. V., & Pearson, T.H. (Eds.). *Modern and Ancient Continental Shelf Anoxia*. Geological Society of London Special Publication. pp. 335 - 51.
- Prauss, M., & Riegel, W. 1989. Evidence from phytoplankton associations for causes of black shale formation in epicontinental seas. *Neues Jahrbuch für Geologie und Paläontologie Monatshefte*. Vol. 1989. pp. 671 - 682.
- Rahman, M., Kinghorn, R.R.F., & Gibson, P.J. 1994. The organic matter in oil shales from the Lowmead Basin, Queensland, Australia. *Journal of Petroleum Geology*. Vol. 17. pp. 317 - 325.
- Raup, D.M., & Sepkoski, J.J.Jr. 1984. Periodicity of extinctions in the geologic past. *Proceedings of the National Academy of Sciences, USA*. Vol. 81. pp. 801 - 805.
- Rauscher, R., Schuler, M., & Benalloulhaj, N. 1986. Les conditions de dépôt des schistes bitumineux et des phosphates Maastrichtiens au Maroc: une approche palynologique. *Documents du Bureau Recherches Géologique et Minières*. Vol. 110. pp. 127 - 139.
- Rauscher, R., Soncini, M.J., Benalloulhaj, S., Trichet, J. 1990. Les phosphates sédimentaires, un milieu de conservation exceptionnel de la matière organique. Apports de la géochimie organique et de la palynologie. *Comptes Rendus Academie des Sciences Paris, Ser. II*. Vol. 310. 613 - 618.
- Rauscher, R., & Schmitt, J.-P. 1990. Recherches palynologiques dans le Jurassique d'Alsace (France). *Review of Palaeobotany and Palynology*. Vol. 62. pp. 107 - 156.
- Rawson, P.F. 1973. Lower Cretaceous (Ryazanian - Barremian) marine connections and cephalopod migrations between the Tethyan and Boreal realms. In: Casey, R. & Rawson, P.F. (Eds.). *The Boreal Lower Cretaceous*. Geological Journal Special Issue No. 5. pp. 131 - 144.
- Rawson, P.F., Curry, D., & Dilley, F.C. 1978. A correlation of Cretaceous rocks in the British Isles. *Geological Society of London Special Report*, 9. pp. 1 - 70.
- Rawson, P.F., & Riley, L.A. 1982. Latest Jurassic-Early Cretaceous events and the "Late Cimmerian Unconformity" in North Sea Area. *American Association of Petroleum Geologists Bulletin*. Vol. 66. pp. 2628 - 2648.
- Raynaud, J.F. 1978. Principaux dinoflagellés caractéristiques du Jurassique Supérieur d'Europe du Nord. *Palinologia. Número Extraordinario*. Vol. 1. pp. 387 - 405.

- Reid, P.C., & Harland, R. 1977. Studies of Quarternary dinoflagellate cysts in the North Atlantic. *American Association of Stratigraphic Palynologists Contribution Series*, 5A. pp.147 - 169.
- Reyre, Y. 1973. Palynologie du Mésozoïque Saharien. Traitement de données par l'Informatique et applications à la Stratigraphie et à la Sédimentologie. *Mémoires du Muséum National d'Histoire Naturelle, Paris*. C. 27. 284 pp.
- Riding, J.B. 1984. Dinoflagellate cyst range-top biostratigraphy of the uppermost Triassic to lowermost Cretaceous of northwest Europe. *Palynology* Vol. 8. pp. 195 - 210.
- Riding, J.B., Fedorova, V.A., & Ilyina, V.I. in press. Jurassic and lowermost Cretaceous dinoflagellate cyst biostratigraphy of the Russian Platform and northern Siberia, Russia. *American Association of Stratigraphic Palynologists Contributions Series*.
- Riding, J.B., & Ioannides, N.S. 1996. A review of Jurassic dinoflagellate cyst biostratigraphy and global provincialism. *Bulletin de la Société Géologique, France*. Vol. 167. pp. 3 - 14.
- Riding, J.B., & Sarjeant, W.A.S. 1985. The role of dinoflagellate cysts in the biostratigraphical subdivision of the Jurassic System. *Newsletters on Stratigraphy*. Vol. 14. pp. 96 - 109.
- Riding, J.B., & Thomas, J.E. 1988. Dinoflagellate cyst stratigraphy of the Kimmeridge Clay (Upper Jurassic) from the Dorset coast, southern England. *Palynology*. Vol. 12. pp. 65 - 88.
- Riding, J.B., & Thomas, J.E. 1992. Dinoflagellate cysts of the Jurassic System. In: Powell, A. J. (Ed.). *A Stratigraphic Index of Dinoflagellate Cysts*. Chapman & Hall. pp. 7 - 97.
- Riding, J.B., & Thomas, J.E. 1997. Marine palynomorphs from the Staffin Bay and Staffin Shale formations (Middle-Upper Jurassic) of the Trotternash Peninsula, NW Skye. *Scottish Journal of Geology*. Vol. 33. pp. 59 - 74.
- Riley, L.A. 1974. A palynological investigation of Upper Jurassic-basal Cretaceous sediments from England, France and Iberia. Unpublished PhD thesis, The Open University, Milton Keynes.
- Riley, L.A., & Fenton, J.P.G. 1984. Palynostratigraphy of the Berriasian to Cenomanian sequence at Deep Sea Drilling Project Site 535, Leg 77, southeastern Gulf of Mexico. *Initial Reports of the Deep Sea Drilling Project*. Vol. 77. pp. 675 - 690.
- Riley, L.A., Harker, S.D., & Green, S.C.H. 1992. Lower Cretaceous palynology and sandstone distribution in the Scapa Field, UK North Sea. *Journal of Petroleum Geology*. Vol. 15. pp. 97 - 110.
- Riley, L.A., & Sarjeant, W.A.S. 1972. Survey of the stratigraphic distribution of dinoflagellates, acritarchs and tasmanitids in the Jurassic. *Geophytology*. Vol. 2. pp. 127 - 139.
- Riley, L.A., & Sarjeant, W.A.S. 1977. Age de quelques assemblages de dinoflagellés et acritarches du Kimméridgien (Jurassique Supérieur) du Boulonnais, nord de la France.

- Rogers, J., & Bremner, J.M. 1991. The Benguela System. Part VII. Marine-geological aspects. *Oceanography and Marine Biology Annual Review*. Vol. 29. pp. 1 - 85.
- Rossignol, M. 1961. Analyse pollinique de sédiments marins Quarternaires en Israel. 1. Sédiments récents. *Pollen et Spores*. Vol. 3. 303 - 324.
- Rovnina, B.V., Markova, L.G., & Purtova, S.I. 1986. Palynology and Petroleum Geology of Western Siberia. *Review of Palaeobotany and Palynology*. Vol. 48. pp. 373 - 376.
- Ruffell, A.H., & Rawson, P.F. 1994. Palaeoclimate control on sequence stratigraphic patterns in the Late Jurassic to Mid Cretaceous, with a case study from eastern England. *Palaeogeography, Palaeoclimatology, Palaeoecology*. Vol. 110. pp. 43 - 54.
- Saks, V.N., Basov, V.A., & Dagit, A.A. 1971. Paleozoogeographica morei borealnogo poyasa v yure i neokome. In: *Problemy obshchei i regionalnoy geologii*. Trudy Instituta Geologii i Geofizika, SO, AN SSSR. (Nauka, Novosibirsk). pp. 179 - 211.
- Saks, V.N., Basov, V.A., Zakharov, V.A., Nalnjaeva, T.I., & Shul'gina, N.I. 1975. Jurassic/Cretaceous boundary, position of the Berriasian in the Boreal realm and correlation with Tethys. *Memoires de la Bureau de Recherches Geologiques et Minieres*. Vol. 86. pp. 135 - 141.
- Saks, V.N., & Nalnyaeva, T.I. 1973. Belemnite assemblages from the Jurassic-Cretaceous boundary beds in the Boreal realm. In: Casey, R. & Rawson, P.F. (Eds.). *The Boreal Lower Cretaceous*. Geological Journal Special Issue No. 5. pp. 393 - 400.
- Saks, V.N., & Sazonova, I.G. 1975. Evolution of concepts on the boundary between the Jurassic and Cretaceous systems and the Berriasian stage. In: Saks, V. N. (Ed.). *The Jurassic-Cretaceous Boundary and the Berriasian Stage in the Boreal Realm*. pp. 4 - 11.
- Saks, V.N., & Shul'gina, N.I. 1973. Correlation of the Jurassic/Cretaceous boundary beds in the Boreal realm. In: Casey, R., & Rawson, P.F. (Eds.). *The Boreal Lower Cretaceous*. Geological Journal Special Issue No. 5. pp. 387 - 392.
- Saks, V.N., & Shulgina, N.I. 1974. Basic problems of the Upper Volgian, Berriasian and Valanginian stratigraphy of the Boreal Zone. *Acta Geologica Polonica*. Vol. 24. pp. 543 - 560.
- Saks, V.N., Shul'gina, N.I., Zakharov, V.A., & Ivanova, E.F. 1975. Chapter 7. Paleozoogeographic zoning (Volgian-Valanginian). In: Saks, V. N. (Ed.). *The Jurassic-Cretaceous Boundary and the Berriasian Stage in the Boreal Realm*. pp. 306 - 316.
- Salvador, A. 1994. *International Stratigraphic Guide*. International Union of Geological Sciences and Geological Society of America, Inc. Boulder. 214 pp.
- Sander, P.M., & Gee, C.T. 1990. Fossil charcoal: techniques and applications. *Review of Palaeobotany and Palynology*. Vol. 63. pp. 269 - 279.
- Sarjeant, W.A.S. 1959. Microplankton from the Cornbrash of Yorkshire. *Geological Magazine*. Vol. 96. pp. 329 - 347.
- Sarjeant, W.A.S. 1960. New Hystrichospheres from the Upper Jurassic of Dorset. *Geological Magazine*. Vol. 97. pp. 137 - 144.
- Sarjeant, W.A.S. 1962a. Microplankton from the Amphill Clay of Melton, South Yorkshire. *Palaeontology*. Vol. 5. pp. 478 - 497.

- Sarjeant, W.A.S. 1962b. Upper Jurassic microplankton from Dorset, England. *Micropalaeontology*. Vol. 8. pp. 255 - 268.
- Sarjeant, W.A.S. 1964. The stratigraphic application of fossil microplankton (dinoflagellates and hystrichospheres) in the Jurassic. *Colloque du Jurassique, Luxembourg 1962*. Volume des Comptes Rendus et Mémoires de l'Institut Grand Ducal, Section des Sciences naturelles. Physique et Mathématiques, Luxembourg. pp. 441 - 448.
- Sarjeant, W.A.S. 1975. Triassic and Jurassic dinoflagellates. In: *Proceedings of a forum on dinoflagellates held at Anaheim, California, 1973, as part of the 6th Annual Meeting, American Association of Stratigraphic Palynologists, Contributions Series. 4*. pp. 51 - 63.
- Sarjeant, W.A.S. 1982. Dinoflagellate cyst terminology, a discussion and proposals. *Canadian Journal of Botany*. Vol. 60. pp. 922 - 945.
- Sarjeant, W.A.S. 1984. A restudy of some dinoflagellate cysts and an acritarch from the Malm (Upper Jurassic) of southwest Germany. *Palaeontographica Abt. B*. Vol. 191. pp. 154 - 177.
- Sarjeant, W.A.S., Lacalli, T., & Gaines, G. 1987. The cysts and skeletal elements of dinoflagellates; speculations on the ecological causes for their morphology and development. *Micropalaeontology*. Vol. 33. pp. 1 - 36.
- Sarjeant, W.A.S., Volkheimer, W., & Zhang, W.P. 1992. Jurassic palynomorphs of the Circum-Pacific region. In: Westermann, G.E.G. (Ed.). *The Jurassic of the Circum-Pacific*. International Geological Correlation Programme Project 171: Jurassic of the Circum-Pacific. pp. 273 - 295.
- Sasonova, J.G., & Sasonov, N.T. 1983. The Berriasian of the European Realm. *Zitteliana*. Vol. 10. pp. 439 - 446.
- Sawyer, M.J., & Keegan, J.B. 1996. Use of palynofacies characterization in sand-dominated sequences, Brent Group, Ninian Field, UK North Sea. *Petroleum Geoscience*. Vol. 2. pp. 289 - 297.
- Scheidt, G., Littke, R. 1989. Comparative organic petrology of interlayered sandstones, siltstones, mudstones, and coals in the Upper Carboniferous Ruhr Basin, northwest Germany, and their thermal history and methane generation. *Geologische Rundschau*. Vol. 78. 375 - 90.
- Scotchman, I.C. 1991. Kerogen facies and maturity of the Kimmeridge Clay Formation in southern and eastern England. *Marine and Petroleum Geology*. Vol. 8. pp. 278 - 295.
- Scott, R.W., & Kidson, E.J. 1977. Lower Cretaceous depositional systems, west Texas. In: Bebout, D. G., & Loucks, R.G. (Eds.). *Cretaceous carbonates of Texas and Mexico: Applications to subsurface exploration*. Reports of Investigations of the Bureau of Economic Geology, University of Texas at Austin. pp. 169 - 181.
- Scull, B.,J., Felix, C.J., McCaleb, S.B., & Shaw, W.G. 1966. The interdisciplinary approach to paleoenvironmental interpretations. *Transactions of the Gulf Coast Association of Geological Societies*. Vol. 16. pp. 81 - 117.
- Senftle, J.T., Brown, J.H., & Larter, S.R. 1987. Refinement of organic petrographic methods for kerogen characterisation. *International Journal of Coal Geology*. Vol. 7. pp. 105 - 117.
- Sepkoski, J.J.Jr., & Raup, D.M. 1986. Periodicity of marine extinction events. In: Elliott, D. K. (Ed.). *Dynamics of Extinction*. Wiley & Sons. pp. 3 - 36.

- Sey, I.I., & Kalcheva, E.D. 1999. Lower Berriasian of Southern Primorye (far-east Russia) and the problem of Boreal-Tethyan correlation. *Palaeogeography, Palaeoclimatology, Palaeoecology*. Vol. 150. pp. 49 - 63.
- Shul'gina, N. I. 1975. Boreal ammonites at the turn of the Jurassic and Cretaceous and their correlation with Tethyan ammonites. 86. pp. 142 - 146.
- Shul'gina, N.I., Burdykina, M.D., Basov, V.A., & Arhus, N. 1994. Distribution of ammonites, Foraminifera and dinoflagellate cysts in the Lower Cretaceous reference sections of the Khatanga Basin, and Boreal Valanginian biogeography. *Cretaceous Research*. Vol. 15. pp. 1-16.
- Sittler, C., & Schuler, M. 1991. Une méthode d'analyse quantitative absolue de la fraction organique constituant le palynofaciès d'une roche sédimentaire. *Palynosciences*. Vol. 1. pp. 59 - 68.
- Sittler, C., & Ollivier-Pierre, M.F. 1994. Palynology and palynofacies analysis: some essential clues to assess and identify West-European Tertiary depositional environments in terms of relative high or lowstands. Application to the case of three Eocene and Oligocene sections in France. *Bulletin des Centres de Recherches Exploration-Production Elf Aquitaine*. Vol. 18. pp. 149 - 163.
- Skolnick, H. 1958. Observations on fusain. *American Association of Petroleum Geologists Bulletin*. Vol. 42. pp. 2223 - 2236.
- Slansky, M. 1986. *Geology of Sedimentary Phosphates*. North Oxford Academic. 210 pp.
- Smelror, M. 1986. Jurassic and Lower Cretaceous palynomorph assemblages from Cape Flora, Franz Joseph Land, Arctic, U.S.S.R. *Norsk geologisk Tidsskrift*. Vol. 66. pp. 107 - 119.
- Smelror, M., & Leereveld, H. 1989. Dinoflagellate and acritarch assemblages from the Late Bathonian to Early Oxfordian of Montagne Crussol, Rhone Valley, southern France. *Palynology*. Vol. 13. pp. 121 - 141.
- Smythe, M., Jian, F.X., & Ward, C.R. 1992. Potential petroleum source rocks in Triassic lacustrine-delta sediments of the Gunnedah Basin, Eastern Australia. *Journal of Petroleum Geology*. Vol. 15. pp. 435 - 450.
- Spackman, W., & Thompson, R. 1963. A coal constituent classification designed to evolve as knowledge of coal composition evolves. *Comptes Rendus du le sanciemme Congres Internationale du Stratigraphé et Geologie du Carbonifère*. Vol. 1. pp. 239 - 254.
- Stanley, D.J. 1986. Turbidity current transport of organic-rich sediments: alpine and Mediterranean examples. *Marine Geology*. Vol. 70. pp. 85 - 101.
- Staplin, F.L. 1969. Sedimentary organic matter, organic metamorphism, and oil and gas occurrence. *Bulletin of Canadian Petroleum Geology*. Vol. 17. pp. 47 - 66.
- Steffen, D., & Gorin, G. 1993a. Palynofacies of the Upper Tithonian-Berriasian deep-sea carbonates in the Vocontian Trough (SE France). *Bulletin des Centres de Recherche Exploration - Production Elf Aquitaine*. Vol. 17. pp. 235 - 247.
- Steffen, D., & Gorin, G.E. 1993b. Sedimentology of organic matter in Upper Tithonian - Berriasian deep-sea carbonates of south-east France: Evidence of eustatic control. In: Katz, B. J. & Pratt, L. (Eds.). *Source rocks in a sequence stratigraphic*

- framework. *American Association of Stratigraphic Palynologists, Studies in Geology*. pp. 49 -65.
- Stockmarr, J. 1971. Tablets with spores used in absolute pollen analysis. *Pollen et Spores*. Vol. 13. pp. 615 - 621.
- Stockmarr, J. 1972. Determination of spore concentration with an electronic particle counter. *Danmarks Geologiske Undersøgelse. Årbok*. pp. 87 - 89.
- Stover, L.E., Brinkhuis, H., Damassa, S.P., de Vertaull, L., Helby, R.J., Monteil, E., Partridge, A.D., Powell, A.J., Riding, J.B., Smelror, M., & Williams, G.L. 1996. Chapter 19. Mesozoic - Tertiary dinoflagellates, acritarchs and prasinophytes. In: Jansonius, J. & McGregor, D.C. (Eds.). *Palynology: Principles and Applications*. American Association of Stratigraphic Palynologists Foundation. pp. 641 - 750.
- Summerhayes, C.P. 1981. Organic facies of Middle Cretaceous black shales in deep North Atlantic. *American Association of Petroleum Geologists Bulletin*. 65. pp. 2364 - 2380.
- Summerhayes, C.P. 1983. Sedimentation of organic matter in upwelling regimes. In: Theide, J. & Suess, E. (Eds.). *Coastal Upwelling: Its Sediment Record Part B: Sedimentary Records of Ancient Coastal Upwelling*. NATO Conference Series IV. pp. 29 - 72.
- Summerhayes, C.P. 1987. Organic-rich Cretaceous sediments from the North Atlantic. In: Brooks, J. & Fleet, A.J. (Eds.). *Marine Petroleum Source Rocks*. Geological Society of London Special Publication. pp. 301 - 316.
- Tappan, H. 1980. *The Paleobiology of Plant Protists*. Freeman., San Fransisco. 1028 pp.
- Tavera, J.M., Aguado, R., Company, M., & Oldriz, F. 1994. Integrated biostratigraphy of the Durangites and Jacobi zones (J/K boundary) at the Puerto Escaño section in southern Spain (Province of Cordoba). *Geobios*. Vol. 17. pp. 469 - 476.
- Taylor, J.C.M. 1981. Zechstein facies and petroleum prospects in the central and northern North Sea. In: Illing, L. V. & Hobson, G.D. (Eds.). *Petroleum Geology of the Continental Shelf of North-West Europe*. Heyden., London. pp. 176 - 185.
- Theodorova, V.A. 1980. Microphytoplankton from the Early Cretaceous epicontinental seas of the European part of the USSR. In: *4th International Palynological conference, Lucknow*. Vol. 2. pp. 368 - 376.
- Thomas, J.E., & Cox, B.M. 1988. The Oxfordian - Kimmeridgian stage boundary (Upper Jurassic): Dinoflagellate cyst assemblages from the Harome Borehole, North Yorkshire, England. *Review of Palaeobotany and Palynology*. Vol. 56. pp. 313 - 326.
- Thusu, B., & van der Eem, J.G.L.A. 1985. Early Cretaceous (Neocomian-Cenomanian) palynomorphs *Journal of Micropalaeontology*. Vol. 4. pp. 131 - 150.
- Thusu, B., van der Eem, J.G.L.A., El-Mehdawi, A., & Bu-Argoub, F. 1988. Jurassic-Early Cretaceous palynostratigraphy in northeast Libya. In: El-Arnauti, A., Owens, B., & Thusu, B. (Eds.). *Subsurface Palynostratigraphy of Northeast Libya*. Garyounis University Publications, Benghazi. pp. 171 - 213.
- Thusu, B., & Vigran, J.O. 1985. Middle - Late Jurassic (Late Bathonian - Tithonian) Palynomorphs. *Journal of Micropalaeontology*. Vol. 4. pp. 113 - 130.

- Tissot, B., Durand, B., Espitalité, J., & Combaz, A. 1974. Influence of nature and diagenesis of organic matter in formation of petroleum. *American Association of Petroleum Geologists Bulletin*. Vol. 58. pp. 499 - 506.
- Tissot, B., & Welte, D.H. 1984. *Petroleum Formation and Occurrence*. Springer-Verlag, Berlin. 699 pp.
- Traverse, A. 1988. *Paleopalynology*. Unwin Hyman. London. 600pp.
- Tribovillard, N.-P., & Gorin, G.E. 1991. Organic facies of the Early Albian Niveau Paquier, a key black shale horizon of the Marnes Bleues Formation in the Vocontian Trough (Subalpine Ranges, SE France). *Palaeogeography, Palaeoclimatology, Palaeoecology*. Vol. 85. pp. 227 - 237.
- Tschudy, R.H. 1969. Relationship of palynomorphs to sedimentation. In: Tschudy, R. H. & Scott, R.A. (Eds.). *Aspects of Palynology*. John Wiley & Son, New York. pp. 79 - 102.
- Tuwani, A.O., & Tyson, R.V. 1994. Organic facies variations in the Westbury Formation (Rhaetic, Bristol Channel, S.W. England. *Organic Geochemistry*. Vol. 200. pp. 1001 - 1014.
- Tyson, R.V. 1984. Palynofacies investigation of Callovian (Middle Jurassic) sediments from DSDP Site 534, Blake-Bahama Basin, western central Atlantic. *Marine and Petroleum Geology*. Vol. 1. pp. 3 - 13.
- Tyson, R.V. 1987. The genesis and palynofacies characteristics of marine petroleum source rocks. In: Brooks, J. & Fleet, A.J. (Eds.). *Marine Petroleum Source Rocks*. Geological Society of London Special Publication. 26. pp. 47 - 67.
- Tyson, R.V. 1989. Late Jurassic palynofacies trends, Piper and Kimmeridge Clay Formations, UK onshore and northern North Sea. In: Batten, D. J. & Keen, M.C. (Eds.). *Northwest European Micropalaeontology and Palynology*. British Micropalaeontology and Palynology Series. Ellis Horwood. pp. 135 - 172.
- Tyson, R.V. 1993. Palynofacies analysis. In: Jenkins, D. G. (Ed.). *Applied Micropalaeontology*. Kluwer Academic Publishers. pp. 153 - 191.
- Tyson, R.V. 1995. *Sedimentary Organic Matter. Organic facies and palynofacies*. Chapman & Hall, London. 615 pp.
- Tyson, R.V., & Pearson, T.H. 1991. Modern and ancient continental shelf anoxia: an overview. In: Tyson, R. V. & Pearson, T.H. (Eds.). *Modern and Ancient Continental Shelf Anoxia*. Geological Society of London Special Publication. pp. 1 - 24.
- van Bergen, P.F., & Kerp, J.H.F. 1990. Palynofacies and sedimentary environments of a Triassic section in southern Germany. In: Fermont, W. J. J. & Weegink, J.W. (Eds.). *International Symposium on Organic Petrology*. Mededelingen Rijks Geologische Dienst. pp. 23 - 31.
- van Bergen, P.F., Janssen, N.M.M., Alferink, M., & Kerp, J.H.F. 1990. Recognition of organic matter types in standard palynological slides. *Mededelingen Rijks Geologische Dienst*. Vol. 45. pp. 9 - 21.
- van de Laar, J.G.M., & Fermont, W.J.J. 1990. The impact of marine transgressions on palynofacies: the Carboniferous Aegir marine band in borehole Kemperkoul-1. In: *Proceedings: International Symposium on Organic Petrology*. Mededelingen Rijks Geologische Dienst. Vol. 45. pp. 75 - 89.

- van der Zwan, C.J. 1990. Palynostratigraphy and palynofacies reconstruction of the Upper Jurassic to lowermost Cretaceous of the Draugen Field, offshore mid Norway. *Review of Palaeobotany and Palynology*. Vol. 62. pp. 157 - 186.
- Van Helden, B.G.T. 1986. Dinoflagellate cysts at the Jurassic/Cretaceous boundary, offshore Newfoundland, Canada. *Palynology*. Vol. 10. pp. 181 - 199.
- van Pelt, R. S., & Habib, D. 1988. Dinoflagellate species abundance and organic facies in Jurassic Twin Creek Limestone signal episodes of transgression and regression. In: *Abstracts, 7th International Palynological Congress*. Brisbane. p. 168.
- van Waveren, I. M. 1989. Palynofacies analysis of surface sediments from the north-eastern Banda Sea (Indonesia). *Netherlands Journal of Sea Research*. Vol. 24. pp. 501 - 509.
- van Waveren, I., & Visscher, H. 1994. Analysis of the composition and selective preservation of organic matter in surficial deep-sea sediments from a high-productivity area (Banda Sea, Indonesia). *Palaeogeography, Palaeoclimatology, Palaeoecology*. Vol. 112. pp. 85 - 111.
- Vasicek, Z., Michalik, J., & Borza, K. 1983. To the Neocomian biostratigraphy in the Krizna-Nappe of the Strazovske Vrchy Mountains (northwestern Central Carpathians). *Zitteliana*. Vol. 10. pp. 467 - 483.
- Venkatachala, B. S. 1981a. Differentiation of amorphous organic matter types in sediments. In: Brooks, J. (Ed.). *Organic Maturation Studies and Fossil Fuel Exploration*. Academic Press. pp. 177 - 200.
- Venkatachala, B. S. 1981b. Hydrocarbon source rock evaluation - a new palynological approach. *Petroleum Asia Journal*. Vol. 4. pp. 79 - 93.
- Venkatachala, B.S. 1984. Finely divided organic matter - its origin and significance as hydrocarbon source material. *Bulletin of the Oil and Natural Gas Commission*. Vol. 21. pp. 23 - 45.
- Venkatachala, B.S., & Kar, R.K. 1968. Dinoflagellate and hystrichosphaerid fossils from Katrol (Upper Jurassic) sediments of Kutchch, W. India. *Current Science*. Vol. 37. pp. 408 - 410.
- Venkatachala, B.S., Rawat, M.S., & Singh, R.N. 1984. Source rock palynology of the Tapti, Dahanu and Tarapur areas around Surat Depression, Bombay offshore region. *Petroleum Asia Journal*. Vol. 7. pp. 190 - 199.
- Vigran, O.V., & Thusu, B. 1975. *Illustrations of Norwegian microfossils. Illustrations and distribution of the Jurassic palynomorphs of Norway*. Royal Norwegian Council for Scientific and Industrial Research (NTNF) Continental Shelf Division. Publication No. 65. 55 pp.
- Vozzhennikova, T.F. 1960. Paleoalgologicheskaya kharakteristika Mesokaynozoyshih otlozheniy Zapadno - Siborskoy Nizmennosti. *Geologiy i Geophysica*. Vol. 1. pp. 7 - 64.
- Vozzhennikova, T.F. 1963. Pirrofitovye Vodorosli. In: Orlov, Y. A. (Ed.). *Osnovy Paleontologii* 14. pp. 179 - 185.
- Vozzhennikova, T.F. 1965. *Vedenie v izuchenie iskopaemykh Peridineevykh vodoroslei (Introduction to the study of fossil Peridiniens algae)*. Akademiya Nauk SSSR, Simbirskae Otdelenie Instituta Geoplogii i Geophysiki, Izdatelstvo 'Nauka', Moskva. 156 pp.

- Vozzhennikova, T.F. 1967. *Fossil Peridinae from Jurassic, Cretaceous and Paleogene deposits of the USSR*. Nauka., Moscow., 347 pp.
- Wall, D. 1971. The lateral and vertical distribution of dinoflagellates in Quaternary sediments. In: Funnell, B. M. & Riedel, W.R. (Eds.). *The Micropalaeontology of the Oceans*. Cambridge University Press. pp. 399 - 405.
- Wall, D., & Dale, B. 1974. Dinoflagellates in late Quaternary deep-water sediments of Black Sea. In: Gogens, E. T., & Ross, D.A. (Eds.). *Black Sea - Geology, Chemistry and Biology*. American Association of Petroleum Geologists Memoir. pp. 364 - 380.
- Wall, D., Dale, B., Lohmann, G.P., & Smith, W.K. 1977. The environmental and climatic distribution of dinoflagellate cysts in modern marine sediments from regions in the north and south Atlantic oceans and adjacent seas. *Marine Micropalaeontology*. Vol. 2. pp. 121 - 200.
- Wang, K.F., Zhang, Y.L., & Sun, Y.H. 1982. The spore-pollen and algae assemblages from the surface layer sediments of the Yangtze River delta. *Acta Geographica Sinica*. Vol. 37. pp. 261 - 271.
- Warren, J. S. 1967. Dinoflagellates from the Upper Jurassic and Lower Cretaceous rocks on the west side of the Sacramento Valley, California. Unpublished PhD thesis, Stanford University.
- Warren, J. S. 1973. Form and variation of the dinoflagellate *Sirmiiodinium grossi* Alberti, from the Upper Jurassic and Lower Cretaceous of California. *Journal of Palaeontology*. Vol. 47. pp. 101 - 114.
- Waterhouse, H.K. 1999. Regular terrestrially-derived palynofacies cycles in irregular marine sedimentary cycles, Lower Lias, Dorset, UK. *Journal of the Geological Society*. Vol. 156. pp. 1113 - 1124.
- Wheeler, J.W., & Sarjeant, W.A.S. 1990. Jurassic and Cretaceous palynomorphs from the central Alborz Mountains, Iran: Their significance in biostratigraphy and palaeogeography. *Modern Geology*. Vol. 14. pp. 267 - 374.
- Whitaker, M.F. 1984. The use of palynofacies and palynostratigraphy in the definition of Troll Field Geology. In: *6th Offshore Northern Seas Conference & Exhibition- reduction of uncertainties by innovative reservoir geomodelling*. Norskpetroleum forening. Article G6. pp. 50.
- Whitaker, M.F., Giles, M.R., & Cannon, S.J.C. 1992. Palynological review of the Brent Group, UK Sector, North Sea. In: Morton, A. C., Haszeldine, R.S., Giles, M.R., & Brown, S. (Eds.). *Geology of the Brent Group*. Geological Society, London, Special Publication No. 61. pp. 169 - 202.
- White, A.W., & Lewis, C.M. 1982. Resting cysts of the toxic, red tide dinoflagellate *Gonyaulax excavata* in Bay of Fundy sediments. *Canadian Journal of Fisheries and Aquatic Sciences*. Vol. 39. pp. 1185 - 1194.
- White, J.M. 1988. Methodology of the exotic spike: differential settling of palynomorphs during sample preparation. *Pollen et Spores*. Vol. 30. pp. 131 - 148.
- Wiedmann, J. 1975. The Jurassic/Cretaceous boundary as one of the Mesozoic system boundaries. *Memoires de la Bureau des Recherches Geologiques et Minières*. Vol. 86. pp. 358 - 362.
- Wierzbowski, A., & Århus, N. 1990. Ammonite and dinoflagellate cyst succession of an Upper Oxfordian - Kimmeridgian black shale core from the Nordkapp Basin, southern Barents Sea. *Newsletters on Stratigraphy*. Vol. 22. pp. 7 - 19.

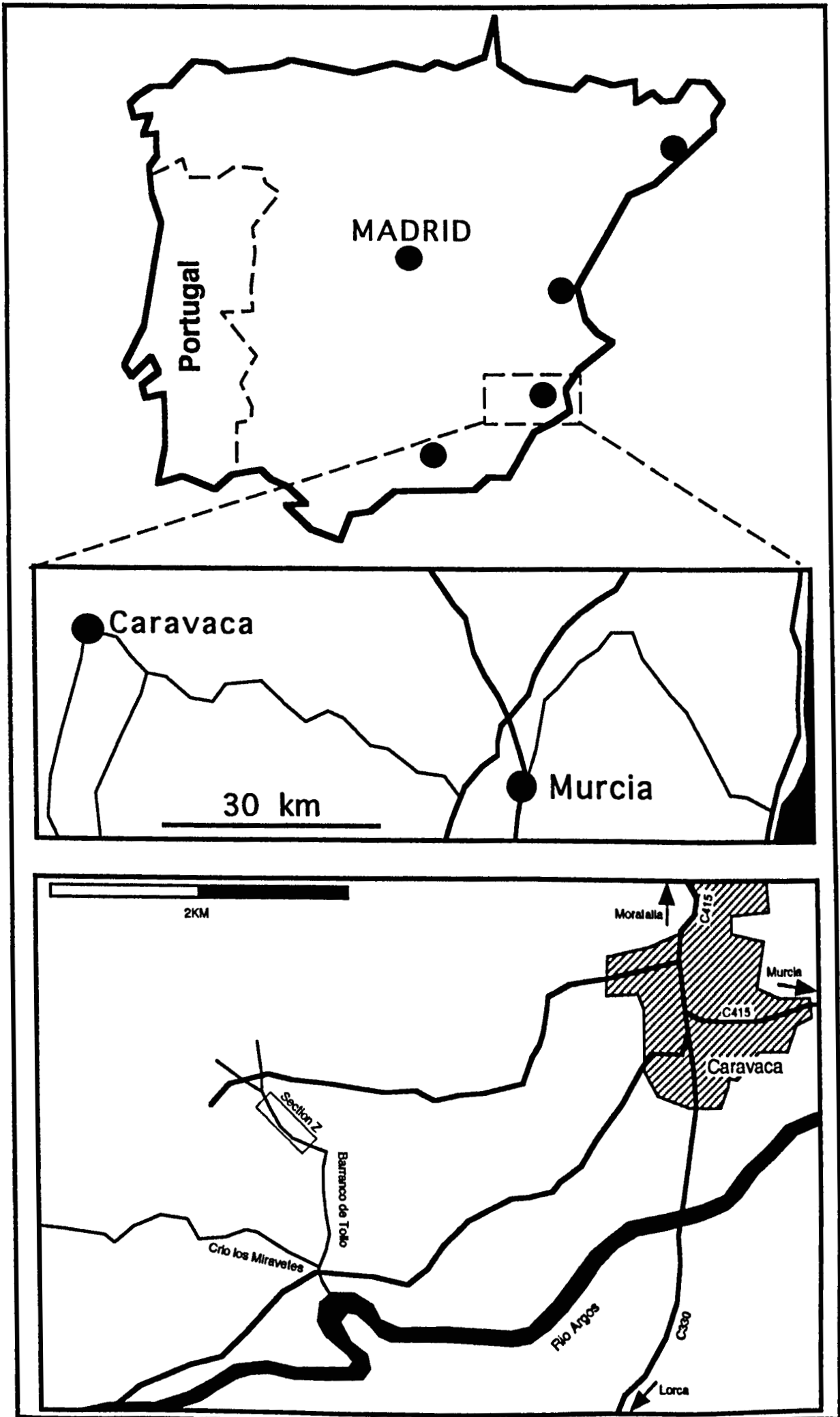
- Wiggins, V.D. 1969. Two Lower Cretaceous dinoflagellate species from Alaska. *Micropalaeontology*. Vol. 15. pp. 145 - 150.
- Wiggins, V.D. 1972. Two new Lower Cretaceous dinoflagellate genera from southern Alaska. *Review of Palaeobotany and Palynology*. Vol. 14. pp. 297 - 308.
- Wignall, P.B. 1991. Test of the concepts of sequence stratigraphy in the Kimmeridgian (Late Jurassic) of England and northern France. *Marine and Petroleum Geology*. Vol. 8. pp. 430 - 441.
- Williams, D.B., & Sarjeant, W.A.S. 1967. Organic walled microfossils as depth and shoreline indicators. *Marine Geology*. Vol. 5. pp. 389 - 412.
- Williams, G.L. 1975. Dinoflagellate and spore stratigraphy of the Mesozoic-Cenozoic, offshore eastern Canada. *Geological Survey of Canada*. Vol. 2. pp. 107 - 161.
- Williams, G.L. 1978. Palynological biostratigraphy, Deep Sea Drilling Project Sites 367 and 370. *Initial Reports of the Deep Sea Drilling Project*. Vol. 41. pp. 783 - 815.
- Williams, G.L. 1992. Palynology as a palaeoenvironmental indicator in the Brent Group, northern North Sea. In: Morton, A. C., Haszeldine, R.S., Giles, M.R., & Brown, S. (Eds.). *Geology of the Brent Group*. Geological Society, London, Special Publication No. 61. pp. 203 - 212.
- Williams, G.L., & Bujak, J.P. 1985. Palynological Stratigraphy of Deep Sea Drilling Project Site 416. *Initial Reports of the Deep Sea Drilling Project*. Vol. 50. pp. 467 - 495.
- Williams, G.L., Lentin, J.K., & Fensome, R.A. 1998. The Lentin & Williams Index of Fossil Dinoflagellates 1998 Edition. *American Association of Stratigraphic Palynologists Contributions Series Number 34*. 817 pp.
- Wilpshaar, M., & Leereveld, H. 1994. Paleoenvironmental change in the Early Cretaceous Vocontian Basin (SE France) reflected by dinoflagellate cysts. *Review of Palaeobotany and Palynology*. Vol. 84. pp. 121-128.
- Wimbledon, W.A. 1984. The Portlandian, the terminal Jurassic Stage in the Boreal Realm. *7th International Symposium on Jurassic Stratigraphy, Erlangen*. pp. 534 - 549.
- Wimbledon, W.A., & Cope, J.C.W. 1978. The ammonite faunas of the English Portland Beds and the zones of the Portlandian Stage. *Journal of the Geological Society of London*. Vol. 135. pp. 183 - 190.
- Woollam, R., & Riding, J.B. 1983. Dinoflagellate cyst zonation of the English Jurassic. *Institute of Geological Sciences Reports*. Vol. 83. 42pp.
- Wood, G.D., Gabriel, A.M., & Lawson, J.C. 1996. Chapter 3: Palynological techniques - processing and microscopy. In: Jansonius, J. & McGregor, D.C. (Eds.). *Palynology: Principles and Applications*. American Association of Stratigraphic Palynologists Foundation. pp. 29 - 51.
- Wrenn, J.H., & Beckman, S.W. 1981. Maceral and total organic carbon analyses of DSDP drill core 11. In: McGinnis, L. D. (Ed.). *Dry Valley Drilling Project. Antarctic Research Series, American Geophysical Union*. pp. 391 - 402.
- Yegoyan, V.L. 1975. Tithonian and Berriasian boundary is the boundary between the Jurassic and Cretaceous systems. *Memoires de la Bureau des Recherches Geologiques et Minieres*. Vol. 86. pp. 363 - 369.

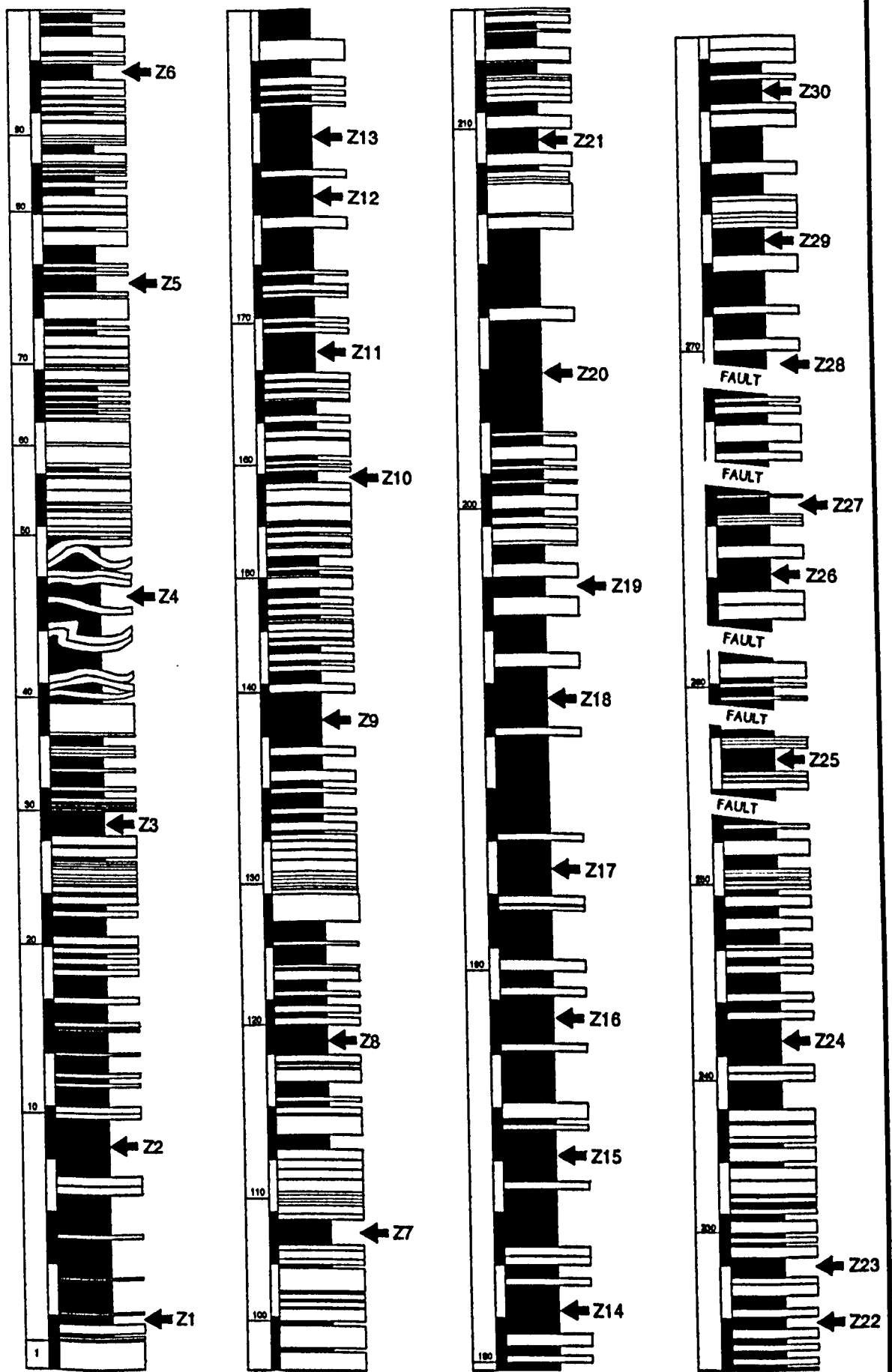
Zakharov, V.A., Bogomolov, Y.I., & Ilyina, V.I. 1997. Boreal Zonal Standard and biostratigraphy of the Siberian Mesozoic. *Geologiy i geophysica*. Vol. 38. pp. 927 - 956.

Zeiss, A. 1986. Comments on the tentative correlation chart for the most important marine provinces of the Jurassic/Cretaceous boundary. *Acta Geologica Hungarica*. Vol. 29. pp. 27 - 30.

Zotto, M., Drugg, W.S., & Habib, D. 1987. Kimmeridgian dinoflagellate stratigraphy in the south-western North Atlantic. *Micropalaeontology*. Vol. 33. pp. 193 - 213.

APPENDIX A

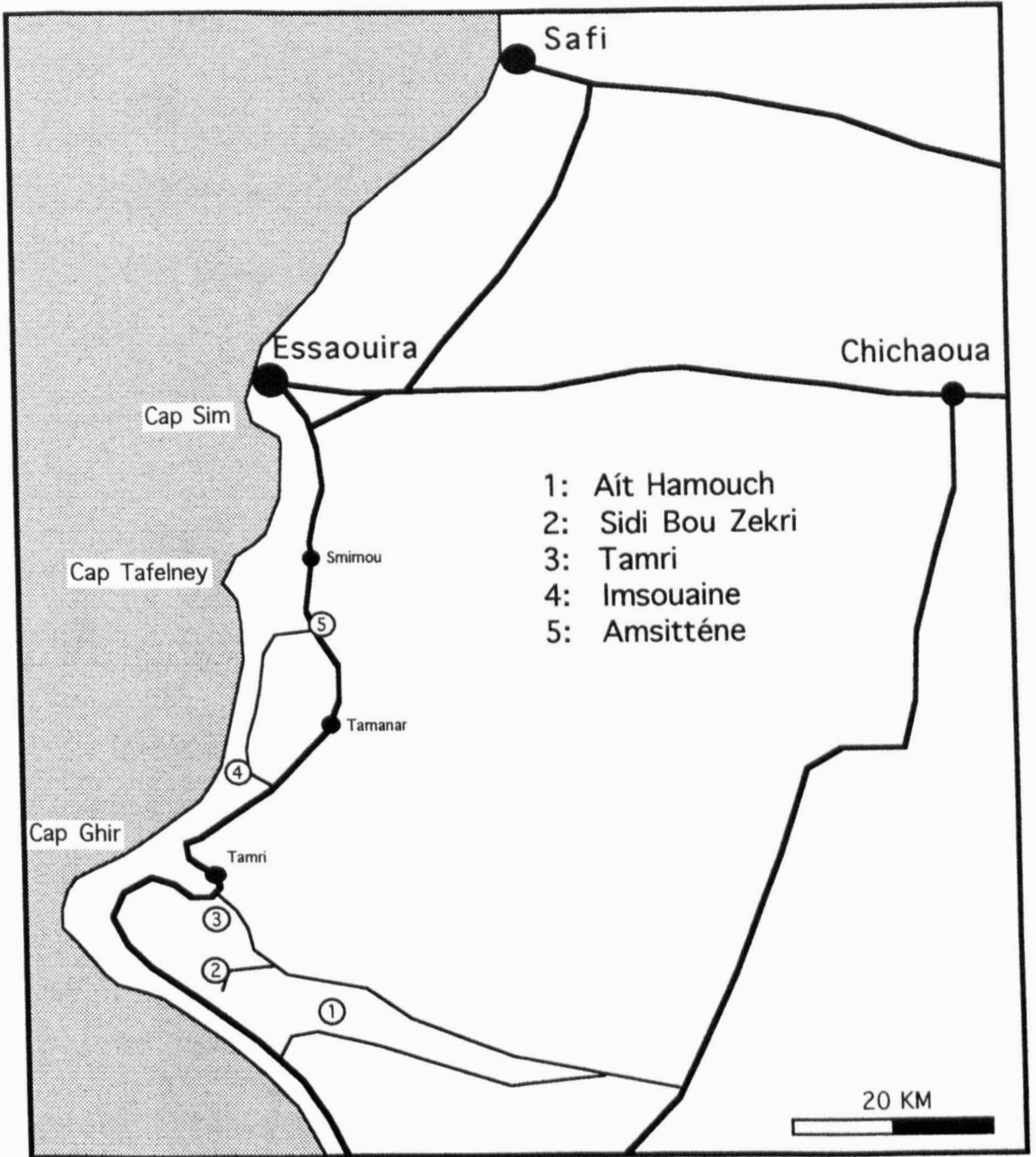


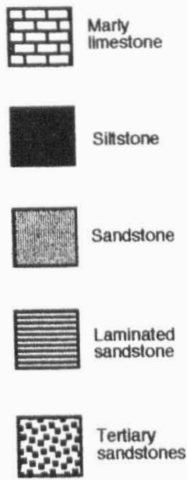


Vertical scale: 1 unit = 1 metre.

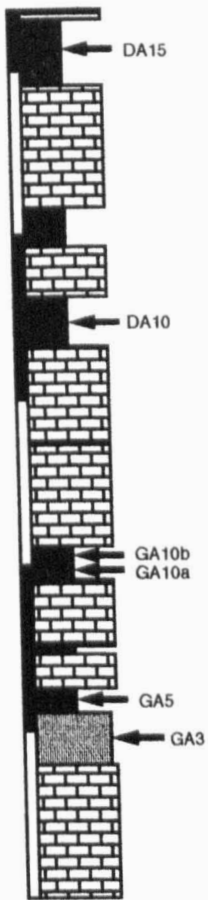
Sedimentary log of Caravaca section Z (Barranco de Tollo) showing position of palynological samples. Redrawn from Hoedemaeker (1981).

APPENDIX B

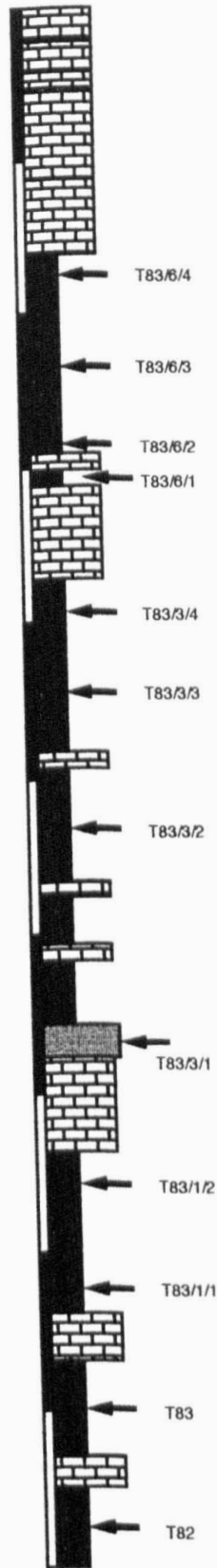




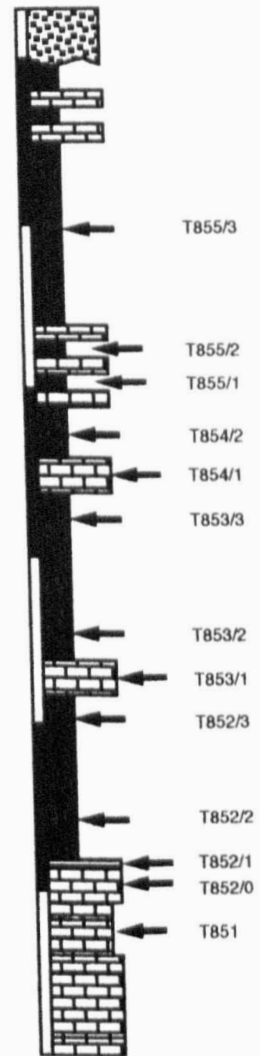
2 Metres
(Both logs)



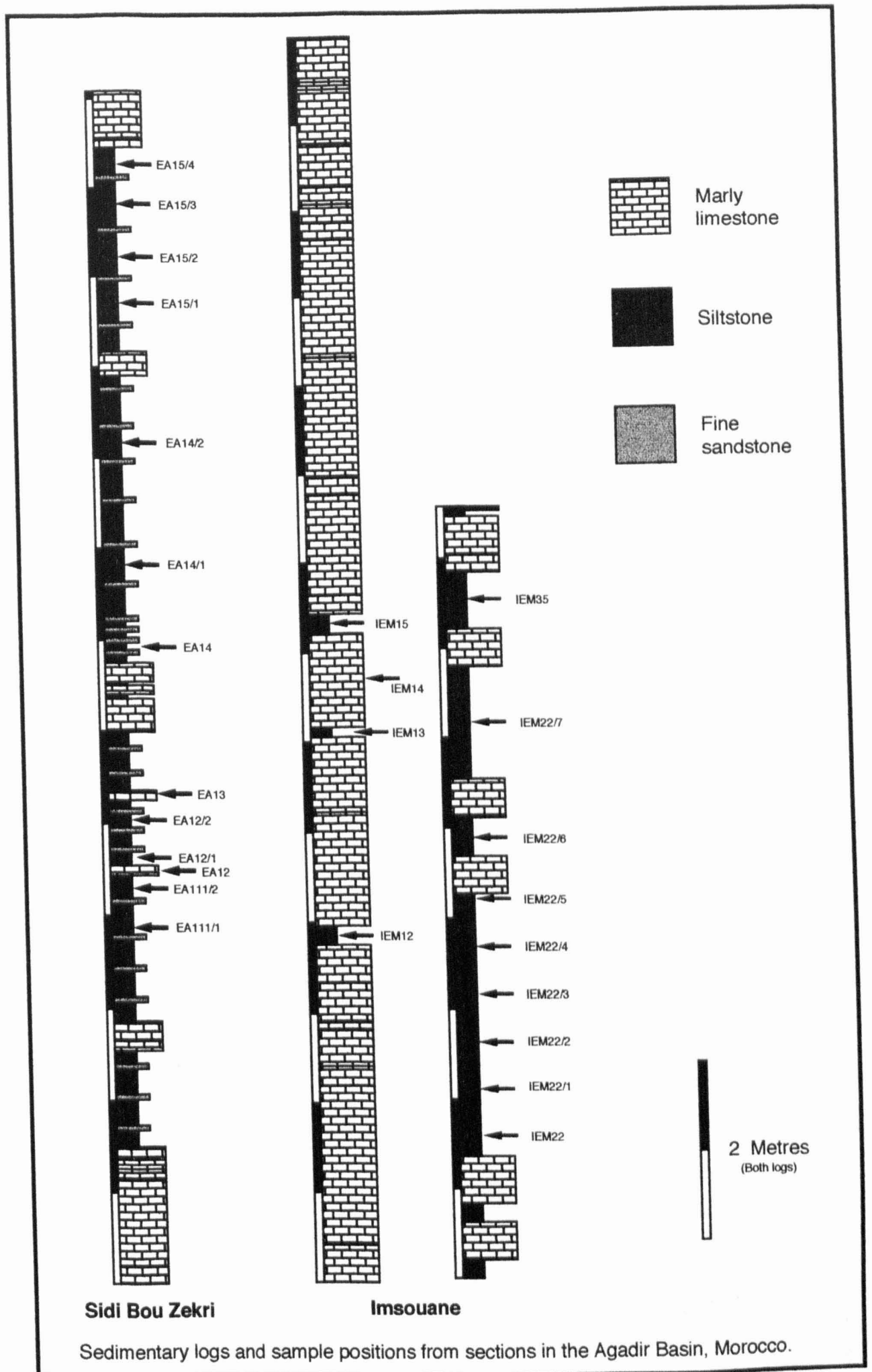
Amstittène

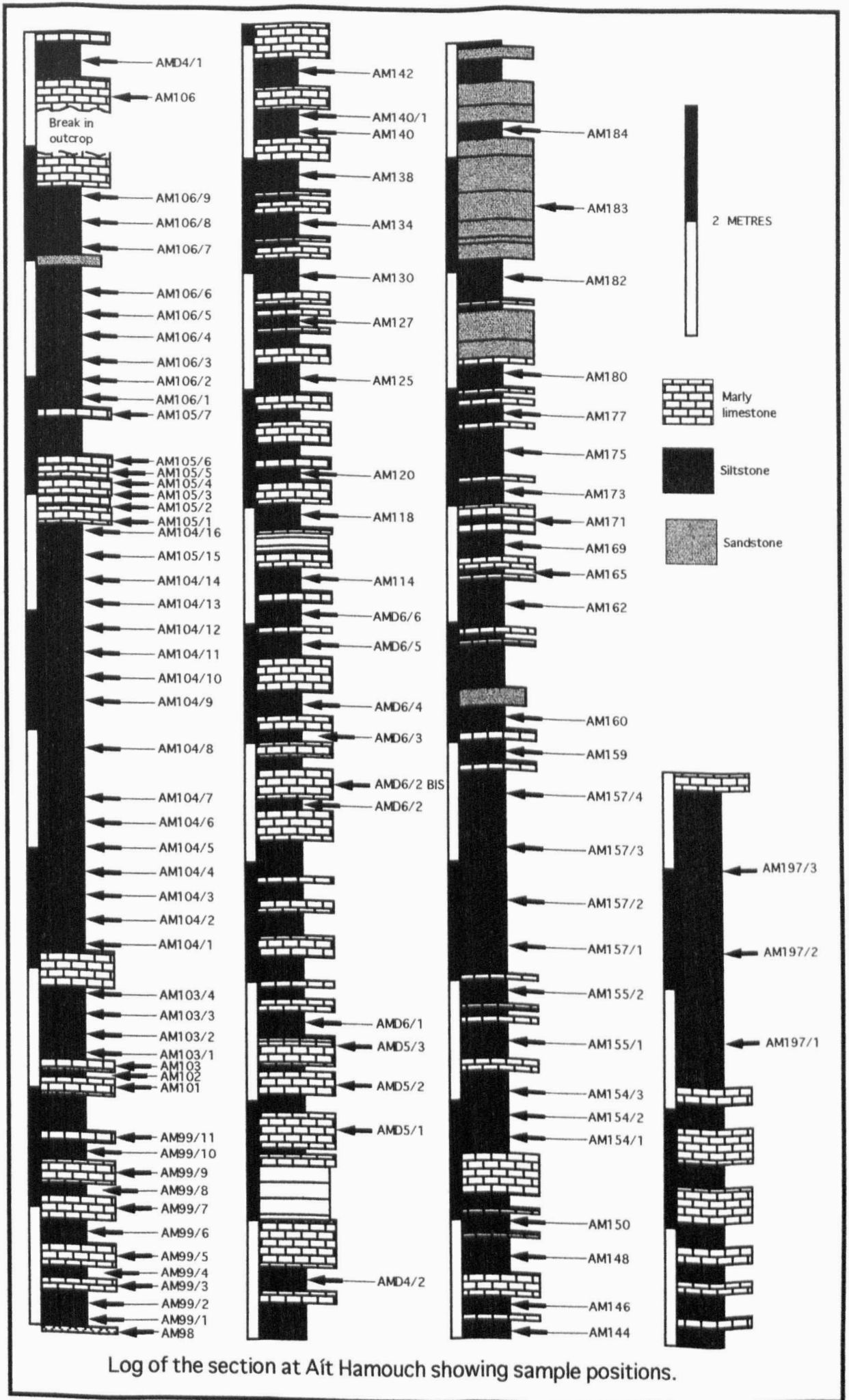


Tamri



Sedimentary logs and sample positions from sections in the Agadir Basin, Morocco.





PLATES

PLATE 1

All figures at x670 magnification unless otherwise stated.

1, 2: *Aprobolocysta pustulosa* sp. nov. Holotype. Slide K17-0/300-3, England Finder coordinates O56/1. **1:** Ventral focus. Note asymmetrical lobate antapex with enlarged pustule. **2:** Dorsal focus.

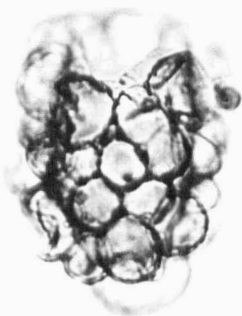
3, 4: *Aprobolocysta pustulosa* sp. nov. Slide K17-0/600-2, England Finder coordinates J43. **3:** Oblique ventral focus. Note the difference in size and spacing of the pustules in comparison to the holotype. **4:** Oblique dorsal focus.

5, 6: *Aprobolocysta pustulosa* sp. nov. Slide K17-0/600, England Finder coordinates H36. **5:** Left lateral focus. Note the manner in which several pustules have joined to form compound pustules. **6:** Right lateral focus.

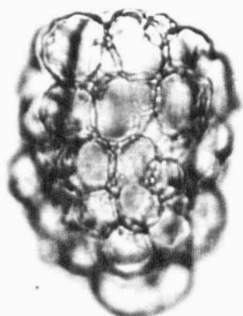
7, 8: *Aprobolocysta pustulosa* sp. nov. Operculum. Slide K17-0/600, England Finder coordinates R57. **7:** Ventral focus. Note the conical apex. **8:** Dorsal focus.

9 - 11: *Aprobolocysta pustulosa* sp. nov. Paratype. Slide K17-0/600, England Finder coordinates Q33. **9:** Probably lateral view. Primary archeopyle suture has only partially formed. Note different size and spacing of the pustules in comparison to the holotype. **10:** Probably lateral view. **11:** Higher magnification showing smaller micro-pustules. x1,100 magnification.

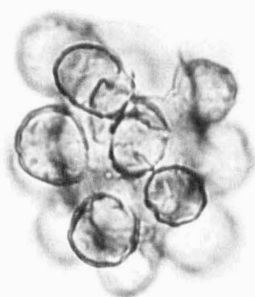
PLATE 1



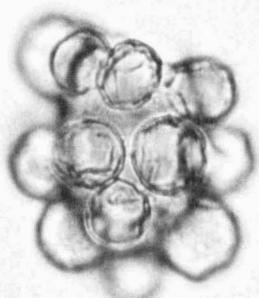
1



2



3



4



5



6



7



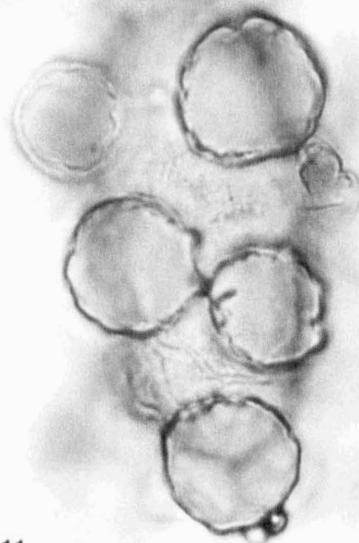
8



9



10



11

PLATE 2

All figures at x670 magnification.

1, 4, 7: *Rhynchodiniopsis magnifica* sp. nov. Holotype. Slide U11-2, England Finder coordinates K28/2. **1:** Ventral focus. **4:** Median focus. Note the slightly elongate oval shape, small rod-like apical horn and high parasutural septa, particularly at the paracingulum. **7:** Dorsal focus. Note gonial 'pseudo-spines' at junctions of the antapical paraplate with the post-cingular series.

2, 5: *Rhynchodiniopsis magnifica* sp. nov. Slide U3-2, England Finder coordinates G55/1. **2:** Ventro-lateral focus in dorso-lateral view. **5:** Dorso-lateral focus.

3, 6, 9: *Rhynchodiniopsis magnifica* sp. nov. Slide U3, England Finder coordinates S57. **3:** Ventro-lateral focus. **6:** Median focus. **9:** Dorsal focus.

8: *Rhynchodiniopsis magnifica* sp. nov. Slide U4, England Finder coordinates Q33/2. Median focus. Note bell-shaped nature of the epicyst and gonial 'pseudo-spines' at the junctions of the apical and pre-cingular paraplate series.

PLATE 2

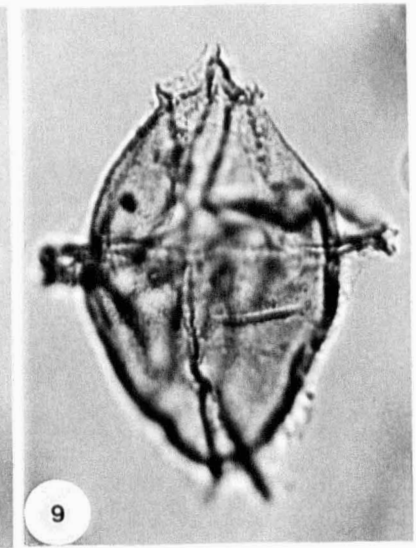
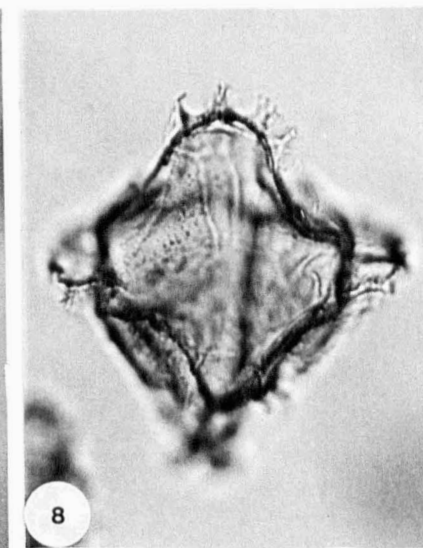
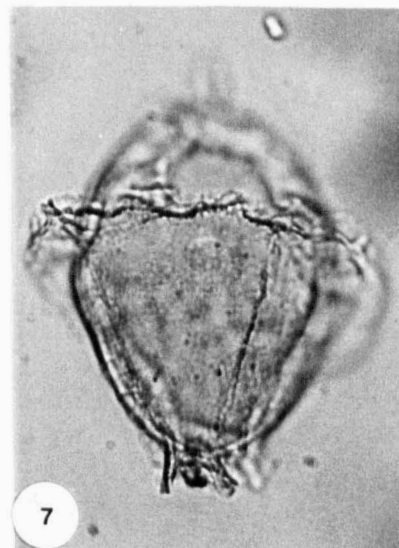
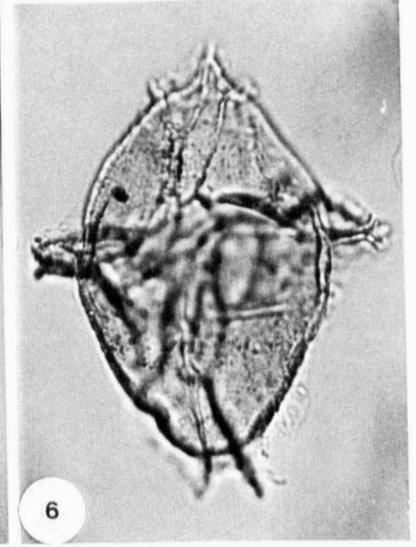
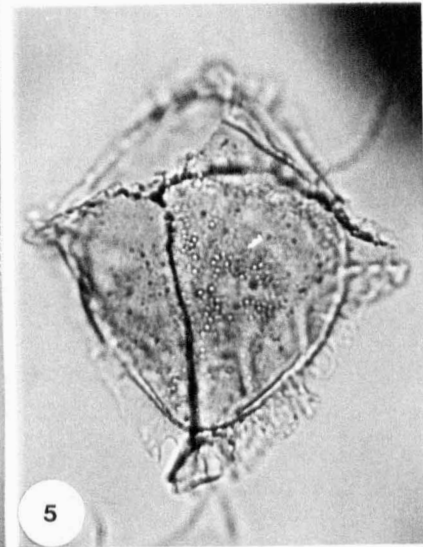
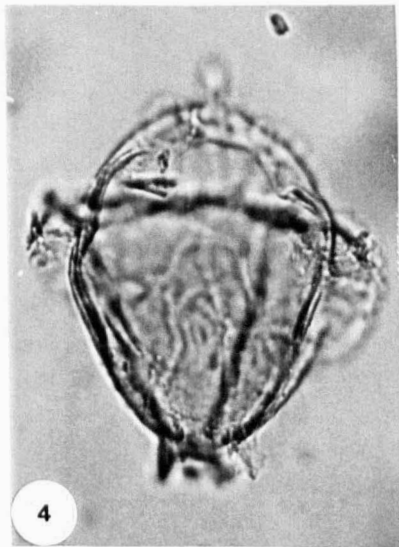
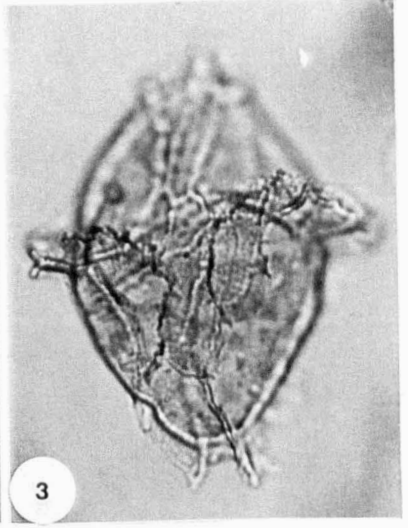
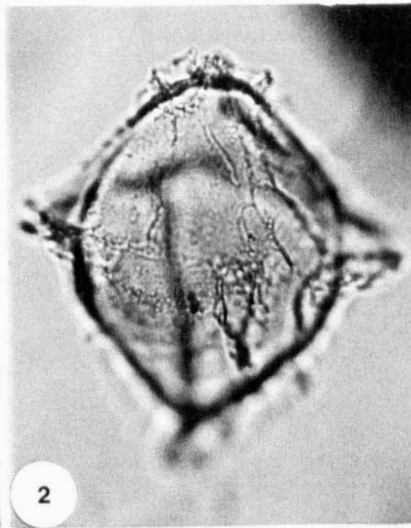
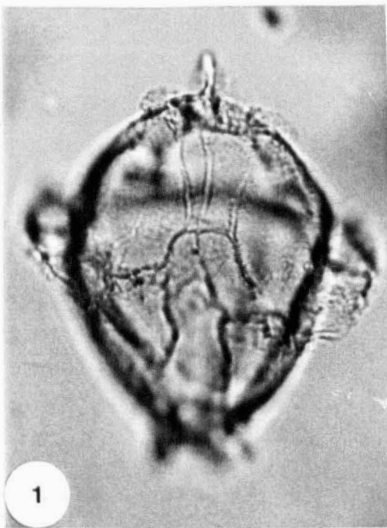


PLATE 3

All figures at x670 magnification unless otherwise stated.

1 - 3: *Rhynchodiniopsis undoryensis* sp. nov. Holotype. Slide U24-2, England Finder coordinates J47/1. **1:** Ventral focus on hypocyst. **2:** Median focus. **3:** Dorsal focus on epicyst.

4 - 6: *Rhynchodiniopsis undoryensis* sp. nov. Paratype. Slide U24-2, England Finder coordinates J40/2. **4:** Ventral focus on hypocyst. Note broader nature of this specimen in comparison to the holotype. **5:** Dorsal focus on epicyst. **6:** Higher magnification of apical region in median focus to emphasise the character of the apical horn. Note also the gonal 'pseudo-spines' at junctions of the apical and pre-cingular paraplate series. x1000 magnification.

PLATE 3

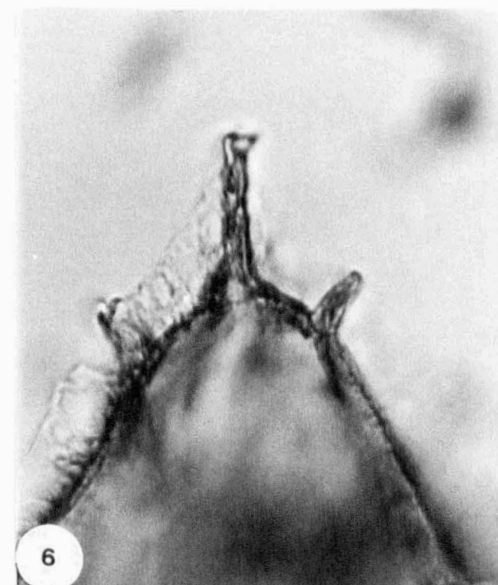
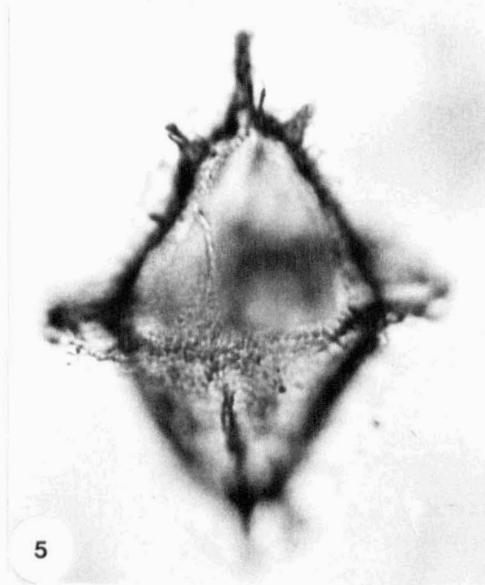
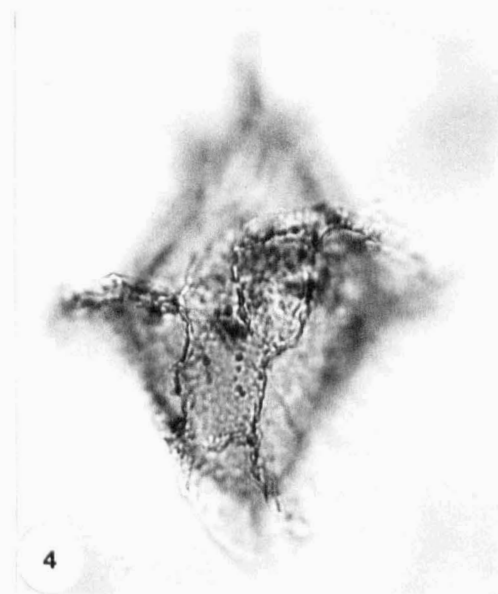
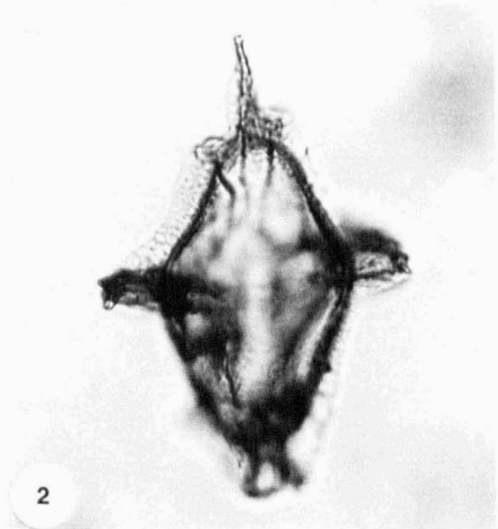
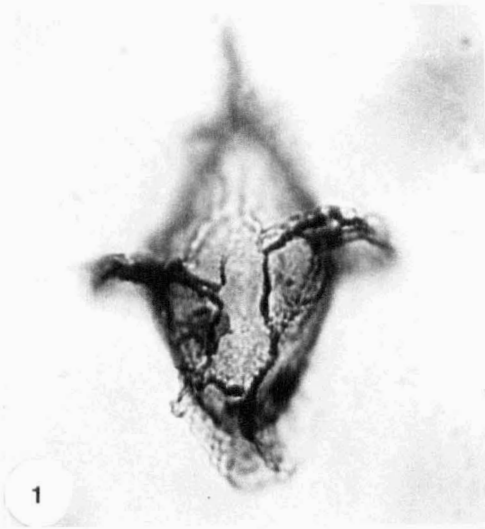


PLATE 4

1, 2: *Lithodinia distincta* sp. nov. Holotype. Slide K17-0/600-3, England Finder coordinates N31/4. **1:** Apical focus. Note the slight dorso-ventral compression. **2:** Median focus showing height of the reticulate sculpture. Both x450 magnification.

3: *Lithodinia distincta* sp. nov. Paratype. Slide K17-0/300-2, England Finder coordinates N61. Apical focus. x450 magnification.

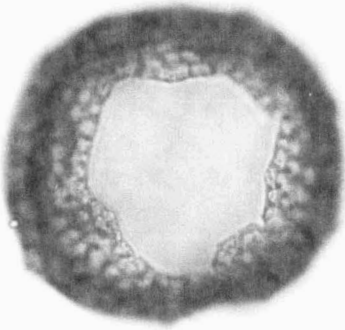
4: *Lithodinia distincta* sp. nov. Slide K17-0/600-2, England Finder coordinates K54. Note the tight, evenly distributed reticulum. x450 magnification.

5: *Lithodinia distincta* sp. nov. Operculum. Slide K17-0/600-3, England Finder coordinates E27/4. x450 magnification.

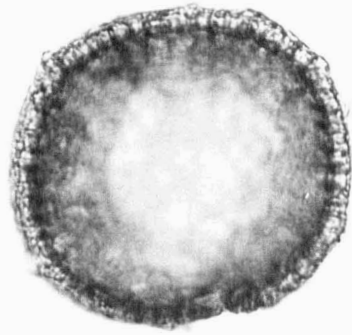
6, 7, 8: *?Cyclonephelium bulbosum* sp. nov. Holotype. Slide K17-0/300, England Finder coordinates K30/3. **6:** Probably ventral focus. Note reduced sculpture in mid-ventral and mid-dorsal (Figure 8) areas, flat antapex with antapical 'tuft' of processes. **7:** Median focus. Primary archeopyle suture has only partially formed. **8:** *?Cyclonephelium bulbosum* sp. nov. Same specimen. Probably dorsal focus. All three x670 magnification.

9, 10: *?Cyclonephelium bulbosum* sp. nov. Paratype. Slide K17-0/600-2, England Finder coordinates N38. **9:** Ventral focus. Note width of opercular attachment, presumably paracingular restriction of cyst ambitus, and bilobed antapex. **10:** Dorsal focus. Note the accessory archeopyle sutures which clearly separate Kofoid paraplate 3". Both x670 magnification.

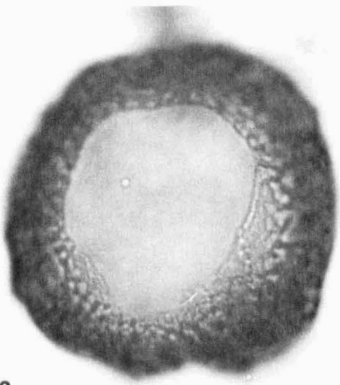
PLATE 4



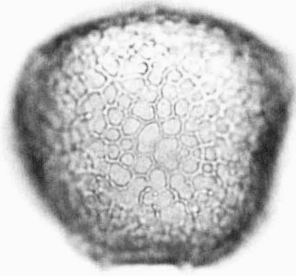
1



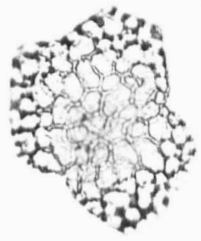
2



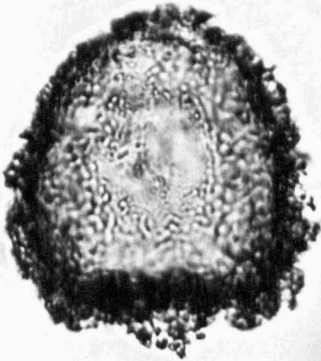
3



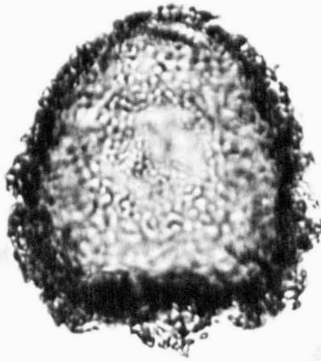
4



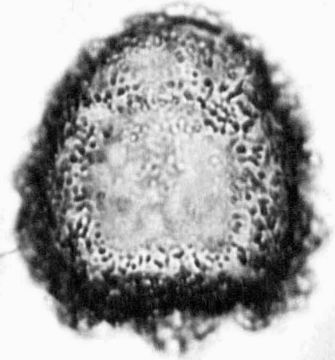
5



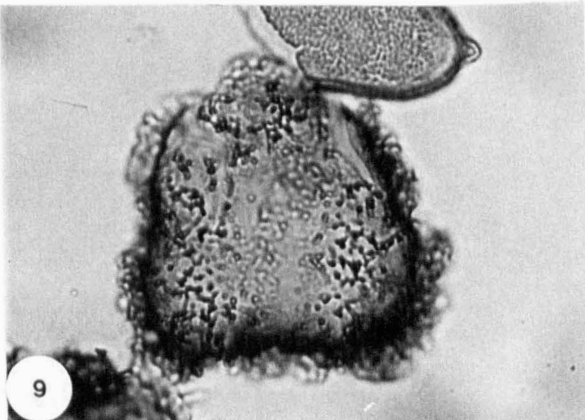
6



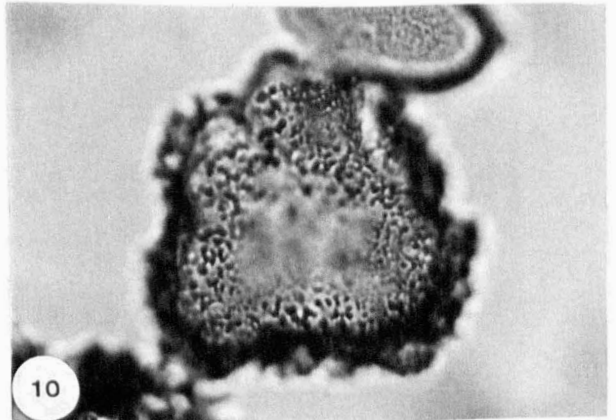
7



8



9



10

PLATE 5

- 1, 2:** *?Thalassiphora robusta* sp. nov.. Holotype. Slide U3-2, England Finder coordinates J41. **1:** Ventral focus. **2:** Dorsal focus. Both x450 magnification.
- 3:** *?Thalassiphora robusta* sp. nov.. Slide U6-2, England Finder coordinates P49/2. x450 magnification.
- 4, 5:** *?Cyclonephelium bulbosum* sp. nov.. SEM stub 6, grid square 1/II. Taken from sample K17. **4:** Ventral view. **5:** Higher magnification of apical region and operculum. Scale bars =20µm.
- 6:** *?Cyclonephelium bulbosum* sp. nov.. SEM stub 4, grid square 4/I. Taken from sample K17. Ventral view. Scale bar =20µm.
- 7:** *Lithodinia distincta* sp. nov.. SEM stub 6, grid square 1/I. Taken from sample K17. Ventral view. Note clear paratabulation. Scale bar =20µm.
- 8:** *Lithodinia distincta* sp. nov.. SEM stub 2, grid square 3/IV. Taken from sample K17. Right lateral view. Note apparent paraplate overlap. Scale bar =20µm.
- 9:** *Lithodinia distincta* sp. nov.. SEM stub 12, grid square 1/I. Taken from sample K17. Left lateral view. Scale bar =20µm.
- 10:** *Lithodinia distincta* sp. nov.. SEM stub 11, grid square 4/III. Taken from sample K17. Apical view, higher magnification to show the two wall layers and spongy nature of the reticulum which supports the periphragm. Scale bar =20µm.
- 11:** *Lithodinia distincta* sp. nov.. SEM stub 12, grid square 1/I. Taken from sample K17. Right lateral view. Higher magnification to show intratabular depressions, presumably where the periphragm 'drapes' into lumina of the supporting reticulum. Scale bar =20µm.
- 12:** *?Thalassiphora robusta* sp. nov.. SEM stub 6, grid square 1/III. Taken from sample U3. Ventral view, uncertain orientation. Note folding of the periphragm where it has collapsed onto the endophragm. Scale bar =20µm.

PLATE 5

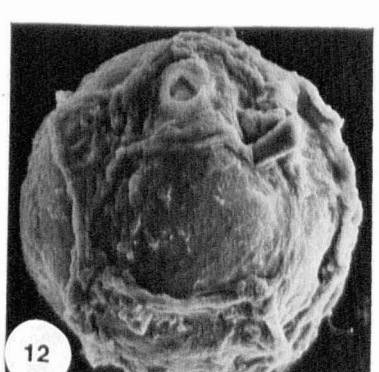
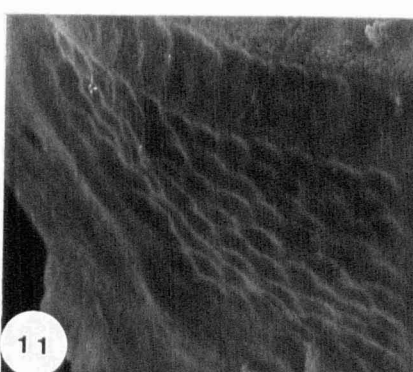
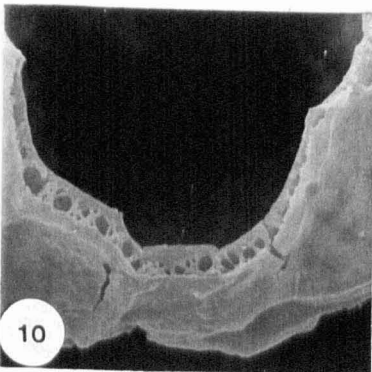
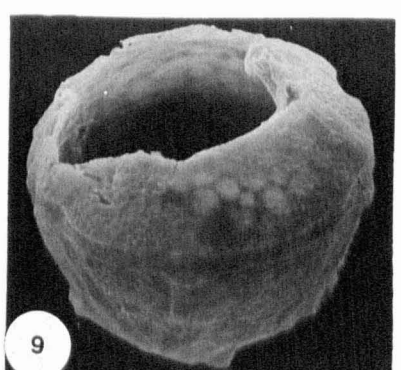
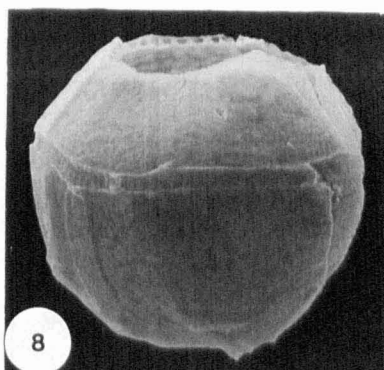
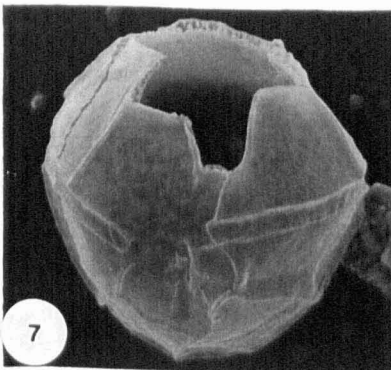
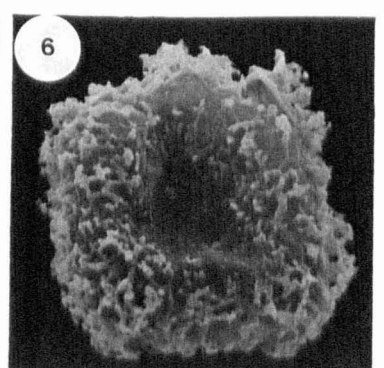
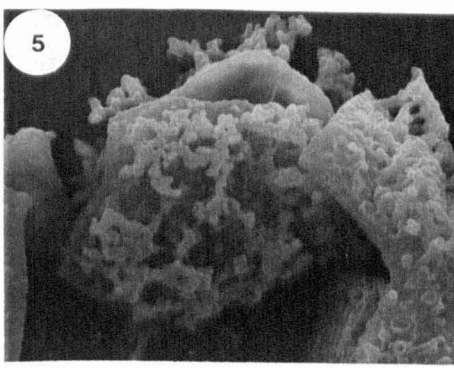
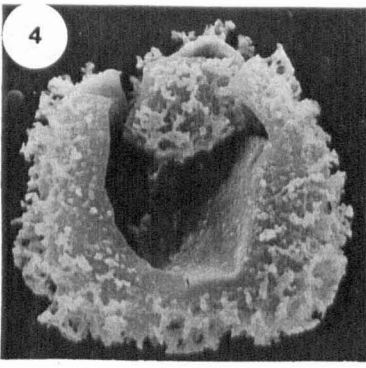
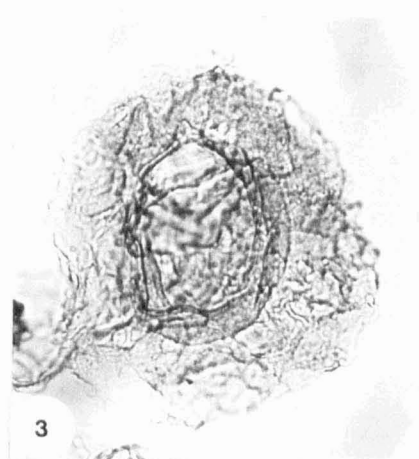
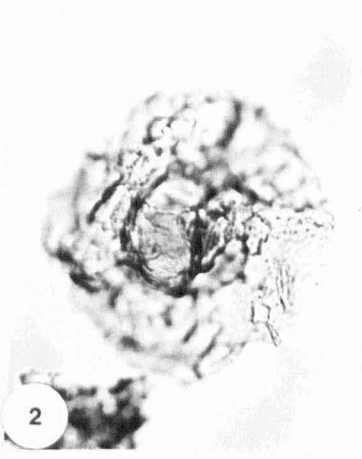
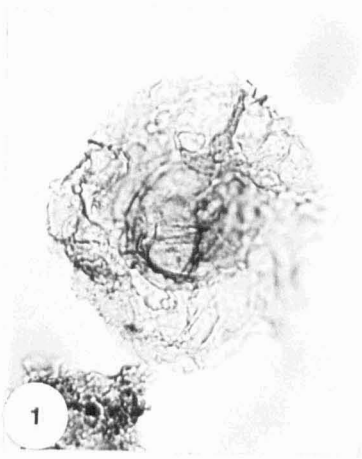


PLATE 6

1: *Aprobolocysta pustulosa* sp. nov.. SEM stub 2, grid square 2/V. Taken from sample K17. Ventro-lateral view. Note the numerous claustra in the periphragm at the base of the pustules. Scale bar =20 μ m.

2: *Aprobolocysta pustulosa* sp. nov.. SEM stub 12, grid square 2/II. Taken from sample K17. Probably Ventral view. Archeopyle has not formed. Note the absence of pustules in the region where the principal archeopyle suture would form. Scale bar =20 μ m.

3: *Aprobolocysta pustulosa* sp. nov.. SEM stub 5, grid square 3/II. Taken from sample K17. High magnification view of the addressed area between pustules showing scabrate to pitted nature of the periphragm in these areas. Scale bar =10 μ m.

4, 5: *Rhynchodiniopsis magnifica* sp. nov.. Paratype. SEM stub 11, grid square 2/IV. Taken from sample K21. **4:** Ventral view. **5:** Higher magnification of apical region showing absence of an apical horn, and the fenestrate nature of the parasutural septa. Scale bar =20 μ m.

6: *Rhynchodiniopsis magnifica* sp. nov.. SEM stub 10, grid square 2/II. Taken from sample U6. Ventral view. Specimen with a more bell-shaped epicyst. Scale bar =20 μ m.

7: *Rhynchodiniopsis undoryensis* sp. nov.. SEM stub 10, grid square 3/I. Taken from sample U24. Dorsal view. Scale bar =20 μ m.

8: *Rhynchodiniopsis undoryensis* sp. nov.. Same specimen, higher magnification of apical region showing reduced length of dorsal epicyst and character of the apical horn. Dorsal view. Scale bar =20 μ m.

9: *Rhynchodiniopsis undoryensis* sp. nov.. SEM stub 10, grid square 3/III. Taken from sample U24. Dorsal view. Scale bar =20 μ m.

PLATE 6

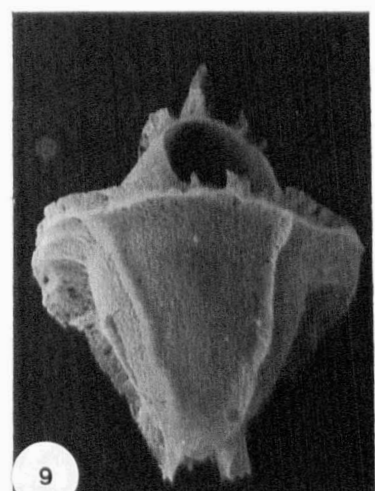
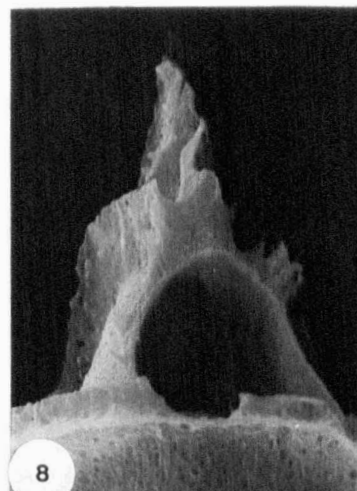
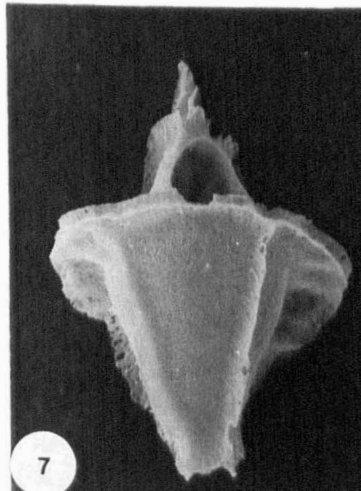
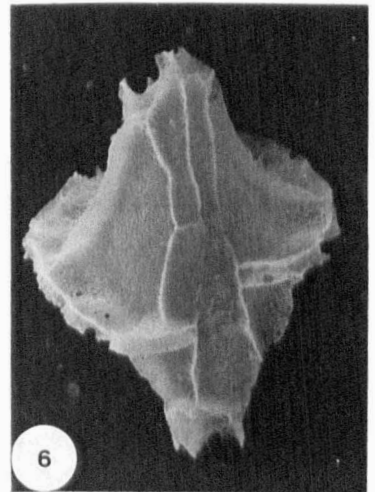
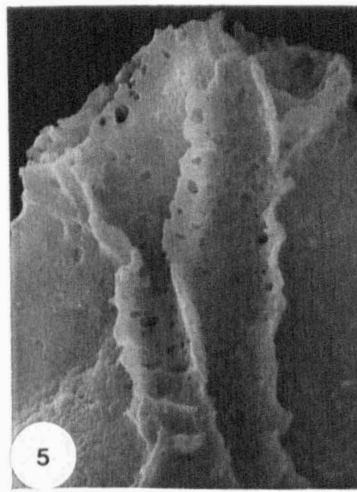
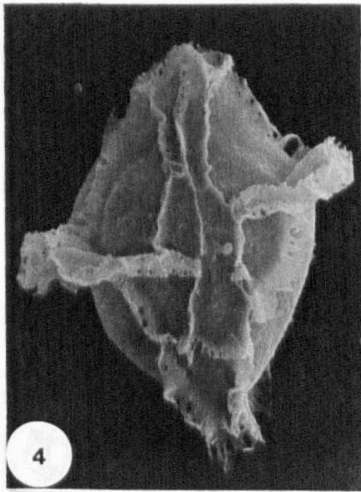
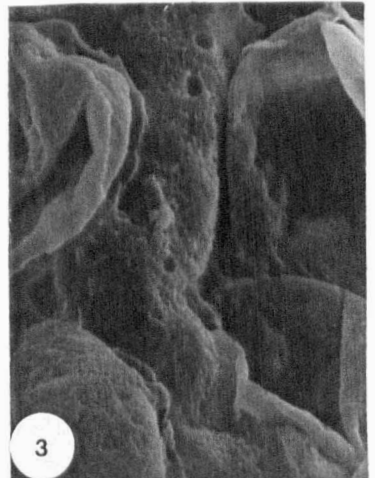
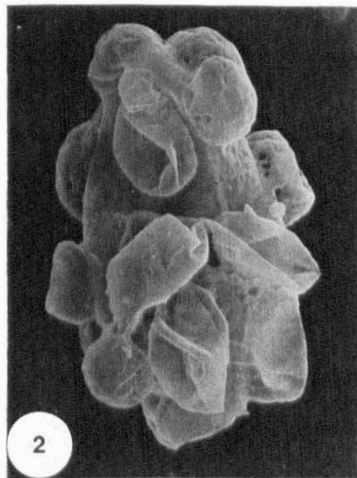
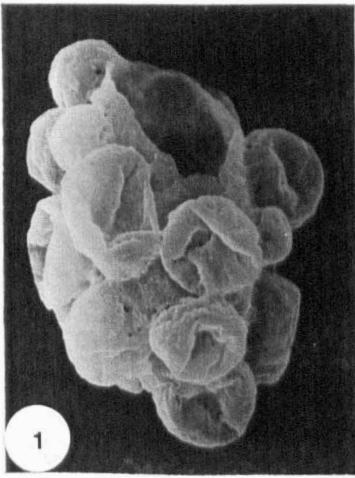


PLATE 7

Key Volgian and Ryazanian taxa

All figures at x450 magnification

- 1:** *Glossodinium dimorphum*. Slide U3-2, England Finder coordinates H54. Ventral focus.
- 2, 3:** *Perisseiasphaeridium ingegerdiae*. Slide K17-0/600-3, England Finder coordinates L49/1. **2:** Ventral focus. **3:** Dorsal focus. Note the loss of paraplate 3" as part of the archeopyle.
- 4:** *Gochteodinia villosa*. Slide K8, England Finder coordinates P53. Left lateral focus
- 5:** *Gochteodinia villosa*. Slide K8, England Finder coordinates M26. Left lateral focus.
- 6:** *Gochteodinia cf. villosa*. Slide K4, England Finder coordinates G23. Left lateral focus.
- 7:** *Circulodinium compta*. Slide K19-60/600, England Finder coordinates H38/3. Ventral focus.
- 8:** *Pseudoceratium pelliferum*. Slide K24, England Finder coordinates F55. Ventral focus.
- 9:** *Pseudoceratium pelliferum*. Slide K27, England Finder coordinates M46/2. Ventral focus.
- 10, 11:** *Muderongia longicorna*. Slide K14, England Finder coordinates E63/2. **10:** Ventral focus. **11:** Dorsal focus.
- 12, 13:** *Batioladinium gochtii*. Slide K17, England Finder coordinates E41/3. Both in oblique focus.
- 14 - 16:** *Cassiculosphaeridia pygmaeus*. Slide K17-0/300, England Finder coordinates K28/2. **14:** Ventral focus. **15:** Median focus. **16:** Dorsal focus.

PLATE 7

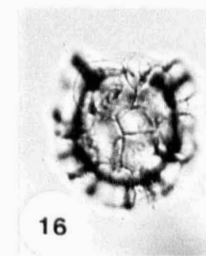
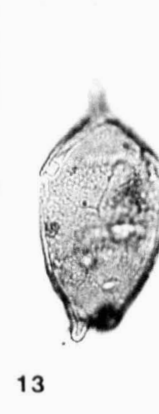
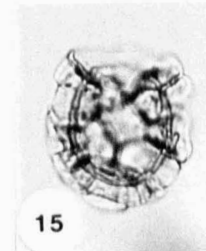
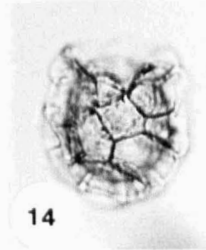
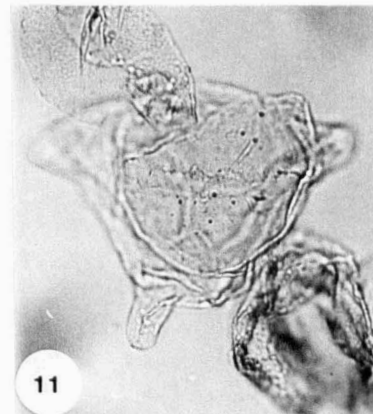
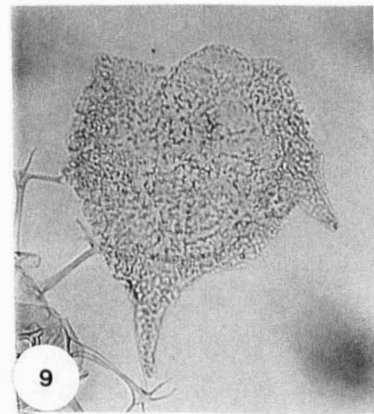
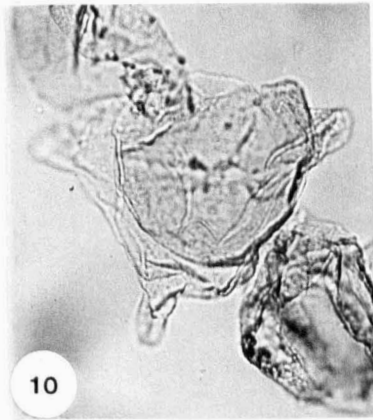
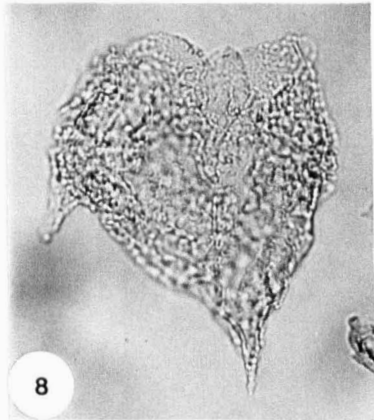
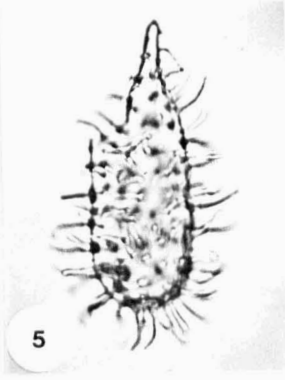
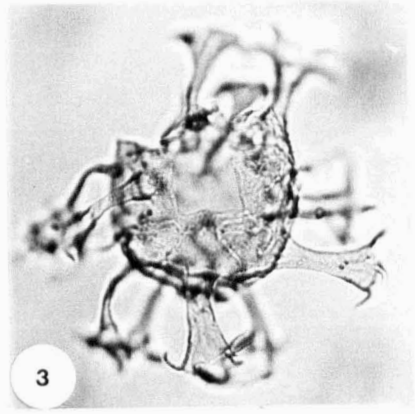
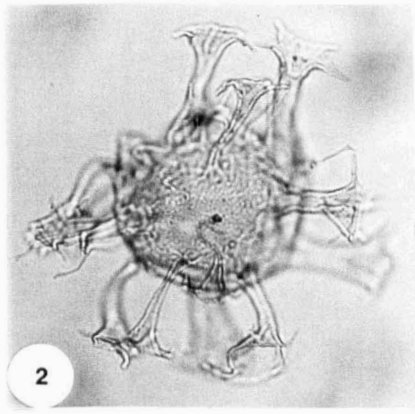
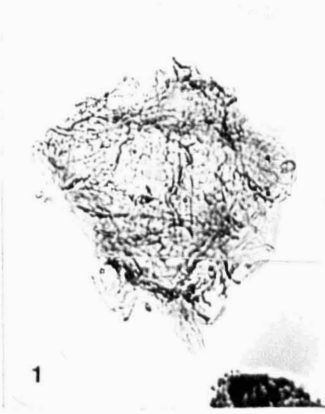


PLATE 8

Key Ryazanian and Valangian taxa

All figures x450 magnification.

1 - 3: *Criproperidinium cf. volkovae*. Slide K17-0/300, England Finder coordinates J35/3. **1:** Ventral focus. Specimen very close to *C. volkovae* in lacking intratabular sculpture on the ventral surface. **2:** Median focus. **3:** Dorsal focus.

4: *Phoberocysta neocomica*. Slide K16, England Finder coordinates L67/1. Ventral focus.

5: *Phoberocysta neocomica*. Slide K16, England Finder coordinates K57. Ventral focus.

6: *Phoberocysta tabulata*. Slide K25-2, England Finder coordinates G49/4. Dorsal focus.

7, 8: *Phoberocysta tabulata*. Slide K25-2, England Finder coordinates Q49. **7:** Ventral focus. **8:** Dorsal focus.

9, 10: *Warrenia brevispinosa*. Slide K19-2, England Finder coordinates K32/1. **9:** Median focus. **10:** Dorsal focus showing 2P archeopyle.

11 - 13: *Warrenia brevispinosa*. Slide K21-2, England Finder coordinates M63/3. **11:** Ventral focus. **12:** Median focus. **13:** Dorsal focus.

PLATE 8

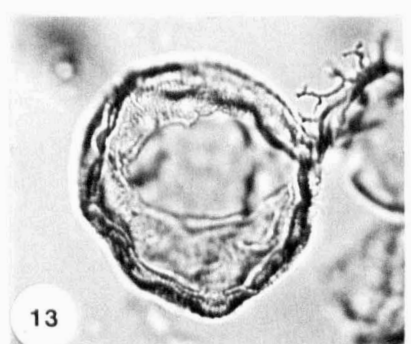
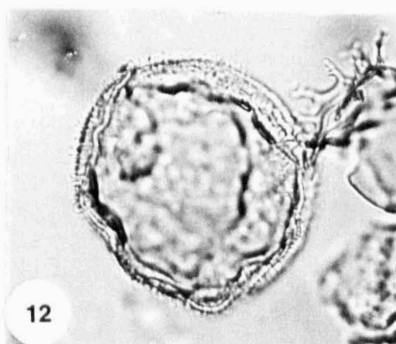
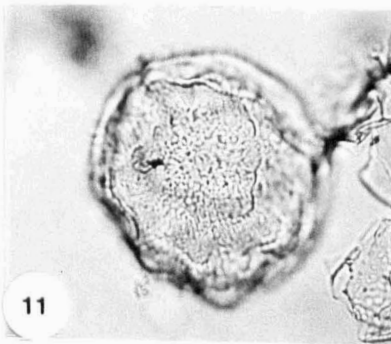
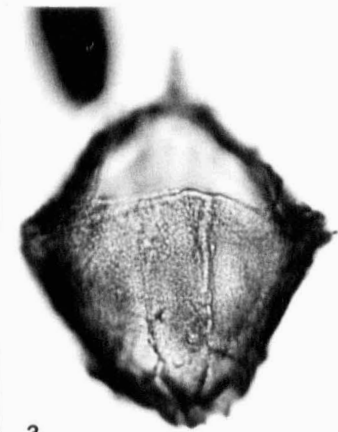
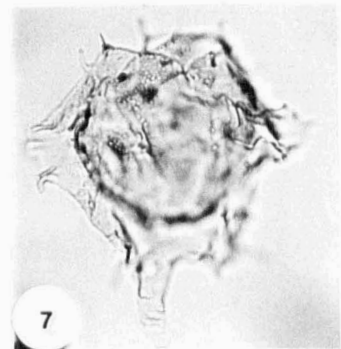
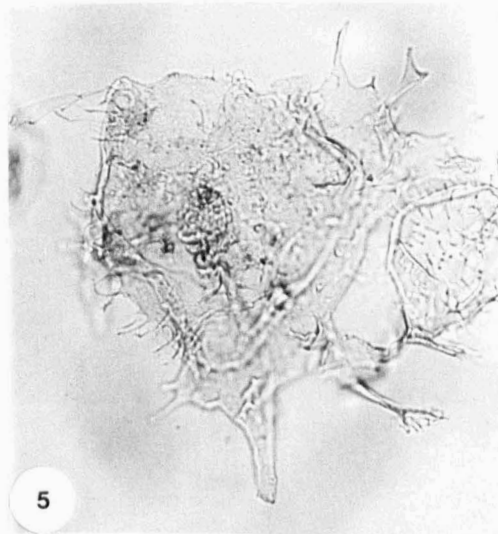
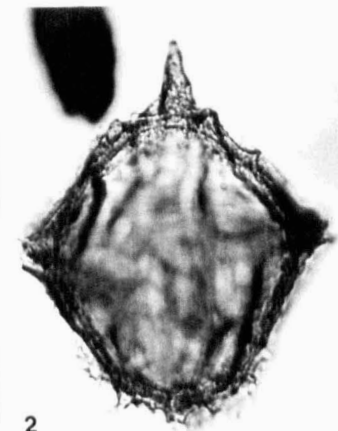
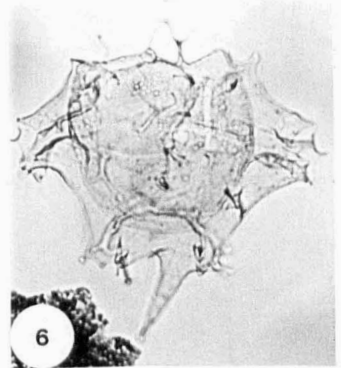
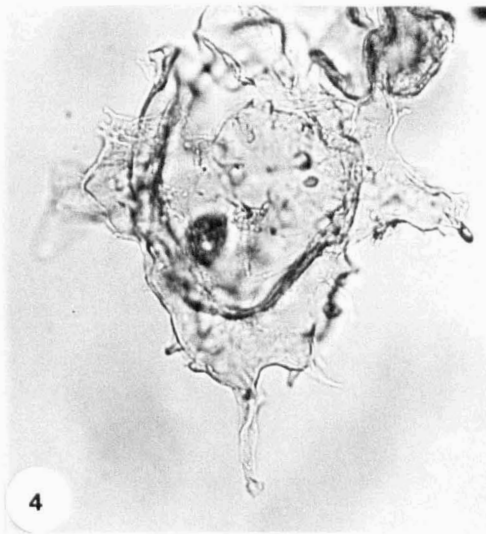
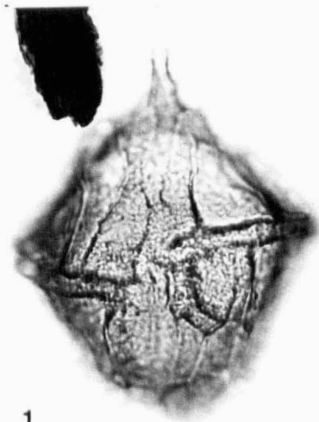


PLATE 9

Key Ryazanian and Valangian taxa

All figures x450 magnification.

1, 2: *Senoniasphaera jurassica*. Slide K8, England Finder coordinates H39. **1:** Ventral focus. **2:** Dorsal focus.

3, 4: *Pseudoceratium* sp. 1. Slide K17-0/300-2, England Finder coordinates M59. **3:** Ventral focus. **4:** Dorsal focus.

5, 6: *Oligosphaeridium complex*. Slide K27, England Finder coordinates J34/3. **5:** Ventral focus. **6:** Dorsal focus.

7, 8: *Spiniferites ramosus*. Slide K17-0/300-2, England Finder coordinates J44. **7:** Vento-lateral focus. **8:** Dorso-lateral focus.

9, 10: *Spiniferites primaevus*. Slide K20-2, England Finder coordinates M31/1. **9:** Ventral focus. **10:** Dorsal focus.

11, 12: *Spiniferites primaevus*. Slide K24-2, England Finder coordinates J46/3. **11:** Ventral focus. **12:** Dorsal focus.

PLATE 9

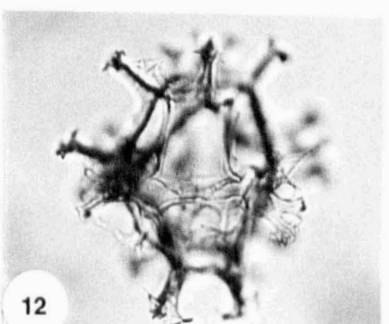
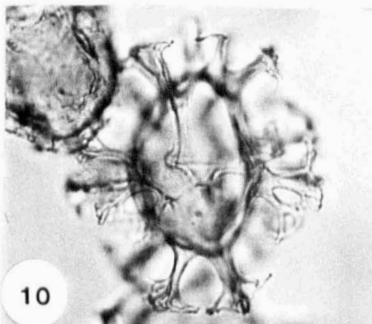
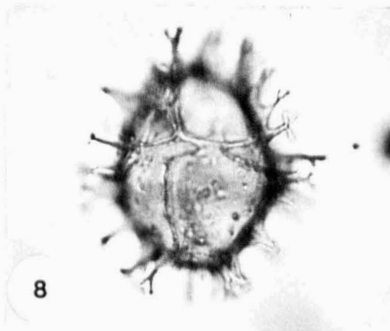
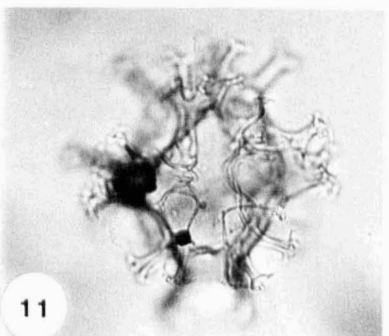
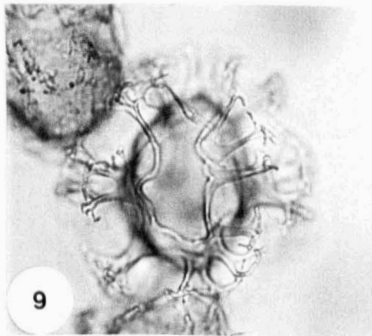
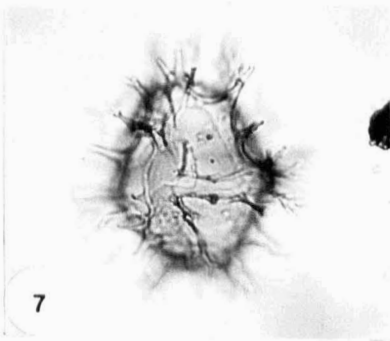
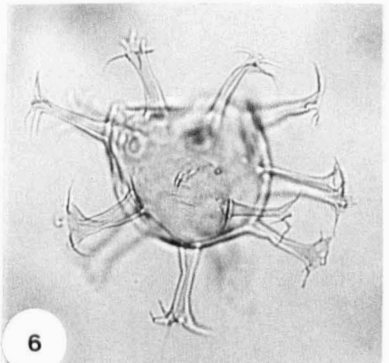
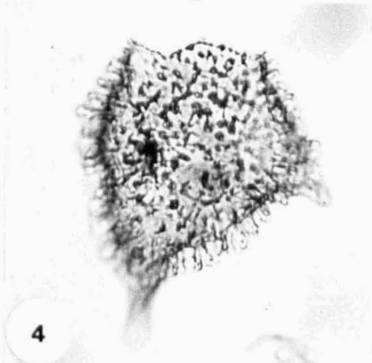
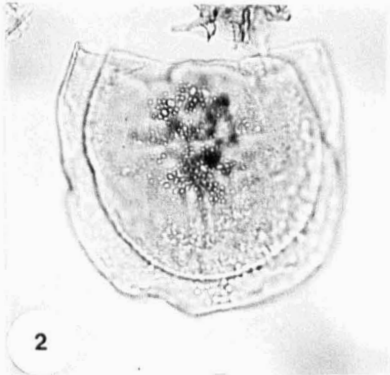
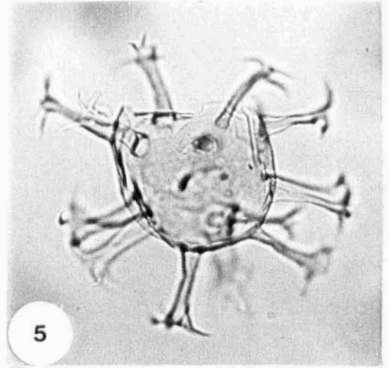
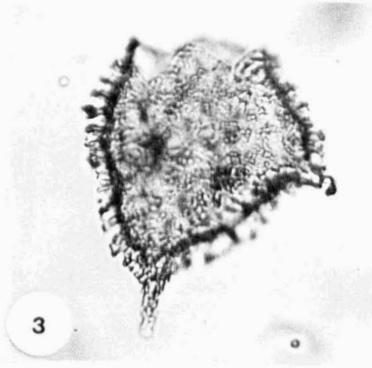
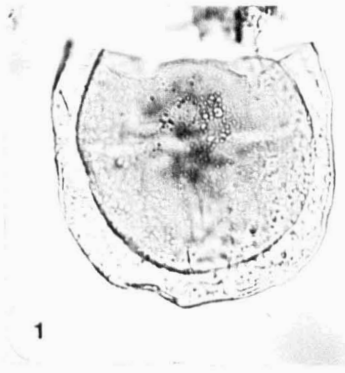


PLATE 10

All figures x450 magnification.

- 1:** *Apteodinium* sp. 1. Slide K14, England Finder coordinates O27. Dorsal focus
- 2, 3:** *Apteodinium* sp. 2. Slide U38, England Finder coordinates L65. **2:** Ventral focus. **3:** Dorsal focus.
- 4:** *Cribooperidinium* sp. 6. Slide U25-2, England Finder coordinates M53. Left lateral focus.
- 5, 6:** *Cribooperidinium nuciforme*. Slide K8, England Finder coordinates M32. **5:** Right lateral focus. **6:** Median focus.
- 7, 8:** *Cribooperidinium* sp. 6. Slide K6, England Finder coordinates H27/1. **7:** Ventro-lateral focus. **8:** Dorso-lateral focus. Note parasutural spines joining distally to form erymnate septa
- 9, 10:** *Cribooperidinium* sp. 1. Slide K6-2, England Finder coordinates H30. **9:** Ventral focus. **10:** Dorsal focus.
- 11, 12:** *Cribooperidinium* sp. 8. Slide K22, England Finder coordinates J39/3. **11:** Ventral focus. Note large intratabular tuberculae. **12:** Dorsal focus.
- 13, 14:** *Cribooperidinium* sp. 7. Slide U3, England Finder coordinates T39/3. **13:** Ventral focus. **14:** Dorsal focus.
- 15:** *Cribooperidinium* sp. 5. Slide U29-2, England Finder coordinates R33/4. Lateral view of hypocyst showing distinctive echinate antapical septa.

PLATE 10

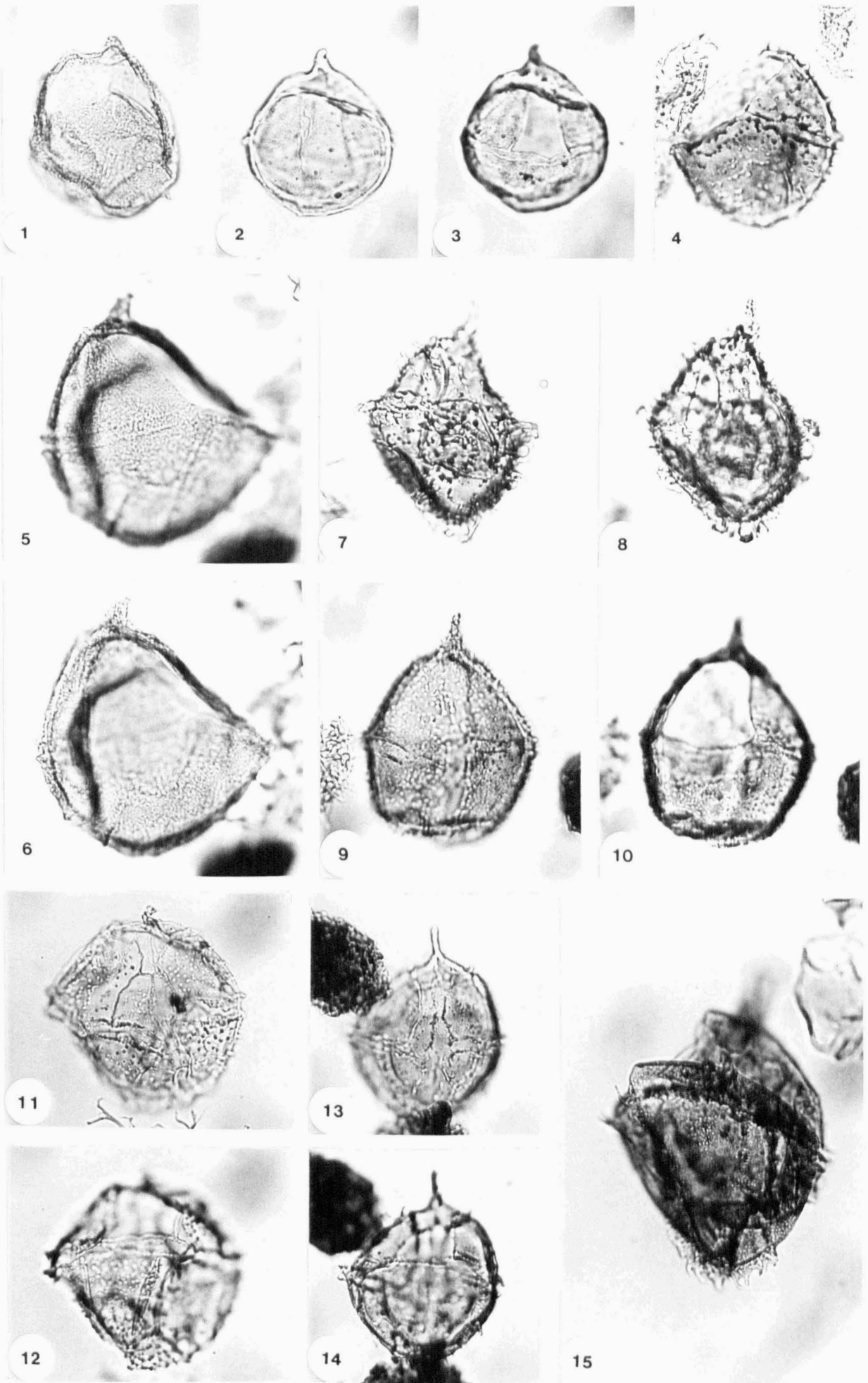


PLATE 11

All figures x450 magnification

1, 2: *Cribroperidinium* sp. 3. Slide K24, England Finder coordinates T56/1. **1:** Lateral focus. **2:** Median focus. Note the antapical projection.

3, 4: *Cribroperidinium* cf. *perforata*. Slide K6, England Finder coordinates G43/1. **3:** Vento-lateral focus on hypocyst. **4:** Dorso-lateral focus on epicyst.

5, 6: *Cribroperidinium* sp. 4. Slide K5, England Finder coordinates Q54. **5:** Ventral focus. Note the 'whispy' nature of the apical horn. **6:** Dorsal focus.

7, 8: *Cribroperidinium* *erymnoseptatum*. Slide U3, England Finder coordinates O39/3. **7:** Ventral focus of on hypocyst. **8:** Dorsal focus on epicyst.

9, 10: *Trichodinium* cf. *ciliatum*. Slide K8-2, England Finder coordinates P39/2. **9:** Ventral focus. **10:** Dorsal focus. Note that the sculpture is restricted to short conules.

11, 12: *Trichodinium* *ciliatum*. Slide K8-2, England Finder coordinates O35. **11:** Median focus. **12:** Dorsal focus.

13, 14: *Trichodinium* sp. 1. Slide U3, England Finder coordinates C32/3. **13:** Right lateral focus. **14:** Left lateral focus. Note the development of parasutural ridges.

PLATE 11

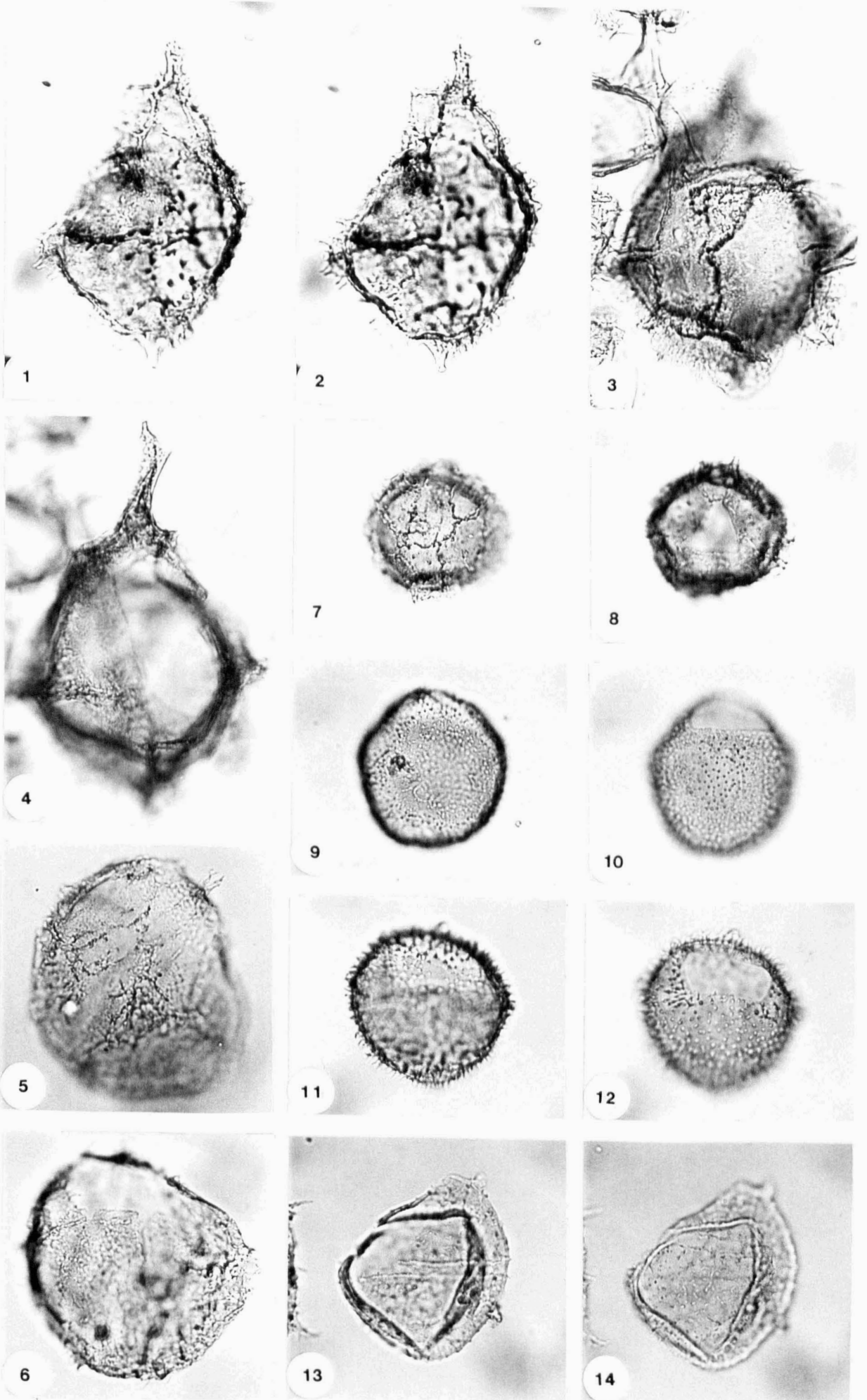


PLATE 12

All figures x450 magnification.

1, 2: *Gonyaulacysta* sp. 1. Slide K17-0/600, England Finder coordinates H37/3. **1:** Ventral focus. **2:** Median focus. Note the high gonal spines which occasionally furcate.

3, 4: *Wrevittia fastigiata*: Slide K9-2, England Finder coordinates R60. **3:** Ventral focus. **4:** Dorsal focus. Note the high denticulate to echinate parasutural septa.

5, 6, 7: *Gonyaulacysta* cf. *centriconnata*. Slide K3, England Finder coordinates E39/3. **5:** Ventral focus. **6:** Median focus. **7:** Dorsal focus. Note the suturocavate, denticulate septa, but lack of significant apical cavation.

8: *Stanfordella exsanguia*. Slide U22-2, England Finder coordinates P56/2 Dorso-lateral focus.

9, 10: *Gonyaulacysta* sp. 4. Slide K14, England Finder coordinates P44/2. **9:** Ventral focus. **10:** Dorsal focus. Note the small apical horn and intratabular tuberculae.

11, 12: *Gonyaulacysta* sp. 4. Slide K3, England Finder coordinates O51/4. **11:** Ventral focus. **12:** Dorsal focus.

13: *Wrevittia* cf. *helicoidea*. Slide K3-2, England Finder coordinates R50. Lateral focus. Note the smooth distal edges on the parasutural septa.

14, 15: *Wrevittia* cf. *helicoidea*. Slide K3-2, England Finder coordinates E60. **14:** Ventral focus. **15:** Dorsal focus.

16, 17: *Gonyaulacysta* sp. 3. Slide K3, England Finder coordinates O51/4. **16:** Ventral focus. **17:** Dorsal focus. Note the closely adpressed wall layers.

18, 19: *Gonyaulacysta pectinigera*. Slide K14, England Finder coordinates M69/3. **18:** Ventro-lateral focus. **19:** Dorso-lateral focus.

20, 21: *Gonyaulacysta pectinigera*. Slide U31/2, England Finder coordinates J35. **20:** Latera focus. **21:** Lateral focus.

22: *Spiniferites* sp. 2. Slide K19-60/600, England Finder coordinates J57. Dorsal focus. Note antapical (ventral) cavation.

23, 24: *Spiniferites* sp. 1. Slide K20, England Finder coordinates O54/1. **23:** Ventral focus on hypocyst. **24:** Dorsal focus on epicyst.

25, 26: *Spiniferites* sp. 1. Slide K19-2, England Finder coordinates G33/3. **25:** Left-lateral focus on epicyst **26:** Right-lateral focus on hypocyst.

PLATE 12

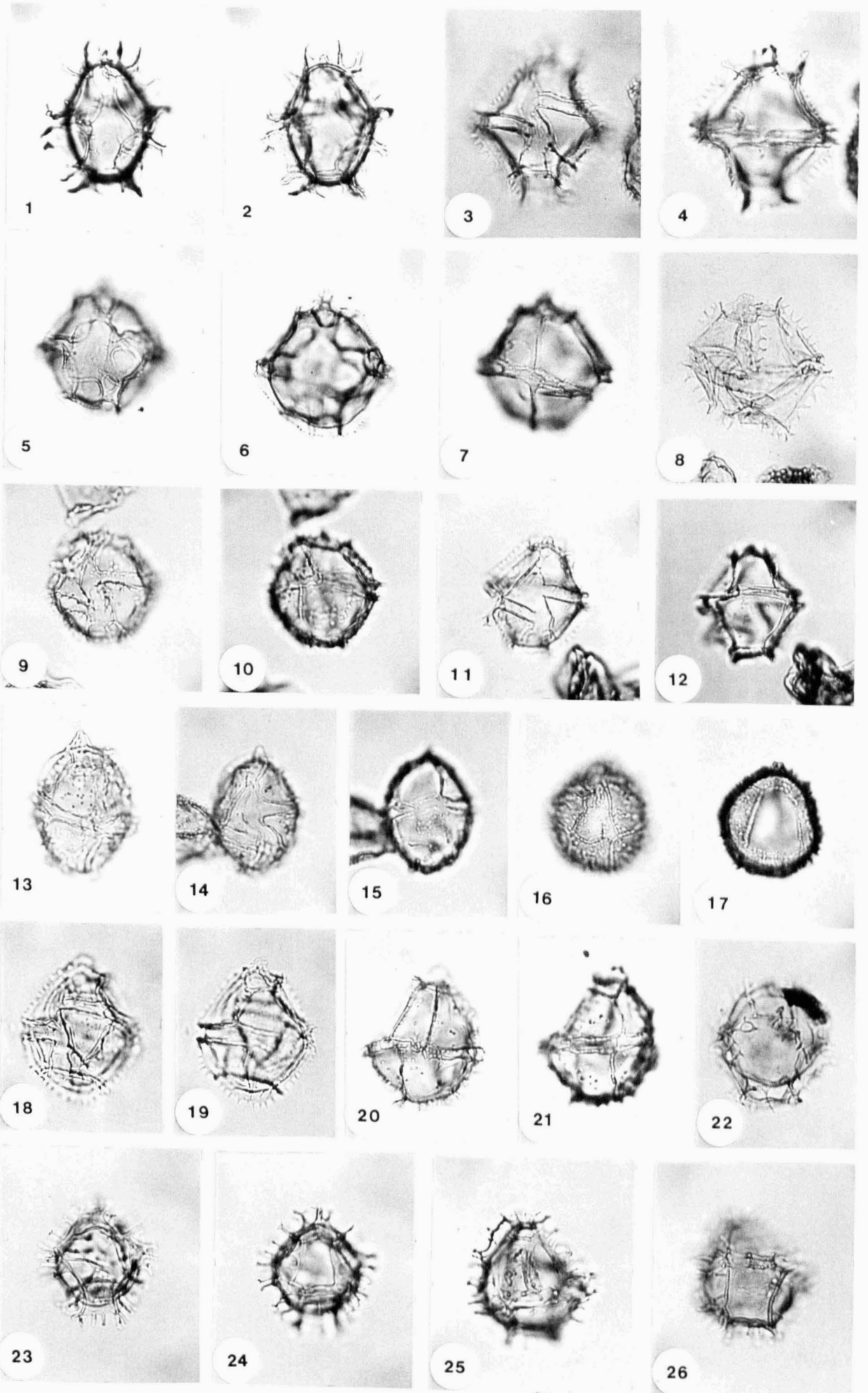


PLATE 13

All figures x450 magnification

1, 2, 3: *Endoscrinium campanula*. Slide K17-0/300-2, England Finder coordinates K41/4. **1:** Ventral focus. **2:** Median focus. **3:** Dorsal focus.

4, 5: *Endoscrinium pharo*. Slide K17-0/300, England Finder coordinates L30/3. **4:** Ventral focus. **5:** Dorsal focus.

6: *Endoscrinium anceps*. Slide U5/2, England Finder coordinates D43/2. Dorsal focus.

7, 8: *Endoscrinium granulatum*. Slide K14-2, England Finder coordinates O41/4. **7:** Lateral focus on hypocyst. **8:** Lateral focus on epicyst.

9, 10: *Leptodinium subtile*. Slide U4, England Finder coordinates L67/2. **9:** Ventral focus on epicyst. Note the sulcal claustrum. **10:** Dorsal focus on hypocyst.

11, 12: *Cribroperidinium* sp. 8. Slide U24-2, England Finder coordinates L49/2. **11:** Ventral focus. **12:** Dorsal focus. Note the short spines surmounting the parasutural ridges, and the dextrally offset nature of paraplate 3" against the septum between 4" and 5", which separates this species from *Leptodinium*.

13, 14: *Leptodinium subtile*. Slide U5, England Finder coordinates L38/3. **13:** Left lateral focus. **14:** Right-lateral focus.

PLATE 13

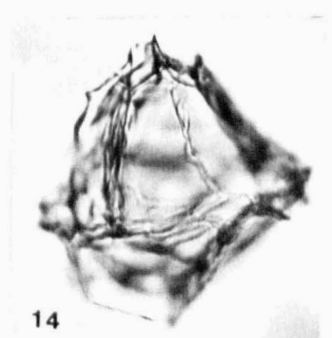
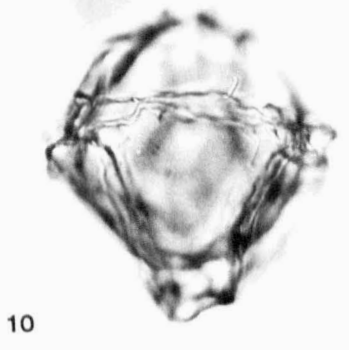
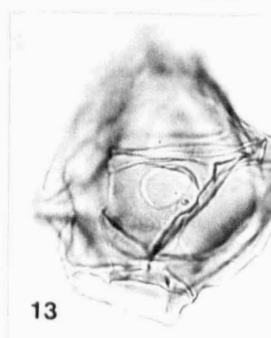
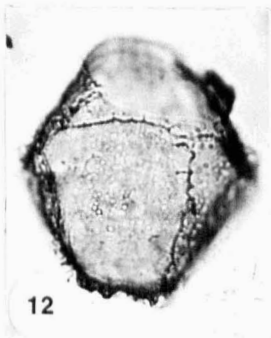
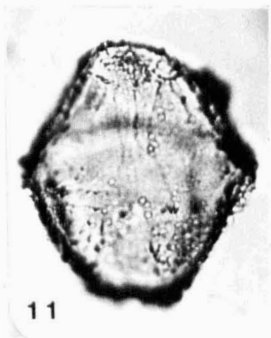
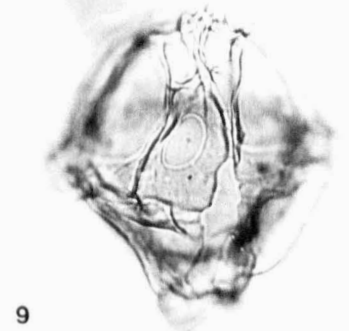
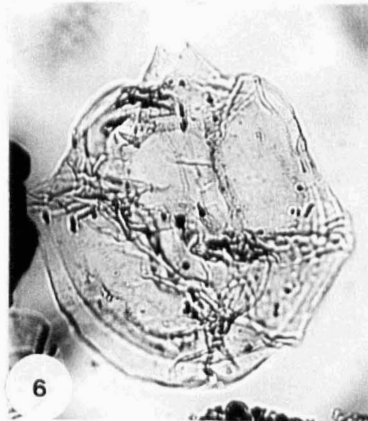
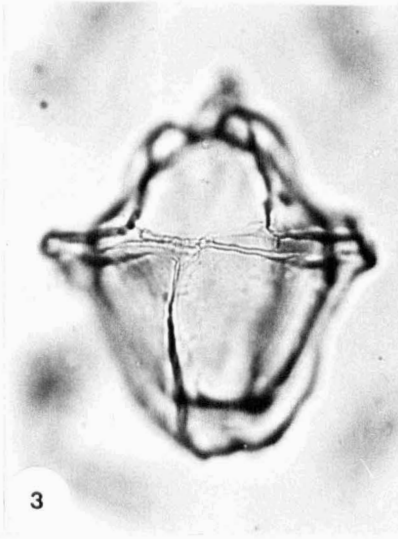
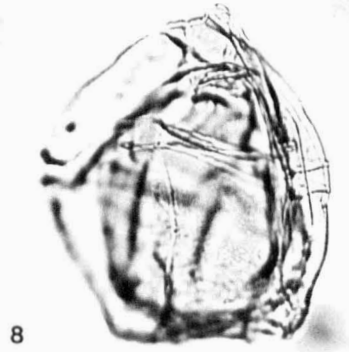
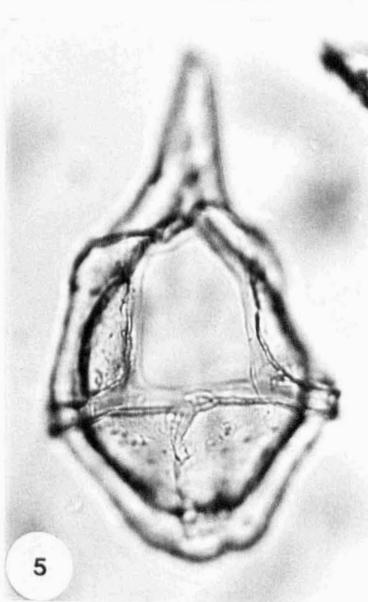
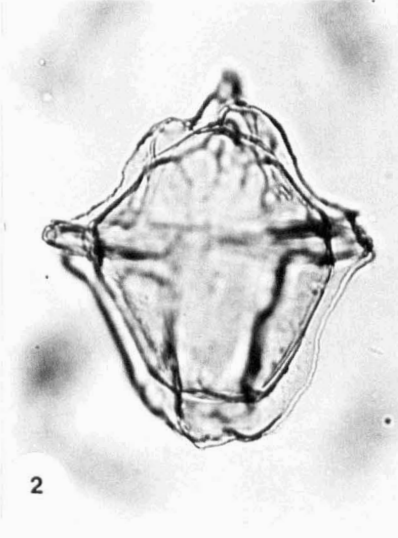
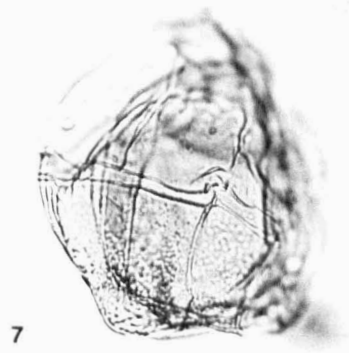
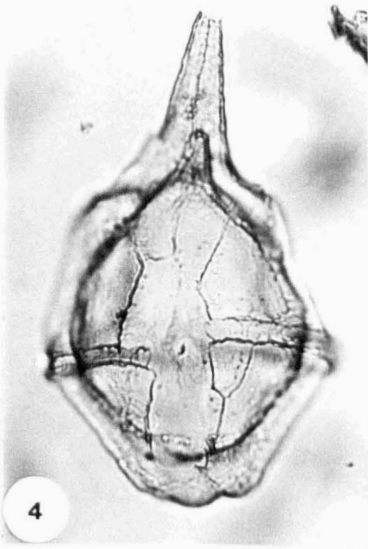
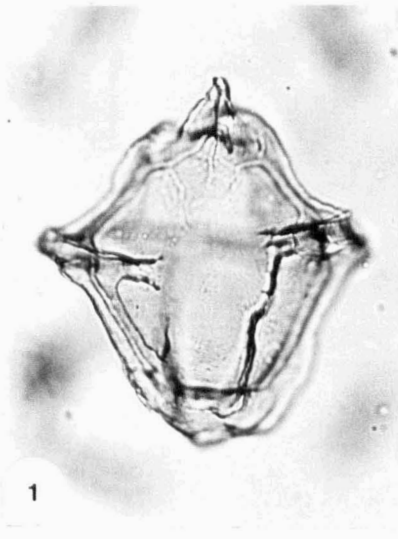


PLATE 14

All figures x450 magnification.

1, 2, 3: *Chlamydophorella nyei*. Slide K8, England Finder coordinates M40/3. **1:** Ventral focus. **2:** Median focus. **3:** Dorsal focus.

4, 5: ?*Lagenadinium membranoideum* Slide U31-2, England Finder coordinates K39/2. **4:** Ventro-lateral focus. **5:** Dorso-lateral focus. Note the large post-cingular corona which separates this monospecific genus from *C. nyei*.

6: *Dingodinium cerviculum*. Slide U23-2, England Finder coordinates L44/3. Ventral focus on epicyst.

7: *Dingodinium cerviculum*. Slide K14, England Finder coordinates D32/3. Lateral focus.

8, 9: *Dingodinium* sp. 1. Slide K21-2, England Finder coordinates L37/2. **8:** Lateral focus on epicyst. **9:** Lateral focus on hypocyst.

10: *Sirmiodinium grossi*. Slide K17-0/600, England Finder coordinates N34/1. Ventral focus.

11, 12: *Ambonosphaera staffinensis*. Slide K17, England Finder coordinates D65/4. **11:** Ventral focus. **12:** Dorsal focus.

13: *Walloodium krutschzi*. Slide K20-2, England Finder coordinates R40/4. Probably lateral focus.

14: *Walloodium lunum*. Slide K17-0/300-2, England Finder coordinates N36/1. Lateral focus.

15: *Tubotuberella* cf. *apatela*. Slide K7, England Finder coordinates T41/2. Dorsal focus. Note perforations on antapical projection of the periphragm.

16, 17: *Tubotuberella* cf. *apatela*. Slide U23-2, England Finder coordinates N29. **16:** Ventral focus. **17:** Dorsal focus.

18: *Tubotuberella apatela*. Slide U22-2, England Finder coordinates R54/1. Dorsal focus.

19, 20: *Tubotuberella apatela*. Slide U23-2, England Finder coordinates N29. Specimen with an antapical lobe on the endophragm. **19:** Median focus. **20:** Dorsal focus.

21: *Tubotuberella dentata*. Slide U22, England Finder coordinates G29/1. Dorsal focus.

22: *Walloodium cylindricum*. Slide K17-0/600, England Finder coordinates K50/3. Probably lateral focus.

23: *Walloodium cylindricum*. Slide K17-0/300-2, England Finder coordinates K37. Probably lateral focus.

24, 25: *Athigmatocysta* sp.. Slide K17-0/300-2, England Finder coordinates Q41/3. **24:** Lateral focus on epicyst. **25:** Lateral focus on hypocyst.

PLATE 14

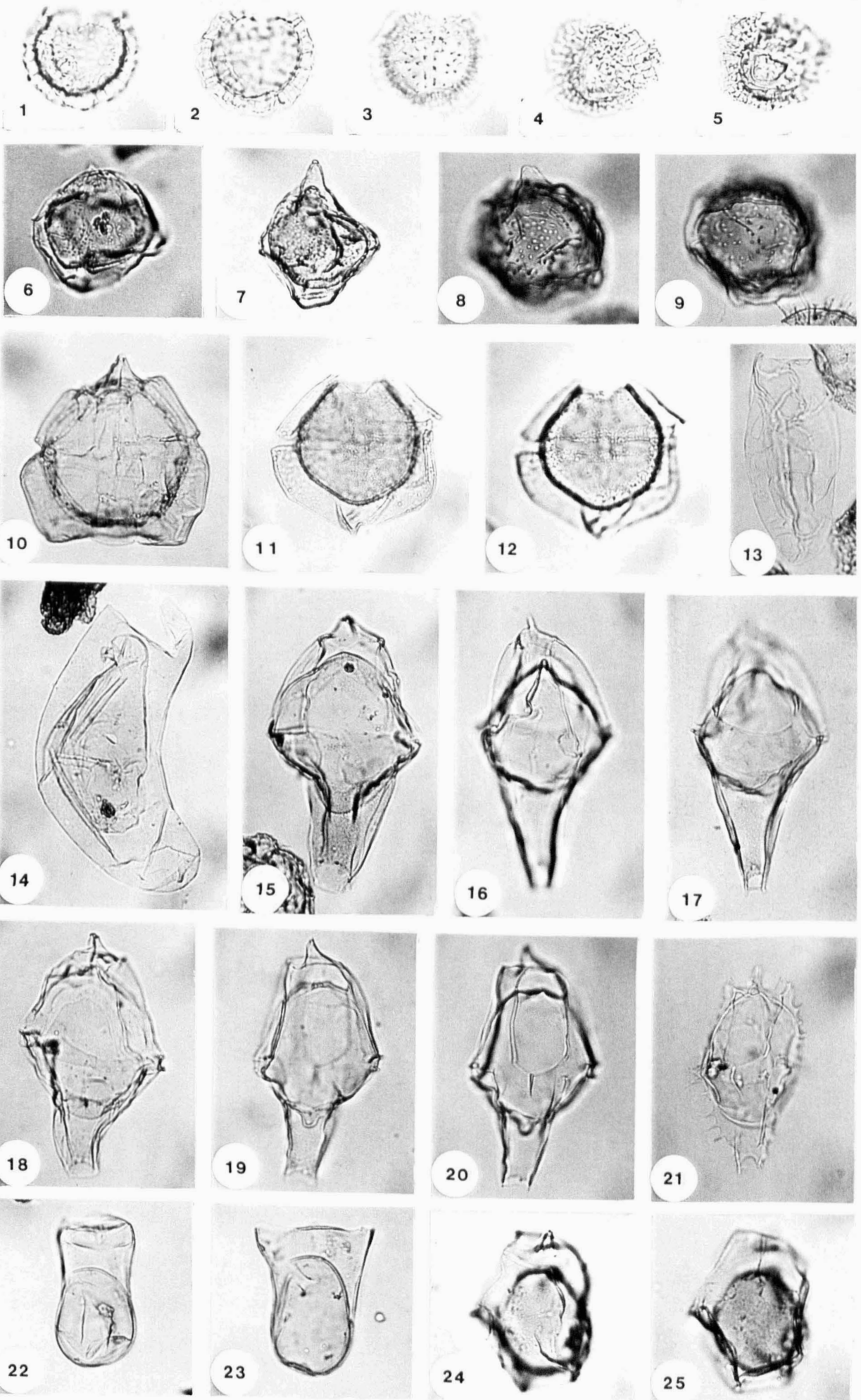


PLATE 15

All figures x450 magnification.

- 1: *Batiacasphaera* sp. 1. Slide U5, England Finder coordinates G35. Ventral focus.
- 2, 3: *Batiacasphaera* sp. 1. Slide U24-2, England Finder coordinates J48/3. 2: Ventral focus. 3: Dorsal focus.
- 4: "*Batiacasphaera fenestrata*" taxon-group. Slide K17, England Finder coordinates Q47. Ventral focus on epicyst.
- 5: "*Batiacasphaera fenestrata*" taxon-group. Slide K17-3, England Finder coordinates B61/2. Ventral focus.
- 6: *Batiacasphaera* sp. 2. Slide K25/2, England Finder coordinates N48/2. Lateral focus.
- 7: "*Circulodinium ciliatum*" taxon-group. Slide U10-2, England Finder coordinates E55/1. Uncertain orientation.
- 8: *Kallosphaeridium* sp. 2. Slide U3/2, England Finder coordinates Q57/2. Ventro-lateral focus.
- 9: *Batioladinium longicornutum*. Slide K14, England Finder coordinates N56/1. Ventro-lateral focus.
- 10, 11: *Microdinium* sp. 1. Slide K17-2, England Finder coordinates H46/4. 10: Lateral focus. 11: Lateral focus.
- 12: *Chytroeisphaeridia cerastes*. Slide K17, England Finder coordinates R58/3. Dorso-lateral focus.
- 13: *Chytroeisphaeridia chytroeides*. Slide K17-0/300, England Finder coordinates R52/3. Dorsal focus.
- 14: *Chytroeisphaeridia chytroeides*. Slide U5, England Finder coordinates J35. Dorso-lateral focus.
- 15: *Kallosphaeridium* sp. 1. Slide U21, England Finder coordinates L47/4. Ventral focus.
- 16: *Circulodinium copei*. Slide K3, England Finder coordinates C59. Ventral focus.
- 17: *Kalyptea* sp. 1. Slide K20-2, England Finder coordinates R33/2. Lateral focus.
- 18: *Pareodinia prolongata*. Slide U10/2, England Finder coordinates R33/2. Ventral focus.
- 19: *Batioladinium varigranosum*. Slide K17-0/300-2, England Finder coordinates H33. Lateral focus.
- 20: *Batioladinium* sp. 1. Slide U6, England Finder coordinates J55. Dorsal focus.
- 21: *Batioladinium varigranosum*. Slide U21, England Finder coordinates L47/4. Lateral focus.
- 22: *Pareodinia ceratophora*. Slide K14, England Finder coordinates G50/1. Dorsal focus.
- 23: *Aprobolocysta neista*. Slide K25, England Finder coordinates N27/2. Ventral focus.

PLATE 15

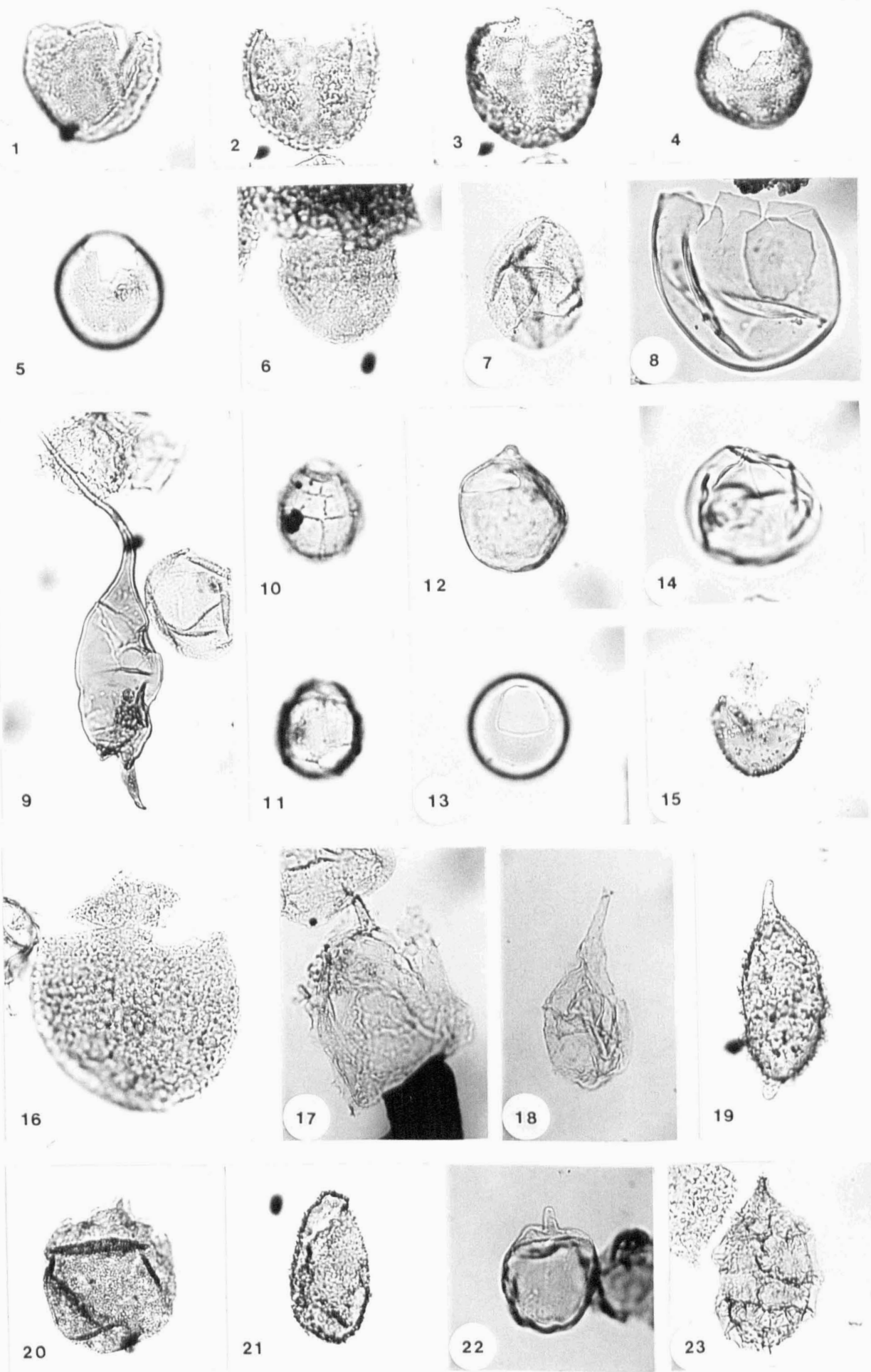


PLATE 16

All figures x450 magnification

1, 2: *Cassiculosphaeridia magna*. Slide K14, England Finder coordinates F49/3. **1:** Left lateral focus. **2:** Right lateral focus.

3, 4: *Cassiculosphaeridia magna*. Slide K17-0/600-2, England Finder coordinates H29/3. **3:** Left lateral focus. **4:** Right lateral focus.

5: *Cassiculosphaeridia magna*. Slide K3, England Finder coordinates M55/2. Lateral focus.

6: *Valensiella ovula*. Slide K17-0/600-3, England Finder coordinates J53. Ventral focus.

7, 8: *Lithodinia bulloidea*. Slide K27, England Finder coordinates J55/4. **7:** Lateral focus. **8:** Lateral focus.

9, 10, 11: *Lithodinia* sp. 2. Slide K17-0/300-3, England Finder coordinates G54. **9:** Ventral focus. **10:** Median focus. **11:** Dorsal focus.

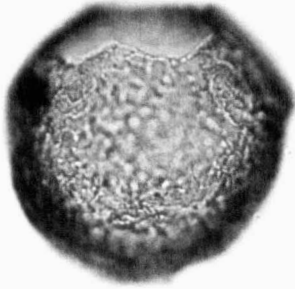
12: *Lithodinia acranitabulata*. Slide K25-30/600, England Finder coordinates L33/4. Ventral focus.

13: *Isthmocystis distincta*. Slide K17-0/300-3, England Finder coordinates K58. Apical focus.

14: *Mendicodinium reticulatum*. Slide K17, England Finder coordinates K41. Probably ventral focus.

15, 16: *Isthmocystis distincta*. Slide K17-0/300-3, England Finder coordinates E34/2. **15:** Ventral focus on epicyst. **16:** Dorsal focus on hypocyst.

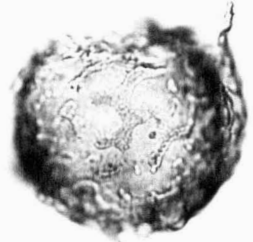
PLATE 16



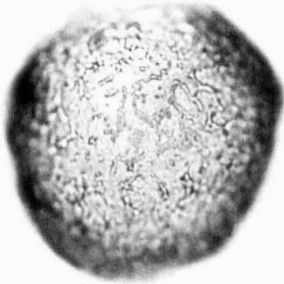
1



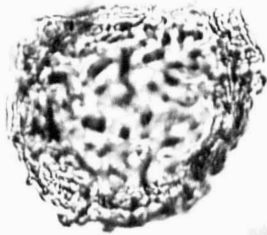
3



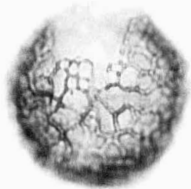
5



2



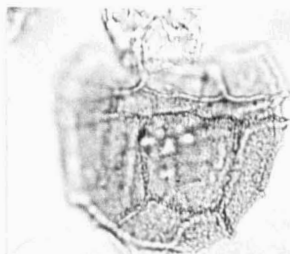
4



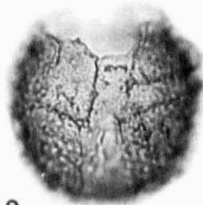
6



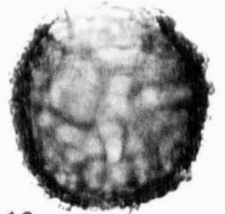
7



8



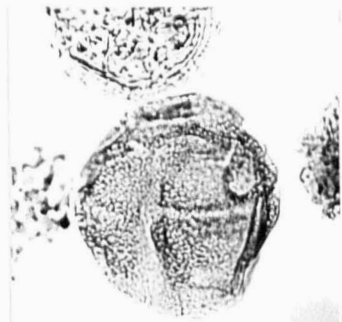
9



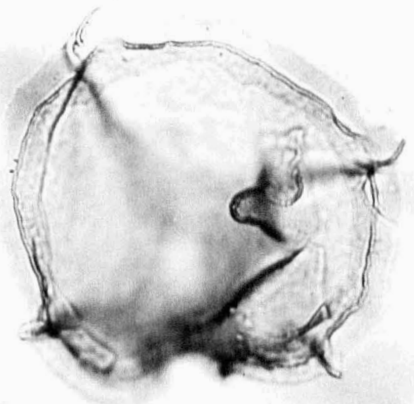
10



11



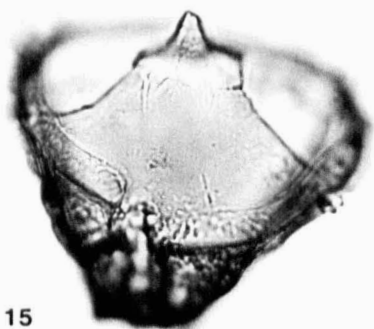
12



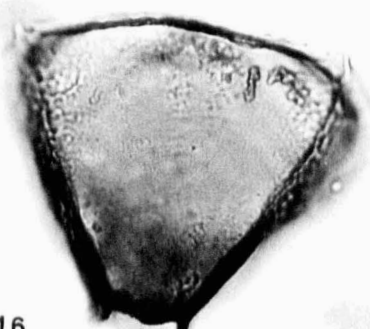
13



14



15



16

PLATE 17

All figures x450 magnification.

- 1:** "*Cleistosphaeridium aciculum*" taxon-group. Slide K15, England Finder coordinates M53/1. Lateral focus.
- 2:** "*Cleistosphaeridium aciculum*" taxon-group. Slide K17-0/300, England Finder coordinates K43/1. Uncertain orientation.
- 3:** "*Cleistosphaeridium aciculum*" taxon-group. Slide K17-0/300, England Finder coordinates T52/4. Dorsal focus on hypocyst
- 4:** *Cometodinium ?whitei*. Slide U19-2, England Finder coordinates K33/3. Probably dorsal focus.
- 5, 6, 7:** *Impletosphaeridium* sp. 1. Slide K19, England Finder coordinates L35/2. **5:** Ventral focus. **6:** Median focus. **7:** Dorsal focus. Note the absence of an ectophragm.
- 8:** *Downiesphaeridium* sp. 2. Slide K19-2, England Finder coordinates J36/3. Dorsal focus.
- 9:** *Downiesphaeridium* sp. 1. Slide K13, England Finder coordinates J42/2. Lateral focus.
- 10:** *Dapsillidium multispinosum*. Slide K20-2, England Finder coordinates G30/3. Uncertain orientation.
- 11, 12:** *Sentusidinium* sp. 3. Slide U3, England Finder coordinates U41/2. **11:** Ventral focus. **12:** Dorsal focus.
- 13:** *Sentusidinium riultii*. Slide K14, England Finder coordinates G36. Dorsal focus.
- 14:** *Sentusidinium* cf. sp. 3. Slide K25-0/600, England Finder coordinates H65. Dorsal focus.
- 15:** *Sentusidinium* cf. sp. 3. Slide K25-0/600, England Finder coordinates K37. Lateral focus.
- 16, 17:** *Sentusidinium* sp. 4. Slide K16, England Finder coordinates E33/3. **16:** Ventral focus. **17:** Dorsal focus.
- 18, 19:** *Sentusidinium* sp. 4. Slide K16, England Finder coordinates J43/2. **18:** Lateral focus. **19:** Lateral focus.
- 20:** *Prolixosphaeridium mixtispinosum*. Slide U13, England Finder coordinates T48. Lateral focus.
- 21:** *Prolixosphaeridium parvispinum*. K17-0/300, England Finder coordinates K28. Ventral focus.
- 22:** *Prolixosphaeridium parvispinum*. K17-0/600, England Finder coordinates H25/4. Ventral focus.
- 23:** *Tanyosphaeridium magneticum*. U10, England Finder coordinates K55. Ventral focus.
- 24:** *Tanyosphaeridium isocalamum*. U22-2, England Finder coordinates U39/2. Dorsal focus.
- 25:** *Bourkinidium* sp. 1. U31-2, England Finder coordinates J36/3. Ventral focus.

PLATE 17

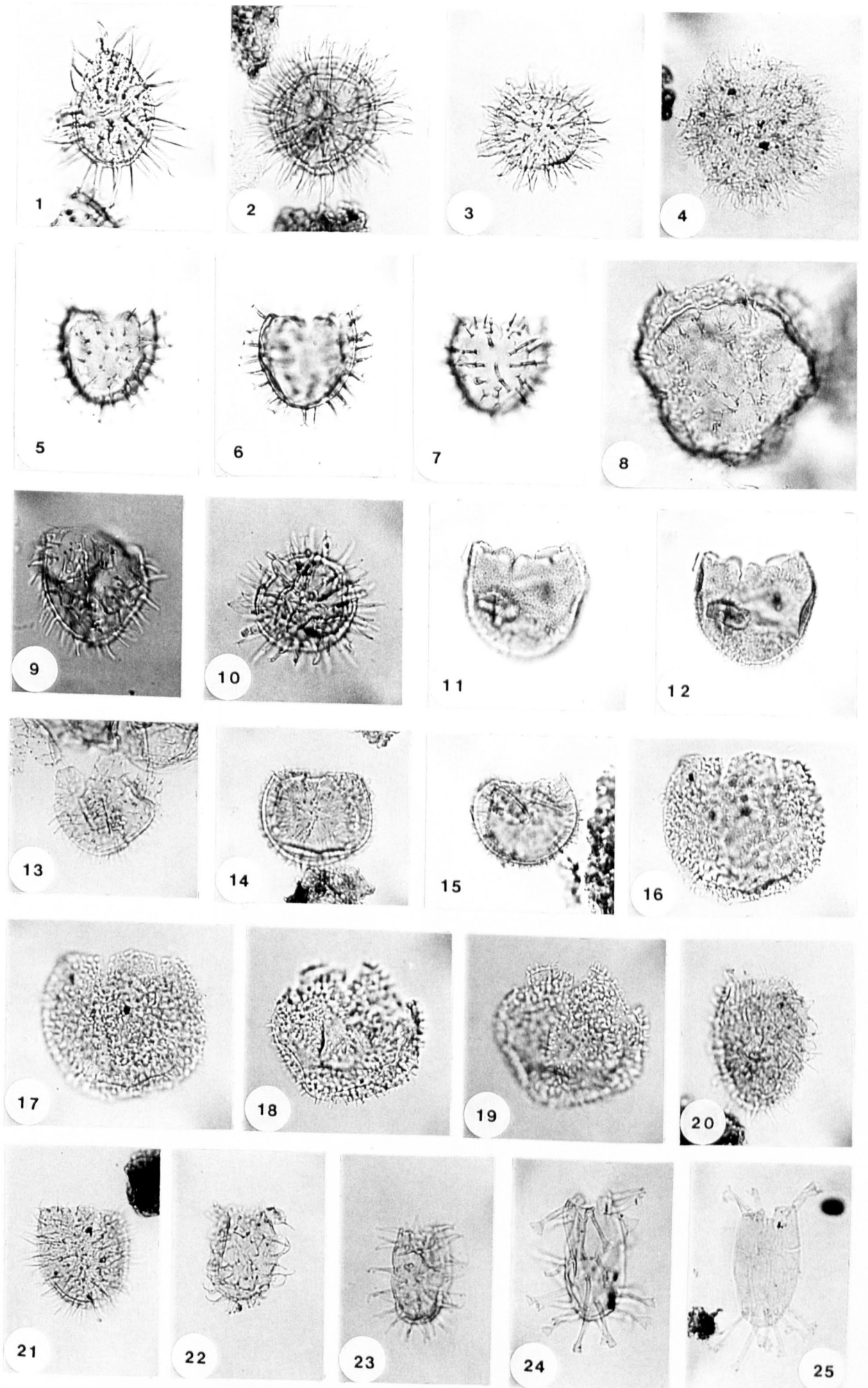


PLATE 18

All Figures x450 magnification.

1, 2, 3: *Tehamadinium daveyi*. Slide K8-2, England Finder coordinates O31. **1:** Ventral focus. **2:** Median focus. **3:** Dorsal focus. Note the absence of an ectophragm.

4, 5, 6: *Tehamadinium evittii*. Slide K6-2, England Finder coordinates H42/1. **1:** Left lateral focus on epicyst. **2:** Median focus. **3:** Right lateral focus on hypocyst.

7, 8: *Tehamadinium sousense*. Slide U10, England Finder coordinates O62. **7:** Ventral focus. **8:** Dorsal focus.

9: *Tehamadinium sousense*. Slide U5, England Finder coordinates G35. Dorsal focus.

10: *Tehamadinium* sp. 1. Slide K8, England Finder coordinates N45/2. Ventro-lateral focus.

11, 12, 13: *Tehamadinium konarae*. Slide K17-0/300, England Finder coordinates R64/4. **11:** Ventral focus on hypocyst. **12:** Median focus. **13:** Dorsal focus on epicyst.

14: *Protoellipsodinium* sp. 1. Slide K17, England Finder coordinates J34/3. Dorsal focus.

15: *Protoellipsodinium* sp. 1. Slide K17, England Finder coordinates K66/4. Lateral focus.

16, 17: *Warrenia* sp. 1 Slide K3, England Finder coordinates S25. **16:** Ventral focus. **17:** Dorsal focus.

18: *Lagenorhysis delicatula*. Slide K20-2, England Finder coordinates G39-2. Dorsal focus.

PLATE 18

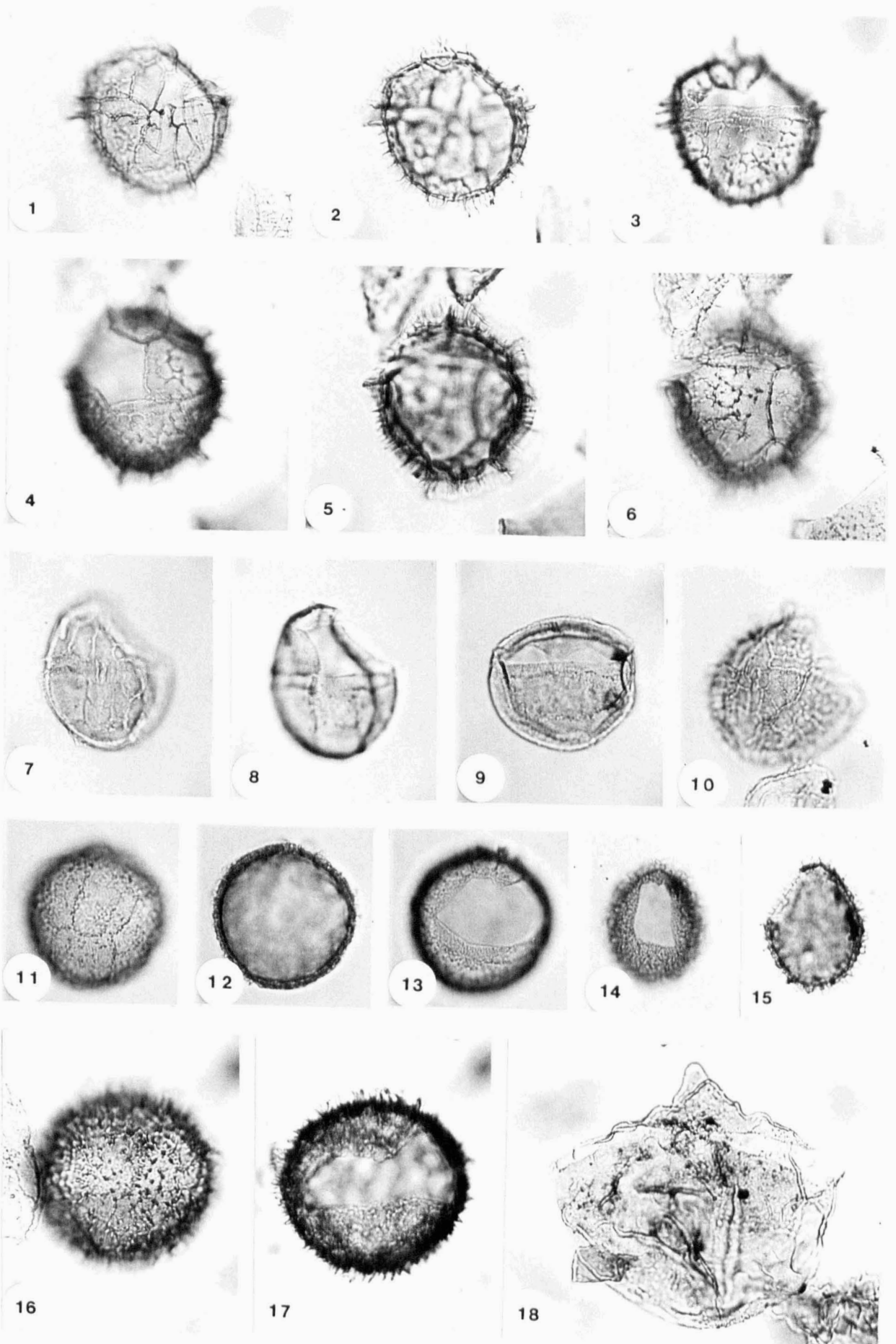


PLATE 19

All figures x450 magnification.

1, 2, 3: *Tenua hystrix*. Slide U21, England Finder coordinates M50. Specimen with reduced sculpture in mid-dorsal and mid-ventral areas. **1:** Ventral focus. **2:** Median focus. **3:** Dorsal focus. Note the absence of an ectophragm.

4, 5: *Tenua hystrix*. Slide U3-3, England Finder coordinates N38/1. **4:** Dorsal focus. **5:** Median focus.

6, 7: *Tenua cf. hystrix*. Slide K14, England Finder coordinates S33. **6:** Dorsal focus. **7:** Ventral focus.

8: *Tenua cf. hystrix*. Slide K24, England Finder coordinates T30/4. Ventral focus.

9, 10: *Tenua hystrix*. Slide K17-0/300, England Finder coordinates F64/4. **9:** Ventral focus. **10:** Median focus.

11, 12: *Amphorula expiratum*. Slide K9, England Finder coordinates F46/3. **11:** Lateral focus. **12:** Median focus.

13, 14: *Ellipsodinium cinctum*. Slide K9, England Finder coordinates G35/3. **13:** Lateral focus. **14:** Median focus.

15, 16: *Egmontodinium polyplacophorum*. Slide K8, England Finder coordinates G24/4. **15:** Lateral focus. **16:** Median focus.

17: *Egmontodinium torynum*. Slide K14, England Finder coordinates H55. Lateral focus.

18: *Egmontodinium* sp. 1. Slide U16-2, England Finder coordinates M44/2. Probably ventral focus.

19, 20, 21: *Epiplosphaera gochtii*. Slide K17-0/300, England Finder coordinates G53/4. **19:** Ventral focus. **20:** Median focus. **21:** Dorsal focus.

PLATE 19

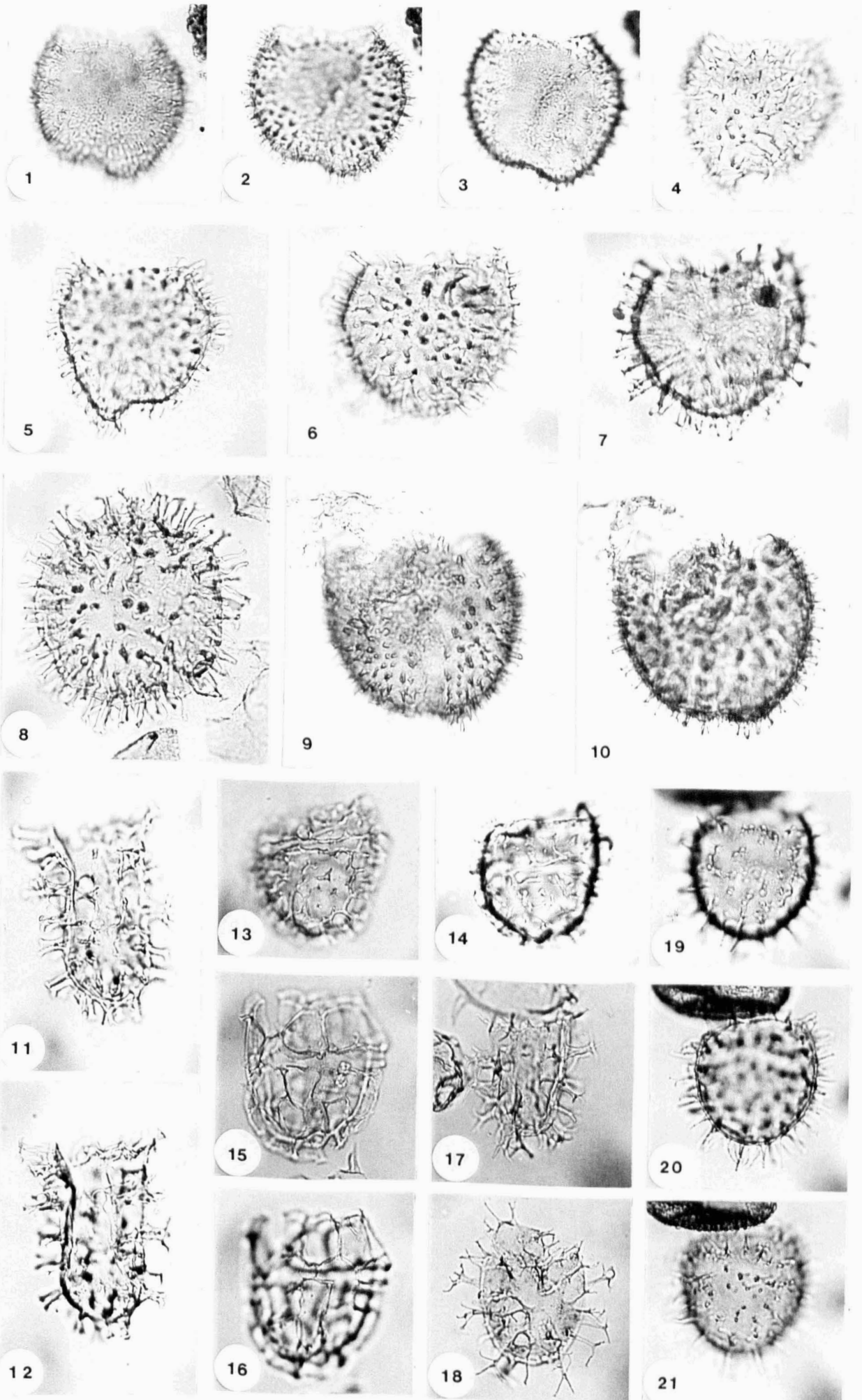


PLATE 20

All figures x450 magnification.

- 1:** *Hystrichosphaerina schindewolfii*. Slide K25-30/0, England Finder coordinates K30/2. Ventral focus.
- 2:** *Stiphrosphaeridium anthophorum*. Slide K8-2, England Finder coordinates O60/2. Dorsal focus.
- 3, 6:** *Systematophora areolata*. Slide U10, England Finder coordinates G55/2. **3:** Lateral focus. **6:** Lateral focus.
- 4:** *Systematophora daveyi*. Slide U11-2, England Finder coordinates S61. Dorsal focus.
- 5:** *Stiphrosphaeridium dictyophorum*. Slide K14, England Finder coordinates F31. Dorsal focus.
- 7:** *Systematophora palmula*. Slide K15, England Finder coordinates L59. Dorsal focus.
- 8:** *Hystrichodinium pulchrum* var. 1. Slide U6, England Finder coordinates J34. Ventral focus.
- 9:** *Hystrichodinium pulchrum* var. 2. Slide K25-30/600, England Finder coordinates M55/1. Ventral focus.
- 10, 11:** *Hystrichodinium pulchrum* var. 1. Slide K17-0/300-2, England Finder coordinates M55/3. Three-dimensionally preserved specimen. **10:** Ventral focus. **11:** Dorsal focus.
- 12:** *Hystrichodinium pulchrum* var. 1. Slide K17-0/300-3, England Finder coordinates O52/4. Three-dimensionally preserved specimen. Lateral focus.

PLATE 20

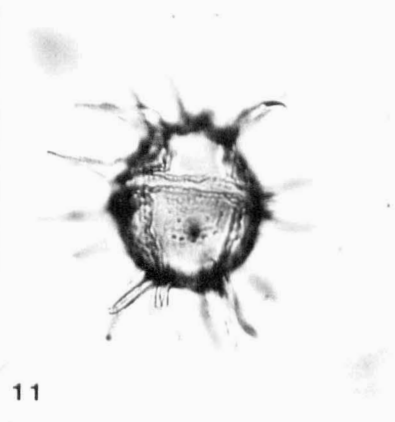
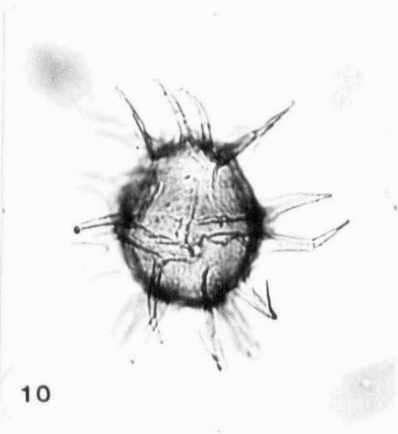
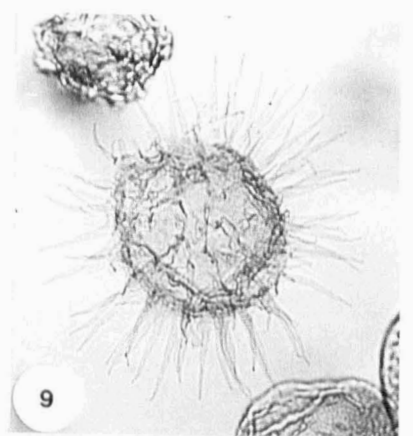
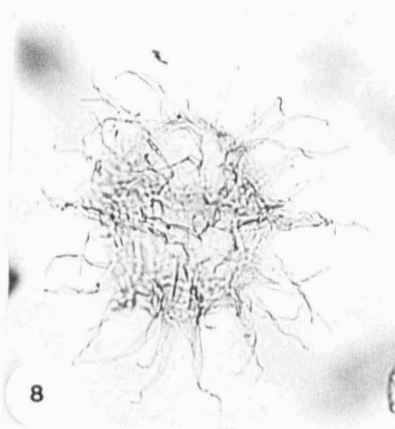
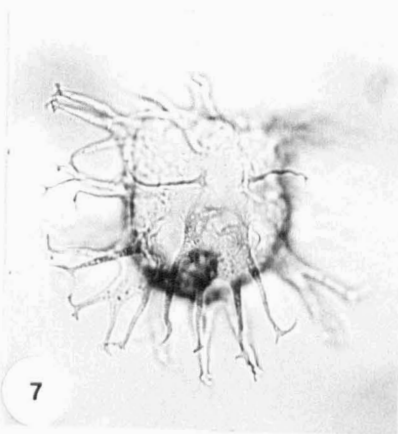
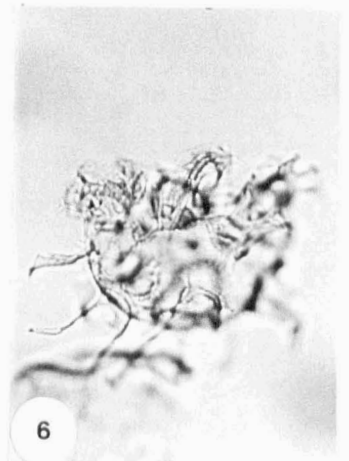
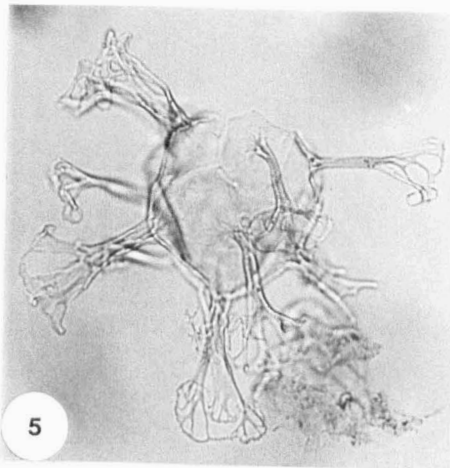
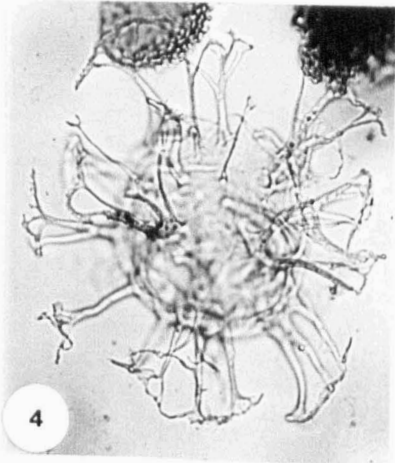
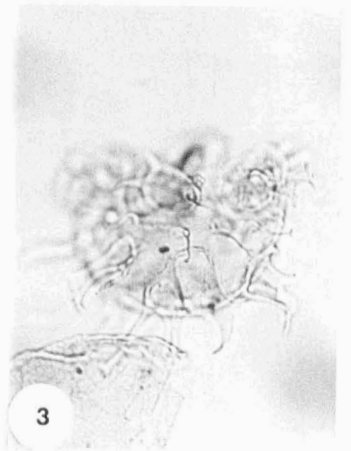
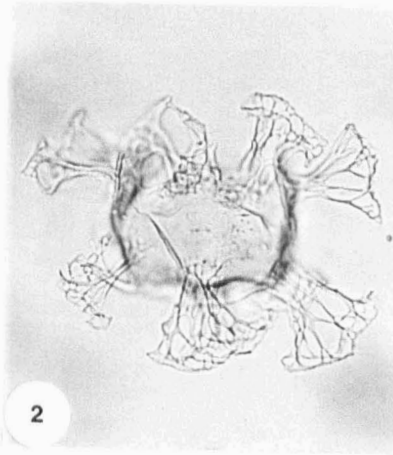
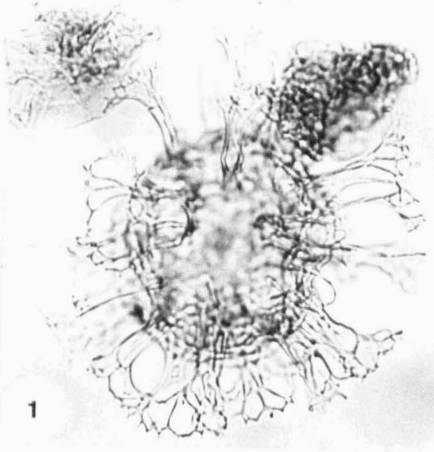


PLATE 21

All figures x450 magnification.

1, 2, 3: *Kleithriasphaeridium fasciatum*. Slide K19-60/600, England Finder coordinates L52.
1: Ventral focus. **2:** Median focus. **3:** Dorsal focus.

4, 5, 6: *Kleithriasphaeridium corrugatum*. Slide K17-0/300-3, England Finder coordinates M45. **4:** Ventral focus. **5:** Median focus. **6:** Dorsal focus.

7, 8, 9: *Kleithriasphaeridium eoinodes*. Slide K17-0/300-2, England Finder coordinates M62/3. **7:** Ventral focus. **8:** Median focus. **9:** Dorsal focus.

10, 11: *Kleithriasphaeridium porosispinum*. Slide K3, England Finder coordinates K68. **10:** Ventral focus. **11:** Dorsal focus.

12: *Hystrichosphaeridium petilum*. Slide K4-2, England Finder coordinates S34. Ventral focus.

13, 14: *Kleithriasphaeridium* cf. *eoinodes*. Slide K9, England Finder coordinates P49/4. **13:** Left lateral focus. **14:** Right lateral focus.

15: *Oligosphaeridium totum*. Slide K27-2, England Finder coordinates M50. Dorsal focus.

16: *Heslertonia* sp 1. Slide U3-2, England Finder coordinates M36. Lateral focus.

PLATE 21

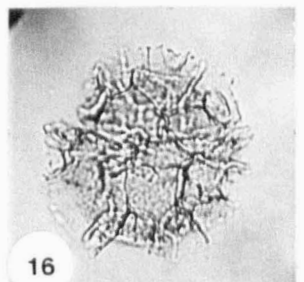
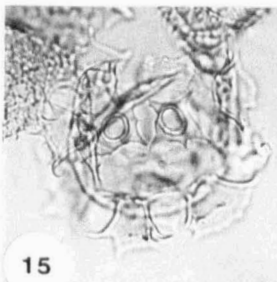
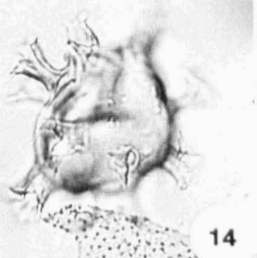
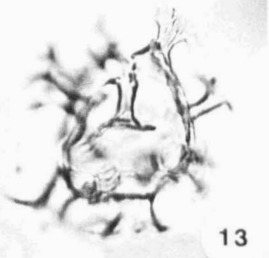
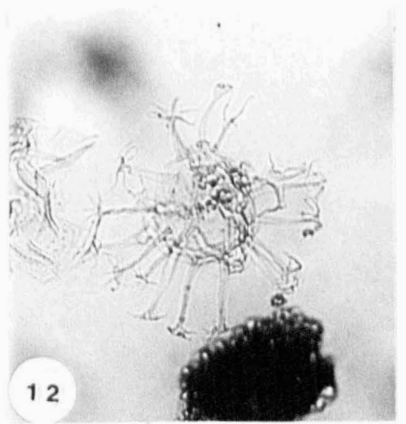
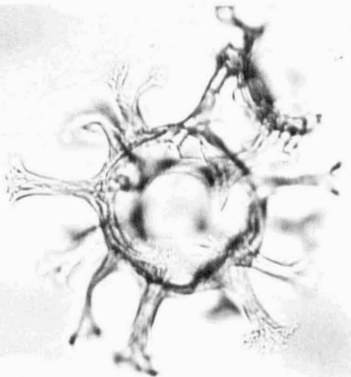
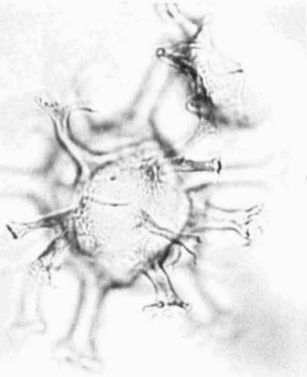
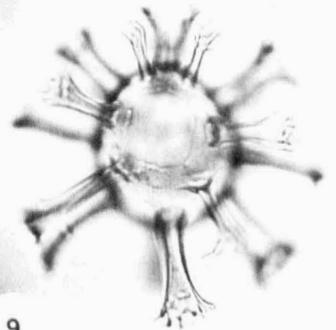
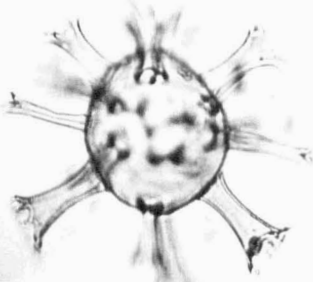
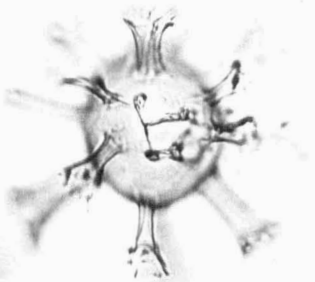
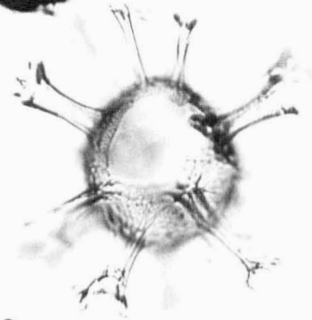
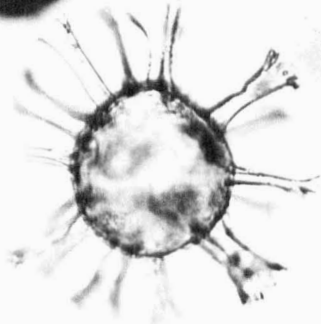
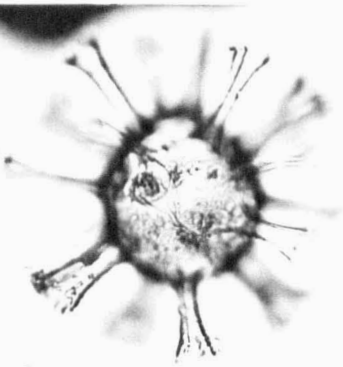
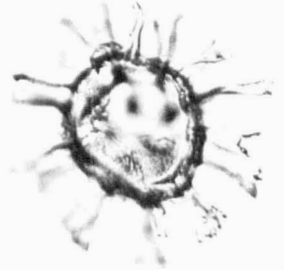
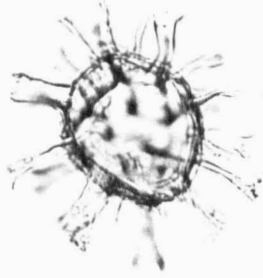
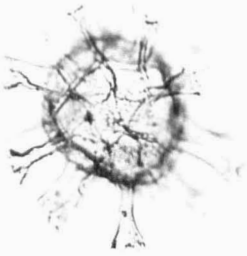


PLATE 22

All figures x450 magnification.

1, 2, 3: *Achomosphaera neptuni*. Slide K17-0/300-2, England Finder coordinates R43. **1:** Ventral focus. **2:** Median focus. **3:** Dorsal focus.

4: *Cymosphaeridium validum*. Slide U38, England Finder coordinates N47/4. Antapical focus.

5, 6: *Avellodinium falsificum*. Slide K24-2, England Finder coordinates E28/3. Both lateral focus.

7: *Nelchinopsis kostromiensis*. Slide U36-2, England Finder coordinates K35/1. Ventro-lateral focus.

8, 9: *Exochosphaeridium phragmites*. Slide K17-0/300, England Finder coordinates G52/2. **8:** Ventral focus. **9:** Dorsal focus.

10: *Dichadogoyaulax chondrum*. Slide U10-2, England Finder coordinates F40/2. Lateral focus.

11, 12: *Muderongia australis*. Slide K17-0/300, England Finder coordinates K42/2. **11:** Ventral focus. **12:** Dorsal focus. Note the small lobes in the endophragm corresponding to horn positions in the periphragm.

13: *Gochteodinia antennata*. Slide K2, England Finder coordinates L38. Lateral focus.

14: *Gochteodinia tuberculata*. Slide K2, England Finder coordinates U38/3. Lateral focus.

15, 16: *Exochosphaeridium phragmites*. Slide K15, England Finder coordinates C54. **15:** Ventral focus. **16:** Dorsal focus. Specimen with apical process and numerous other furcating processes.

PLATE 22

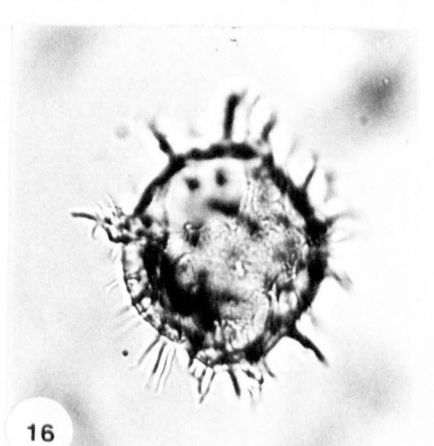
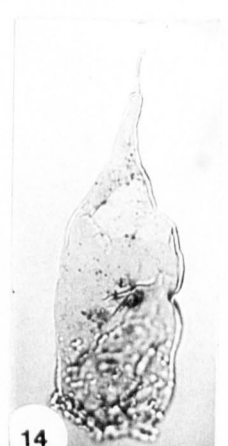
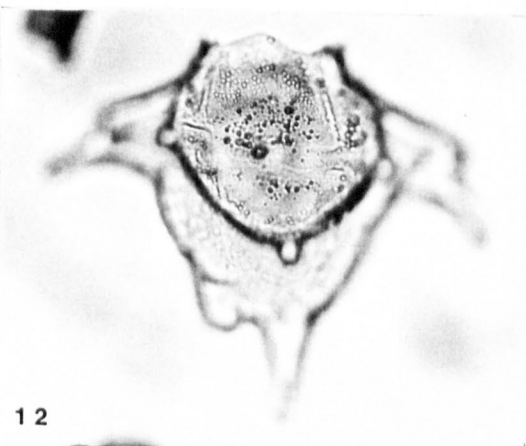
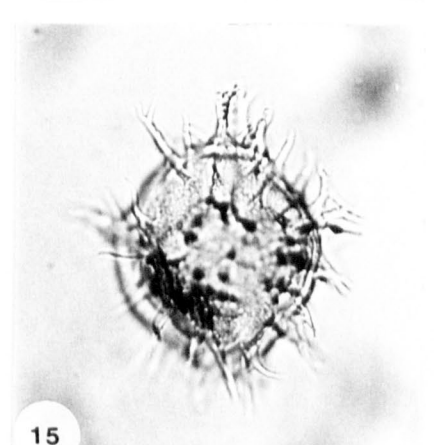
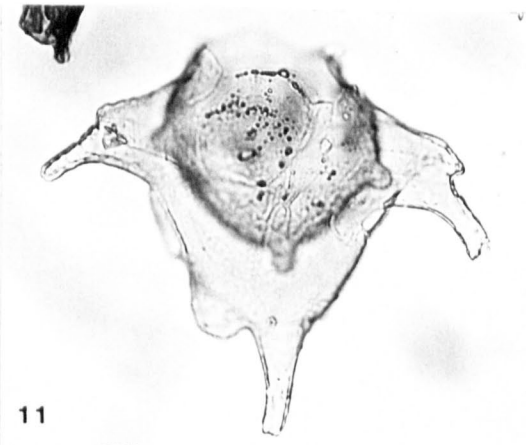
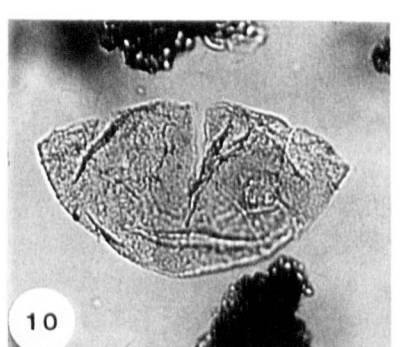
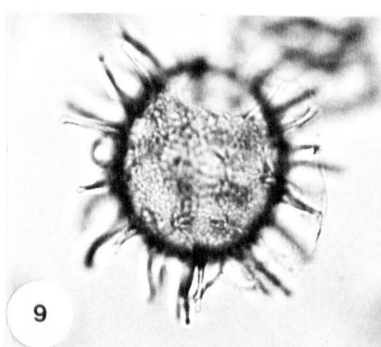
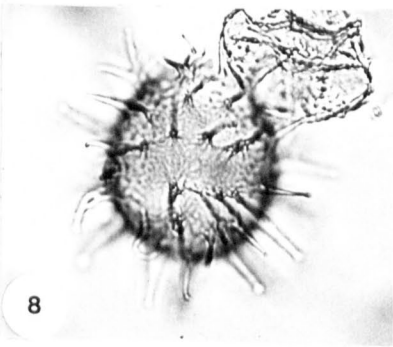
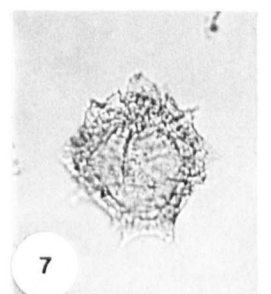
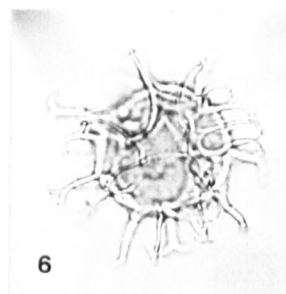
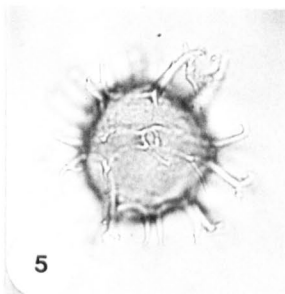
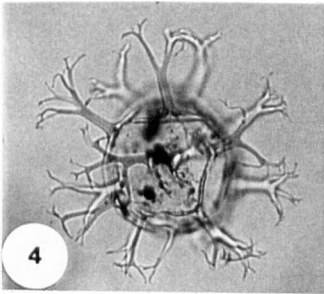
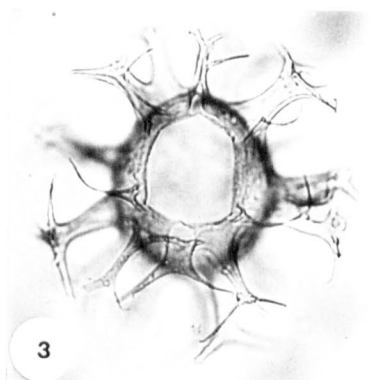
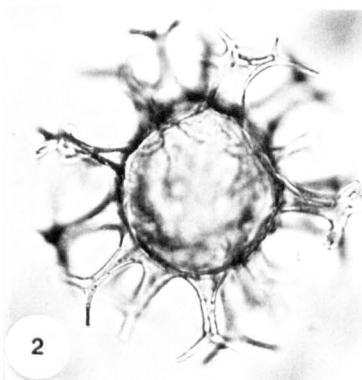
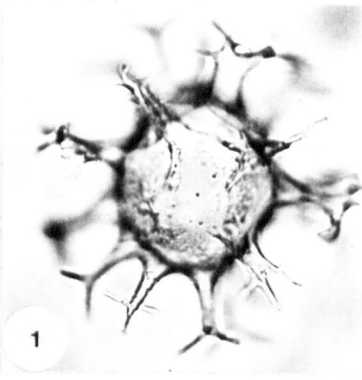


PLATE 23

All scale bars = 20µm.

- 1:** *Gochteodinia villosa*. SEM stub 9, grid square 2/II. Taken from sample K8. Dorsal view.
- 2:** *Endoscrinium pharo*. SEM stub 3, grid square 2/II. Taken from sample K17. Ventral view. Note large sulcal claustrum.
- 3:** *Endoscrinium pharo*. SEM stub 12, grid square 1/II. Taken from sample K17. Dorsal view.
- 4:** *Warrenia* sp. 1. SEM stub 9, grid square 3/III. Taken from sample K8. Dorsal view.
- 5:** *Tehamadinium daveyi*. SEM stub 7, grid square 4/II. Taken from sample K8. Ventral view.
- 6:** *Tehamadinium daveyi*. SEM stub 9, grid square 3/III. Taken from sample K8. Dorsal view.
- 7:** *Tehamadinium daveyi*. SEM stub 4, grid square 4/III. Taken from sample K8. Higher magnification of sculpture showing how the intratabular spines are usually linked.
- 8:** *Isthmocystis distincta*. SEM stub 11, grid square 4/I. Taken from sample K21. Ventral view.
- 9:** *Warrenia brevispinosa*. SEM stub 10, grid square 2/III. Taken from sample K20. Dorsal view.
- 10:** *Exochosphaeridium phragmites* SEM stub 12, grid square 1/IV. Taken from sample K17. Right dorso-lateral view.
- 11:** *Gonyaulacysta* sp. 1. SEM stub 12, grid square 5/x. Taken from sample K17. Ventral view.
- 12:** *Achomosphaera neptuni*. SEM stub 12, grid square 5/II. Taken from sample K17. Left dorso-lateral view.

PLATE 23

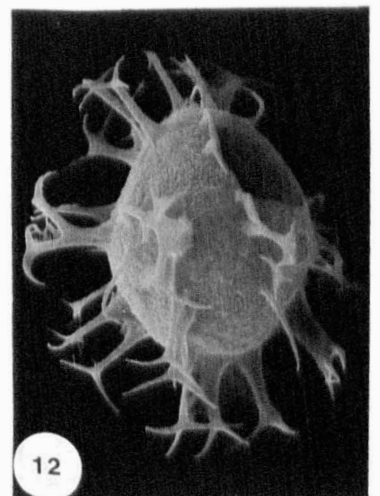
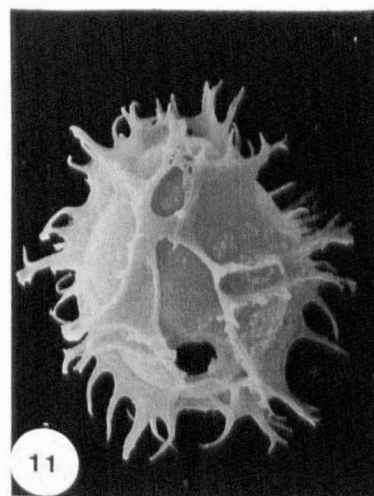
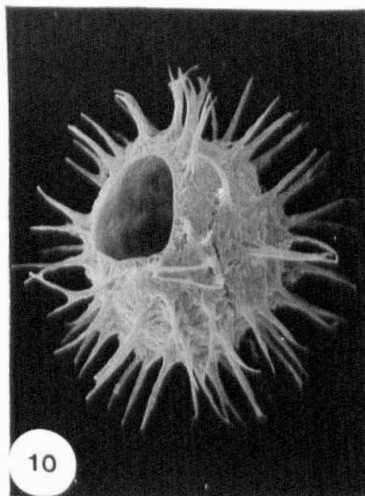
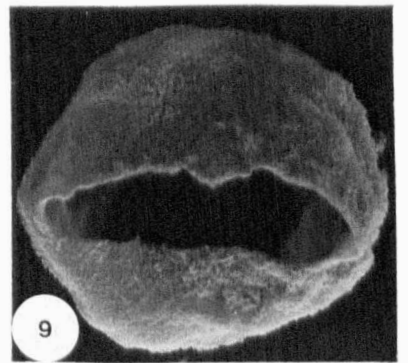
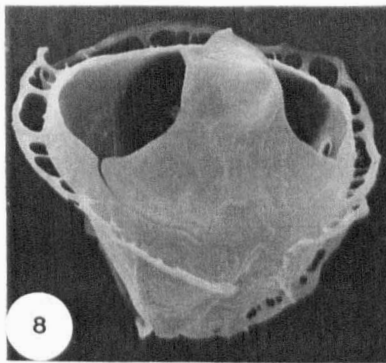
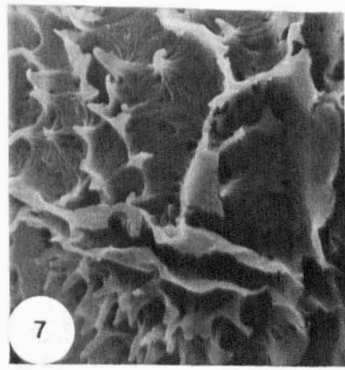
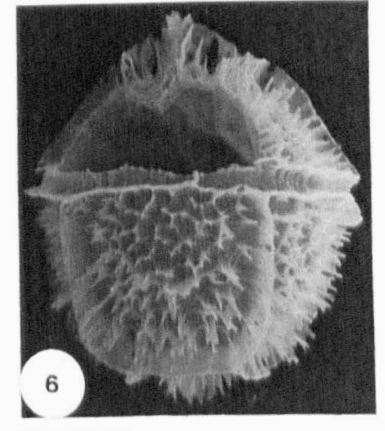
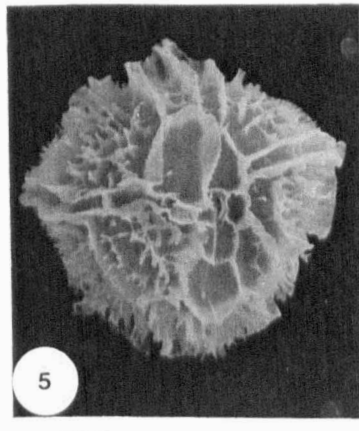
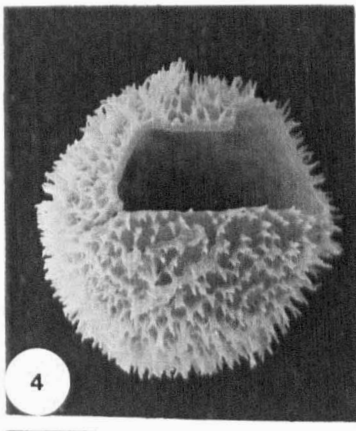
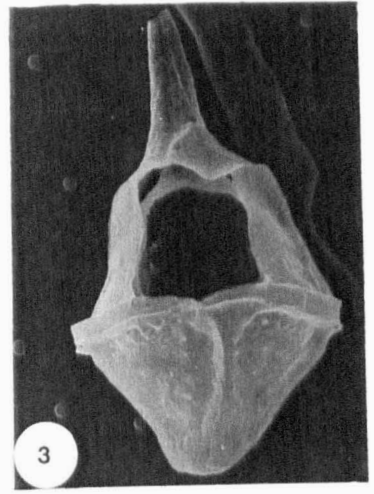
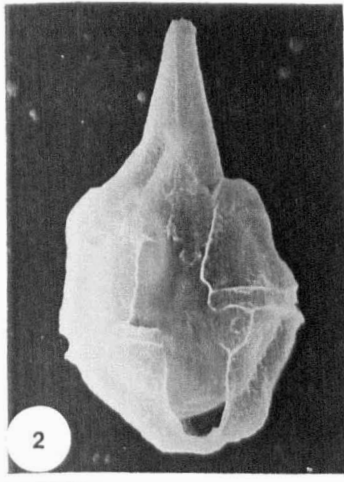
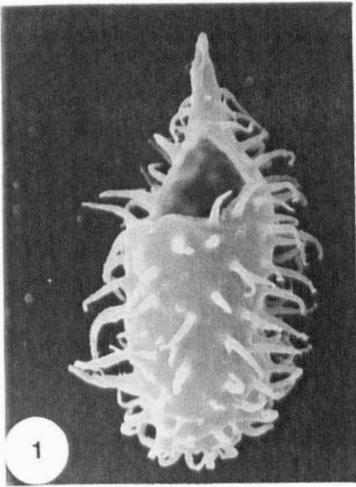


PLATE 24

All scale bars = 20 μ m.

- 1: *Cribroperidinium* cf. *volkovae*. SEM stub 4, grid square 1/II. Taken from sample K17. Dorsal view. Note the intratabular tuberculae.
- 2: *Cribroperidinium* sp. 8. SEM stub 7, grid square 2/II. Taken from sample U21. Dorsal view.
- 3: *Cassiculosphaeridia pygmaeus*. SEM stub 6, grid square 2/II. Taken from sample K17. Probably lateral view.
- 4: *Cribroperidinium* cf. *volkovae*. SEM stub 6, grid square 3/II. Taken from sample K17. Ventral view. Again note the intratabular tuberculae.
- 5: *Cribroperidinium* sp. 5. SEM stub 2, grid square 4/II. Taken from sample K17. Left dorso-lateral view.
- 6: *Rhynchodiniopsis* sp. 1. SEM stub 10, grid square 3/II. Taken from sample K20. Ventral view.
- 7: *Cribroperidinium* sp. 2. SEM stub 5, grid square 4/II. Taken from sample K14. Left lateral view.
- 8: *Phoberocysta neocomica*. SEM stub 8, grid square 3/II. Taken from sample K24. Ventral view.
- 9: *Phoberocysta tabulata*. SEM stub 8, grid square 3/IV. Taken from sample K24. Ventral view.
- 10: *Trichodinium ciliatum*. SEM stub 6, grid square 1/II. Taken from sample K17. Ventral view.
- 11: *Trichodinium ciliatum*. SEM stub 5, grid square 3/I. Taken from sample K14. Dorsal view.
- 12: *Trichodinium* cf. *ciliatum*. SEM stub 11, grid square 5/IV. Taken from sample K14. Dorso-lateral view. Note shorter spine length.

PLATE 24

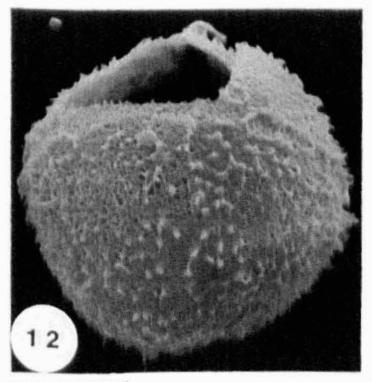
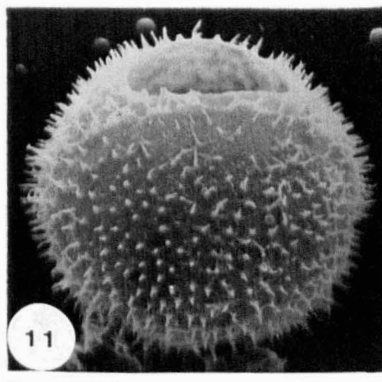
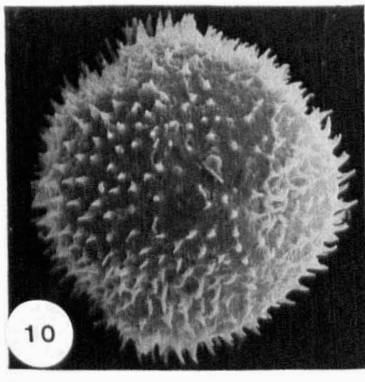
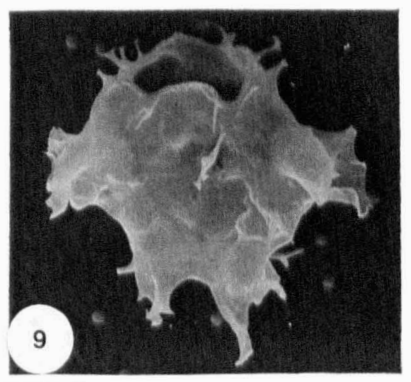
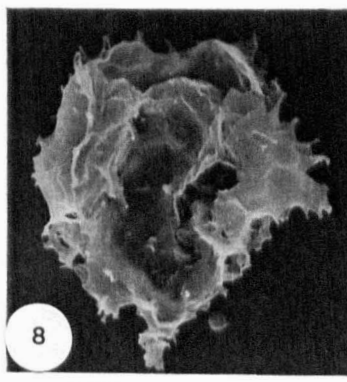
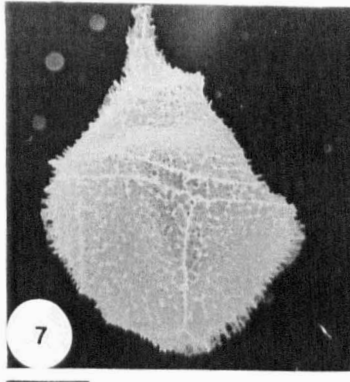
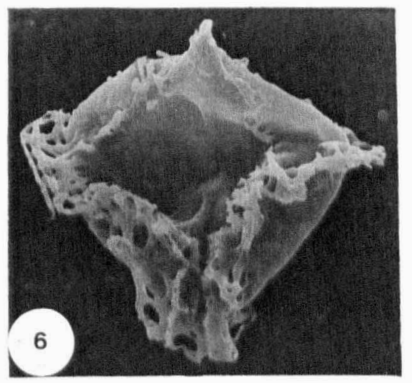
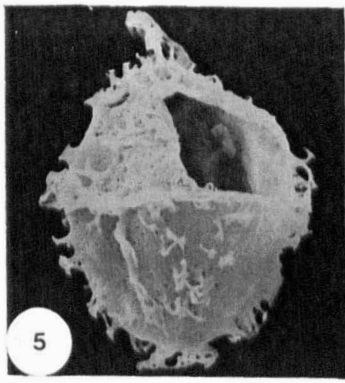
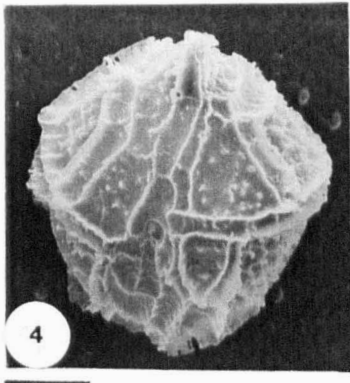
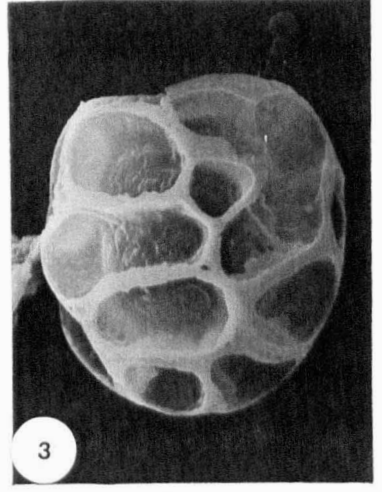
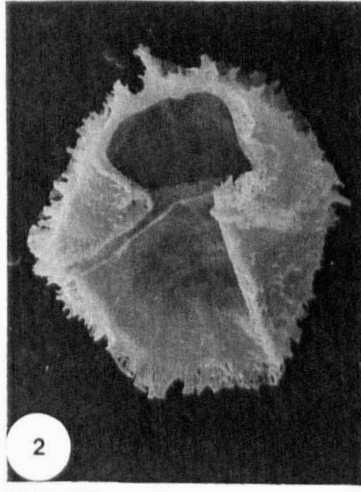
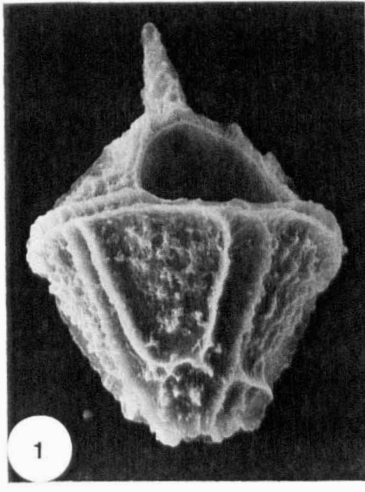


PLATE 25

All scale bars = 20 μm unless otherwise stated.

- 1:** *Batiacasphaera* sp. 1. SEM stub 2, grid square 1/I. Taken from sample K17. Ventral view.
- 2:** *Sentusidinium* sp. 3 SEM stub 11, grid square 1/III. Taken from sample K21. Dorsal view.
- 3, 6:** *Dingodinium cerviculum*. SEM stub 12, grid square 2/II. Taken from sample K17. **3:** Ventral view. **6:** Enlarged view of sulcal claustrum showing sculpture of both wall layers. Scale bar = 10 μm .
- 4:** *Tenu hystrix*. SEM stub 12, grid square 2/III. Taken from sample K17. Ventral view.
- 5:** *Tenu hystrix*. SEM stub 8, grid square 3/I. Taken from sample K24. Dorsal view.
- 7:** *Hystrichodinium pulchrum* var 1. SEM stub 11, grid square 3/II. Taken from sample K17. Ventral view of three-dimensionally preserved specimen.
- 8:** *Hystrichodinium pulchrum* var 1. SEM stub 4, grid square 2/II. Taken from sample K17. Lateral view of three-dimensionally preserved specimen.
- 9:** *Epiplosphaera gochtii*. SEM stub 6, grid square 2/I. Taken from sample K17. Dorsal view.
- 10:** *Endoscrinium campanula*. SEM stub 12, grid square 7/IX. Taken from sample K17. Dorsal view.
- 11:** *Gonyaulacysta pectinigera*. SEM stub 12, grid square 4/IV. Taken from sample K17. Dorso-lateral view.
- 12:** *Egmontodinium torynum*. SEM stub 5, grid square 2/IV. Taken from sample K8. Probably lateral view.

PLATE 25

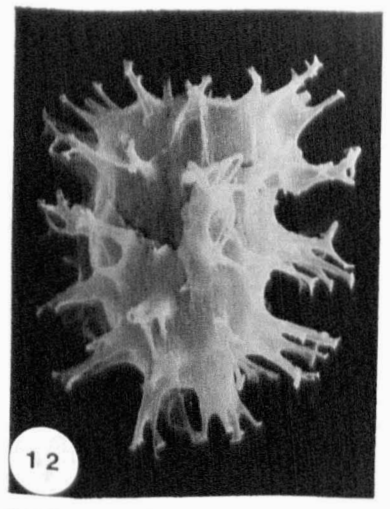
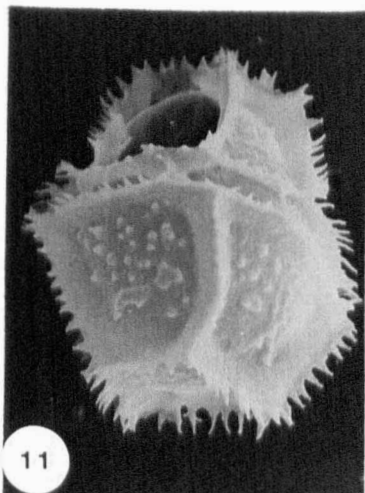
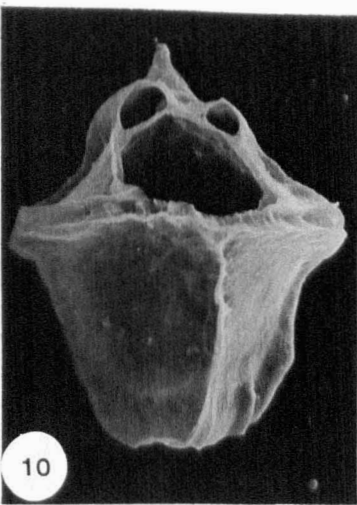
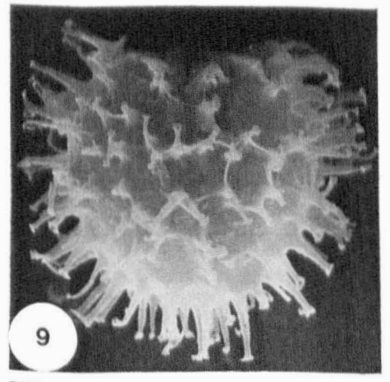
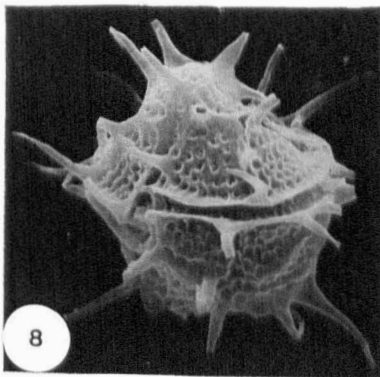
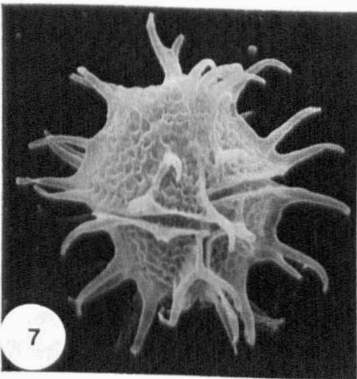
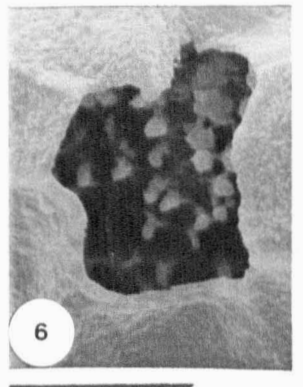
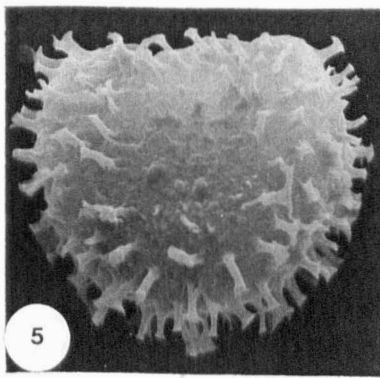
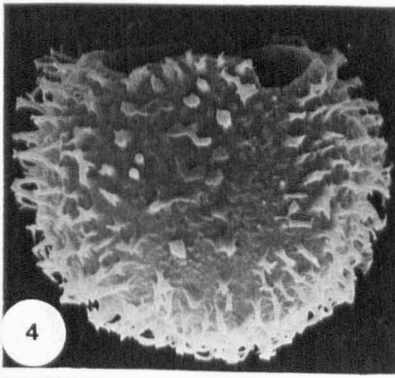
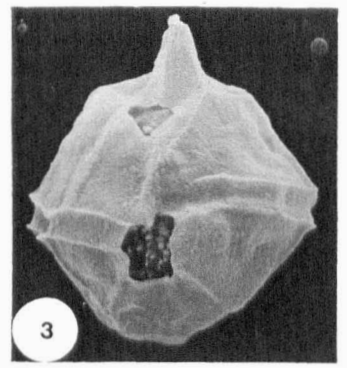
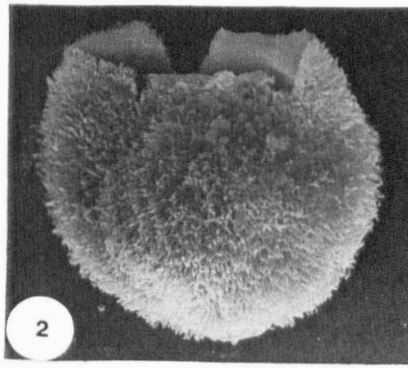
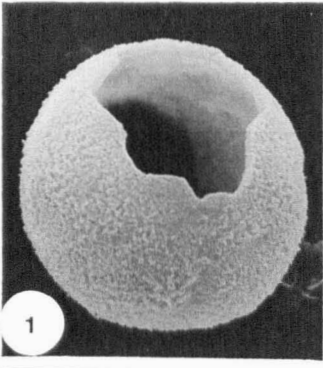
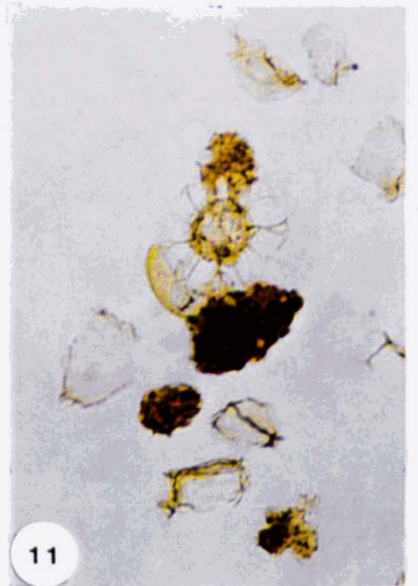
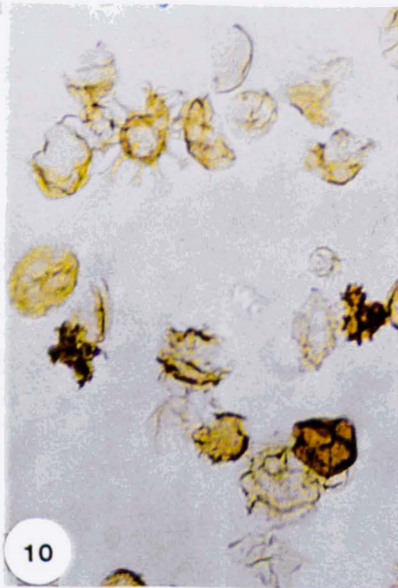
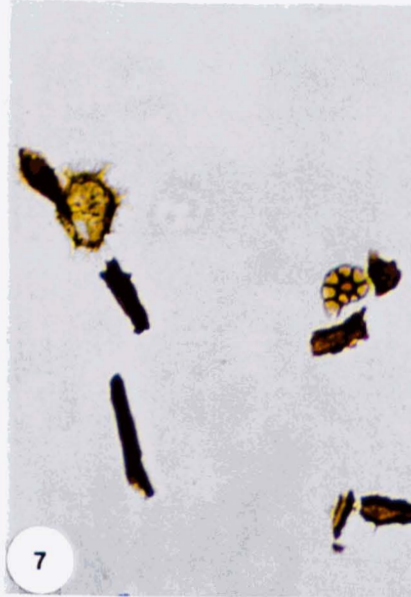
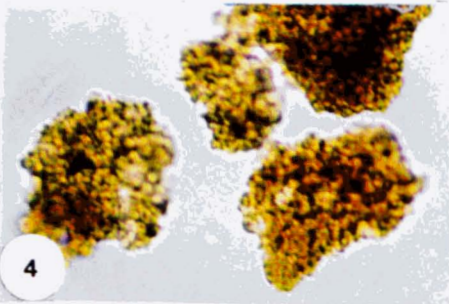
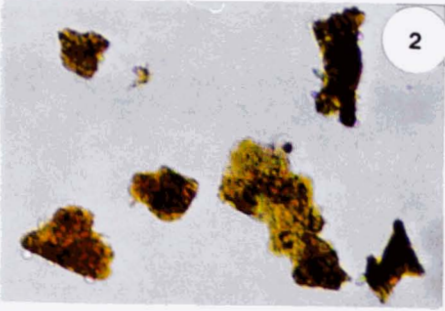
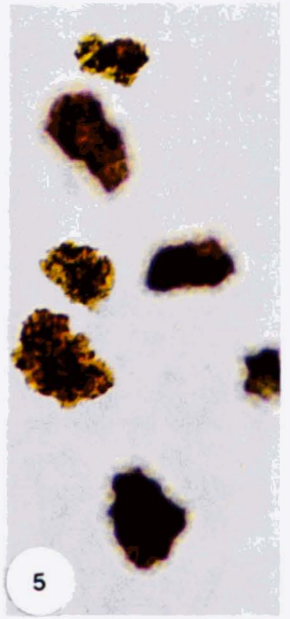
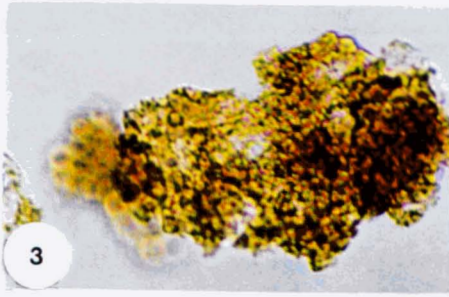
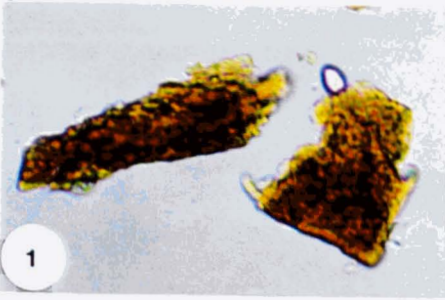


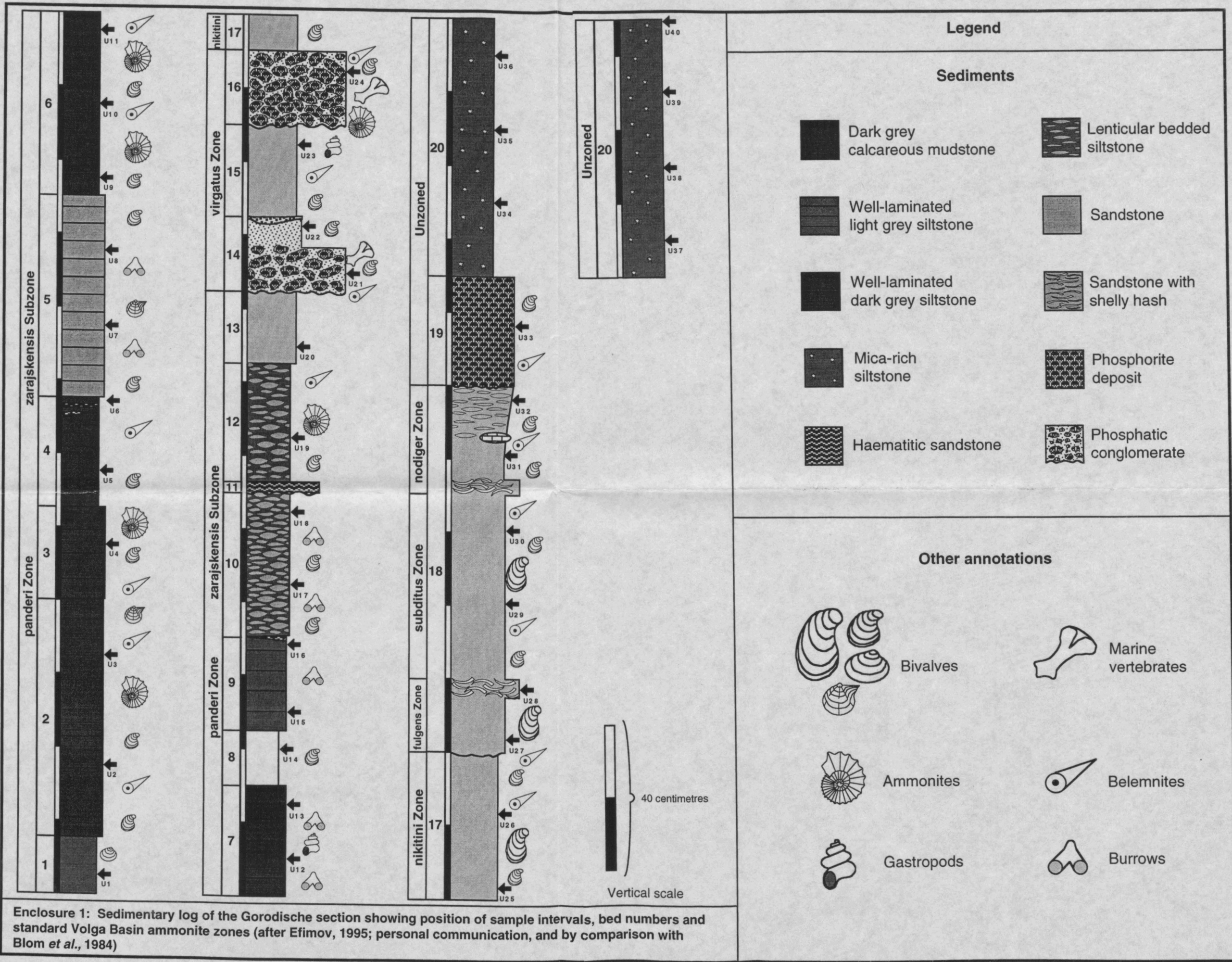
PLATE 26

- 1: Type 3 AOM from sample K10. x320 magnification.
- 2: Type 3 AOM from sample K10. x170 magnification.
- 3: Type 1 AOM from sample U2. x320 magnification.
- 4: Type 1 AOM from sample U2. x320 magnification.
- 5: Type 1 AOM from sample U8. x170 magnification.
- 6: Phytoclast-dominated palynofacies from sample U34. Characterised by frequent large and angular particles of brown and black wood and a poorly sorted assemblage. Black wood usually carbonised due to extended residence times at the sediment/water interface. x170 magnification.
- 7: Tracheid-dominated palynofacies from sample K17. Also abundant are dinoflagellate cysts and microforams. x170 magnification.
- 8: Tracheid-dominated palynofacies from sample K17. x170 magnification.
- 9: Dinocyst-dominated palynofacies from sample U26. x170 magnification.
- 10: Dinocyst-dominated palynofacies from sample K14. x170 magnification.
- 11: Dinocyst-dominated palynofacies with abundant Type 1 AOM from sample U10. x170 magnification.

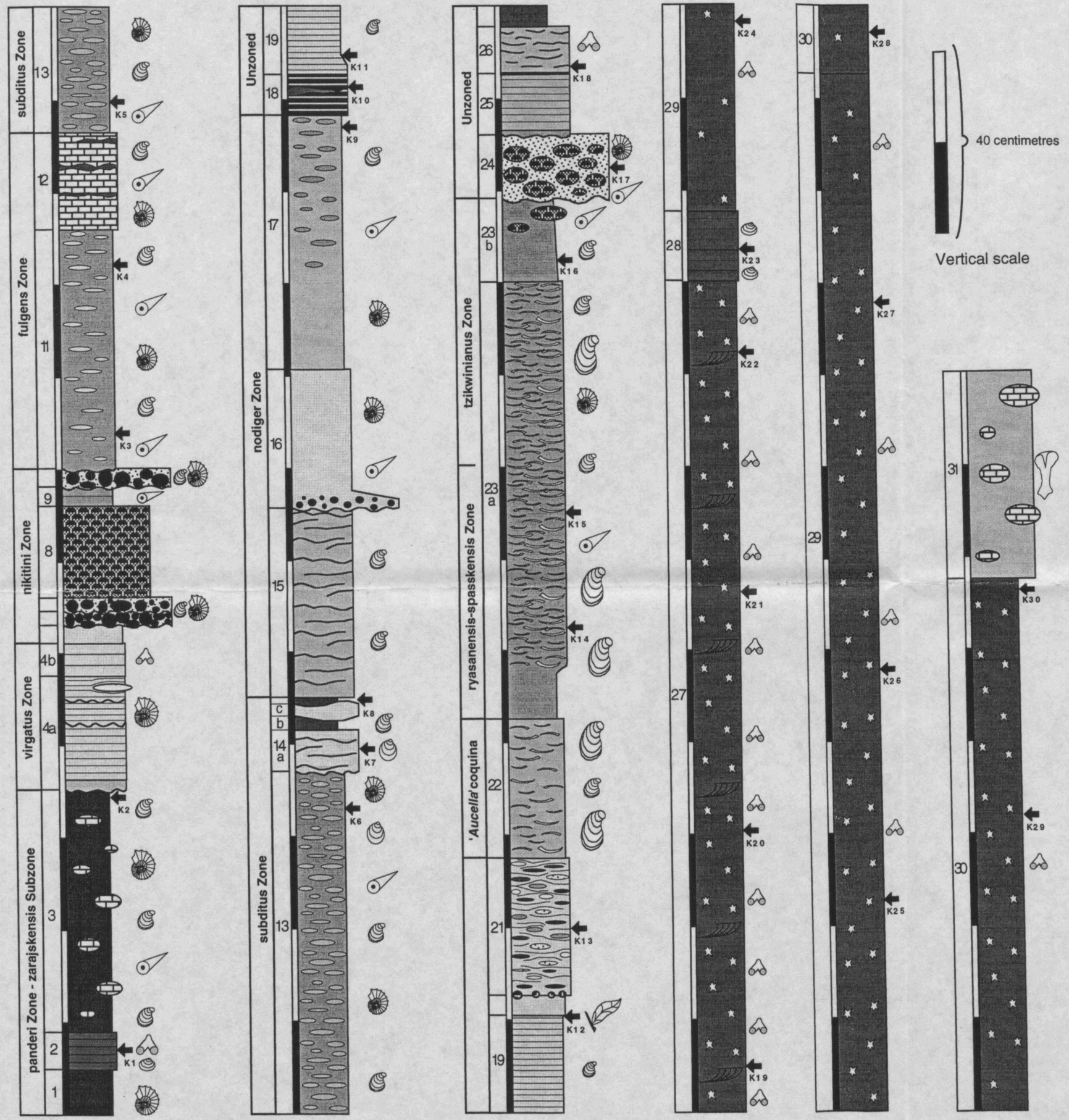
PLATE 26



CONTAINS DISKETTE



Enclosure 1: Sedimentary log of the Gorodische section showing position of sample intervals, bed numbers and standard Volga Basin ammonite zones (after Efimov, 1995; personal communication, and by comparison with Blom *et al.*, 1984)



Legend

Sediments	
Limestone Dark grey calcareous mudstone Well-laminated siltstone Mica-rich siltstone Bituminous shale Thinly bedded sandstone Sandstone with phosphatic concretions	Lenticular bedded siltstone Lenticular bedded sandstone Sandstone with calcareous concretions Siltstone with phosphatic concretions Wavy / flaser bedded sandstone Sandstone Sandstone with shelly hash Phosphoritized sandstone Conglomerate
Other annotations	
Bivalves Ammonites Plant fragments	Burrows Belemnites Marine vertebrates

Enclosure 2: Sedimentary log of the Kashpir section, showing sample positions and ammonite zonation. Beds 27 - 31 are unzoned by ammonites although suggested to be of Valanginian to Hauterivian age (Sazonova, 1972; Blom, 1984).